DOCTOR OF PHILOSOPHY

Applying effectoromics and genomics to identify resistance against Rhynchosporium commune in barley

Griffe, Lucie L.

Award date:
2017

DOCTOR OF PHILOSOPHY

Applying effectoromics and genomics to identify resistance against *Rhynchosporium commune* in barley.

Lucie L. Griffe

January 2017

University of Dundee

Table of contents

List of illustrations

List of tables

Acknowledgments

Firstly, I would like thank my supervisors Anna Avrova, Ingo Hein and Paul Birch at the James Hutton Institute and the University of Dundee for giving me the opportunity to do a PhD. I am also thankful to them and to Robbie Waugh for trustingly giving me the freedom to divert from my initial project by adding a supplementary strategy of study which considerably added value to my PhD and increased my knowledge. That move probably saved my PhD and would not have been possible without the help, guidance and encouragements of Mark Looseley to whom I am extremely grateful.

Thanks to the BBSRC for funding the research and the Crop Improvement Research Club members for the encouragements. Thanks to Paul Nicholson for hosting me in his lab during my last year.

Thanks to colleagues who helped me in any ways and made my PhD possible particularly Bill Thomas, Micha Bayer and Adokiye Berepiki. A big thanks to friends from the JHI who never let me down and became my Scottish family particularly my friends Adeline who was and is always available for anything providing me the strength to carry on, Daniel for sharing, discussing and understanding our exciting results, Louise for warming up the lab with our laugh, Camille and Fulvia for sharing all these entertaining lunches, (Italian) dinners and time out, Maelle for her friendship and support, Sophie for her experienced scientific support and Julie for chats and support.

Thanks to the John Jones team for sharing facilities and knowledge. Thanks to the staff of the JHI facilities such as the media kitchen, glasshouse and particularly to the engineering team who comprehensively and kindly deal with stressed PhD students' requirement.

Thanks to my old friends Justine and Elodie for coming for visit, being such good friends and sharing our respective PhD life issues which probably only another PhD student could ever understand.

A last but special thanks to my family for believing in me and always letting me accomplish whatever I wanted to, to Sigma who was strong moral support and finally to Hadrien for his help, optimism, support and endless patience through all my PhD giving me the courage to finish.

Declaration

I certify that I am the author of the thesis. All references cited have been consulted. The work and according results presented have been generated by myself unless otherwise stated, and it has not been previously accepted for a higher degree.

Lucie L. Griffe

Abstract

Rhynchosporium commune is one of the most destructive fungal pathogens of barley worldwide. It causes scald, responsible for reduced grain quality and yield losses of up to 40%. This project aimed to identify genetic resistance in barley using two different approaches: an effector approach through the identification of important pathogen virulence factors and their barley targets, and a genomics association approach.

Numerous secreted effectors have been identified in many phytopathogens including *R. commune*. *Rrs1* resistance, recognising the *R. commune* avirulence protein - AvrRrs1 (NIP1) has been deployed in the field to prevent infection but has soon proven ineffective. *R. commune* has managed to overcome this resistance by alteration or deletion of the *NIP1* gene as it is not essential for pathogenicity. However, our field trial data suggests that *Rrs1* remains an important component of resistance to *R. commune* in the field. Resistance genes recognising more essential *Avr* genes are likely to be more durable and as a consequence, the discovery of novel *R. commune Avr* genes is fundamental for the implementation of an integrated pest management approach to prevent this disease.

Recent sequencing of the *R. commune* genome allowed identification of putative effectors. Expression of 26 potential effectors with low sequence variability in 9 sequenced *R. commune* strains have been analysed during barley infection. The best genes were selected for gene disruption and individual expression in barley cultivars and landraces using the Barley Stripe Mosaic Virus (BSMV) – based expression system to see if they are recognised by the plant. The work also focused on candidate effectors with putative functions. A putative protease inhibitor was chosen for functional characterisation but its function and importance for pathogenicity could not be confirmed. In addition, high amount of the candidate protein appeared to be toxic for barley and *Nicotinana benthamiana*. Two SA (salicylic acid)-related putative effectors were also chosen for further characterisation and revealed a direct link between the SA pathway of barley and *R. commune.* The results of this project suggest that *R. commune* might be able to manipulate the SA

pathway of the host confirming the existence of a biotrophic phase of the fungus.

The genomics association approach to identify resistance genes against *R. commune* in barley used a Genome Wide Association Scan (GWAS) using a combination of three years of disease nursery field trial data for a collection of over 500 elite spring barley cultivars. This analysis identified a number of quantitative trait loci (QTL) in barley genome regions previously shown to contain major resistance genes such as *Rrs1* on chromosome 3H, *Rrs2* on chromosome 7H, *Rrs3* on chromosome 4H, *Rrs4* on chromosome 3H, *Rrs13* on chromosome 6H, *Rrs14* on chromosome 1H and *Rrs16* on chromosome 4H, as well as novel QTL. The work was focused on *Rrs1* resistance. *R. commune* strains producing a type of NIP1 effector, recognised by barley lines containing *Rrs1*, were used to confirm the resistance in predicted *Rrs1* barley cultivars. The *Rrs1* interval has been narrowed down to 3 Mbp, and high resolution mapping led to the identification of 3 SNP markers which perfectly discriminated $Rrs1_{Rh4}$ lines from susceptible lines. These diagnostic markers will provide a useful breeding tool for improving the design of new varieties allowing the incorporation of the *Rrs1* resistance. This research takes us a step closer towards cloning the first barley major resistance (*R*) gene against *R. commune,* which is likely to be present only in *Rrs1* lines and have a kinase domain very similar to the one in a putative wall associated kinase found within the *Rrs1* interval in the genome assembly of susceptible cultivar Morex. It will also help us to better understand *R. commune*-barley pathosystem and to identify further *R* genes.

I. Chapter 1: General introduction

I.1. Plant pathogens in human history

All kinds of plant pests and pathogens, including viruses, bacteria, oomycetes and fungi have been involved in many dramatic periods in human history. They destroyed harvests, forced people to change diet and/or location to avoid famine, caused huge economic losses and stimulated the improvement of agricultural practices, habits, techniques and the development of science.

The most famous example is the potato late blight caused by the Oomycete *Phytophthora infestans* which caused the Irish “Great Famine” in the 1840s: 1.5 million Irish people died and a similar number emigrated (Fry and Goodwin 1997). This unexpected epidemic stimulated the development of plant pathology as a discipline to investigate the nature of plant disease. More recently in 1960 bacterial leaf blight led to up to 75% reduction in yield of rice in South and South-East Asia and Japan, due to the massive use of susceptible dwarf high-yielding varieties (NiÑO-Liu et al. 2006). Farmer varieties and wild material throughout the world were incorporated into breeding programmes to generate new resistant varieties.

Fungi can be devastating pathogens as well. In 1970-1972 southern corn leaf blight, caused by Race T of the fungus *Bipolaris (Helminthosporium) maydis* ravaged fields resulting in an estimated loss of about 1 billion dollars (Ullstrup 1972; Cai et al. 2003). Losses of 50% or more were common in some areas of the US mainly because US maize was highly susceptible (Tatum 1971). The food energy losses were considered to be greater than those caused by the potato late blight epidemic of the 1840's but human losses were low as maize mainly served to feed animals. Since February 2016, Bangladesh wheat fields are being devastated by a new fungal disease spreading to an estimated 15000 hectares with up to 100% yield losses forcing farmers to burn wheat fields to contain the disease. Transcriptome sequencing, phylogenomic and population genomic analyses of infected leaf samples revealed that the epidemic was caused by a *Magnaporthe oryzae* strain related to the South American blast fungus. This fungus, specialized in infecting rice seems to have evolved to infect wheat and was originally identified in 1985 in Brazil causing serious wheat

production losses in the warmer wheat growing areas of South America (Islam et al. 2016; Malaker et al. 2016). The emergency of the situation solicited the scientific community to fight against this new threat and the Open Wheat Blast website was created making the data accessible to whoever would like to help.

In Europe, and more specifically in France, an insect, the grape phylloxera, *Daktulosphaira vitifoliae* destroyed most of the vineyards in the late 19th century. The grape phylloxera arrived from the United States in the 1850s and caused weakening and wounding on roots while feeding, promoting fungal infection (Granett et al. 1998). This epidemic develops the use of hybridisation with resistant varieties but grafting with American resistant rootstock was the preferred method and saved the European wine industry (Melnyk and Meyerowitz 2015). The last example relates to Cassava mosaic disease (CMD) caused by whitefly borne viruses that caused an epidemic that broke out in Uganda during the early- to mid 1990's (Otim-Nape and Thresh 1998; Alabi 2011). Chemical control of the whitefly vector has been sought and efforts have been made to breed new resistant varieties (Alabi 2011).

I.2. Plant infection

I.2.1. The plant-pathogen interactions model

Plants are immobile living systems; they cannot move to avoid an unfriendly environment or biotic pressures such as pathogens. Plants are constantly under pathogen pressure and the fact that plants have evolutionally survived until now indicates that most plants are resistant to most plant pathogens. As a consequence, plants must have developed a system to be able to fight, more or less efficiently against their pathogens. The gene-for-gene interaction hypothesis, firstly described by Flor (1955) illustrates the relation between the plant gene called resistance (R) gene and the pathogen gene called avirulence (*avr*) gene. Plants carrying a specific R gene are resistant to a pathogen with biotrophic phase carrying the corresponding avr gene, and therefore used in breeding programmes as sources of major resistance (Flor 1971; Robinson 1987). This gene-for-gene relationship is the basis of the plant immune system called the innate immunity- a system able to detect and stop pathogens during the biotrophic phase by inducing systemic signals (Chisholm et al. 2006; Jones

and Dangl 2006; Boller and He 2009). Like mammals, the plant immune system can discriminate between self and non-self. The current thinking is that the plant immune system has two strategies: one involving the use of transmembrane pattern recognition receptors (PRRs) recognising pathogen-associated molecular patterns (PAMPs) (Zipfel and Felix 2005) and the second using nucleotide binding (NB) and leucine rich repeat (LRR) (NB-LRR) domain proteins, products of classical R genes, recognising pathogen-encoded effectors (Dangl and Jones 2001). At present, the plant immune system is represented as a 'zigzag' model containing four phases (Figure I-1). During the first phase, PAMPs are being recognised by PRRs resulting in PAMP-triggered immunity (PTI), stopping or slowing down pathogen colonisation. During the second phase, pathogens produce proteins involved in pathogenicity called effectors and possibly disabling PTI resulting in effector-triggered susceptibility (ETS). In the third phase, an effector is directly or indirectly recognized by NB-LRR proteins, resulting in effector-triggered immunity (ETI). ETI has a similar effect to PTI but often results in plant cell death called hypersensitive response (HR) and disease resistance thanks to its faster and stronger effect. HR allows the spread of the disease during biotrophic infection to be stopped but can be a disadvantage against necrotrophic pathogens. The fourth phase describes the ability of pathogens to evolve to avoid ETI by losing or modifying the recognized effector gene, or to suppress ETI using extra effectors (Jones and Dangl 2006).

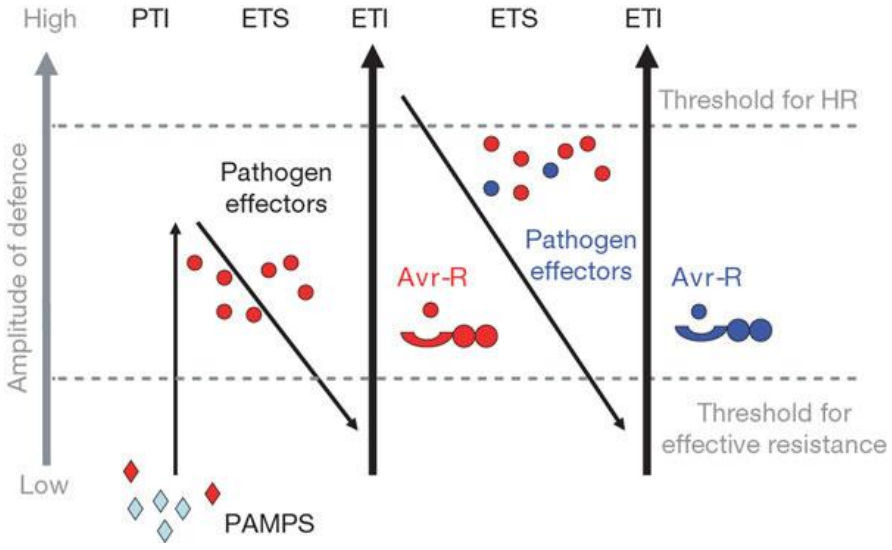

Figure I-1: A zigzag model explaining the quantitative response of the plant immune system (Jones and Dangl 2006). PAMPs (or DAMPs) are detected via PRRs activating PTI. Effectors delivered by pathogen disable PTI or trigger ETI preventing the feeding and growth of the pathogen by the induction of HR.

Plant defences and pathogen actions are different depending on the lifestyle of the pathogen, whether it is a biotroph - feeding from living host tissue, or a necrotroph - killing host tissue before feeding (Glazebrook 2005), or a hemibiotroph - colonising the living host tissue before moving on and sometimes inducing cell death (Horbach et al. 2011; Doehlemann and Hemetsberger 2013).

I.2.2. PAMPs and PTI

PAMPs are defined as molecules that are conserved and important to the microbial lifestyle, and that are secreted or released from cells of microorganisms (Medzhitov and Janeway 1997). For example, bacterial flagellin contains a 22 amino acid -long peptide, flg22, that activates PTI in tomato and Arabidopsis via binding to the LRR receptor-like kinase (LRR-RLK) flagellin-sensitive 2 (FLS2) (Meindl et al. 2000; Chinchilla et al. 2006; Boller and Felix 2009) (Figure 2). Fungal chitin triggers immunity in rice thanks to LysM receptor-like proteins CEBiP and OsCERK1 (Shimizu et al. 2010) and in Arabidopsis thanks to CERK1 (Miya et al. 2007). In addition, DAMPs, for danger-associated molecular patterns are molecules released during infection by the plant and being detected as a PAMP (Huffaker and Ryan 2007). For example, AtPep1 is a 23-aa endogenous peptide from Arabidopsis that activates PTI through a LRR-RLK called PEPR1 (Yamaguchi et al. 2006).

PTI induces basal defence activation with the production of phytohormones such as salicylic acid (SA) and jasmonic acid (JA) which are important factors of the signal transduction activating plant defences (Dong 1998; Doehlemann and Hemetsberger 2013). SA-dependent responses are specific to biotrophic pathogens and trigger several complex processes such as reactive oxygen species (ROS) accumulation, systemic acquired resistance (SAR), pathogenesis-related (PR) gene activation, callose deposition and activation of a mitogen-activated protein kinase (MAPK) cascade to induce defence gene expression and, in some cases, lead to hypersensitive response (HR) (Morel and Dangl 1997; Cao et al. 1998; McDowell and Dangl 2000; Nicaise et al. 2009). However, HR is an inconvenient strategy against necrotrophic pathogens. Necrotrophs are controlled by the antagonistic JA-dependent signalling triggering the secretion of defence compounds called phytoalexins

with antimicrobial activity, such as pathogens cell membrane damage caused by camalexin (Ahuja et al. ; Memelink et al. 2001).

I.2.3. Effectors, suppression of PTI, ETI and manipulation of plant host

Effectors are secreted small proteins used by pathogens to manipulate plant processes to their benefit, but some may also trigger plant immune responses (Stergiopoulos and de Wit 2009; Pelgrom and Van den Ackerveken 2016). Depending on the infection strategy, the pathogens can deploy apoplastic effectors often represented by cysteine-rich proteins for the stability in the apoplast, or/and cytoplasmic effectors such as the RXLR and CRN families in Oomycetes (Kamoun 2006).

PTI suppressor: The oomycete *P. infestans* is a well-studied example which uses apoplastic and cytoplasmic effectors. For example, it uses EPI1, a Kazal-like serine protease inhibitor to inhibit and interact with (among other things) the pathogenesis-related subtilisin-like serine protease of tomato in the apoplast to disable the PTI activation of P69B protein induced by multiple plant pathogens, including *P. infestans* (Tian et al. 2004; Tian et al. 2005). Other examples include the potato cyst nematode *Globodera rostochiensis* using GrCEP12 peptide to increase the susceptibility of the host by suppressing host basal defence, and bacterial pathogen *Streptomyces scabiesis* which is able to suppress flg22-mediated PTI in *N. benthamiana* (Chen et al. 2013).

ETI and ETI suppression: In *P. infestans* ETI was effectively working against the cytoplasmic effector Avr3a recognised by the R3a resistance protein (Armstrong et al. 2005). However, a different allele of Avr3a was identified containing 2 SNPs coding for a form of Avr3a which is able to avoid recognition. In addition, Avr3a was shown to suppress the recognition of INF1, a PAMP triggering HR in *N. benthamiana* (Kamoun et al. 1998; Bos et al. 2006). In *Pseudomonas syringae* the secreted protein HopPtoD2 was shown to be able to supress HR elicited by an avirulent strain on *N. benthamiana* thanks to its protein tyrosine phosphatase activity (Espinosa et al. 2003). In addition, *Fusarium oxysporum* f. sp. *lycopersici* secreting Avr1 effector in the xylem of tomato is a perfect example illustrating the constant evolutionary fight between pathogens and their hosts. Two R genes I-2 and I-3 have evolved to allow recognition of Avr2 and

Avr3 effectors, respectively. However, the pathogen evolved to produce Avr1 effector to suppress Avr2 and Avr3 recognition, thereby promoting tomato evolution to itself acquire the gene *I,* the product of which specifically recognises Avr1 without being sensitive to Avr1 suppression (Houterman et al. 2008).

Host manipulation upstream of plant defence responses: Plant pathogens seem to share the mechanism used to manipulate the production of SA by the host. For example, *Ustilago maydis* secretes and translocates chorimate mutase Cmu1 into the plant cells to manipulate the shikimate pathway to slow down the production of SA by prioritising the tyrosine and phenylalanine synthesis pathway though the conversion of chorismate to prephenate (Djamei et al. 2011). In addition, chorimate mutase was reported to be an important virulence factor in *Xanthomonas oryzae pv. oryzae* (Degrassi et al. 2010) and the soybean cyst nematode *Heterodera glycines* (Bekal et al. 2003). Moreover, *Phytophtora. sojae* and *Verticillium dahlia* seem to use another strategy to disrupt the SA pathway: they produce isochorismatases, unconventionally secreted proteins essential for pathogenicity which suppress SA-mediated PTI *in planta* by consuming SA pathway precursors (Liu et al. 2014).

Host manipulation unrelated to plant defence processes: Pathogens can also use effectors to directly manipulate other plant processes to improve their environment. For example, the AvrBs3 effector family from *Xantomonas campestris pv. vesicatoria,* also known as TAL (transcription activator-like) effectors work as transcription factors inducing expression of plant genes related to cell size (Kay et al. 2007), resulting in cell hypertrophy which promotes bacterial dispersal (Marois et al. 2002). However, the AvrBs3 effector appeared to be itself activating ETI through the pepper Bs3 resistance gene, inducing recognition mediated by promoter activation (Romer et al. 2007).

The above examples show that effectors can be very variable and target many mechanisms to promote host colonisation. This variability of function and the fact that the function of most effectors remains unknown does not help with the identification of new effectors, potential target of resistance genes. So far, effectors have been identified by differential study comparing transcription or

protein presence and quantity during different phases of infection or by similarities with known effectors.

I.2.4. Plant genes and mechanisms involved in resistance

Plant defence mechanisms are very complex, depend on the pathogen infection strategy and involve a multitude of different kinds of genes, many of which still remain unknown. A few examples are going to be listed and described.

Receptors: Receptors are a part of the first layer of resistance processes thanks to their role in sensing the presence of the pathogen with the aim of transmitting the signal to the rest of the cell/plant (Figure I-2). Extracellular receptors recognising PAMPs, PAMP recognition receptors (PRRs) and apoplastic effectors include membrane proteins called receptor-like kinases (RLK) and receptor-like proteins (RLPs). RLKs contain extracellular receptor domain, a transmembrane domain and an intracellular kinase domain, while RLPs contain an extracellular receptor domain and a transmembrane domain but lack a cytoplasmic kinase domain (Zipfel 2014) and are thought to interact with other kinases for signalling (Böhm et al. 2014). RLKs are sorted into different families depending on their ligand such as LRR-RLKs, LysM domain-RLKs, Lectin-RLK, Wall-associated-kinase-RLK (WAK) and many others. Most PRRs interact with the Brassinosteroid insensitive 1-Associated Kinase 1 (BAK1). For example, in *A. thaliana*, the LRR-RLK FLS2 and BAK1 form a complex which is necessary for positive regulation of signalling though PRR of the bacterial PAMP flagellin (Chinchilla et al. 2007). Another example showed that the *Arabidopsis. thaliana* lectin receptor kinase LecRK-I.9 provided an increase of resistance to *P. infestans* in potato and *N. benthamiana* though the probable activation of protease inhibitors (Bouwmeester et al. 2014). In maize, a WAK-RLK called ZmWAK-RLK1 at *Htn1* locus have been shown to delay the lesion formation and to provide partial resistance to northern corn leaf blight potentially thanks to the ability of WAK to sense changes to the cell wall structure induced by the pathogen infection by detecting oligogalacturonides (Brutus et al. 2010; Hurni et al. 2015).

Intracellular receptors NB-LRR recognise intracellular effectors in the cytoplasm of plant cells through LRR motifs. They also form complexes, as in the case of the *A. thaliana* protein RPM1 which associates with HSP90 in the cytoplasm of

the cell to switch on disease resistance processes in response to *P. syringae* (Hubert et al. 2003).

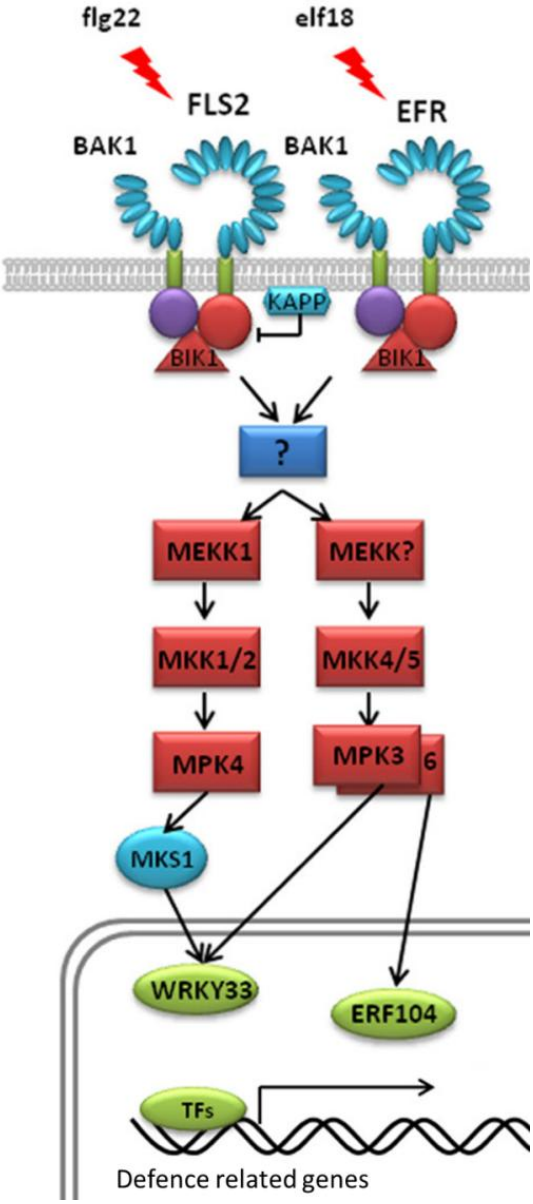

Figure I-2: Diagram illustrating plant defence mechanism from PAMP perception. PAMPs are inducing plant defence relate gene through the action of receptor, MAPK cascade activation, transcriptional factor translocation to the nucleus and induction of plant related genes (adapted from Park et al. (2012))

Mitogen-activated protein kinases (MAPKs): MAPKs are highly conserved and are the main and earliest component of intracellular signal transduction downstream of receptors and are activated by phosphorylation (Figure I-2). Several studies have shown that MAPK cascades (succession of MAPK three-kinase) play an important role in plant defence responses and are likely to be one of the converging points in the defence signalling network (Zhang and Klessig 2001).They activate responses such as the biosynthesis and signalling

of plant stress and defences hormones, ROS generation, stomatal closure, defence genes activation, phytoalexin biosynthesis, cell wall strengthening, and HR cell death (Meng and Zhang 2013). For example, in Arabidopsis, two MAPK: MPK3 and MPK6 play roles in PTI activation through DAMP activation due to oligogalacturonides (OGs) release during *Botrytis cinerea* infection (Galletti et al. 2011) and activation of the WAK1 receptor (Brutus et al. 2010). In addition, in parsley, *P. sojae*-derived oligopeptide elicitor Pep25 binds to a plasma membrane receptor activating ETI through a MAPK which is translocated to the nucleus and possibly interacts with transcription factors activating the expression of defence genes (Ligterink et al. 1997).

Transcription factors: Regulators of transcription play an important role in plant defence (Eulgem and Somssich 2007) (Figure I-2) and are represented by several families such as ERF, MyB and WRKY, positively or negatively regulating defence-related genes (Eulgem 2005). For example, in rice, the SA-inducible *WRKY45* gene was shown to promote resistance against blast fungus *Magnaporthe grisea* (Shimono et al. 2007); the overexpression of the cotton *GhWRKY15* seems to contribute to the alteration of defence resistance to viral and fungal infections in tobacco (Yu et al. 2012), and overexpression of *VvWRKY33* in grapevine leaves increases resistance to *Plasmopara viticola* and reduces pathogen sporulation by up to 70% (Merz et al. 2015).

Transporters: ATP-binding cassette (ABC) transporters are membrane structures mediating the translocation of molecules across the membrane and are involved in a large range of processes such as polar auxin transport, lipid catabolism, xenobiotic detoxification, stomatal function and disease resistance (Rea 2007) and actively participate in the fight against pathogens. For example, NpPDR1, ATP-binding cassette transporter of *Nicotiana plumbaginifolia* has been suggested to transport the diterpene sclareol, an antifungal compound, and to be involved in JA-dependent defence and provides resistance against *B. cinerea* (Stukkens et al. 2005). In addition, the wheat gene *Lr34* encoding an ABC transporter has been shown to provide multiple resistances to leaf rust (*Puccinia triticina*), stripe rust (*Puccinia striiformis f.sp. tritici*), stem rust (*Puccinia graminis f.sp. tritici*) and powdery mildew (*Blumeria graminis f.sp. tritici*) in wheat (Ellis et al. 2014); to leaf rust in durum wheat; (Rinaldo et al. 2016); to leaf rust and powdery mildew in barley (Risk et al. 2013); to blast

disease (*M. oryzae*) in rice (Krattinger et al. 2015); and to rust and northern corn leaf blight (*Exserohilum turcicum*) in maize (Sucher et al. 2016).

Protease inhibitors: Protease inhibitors (PIs) are an efficient means of protection against proteases released by pathogens during infection by preventing the action of pathogenic proteases on plant proteins by usurping or modifying the binding site. PIs are activated by PTI in particular by necrotrophic pathogens, insects and herbivores (Mengiste 2012; Zhu-Salzman and Zeng 2015). Plant PIs have been divided into 10 main families based on sequence similarity, the similarity of protein folds of the inhibitory domains and the specific protease targeted (Habib and Fazili 2007). Transgenic plants expressing heterologous PIs have been shown to be resistant to certain pests and pathogens. For example the potato proteinase inhibitor II gene *pin2* was introduced into japonica rice varieties which resulted in an accumulation of protein increasing the resistance to an insect named pink stem borer (*Sesamia inferens*) (Duan et al. 1996). The bean α-amylase inhibitor 1 αAI-1 introgressed into peas provided complete protection against the pea weevil (*Bruchus pisorum*) in pea seed and under field condition (Morton et al. 2000). More recently, a subtilisin-chymotrypsin inhibitor appeared to be induced during stripe rust infection of wheat and involved in plant resistance (Huang et al. 2013).

Gene silencing: Gene silencing is the downregulation of gene expression by non-coding RNAs called double-stranded RNA (dsRNA) which are able to inhibit gene expression by causing the degradation of messenger RNA (mRNA) and by altering the transcriptional activities through the induction of DNA methylation. dsRNAs are produced by transcription from both DNA strands by RNA-dependent RNA polymerase and cut into short interfering RNA (siRNA) by Dicer. Then single stranded siRNAs are carried by Argonaute which cleaves mRNA complementary to the loaded siRNA (Baulcombe 2004; Vetukuri et al. 2011). Gene silencing was found to be a plant defence mechanism which is activated in particular against viruses and transposable elements (Waterhouse et al. 2001). Suppression of posttranscriptional gene silencing (PTGS) was shown to be one of the counter-defence strategies by DNA and RNA viruses (Voinnet et al. 1999). In addition, *P. syringae* carrying the effector *avrRpt2* was reported to be inducing an endogenous siRNA called nat-siRNAATGB2 during infection of *A. thaliana* by repressing a putative negative regulator of the RPS2

disease resistance gene required for race-specificity (Katiyar-Agarwal et al. 2006).

The examples of plant genes and mechanisms involved in resistance listed above show that plants evolved alongside their pathogens and developed a set of mechanisms to fight against all kind of pathogens and their diverse infection strategies and effectors.

I.3. Barley

I.3.1. General information

Barley (*Hordeum vulgare*) is a cereal that originated in west Asia in various sites of the Fertile Crescent in the Middle East. Like wheat and rye it was domesticated about 10000 years ago (Badr et al. 2000; Khoury et al. 2016). Barley is the fourth most important cereal crop, cultivated on 48 million hectares spanning ~100 countries with over 144m tonnes produced in 2014 (faostat.fao.org). Europe produces almost 60% of the global barley crop with around 86m tonnes produced in 2013, making it the fifth largest crop. Most barley is used as a carbohydrate source in animal feed but in the UK the crop's most valuable use is in malting for the production of beer and whisky (Newton et al. 2011). There is also increasing interest in barley's potential health-food properties, e.g., lowering LDL cholesterol, contributing positively to diabetics' diets and reducing colon cancer incidence (Johansson et al. 2013; Sullivan et al. 2013; Thompson et al. 2016).

I.3.2 Barley genome

Barley is a diploid with a large haploid genome of 5.1 Gbp which have been recently sequenced (Mayer et al. 2012). Barley is widely used as a model crop for adaptation to climate change (Dawson et al. 2015), plant breeding methodology and genetics (Yin et al. 1999), cytogenetics (Heneen 2010), pathology and virology (Thackray et al. 2009), and biotechnology studies (Akar et al. 2004).

I.3.3. Barley pathogens

Unfortunately, yield losses occur in barley due to biotic factors such as fungal and viral infection, pests and weeds (Oerke and Dehne 2004), and resistance adaptability of the crop requires improvement. Fungal pathogens represent the main constraint to barley production and barley is mainly susceptible to five fungal pathogens. Net blotch is caused by *Pyrenophora teres*, and induces yield losses of 10%–40% (Liu et al. 2011) (Figure I-3a). Brown rust (or leaf rust) is caused by *Puccinia hordei,* can in some areas cause yield losses close to 30% (Qi et al. 1998) (Figure I-3b). Powdery mildew is due to *B. graminis,* an obligate biotrophic fungus causing considerable yield losses throughout the world (Tucker et al. 2015) (Figure I-3c). Foot rot (or Spot blotch) caused by *Cochliobolus sativus*, is one of the most common and economically important diseases of barley and can cause more than 30 % yield loss and significantly impact the malting quality of barley (Wang et al. 2016) (Figure I-3d). Scald (or leaf blotch) is caused by *R. commune* inducing up to 45% of yield losses and a decrease in grain quality (Avrova and Knogge 2012) (Figure I-3e).

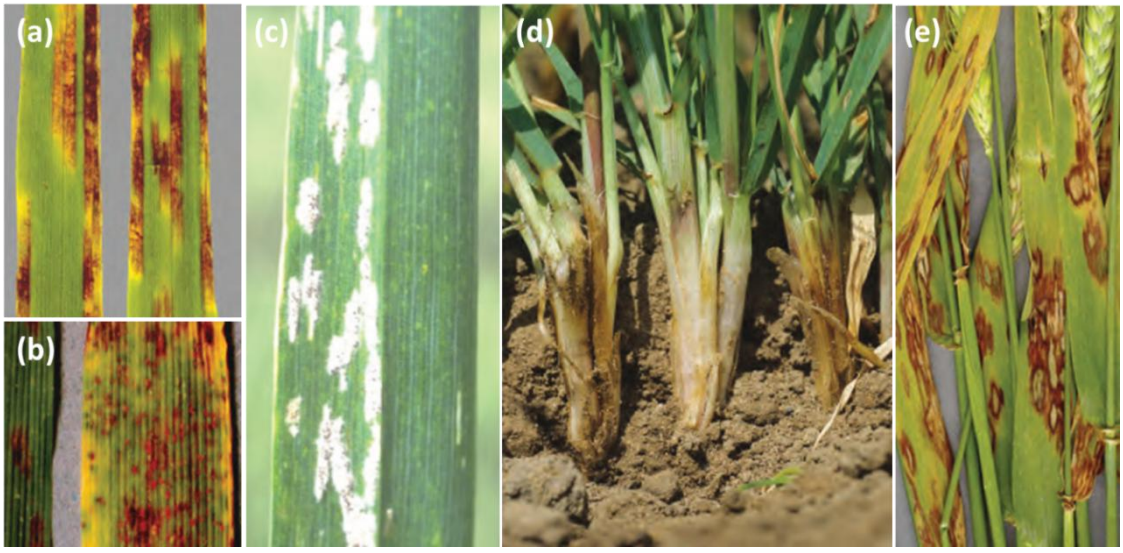

Figure I-3: Picture illustrating the 5 main barley diseases. Barley infection with (a) *P. teres,* (b) *P. hordei,* (c) *B. graminis,* (d) *C. sativus*, (e) *R. commune.* (pictures from encyclopaedia of cereal diseases - BASF UK)

I.4. *Rhynchosporium commune*

I.4.1. General information

R. commune is an ascomycete fungal pathogen causing one of the most economically significant and destructive disease of barley worldwide known as

leaf scald (or leaf blotch) (Avrova and Knogge 2012; AHDB 2016). Barley scald affects grain quality and decreases yield by up to 40 % when conditions are favourable for disease development by infecting leaves, leaf sheaths and ears (Xi et al. 2000). CropMonitor national survey 2005 data indicated that Rhynchosporium involved a national yield loss worth £7.2 million (at £150/t) despite treatment (AHDB 2016). This fungus occurs in cool temperature areas and is very important in the UK; particularly in Scotland, Northern Ireland, Wales and the west of England (AHDB 2016) (Figure I-4a). *R. commune* was first isolated from rye and described as *Marsonia secalis Oud*, by Oudemans (1897) in the Netherlands and in Germany by Frank (1897). The fungus was reclassified into the new genus *Rhynchosporium graminicola* thanks to its typical beak-shaped one-septate conidia by (Heinsen 1901). The first recorded description of the pathogen in the UK happened in 1919 (Brooks 1928) and was renamed as *Rhynchosporium secalis* due to its ability to infect barley, rye, triticale and other grasses by Davis (1922). In 2011, phylogenetic analysis of DNA sequence data of *R. secalis* isolates originating from cultivated barley, rye, triticale and other grasses split them into 3 different species according to their respective hosts, Rhynchosporium isolates infecting *Hordeum spp*. (including cultivated barley) and *Bromus diandrus* belong to a the *R. commune* species, Rhynchosporium isolates infecting rye and triticale belong to *R. secalis* species and isolates infecting *Agropyron spp.* represent a distinct species of Rhynchosporium, namely *R. agropyri* (Zaffarano et al. 2011).

I.4.2. Life cycle

R. commune has been classified as a hemibiotroph (Perfect and Green 2001; Oliver and Ipcho 2004); despite producing necrotic lesions, it has a long asymptomatic phase during which it is able to colonise the host tissues and even sporulate (Zhan et al. 2008; Thirugnanasambandam et al. 2011; Avrova and Knogge 2012). *R. commune* is a polycyclic pathogen, with primary inoculum coming from crop debris left in the field, and infected seed (Davis and Fitt 1992; Fitt et al. 2010). Conidia land on the surface of barley helped by water droplets and germinate within the first 24 h (Linsell et al. 2011), generating a germ tube which directly penetrates the cuticle (Jones and Ayres 1974) or occasionally the stomata pore (Ayesu-Offei and Clare 1970) with the help of

appressoria helping to break the cuticle by pressing (Horbach et al. 2011; Linsell et al. 2011) and releasing degradative enzymes (Ayesu-Offei and Clare 1970) (Figure I-5). After penetration of the cuticle, fungal hyphae grow with closely spaced septae and align themselves parallel to the leaf surface along the junction between epidermal cells and above the anticlinal walls forming a subcuticular stroma (Jones and Ayres 1974; Lehnackers and Knogge 1990; Linsell et al. 2011; Thirugnanasambandam et al. 2011) followed by the collapse of underlying mesophyll cells two weeks after penetration (Steiner-Lange et al. 2003). Incompatible interactions characterised by limited growth with random pattern is observed during infection of resistant barley (Thirugnanasambandam et al. 2011), which is likely due to a recognition mechanism involving the activation of plant defences such as reactive oxygen species (ROS) and pathogenicity related protein (PR) (Steiner-Lange et al. 2003). New conidia are produced on top of thick hyphae, which protrude from the stroma or through the leaf cuticle (Jørgensen et al. 1993; Horbach et al. 2011). Secondary infection comes from freshly produced conidia spread by splash dispersal to the upper leaves (Figure I-4b).

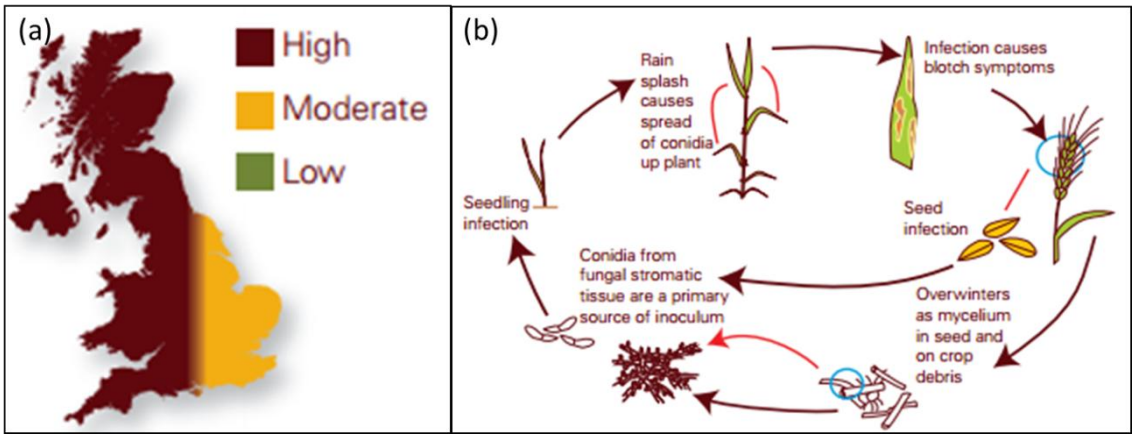

Figure I-4: Occurrence and life cycle of *R. commune*. (a) Picture illustrating the occurrence of *R. commune* in UK. (b) Picture illustrating the life cycle of *R. commune.* (Pictures from AHDB (2016)

I.4.3. *R. commune* is a hemibiotrophic fungus

Due to the necrotic lesion produced by *R. commune*, it was considered for a long time as a necrotrophic fungus. However, *R. commune* does not seems to feed from dead of dying host tissue whereas necrotrophic pathogens do, and it does seem to feed like a biotrophic fungal pathogen although it remains constrained to the apoplast and does not produce haustoria (Carris et al. 2012).

We know now that several generations of the pathogen may occur before symptoms appear (Horbach et al. 2011) (Figure I-5), and that the fungus feeds biotrophically during the long asymptomatic phase (Davis et al. 1994). Moreover, *R. commune* has a limited host range restricted to closely related species including barley, other *Hordeum* species and *Bromus diandrus* while necrotrophic pathogens are usually generalists, growing on a wide range of host species, rather than specialising on a restricted range of hosts (Carris et al. 2012). As a consequence, the *R. commune* lifestyle cannot be classified as necrotrophic or biotrophic but is described as hemibiotrophic with a long symptomless growth phase before producing new conidia by sporulation and finally inducing visible necrosis (Oliver and Ipcho 2004; Zhan et al. 2008; Avrova and Knogge 2012). *R. commune* is not the only pathogen showing this kind on infection strategy: *Cladosporium fulvum* is a hemibiotrophic fungus infecting the intercellular compartment of tomato (Perfect and Green 2001) and *Zymoseptoria tritici* (formerly *Mycosphaerella graminicola)* lives in the apoplast of wheat and rye, feeding without the use of haustoria for 8-11 days prior to the apparition of necrotic symptoms necessary to finish the life cycle (Sánchez-Vallet et al. 2015). Unlike *Z. tritici*, *R. commune* does not need a necrotrophic phase to complete its life cycle and there is no evidence of *R. commune* benefiting from the necrotrophic phase characterised by the collapse of epidermal and mesophyll cells as, by that time, the front of the infection has moved away from the necrotic part of the leaf (Avrova and Knogge 2012).

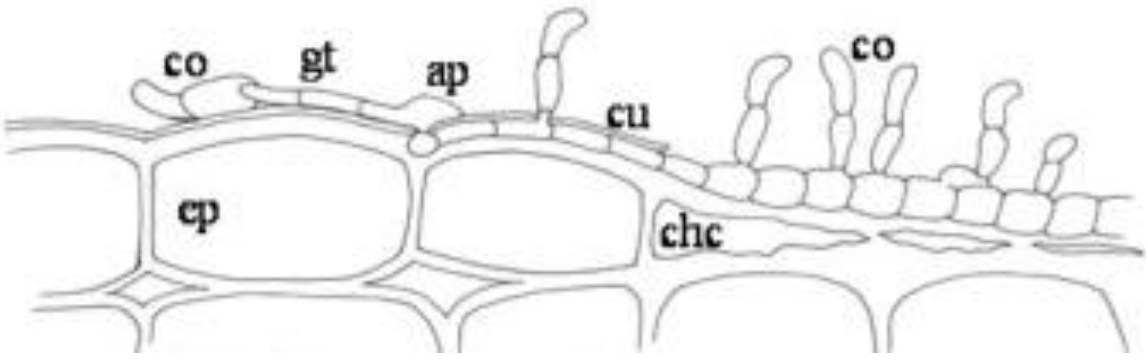

Figure I-5: Illustration of the infection of *R commune*. The conidium (co) of the fungus forms a germ tube (gt) and an appressorium (ap) on the surface of its host plant. After penetration through the cuticle (cu), thin hyphae grow subcuticularly, on top of epidermal cells (ep) followed by thick hyphae with short cells, which emerge from the cuticle on the leaf surface and form new conidia. Thick hyphae induce the collapse of epidermal cells.

I.4.4. Occurrence, disease symptoms and worldwide spread

Several factors can influence the development and severity of *R. commune* infection. The disease being mainly propagated by crop debris left in the field, the soil on which barley will be grown can be a reservoir of disease depending on the level of infection in previous years (Polley 1971) and the quantity of straw on soil surface during sowing, since *R. commune* is able to survive on straw for about 1 year (Ozoe 1956; Skoropad 1959). Continuous barley cultivation and more specifically cultivation of spring barley (Hansen and Magnus 1969) as well as the reduction of tillage induced an increase in the occurrence of the disease caused by *R. commune* (Ardvison 1999). In addition, the occurrence of the disease is dependent on *R. commune* sporulation which is influenced by moisture, temperature, and location of leaves in relation to the soil, therefore the duration of the freezing period and the number of alternating wet and dry periods in the autumn and spring can affect the germination efficiency of conidia (Skoropad 1966). Moreover, plant density and nutrition influence the disease as dense planting will favour the spread of disease by splashing (Ozoe 1956).

In the first instance, leaf symptoms appear as pale grey oval lesions and then the centre of the lesion becomes pale green or pale brown surrounded by a dark brown margin (Davis and Fitt 1990; Lehnackers and Knogge 1990; Avrova and Knogge 2012). Ear infection can also happen resulting in a decrease of the grain quality even when the disease remains asymptomatic (Lee et al. 2001). Indeed, infected grains promote the transmission of the disease in the field (Habgood 1971). Long distance transport of infected seed may be responsible for the spread of the disease worldwide (Lee et al. 2001), in particular by recent human migration to California and Australia (Brunner et al. 2007) (Figure I-6). *R. commune* may not have originated in the Fertile Crescent, but spread from northern Europe after host switch from a wild grass onto cultivated barley shortly after barley was introduced into northern Europe. Then, Neolithic farmers moved infected seed from north to south through trade up to the Fertile Crescent (Brunner et al. 2007) (Figure I-6).

Figure I-6: Worldwide distribution of *R. commune*. Red arrows indicate migration routes of R. commune around the world. Yellow arrows are migration routes of Neolithic farmers into Europe adapted from Brunner et al. (2007) by Avrova and Knogge (2012).

I.4.5. Genetic variability

R. commune can be split into different races, which can infect specific cultivars with different resistance genes in different geographical locations showing a great environmental and host adaptability (Walters et al. 2012). For example, Ceoloni (1980) described differential pathogenic variation of 17 races of *R. commune* on 13 barley cultivars. The use of molecular markers has helped to better understand genetic diversity. McDonald et al. (1999) found high genetic diversity within a small spatial scale using RFLP markers but higher levels of variation were found between isolates from different hotspots determined by AFLPs (Williams et al. 2003). The sexual stage of *R. commune* has not been found and the source of this high level of genetic diversity is not known but AFLP variation within hotspots suggests a high rate of mutation within a few asexual cycles of fungal infection (Williams et al. 2003).

I.4.6. *R. commune* effectors identified so far

Necrosis-inducing peptides (NIPs): Use of culture filtrate of *R. commune* allowed the identification of 3 small toxic compounds called NIP1, NIP2 and NIP3 inducing disease symptoms like necrotic lesions on barley leaves (Wevelsiep et al. 1991). Moreover, NIP1 and NIP3 were found to stimulate the phosphohydrolyzing activity of the Mg2+-dependent, K+-stimulated H+-ATPase

of plasma membrane of barley leaves (Wevelsiep et al. 1993) but the function of NIP2 remains unknown. The 3 NIPs showed upregulation during barley infection and deletion mutants were generated and tested on different barley genotypes showing differential growth and recognition events depending on the host genotype, suggesting that the 3 NIP effectors are involved in pathogenicity and activate plant defences (Kirsten et al. 2012).

NIP1: NIP1 effector was one of the first *Avr* genes to be identified in fungal plant pathogens and has been intensively studied since it was identified to be recognised by barley genotypes carrying *Rrs1* resistance (Rohe et al. 1995). Interestingly, NIP1 does not trigger HR (Hahn et al. 1993) but can induce the expression of plant defence genes such as pathogenesis-related (PR) proteins (Steiner-Lange et al. 2003). During infection, NIP1 is secreted into the apoplast at an early time point during the infection, and passes through the cell wall to stimulate H+ ATPase pump to disturb essential cellular processes and force the cells to collapse (Wevelsiep et al. 1993), but the mechanism remains unclear. Binding studies of NIP1 revealed a single class of binding sites with identical binding characteristics independently of the presence of *Rrs1* resistance gene and independently of the avirulence activity of NIP1 suggesting that the *Rrs1* gene does not encode the NIP1 receptor and that an extra event is necessary for recognition and to trigger race-specific plant defence activation such as a hypothetic conformational change of the target protein or an additional protein involved in the protein complex (van't Slot et al. 2007). As mentioned before, *R. commune* is a variable pathogen able to adapt to the environment and under the strong selective pressure of *Rrs1*-carrying cultivars which are able to recognise NIP1, *R. commune* lost or modified NIP1 to avoid recognition and enable fungal growth (Rohe et al. 1995; van't Slot et al. 2007; Avrova and Knogge 2012). Schurch et al. (2004) has analysed the frequency and the conservation of NIP1 in different geographic populations on four continents, revealing 45% deletion frequency of NIP1 among 614 isolates and 14 polymorphic NIP1 types suggesting that NIP1 is not essential for pathogenicity.

I.5. *R. commune* disease management

I.5.1. Agronomic practices and pathogen free seeds

As mentioned above, agronomic practices such as seed treatment, crop rotation, tillage and grazing are important ways of controlling the occurrence of the disease, by limiting primary inoculum (Ardvison 1999; Elen 2002). Indeed, the continuous use of the same crop promotes the establishment of a pathogenic soil population and reduced tillage increases the biomass and survival of the pathogen which has not been buried deeper in the soil (Walters et al. 2012). Another major direct influence on the health of barley is the selection of pathogen free seeds as shown by Fountaine et al. (2010) indicating that seed infection was the main source of inoculum in barley. To finish, late sowing seems to decrease the primary infection of winter barley seedling by limiting the exposure to *R. commune* inoculum present on crop debris (Zhan et al. 2008).

I.5.2. Fungicides

Despite the use of good agronomic practices, infection can still happen in the field due to infected seeds or small droplets carried by the wind over a long distance (Fitt et al. 1989). Barley can be protected by the use of fungicides to control the levels of disease. However intensive use of fungicides, together with the fact that *R. commune* is a relatively highly genetically diverse pathogen able to rapidly adapt to the environment has reduced fungicide efficacy (Walters et al. 2012). *R. commune* has a long asymptomatic phase, which makes it hard to predict when or if fungicides need to be applied. Conidia may have germinated on the crop but without producing visible symptoms, so the only way of assaying the presence of *R. commune* in the field before the first symptoms appear is by using PCR (Fountaine et al. 2010) . However AHDB (2016) recommended the use of fungicide in autumn if early symptoms cause extensive leaf damage, and in early spring if symptoms occur before the main fungicide timing in spring for additional eradication. In wet conditions, later protection of upper leaves may be carried out. Methyl benzimidazole carbamates (MBCs) and the demethylation inhibitors (DMIs) are the groups of fungicides efficiently controlling *R. commune* infection of barley until 1990 when

Kendall et al. (1994) detected and described the first MBC fungicide resistance in *R. commune* field strains. The frequency of MBC resistant strains increased significantly throughout England, Wales and Northern Ireland reaching up to 40% of resistant strains detected in Northern Ireland (Taggart et al. 1999), leading to a reduction in the use of MBCs.

I.5.3. Resistant cultivars

Varietal resistance is an effective way of providing protection against initial infection and is another important method of disease control. *R* genes trigger plant defence responses by directly or indirectly recognising the product of Avr genes expressed by pathogen during infection. However, due to the simple genetic architecture of this interaction, major gene-mediated resistance can be broken down after only a short period of commercial cultivation (Newton et al. 2001b; Abang et al. 2006), unless the Avr gene products are essential for the pathogen. A number of studies have reported partial resistance genes that reduce Rhynchosporium severity. As these rely on less specific interactions with the pathogen, the selection pressure of partial resistance on the pathogen is less strong than major gene resistance; so partial resistance genes are likely to be more durable (Poland et al. 2009), but the limited magnitude of their effect means that they are unlikely to offer good levels of varietal resistance if used in isolation. The best way of increasing the effectiveness of these various crop protection tools, is through adopting an integrated approach to disease management, using a combination of fungicides, agronomic practices and good levels of varietal resistance. The use of resistant varieties carrying polygenic (and therefore more durable) resistance (both major *R* genes and quantitative resistance) with complementary effects to control the disease in the field is the most sustainable and cost effective method of protecting the considerable breeding effort required to identify and incorporate resistance genes into elite varieties. However, the generation of polygenic resistance is not feasible for commercial breeders using only phenotypic selection, and as such, there is a requirement, not only for new sources of resistance, but also for the identification of closely linked markers for marker assisted breeding.

I.6. Useful tools for crop improvement

I.6.1. Genetic markers and their use

Morphological markers: Historically, Mendelian morphological characters were the first genetic markers to be used for plant breeding. These markers are easily observable morphological traits such as colour, and shape of different organs which can be linked with other agronomic traits and as a consequence used to distinguish individuals (Kadivel et al. 2015).

Molecular markers: Genetic markers are based on DNA sequences containing variation between individuals or species with a known genetic or physical location in the genome used for genetic analysis, genetic improvement and gene identification. There are 3 categories of markers called first, second and third generation markers. The first generation molecular markers includes markers based on restriction fragment length polymorphism (RFLP) which can be time consuming, labour intensive and involves the use of expensive and radioactive/toxic reagents (Agarwal et al. 2008). Randomly amplified polymorphic DNA (RAPD) is a PCR-based technique generating markers that are rarely co-dominant preventing the distinction between heterozygous and homozygous. (Agarwal et al. 2008; Khan 2015). The second-generation molecular markers use amplified fragment length polymorphism (AFLP), a technique which combines the power of RFLP with PCR-based technology leading to saturating genomic regions with high powers of discrimination and reproducibility (Savelkoul et al. 1999; Agarwal et al. 2008). Simple sequence repeats (SSRs or microsatellites) markers are codominant and reproducible PCR-based assay leading to highly polymorphic assays compared with other genetic markers (Agarwal et al. 2008; Miah et al. 2013). The third generation molecular markers utilise SNPs, the most abundant molecular markers which are widely distributed throughout genomes. These are used in high throughput genotyping methods such as DNA chips and Kompetitive allele-specific PCR (KASP) technology (Agarwal et al. 2008; Hiremath et al. 2012).

Fine mapping: Fine mapping is a method used to localise the locus of a gene involved in a specific trait based on the use of recombination events after backcrossing and monitored by the study of polymorphic markers (Boopathi

2013). In plants, this technique was used for the identification of several quantitative trait loci (QTL), controlling yield, biotic and abiotic resistance, maturity date, flowering, quality etc. in segregating populations from a cross between different cultivars of the same species or from a cross with a wild related species, often a source of greater genetic diversity. Moreover, the identification of markers tightly linked with a trait is a useful tool for marker-assisted selection (MAS) for applied breeding programmes. For example, in peach, fine mapping allowed breeders to narrow down from 3.56 Mb to 220 kb the interval for a major locus controlling maturity and led to the identification of a candidate gene controlling ripening time, a crucial factor for marketing of fresh fruit. SSR markers could be used for marker-assisted selection and breeding of new cultivars with differing maturity date extending the market season (Pirona et al. 2013). In rice, a QTL for grain weight named *gw8.1* was detected on chromosome 8 in an interval of about 306.4 kb using a backcross population derived from a cross between the Korean japonica cultivar Hwaseongbyeo and the wild related species *Oryza rufipogon*. The introgression of *gw8.1* caused a 19.3% yield increase and SSR markers tightly linked to *gw8.1* will facilitate cloning of the gene responsible for this yield increase and will be able to be used for MAS (Xie et al. 2006). Moreover, fine mapping and MAS are useful tools for combining genes such as resistance genes in the same cultivar; this strategy is called pyramiding. Hittalmani et al. (2000) pyramided three major genes Pi1, Piz-5 and Pita respectively on chromosomes 11, 6 and 12, for resistance against *M. grisea* by fine-mapping using closely linked RFLP markers for each gene and these genes are at present being deployed into agronomically superior rice varieties by MAS. More recently, Yamanaka et al (2015) created pyramided soybean lines carrying multiple resistance genes against Asian soybean rust. Lines had highly resistant phenotypes and were useful in soybean breeding for conferring broad spectrum, strong resistance to Asian soybean rust strains that are virulent to the varieties carrying single resistance genes.

Association genetics: Association genetics or genome-wide association scan (GWAS) is a technique allowing to look for associations between DNA sequence variants like SNPs and a trait (or phenotype) of interest in a gene pool or collection of individuals (Rafalski 2010). SNPs for which one allele is

statistically more highly represented in one specific phenotypic group are then reported as being associated with the phenotype (Donnelly 2008). This strategy was developed for human genetics because biparental populations were not available and inconceivable for studies such as fine mapping (Waugh et al. 2014b). In human research, GWAS was used to identify genes for more than 70 common diseases (Donnelly 2008), and the constant improvement and accessibility of genotyping technique promoted the use of this strategy. As an example, a GWAS identified a total of 22 loci associated with schizophrenia using 39,239 SNPs and a “collection” of 11,850 Swedish subjects (Ripke et al. 2013). GWAS was ultimately adapted to plants, providing an opportunity to identify and fine-map traits directly in elite plant breeding material or collections derived from wild populations and germplasm using an increased genetic resolution with more alleles than are found in biparental population (Waugh et al. 2009; Rafalski 2010; Waugh et al. 2014b). For example in plants, 287 elite spring wheat lines and 18,704 SNPs were used for the identification of association with grain yield identifying 31 loci that explained 5–14 % of the variation in individual traits (Sukumaran et al. 2015). 768 barley breeding lines and 1,536 SNP markers were used for the identification of association with Fusarium head blight (FHB) resistance and revealed four QTL for FHB severity and eight QTL for the DON concentration (Massman et al. 2011). 399 Spring-type and 204 Winter-type elite barley cultivars from north-western Europe and 9K barley iSelect SNP genotyping platform were used to identify the association with (1,3;1,4)-β-glucan grain content required at low level for brewing and distilling and at high levels for positive impacts on human health (Houston et al. 2014).

I.6.2. Genome sequencing

In plants, genome sequencing aims to identify important genes for agronomy and develop novel markers in model and non-model species (Edwards and Batley 2010). The first crop genome sequenced was rice (Goff et al. 2002) but at present, all crops are in the process or already sequenced such as *Brassica rapa* (Wang et al. 2011), potato (Xu et al. 2011), tomato (Consortium 2012), barley (Mayer et al. 2012), wheat (Mayer et al. 2014). Next generation sequencing (NGS) technologies allows us to sequence and resequence entire

plant genomes (and related genomes), exomes and transcriptomes more efficiently and economically and in greater depth than ever before (Varshney et al. 2009). Moreover, NGS is useful to study the expression of genes, population biology and to develop new SNP-based markers, improving association mapping, fine mapping, genetic map construction, and alien introgression (Varshney et al. 2009).

As an example, RNA sequencing and transcriptome analysis of the turf grass species Tall fescue (*Festuca arundinacea* Schreb.) during high temperature stress allowed the identification of 49 functional gene subcategories in response to heat stress which could help to improve forage production in high-temperature region (Hu et al. 2014). Moreover, transcriptome analysis can help to reduce the number of candidate genes identified in a QTL as shown by Xu et al. (2015) which facilitated the genetic improvement of rapeseed, identified lipid-related candidate genes using *B. napus* pod RNA-sequencing and transcriptome analysis at different stages of development. This strategy allowed the identification of 33 candidate genes affecting seed oil content by combining differentially expressed genes identified during the analysis with QTL mapping results. In addition, RNA sequencing can be used as a genotyping method as demonstrated by Kim et al. (2011) which used RNA sequencing on Soybean Near-Isogenic Lines (NILs) carrying resistant and susceptible alleles against Bacterial leaf pustule (BLP) disease caused by *Xanthomonas axonopodis*. The analysis indicated that 134 genes were significantly differentially expressed between the BLP-resistant and BLP-susceptible lines involved in basal defence mechanisms such as the recognition of PAMPs or DAMPs, high level of accumulation of pathogenesis-related PR1 and PR14 products and JA-signalling pathway possibly contributing to BLP resistance in soybean. Moreover, only a small part of genomes correspond to coding sequences. For example, in wheat, only 93 Mbp of cDNA sequences were assembled on the 17 Gbp genome sequence meaning that wheat genome is composed of only 0.5% coding sequence (Brenchley et al. 2012). Consequently, exome capture (or whole exome) a strategy for selectively sequencing complete coding regions is a faster and the more efficient way to study exome variation in several species or races. An example of whole-genome sequencing and intensive analysis of the undomesticated ancestor of *Glycine max* (*G. soja Sieb. and Zucc.*) showed

that *G. soja* is ~0.31% different from that of *G. max* and suggested that the crop appeared before the relatively recent event of domestication (6,000~9,000 years ago) (Kim et al. 2010). In addition, in barley, exome sequencing of a collection of 267 geographically diverse landraces and wild relatives showed an association between variability and geographic location suggesting environmental adaptation (Russell et al. 2016). To summarise, NGS is a useful tool to improve knowledge about population biology and the history of a crop.

I.6.3. Microarrays

Microarrays (or gene chips, biochip) are molecular tools based on the hybridisation of DNA fragments arrayed on solid support to radioactively or fluorescently labelled specific DNA probes. The strength of the hybridization signals is scanned using laser scanning or confocal laser fluorescence microscopy techniques and analysed by computational methods (Duggan et al. ; Wu et al. 2015). Microarrays are used for various purposes such as Oligo microarray for cDNA quantification and gene expression profiling, SNP chip for genotyping and MiRNA microarray for microRNA expression studies. They all contain DNA fragments which are selected using database such as Genbank, Unigene or EST libraries to cover the maximum number of genes (Wu et al. 2015).

Gene expression profiling: Microarrays are widely used in plants for expression profiling and are available for some crop species such as rice, barley, wheat, maize, tomato, soybean and model species such as Arabidopsis, tobacco and *Medicago*; they are being used to understand and improve agronomic characteristics such as yield, quality and resistance (Wu et al. 2008). As an example, transgenic rice plants overexpressing *OsNAC5* with larger root diameter and showing an increase of yield, particularly in drought conditions, compared to non-transgenic controls were used in microarray experiments comparing normal and drought growth condition. The analysis identified 25 up-regulated genes, some of which were implicated in root growth and development demonstrating that *OsNAC5* enhances drought tolerance and grain yield under field conditions thanks to its ability to promote the significant enlargement of roots (Jeong et al. 2013). Microarrays can also help to discover new genes and build expression networks by studying the co-expression of

groups of genes. For example, an Arabidopsis cDNA microarray representing 7000 independent full-length transcripts was hybridised to cDNA obtained for material under various treatments, such as hormones, pathogen-inoculation, UV stress, heavy metal stress, mechanical wounding, drought, high salinity and low temperature and showed crosstalk between abiotic and biotic stresses regulated by the cytochrome P450 gene family (Narusaka et al. 2004).

Genotyping: SNP microarrays for genotyping are a powerful tool for plant breeding, particularly for previously described genome association and fine mapping. For example, genome-wide SNP discovery in peach was carried out to develop a SNP genotyping array platform using 56 peach breeding accessions, leading to the discovery of almost 7,000 validated SNPs, a resource usable for genetic studies in peach and related stone fruit (Verde et al. 2012). In wheat, an array including about 90,000 gene-associated SNPs was developed to characterize genetic variation in wheat populations resulting in a total of 41,704 SNP markers that have been unambiguously genetically mapped on the 21 wheat chromosomes, an invaluable resource that can be used for diversity and genetic studies (Wang et al. 2014).

miRNA expression profiling: miRNA microarrays are tools to study the expression of non-coding miRNAs, a class of gene expression regulators known to regulate the development and stress response in plant by cleaving mRNAs (Carrington and Ambros 2003; Chen 2009). For example, 18 cold-responsive miRNAs were identified in rice using microarrays (Lv et al. 2010) and 14 stress-inducible miRNAs were identified in *A. thaliana* using microarray data. Three of them were induced by high-salinity, drought and cold, thereby revealing high regulatory cross-talk between miRNA responses to environmental stresses (Liu et al. 2008).

I.6.4. Generation of point mutations

Tilling: Targeting Induced Local Lesions IN Genomes (TILLING) is a molecular biology method, allowing the identification of point mutations, such as those induced by EMS (Ethyl methanesulfonate). It uses denaturing HPLC or crude celery juice extract containing CEL 1 endonuclease which detects and digests mismatches in heteroduplexes created by melting and annealing PCR amplification products of heteroallelic DNA (McCallum et al. 2000; Uauy et al.

2009). This strategy has been widely used in several plant species such as maize (Till et al. 2004), wheat (Slade et al. 2005; Uauy et al. 2009), rice (Till et al. 2007), sorghum (Xin et al. 2008), Arabidopsis (Greene et al. 2003), *Lotus japonicas* (Perry et al. 2003), soybean (Cooper et al. 2008), *B. napus* L. (Harloff et al. 2014), tomato (Minoia et al. 2010), etc. It is a great tool for reverse genetics, allowing the identification of the function of a gene with a known sequence in individuals carrying point mutations in any gene of interest. For example in tomato, TILLING was used to create mutants in 2 translation initiation factor families (eIF4E and eIF4G) representing susceptibility factors required for resistance against potyviruses, and revealed that translation initiation factors family eIF4E has a role in plant susceptibility to viruses (Piron et al. 2010).

MutRenSeq and MutMap+: Recent advances in genome sequencing technology massively improved the speed of generation and the accessibility of genomic data. As a consequence, new techniques appeared like Mutmap (Abe et al. 2012), MutMap+ (Fekih et al. 2013) and MutRenSeq (Steuernagel et al. 2016), allowing the rapid identification of point mutations by combining chemical mutagenesis with exome capture and sequencing (Steuernagel et al. 2016). This strategy could be adapted in all crops and lead to a fast identification of R genes (Steuernagel et al. 2016). For example MutMap already proved its efficiency by accelerating breeding of a salt-tolerant rice cultivar which became necessary after the tsunami that inundated Japanese fields in 2011 and contaminated them with seawater (Takagi et al. 2015).

I.6.5. Genetic Modification (GM) technology tools

In recent years, new advances in transgenic technology and genetic engineering have provided powerful and innovative tools to improve laborious and time consuming conventional crop breeding methods (Knight 2003, Kamthan et al. 2016). However, the cultivation of genetically modified crops introgressed with genes from distantly related organism remains limited due to public reluctance, even though they can provide higher yield, nutritional value, enhanced stress tolerance and wider adaptability (Kamthan et al. 2016). As a consequence, researchers developed alternative concepts involving transformation of plants with genetic material derived from the same species or

from closely related species. Introgression of un-related genes in a species is mainly used as a transgenic tool in research, even though transgenic plants are currently being consumed throughout the world (Kamthan et al. 2016), such as papaya resistant to papaya ringspot virus (PRSV) (Gonsalves et al. 2000), or produced for industrial application like altered lignin content wood trees for paper production (Baucher et al. 2003).

Transient expression: Transient expression is a technique that uses *Agrobacterium tumefaciens* or microprojectile bombardment to deliver and express specific genes of interest in a plant tissue (Scholthof et al. 1996) (Christou 1992). For crop improvement, transient expression is a faster and more flexible method than generating stable transgenic plants which allows testing a gene candidate which might have an effect on an agricultural trait without going through the long stage of *in vitro* culture, and gives the opportunity to study the effect of the genes of interest at any stage of the development. In addition, transient expression does not necessarily involve the introduction of an antibiotic resistance gene into the plant, which is a major cause of public concern due to potential risk of escape of resistance markers into the environment (Kamthan et al. 2016). However, transient expression is not feasible in all species. *Agrobacterium tumefaciens* mediated transient expression is widely used in dicots and allowed the expression of genes in tomato, potato, lettuce and model plants such as Arabidopsis, tobacco and *N. benthamiana* (Bendahmane et al. 2000; Wroblewski et al. 2005; Sparkes et al. 2006; Sheludko et al. 2007). For example *A. tumefaciens*- mediated transient expression allowed the identification of *Rx2* disease resistance gene against potato virus X (PVX) by expressing the PVX coat protein elicitor inducing HR only in the presence of *Rx2* (Bendahmane et al. 2000), and the transient expression of the *Bs2* pepper gene in tomato conferred resistance to strains of *X. campestris pv. vesicatoria* (Tai et al. 1999). Unfortunately, *A. tumefaciens*-mediated transient expression is highly inefficient in monocots and in particular in graminaceous monocots such as wheat, rice and corn, but transient expression could be achieved in barley, rice and wheat and allowed the transient expression of the GUS reporter gene in rice and wheat and chloramphenicol acetyltransferase (CAT) in barley (Wang et al. 1988; Kartha et al. 1989). Alternatively, a barley Stripe Mosaic Virus (BSMV) delivery system

can be used to transiently and systemically express genes after propagation of the virus in *N. benthamina* and sap inoculation of barley and wheat (Lee et al. 2012). It was used to express the ToxA effector protein from Pyrenophora *tritici-repentis*, causing tan spot disease in wheat (Manning et al. 2010). The NIP1 effector protein from *R. commune* was also expressed in a barley genotype carrying *Rrs1* resistance gene to confirm the race specificity of the plant defence reaction (Rohe et al. 1995). In addition, BSMV can be used for gene-silencing to silence plant genes and is called virus-induced gene-silencing (VIGS) which allowed the functional analysis of Lr21-mediated leaf rust resistance pathway in wheat (Scofield et al. 2005). It can also be used to silence pathogen genes and is called host-induced gene silencing (HIGS) and allowed the silencing of the effector gene *Avra10*, which resulted in reduced fungal development of *B. graminis* (Nowara et al. 2010).

Generation of transgenic plants: The generation of transgenic plants have some of the same limitation as transient expression. It can be achieved using *A. tumefaciens* transformation or microprojectile bombardment but is followed by regeneration of the plant from a transformed cell and allows the study of a gene effect in the full plant rather than in localised plant tissue or in protoplasts (Kamthan et al. 2016). Transgenic plant generation is widely used in crop research and allowed the identification of resistance genes such as potato proteinase inhibitor II pin2 gene introgressed into rice and providing resistance against insects (Duan et al. 1996), or a fungal gene encoding glucose oxidase introgressed into potato which increased H_2O_2 levels leading to strong resistance to bacterial soft rot disease caused by *Erwinia carotovora* sub sp *carotovora* (Wu et al. 1995). It also allowed the improvement of plants for other agronomic traits such as salt tolerance in tomato (Zhang and Blumwald 2001) and yield and quality in brassica (Zhang et al. 2001).

Genetic engineering strategies: Genetic engineering provides different strategies for transgenic or transient expression studies in plants. The function of a gene and its importance for pathogenicity can be studied and tested by overexpression under the control of a strong constitutive promoter as illustrated by Li and Steffens (2002) who improved bacterial disease resistance in tomato through overexpression of polyphenol oxidase. Until recently, the study of the effect of a gene by suppression (or knock-out) of the gene was not feasible and

gene silencing was used as an alternative by regulating the expression of the gene through the use of artificial miRNAs (amiRNAs) synthesized in vitro or by transgenic expression of a double-stranded precursor that folds back on itself as a hairpin (Hannon and Rossi 2004). This strategy allowed a better characterisation of SGT1, which had been shown by silencing to upregulate HR-like cell death protein MEK2DD, suggesting that SGT1 is required for HR-like cell death (Ichimura et al. 2016). Moreover, genes of interest can be tagged to allow production of tagged proteins for protein purification or for subcellular and macro localisation if the tag is coding for a fluorescent protein such Green Fluorescent Protein (GFP), Red Fluorescent Protein (RFP) and Yellow Fluorescent Protein (YFP). Quantifying and localising proteins in a particular plant tissue or subcellular location under specific circumstances can help to characterise gene function as showed by (Dong et al. 2008) who demonstrated the regulation of ETR1 ethylene receptor by RTE1 thanks to the subcellular co-localization of the two proteins.

In addition, insertional mutagenesis can be used as a forward and reverse genetics tool by inserting promoter trap or gene trap inserts. Promoter trapping allows the generation of a mutant collection with a random insertion of a reporter gene such as GUS which in some cases takes place downstream of a native gene promoter, possibly disrupting the expression of the gene but allowing the study of the condition and macroscopic location of the gene controlled by the trapped promoter (Topping et al. 1994). In rare cases, the random promoter trap vector insertion allows the reporter to be in frame with the native gene generating a tagged protein, allowing conditional and subcellular localisation without disrupting the function of the gene; this leads to promoter and gene trapping (Alvarado et al. 2004). Gene trapping or activation tagging allow the generation of mutant collections with a random insertion of a promoter which in some cases happens just upstream of an open reading frame, leading to an increase of the expression of these genes if an enhancer promoter is used such as CaMV 35S; or leading to a tissue-specific or inducible expression if different promoters are used (Nakazawa et al. 2003).

Recently, a new technique has been developed: the clustered regularly interspaced short palindromic repeat (CRISPR) -associated (Cas) type II prokaryotic adaptive immune system has been used to develop an effective tool

allowing targeted genome editing (Cong et al., 2013; Jinek et al., 2012; Mali et al., 2013). The key components of this system are the endonuclease Cas9, CRISPR RNA (crRNA), and transactivating crRNA. The bacterial Cas9 engineered endonucleases based on bacterial Cas9 endonuclease has been adapted for use in plants, animals, fungi and oomycetes (Hsu et al. 2014) and can be directed by short RNAs to induce precise cleavage at endogenous genomic locus (Cong et al. 2013). The CRISPR system is a bacterial immune mechanism deployed against non-host nucleic acids, such as viruses or plasmids (Barrangou et al. 2007). The CRISPR/Cas9 system was used in rice to generate single, double and triple knockout mutants of cyclin dependent kinase (CDK) gene family members (Endo et al. 2014). In addition, CRISPR/Cas9 has been successfully used in other plant species including wheat, sorghum, tobacco, soybean, maize (Hsu et al. 2014; Jacobs et al. 2015; Svitashev et al. 2015) and is currently revolutionising genetics and molecular biology approaches for plants and their pathogens (Doudna and Charpentier 2014).

I.7. Barley resistance against *R. commune*

Several major resistance genes and quantitative trait loci (QTL) against *R. commune* have already been mapped (Figure I-7). *Rrs1* on chromosome 3H (Hofmann et al. 2013), *Rrs2* on chromosome 7H (Hanemann et al. 2009), *Rrs3* on chromosome 4H (Bjørnstad et al. 2002; Grønnerød et al. 2002), *Rrs4* on chromosome 3H (Patil et al. 2003) and *Rrs15b* on chromosome 2H (Schweizer et al. 2004) originated from *H. vulgare*, but wild *Hordeum* species have also been used as a source of resistance. *Rrs12* on chromosome 7H (Abbott et al. 1991), *Rrs13* on chromosome 6H (Abbott et al. 1991), *Rrs14* on 1H (Garvin et al. 2000) and *Rrs15a* on chromosome 7H (Genger et al. 2003; Genger et al. 2005) were introgressed from *Hordeum vulgare ssp. spontaneum,* while *Rrs16* on chromosome 4H (Pickering et al. 2006) was introduced from *Hordeum bulbosum*. So far, none of these genes have been cloned.

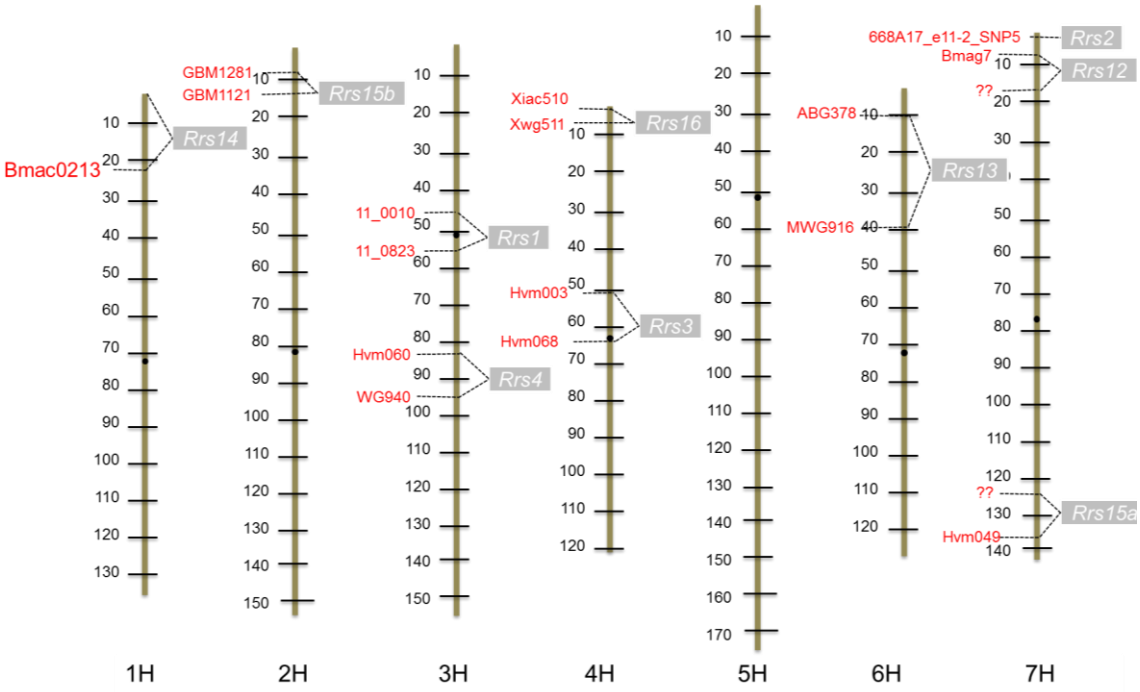

Figure I-7: Genetic map illustrating *R. commune* resistance locations in the barley genome identified so far. Names of resistances are indicated in grey boxes and their flanking markers are red names. *Rrs1* on 3H (Hofmann et al. 2013), *Rrs2* on 7H (Hanemann et al. 2009), Rrs3 oh 4H (Bjørnstad et al. 2002; Grønnerød et al. 2002), *Rrs4* on 3H (Patil et al. 2003), *Rrs15b* on 2H (Schweizer et al. 2004), *Rrs12* on 7H (Abbott et al. 1991), *Rrs13* on 6H (Abbott et al. 1991), *Rrs14* on 1H (Garvin et al. 2000) and *Rrs15a* on 7H (Genger et al. 2003) and *Rrs16* on 4H (Pickering et al. 2006)

I.7.1. *Rrs1*

The first resistance locus mapped was *Rrs1* on chromosome 3H (Thomas et al. 1995) and to date more than 11 different *Rrs1* alleles have been described (Bjørnstad et al. 2002; Hofmann et al. 2013) leading to a debate over whether *Rrs1* is a complex locus comprising multiple tightly linked genes, or different alleles of the same *R* gene. The functional effect of *Rrs1* seems to be the prevention of penetration and subcuticular growth (Lehnackers and Knogge 1990; Carisse et al. 2000; Thirugnanasambandam et al. 2011) of *R. commune* strains carrying NIP1 (Rohe et al. 1995). NIP1 is an avirulence gene, which does not trigger hypersensitive response (HR) during plant pathogen interaction (Hahn et al. 1993). It has been shown to interact with the barley plasma membrane H^+-ATPase independently of the barley genotype suggesting that at least one additional (genotypically dependant) mechanism is involved in activating the resistance, such as another protein or a conformational change of the target, induced by NIP1 interaction with the plasma membrane (van't Slot et al. 2007).

The closest markers for *Rrs1* were identified using large DH-mapping populations generated by crossing Spanish landrace-derived lines, SBCC145 and SBCC154 (with outstanding resistance to scald) to the susceptible cultivar Beatrix. The genetic distance between *Rrs1* and these flanking markers is 1.2 cM for 11_0010 (iSelect name: 11_10005) proximally and 0.9 cM for 11_0823 (iSelect name: 11_10728) distally, which corresponds to a physical distance of just under 9 Mb (Hofmann et al. 2013).

I.7.2. *Rrs2*

So far *Rrs2* is the only scald resistance locus for which diagnostic markers have been developed (Hanemann et al. 2009). The *Rrs2* gene was fine mapped using an Atlas(*Rrs2*) × Steffi mapping population allowing the discovery of an interval of 0.08 cM between markers 693M6_6 and P1D23R on barley chromosome 7HS (Hanemann et al. 2009). Within that interval, a family of 6 putative Pectin Esterase Inhibitor (PEI) genes were identified where 4 of them showed haplotypes SNPs distinguishing between resistant and susceptible cultivars of barley (HvPEI2, HvPEI3, HvPEI4 and HvPEI6). Unfortunately, over-expression of the putative resistant alleles of the tested candidate genes *HvPEI2*, *HvPEI3* and *HvPEI4* did not provide a high level of resistance against *R. commune* but HvPEI4-overexpressing lines conferred an improvement of the resistance level suggesting that the action of multiple PEI genes may be requires to confer Rrs2 resistance, or HvPEI6 may be Rrs2 and needs to be tested in transgenic over-expression plants, or that *Rrs2* may be absent from the available sequence information of the susceptible cultivar Morex used to identify candidate genes (Marzin et al. 2016).

I.7.3. Others mapped resistances

The *Rrs3* resistance gene is located on 4H and was mapped by Bjørnstad et al. (2002) and Grønnerød et al. (2002) but not confirmed in a DH population from a cross between the susceptible Ingrid and the Ethiopian landrace Abyssinian due to heterogeneity in the Abyssinian accession (Grønnerød et al. 2002).

Chromosome 3H, already described as a major source of resistance to Rhynchosporium (Zhan et al. 2008) contains previously described *Rrs1* and *Rrs4* resistance gene mapped by Patil et al. (2003) using a DH progeny from a

cross between the susceptible cultivar Ingrid and the resistant accession CI 11549 (Nigrinudum). *Rrs4* is often confused with *Rrs1* due to their proximity, 22cM away from each other (Patil et al. 2003). *Rrs15*(b) is a resistance identified thanks to DH lines of the cross Igri × Triton on chromosome 2H in a 23 cM interval between GBM1121 and GBM1281 that explained almost 80% of the phenotypic variance (Wagner et al. 2008).

I.7.4 Resistance genes from related *Hordeum* species

Related wild species such as *H. vulgare ssp. spontaneum* and *H. bulbosum* are a good source of resistance genes (Abbott et al. 1991; Pickering and Johnston 2005).

Rrs12 resistance gene was mapped thanks to a cross between clipper and a *H. vulgare* ssp *spontaneum* (Abbott et al. 1991) to the chromosome 7H at 10.5cM away from microsatellites Bmag7(Genger et al. 2003). *Rr12* appeared to be located close to *Rrs2* and as a concequence it was suggested that *Rr12* could ba an allele of *Rrs2* until the Hanemann et al. (2009) made huge improvements to the map.

Rrs13 was introgressed from wild barley *H. vulgare ssp. spontaneum* generating BC line 30 for marker assisted selection in barley breeding programmes (Abbott et al. 1991; Abbott et al. 1995). It is located on chromosome 6H flanked by 2 RFLP markers at 7.3 cM from Cxp3 and 26.4 cM from ABG458. Genger et al. (2003) narrowed down the interval to between 11.7 cM from Cxp3 and 10.8 cM from MWG916. Allelic differences of *Rrs13* were suggested due to a slightly different seedling response to *R. commune* between lines carrying resistance at the *Rrs13* locus (Genger et al. 2005).

Rrs14 is a resistance located on the 1H chromosome near marker Bmac0213 identified in a population developed with the wild barley accession OUH602 as the donor parent (Yun et al. 2006). This resistance was also mapped 10.8 cM away from HOR1 and 1.8 cM away from HOR2 by Garvin et al. (2000) in a population of the Australian cultivar Clipper with the wild barley *H. vulgare* ssp. *spontaneum* from Mehran, Iran (Garvin et al. 1997). Garvin et al. (2000) described consistent protection for 2 consecutive years of up to 88 % less leaf damage observed for the *Rrs14* line compared to Clipper.

Rrs15(a) is a resistance gene derived from wild barley *H. vulgare* ssp. *spontaneum*, located on the long arm of chromosome 7H between the centromeric region and 11.5 cM from microsatellite markers HVM49 (Genger et al. 2005). *Rrs15*(a) and *Rrs13* were tested together for pyramiding breeding and showed a beneficial effect of the digenic resistance in the field with no yield penalty (Brown et al. 1996).

Rrs16 is a resistance located on 4H transferred from *H. bulbosum* genotype A17/1 to *H. vulgare* cv Emir after embryo rescue of a partially fertile triploid hybrid and backcrossing to generate a population and carry on fine mapping. *Rrs16* was localised between Xiac510 and Xiac511 at 0.3 and 0.1 cM respectively. Lines with an introgressed *Rrs16* appeared to be highly resistant in Canada, Japan and Mexico without yield penalty (Pickering et al. 2006) .

I.7.5 Height related resistance

Height of barley plants is an important trait for *R. commune* resistance and seems to control the disease in the field and reflects the developmental effects of severe infection. The semi-dwarfing gene sdw1 mapped by (Malosetti et al. (2011)) around SNP marker 11_10867 was identified as a resistance QTL in previous studies. This is thought to be due to the limited splash dispersion on tall cultivars (Looseley et al. 2012; Walters et al. 2012; Looseley et al. 2015).

I.8. Aims of the project

The main project aim is to identify resistance against *R. commune* in barley through the use of two different strategies. The first strategy applies an effectoromics approach based on the fact that resistance genes recognising more essential *Avr* genes are likely to be more durable. As a consequence, novel and essential *R. commune Avr* effectors need to be discovered to be able to identify their barley targets and potentially new resistance. The second strategy applies a genomics approach to identify and/or characterise new or mapped resistance against *R. commune* in barley through the use of a Genome Wide Association Scan (GWAS) in a collection of UK spring barley elite varieties. This approach will survey all the resistance present in UK spring barley elite varieties and provide valuable information about them for barley breeding.

II. Chapter 2: General materials and methods

II.1. Culturing and storage of pathogens

For long-term storage, concentrated *R. commune* spore suspension was poured onto silica gel. Silica gel needs to be dry heated for 20min at 121°C and chilled before use. Silica gel beads of *R. commune* strains from the culture collection at the James Hutton Institute were cultivated in sterile Petri dishes on CZV8CM agar medium at 18°C in the dark. Strains were transferred onto fresh plates by spreading spores from the surface of sporulating agar plug every 12 to 16 days (depending on the strain) with 500µl of water on a new plate.

II.2. *R. commune* conidia harvesting

12 to 16-day-old sporulating plates were scraped with a sterile spatula, and the fungal matter was transferred into sterile distilled water. The fungal suspension was thoroughly mixed by vortexing allowing spores to be released into the water followed by a filtration through a 60 µM filter unit. The flow-through containing conidia were spun down for 5 min at 1600 x g and washed with sterile distilled water 3 times.

II.3. *R. commune* infection assays

II.3.1 Detached leaf assay

Optic cultivar seeds were sown in seed trays filled with JHI soil and grown in plastic seed propagator. Two cm leaf sections of two weeks old plants were placed in clear rectangular boxes containing 0.5% distilled water agar supplemented with 0.01% of benzimidazole in sterile conditions. Before adding the inoculum to each leaf, the centre of each leaf was gently brushed with the paintbrush to remove the surface wax layer. 10 µl of 10^5 conidia/mL inoculum were pipetted onto the surface of each leaf section, where the surface had been brushed. Boxes were kept in illuminated incubator set at 17°C.

II.3.2 “Attached” leaf assay

Optic cultivar seeds were sown along the longer side at 1–2 cm from the side wall of seed tray filled with JHI soil and grown in a plastic seed propagator. Three weeks after sowing, barley plants were prepared for the inoculation by gently bending the second and/or third leaves over a short tray placed upside down used as an inoculation platform (Figure II-1). Double-sided tape between the leaves and platform was used to keep leaves horizontal complemented by extra tape on top of leaf extremities to secure the experiment against humidity. Barley bended leaves were drop-inoculated with 2 10 μL drops of conidia suspension (10^^{7} spore/mL, 0.1% Tween 20). After inoculation, plants were kept at 18°C in the dark for the first 24 h.

Figure II-1: Picture illustrating the plant preparation for inoculation developed as an alternative to the detached leaf assay and named “attached leaf assay”

II.4. RNA extraction and cDNA synthesis

Total RNA was extracted from frozen spores and germinated conidia using an RNeasy plant mini kit from Qiagen, following manufacturer’s protocol. mRNA was extracted from inoculated leaves using Dynabeads Oligo(dT)25 mRNA

Purification kit from Life Technologies, following manufacturer's protocol. All RNA extracted was treated with DNAse using a Turbo DNA-free kit from Thermo Fisher Scientific following the manufacturer's procedure. Leaf sample mRNA was concentrated by precipitation adding 0,1 volume of 3 M sodium acetate and 2,5 volume of 80 % ethanol, then freezing at -70°C for 1 h, and spinning down for 30 min at full speed to precipitate the mRNA. Pellets were washed 2 times with 500 µL of 80% ethanol and re-suspended into 6 µL of distilled water after ethanol evaporation. RNA yield was measured using a NanoDrop Micro Photometer (NanoDrop Technologies, Inc., Rockland, USA).

First strand cDNA for real-time RT-PCR was synthesised from 1-5 µg of total RNA or 30-100 ng of mRNA using a superscript III Reverse Transcriptase from Life Technologies following the manufacturer's procedure.

II.5. Expression profiling

Expression data were obtained by running 2-4 technical repeats of each sample in a 12 µL PCR reaction in a 96 well plate. Each sample contained 6 µL of 2x SYBR® Select Master Mix (Applied Biosystems), 1µL of each primer at 300 µM and 1 µL of template or water for no template controls. SYBR green qPCR assays for gene expression analysis were carried out with SYBR® Select Master Mix (Applied Biosystems) and monitored on a BioRad DNA engine coupled with a Chromo 4 real-time PCR detector as described in Avrova et al. (2003) using specific primers. All reactions were heated to 95°C for 10 min, followed by 40 cycles of 95°C for 15 sec and 60°C for 1 min. Melting curves were checked for each sample to ensure that single product of the right size was amplified in each case. The comparative Ct method (ΔΔCt) was used to calculate the relative expression.. Relative expression was calculated using the equation: relative expression= $(E_{target})^{\Delta Cttarget(control-sample)}$/ $(E_{ref})^{\Delta Ctref(control-sample)}$ where E (the efficiency of each primer pair) was evaluated on a slope of a standard curve generated using a serial dilution (4 dilution points-2 fold dilution) of the mixed sample (E = 10^(-1/ slope)-1) and $(E_{ref})^{\Delta Ctref}$ were the geomean of the different ref genes used $(E_{ref})^{\Delta Ctref}$.

Relative abundance of candidate genes was calculated using the comparative Ct method (ΔCt) and compared to actin abundance in the same sample.

II.6. Agarose gel

PCR amplification was checked by loading a mixture of PCR product and DNA gel loading buffer Dye (6X) from Thermo Fisher Scientific onto a 1% agarose gel (1g of agarose for 100 ml of TBE (0.1M Tris base, 0.1 M boric acid, 2 mM EDTA) supplemented with 0.001% SYBR safe DNA intercalator from Thermo Fisher Scientific . Agarose gels were run in TBE buffer for approximatively 20 min at 150 V. PCR amplification products were visualised under UV light comparing to 1 kb DNA ladder (Thermo Fisher Scientific).

II.7. Yeast (*Saccharomyces cerevisiae*) competent cells preparation

Yeast strains were cultivated from a fresh plate (i.e. less than 1 week old) into 10 mL YPD and cultured overnight at 30°C. 2 flasks each containing 300 mL of YPD were inoculated with 5 mL of the overnight culture and grown at 30°C until the OD600 nm rose to between around 0.6 – 0.8. Yeast cells were harvested into 50 mL falcon tubes by centrifugation (3000 x g, 5 min), washed once with 50 ml of sterile water after pooling cells in 2 50 mL falcon tubes and harvested by centrifugation (3000 x g, 5 min). Cells in each falcon tube were washed with 40 mL of SORB and harvested by centrifugation (3000 x g, 5 min). Cells in each falcon tube were re-suspended in a total volume of 2160 µl SORB and 240 µL of boiled ice cooled carrier salmon sperm DNA. 50 µL aliquots of cells were dispensed into 1.5 mL tubes at room temperature and then placed at -80°C without snap-freezing.

II.8. Yeast Recombinational Cloning (YRC) transformation

Yeast recombinational cloning (YRC) (Oldenburg et al. 1997) is a technique allowing the creation of DNA cassettes composed of multiple DNA fragments amplified by PCR in *S. cerevisiae*. This strategy uses the natural DNA recombining ability of yeast to clone PCR fragments containing defined extensions.

DNA mix (1 µL of linearised plasmid at 100 ng/µL and 3 µL of each recombining PCR fragment) was directly added into thawed competent cells of *S. cerevisiae* strain FY834 (FGSC), mixed with 360 µL of PEG/LiAC solution and incubated

for 30 min at room temperature after a brief vortex. After incubation, 47 µL of DMSO were added and incubated at 42°C for 15 min after another brief vortex. 1 mL of sterile distilled water was added to the transformation tube and centrifuged at 12,000 x g for 15 s. 1.3 mL of supernatant was removed to resuspend cells in ~150 µL. 20% of total volume was plated onto SC-ura plates and remaining 80% were added to 20 mL of liquid SC-ura before 2-3 days incubation at 30°C (180 rpm for flasks). After each transformation the number of colonies on the plate was compared to the control plate transformed with the open vector to observe the rate of re-ligation of the vector.

II.9. *R. commune* conidia transformation by electroporation

Conidia were collected by centrifugation at 1600 x g for 5 min then washed 3 times with 1 M sorbitol by spin down (1600 x g for 5 min) and resuspension. With the last wash, conidia were resuspended into a volume of around 200 µL. Conidia were transferred into an ice cold eppendorf tube containing 0.5 to 1 µg of sequenced DNA cassette fragment and incubated on ice for 5 min. The mixture was dispensed into an ice cold electroporation cuvette and pulsed at 1.25 kV. Cells were then transferred to a falcon tube containing 25mL of PDB+1M sorbitol and 25 µL 100 mM ampicillin to prevent bacterial contamination . The falcon tube was incubated on a rocker overnight at 18 °C. Transformed conidia were harvested by centrifugation, resuspended in 2mL and aliquots were spread on CZV8CM agar medium selection plates supplemented with 100 mM hygromycin for mutant selection and 100 mM ampicillin against contamination. 2-3 weeks after spreading, single colonies were transferred to a fresh plate supplemented with 100 mM hygromycin and 100 mM ampicillin to be sure that the transformation is stable and ready to be genotyped 4 weeks later.

II.10. *R. commune* DNA extraction

The DNA extraction protocol was adapted from Cenis (1992). 4 weeks after transferring onto a fresh plate, half of the transformant colonies were collected in a 2ml eppendorf tube. 300 µl of SDS extraction buffer (200 mM Tris HCl pH 8.5, 250 mM NaCl, 25 mM EDTA, 0.5% SDS) and 1 measure (approx. 200 mg) of small glass beads were added to the tube followed by disruption of mycelium in a tissue lyser (bead beater) for 2 cycles at 30 s/cycle. After disruption, tubes

were briefly centrifuged at 16,000 x g for 15 second, 150 µl of 3M sodium acetate pH 5.5 were added and tubes were incubated for 10 min at -20°C. After incubation, tubes were centrifuged at 16,000 x g for 5 min and supernatant was transferred to a fresh tube. 2.5 x sample volume of ethanol were added to fresh sample tubes and tubes were centrifuged at 16,000 x g for 30 min to pellet DNA. Pellets were washed in 150 µl 70% ethanol and centrifuged at 16,000 x g for 2 min. After removing supernatant and air drying the DNA pellet, DNA was re-suspend in 10 µl of sterile water.

II.11. Instantaneous electrocompetent *A. tumefaciens* cell preparation and transformation

LBA4404 strain was kindly provided by Dr Laura Stevens. GV0131 strain was kindly provided by Dr Camille Lenoir. Agrobacterium strains were grown in 15 mL of liquid culture for 24 h prior to transformation in LB supplemented with 50 µg/ml rifampicin and 50µg/ml gentamycin for GV0131 strain to select for helper plasmid. Cells were centrifuged at 10,000x g for 1 min and washed with 10 mL ice cold and sterile 10 % glycerol 4 times. Cells were re-suspended in 200 µL of ice cold 10 % glycerol. 30 µL aliquots were used immediately for transformation by electroporation using a MicroPulser set to “Agro”.

II.12. *A. tumefaciens* agroinfiltration into *N. benthamiana*

Agrotransformant were grown in liquid LB containing the appropriate antibiotic and incubate for approximately 20-22 hrs at 28°C on a shaker at 250 rpm. Cells were centrifuged for 20 min at 1000 x g at 15-17°C and resuspended in an inoculation buffer (10 mM MgCl2, 10 mM MES pH 5.6 supplemented with 150 µM acetosyringone) to a final OD600=0.5. 3H after cell suspension preparation, Agrobacterium cell suspensions were infiltrated into leaves of 3-4 week-old *N. benthamiana* using a 1mL syringe.

II.13. SDS-Page Electrophoresis and Western blotting

NuPAGE™ Novex™ 4-12 % Bis-Tris Protein Gels were used for SDS-Page electrophoresis and Western blotting. For a fast protein expression check-up, 5 leaf discs of 5 mm diameter were directly grinded in 100 µl of loading buffer in an Eppendorf tube with a micropertal before boiling for 5 min at 95^{o}C. 12 µL of

CO-IP, pulldown or fast protein extraction samples and 8 µl of Novex Sharp Pre-Stained Protein Standard (Thermo Fisher Scientific) were loaded into the gel. Gels were run and transferred to a nitrocellulose membrane using a XCell SureLock™ Mini-Cell Electrophoresis system following the manufacturer's protocol. Blots were blocked with 5% milk in PBST blocking solution (137 mM NaCl, 2.7 mM KCl, 10 mM Na_2HPO_4, 1.8 mM KH_2PO_4, 0.5% Tween 20) for 1 h, then incubated with the primary or conjugated horseradish peroxidase appropriate antibody and conditioned in blocking buffer, then washed three times in blocking buffer for 5 minutes, then incubated in blocking buffer with the secondary appropriate horseradish peroxidase antibody, if applicable. Blots were washed three times in blocking buffer for 5 min and after a final wash in PBS washing solution (137 mM NaCl, 2.7 mM KCl, 10 mM Na_2HPO_4, 1.8 mM KH_2PO_4) for 15 min proteins were detected using Chemiluminescent Western Blot Detection kit SuperSignal™ West Pico chemiluminescent substrate (Fisher Scientific) and visualized on CL-XPosure film (Thermo Fisher Scientific). Total proteins were observed on the nitrocellulose membrane after incubating for 5 min in Ponceau Red Stain solution (0.5 % Ponceau Red [w/v] (Sigma) + 1% Acetic Acid [v/v]) and washing progressively with clean water. Antibodies used are described in Table II-1.

Table II-1: List of antibody and utilisation condition used for Western blotting

Antibody	Dilution	Condition
Anti-V5-HRP Mouse Monoclonal Antibody HRP conjugated (Novex)	1/5000	1H at room temperature
Rat monoclonal GFP antibody [3H9] (Chromotek)	1/1000	Overnight at 4C
Rat monoclonal RFP antibody [5F8] (Chromotek)	1/1000	Overnight at 4C
Goat anti-Rat IgG−Peroxidase antibody (Sigma)	1/10000	1H at room temperature
Mouse Tetra His Antibody, BSA-free (Qiagen)	1/5000	Overnight at 4C
Rabbit anti-Mouse IgG–Peroxidase antibody (Sigma)	1/5000	1H at room temperature
Anti-HA-Peroxidase, High Affinity (Sigma)	1/500	1H at room temperature

II.14. Gateway cloning

Candidate genes selected were amplified using fungal or barley cDNA and primer specifically designed to be able to tag protein in N or C terminal location using gateway plasmid. Attb extensions were added to primers for cloning. BP enzyme (Thermo Fisher Scientific) was used to clone PCR insert into donor vector pDONR201 and pDONR207 following manufacturer's recipe for

transformation into Library Efficiency® DH5α™ competent E. coli (ThermoFisher Scientific) following manufacturer's procedure. pDONR201 and pDONR207 *E.coli* transformants were grown on LB agar plate respectively supplemented with 50 µg/ml kanamycin or 8 µg/ml gentamycin. After colonies PCR check with sequencing primers, plasmids were extracted from E.coli liquid culture using miniprep kit from Qiagen following manufacturer's procedure and sequenced to check the insertion using M13 Sequencing Primers: Forward: GTAAAACGACGGCCAGT, Reverse: CAGGAAACAGCTATGAC.

Successfully cloned vectors were used to transfer insert into expressing vector using LR enzyme following manufacturer's recipe and transformed into Library Efficiency® DH5α™ competent *E. coli* (Thermo Fisher) following manufacturer procedure. pB7FGW2, sec-gfp-pK7GW2, pB7GWF2 and pB7GWR2 *E.coli* transformants were grown on LB agar plate supplemented with 100 µg/ml spectinomycin. pDONR207 donor vector clones were specifically used for the transfer into pMdc43 to be able to successfully select *E.coli* transformants using LB agar plate supplemented with 50 µg/ml kanamycin. Transfer to pB7FGW2 vector allowed the expression of C-terminal GFP tagged protein. Transfer to sec-gfp-pK7GW2 vector allowed the expression and secretion of C-terminal GFP tagged protein. Transfer to pB7GWF2 vector allowed the expression of N-terminal GFP tagged protein. Transfer to pB7GWR2 vector allowed the expression of N-terminal RFP tagged protein. Transfer to pMdc43-spmRFP vector allowed the expression and secretion of N-terminal RFP tagged protein.

II.15. Confocal microscopy observation of tagged proteins

Subcellular localisations were done 3-4 days post infiltration (DPI). Leaves were infiltrated with water before mounting on a microscope slide. Imaging was performed on a Leica SP2 confocal microscope using excitation wavelengths of 488nm for GFP, 561nm for RFP and on a separate channel between 650 and 700nm chlorophyll autofluorescence signal was collected.

II.16. *A. tumefaciens* transient expression of effector candidate in *N. benthamiana* to boosts pathogen infection

A. tumefaciens cell suspension was prepared as described before for infiltration but diluted to an OD_{600}=0.1 for the cells carrying the expression vector and to

an OD_{600}=0.05 for the cells carrying P19. 6 week-old *N. benthamiana* plants were infiltrated with cell suspension by doing 4 distinct 1.5cm spots (2 on each side of the leaf). On one side, candidate effector was transiently expressed and the empty vector was agroinfiltrated on the other side of the leaf. 24h after infiltration, each infiltration spot was inoculated with 10 µL of *P. infestans* strain TdTomato10xx cell suspension kindly provided by Dr Hazel McLellan. *P. infestans* lesions were measured 1 week after infection.

A similar assay was carried out using *B. cinerea* instead of *P. infestans.* A 7 µL of spore solution at a concentration of $5X10^4$ Cfu/mL was kindly provided by Daniel de Vega Perez. *B. cinerea* lesions were measured 2 DPI.

III. Chapter 3: Identification of effector candidates in *R. commune*

III.1. Introduction

The most sustainable method of protecting barley from *R. commune* is the identification of host resistance genes for the subsequent development of resistant cultivars. Recent advances in high-throughput sequencing technologies and developments in fungal genomics allowed the development of a new strategy to identify resistance genes in plants through the study of effector proteins secreted by the pathogen. Effector-assisted germplasm screening can accelerate the identification and transfer of resistance genes to elite cultivars. Indeed, effector identification improves the understanding of fungal pathogenesis through the study of their genomic sequence, their function and their interaction with target proteins in the plant.

Effector identification can be achieved by different strategies. The genomics approach is based on sequencing data and requires high throughput bioinformatics to identify potential candidates carrying typical characteristics and comparing them with already known effectors (Saunders et al. 2012). Sequencing data of several strains can be used to identify SNPs in genes that could indicate functional polymorphism between strains where one version of the protein is the avirulent allele and the other version is the virulent allele and this information can be used for association genomics by examining DNA polymorphism of candidate genes between different strains and look for differential pathogenicity on different plant genotypes as illustrated by Yoshida et al. (2009). Transcriptomics and RNAseq can also be used to validate candidate effectors, particularly when different tissues are studied. For example Cantu et al. (2013) used RNAseq analysis to identify transcripts encoding secreted proteins enriched in wheat yellow (stripe) rust haustoria compared to infected wheat tissue indicating that these proteins must be important at early stages of infection. In addition, expression profiling of candidate effector genes can be used to identify differential expression patterns suggesting that candidate effectors may be involved at different stages of the infection indicating sequential waves of expression of different sets of effectors already

described by Win et al. (2012). As an alternative, proteomics can be associated with transcriptomics to identify candidate effectors, and were successfully used to identify effector proteins from the salivary glands of the pea aphid using mass spectrometry (Carolan et al. 2011).

Penselin et al. (2016) recently sequenced, assembled and annotated the genomes of different *Rhynchosporium* species and allowed the identification of putative effectors. The genome of *R. commune*, isolate UK7, was screened for candidate genes coding for proteins with classical criteria of apoplastic effectors such as small protein size with a predicted signal peptide, no transmembrane helices and high cysteine content, allowing the identification of 146 putative effector genes. So far, in *R. commune*, seven candidate effector genes (*RcSP1*, *RcSP2, RcSP3, RcSP4, RcSP5, RcSP6, RcSP9*) were studied by thorough expression analysis and the generation of deletion strains revealing significant quantitative effects on fungal growth and symptom (Penselin et al. 2016).

The aim of this study was to identify and characterise new important effectors from *R. commune.*

III.2. Materials and methods

III.2.1. Infection time course

200 seedlings of susceptible cultivar Optic were grown under lab condition at 18°C in plastic seed propagator filled with JHI soil (1200 L peat, 400 L sand, 2.5 kg dolomite limestone, 2.5 kg ground limestone, 100 L perlite, 1.5 kg Synchrostart fast release fertiliser (12 N: 14 P: 24 K: 3 MgO), micronutrients (B, Cu, Fe, Mn, Mo, Zn), containing Intercept insecticide). One week old seedlings were spray-inoculated with 20 mL of *R. commune* strain L2A spore suspension (10^7 spore/mL, 0.1% Tween 20). Tween 20 solution allows conidia solution droplets to sticks to barley leaves. During the first 48h, plants were kept in the dark at 100 % humidity in a plastic bag, then kept at a relative humidity of 80%.

Leaf sampling was carried out at 1, 2, 3, 4, 6, 8, 10 and 14 days post inoculation (DPI). These time points are covering several stages of barley infection by *R. commune*: spore germination and penetration (1-3 DPI), biotrophic interaction with hyphae growth under the cuticle (3-6 DPI), and transition phase between biotrophy and necrotrophy (8-14 DPI). Five leaf sections from five different plants were taken for each time point, pooled, frozen in liquid nitrogen and then stored at -80°C. Additional inoculated leaf samples were collected at 4, 7, 9 DPI for trypan bleu staining and light microscopy to confirm the infection. Inoculated plants were kept for 3 weeks and necrotic lesions could be observed at 21 DPI.

III.2.2. Lactophenol Trypan Blue Staining of leaf material

Leaves were immerged in lactophenol trypan blue solution (10mL Lactic Acid, 10 mL glycerol, 10 g phenol, 10 mg trypan Blue, 10 mL distilled water) and heated at 90°C for 5 min. After incubation, leaf segments were immerged into chloral hydrate solution (2.5 g/mL) until de-stained. De-stained leaf segments were observed using a light microscope.

III.2.3. Real-time primers of candidate effectors and *R. commune* reference genes

Real-time primers for candidate genes and reference gene controls were designed using Primer Express software and following the manufacturer's procedure for primer design (Table III-1). The expression of each gene was

determined relative to actin, c-4 methyl sterol oxidase and acyl-CoA desaturase genes showing very small difference of level of expression during infection and used as constitutively expressed endogenous controls.

Table III-1: Genes chosen for expression analysis and their qPCRprimers.

Genes accession	Genes name in strain 13-13	primers name	primer sequence 5' - 3'
CZS88923.1	**rsu3_01912**	1912_29F	tcctactgcttgccctcttca
		1912_98R	gcctcagaacggatcagagaa
CZT04885.1	**rsu3_03236**	3236_57F	ccatacccaggcgtcgtaag
		3236_106R	atgtgctccgagtaagcaacag
CZT45822.1	**rsu3_03870_g**	3870_266F	attgtaccggtggagctgttct
		3870_328R	gagctgaacaaagtccaggagatt
CZS96653.1	**rsu3_03882**	3882_178F	cctaccgacggcatgca
		3882_262R	ccctcagaaatccgctcttg
CZS95721.1	**rsu3_00045_g**	45_169F	actaccgctgccacgtcttg
		45_245R	cggcttgagcagcactca
CZS99974.1	**rsu3_00144_g**	144_18F	ttcagtccttgcgcttgct
		144_91R	ctggccatgacacaatgattg
CZS91091.1	**rsu3_02682_g**	2682_263F	actggtctacctttcaagcatcaa
		2682_345R	caatacagctagcgaaacaccaa
CZT09278.1	**rsu3_03570_g**	3570_183F	tcgtgctgccactccttgt
		3570_257R	tggccggtgatggattg
CZS96945.1	**rsu3_09566_g**	9566_272F	tggatggatcgattgggtaca
		9566_343	caaaaccaccccgataagca
CZS99494.1	**rsu3_07985_g**	7985_222F	gcgtacattttccgcatcact
		7985_288R	tccccaagctcgaatttctct
CZS90987.1	**rsu3_04426_g**	4426_62f	cacctgttgctgctcctgaa
		4426_129R	aatgagaggaactgctcgagctt
CZS99554.1	**rsu3_05502_g**	5502_32F	ttcccctctcctacgctcttc
		5502_110R	atctcatcacgaccgagtactttg
CZT04607.1	**rsu3_09280_g**	9280_22F	cgactcttgcgggtttcact
		9280_91R	gcgcagggatagtcgtgttt
CZT46111.1	**rsu3_11923_g**	11923_153F	cgatagcggcttcatcaactg
		11923_219R	ttcgcaggctgggatgata
CZT46883.1	**rsu3_12059_g**	12059_3F	gctgttcacgaagcaaatcatc
		12059_76R	ttggagtggcaactaccacagat
CZS89773.1	**rsu3_01835_g**	1835_133F	acgattgacaaggcggaaac
		1835_207R	tggtgtcacgccgttgttac
CZS88276.1	**rsu3_03792_g**	3792_380F	caacgactgcccctccaa
		3792_446R	gaggcggcgccagttac
CZT46925.1	**rsu3_05260_g**	5260_347F	cttgccgtgcggatcatc
		5260_417R	cgcggaagagctggttgt
CZT44527.1	**rsu3_06458_g**	6458_87F	ggcaaacgcggaccaa
		6458_157R	tcgctgcgttgttgatgtagata
CZT11549.1	**rsu3_06926**	6926_22F	gttctcgccttcgctgctt
		6926_93R	tggtgctgatcgacatgaatc

CZT05306.1	**rsu3_07190_g**	7190_270F	tccaacggtcacggttactg
		7190_345R	caatatcatagcccgagtcgtacat
CZT09389.1	**rsu3_08360_g**	8360_78F	gaccgtctgcatccaaaatctat
		8360_151R	ccggctggagatcgaaact
CZT07829.1	**rsu3_09063_g**	9063_327F	cctcaagcaatgtatccagcaa
		9063_397R	ccgaagccccggttgt
CZT00822.1	**rsu3_07595_g**	7595_266F	cacaggcgcagggtcaag
		7595_337R	taggagggcaagaggtgtaaagg
CZS95828.1	**rsu3_11823_g**	11823_273F	gtggttccattgggacgttt
		11823_348R	atgagtactgccctctggaccat
CZS97498.1	**rsu3_12695_g**	12695_172F	acccaaaaccgcaccaact
		12695_234R	gaaccagccgggttgga
CZT03605.1	**rsu3_02291_g**	2291_220F	gctcagtgcaaactcaacacagt
		2291_296R	ggtccgacgacccaggtatt
CZT41612.1	**Chorismate mutase**	F-CMA	tccccaacgggaccttatg
		R-CMA	gttgggcgtttatggcattta
CZT49407.1	**Isochorismatase hydrolase**	F-ISC	ccgatctcgaggagttcttg
		R-ISC	cgtactcacacagacatgcg
CZT46230.1	**Actin**	Rs214-08387actinTMF	gcgaggacgaccaacgat
		Rs214-08387actinTMR	aatgtgtaaggccggtttcg
CZT04694.1	**c-4 methyl sterol oxidase**	Rs214-08818c-4TMF	ggtgggattacatgatggacact
		Rs214-08818c-4TMR	ctggaccttctttgccttcttc
CZT43859.1	**acyl-CoA desaturase**	Rs214-08456 acyl TMF	cgctggtgttgtccacgat
		Rs214-08456 acyl TMR	cttgccaataccggaggtgat

III.2.4. Expression profiling of the infection time course sample

The relative expression analysis was carried out as described previously. The relative expression of the *RcCDI1* effector gene was analysed as a positive control to validate the quality of infection time course sample. .

III.2.5. Yeast recombinational cloning strategy for KO cassette generation

Primers were specifically designed to amplify 1 kb to 1.5 kb on each flanking regions of the targeted gene with the defined 30 bp extension shown as two letters on Figure III-1a. Flanking regions amplified by PCR with extensions were combined with the resistance marker (promoter and hygromycin gene annotated as hph Figure III-1c) amplified by PCR and a linearised pRS426 plasmid with complementary defined extensions (Figure III-1b,c). The DNA fragments were assembled together with the vector during transformation into *S. cerevisiae* via its endogenous recombination system (Figure III-1d).

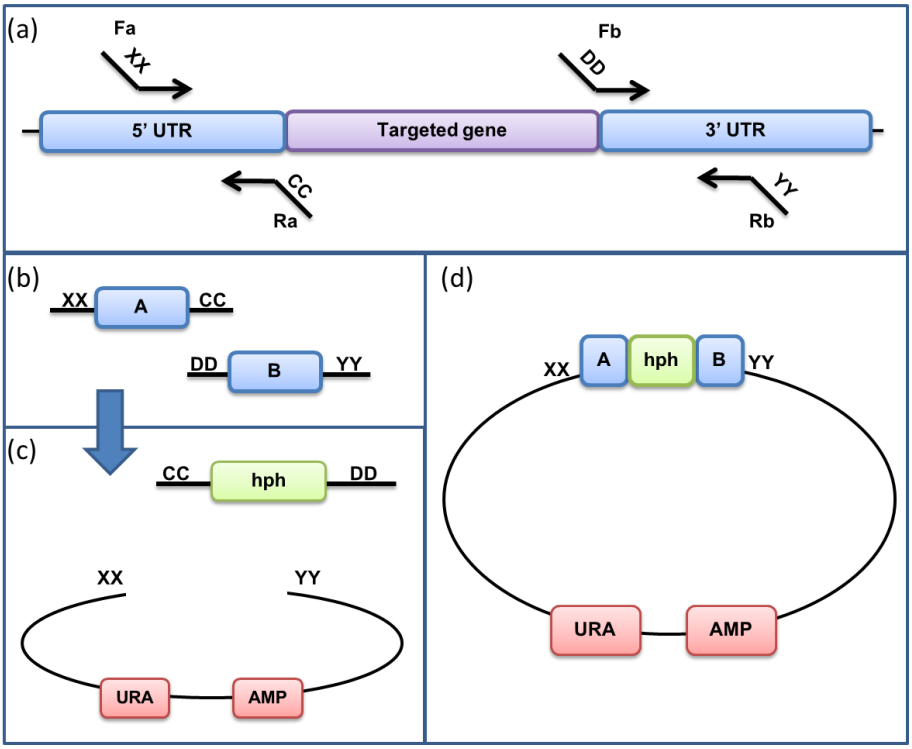

Figure III-1: Yeast recombinational cloning strategy. (a) Flanks of target genes are amplified by PCR using primers carrying appropriate extension (XX, CC to generate the flank A; DD, YY to generate the flank B). (b-c) PCR amplified flanks A and B are combined with the PCR amplified Hygromycin resistance cassette (hph) carrying CC and DD extensions and the open plasmid carrying XX and YY extensions, URA gene for yeast selection on media lacking Uracil amino acid and AMP for ampicillin resistance gene for bacterial selection. (d) Assembled plasmid with hygromycin resistance cassette surrounded by gene target gene flanks A and B for homologous recombination

The pRS426 plasmid was linearised by digesting the plasmid using 1 µg of plasmid with XhoI/BamHI for 1 h at 37°C following the manufacturer's instructions followed by a 20 min incubation at 65°C. Digested plasmid was used as phusion PCR template using YY-fw- PmeI-extgtttaaacttgttatccgctcacaattccacac and XX-rv-PmeI-extgtttaaacggcccgcaccgatc primers with a 70°C annealing temperature.

III.2.6. Split marker strategy

Split marker is a technique of transformation allowing an increase of efficiency of homologous recombination (Fu et al. 2006). Instead of transforming with the full cassette, 2 splits of the cassette (one left flank plus the truncated gene marker and right flank plus truncated gene marked) were amplified for *R. commune* transformation (Figure III-2a). The overlapping region of the gene marker is present on both splits that will recombine because of the homology and restore the full sequence of the gene marker and create a resistant mutant

(Figure III-2b). This process limits false positive transformants induced by ectopic insertion of the full cassette by the introduction of a non-functional marker gene, but induces a less efficient transformation because 3 events are now necessary to obtain a functional gene marker (Figure III-2b).

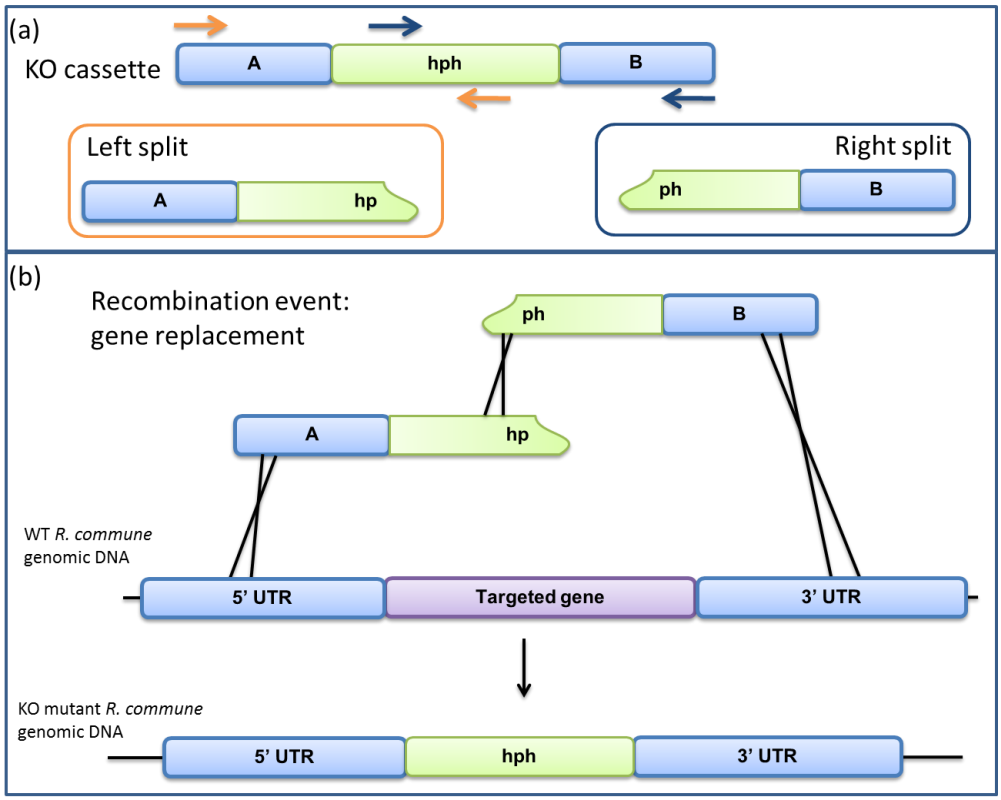

Figure III-2: Split marker transformation strategy. (a) KO cassette overlapping fragments are amplified by PCR using specific primers indicated by orange arrow for the left split fragment and blue arrow for the right split fragment. (b) Gene replacement of targeted gene on genomic DNA by hygromycin cassette. The 3 recombination events are illustrated by crossing lines between flanks and overlapping hygromycin sequences of 2 splits ideally generating KO mutant due to the gene replacement of the target gene by hygromycin

III.2.7. *R. commune* KO transformants genotyping

1 µl of DNA was used for PCR genotyping. An Actin primer pair was used at 0.5 µM for control of DNA quality. Genotyping primers Fgen and Rgen were specifically designed for each specific target gene. The Fgen primer was specifically designed upstream of the 5'UTR to be specific to WT DNA only (Figure III-3). The Hph-stop-rv primer was specifically designed at the end of the marker gene and was used with Fgen primer to screen for the replacement of the targeted gene with the hph marker gene (Figure III-3a). Hph-start-fw and hph-stop-rv were used together to screen for the integration of overlapping DNA fragments into the *R. commune* gDNA (Figure III-3a). The Rgen primer

specifically designed in the target gene was used with Fgen to screen for the presence of the targeted gene (Figure III-3b).

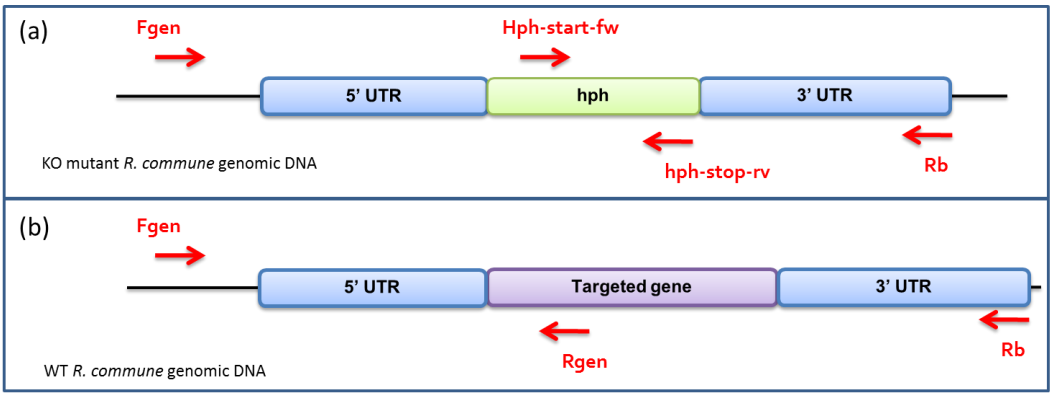

Figure III-3: Genotyping strategy. Red arrows and names represent the location of primers used for genotyping *R. commune* transformants.

III.2.8. BSMV-VOX Ligation-independent cloning and *E. coli* transformation

BSMV-VOX Ligation-independent cloning

An aliquot of BSMVγ-b-2A plasmid linearised with *ApaI* and treated with dTTP T4 polymerase were kindly provided by Olaya Ruiz and Wing-Sham Lee. Phusion PCR was used to amplify candidate genes using specific primers. PCR products were treated with dATP T4 DNA polymerase using 5.2 µL of a gel-purified PCR product (Qiagene kit) mixed with 4.8 µL of the master mix (60 µL of water, 10 µL of 100 mM dATP, 2 µL 100 x BSA (NEB), 20 µL of 10 × T4 DNA Polymerase buffer (NEB) and 4 µL of T4 DNA Polymerase (NEB)). Samples were incubated for 30 min at 22°C followed by a 15 min incubation at 75°C to inactivate the enzyme. For the ligation, 10 µL of T4 DNA polymerase treated PCR product was mixed with 2 µL of T4 DNA polymerase treated BSMV-γ-b-2A and incubated at 65°C for 2 min, then for 10-15 min at room temperature.

BSMV-VOX Ligated plasmid transformation into *E. coli*

2 µL of ligation mix was used for transformation of 20 µL chemically competent *E. coli* strain JM109 (Promega) following the manufacturer's procedure. Cells were spread out on LB agar plate supplemented with 50 µg/mL of kanamycin. BSMV-γ-b-2A-constructs were extracted from *E.coli* liquid culture using the

miniprep kit from Qiagen following the manufacturer's procedure. BSMV-γ-b-2A-constructs were sequenced to check the insertion.

III.2.9. Transformation of BSMV-γ-b-2A-construct into *A.tumefaciens* and agroinfiltration of *N. benthamiana*

A. tumefaciens transformation

BSMV-γ-b-2A-constructs were transformed by electroporation into *A. tumefaciens* strain GV3101 carrying the virulence helper plasmid pMP90. 20 µL of ice cold electro-competent cells, kindly provided by Olaya Ruiz, were combined with 1 µL of plasmid DNA and incubated on ice for 3 min. Mixtures were transferred to an ice cold electroporation cuvette prior to one pulse electroporation using a MicroPulser set to "Agro". Cells were immediately transferred to a sterile 14 mL tube containing 1 ml of LB broth and incubated for 2 h at 28°C with shaking at 250 rpm. After incubation, cells were plated on LB agar plates supplemented with 50 µg/mL kanamycin, 100µg/mL rifampicin and 25 µg/mL gentamycin. Plates were incubated for 3-4 days at 28°C.

A. tumefaciens agroinfiltration into *N. benthamiana*

Before agroinfiltration BSMV-γ-b-2A-construct agrotransformants were prepared as described previously with the following modification. Cells were resuspended in an inoculation buffer (10 mM MgCl2, 10 mM MES pH 5.6 supplemented with 150 µM acetosyringone) to a final OD_{600}=1.5. The 3 BSMV agrotransformants were equally mixed together and incubated at room temperature for 3 h. Agrobacterium cell suspensions were infiltrated into leaves of 4 week-old *N. benthamiana* using a 1mL syringe.

III.2.10. Barley plant inoculation with sap from agroinfiltrated *N. benthamiana* plants and scoring

SAP preparation

3-5 days post agroinfiltration, 1 g of *N. benthamiana* infiltrated leaf tissue with visible virus symptoms were grinded with 3 mL of 10 mM potassium phosphate buffer pH 7, using a mortar and pestle chilled on ice. Saps were filtered through cheese cloth and 1% w/v Celite® was added to serve as an abrasive.

Barley inoculation conditions

The first and second leaf of 10 week old barley plants were inoculated by dipping gloved fingers in the sap preparation before gently pulling the leaves between the thumb and index finger. Leaves were sprayed with water 10 min after the inoculation to let the plant absorb the virus but remove buffer and residual Celite®. Inoculated plants were covered with a large transparent plastic box and left to recover in low light overnight followed by standard growth conditions: 16 h day / 8 h night, 20-23°C (night-day).

BSMV-VOX scoring

The rate of infection was calculated by counting the number of plans infected compared to the number of plants inoculated at 12 DPI. BSMV-VOX development was observed at 10 and 12 DPI on each of 4 replicates of each line inoculated recording the presence of infection, mosaic, necrosis, strong necrosis, weak necrosis, dry tips, chlorotic leaves and dead new leaves on third and fourth uninoculated leaves. Barley response to the construct was classified from 0 to 5 according to the annotation. Rating scores are 0 for no infection, 1 for mosaic, 2 for more severe mosaic, 3 for necrosis of the tip and weak necrosis, 4 for necrosis and 5 for strong necrosis.

III.2.11. Cloning into pEAQ-HT vector for agroinfiltration into *N. benthamiana*

Restriction digestion and ligation

Restriction digestion of PCR fragments and the pEAQ-HT vector were carried out following the manufacturer's recipe and incubated for 2 h at 37^{o}C before the enzyme inactivation for 15min at 65^{o}C. Ligation with T4 DNA ligase was carried out overnight at 4^{o}C in a 10 µl reaction with 25 ng of digested plasmid, 120 ng of digested PCR fragment, 1 µl of T4 DNA ligase (NEB) and 1 µL of 10 X Buffer.

Transformation in *E. coli* and screening

2 µL of ligation product were used to transform One Shot TOP10 Chemically Competent *E. coli* (Thermo Fisher Scientific) following the manufacturer's procedure. Cells were spread on LB agar plates supplemented with 50 µg/mL

kanamycin. After colony PCR check with sequencing primers, plasmids were extracted from *E. coli* liquid culture using the miniprep kit from Qiagen following the manufacturer's procedure and sequenced to check the insertion using Forward: gttttcccgtggttttcgaacttg and Reverse: gcacaccgaataacagtaaattcaaactaaag primers located respectively in 5' and 3' UTR.

III.2.12. PCRs

Amplification of DNA fragments for transformation cassette generation

Amplification of DNA fragments to be used for transformation cassette generation was carried out using Phusion high fidelity polymerase and following the manufacturer's instructions and thermocycler conditions using primers specifically designed to amplify selected fragments (Table III-2).

Table III-2: List of primers used to amplify DNA fragments for generation of KO cassettes. amplify DNA fragments for generation of KO generation cassettes. Approximately 1 Kb flanking region on each side of target gene was amplified using Fa/Ra and Fb/Rb primer pairs from *R. commune* genomic DNA template. Fa, Ra, Fb, and Rb primers contain XX, CC, DD, YY extensions at 5' respectively. PtrpC promoter and hygromycin resistance gene were amplified together using specific primers with CC extension at 5' of forward primer and DD at 5' of reverser primer from pGFP-HPH template.

Target gene	Primer name	Primer sequence 5'-3'
rsu3_00144_g	Fa-144	GGAAGGGCGATCGGTGCGGGCCGTTTAAACCGACTCGAGCGTATGAGTCC
	Ra-144	TTGTGTCATGAATTAACAGTTAACGAATACTGAGGGTCTTCTGAGAGCGG
	Fb-144	TTAGTGTCAAACAGTCAAACCAGTTCTACGGGCCTGCAATGAAGCATACG
	Rb-144	TGGAATTGTGAGCGGATAACAAGTTTAAACGATTCCGAGATCGCATACCC
rsu3_07985_g	Fa-7985	GGAAGGGCGATCGGTGCGGGCCGTTTAAACTCCCCAAACTCCTCTTCTCG
	Ra-7985	TTGTGTCATGAATTAACAGTTAACGAATACTGCAGCAGAAGTACGATTTTTG
	Fb-7985	TTAGTGTCAAACAGTCAAACCAGTTCTACGACGAGGACAGGCAGGCC
	Rb-7985	TGGAATTGTGAGCGGATAACAAGTTTAAACTGCATGGTCTTTGGCCC
rsu3_05502_g	Fa-5502	GAAGGGCGATCGGTGCGGGCCGTTTAAACCGTCGATTTCTTTTCAGCTG
	Ra-5502	TTGTGTCATGAATTAACAGTTAACGAATACTGAATGCCAAAGTACAGGTC
	Fb-5502	TTAGTGTCAAACAGTCAAACCAGTTCTACGGGGAAGTGTCAAACTCGAAG
	Rb-5502	TGGAATTGTGAGCGGATAACAAGTTTAAACTTACTCACGCAGAATTTGGC
rsu3_09280_g	Fa.1-9280	GAAGGGCGATCGGTGCGGGCCGTTTAAACGCAGGAGCATCTCGAAGACC

	Ra.1-9280	TTGTGTCATGAATTAACAGTTAACGAATACCTGGATGAAGTTTCGAGATTGG
	Fb-9280	TTAGTGTCAAACAGTCAAACCAGTTCTACGCGTGGAGATGTCTTCAACGAC
	Rb-9280	TGGAATTGTGAGCGGATAACAAGTTTAAACGTTGTTGTGTTGTGTTGAGGG
rsu3_07190_g	Fa-7190	GAAGGGCGATCGGTGCGGGCCGTTTAAACGACAGGTACAGCCACCTTTG
	Ra-7190	TTGTGTCATGAATTAACAGTTAACGAATACACTCGGTTCCAATGAGGTG
	Fb-7190	TTAGTGTCAAACAGTCAAACCAGTTCTACGAGGGGCCTGAAAGGAGCAAG
	Rb-7190	TGGAATTGTGAGCGGATAACAAGTTTAAACTGATGAGGGTATCGGAAGCG
rsu3_06458_g	Fa-6458	GAAGGGCGATCGGTGCGGGCCGTTTAAACGCCTGTAGAGCGCTAAATGC
	Ra-6458	TTGTGTCATGAATTAACAGTTAACGAATACGGCAAATAGTGTTGCTTGGG
	Fb-6458	TTAGTGTCAAACAGTCAAACCAGTTCTACGGTCGGCATTGAGATTTAAGG
	Rb-6458	TGGAATTGTGAGCGGATAACAAGTTTAAACTGCTACCGCTGCAGTCTC
rsu3_03792_g	Fa-3792	GAAGGGCGATCGGTGCGGGCCGTTTAAACGTCTTCTCGTTGCAATTCCC
	Ra-3792	TTGTGTCATGAATTAACAGTTAACGAATACCAAGTAGTGGGGGTGGAGAG
	Fb-3792	TTAGTGTCAAACAGTCAAACCAGTTCTACGTGCATAGATATTTGCGTCGG
	Rb.1-3792	TGGAATTGTGAGCGGATAACAAGTTTAAACCGCTCACTACGCTCACTACC
rsu3_03882_g	Fa-3882	GAAGGGCGATCGGTGCGGGCCGTTTAAACTAAAGTCGAACCACGATACG
	Ra-3882	TTGTGTCATGAATTAACAGTTAACGAATACGAGGTAAGACGTCTGATGTGAG
	Fb-3882	TTAGTGTCAAACAGTCAAACCAGTTCTACGGGTAGAGGGAAAACAAGGCG
	Rb-3882	TGGAATTGTGAGCGGATAACAAGTTTAAACGCTCGCTTAATTCCGTGTTTAC
rsu3_11823_g	Fa-11823	GAAGGGCGATCGGTGCGGGCCGTTTAAACTCGTCTACGAGAAGGTCAGC
	Ra-11823	TTGTGTCATGAATTAACAGTTAACGAATACGCGATGAAGATTATTGAGGG
	Fb-11823	TTAGTGTCAAACAGTCAAACCAGTTCTACGAGATGGAATGTTGAGGTTGG
	Rb-11823	TGGAATTGTGAGCGGATAACAAGTTTAAACAAATTGAACCAGATTCCCG
rsu3_01835_g	Fa-1-1835	GAAGGGCGATCGGTGCGGGCCGTTTAAACACAGGTAGGGTATGCTTGGC
	Ra-1-1835	TTGTGTCATGAATTAACAGTTAACGAATACGGTATGGTAGATGGATGTGGG
	Fb-1835	TTAGTGTCAAACAGTCAAACCAGTTCTACGCTTTCAGAACTTCAAGAGCTTAAGG
	Rb-1835	TGGAATTGTGAGCGGATAACAAGTTTAAACATCTTGCAGGTATGGCCTTG
PtrpC promotor + hygromycin gene	CC-ext-PtrpC-Fw	GTATTCGTTAACTGTTAATTCATGACACAAtgatattgaaggagcacttttttggg
	DD-ext-hph-rv	CGTAGAACTGGTTTGACTGTTTGACACTAActattcctttgccctcggacg

Amplification of DNA fragments for yeast transformants screen

Yeast transformants were screened by PCR using Phusion high fidelity DNA polymerase and as a template 1 µl of yeast suspension incubated in 20 µl of 20 mM NAOH for 15 min at 70°C. Expected size bands were purified with MiniElute PCR Purification Kit from Qiagen following the manufacturer's procedure but eluted in 15 µl only for high DNA concentration. DNA cassettes were sequenced using forward and reverse primers located on CC and DD extensions (Table III-3) to confirm the success of the cloning and the authenticity of fragments.

Table III-3: List of primers used to sequence DNA cassettes created for the generation of *R. commune* KO mutant.

Primer name	Primer sequence 5'-3'
CC-fw	gtattcgttaactgttaattcatgacac
CC-rv	ttgtgtcatgaattaacagttaacg
DD-fw	ttagtgtcaaacagtcaaaccag
DD-rv	cgtagaactggtttgactgtttg

Amplification of DNA fragments for *R. commune* transformation

Amplification of DNA fragments to be used for *R. commune* transformation was carried out using Phusion high fidelity DNA polymerase following the manufacturer's instructions and thermocycler conditions using primers specifically designed to amplify selected fragments (Table III-4).

Table III-4: Primers used for amplification of DNA fragments for *R. commune* transformation into YRC plasmid created. For split marker transformation strategy, 2 splits were amplified using primer described in the table. For full cassette transformation, XX-fw/YY-rv pair was used to amplify the entire fragment.

Amplicon	Primer name	Primer sequence 5'-3'	Annealing temperature
Left split	XX-fw	ggaagggcgatcggtgcg	74
	hph-split-rv	gacgattgcgtcgcatcgac	72
Right split	hph-split-fw	gggcgaagaatctcgtgctttcag	73
	YY-rv	gtgtggaattgtgagcggataacaag	70

Amplification of DNA fragments for *R. commune* mutant genotyping

Amplification of DNA fragments to be used for *R. commune* mutant genotyping was carried out using Phire DNA polymerase following the manufacturer's recipe and thermocycler conditions using primers specifically designed to amplify *R. commune* genomic region for mutant genotyping (Table III-5).

Table III-5: Primers used for *R. commune* transformants genotyping. Fgen/Rgen primer pair specific to each gene was used to screen for the presence of targeted gene. Fgen/ hph-split-rv (from Table 2) primer pair was specifically used to screen for the replacement of the target gene by the cassette. Act-fw/Act-rv primer pair was used as a control attesting of the quality of the DNA used in the PCR.

Target gene	Primer name	Primer sequence 5'-3'
rsu3_03882_g	Fgen-3882	ctgtccccttatgatagcttcccc
	Rgen-3882	cctgatgagaaagagacgtgagc
rsu3_07190_g	Fgen-7190	ccaactcgattgcatgtcaatacc
	Rgen-7190	ccgtgaccgttggagtaacagg
rsu3_06458_g	Fgen-6458	cgtatttatctacgcgatcgcagac
	Rgen-6458	attctttgtgcctgagatgaagacg
rsu3_07985_g	Fgen-7985	caccttatcatacaaccaaaccttc
	Rgen-7985	cctcgtagttctgctggtacc
rsu3_05502_g	Fgen-5502	tataattggctgtcatatagtaccgc
	Rgen-5502	cccaaaaggctaggattcc
rsu3_00144_g	Fgen-144	ggctctttccatgttcttagcat
	Rgen-144	ttatactcgtgggttatcattccg
hph	Hph-start-fw	atgaaaaagcctgaactcaccg
	Hph-stop-rv	ctattcctttgccctcggacg
actin	Act fw 70	gggacgacatggagaagatctgg
	Act rv 70	agctcgtatgacttctccaagctgg

Amplification of DNA fragments for *R. commune* effector cloning into pEAQ-HT vector

Amplification of DNA fragments to be used for effector cloning into pEAQ-HT vector was carried out using Phusion high fidelity DNA polymerase following the manufacturer's recipe and thermocycler conditions using primers specifically designed to amplify genes from cDNA and specifically designed to contain the *NruI* and *XmaI* restriction sites (Table III-6).

Table III-6: Primers used for *R. commune* candidate genes amplification for cloning into the pEAQ-HT vector. Primers specifically designed to contain the *Nru*I and *Xma*I restriction sites.

Target gene	Primer name	Primer sequence 5'-3'
rsu3_00144_g	FpEAQ-HT-144	TCGCGAATGAAGTTCACCATATTTTCAGTCCTTG
	RpEAQ-HT-144	cccgggGGATCCGCTATTGATCGAGACC
rsu3_07985_g	FpEAQ-HT-7985	TCGCGAATGACACAAATACTCCTCTCCCTTCTC
	RpEAQ-HT-7985	cccgggCAACAGACCCTTCCTCGCC
rsu3_03882_g	FpEAQ-HT-3882	TCGCGAATGGTCACCCTTCCCAAGC
	RpEAQ-HT-3882	cccgggCCAATCATGTCCCTTCAAACTG
rsu3_06458_g	FpEAQ-HT-6458	TCGCGAATGATCACTCCTAGAATCCTTTGTCTTTC
	RpEAQ-HT-6458	cccgggGTACTGCTTGATGGCCCATCTG

III.3. Results

III.3.1. Infection time course

The barley - *R. commune* infection time course was monitored by light microscopy, which allowed the visualisation of conidia germination, mycelial growth and penetration of trypan blue stained leaf sections during the early time point of the infection (Figure III-4). At the end of the infection time course, lesions were observed attesting to the success of infection during the time course (Figure III-5).

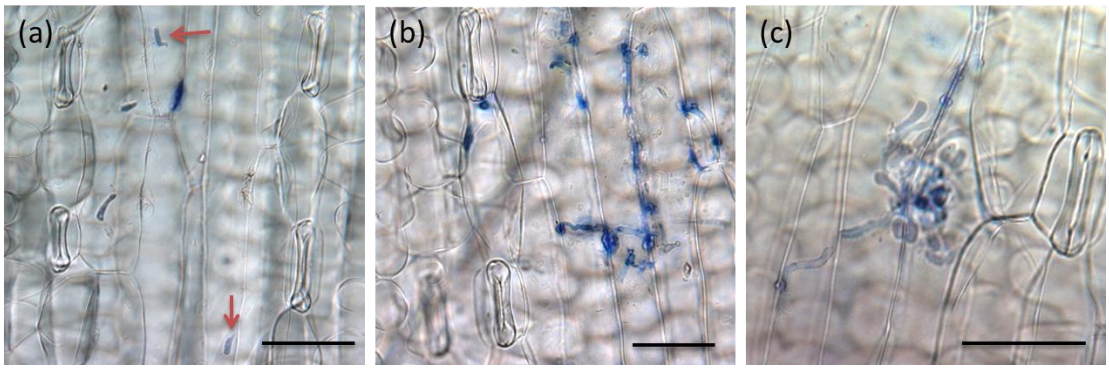

Figure III-4: Light microscopy pictures of infection time course trypan blue stained leaf sections. Leaves sections were collected at 4 days post inoculation (DPI) (a), 7 DPI (b) and 9 DPI (c). *R commune* conidia and hyphae chitin is stained in blue by the trypan blue. (a) Red arrows are pointing to germinating spores. (b,c) Hyphae grew, penetrated the cuticle and grew alongside the cell walls of the epidermal cells. Scale bar represents 50 µm

Figure III-5: Picture of *R. commune* time course barley leaves with lesions at 21 DPI

III.3.2. Selection of putative candidate effectors for transcriptional analysis

Recent sequencing and genome annotation of 9 strains of *R. commune* allowed the generation of a list of 70 conserved in these strains genes with classical features of effectors such as small protein size (up to 225 amino acids) with

signal peptide for secretion and a high number of cysteine amino acids for protein stability in the apoplast. Proteins were predicted to have a signal peptide using TargetP 1.1 (SP>0.5), and TMHMM 2.0 with default settings was used to predict that these proteins did not contain any transmembrane domains. These candidates were genes with homologues in other fungi (using standard cut off of 1e-04 and BLASTx) meaning that they are not specific to *R. commune* but are probably important proteins particularly for infection if conserved between other plant pathogens. An important candidate effector must be conserved between *R. commune* stains, for this reason, putative candidate effector genes were selected based on their limited protein sequence variability within the 9 sequenced strains. Other selecting factors were used such as association between the amino acid differences and virulence/avirulence phenotype on different barley cultivars, evidence of expression in germinated conidia and/or 3DPI, presence in other plant pathogens and a pathogenicity-related putative function. Recent updates provided by Dr Anna Avrova of virulence testing of the different strains of *R. commune* did not allow the identification of a correlation between the amino acid differences of the genes from the list of 70 conserved genes with classical features of effector and virulence/avirulence phenotypes on different barley cultivars. However, a total of 27 genes where selected from that list for transcriptional analysis: *rsu3_00144_g*, *rsu3_03570_g*, *rsu3_05260_g*, *rsu3_05502_g*, *rsu3_11923_g*, *rsu3_12059_g* and rsu3_12695_g were selected due to evidence of expression in germinated conidia and/or at 3 DPI. *rsu3_06458_g*, *rsu3_01835_g*, *rsu3_07190_g*, *rsu3_09063_g*, *rsu3_11823_g*, *rsu3_03236_g*, *rsu3_03870_g*, *rsu3_03882_g* and rsu3_08360_g were selected on their limited protein sequence variability within the 9 sequenced strains. *rsu3_09280_g*, *rsu3_07985_g*, *rsu3_03792_g*, *rsu3_00045_g*, *rsu3_04426_g* and *rsu3_01912_g* were selected on their limited protein sequence variability within the 9 sequenced strains and due to evidence of expression in germinated conidia and/or 3 DPI. *rsu3_02291_g, rsu3_07595_g, rsu3_06926_g, rsu3_02682_g* and *rsu3_09566_g* were selected due to evidence of expression in germinated conidia and/or 3 DPI even if 3 or more different amino acid alleles were observed (

Table **III**-**7**). New annotation of *R. commune* sequences allowed the identification of 2 extra putative candidates due to their interesting putative

function. RcCM is a putative secreted chorismate mutase and RcISC is a putative non-secreted isochorismatase hydrolase.

Table III-7: List and features of putative candidate effectors selected for transcriptional analysis. Genes highlighted in green were detected by RNAseq in 3 DPI sample, genes highlighted in yellow were detected by RNAseq in germinated conidia sample, genes highlighted in red were detected by RNAseq in germinated conidia sample and 3 DPI sample and uncoloured genes were not detected by RNAseq. Amino acid differences for each gene are listed for each sequenced strain in the appropriated column. Genes missing from the *R. commune* strain genome sequence data are in white.

R. commune putative effector	*R.commune* strains									size (aa)	Number of Cysteines
	13-13	214	L2A	L32B	L43D	L73A	L77	UK7	AU2		
rsu3_00144_g	identical									97	1
rsu3_03570_g	identical									196	8
rsu3_05260_g	identical									214	12
rsu3_05502_g	identical									128	8
rsu3_11923_g	identical									200	8
rsu3_12059_g	identical									61	4
rsu3_12695_g	identical									225	4
rsu3_09280_g	identical								Missing gene	191	5
rsu3_07985_g	G	G	G	G	G	G	G	G	R	124-173	6
rsu3_03792_g	K	K	K	K	K	K	K	K	R	168	8
rsu3_00045_g	A	A	A	A	A	A	A	T	A	216	8
rsu3_01912_g	DC-Q	DC-Q	DC-Q	DC-Q	DC-H	DC-Q	DC-Q	DC-H	ES-H	224	9
rsu3_02291_g	V-F-E-T-G-T	V-F-E-N-G-T	V-V-G-T-R-N	V-V-E-T-G-T	V-V-G-T-R-N			V-V-G-T-R-N	I-V-G-T-G-T	206	4
rsu3_04426_g	A	T	A	T	A	A	A	T	A	127	4
rsu3_07595_g	P-V-GS	P-V-GS	P-V-GS	P-G--A	S-V-GS	P-V-GS	P-V-GS	P-G----	P-V-GS	220	4
rsu3_06926_g	E-T-M-Y	E-T-M-Y	E-A-M-H	Q-T-M-Y	E-T-M-Y	E-T-M-Y	E-T-M-H	Q-T-M-Y	Q-T-M-Y	222	4
rsu3_02682_g	217aa A-T-T-Q	T-AT-Q no stop						188aa A-T-T-Q	188aa A-T-A-K	217	6
rsu3_09566_g	V-D-N-L	G-D-N-L	G-D-N-F	G-N-D-F	3' end missing			G-N-D-F	G-N-D 177aa	196	5
rsu3_06458_g	D	D	N	D	D	D	D	D	D	193	4
rsu3_01835_g	V-P-R-G	V-P-R-G	V-P-R-G	V-P-R-G	V-P-R-G	V-P-R-G	V-P-R-G	V-P-R-G	I-R-G-D	88	10
rsu3_07190_g	P	P	P	P	P	P	P	P	-	129	10
rsu3_09063_g	S	S	S	S	S	S	S	T	S	181	6
rsu3_11823_g	R-I-V-L	P-L-V-L	R-I-V-L	P-L-F-V	P-L-F-V	R-I-V-L	R-I-V-L	P-L-V-L	P-L-F-V	132	6
rsu3_03236_g	G	S	G	S	S	G	S-D	S	G	162	6
rsu3_03870_g	L-QRN	P-QRN	L-QRN					P-FKP	P-QRN	130	8
rsu3_03882_g	N	D	N	N	D	N	N	D	D	185	4
rsu3_08360_g	S-D	S-D	I-D	I-D	I-D	S-D	S-D	S-D	S-D	144	5

III.3.3. Transcriptional analysis of *R. commune* candidate effector genes during the infection time course

No working qPCRprimers could be designed for *rsu3_02291_g* probably due to the high variability of the gene sequence. The relative expression of the *RcCDI1* effector gene showed the expected pattern of upregulation at 3 DPI confirming the successful infection development during the time course (Figure III-6).

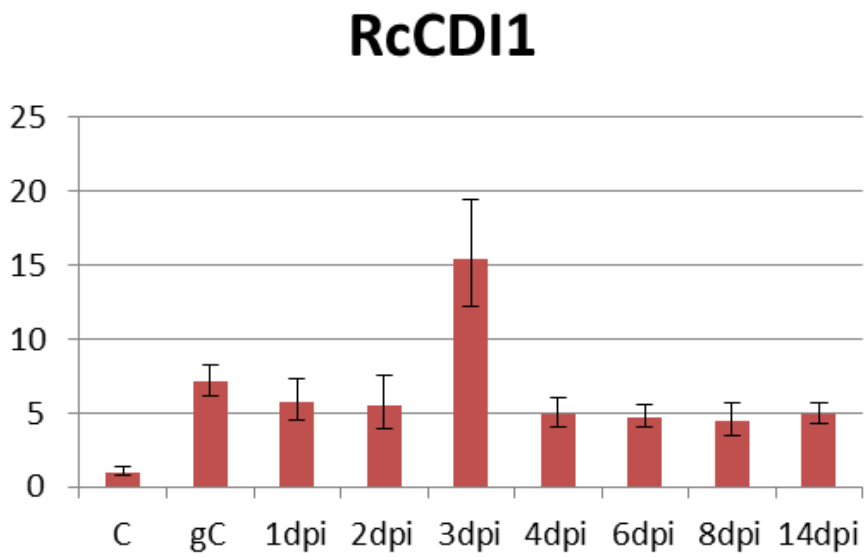

Figure III-6: Relative expression of *R. commune* effector RcCDI1. Relative expression was measured in C=Conidia, gC= germinated Conidia and at 1, 2, 3, 4, 6, 8, 14 days post inoculation (DPI). Error bars represent standard deviations calculated using technical repeats.

Putative candidate effector genes not upregulated during the infection.

4 out of 27 genes were not upregulated during infection compared to their relative expression in conidia and germinated conidia. *rsu3_03570_g, rsu3_04426_g* and *rsu3_05260_g* relative expression during infection is clearly not higher than in conidia and/or germinated conidia, while *rsu3_08360_g* relative expression stayed very low in all samples expect for a slight increase at 6 DPI (Figure III-7).

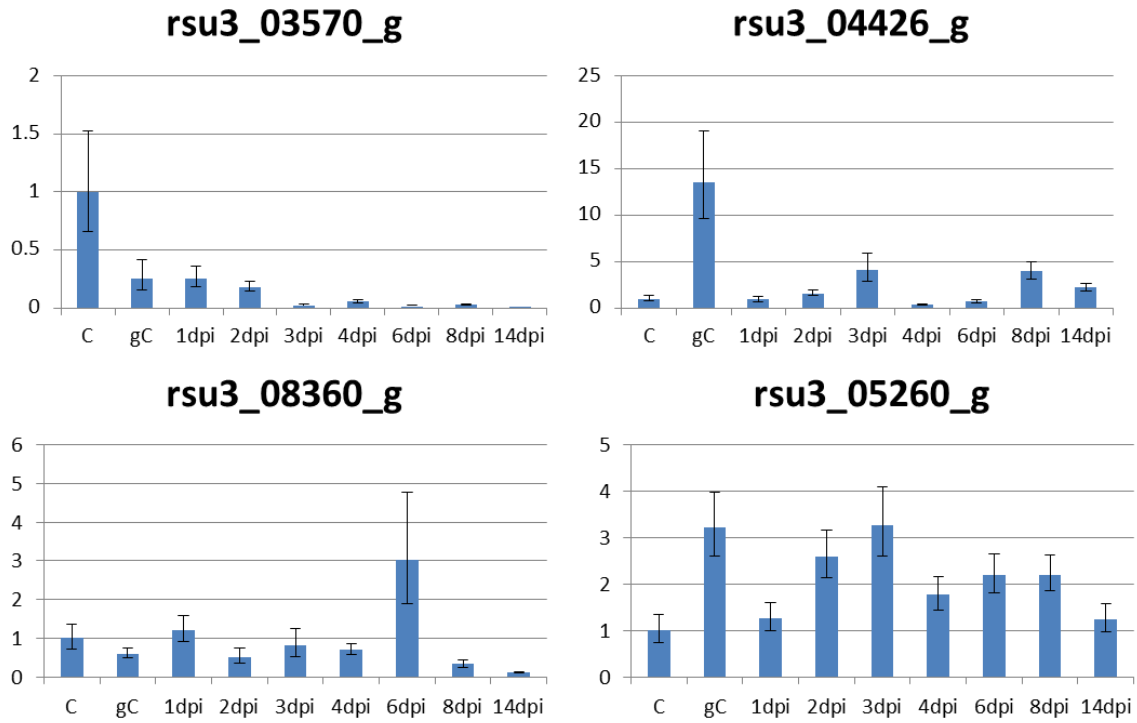

Figure III-7: Relative expression of *R. commune* putative candidate effectors not upregulated during inoculation. Relative expression was measured in C=Conidia, gC= germinated Conidia, and at 1, 2, 3, 4, 6, 8, 14 days post infection (DPI). Error bars represent standard deviations calculated using technical repeats.

The 24 remaining candidate genes were sorted into different groups according to their relative expression pattern.

Group 1: Putative candidate effectors with transcript levels peaking at 1 DPI

The group contains 7 genes all of which were upregulated during infection compared to conidia and germinated conidia (Figure III-8). Moreover, *rsu3_00144_g, rsu3_07190_g, rsu3_03236_g, rsu3_07985_g* and *rsu3_09280_g* showed a clear upregulation from 1 DPI followed by a decrease. *rsu3_03792_g* and *rsu3_03870_g* where classified in that group according to their high upregulation at 1 DPI but the size of the technical error bars could indicate that the higher expressing sample could be 2 DPI and 3 DPI for candidate genes *rsu3_03236_g* and *rsu3_03870_g* respectively.

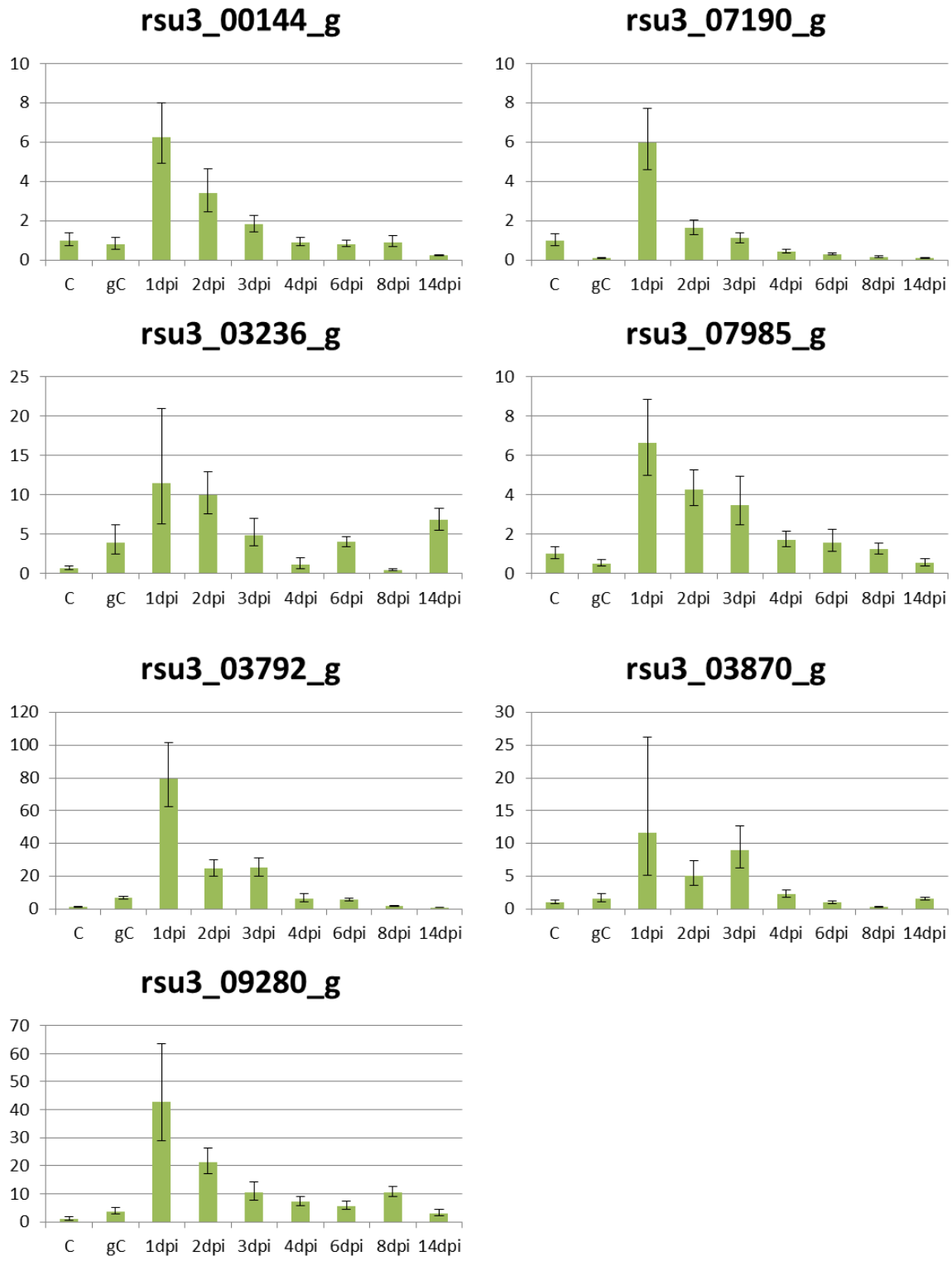

Figure III-8: Relative expression of *R. commune* putative candidate effectors upregulated at 1 DPI. Relative expression was measured in C=Conidia, gC= germinated Conidia, and at 1, 2, 3, 4, 6, 8, 14 days post inoculation (DPI). Error bars represent standard deviations calculated using technical repeats.

Group 2: Putative candidate effectors with transcript abundance peaking at 2-3 DPI

The group contains 9 genes, all of which were upregulated during infection compared to conidia and germinated conidia. Moreover *rsu3_05502_g, rsu3_07595_g, RcCM, RcISC, rsu3_09566_g, rsu3_12059_g* and *rsu3_02682_g* showed an increasing upregulation until 2 DPI compared to conidia and germinated conidia followed by a decrease. Candidate genes *rsu3_06926_g* and *rsu3_11923_g* showed an upregulation from 2 DPI compared to conidia and germinated conidia followed by a decrease (Figure III-9).

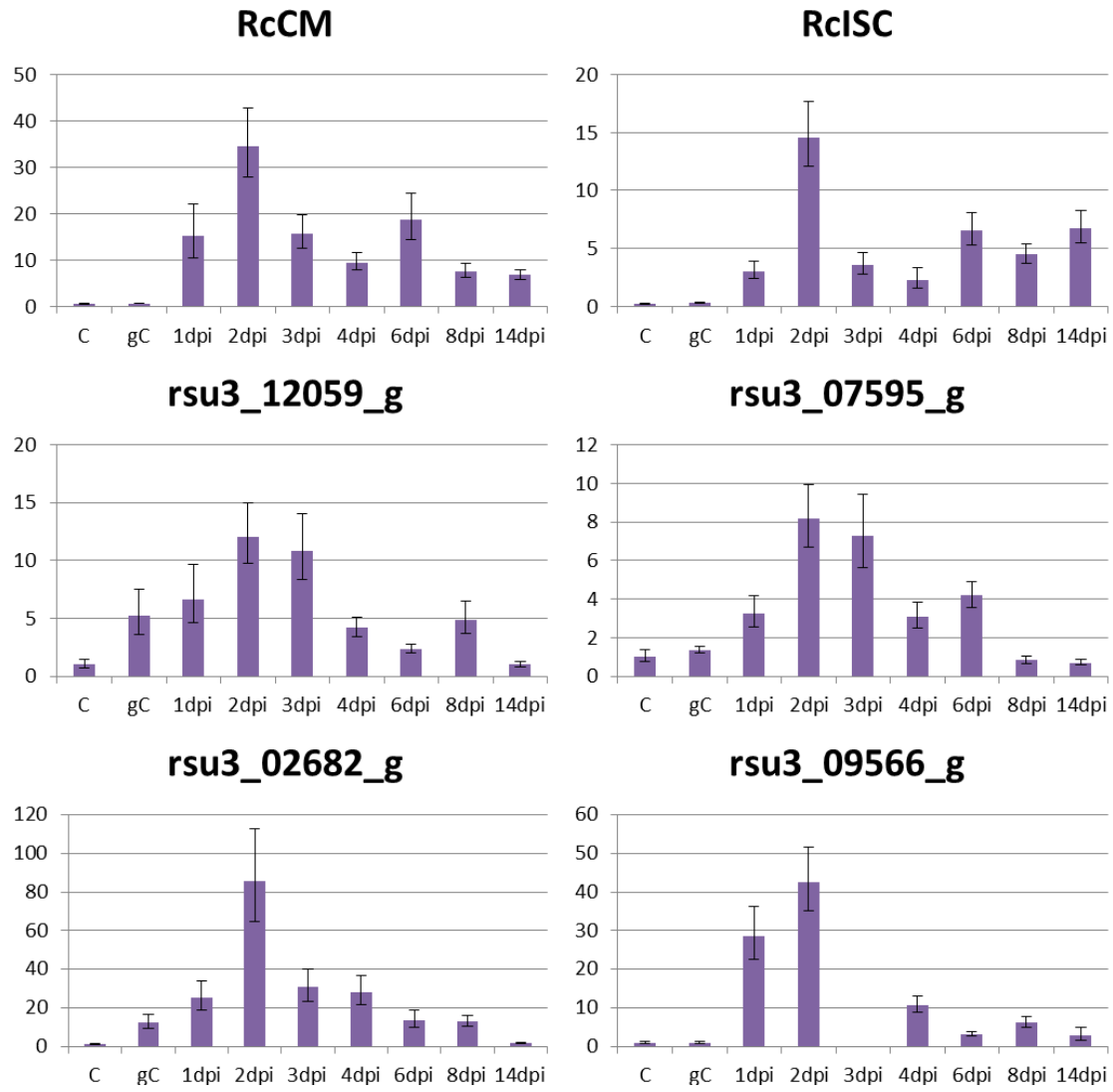

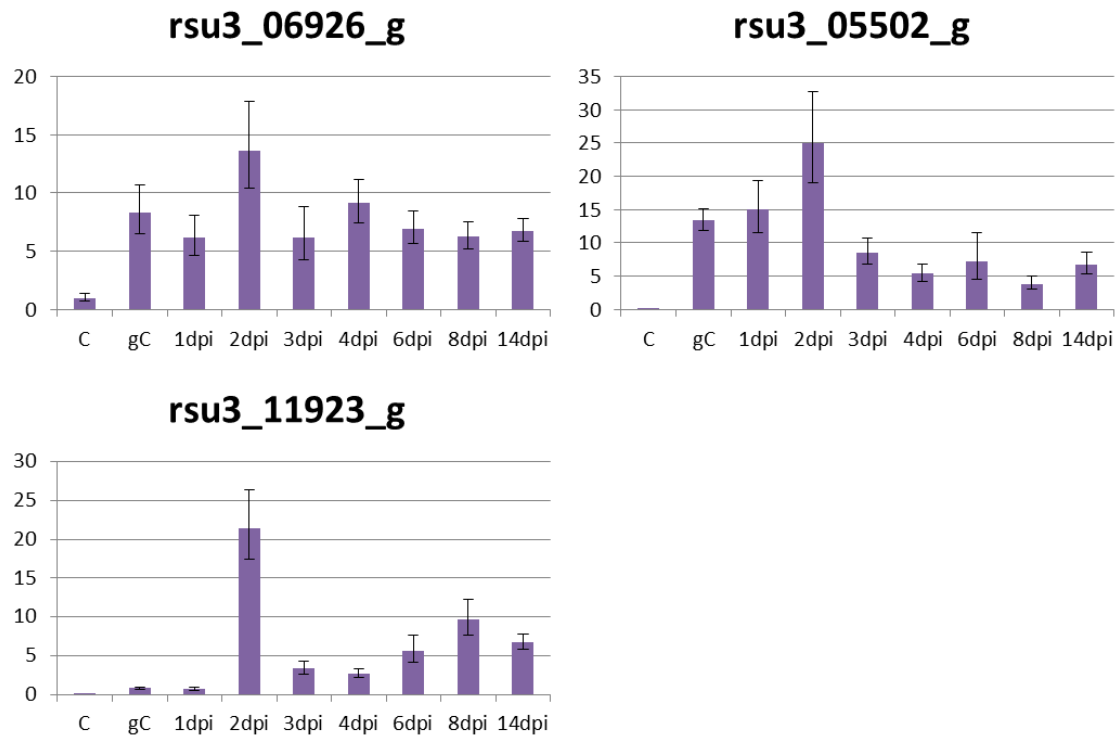

Figure III-9: Relative expression of *R. commune* putative candidate effectors peaking at 2-3 DPI. Relative expression was measured in C=Conidia, gC= germinated Conidia, and at 1, 2, 3, 4, 6, 8, 14days post inoculation. Error bars represent confidence intervals calculated using technical repeats.

Group 3: Putative candidate effectors with transcript abundance peaking at 3 DPI

The group contains 4 genes showing a similar pattern of relative expression to that of *RcCDI1* with an upregulation at 3 DPI followed by a decrease compared to conidia and germinated conidia sample. *rsu3_01835_g* showed an increase in transcript abundance until 3 DPI followed by a decrease compared to conidia and germinated conidia sample. The transcript abundance of *rsu3_09063_g* and *rsu3_11823_g* was higher at 3 DPI but 1 DPI samples showed an upregulation compared to conidia and germinated conidia samples. *rsu3_00045_g* was classified in that group according to its higher upregulation at 3DPI but the confidence interval suggests that it could be equally abundant at 2 DPI (Figure III-10).

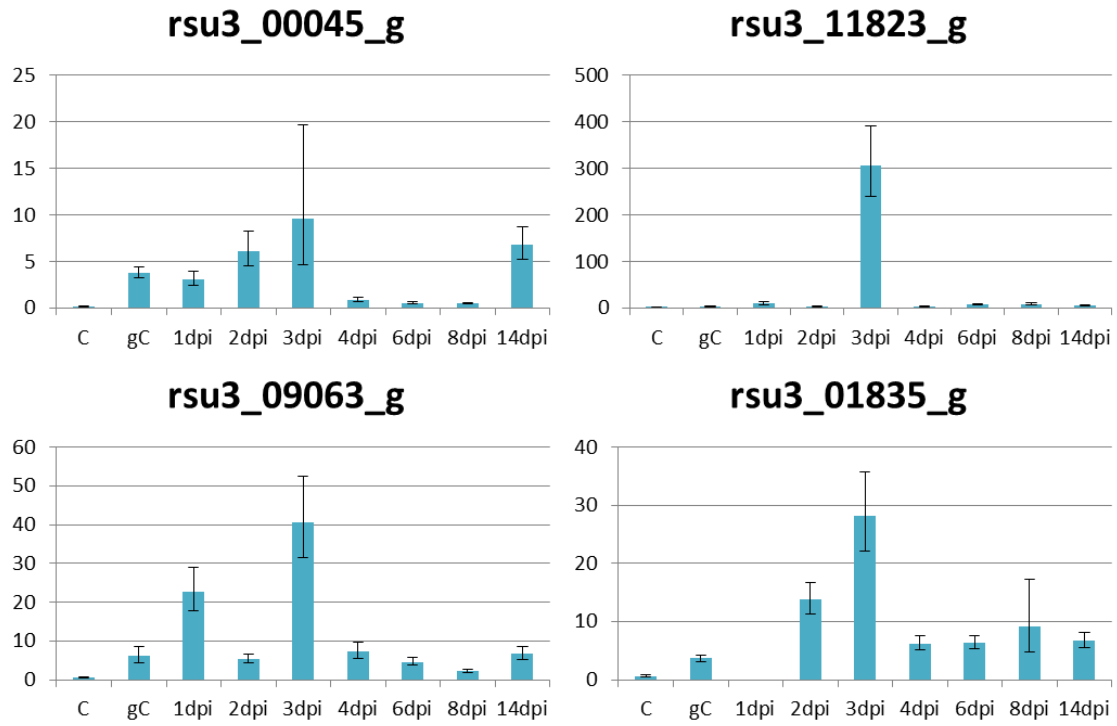

Figure III-10: Relative expression of *R. commune* putative candidate effectors with expression levels peaking at 3 DPI. Relative expression was measured in C=Conidia, gC= germinated Conidia, and at 1, 2, 3, 4, 6, 8, 14 days post inoculation (DPI). Error bars represent standard deviations calculated using technical repeats.

Group 4: Putative candidate effectors upregulated at late stage of infection

Group contains 4 genes showing late upregulation during the infection compared to conidia and germinated conidia sample (Figure III-11). Transcript abundance of *rsu3_03882_g* and *rsu3_06458_g* increased up to 6 DPI followed by a decrease compared to conidia and germinated conidia samples. Transcript abundance of *rsu3_01912_g* and *rsu3_12695_g* increased up to the last time point of 14 DPI compared to conidia and germinated conidia samples.

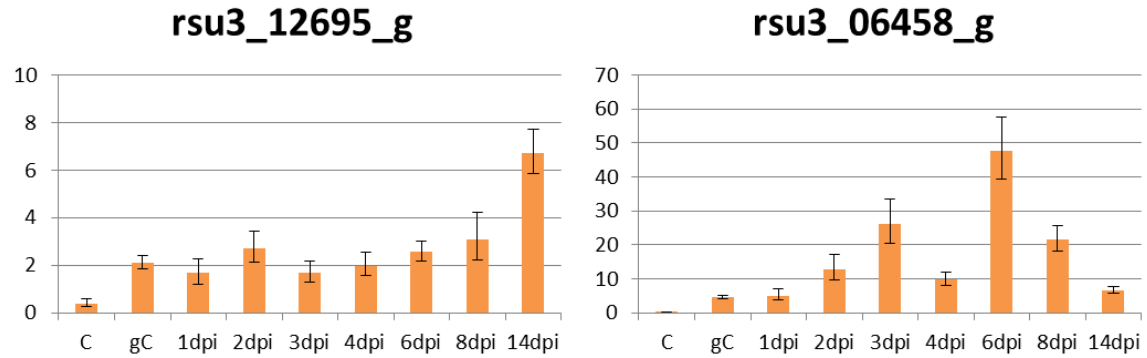

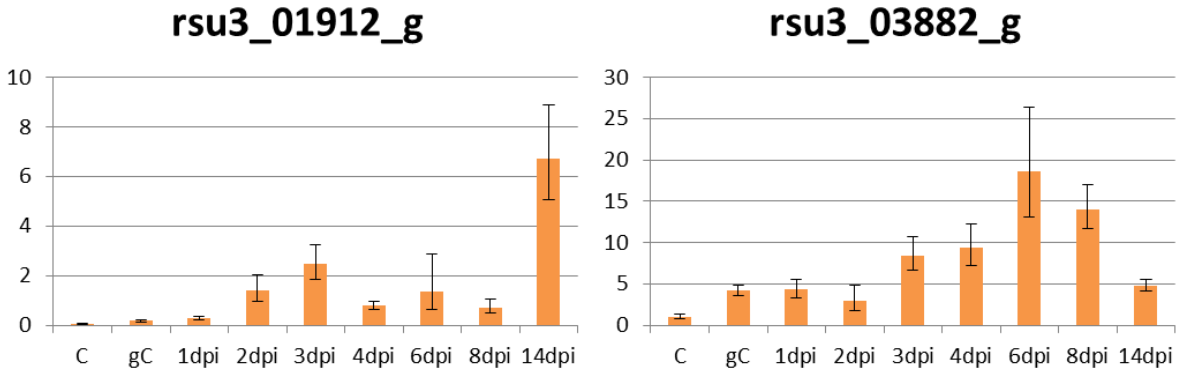

Figure III-11: Relative expression of *R. commune* putative candidate effectors upregulated late during the infection. Relative expression was measured in C=Conidia, gC= germinated Conidia, and 1, 2, 3, 4, 6, 8, 14 days post inoculation (DPI). Error bars represent confidence intervals calculated using technical repeats.

III.3.4. Candidate genes transcript abundance relative to actin transcript abundance

Candidate genes transcript abundance relative to actin transcript abundance was calculated to identify the quantity of transcript produced in each sample compared to the highly expressed gene actin. Results are summarised in Table III-8.

Table III-8: Transcript abundance of the candidate effector genes at the peak of their expression relative to actin.

Gene name	Transcript abundance relative to actin	Sample	Gene name	Transcript abundance relative to actin	Sample
rsu3_00144_g	20.2	1 DPI	rsu3_11923_g	0.3	2 DPI
rsu3_07190_g	18.8	1 DPI	rsu3_07595_g	39.1	3 DPI
rsu3_05502_g	14.7	1 DPI	RcCDI1	11.9	3 DPI
rsu3_07985_g	7.1	1 DPI	rsu3_12059_g	1.7	3 DPI
RcCM	2.2	1 DPI	rsu3_05260_g	1.6	3 DPI
rsu3_02682_g	1.8	1 DPI	rsu3_00045_g	1.1	3 DPI
rsu3_09280_g	1.1	1 DPI	rsu3_11823_g	0.8	3 DPI
rsu3_03792_g	0.3	1 DPI	rsu3_04426_g	0.6	3 DPI
rsu3_06926_g	0.1	1 DPI	rsu3_01912_g	0.4	3 DPI
rsu3_03870_g	0.1	1 DPI	rsu3_09063_g	0.0	3 DPI
rsu3_12695_g	0.1	1 DPI	rsu3_01835_g	0.0	3 DPI
rsu3_09566_g	0.1	1 DPI	rsu3_06458_g	1.5	6 DPI
rsu3_03236_g	0.0	1 DPI	rsu3_03882_g	1.3	6 DPI
rsu3_08360_g	0.0	1 DPI	rsu3_03570_g	5.4	conidia
RCisc	4.3	2 DPI			

III.3.5. Selection of genes for KO mutant generation and BSMV-VOX screening

Expression profiling allowed prioritising 10 out of 22 candidate effector genes for KO mutant generation. Candidate genes were selected based on their relative expression level and pattern during infection, relative transcript abundance compared to actin, putative function and presence of homologues in other plant pathogens. These candidates were genes shared with other fungi meaning that they are not only present in *R. commune* but are probably proteins important for infection if conserved between other plant pathogens. Candidate genes were selected from the 4 relative expression groups as genes upregulated at different stages of infection could play different roles of importance for pathogenicity. However, group 1 was prioritised due to the fact that if proteins are essential and important, they must be expressed as soon as possible during the infection to allow a fast and efficient infection in order to ensure growth and survival during the infection. *rsu3_00144_g, rsu3_07985_g, rsu3_05502_g, rsu3_07190_g, rsu3_03882_g* and *rsu3_06458_g* were selected due to their high transcript abundance and the presence of gene homologues in other plant and cereal pathogens. In addition, *rsu3_00144_g* and *rsu3_06458_*g presented interesting putative functions. *rsu3_03792_g, rsu3_11823_g* and *rsu3_01835_g* transcript abundance was lower than that of the actin transcript but they were selected due the presence of homologous gene in other plant and cereal pathogens. Moreover, *rsu3_03792_g* and *rsu3_01835_g* putative functions seem to be related to pathogenicity (Table III-9).

Table III-9: Candidate genes selected for KO mutants generation. Fungal species in green are cereal pathogens.

Gene name	size aa	Number of Cysteines	Peak transcript abundance and the time point	Transcript pattern group	Putative function	Plant pathogen homologue (BlastP)
rsu3_00144_g	97	1	20.2 at 1DPI	1	strong similarity to serine proteinase inhibitor	*Sclerotinia sclerotiorum*, *Sclerotinia borealis*, *Z. tritici*
rsu3_07985_g	124-173	6	7.1 at 1DPI	1	Putative long chronological lifespan protein 2	*B. cinerea*, *F. oxysporum*, *Ustilaginoidea virens*
rsu3_05502_g	124	8	14.7 at 1DPI	2	hypothetical protein	*S. borealis*, *B. cinerea*, *S. sclerotiorum*
rsu3_09280_g	191	5	1.1 at 1DPI	1	Thioredoxin-like protein link to thermal stress	*Marssonina brunnea*, *Verticillium alfalfae*
rsu3_07190_g	129	10	18.8 at 1DPI	1	hypothetical protein	*S. sclerotiorum*, *B. cinerea*, *S. borealis*
rsu3_03882_g	185	4	1.3 at 6DPI	4	hypothetical protein	, *M. oryzae*, *Z.tritici*, *F.oxysporum*
rsu3_06458_g	193	4	1.5 at 6DPI	4	Pathogen effector domain; putative necrosis-inducing factor	*Parastagonospora nodorum*, *Stagonospora sp*, *Fusarium graminearum*,
rsu3_03792_g	168	8	0.3 at 6DPI	1	CFEM domain; fungal specific cysteine rich domain found in proteins with roles in fungal pathogenesis	*Marssonina brunnea*, *B. cinerea*, *S. borealis*
rsu3_11823_g	132	6	0.8 at 6DPI	3	hypothetical protein	*M. oryzae*, *Stagonospora sp.* , *Pyrenochaeta sp*
rsu3_01835_g	88	10	0.007 at 3DPI	3	Putative Cytochrome P450	*Macrophomina phaseolina*, *P. nodorum*, *Bipolaris oryzae*

III.3.6. KO mutant generation and screening

KO-mutant generation in plant pathogens is a method used to identify and characterise effectors by knocking out the gene candidate and testing the mutant for pathogenicity. This method could identify whether the gene is

important for pathogenicity if KO-mutant shows a decreased pathogenicity on susceptible barley lines or to identify whether the effector was recognised by the plant if the KO-mutants show the ability to infect previously resistant lines. Because the method used was identical for all candidates, results will be illustrated by the processes of cassette creation for 3 or 4 different candidates only. KO cassettes were generated to be used on 2 different *R. commune* strains: L2A and AU2. To avoid disrupting possible genes in flanking regions of targeted genes, specific KO cassettes were created for both strains due to SNPs located in some flanking region.

Summary of KO mutants' generation and screening

A total of 12 different cassettes were generated by Yeast recombinational cloning (YRC). 9 out of 12 were successfully sequenced. 11 transformation attempts were carried out and 7 were successful. Details are resumed in the Table III-10.

Table III-10: Summary of KO mutant cassettes generated, transformation processed and colonies screened. SNP on flank column indicates if there is SNPs in flanks between the 2 strains X indicates sequencing issue in one of the flank.

	Strain	L2A		AU2		L2A			AU2			
Gene name	SNP on flank	Cloning achieved	Sequencing achieved	Cloning achieved	Sequencing achieved	Transformation	Subcultured	Genotyped	Transformation		Subcultured	Genotyped
rsu3_00144_g	No	✓	✓			1 fail			1 fail	✓	121	87
rsu3_07985_g	Yes	✓	✓	✓	✓	1 fail			✓		120	84
rsu3_05502_g	Yes	✓	✓	✓	✓				✓		125	44
rsu3_9280_g	Yes	✓	X	✓	X							
rsu3_07190_g	No	✓	✓			1 fail			✓		100	49
rsu3_03882_g	No	✓	✓						✓		125	75
rsu3_06458_g	No	✓	✓			✓	125	71	✓		75	36
rsu3_3792_g	Yes	✓	✓	✓	X							
rsu3_11823_g	No	✓										
rsu3_1835_g	Yes											

Cassette generation by YRC strategy

KO cassettes were generated to be used for 2 different strains: L2A and AU2. To avoid disrupting possible genes in flanking regions of targeted genes, specific KO cassettes were created for both strains due to SNPs located in

some flanking region. Flanking regions of candidates were successfully amplified by PCR with an expected size around 1kb (Figure III-12).

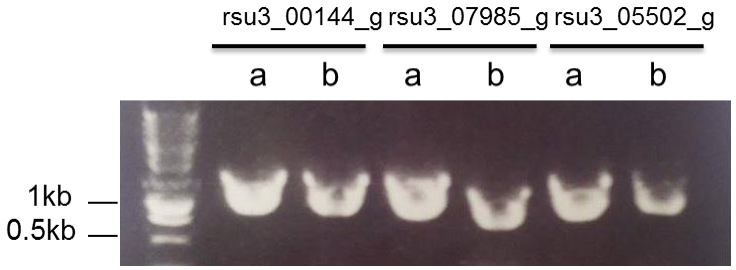

Figure III-12: Agarose gel of amplicons of flanking fragments of candidate genes. Expected size: rsu3_00144_g flank a: 1134bp, rsu3_00144_g flank b: 1175bp, rsu3_07985_g flank a: 1132bp, rsu3_07985_g flank b: 932bp, rsu3_05502_g flank a: 1124bo, rsu3_05502_g flank b: 1176bp.

Yeast colonies were screened by amplifying 2 products by PCR. PCR products showing the expected size and sequence were used for *R. commune* transformation (Figure III-13).

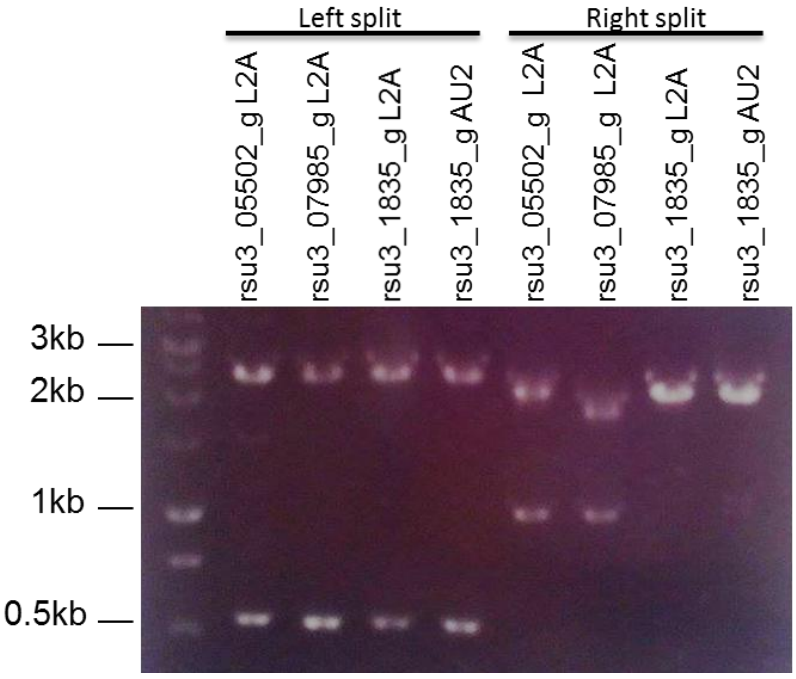

Figure III-13: Agarose gel of PCR amplification of cassettes splits. Left split (LS) and Right split (RS) of 4 different construct. Expected size: LS of rsu3_05502_gL2A: 2424pb, RS of rsu3_05502_gL2A :2076pb, LS of rsu3_07985_gL2A: 2432bp, RS of rsu3_07985_gL2A: 1832 bp,, LS of rsu3_1835_gL2A/AU2:2374pb, RS of rsu3_1835_gL2A/AU2:2134pb.

Transformants subcultivation

Hygromycin efficiency for selecting *R. commune* transformants was tested by comparing the growth of wild type (WT) *R. commune* on plate supplemented or not with hygromycin. Growth of WT *R. commune* was observed on selective

media from 20 day after spreading due to hygromycin instability over time (Figure III-14.a).

Transformants were spread on non-selective plates used for health and growth control (Figure III-14.b). No growth on non-selective plate would indicate that the transformation procedure killed all the conidia. Equivalent speed of growth on selective and non-selective plates indicated that hygromycin is inefficient which happens when it gets too old.

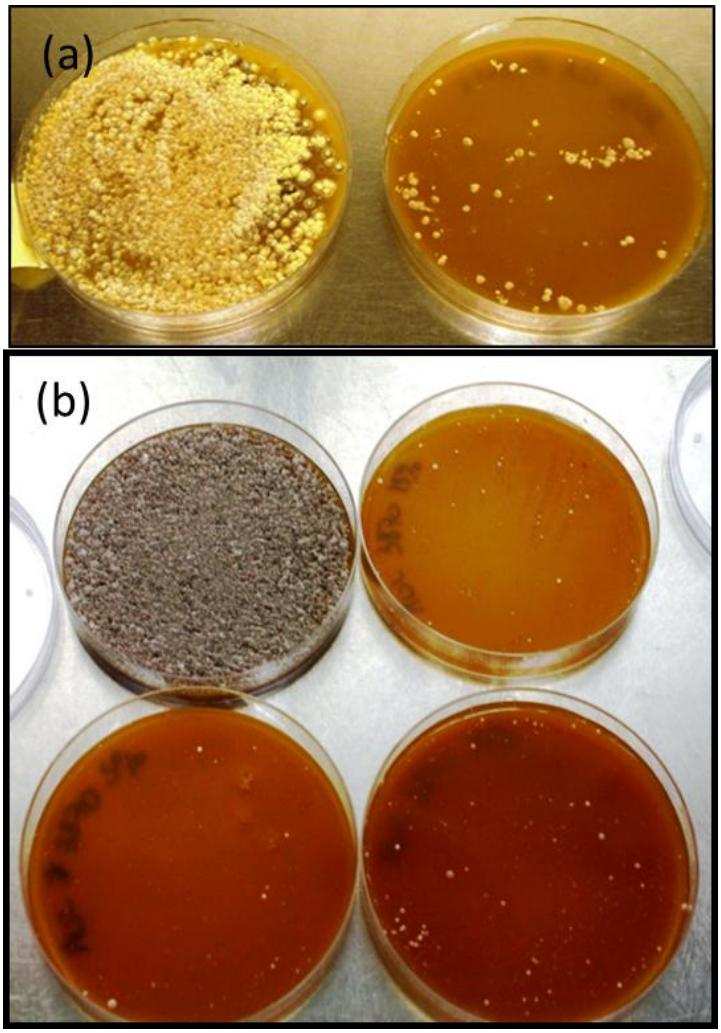

Figure III-14: Picture of *R. commune* growth. (a) *R. commune* WT strain L2A growth 22 days after spreading on CZV8CM agar medium (left) and CZV8CM agar medium supplemented with 100 mM hygromycin and 100 mM Ampicillin (right). (b) *R. commune* transformants growth 17 days after spreading on CZV8CM agar medium (top left) and CZV8CM agar medium supplemented with 100 mM hygromycin and 100 mM ampicillin (others three plates).

Transformant colonies of 1mm minimum diameter from selective plate (Figure III-14.b) were subcultured onto a fresh plate (Figure III-15) up to when colonies started to appear on selective plates spread with WT *R. commune* to select stable transformants and avoid screening non-selected colonies.

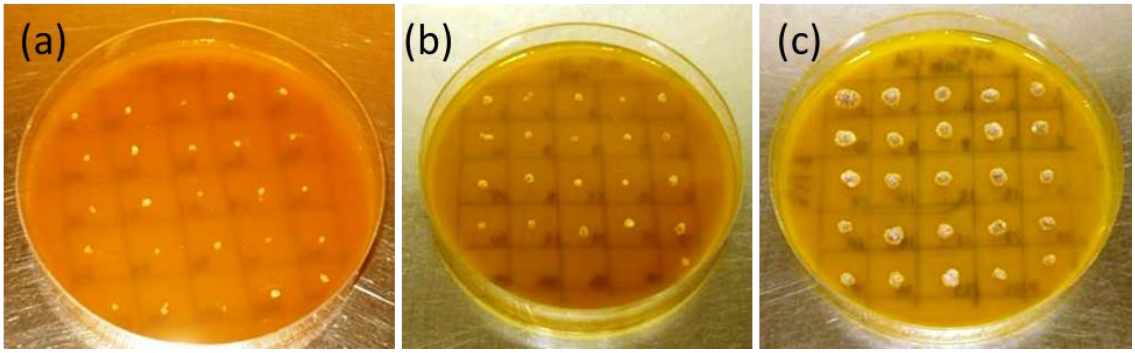

Figure III-15: Pictures of subcultured transformants. Colonies were subcultured on fresh CZV8CM agar medium supplemented with 100 mM hygromycin and 100 mM ampicillin 1 (a), 5 (b) and 28 (c) days after subcultivation.

Transformants genotyping

A total of 791 colonies were subcultivated but not all of them were screened since unstable transformants died and contamination forced me to discard some others. 446 transformants out of 791 total subcultivated colonies were genotyped. No positive colonies were observed by PCR screening of hph replacement in the targeted region (Figure III-16). However, the lack of existing positive PCR control prevented definitive conclusions from being made. The absence of bands when screening for the presence of targeted genes in transformants could be a sign of a missing gene due to gene replacement (Figure III-16).

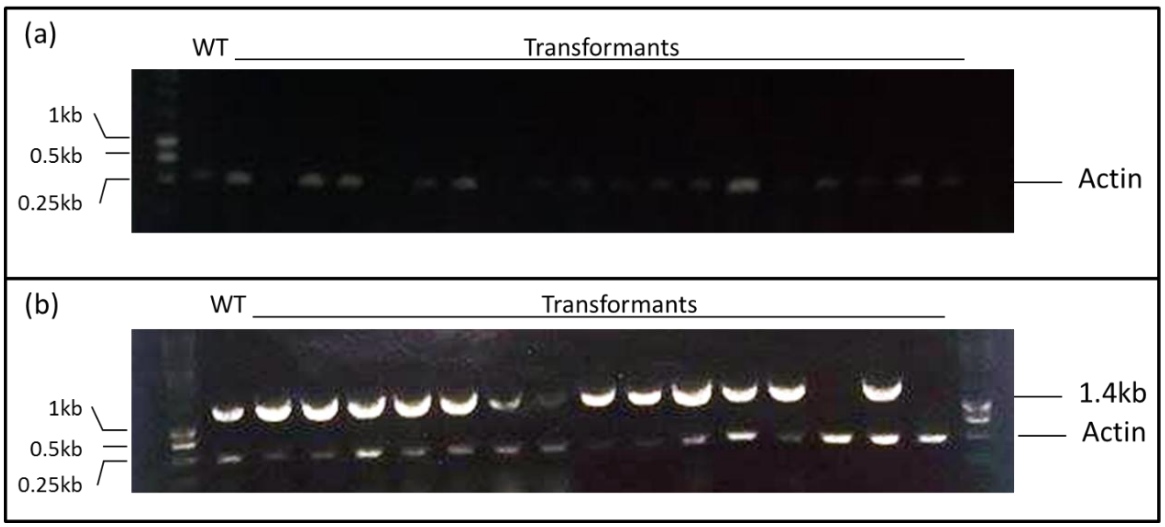

Figure III-16: Agarose gel pictures of rsu3_00144_g KO mutant screen. (a) PCR using Fgen and hph-stop-rv for gene replacement by KO cassette screen and actin primer for DNA control. (b) PCR using Fgen and Rgen for targeted gene presence screen and actin primer for DNA control. Expected size: actin: 250pb, targeted gene presence: 1.4kb.

Ambiguous transformants showing missing PCR amplification were retested individually including a PCR test for full fragment hph gene.

Retest of individual colonies did not allow identification of colonies with gene replacement, however fully recombined hph gene fragment could be detected in transformants meaning that transformation worked and recombination happened (Figure III-17). To avoid the issue of lacking a positive control when screening for gene replacement, a PCR reaction amplifying from upstream of the 5'UTR to the end of the flank b allowed me to compare the size between WT and transformants and revealed that they all had the amplicon same size while transformants must be 1kb bigger meaning that targeted genes were not knocked out (Figure III-17).

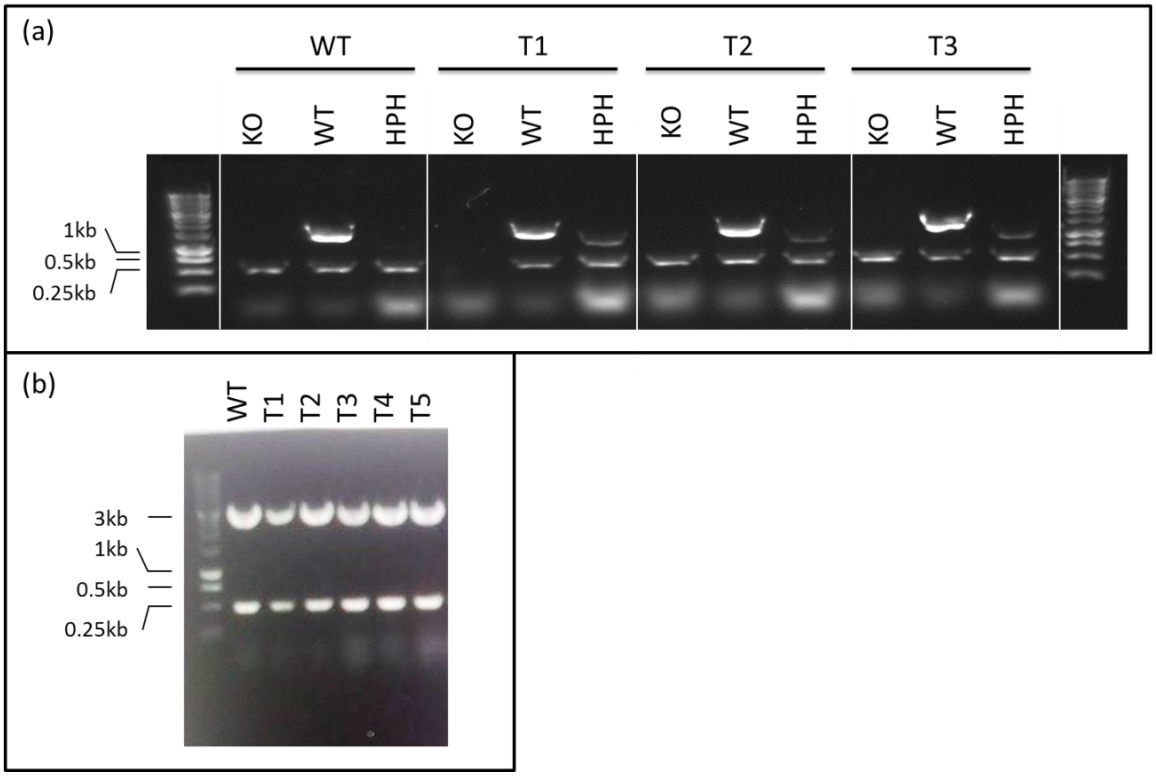

Figure III-17: Agarose gel with PCR products from ambiguous rsu3_00144_g KO transformants. WT, T1, T2, T3, T4 and T5 are arbitrary names of transformants. (a) KO: PCR using Fgen and hph-stop-rv primers for gene replacement by KO cassette screen and actin primers for DNA control, WT: PCR for targeted gene presence screen and actin for DNA control, HpH: PCR for hygromycin gene and actin for DNA control. HpH amplicon expected size: 1kb. , actin amplicon expected size: 250pb. (b) PCR using Fgen and Rb primers for DNA amplicon comparison between WT and transformants. Expected size: WT: 2,8kb, KO mutant: 3.8Kb.

III.3.7. BSMV mediated tools.

Transient expression using plant virus vectors known as virus-mediated overexpression (VOX) is useful for the production of a recombinant protein. Screening of different barley genotypes for novel sources of resistance using VOX of pathogen effectors can help to characterise and identify real effectors

and determine which cultivars are recognising the effector. BSMV-VOX system is capable of expressing only relatively small (up to ~ 160 amino acid residues) heterologous proteins produced as a C-terminal fusion to the BSMV γb via the FMDV 2A peptide bridge.

Use of BSMV-VOX system to deliver candidate effectors to a set of lines and investigate for recognition symptoms

BSMV-VOX constructs and assays with selected candidate effectors were processed by our collaborator Dr Olaya Ruiz at Rothamsted Research. In addition, two BSMV-VOX constructs delivering a version of the RcCM candidate effector with or without signal peptide; and 2 different BSMV-HIGS constructs targeting *R. commune* B-tubulin were engineered by myself.

*Summary of *R. commune* candidate effectors screened.

Fours candidate effectors (rsu3_00144_g, rsu3_07985_g, rsu3_04426_g and rsu3_05502_g) expressed using BSMV-VOX were tested in a selected list of barley lines and were scored (Table III-11). Barley lines tested were chosen for their compatibility with BSMV.

Table III-11: Barley line tested for recognition of 4 candidate effectors expressed using BSMV-VOX. rsu3_00144_g, rsu3_07985_g, rsu3_04426_g and rsu3_05502_g candidate effectors were tested. Symptoms annotation indicates 1 for mosaic, 2 for more severe mosaic, 3 for necrosis of the tip and weak necrosis, 4 for necrosis and 5 for strong necrosis (in red).

	Class of symptoms			
Lines tested	**rsu3_00144_g**	**rsu3_07985_g**	**rsu3_04426_g**	**rsu3_05502_g**
Abyssinian (6 row)	2		2	2
Astrix	4	1	4	4
Athene	4	1	4	2
Atlas	4	1	2	4
Atlas 46	5	1	4	5
Black Hulless	5	4		4
Cadenza wheat	4	1	2	3
CI 11549	4	4	4	2
Flagon	4	1	2	2
Igri	1	4	1	
JLB_37-002	4		4	
JLB_37-012	3		5	3
Pirate	4	4	1	2
Retriever	1	1	4	
SLB_03-026	1	1	2	2
SLB_03-029	1	1	4	
SLB_03-054	3		4	4
SLB_05-030	4			

SLB_05-053	4	1	4	
SLB_09-049	4	1	4	
SLB_10-007	4	1		2
SLB_10-009	4	1	4	
SLB_12-002	4	1		
SLB_19-009	4		4	1
SLB_19-011	4	1	1	
SLB_19-034	3		3	4
SLB_19-094	4		4	2
SLB_22-004	5		4	2
SLB_22-012	4	1	4	
SLB_22-013	4	1	2	3
SLB_22-014	3		4	2
SLB_22-065	2	1	4	2
SLB_22-066	4	1	4	2
SLB_30-010	3			2
SLB_30-014	4	0	4	
SLB_30-031				4
SLB_30-048	4	1		
SLB_32-014	4	1		
SLB_32-020	2			
SLB_34-007	1			
SLB_34-018	4	1	4	3
SLB_34-030	4	1	4	
SLB_34-063	5		4	4
SLB_34-074			3	4
SLB_34-076	4	4	4	5
SLB_40-038	4	1	4	
SLB_40-089	4	1	4	3
SLB_42-003	1	1		0
SLB_42-008	4	1	4	
SLB_49-036	4	1	2	2
SLB_49-048	2	1		4
SLB_58-012	4	1	4	
SLB_58-019				
SLB_58-021	4	1	4	
SLB_66-023	4	0		
SLB_66-024			4	3
SLB_66-058	4	1	4	3
SLB_67-007	4	1		
SLB_67-008	4	1		3
SLB_67-015	4	0	4	
Suzuka	4	1	4	4
Westminster	4	0	4	

*Testing of barley germplasm for recognition of rsu3_00144_g expressed using BSMV-VOX

BSMV-VOX construct expressing rsu3_00144_g processed by Dr Olaya Ruiz will be presented as an example. A total of 57 barley lines previously shown to

be compatible with BSMV-WT were tested with BSMV-VOX-rsu3_00144_g. During the procedure, no BSMV-WT inoculations were carried out as a control on the same test lines, which prevents any comparison with the tested construct. However Atlas 46 plants were inoculated with BSMV-VOX-NIP1, the well characterised interaction used as a control which shows necrosis due to the recognition of NIP1 by the plant expressing the cognate resistance gene *Rrs1*. Scores are summarised in Table III-11 together with results of screening with 3 other candidate effectors. Some symptoms are illustrated in Figure III-18. Three lines, Black Hulless, a line super susceptible to BSMV used as an infection control, Atlas 46 and the potentially interesting SLB-22-004 line showed a category 5 strong necrosis. Unexpectedly, most of the lines presented category 4 necrosis. However, the lack of BSMV-WT infection control on the same line did not allow us to conclude whether the necrosis was due to the virus itself or the presence of our candidate effector in the plant. Moreover, because the delivered effector was untagged, the presence of the protein could not be proven and tests for construct stability *in planta* were not carried out to be sure that the virus was still there.

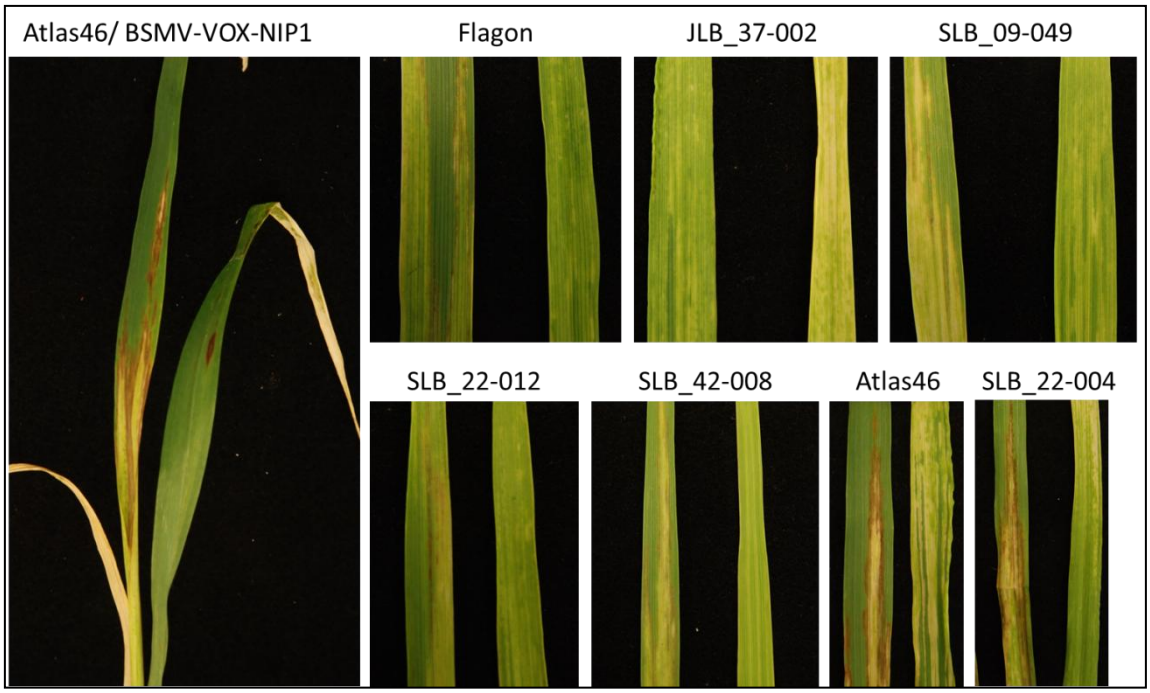

Figure III-18: Pictures of the symptoms induced by the BSMV delivering candidate effectors. BSMV was used to deliver rsu3_00144_g in a set of lines compared to the symptoms observed during the interaction Atlas 46/NIP1. For each picture, the leaf on the left is the third leaf and the leaf on the right is the fourth leaf. Pictures were provided by Dr Olaya Ruiz.

*Stability of BSMV-VOX constructs

The high variability of the BSMV-VOX assay carried out at Rothamsted Research, together with the lack of routine use of BSMV comparative control and expression stability test made me check the stability of BSMV-VOX constructs by RNA extraction from infected plants and PCR amplification from cDNA using construct specific primers. The presence of effectors could not be verified by Western blotting since proteins were untagged and no antibodies specific to the effector were available. The size of the PCR amplicon from infected leaves was compared to the expected size of the amplicon of pure plasmid constructs created for the delivery of the candidate effector. A general reduction in size of constructs in infected plants was observed over time. At 7 DPI, the *rsu3_07612_g* full-length construct was still detected, but shorter bands were observed, while the *rsu3_02410_g* full-length construct was almost undetectable and a strong shorter band was observed (Figure III-19.a). At 10 DPI, *RcCM* and *RC-spCM* full-length constructs were undetectable and shorter bands up to a band of the size of the BSMV-WT control were detected for *RC-spCM* indicating construct modification up to a total deletion of the candidate sequence (Figure III-19.a). At 17 DPI, a late time point, *rsu3_03870_g* appeared to be totally missing indicating a lack of infection, *RcCM* full-length construct was missing but the lower band of the size of BSMV-WT indicated a total deletion of the effector (Figure III-19.b). However, the full-length *NIP1* construct seemed to be a more stable construct showing a mixture of full-length construct remaining together with truncated versions of up to the length of BSMV-WT (Figure III-19.b). Stability seems to be dependent on the size of the construct - since *rsu3_07612_g* appeared to be smaller but more stable than *rsu3_02410_g* - and on the candidate sequence.

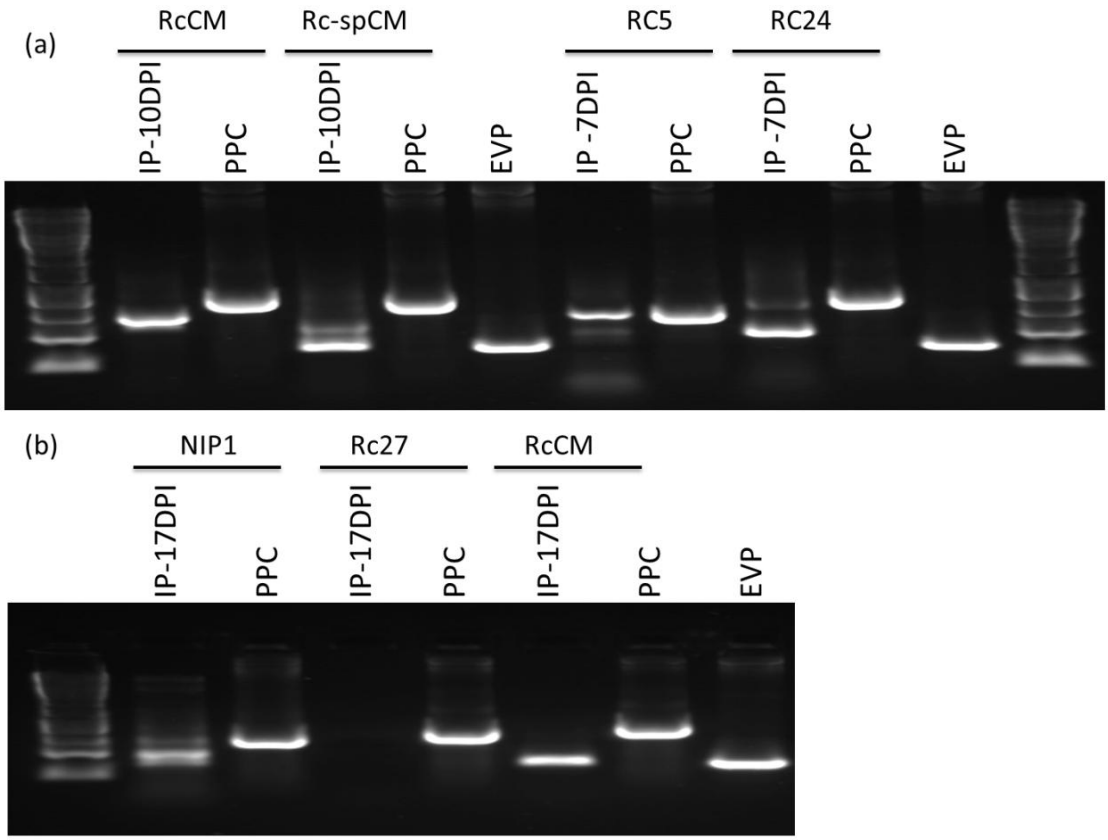

Figure III-19: Stability check of BSMV construct by PCR. PCR amplicons of different BSMV-VOX constructs from infected plants at various days post inoculation (DPI). IP is infected plant, PPC is pure plasmid construct, EVP is empty vector plasmid.

Use of BSMV as a tool to characterise *R. commune* interaction with barley.

BSMV-VOX and BSMV-HIGS could be used to characterise candidate pathogenicity genes and potentially suppress fungal infection. BSMV-VOX of candidate effectors followed by *R. commune* inoculation could indicate whether the overexpression of the effector is helping the fungus to infect or otherwise prevents the infection due to resistance activated following the recognition of the fungal effector. BSMV-HIGS targeting candidate effectors could indicate the importance of the effector for pathogenicity or recognition. However, we need to prove that *R. commune* and BSMV are compatible and that *R. commune* is able to infect BSMV-infected plants. 10 DPI BSMV-infected plants were inoculated with 10^7 conidia of *R. commune* and the fungal infection was visually and microscopically observed until the virus totally destroyed the plants. Due to *R. commune* having a long asymptomatic phase, no clear symptoms could be observed before the plants collapsed and no difference could be observed between the infection of healthy plants and BSMV-infected plants. Necrosis observed 11 DPI with *R commune* of BSMV-infected plants on the middle leaf

are too far from the pale patch indicating the drop inoculation point and must be due to the virus (Figure III-20).

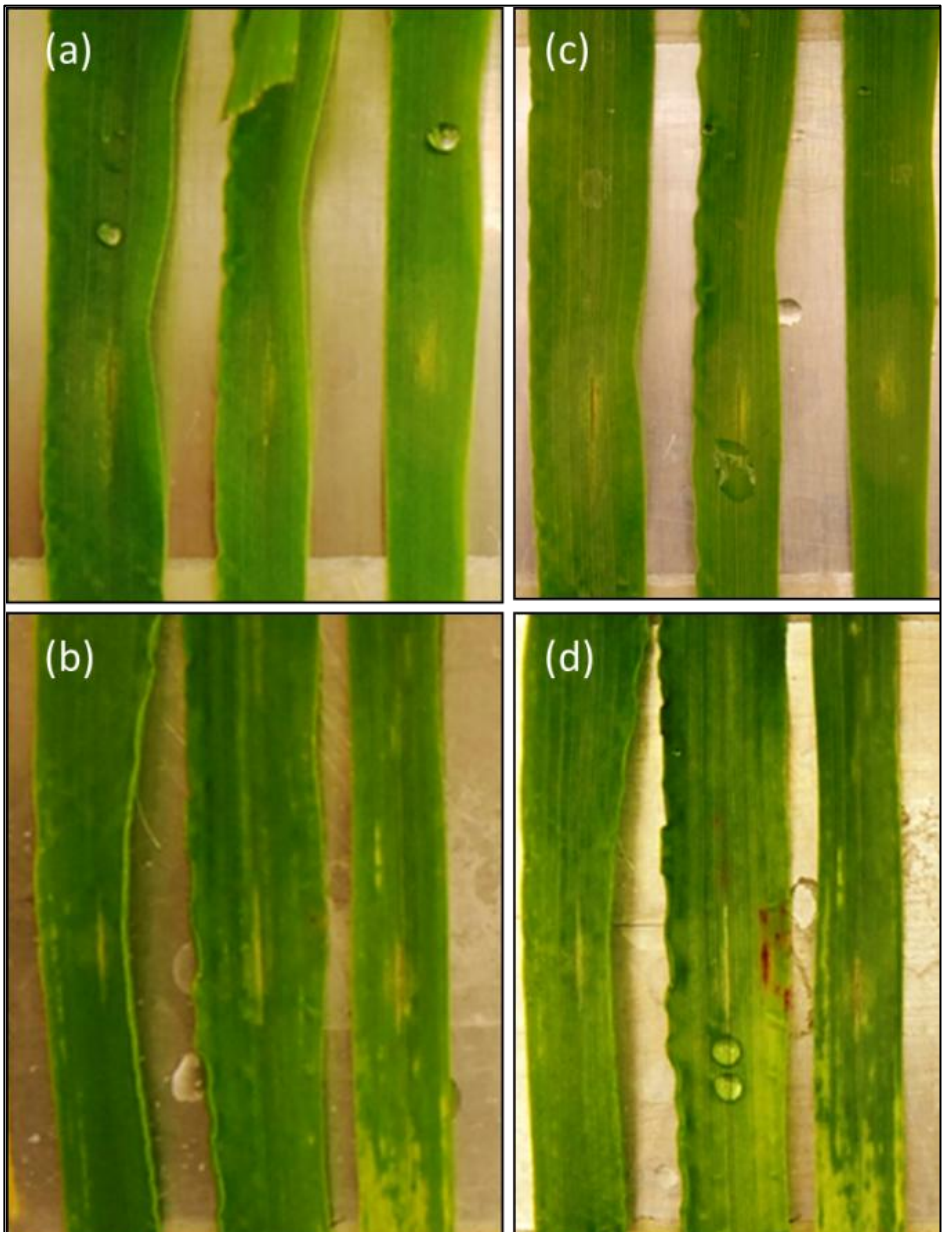

Figure III-20: Pictures of *R commune* infection of healthy barley plants compared to BSMV-infected plants. (a) 5 DPI with *R. commune* of healthy plants, (b) 5 DPI with *R commune* of BSMV-infected plants, (c) 11 DPI with *R. commune* of healthy plants, (d) 11 DPI with *R commune* of BSMV-infected plants.

Microscopy imaging of trypan blue stained infected leaf sections allowed the observation of *R. commune* colonisation and penetration point on the surface of BSMV infected and healthy barley leaves indicating that *R. commune* infection was compatible with BSMV (Figure III-20).

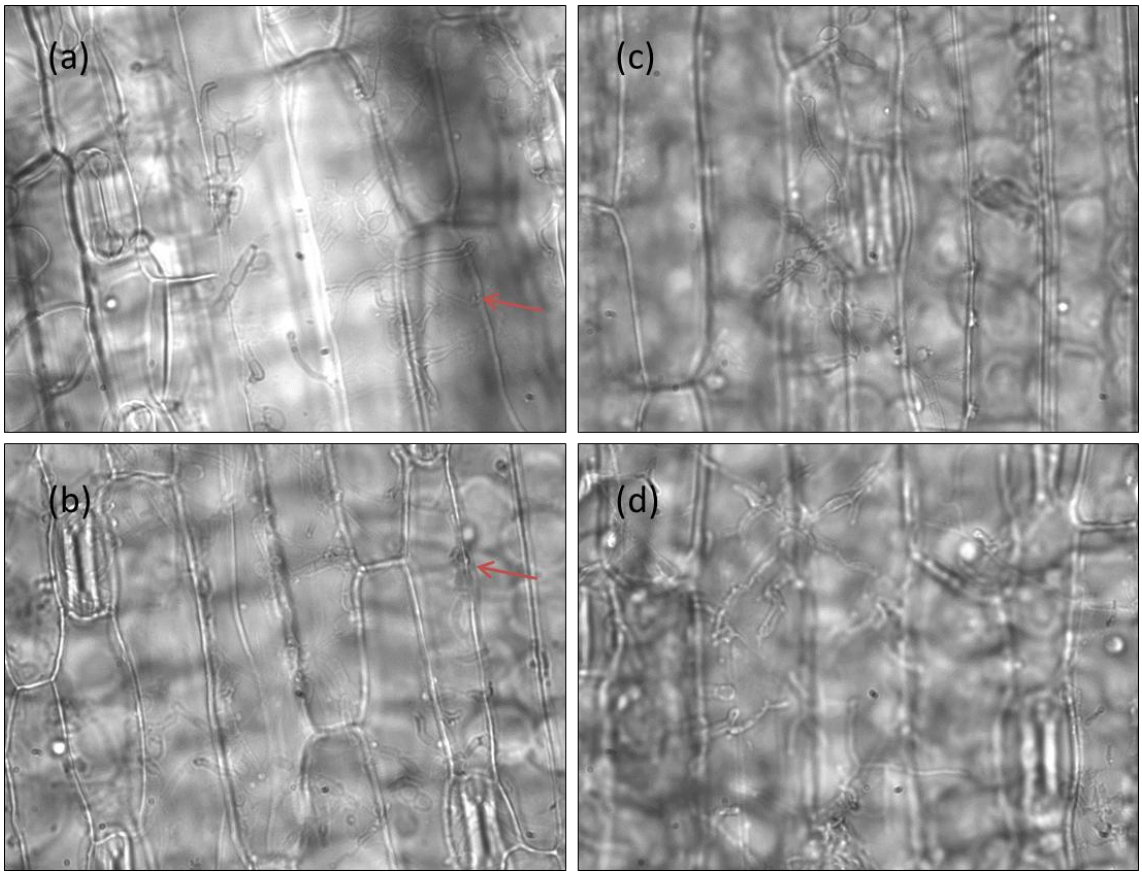

Figure III-21: Black and white light microscopy pictures of barley leaf sections of healthy plants and BSMV-infected plants. BSMV-infected plants infected with *R. commune* were stained with trypan blue. (a) 5 DPI with *R. commune* of healthy plant, (b) 5 DPI with *R commune* of BSMV infected plant, (c) 11 DPI with *R. commune* of healthy plant, (d) 11 DPI with R commune of BSMV infected plant. Penetration points are indicated with red arrows.

As *R. commune* was able to infect BSMV infected barley plants, 2 BSMV-HIGS constructs targeting *R. commune* β-tubulin were generated. SIFI program was use to select cDNA fragment predicted to generate good numbers of effective siRNAs (138 and 124 hits respectively) which do not have any hits in the barley transcriptome. Unfortunately, due to lack of time and facilities, this was not taken any further at the JHI.

III.3.8. pEAQ-HT vector over-expression of *R. commune* candidate effectors in *N. benthamiana*

The BSMV-VOX delivery system in barley presented some limitations in terms of stability relating to the size of the insert. Because of this, this technique seems poorly adapted for functional study of effectors by pulling out effectors from the plant as effectors are untagged. As an alternative, a different system was chosen: transiently expressing tagged candidate effectors in *N.*

benthamiana through the use of the delivery plasmid pEAQ-HT (Sainsbury et al. 2009).

Cloning and agroinfiltration

Four candidate effectors were successfully cloned into the pEAQ-HT vector (Figure III-22) and expressed in *N. benthamiana* to produce and purify the protein. Annotated gene names were shortened to the unique number present in the initial list name of each effector (rsu3_00144_g=144, rsu3_07985_g=7985, rsu3_06458_g=6458 and rsu3_03882_g=3882)

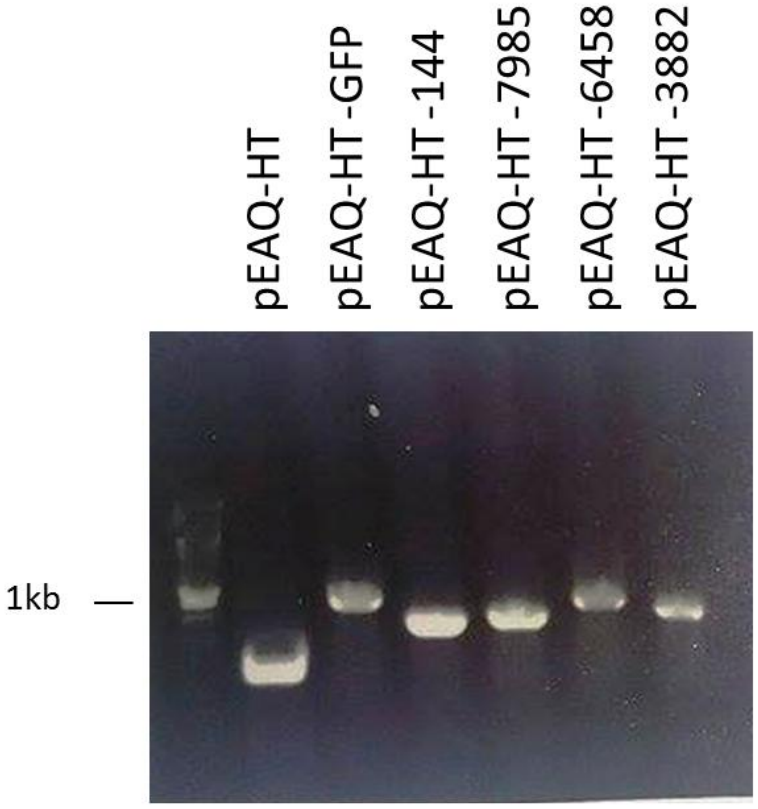

Figure III-22: Agarose gel of colony PCR of pEAQ-HT constructs in *A. tumefaciens*.

5 days post agroinfiltration with pEAQ-HT, the agroexpression of pEAQ-HT-144 induced cell death (Figure III-23.a). UV light pictures allowed to see that agroculture prepared were successfully working as GFP could be visualised on the leaf agroexpressing of pEAQ-HT-GFP. In addition under UV light, pEAQ-HT-144 cell death necrotic infiltration spot showed a light green fluorescence compared to the pEAQ-HT empty control (Figure III-23.b). This fluorescence may be due to the accumulation of fluorescent phenylpropanoid derivatives (phytoalexins) usually associated with HR cell death (Dixon and Paiva 1995; Zhang et al. 2004).

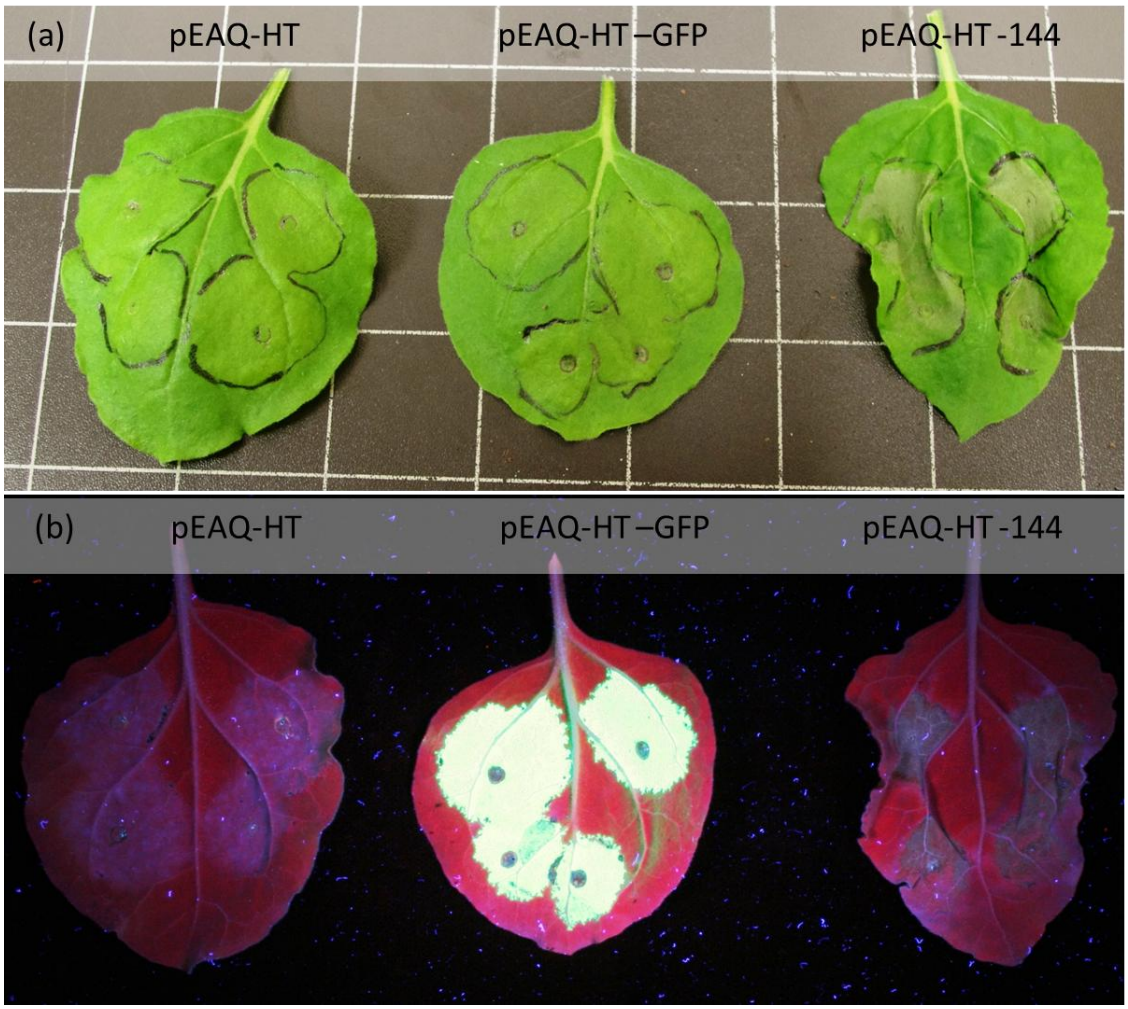

Figure III-23: Pictures of *N. benthamiana* 5 days post agroinfiltration with pEAQ-HT constructs. (a) Light picture of superior face of leaves. (b) UV light picture of inferior face of leaves.

Western blot for candidate effector proteins detection

5 days post agroinfiltration leaf samples were collected for protein presence check by Western blotting. The Western blot successfully detected the P24 his tagged control protein but did not allow the detection of the protein effectors (Figure III-24). However, cell death phenotype with the pEAQ-HT-rsu3_00144_g construct showed that the protein produced has an effect on *N. benthamiana* suggesting that the protein was produced. This phenotype has been observed each of the 4 times that *N. benthamiana* leaves have been infiltrated with pEAQ-HT-rsu3_00144_g.

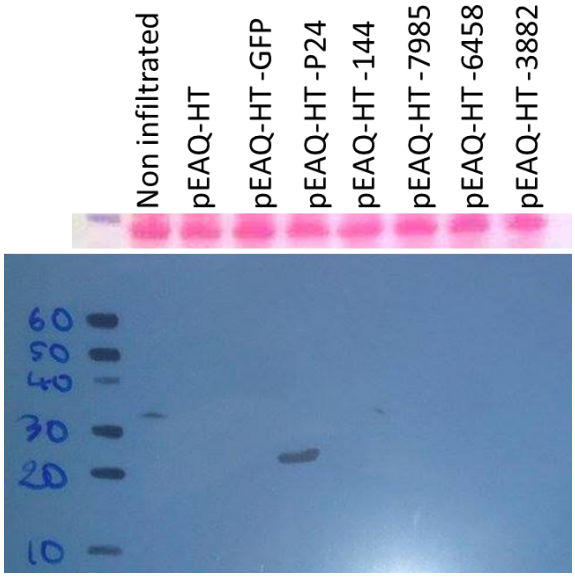

Figure III-24: Western blot for the detection of pEAQ-HT-effector constructs tagged with HIS tag.

PCR detection of candidate effector transcripts

Five days post agroinfiltration, leaf samples were collected for RNA extraction and cDNA synthesis to check transcript presence using qPCR primers for each candidate effectors and make sure that effectors were correctly transiently expressed. For all samples, a specific band was observed for leaf samples of each pEAQ-HT construct. Some nonspecific bands were observed with negative control with water, non-infiltrated plant and pEAQ-HT empty vector infiltration but the size of nonspecific bands was always different to that of pEAQ-HT-construct attesting of the specificity and presence of the transcript (Figure III-25).

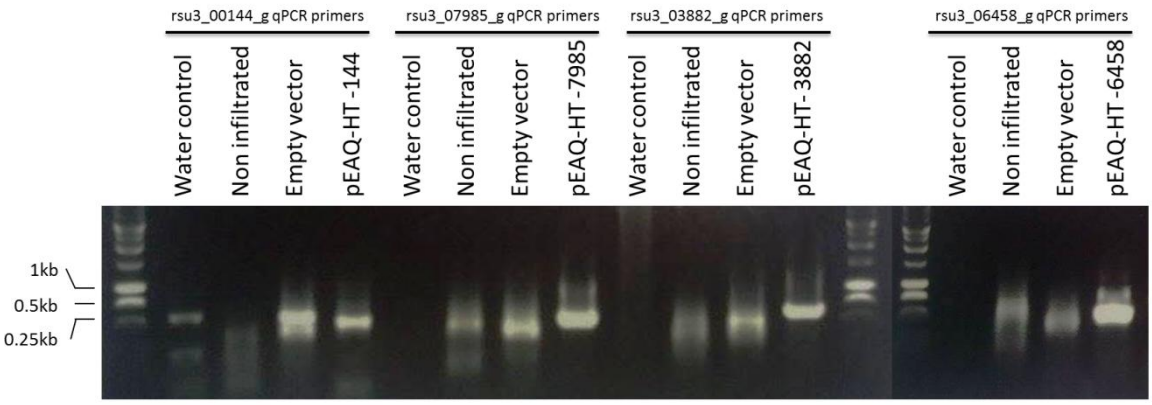

Figure III-25: Agarose gel to check the presence of candidate effector transcripts in *N. benthamiana* agroexpressing leaf sample. in of PCR amplicons using gene-specific qPCRprimers of each candidate effector to detect the transcript in plants agroinfiltrated with pEAQ-HT-constructs.

III.4. Discussion

Recent genome sequencing of 9 *R. commune* strains allowed the annotation and identification of a list of genes with homologues in other fungal species and presenting the classical feature of an apoplastic effector such as short cysteine rich protein with signal peptide (Sperschneider et al. 2015). The virulence testing of sequenced *R. commune* strains on different resistant barley cultivars did not lead to the identification of association between virulence on any of the tested barley lines and SNPs identified in sequences of selected candidate effectors. Candidate genes were selected from the list of candidate effectors based on their limited amino acid sequence variation in sequenced *R. commune* strains, transcript presence in RNAseq data for germinated conidia and/or epidermal strips of barley leaves 3 DPI with *R. commune*, relative expression profiling and quantification, putative function and the presence of homologues in other plant pathogen species. qPCR profiling allowed to sort candidates studied and to prioritise the most promising candidate effectors for further analysis based on their profile and quantification. Microscopic pictures, disease lesions and *RcCDI1* expression profiling confirmed that the infection time course worked and that *R. commune* successfully infected barley plants. However, the use of pooled samples and the lack of biological reps is preventing any statistical analysis which could have confirmed the expression profiling pattern observed and it would have been better to confirm the expression profiling pattern of candidates tested in different biological reps. 23 genes showed an upregulation during infection and 13 of them had a transcript abundance equal or higher than actin -one of the most abundant transcripts - indicating that these transcripts are highly abundant and upregulated during the infection. Candidate genes were sorted in groups according to their pattern of expression but it would have been a good idea to also confirm the allocation of expression patterns in the different groups by hierarchical clustering, which in biology is typically used for classification of gene expression data and which had already been used by Saunders et al (2012) and Guyon et al (2014) to characterise fungal plant pathogen effectors. Candidate effectors were selected when upregulated *in planta,* suggesting an important role during host infection (Kleemann et al. 2012). No candidate appeared to be much more interesting than others, leading to a selection of several candidates mainly from group 1 of

relative expression pattern which showed a fast and strong upregulation at 1 DPI specific to the biotrophic phase and because genes from group 1 would be better target candidates for resistance allowing detection of the fungus at the very early time of the infection providing more time to fight effectively against the pathogen. Due to *R. commune*'s long asymptomatic phase (Avrova and Knogge 2012), group 2 and 3 are considered as biotrophic phase effectors while later upregulated effectors belonging to the group 4 could be involved in the transition to the necrotrophic phase or the necrotrophic phase itself. Genes from group 2, 3 and 4 were selected too as any wave of effector expressed during the infection could have an important role for pathogenicity particularly if genes were also present in other plant pathogens such as cereal pathogens. Discarding gene candidates is risky; we cannot be sure about the potential of any candidate. However working with too many candidates is ambitious but limits the probability of obtaining clear results.

Rsu3_00144_g was selected for its 60% similarity over 98% query coverage to protease propeptide inhibitor from *Glarea lozoyensis* and similarity to proteins from many plant pathogens including cereal pathogens such as *S. sclerotiorum, S. borealis, Z. tritici* for example. Proteinase inhibitors have already been identified to be avirulence genes like the kazal-like extracellular serine protease inhibitor EPI1 from *P. infestans* interacting with the tomato resistance gene P69B related to pathogenicity (Tian et al. 2004). Rsu3_06458_g was selected due to its Hce2 domain (pfam14856) corresponding to the mature part of the Ecp2 effector protein from the tomato pathogen *Cladopsorium fulvum* (Wulff et al. 2009). Rsu3_07985_g, rsu3_05502_g, rsu3_07190_g, rsu3_03882_g and rsu3_11823_g were selected for the presence of gene homologues in many plant pathogens including cereal pathogens. Rsu3_03792_g was selected due to its CFEM domain (pfam05730) coding for fungal specific cysteine rich domain found in some proteins with proposed roles in fungal pathogenesis (Kulkarni et al. 2003) and the presence of gene homologues in many plant pathogens including cereal pathogens. Rsu3_01835_g was selected thanks to its 40% similarity over 94% query cover with Cytochrome P450 in *M. phaseolina* involved in several essential biological process including pathogenicity related (Siewers et al. 2005; Chen et al. 2014). RcCM (secreted chorismate mutase) and RcISC (isochorismatase hydrolase) were selected for their putative

function related to SA pathway, an effective defence against biotrophic plant pathogens (Glazebrook 2005). Moreover, gene homologues from *U. maydis* and *P. sojae* and *V. dahliae* respectively were identified to be important effectors for pathogenicity (Djamei et al. 2011; Liu et al. 2014).

The KO mutant generation strategy is a useful technique to identify whether or not candidate effectors are important for pathogenicity and/or recognised by a specific barley cultivar. The 3 first characterised *R. commune* effectors NIP1, NIP2 and NIP3 were successfully deleted by homologous recombination (Kirsten et al. 2012). Unfortunately, the efficiency of gene replacement by homologous recombination in *R. commune* is very low, with only 1-5 % of the transformants likely to be knock-outs, and it was not successful in our group. Using the split maker strategy (Fu et al. 2006) to reduce the number of false positives did not increase the rate of gene replacement but allowed us to visualise that homologous recombination was happening in *R. commune* thanks to the identification of recombined split cassette in screened mutants. This failure could be due to the fact that we were screening slightly less transformants per construct and using a different method of transformation and strains than Kirsten et al. (2012) who screening over 100 transformants generated by protoplast transformation of *R. commune* strain UK7. Different strains could have different rates of homologous recombination success and it could have been a good idea to try to generate KO mutant in the UK7 strain as a control even if it would have increased the number of cassette generation, transformation and genotyping procedures. Moreover, gene replacement could be dependent on the location of the gene in the genome and the function of the gene, some genes could be more accessible and/or important than others limiting the gene replacement efficiency and the survival of the fungus. Our inability to successfully generate *R. commune* knock out mutants could be due to a mixture of all these reasons. To facilitate the generation of effector replaced mutant strains, we tried to generate a lab strain with KU70 deletion. KU70 protein functions in nonhomologous end-joining of double-stranded DNA breaks, strains with KU70 deletion would potentially be more efficient for gene replacement, as was described in *N. crassa*, *Aspergillus sojae* and *Aspergillus. oryzae* (Ninomiya et al. 2004; Takahashi et al. 2006) . Unfortunately, the gene replacement strain of KU70 could not be generated either. Different methods

can be used as alternative to gene replacements such as CRISPR/Cas9 which have been used to successfully delete effector genes in *U. maydis* and *M. oryzae* (Selin et al. 2016); or gene silencing which was used to knock down Avr3a from *P. infestans* (Bos et al. 2010). The creation of a silencing cassette targeting KU70 was also attempted by yeast recombinational cloning but the identical sense and antisense DNA fragments needed were causing issues for the creation of the cassette and the sequencing. In addition, the chance of identifying an effector with a strong effect on pathogenicity using this technique is low due to the high redundancy of gene sequences or function (Tan et al. 2015). As an example, Saitoh et al. (2012) generated 78 KO mutants of putative secreted proteins expressed during the early stages of infection of *M. oryzae* to find a single mutant showing a severe reduction in blast symptoms. In conclusion, gene replacement appears to be a useful technique but it is limited by its poor efficiency to generate KO mutants followed by the risk to have generated a mutant with no effect on pathogenicity due to gene function redundancy.

Viruses have always been involved in transient expression studies ever since the overexpression promoter P35S from Cauliflower mosaic virus (CaMV) became widely used (Ow et al. 1987). Transient expression using plant virus vectors known as VOX is useful for the production of recombinant proteins in plants. PVX has been widely used for VOX in dicotyledonous plants since 1990s (Chapman et al. (1992) and more recently the cowpea mosaic virus based vector pEAQ-HT has been developed for expression of recombinant proteins in *N. benthamiana* in much higher quantities (Sainsbury et al. 2009). Screening of different barley genotypes for novel sources of resistance using VOX of pathogen effectors has great potential in crop breeding. For instance, this technique confirmed the recognition of NIP1, by the product of the cognate resistance gene *Rrs1*, present in the barley cultivar Atlas 46 (Lee et al. 2012). Unfortunately the BSMV-VOX system is capable of expressing only relatively small (up to ~ 160 amino acid residues) heterologous proteins (Bruun-Rasmussen et al. 2007; Lee et al. 2012). Several barley genotypes were screened for cell death as evidence of the recognition of the effector protein by the product of a potential plant disease resistance gene present in the tested genotype. However, the BSMV expression system is technically challenging.

Firstly, BSMV-VOX may not be enough to trigger recognition, the plant may need extra plant defence activation to establish the recognition and the level of effector expression provided through BSMV-VOX may not in some cases be sufficient to trigger cell death following the recognition event. Another complicating factor is that BSMV itself induces leaf chlorosis and even necrosis of various degree of severity in some barley genotypes, making the phenotyping complicated in particular when no BSMV-WT controls are processed at the same time to compare the symptoms. Necrosis usually appears at >10-14 DPI with VOX constructs. Therefore, the phenotyping is best to be done during a short window post inoculation between 5-14 DPI. Another complicating factor in BSMV-VOX is relatively poor insert stability, especially for the larger inserts (Bruun-Rasmussen et al. 2007; Lee et al. 2012) The stability of some BSMV-VOX constructs throughout the barley infection process was checked to be sure that symptoms observed were caused by heterologous protein expression rather than induced by the virus itself. PCR-based analyses showed that in certain cases, BSMV was able to lose or truncate some of the heterologous inserts. Larger inserts were truncated or deleted earlier than smaller inserts. Also, a positive correlation was observed between the appearance of necrosis and the speed of insert loss/truncation, the less stable constructs were able to induce more rapid development of disease symptoms than the stable ones. In addition, several of the 11 *R. commune* effectors screened in a selection of barley lines induced necrosis in the same lines (data not show because this detail was not related to my candidates). Different putative effectors are very unlikely to be recognised by the same barley lines suggesting that it is probably the BSMV effect which have been reported by the phenotyping rather than the effect of *R. commune* effector. In the future, it will be essential to do the appropriate controls and PCR verification to avoid a misinterpretation of the observed symptoms and maybe to find an alternative system of protein delivery in barley that is less aggressive and more stable than BSMV.

BSMV is also commonly used as a gene silencing tool (Lee et al. 2012). VIGS is used to knock-down expression of plant genes, whereas HIGS is used to reduce expression of genes in the plant pathogen such as described by Yin et al. (2011) silencing wheat stripe rust fungus genes through the plant. One of the pre-requisites required when using these functional genomics tools is the

demonstrated compatibility between BSMV and the second pathogen under investigation. A sequential inoculation of barley with BSMV and a mixture of *R. commune* strains followed by microscopic observation of trypan blue-stained leaves at different time points post fungal inoculation showed that *R. commune* was able to colonise BSMV-infected leaves. Unfortunately, on my return to JHI, due to the impossibility to find a compatible environment, I could not test BSMV-HIGS constructs targeting GFP and *R. commune* β-tubulin during barley infection by *R. commune* to see if BSMV-HIGS can be achieved in this fungal pathogen. Using confocal microscopy and the transgenic GFP-expressing strain to check penetration of the fungus in such conditions would have been ideal. In the absence of an efficient gene knock-out technology for *R. commune* in our lab, BSMV-HIGS would have been a challenging but interesting alternative tool to try for silencing *R. commune* effectors during infection, thereby limiting the variability inherent in comparing two different infection strains (one WT and one silenced or KO mutant). Moreover, HIGS might prove to be an alternative way of preventing disease spread in the field. This strategy has already been successfully used for silencing CYP51 from *Fusarium* species to provide strong resistance to the plant (Koch et al. 2013). One limitation of combining BSMV and *R. commune* is that due to the long asymptomatic phase of *R. commune* and the instability of BSMV constructs, microscopy-monitored phenotyping would be essential, because the time taken by *R. commune* to produce visible symptoms could be longer than the time taken by the virus to remove its insert and destroy the plant. One challenging fact about attempting this technique is that because *R. commune* is an apoplastic fungus growing in-between barley cells (Avrova and Knogge 2012), we do not know if dsRNA produced in the plant cell would be taken up by *R. commune* to come into contact with fungal RNA.

I decided to change strategy and work with the most promising candidates based on their putative function and potential different allele sequences and use the pEAQ-HT vector system of expression in *N. benthamiana,* a virus based overexpressing vector known for its high efficiency (Sainsbury et al. 2009) to produce candidate effector proteins of rsu3_00144_g (putative protease inhibitor), rsu3_07985_g (putative long chronological lifespan protein 2), rsu3_06458_g (contains pathogen effector; putative necrosis-inducing factor

domain) and rsu3_03882_g (2 clear allelic versions of the same gene), and purify them to identify plant targets. Unfortunately, although sequencing did not reveal any issues with the cloning, the 4 candidates tested could not be detected on the Western blot indicating that the protein may be degraded or insoluble or that HIS tag is being cleaved from the protein, which would make detection and purification impossible. However, specific transcripts could be detected by PCR on leaf sample cDNA indicating that the candidate insert is present and that the lack of protein detection is not due to the use of empty vector colonies. The PCR for rsu3_00144_g shows a band in negative control but sizes are slightly different; it would have been good to repeat that experiment. Moreover pEAQ-HT-rsu3_00144_g construct appeared to be inducing cell death at 5 DPI indicating that rsu3_00144_g may have an effect on *N. benthamiana* plants. This cell death could be induced for many reasons. Firstly, pEAQ-HT vectors are known to be producing a high quantity of protein which could be toxic for the plant due to sheer quantity and could therefore induce damage of the leaf tissue (Sainsbury et al. 2009). The second hypothesis is that the function of the protein can be inducing plant cell death. Rsu3_00144_g codes for a putative protease inhibitor, a function described to be involved in PCD (Program Cell Death) by (Solomon et al. (1999)). However, the function of rsu3_00144_g has not been proven yet. The last hypothesis is that rsu3_00144_g is being recognised by the plant inducing a hypersensitive response causing the cell death to prevent the spread of a pathogen as firstly describe by Morel and Dangl (1997).

III.5. Conclusion

Due to the lack of success in generation of KO mutants and poor reliability regarding the BSMV-VOX method, we have no evidence of the importance of candidate effector genes for pathogenicity or of any potential recognition of any of them in barley lines. However, some candidates have an interesting putative function such as a secreted chorismate mutase (RcCM), and an isochorismatase hydrolase (RcISC) which are going to be further studied as well as the rsu3_00144_g putative protease inhibitor which induces cell death on *N. benthamiana*.

IV. Chapter 4: Putative protease inhibitor candidate effector characterisation

IV.1. Introduction

Due to the impossibility of confirming the importance for pathogenicity of candidate effectors by generating KO mutants, the candidate 144 was chosen for its interesting putative function of protease inhibitor and relative expression profile during infection showing upregulation at an early time point during the infection. Indeed, protease inhibitors secreted by the pathogen are a perfect example of PTI or ETI suppression by the pathogen, allowing avoidance of plant defences by the secretion of a protein which inhibits plant protease action.

Moreover, pathogen protease inhibitors have already been shown to play an important role in suppressing the plant immune responses. Firstly, an extracellular serine protease inhibitor (Kazal-like A) named EPI1 from *P. infestans* was shown to target P69B subtilase in tomato, a pathogenesis-related protease (Tian et al. 2004). Another extracellular protease inhibitor from *P. infestans*, EPI10, was shown to be up-regulated during infection of tomato and specifically inhibiting subtilisin A protease and like EPI1, it inhibited P69B subtilase of tomato (Tian et al. 2005). The *P. infestans* effector AVRblb2 was also shown to target papain-like cysteine protease C14 (PLCP) and specifically prevent its secretion into the apoplast at the haustorial interface, significantly enhancing susceptibility of host plants (Bozkurt et al. 2011). Tomato PLCPs were previously shown to play a role in defence response thanks to the selective inhibition of 2 PLCPs: *PIP1* and *RCR3* by the secretion of protease inhibitor *AVR2* by *C.* fulvum (Shabab et al. 2008). More recently, a screen of 43 small, secreted, non-annotated proteins from *P. syringae* potentially expressed during apoplastic colonization of tomato allowed the identification of *Cip1* (*C14*-inhibiting protein-1) inhibiting *C14* and *Pip1* tomato protease (Shindo et al. 2016). Moreover, compatible infection of the monocot maize by *U. maydis* was shown to require Pit2, an inhibitor of apoplastic cysteine proteases disrupting salicylic-acid-associated plant defences (Mueller et al. 2013).

All these examples show that protease inhibitors secreted by plant pathogens play an important role in plant infection.

Our aim was to determine if our candidate 144, with homology to a protease inhibitor, plays a role in plant pathogenicity by confirming its function, studying its plant target and its effect on plant immunity processes.

IV.2. Materials and methods

IV.2.1. *Pichia. pastoris* heterologous protein production system

Construct generation strategy

The candidate gene sequence was amplified by using specific forward primers with AA 5' extension and reverse primers with BB 5' extension corresponding to the recombination site of plasmid p75. The vector was created from pGAPZ by Dr Adokiye Berepiki adding V5 epitope, URA3 gene and 2 micron origin to allow it to be used for YRC, TAG sequences corresponding to mCherry sequence or V5 epitope sequence allowing tagging of our candidate gene and Bleocin resistance gene (BLE) to allow transformation and selection in bacteria using zeocin. A factor is a secretion signal used for extracellular expression in yeast and will allow the secretion of the protein under promotor pGAP and terminator AOX1 control. To reduce background by decreasing the chances of plasmid re-circularisation during YRC, the vector was linearized by PCR generating 2 splits of the vector with corresponding recombination sites (Figure IV-1).

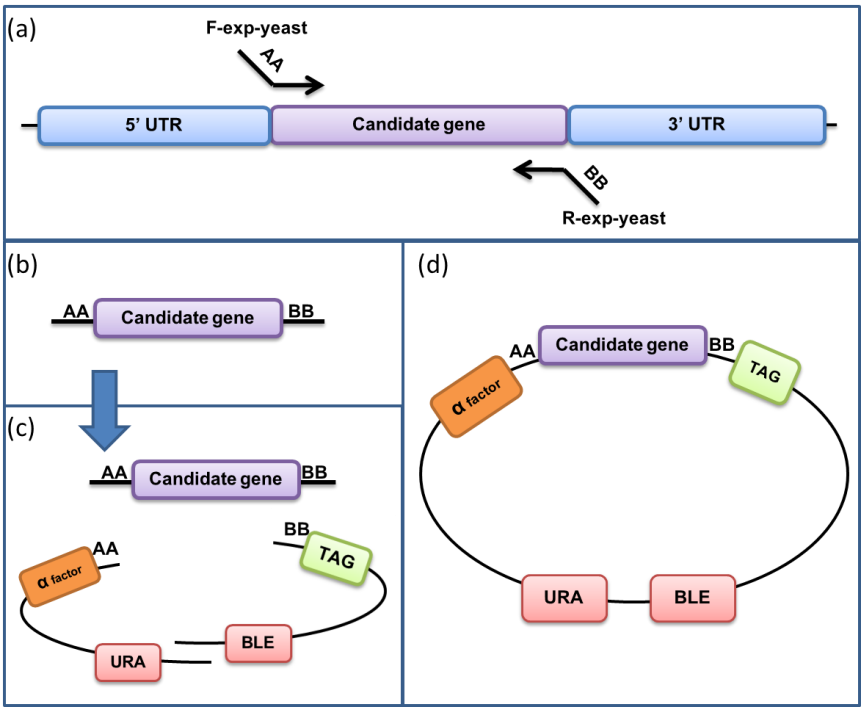

Figure IV-1: Construct generation strategy. (a) Candidate gene is amplified by PCR using primers illustrated by black arrows carrying appropriate extensions (AA and BB) (b) PCR fragment is combined with the split plasmid fragments carrying AA and BB extensions, α factor secretion signal, URA gene for yeast selection on media lacking Uracil amino acid, TAG corresponding to mCherry sequence or V5 sequence and BLE for zeocin resistance gene for bacterial selection.

Yeast transformation and screening of transformants

YRC and screening of transformants was carried out as previously described using appropriated DNA fragments in *S. cerevisiae* strain FY834 with the following modifications. Recombinant plasmids were extracted from yeast using Zymoprep™ Yeast Plasmid Miniprep I kit (Zymoresearch) and transformed into Efficiency® DH5α™ competent *E. coli* (Thermo Fisher Scientific) as described previously. Cells were spread on low salt LB supplemented with 25 µg/mL of zeocine (Melford Laboratories Ltd). Plasmids were purified from *E. coli* using miniprep Qiagen kit and digested with *Pme*I restriction enzyme (NEB). Fragment insertions were cut out from the plasmid and the transformants with fragments of the expected size were checked by sequencing using pGAP-fw-seq and AOX1-TT-rv-seq primers (Table IV-1).

Table IV-1: List of primers used to sequence *P. pastoris* construct

Target gene	Primer name	Primer sequence 5-'3'
***Pichia* cassette**	pGAP-fw-seq	gtccctatttcaatcaattgaa
	AOX1-TT-rv-seq	gcaaatggcattctgacatc

IV.2.2. *P. pastoris* transformation and screening

A successful construct was used to transform *P. pastoris* via electroporation using a protocol from Invitrogen's *Pichia* expression kit manual. Transformants were selected on YPD supplemented with 100 µg/mL of zeocin. *P. pastoris* transformants were screened by colony PCR using as a template 1µL of *P. pastoris* suspension incubated in 20 µL of 20 mM NAOH for 15 minutes at 70°C using multiplex PCR with Pgap-upstream-fw and alpha-factor-rv (10 mM) primers to check the correct insertion into *P. pastoris* genome and 18S-rv-universal 18S-fw-universal (2 mM) primers to be sure that there is good quality DNA for PCR.

IV.2.3. *P. pastoris* heterologous protein production and purification

P. pastoris transformants were grow in YDP or YNB media for 2 to 3 days at 30°C with shaking at 250 rpm. Heterologous protein secreted by *P. pastoris* into the supernatant was collected by centrifugation at 2000 g for 5 min at room temperature. The supernatant can be used for plant infiltration assays and protein expression assays such as Western blot.

Proteins secreted into YNB media were purified and concentrated using vivaspin 20 column with a molecular weight cut off at 10 kDa so anything smaller flows through. Supernatant was transferred to a Vivaspin column to centrifuge at 9000 g for 30 min at 4°C. The flow-through was discarded before 3 washes with 10 mL of HNT buffer (HEPES-KOH 50 mM pH7.4, NaCl 50 mM, tween-20 0.02%) by centrifuging at 9000 g for 20 min at 4°C and discarding the flow-through. Vivaspin columns were centrifuged until the buffer volume in the upper chamber was reduced to 2 mL or less and concentrated protein was recovered from the upper chamber with a pipette.

IV.2.4. Protein quantification

Protein quantification was carried out using Pierce™ BCA Protein Assay Kit (Thermo Fisher Scientific) following manufacturer's protocol and comparing to a BSA standard curve.

IV.2.5. Pull down assay

Co-immunoprecipitation was carried out by collecting 9 discs of 10 mm diameter from 6 hpi of *N. benthamiana* leaves infiltrated with supernatant of *P. pastoris* culture secreting candidate protein 144V5 in YPD or V5 only. Frozen leaf material was ground with a mortar and pestle in liquid nitrogen. 10 mL of GTEN extraction buffer (10% glycerol, 25 mM Tris pH7.5, 1mM EDTA, 150 mM NaCl) and 2% w/v PVPP, 10 mM DTT, 1X protease inhibitor cocktail (Sigma), 0.1% NP40 (Sigma) was added. Samples were centrifuged at high speed to remove debris at 4°C and supernatant was transferred to a new tube. This step was repeated at least once more to remove as much debris as possible. V5 beads were made using Dynabeads® Co-Immunoprecipitation Kit and kindly provided by Dr Adokiye Berepiki. 20 µL of V5 beads were prepared per sample by washing twice in washing buffet (10 mM Tris/Cl pH 7.5; 150 mM NaCl; 0.5 mM EDTA; 1 x Plant Protease Inhibitor). V5 beads were collected using magnetic stand in a 1.5 mL tube and washed 4 times with the washing buffer. Beads were resuspended in 75 µL of sample buffer (NuPAGE® LDS Sample Buffer (4X), 10 mM DTT) and boiled for 5 min at 95°C before separating protein samples from beads with the magnetic stand in a new tube ready for the SDS-PAGE.

IV.2.6. Mass spectrometry

Excised gel sections of 144V5 and V5 sample were processed by Douglas Lamont, Proteomics Facility Manager at the University of Dundee. Samples were analysed by nanoflow liquid chromatography–tandem mass spectrometry (nLC-MS-MS) after trypsin digestion. Proteins IDs were generated by comparison to plant proteome database and 144-V5 protein sequence.

IV.2.7. Gateway cloning

Gateway cloning was carried out as described in previously. Vectors used and generated are listed in Table IV-2.

Table IV-2: List of vectors created and used by gateway cloning. Features of each vector and how they have been created is resumed in resistant been created, feature and size of protein expressed.

Plasmid name	Resistance	Function	Cloned from	Size of the overexpressed protein (kDa)
pDONR201-sp-144-st	kanamycin	Entry vector	144 candidate PCR without signal peptide and stop codon	N/A
pDONR207-sp144	gentamycin	Entry vector	144 candidate PCR without signal peptide and with stop codon	N/A
sec-gfp-pK7GW2-sp-144-st	spectinomycin	C-terminal GFP tagged secreted	pDONR201-sp-144-st	37
pB7FGW2-sp-144-st	spectinomycin	C-terminal GFP tagged	pDONR201-sp-144-st	37
pB7GWR2-sp-144	spectinomycin	N-terminal RFP tagged	pDONR207-sp-144	37
pMdc43-spmRFP-sp-144	kanamycin	N-terminal RFP tagged secreted	pDONR207-sp-144	37
pK7GW2-GFP	spectinomycin	GFP	N/A (empty vector)	27
pK7GW2-RFP	spectinomycin	RFP	N/A (empty vector)	28

IV.2.8. Protease assay using 2,4,6-Trinitrobenzene Sulfonic Acid (TNBSA)

The method was adapted from Thermo Fisher Scientific instruction and Tian et al. (2004) and TNBSA procedure recommendation.

Apoplastic fluid extraction

Apoplastic fluid was extracted from *N. benthamiana* leaves. Leaves were vacuum infiltrated with ice cold reaction buffer (0.1 M sodium bicarbonate, pH 8.5) using a 60 ml syringe. Infiltrated leaves were rolled within muslin clothes before being put into 20 ml syringe. Apoplastic fluid was extracted from rolled infiltrated leaves by gentle centrifugation of the 20 mL syringe in a 50 ml falcon tube for 10 min at 1000 g at 4 °C.

Protease assay

For each sample, 500 µL of reaction buffer or apoplastic fluid was used as pure and diluted protein (450 µg/mL and 250 µg/mL respectively) supplemented with 10 µL of HNT buffer, or 10 µL of 144V5 protein suspension (200 ng) from *P. pastoris* culture supernatant concentrated in HNT or 10 µL of V5 protein suspension from *P. pastoris* empty vector culture supernatant concentrated in HNT or of 2.5 µL of 1000X protease inhibitor cocktail. Samples were incubated for 1h on ice for control and at 25 °C for protease activity. 250 µL of the 0.01% (w/v) solution of TNBSA were added to each sample solution and incubated for 2h at 37°C. 250 µL of 10% Sodium dodecyl sulfate (SDS) and 125 µL of 1 N HCL were added before measuring the absorbance at OD=335 nm. The procedure was repeated using apoplastic fluid that had been concentrated 3X with a freeze dryer and supplemented with 6.5 mg/mL casein substrate.

IV.2.9. 3,3′-Diaminobenzidine (DAB) staining of leaf material

Leaves were immerged in 1 g/L DAB solution for 3h. Leaves were bleached in a solution of 90% ethanol and 5% acetic acid until green discoloration to reveal the brown coloration of DAB.

IV.2.10. PCR

Amplification of DNA fragment for *P. pastoris* cassette generation

Amplification of DNA fragments to be used for transformation construct generation was carried out using Phusion high fidelity polymerase (NEB) following the manufacturer's recipe and thermocycler conditions using primers specifically designed to amplify selected fragments (Table IV-3).

Amplification of DNA fragment for *P. pastoris* transformation screening

Amplification of DNA fragments to screen transformants was carried out using Phire polymerase following the manufacturer's recipe and thermocycler conditions using primers specifically designed to amplify selected fragments (Table IV-3).

Table IV-3: Table of primers used for DNA fragment amplification for *P. pastoris* cassette generation and transformant screening.PCR were prepared using fungal cDNA and plasmid miniprep for p75 splits. F144-exp-yeast black sequence is AA extension and green sequence is specific of the candidate gene. R144-exp-yeast black sequence is BB extension and green sequence is specific of the candidate gene.

Target gene	Primer name	Primer sequence 5'3'
rsu3_00144_g	F144-exp-yeast	GTATCTCTCGAGAAAAGAGAGGCTGAAG CTGTAACCACACCTCAGAAATCAATC
	R144-exp-yeast	AGCTCCGGCACCAGCACCGGCACCAGCT CCGGATCCGCTATTGATCGAG
p75 split 1	alpha-factor-rv	agcttcagcctctctttctcgagagatac
	2-micron-fw-split	gcaacgcgaaagcgctattttac
p75 split 2	BB-fw	ggagctggtgccggtgctg
	2-micron-rv-split	cagtaaacgcgggaagtggagtc
Pichia transformant genotyping	Pgap-upstream-fw	CAGCCTCACATGCGACTATTATCG
Pichia transformant control	18S-fw-universal	ATTGGAGGGCAAGTCTGGTG
	18S-rv-universal	CCGATCCCTAGTCGGCAT

Amplification of candidate 144 DNA fragment for gateway cloning

Amplification of DNA fragments to be used for gateway cloning construct generation was carried out using Phusion high fidelity polymerase (NEB) following the manufacturer's recipe and thermocycler conditions using primers specifically designed to amplify selected fragments (Table IV-4).

Table IV-4: Table of primers used for candidate DNA fragment amplification for gateway cloning. 144FattB1-sp black sequence is attB1 gateway extension sequence and red sequence is specific of the candidate gene. In blue, start codon ATG is added as no start codon was present due to the non-amplification of signal peptide. 144RattB2-stop and 144RattB2 black sequence is attB1 gateway extension sequence and red sequence is specific of the candidate gene.

Primer name	Primer sequence 5'-3'
144FattB1-sp	GGGGACAAGTTTGTACAAAAAAGCAGGCTTCATGGTAACCACACCTC AGAAATC
144RattB2-stop	GGGGACCACTTTGTACAAGAAAGCTGGGTTGGATCCGCTATTGATCG
144RattB2	GGGGACCACTTTGTACAAGAAAGCTGGGTTTTAGGATCCGCTATTGA

IV.2.11. Expression analysis of HR marker genes during expression of the candidate 144 using pEAQ-HT system

Real-time primer of HR marker genes and *N. benthamiana* reference genes

Real-time primers for HR marker genes were designed using Primer Express software and following the manufacturer's procedure for primer design. Elongation Factor (EF), ribosomal protein L23 (L23) and protein phosphatase 2A (PP2A) reference genes and primers for RT-PCR were chosen from Liu et al. (2012) as they were showing stability during infection of *N. benthamiana* with viruses. Primer sequences are listed in Table IV-5.

Primer efficiency was evaluated on a slope of a standard curve generated using a 4 serial dilution of cDNA mixed sample ($E = 10^{(-1/slope)-1}$).

Table IV-5: List of primes used for expression analysis of HR marker genes

Target gene	Primer name	Primer sequence 5'-3'
EF	NBefF	AGCTTTACCTCCCAAGTCATC
	NBefR	AGAACGCCTGTCAATCTTGG
L23	*NBL23F*	AAGGATGCCGTGAAGAAGATGT
	NBL23R	GCATCGTAGTCAGGAGTCAACC
PP2A	PP2AF	GACCCTGATGTTGATGTTCGCT
	PP2AR	GAGGGATTTGAAGAGAGATTTC
MAPK	MapkF	ACAGCTCCCCCAGTATCCAA
	MapkR	CAAGTAGGGGTGGCAGAGC
NOX	NOXF	GCATTGCTCTCAACCACCCT
	NoxR	GTTCTTTGGTCAGTGCTGGTG
PRX	PRXF	TCACATTTGTTTGCCCGACAG
	PRXR	ATCAGTTTGGACCCAGGCAA
PR1	Fpr1	GCGAAAACCTAGCTGAGGGAA
	Rpr1	TCATCGACCCACATCTCAACA
HSP90	FHSP90	GGGACTGTGCAAGGTCATCAA
	Rhsp90	CCAGTGACTAAGCAGCAGGG
SGT1	Fsgt1	CCTTGCAAAAGCTGAACCCT
	Rsgt1	GACACATTAGGCCTCTGCACT

Expression analysis

RNA and cDNA were respectively extracted and produced as previously described from 6 leaf discs per plant. 3 reps of each construct were collected. Leaf discs were collected from non-infiltrated plants (NI), pEAQ-HT-empty vector (EV) infiltrated plants, pEAQ-HT-GFP (GFP) infiltrated plants, pEAQ-HT-144 (candidate 144) infiltrated plants and pGrab-INF1 infiltrated plants.

IV.3. Results

IV.3.1. *P. pastoris* heterologous protein production of putative protease inhibitor protein (named candidate 144)

Candidate 144 was previously shown to be an interesting candidate because it was able to induce cell death in *N. benthamiana* when massively overexpressed with the pEAQ-HT system, a virus-based overexpressing vector known for its high efficiency (Sainsbury et al. 2009). However, despite the clear specific symptoms observed, no protein could be detected and purified to study the protein. For these reasons, I decided to change expression system and the *P. pastoris* heterologous protein production system was used to produce a V5-tagged version of candidate 144 (144V5) to allow its functional characterisation

P. pastoris transformant colonies selection

P. pastoris colonies transformed with p75-144V5 were screened for the presence of the insert and 5 positive colonies were selected to test the production of the protein: colonies 1, 3, 7, 13 and 30 (Figure IV-2).

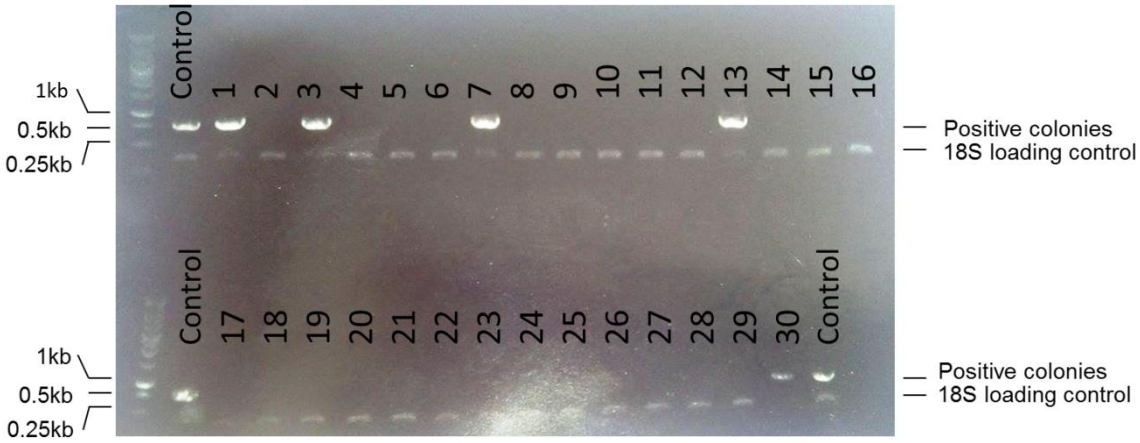

Figure IV-2: PCR screening of 30 *P. pastoris* transformants (1-30). Control lines are PCR with DNA of *P. pastoris* already successfully transformed with a similar construct provided by Dr Adokiye Berepiki. The lower band corresponds to DNA loading control specifically amplifying 18S sequence. The higher band is specific to successfully transformed colonies with DNA fragment of promoter and α factor of the insert.

Selection of the *P. pastoris* transformant producing the highest amount of candidate 144V5

Expression of protein can differ between transformants depending on the localisation of the insertion and whether or not the constructs have been fully

transformed. To check the expression of the protein, Western blot using supernatants of the five successful colonies was carried out to detect V5-tagged protein. Selected transformants of *P. pastoris* appeared to be successfully transformed and expressing our candidate 144V5 at the expected size but at different levels. *P. pastoris* colony 7 appeared to be the most efficient colony while colonies 1, 3 and 30 showed lower quantities of protein and colony 13 showed an almost undetectable level of protein (Figure IV-3).

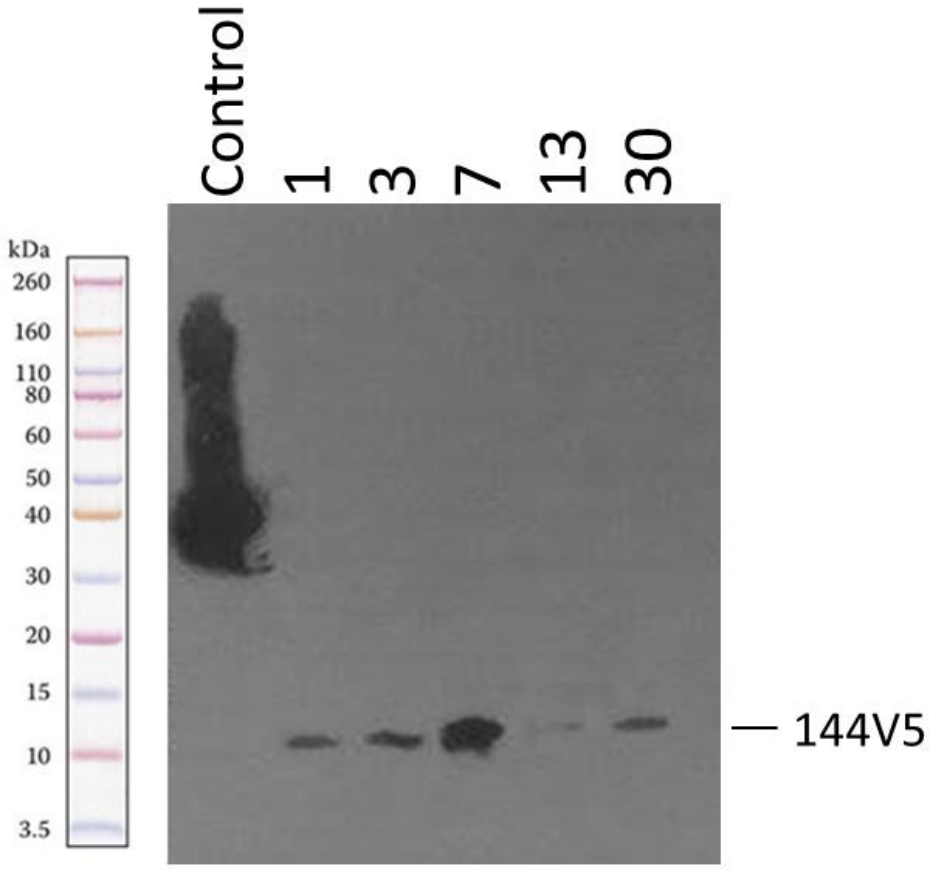

Figure IV-3: Western blot using culture supernatant of positive *P. pastoris* colonies selected (1, 3, 7, 13 and 30). The control *P. pastoris* colony producing a 40kDa V5 tagged protein kindly provided by Dr Adokiye Berepiki. Proteins were detected using HRP conjugated V5 antibody.

IV.3.2. Does infiltration of 144V5 heterologous protein -produced by *P. pastoris*- causes phenotype in *N. benthamiana*?

144V5 heterologous protein produced by *P. pastoris* and secreted into the supernatant was concentrated in HNT buffer using a Vivaspin column. Concentrated protein solution was compared to the non-concentrated solution by Western and showed a clear increase of the protein quantity (Figure IV-4). Moreover, multiple bands of higher weight than expected were observed for

144V5 concentrated sample, an unexpected result for a denatured protein Western, which could be due to strong dimerization and even trimerisation of the protein due to the high concentration (Figure IV-4).

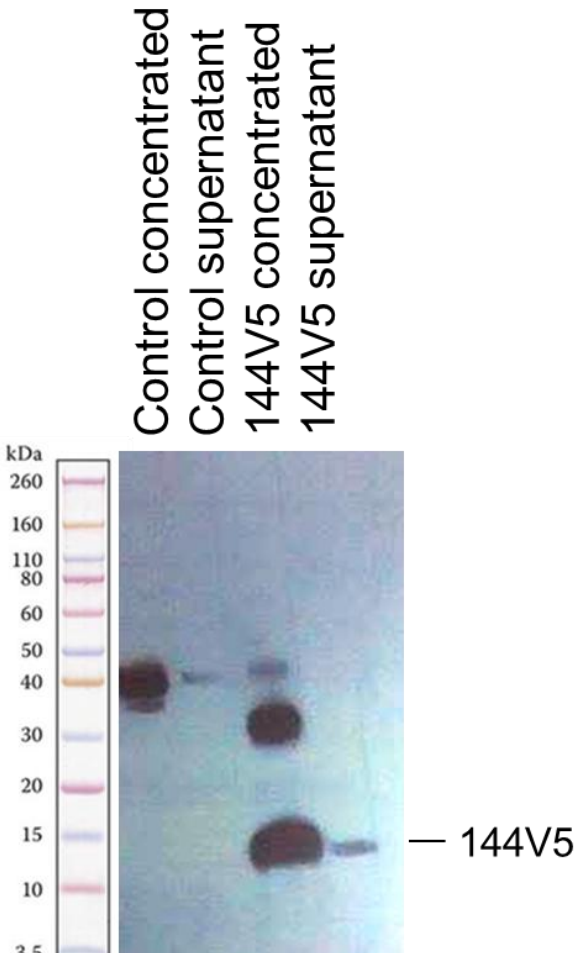

Figure IV-4: Western blot to check the presence of 144V5 after concentration. Proteins were detected using HRP conjugated V5 antibody.

Concentrated protein, dilution of protein in HNT buffer and HNT buffer only were infiltrated into *N. benthamiana* leaves following the map Figure IV-5A. At two DPI, cell death appeared on the infiltrated spot of concentrated protein and 1/10 diluted protein (Figure IV-5). 144V5 may be recognised by *N. benthamiana* or has a toxic effect.

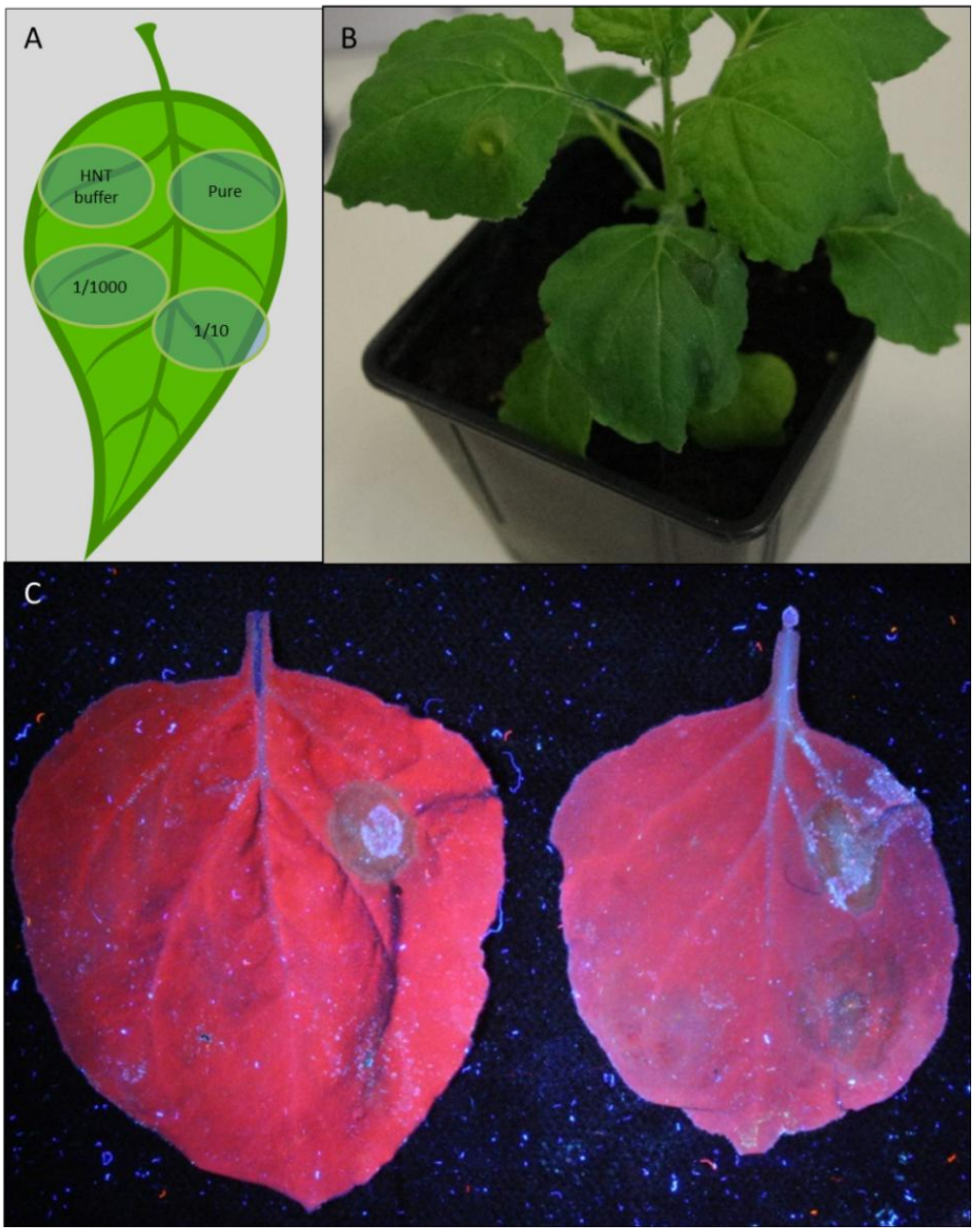

Figure IV-5: 144V5 candidate heterologous protein infiltration into *N. benthamiana.* A: Diagram of the map of infiltration spot in leaves. B: Picture of leaf symptoms 2 days post infiltration (DPI). C: Picture under UV light of leaf symptoms 2 DPI.

IV.3.3. The effect of infiltration of heterologous protein 144 produced by *P. pastoris* into barley

144V5 and V5 epitope only heterologous proteins produced by *P. pastoris* and secreted into the supernatant in the same conditions were concentrated in the same volume of HNT buffer using Vivaspin columns to allow comparison. V5 concentrated supernatant was used as a basal control containing proteins secreted by *P. pastoris* and retained by the column. Protein levels were quantified in both concentrated supernatant solutions and 25 µg/mL and 475

µg/mL were detected in V5 and 144V5 concentrated supernatant solutions respectively. Similar dilutions of 1/5 of V5 and 144V5, resulting in 5 µg/mL and 95 µg/mL solutions respectively, with a higher concentration of 144V5 concentrated supernatant solution of 220 µg/mL, and HNT buffer only were individually spot-infiltrated in seven barley leaves. Barley leaf infiltration does not induce nice circular infiltration spot but a long rectangular shaped spot due to barley cell arrangement. Eight DPI, lesions at the spot of infiltration were scored following the key (Figure IV-6).

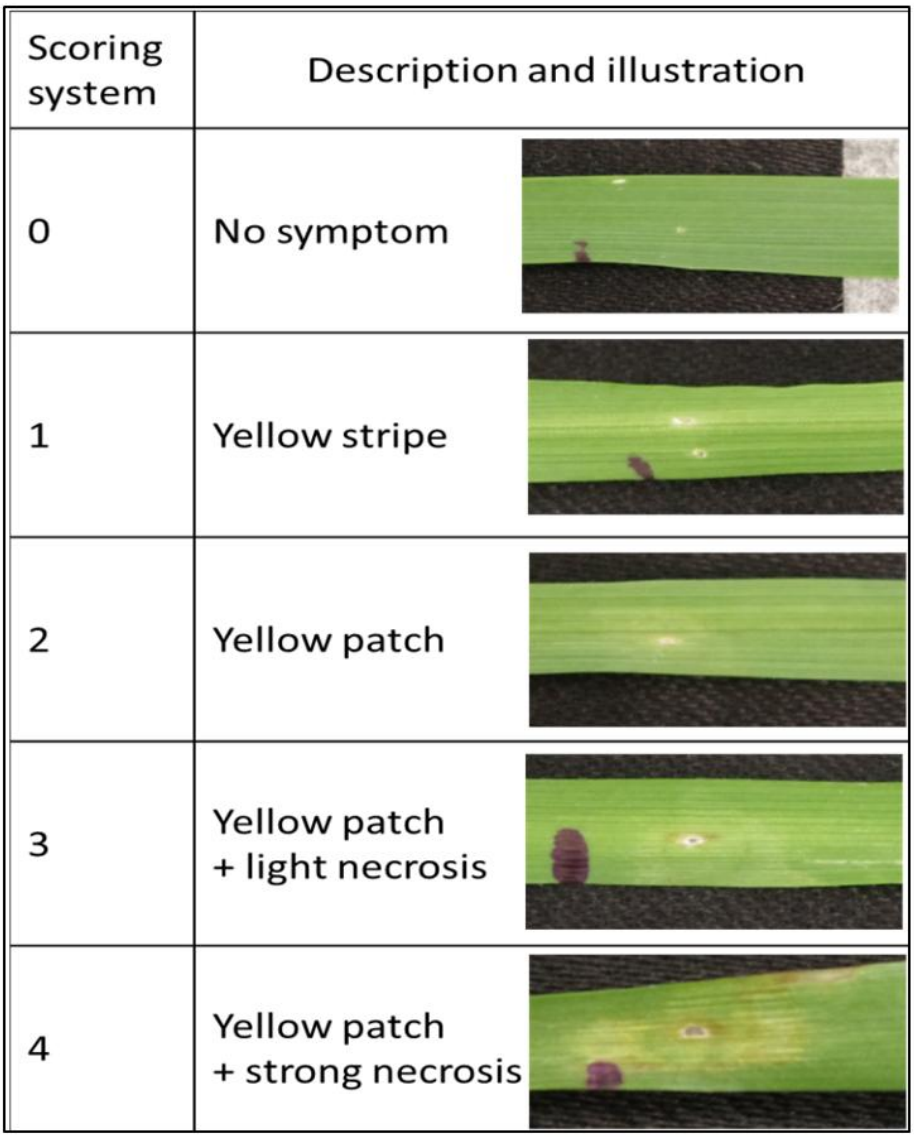

Figure IV-6: Key system used to score lesions induced by infiltration in barley leaves 8 days post infiltration (DPI).

HNT buffer induced light lesion (score 0-1) probably due to the mechanical damage induced by the infiltration. V5 concentrated supernatant induced up to yellow stipe and patches, probably the result of PTI activation due to the

presence of *P. pastoris* secreted proteins in the solution or due to the mechanical damage induced by the infiltration.. Yellow patch and strong necrosis were induced by 144V5 supernatant protein infiltration and seem to be correlating with the increase of the concentration of 144V5. Statistical analysis of mean score lesion showed differential significant responses of spots infiltrated with 144V5 at 220 µg/ml compared to spot infiltrated with HNT or V5 (Figure IV-7). 144V5 may have a toxic effect on barley leaves.

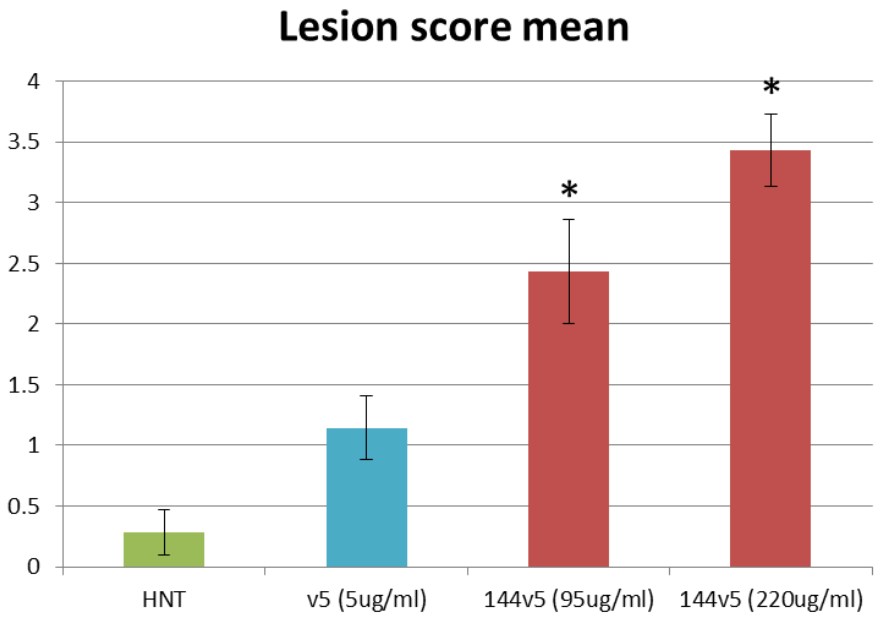

Figure IV-7: Mean score of lesions induced by infiltration in barley. Different solution were infiltrated: HNT buffer only, V5 supernatant (5 µg/mL) at the equivalent dilution to that of 144V5 (95 µg/ml) and 144V5 (220ug/ml). * indicates significant difference of lesion induced by 144V5 compared to HNT and V5 induced response (based on t-test $p<0.05$). Error bars are standard errors between biological replicates.

IV.3.4. Pull down of 144V5 protein and mass spectrometry

To be able to determine the function of candidate 144 and whether 144V5 is causing cell death by being recognised or by having a toxic effect, we decided to study targets of 144V5 by pull down and mass spectrometry. Knowing what 144V5 targets are could confirm the function of the protein and help us understand whether it is recognition, if plant immune system proteins are being pulled down.

After infiltration of 144V5 and V5 only into *N. benthamiana* leaves, 144V5 and V5 were pulled down from protein extraction of infiltrated leaves. A protein gel of pulled down sample showed the same strong band around 55 kDa (probably

Ribulose bisphosphate carboxylase) and around 25 kDa. However, a light smear was observed in the 144V5 sample which could be proteins pulled down together with 144V5. Moreover, a faint band was observed at the expected size of 144V5 confirming the presence of the pulled down protein (Figure IV-8A). V5 is not detectable because is it too small (1.4 kDa) and probably ran out of the gel.

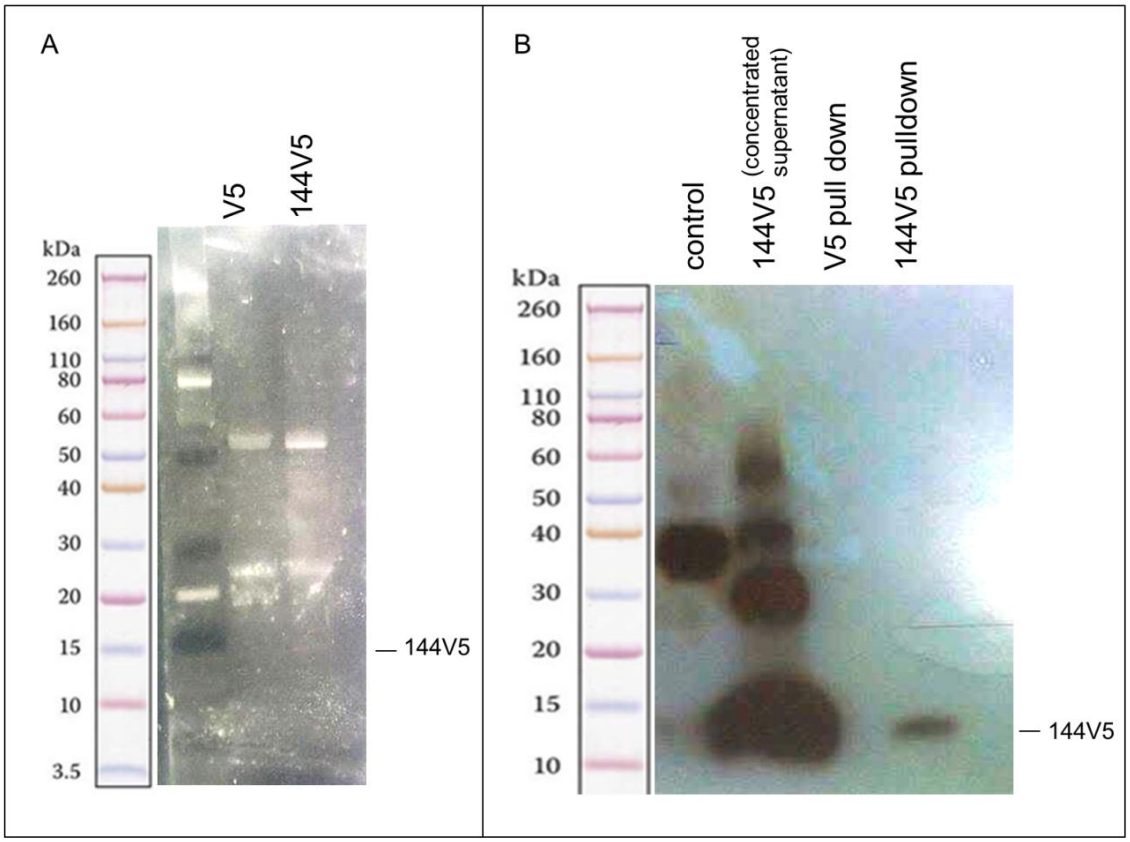

Figure IV-8: Pull down control before the mass spectrometry. A: Protein gel of pulled down sample. B: Western blot of V5 detection control (40kDa), 144V5 concentrated supernatant and pulled down samples. Proteins were detected using HRP conjugated V5 antibody.

Excised gel sections of 144V5 and V5 samples were sent for mass spectrometry after trypsin digestion. Protein IDs were generated by nanoflow liquid chromatography–tandem mass spectrometry (nLC-MS-MS) and comparison to *N. benthamiana* proteome database and 144-V5 protein sequence. Six proteins could be identified in the V5 sample, all involved in metabolic or regulation processes except for accession P86104, which did not have any description but the blast of the sequence revealed that it is Keratin, a human protein due to handling manipulation during the experiment (

Table IV-6).

Table IV-6: List of proteins detected in the pull down of the V5 sample

Accession	Description	Score	Coverage	Biological Process
P48709	Ribulose bisphosphate carboxylase large chain	125.83	36.9	metabolic process
P86104	Unknown protein 1	124.28	100	Keratin (human protein contamination)
Q40460	Ribulose bisphosphate carboxylase/oxygenase activase 1, chloroplastic	109.33	7.69	metabolic process
B9A6I8	Germin like protein	96.28	18.27	regulation of biological process; plant defence
Q0PWS6	Chloroplast pigment-binding protein CP24	81.23	16.73	metabolic process
C9VWR1	Chlorophyll A-B binding protein	73.79	11.76	metabolic process

27 proteins were identified in the 144V5 sample and none of them were proteases but all are involved in metabolic, regulation and transport processes except for two accessions with interesting functions: B7FJ53, involved in response to stimulus; and D7KJP2, involved in response to stimulus, cell communication and defence response (Table IV-7). However, 144-V5 protein was not detected indicating that the pulldown did not precipitate enough protein to be detected by mass spectrometry or that the protein was degraded during the pull down process and as a consequence, 144-V5 target proteins cannot be detected (Table IV-7). We still do not know if candidate 144 is a protease inhibitor or not and if it is being recognised or having a toxic effect on *N. benthamiana.*

Table IV-7: List of protein detected in the pull down of the 144-V5 sample.

Accession	Description	Score	Coverage	Biological Process
P48709	Ribulose bisphosphate carboxylase large chain	242.89	28.3	metabolic process
B9A6I8	Germin like protein	221.02	17.79	regulation of biological process; plant defence
Q8SAQ3	Ribulose bisphosphate carboxylase small chain	208.09	24.78	metabolic process
P14279	Chlorophyll a-b binding protein 5, chloroplastic	206.68	38.4	metabolic process
K4B3P9	Fructose-bisphosphate aldolase	206.04	13.1	metabolic process
A4D0J9	Carbonic anhydrase	202.33	31.64	metabolic process
D6CIA6	Chlorophyll a/b binding protein	192.87	29.61	metabolic process
W5BXM5	Glyceraldehyde-3-phosphate dehydrogenase B	189.47	38.51	metabolic process
F2VJ75	Fructose-bisphosphate aldolase	188.27	15.33	metabolic process
Q40460	Ribulose bisphosphate carboxylase/oxygenase activase 1,	185.71	11.76	metabolic process

K7RYG4	Chloroplast ribulose bisphosphate carboxylase/oxygenase activase beta2	183.4	15.88	metabolic process
O64444	Light harvesting chlorophyll a/b-binding protein	171.91	40.75	metabolic process
E3W0H8	ATP synthase subunit alpha, chloroplastic	144.94	13.02	metabolic process; transport
K4K6D0	ATP synthase subunit alpha, chloroplastic	144.94	13.12	transport; metabolic process
A0A022PPP3	photosystem II CP47 chlorophyll apoprotein	135.43	32.14	metabolic process
D3WES6	Photosystem II CP43 chlorophyll apoprotein	134.5	8.68	metabolic process
A9PIR4	Phosphoglycerate kinase	124.04	10.4	metabolic process
H6SZH3	Photosystem I P700 apoprotein A2	122.4	5.53	metabolic process
Q0PWS6	Chloroplast pigment-binding protein CP24	102.25	16.73	metabolic process
Q0PWS5	Chloroplast pigment-binding protein CP26	96.13	14.74	metabolic process
B7FJ53	chloroplast photosystem II 22 kDa component	87.27	12.98	cell organization and biogenesis; response to stimulus
Q43775	Glycolate oxidase	73.82	20.69	metabolic process
P29302	Photosystem I reaction center subunit II, chloroplastic	70.95	21.08	metabolic process
V9ZA06	Cytochrome f	69.74	19.59	metabolic process
M0XD85	Malate dehydrogenase	68.72	13.82	metabolic process
P22179	Photosystem I reaction center subunit VI, chloroplastic	65.42	30.56	metabolic process
D7KJP2	Catalytic/ coenzyme binding protein	59.06	4.5	metabolic process; response to stimulus; cell organization and biogenesis; cell communication; defence response; regulation of biological process

IV.3.5. Does candidate 144 acts as a protease inhibitor?

To investigate the function of the candidate 144, a protease assay was carried out using *N. benthamiana* apoplastic fluid to see if the presence of 144-V5 protein was preventing the release of amino acids induced by proteases present in the apoplast. Different dilutions of apoplastic fluid and apoplastic fluid supplemented with casein substrate were tested with 144-V5 concentrated protein, V5 concentrated supernatant, and an appropriate control such as HNT buffer for negative control and commercial protease inhibitor cocktail for positive control. Samples were incubated for 1h on ice for control and at 25 °C for

protease activity. In all of the conditions tested, the measure of the absorbance at OD=335 nm did not reveal any difference between samples incubated on ice or at 25°C and between control samples, indicating that the assay did not work and cannot help us to study the function of the protein.

IV.3.6. Overexpression and subcellular localisation of candidate 144 in *N. benthamiana*

Candidate 144 was previously shown to be an interesting candidate because it was able to induce cell death in *N. benthamiana* when massively overexpressed with the pEAQ-HT (Sainsbury et al. 2009). However, despite the clear specific symptoms observed, no protein could be detected. For these reasons, I decided to express the fluorescent tagged version of candidate 144 using a less efficient vector.

GFP tagged protein

Candidate 144 was cloned into pB7FGW2 and sec-gfp-pK7GW2 vector to be overexpressed and tagged with GFP in *N. benthamiana.* Two expressing constructs of 144 were generated: pB7FGW2-sp-144-st expressing a C-terminal GFP tagged and sec-gfp-pK7GW2-sp-144-st expressing a secreted GFP with a C-terminal tag.

The subcellular localisation of the 144 candidate was performed by confocal microscopy and showed a similar localisation to that of GFP from empty vector, 144GFP was located in the cytoplasm and passively diffusing into the nucleus (Figure IV-9A). However, when 144GFP was directed to the apoplast by secretion, discontinuously-shaped cells were observed(Figure IV-9C), a sign indicating that cells may be stressed or that 144GFP is not stable in the apoplast and cannot be detected in the apoplast (Brandizzi et al. 2003). The localisation of secreted 144GFP cannot be compared to the location of the GFP using the empty vector as the empty vector sec-gfp-pK7GW2-EV is not functional due to frame shift in the cloning area sequence (Figure IV-9B).

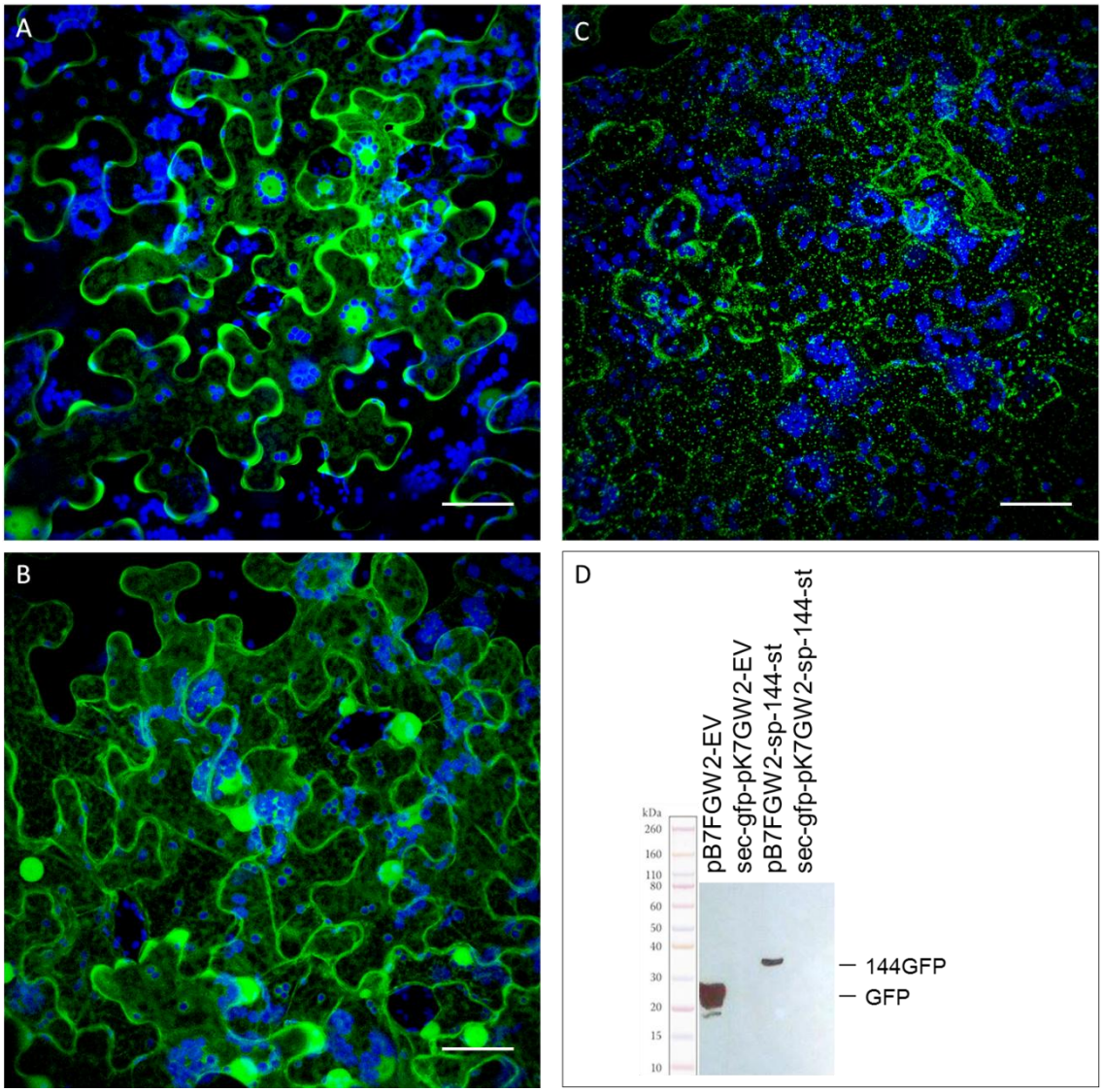

Figure IV-9: Subcellular localisation and Western blot of GFP and GFP tagged 144 protein 5 days post infiltration (DPI). A: pB7FGW2-sp-144-st intracellular expression of 144GFP. B: pB7FGW2-EV intracellular expression of GFP. C: sec-gfp-pK7GW2-sp-144-st expression of 144GFP directed to the extracellular compartment (apoplast). GFP and chlorophyll autofluorescence channels are coloured in green and in blue respectively. Scale bars represent 25 µm. D: Western blot using leaf disc samples collected 5 DPI. Proteins were detected using anti-GFP antibody.

A Western blot with leaf disc samples collected 5 DPI was carried out to check the presence of the 144GFP. GFP was detected in the pB7FGW2-EV sample but was not detected in the non-functional sec-gfp-pK7GW2-EV sample as expected. 144GFP was detected at the expected size expressed with pB7FGW2-sp-144-st but could not be detected with sec-gfp-pK7GW2-sp-144-st possibly due to the cell death induced by 144GFP or its instability *in planta*.

RFP-tagged protein

Expression of GFP-tagged protein seems to have some limitation so candidate 144 was cloned in a vector to be overexpressed and tagged with RFP in *N. benthamiana.* Two expressing constructs of 144 were generated: pB7GWR2-sp-144 expressing an N-terminal RFP tag and pMdc43-spmRFP-sp-144 expressing a secreted N-terminally-tagged RFP.

The subcellular localisation of the 144 candidate was performed by confocal microscopy and showed that 144RFP localised like 144GFP in the cytoplasm and passively diffused into the nucleus. The localisation of 144RFP cannot be compared to the location of the RFP using the empty vector as the empty vector pB7GWR2-EV is not functional and no RFP was detected at the confocal. Moreover, when 144RFP was directed to the apoplast by secretion it behaved like 144GFP showing discontinuously-shaped cells indicating that the phenotype is not due to the instability of the GFP and that cells may be stressed by the secretion of 144. The localisation of secreted 144RFP can be compared to the location of RFP using the empty vector pMdc43-spmRFP-EV which only showed a light localisation shaping cells in the apoplast.

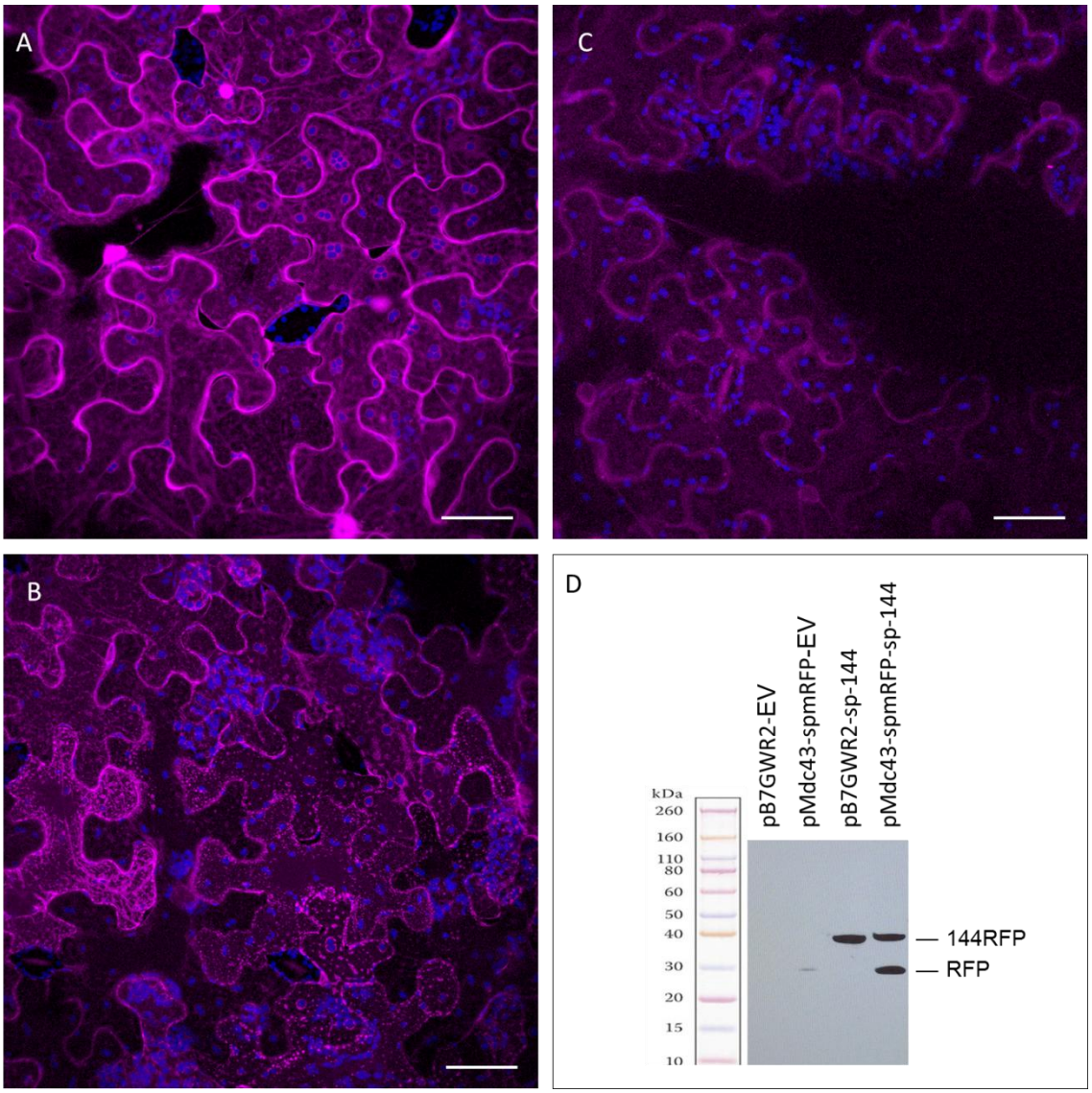

Figure IV-10: Subcellular localisation and Western blot of RFP and 144RFP protein 2 days post infiltration (DPI). A: pB7GWR2-sp-144 intracellular expression of 144RFP. B: pMdc43-spmRFP-sp-144 expression of 144RFP directed to the extracellular compartment (apoplast). C: pMdc43-spmRFP-EV intracellular expression of RFP. RFP and chlorophyll autofluorescence channels are coloured in pink and in blue, respectively. Scale bars represent 25 µm. D: Western blot using leaf disc samples collected 2 DPI. Proteins were detected using anti-RFP antibody.

A Western blot with leaf disc samples collected 2 DPI was carried out to check the presence of the 144RFP. A faint band was detected in the pMdc43-spmRFP-EV sample but was not detected in the non-functional pB7GWR2 sample, as expected. 144RFP was detected expressed with pB7GWR2 and pMdc43-spmRFP-sp-144. However, 144RFP expressed with pMdc43-spmRFP-sp-144 looks slightly bigger than the one expressed with pB7GWR2-sp-144 and could be due to the linker between signal peptide and mRFP sequence in pMdc43-spmRFP-sp-144.

IV.3.7. Study of the effect of the overexpression of candidate 144 in *N. benthamiana* on the pathogen

In order to see whether candidate 144 has an effect on pathogenicity, *N. benthamiana* plants were spot infiltrated with cell suspension. Two distinct 1.5 cm spots where infiltrated on both sides of the leaf. The candidate effector was transiently expressed on one side of the leaf and on the other side the empty vector was agroinfiltrated. Fungal infection was carried out24h after agroinfiltration. If candidate144 has an effect on pathogenicity, the fungal pathogen growth may be boosted. Because *R. commune* is unable to infect *N. benthamiana*, we tested *P. infestans* and *B. cinerea.* The secreted and the cytoplasmic versions of candidate 144 were tested separately with pMdc43-spmRFP-sp-144 and pB7GWR2-sp-144 respectively.

P. infestans boost assay

P. infestans has a hemibiotrophic lifestyle, like *R. commune,* and was chosen to test the pathogenic effect of candidate 144. Infection successfully happened (Figure IV-11a) but no difference in lesion size could be observed from the expression of the candidate RFP144 in the cytoplasm (Figure IV-11b) and the secreted version of RFP144 (Figure IV-11c) compared to empty vector control at 7 DPI.

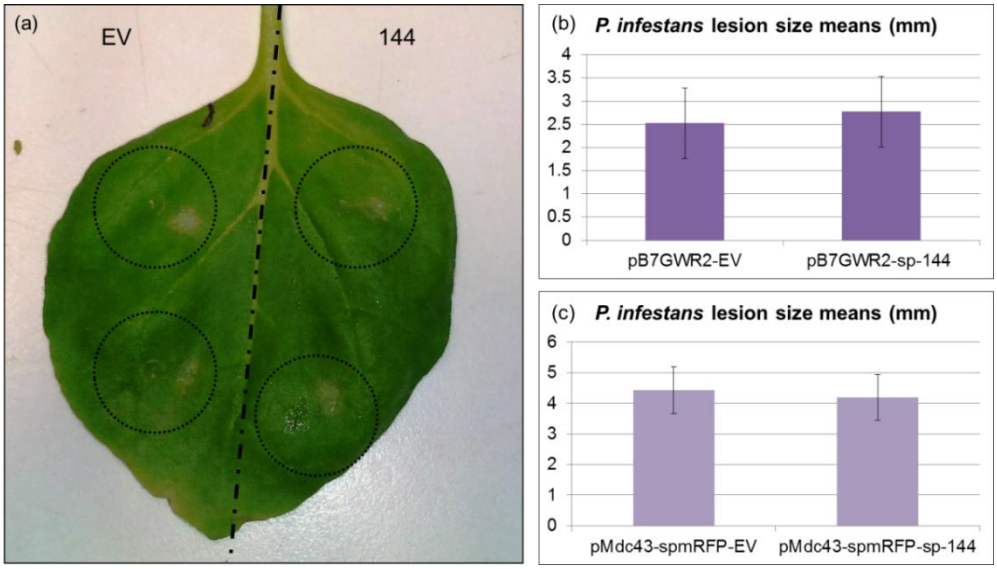

Figure IV-11: *P. infestans* boost assay. (a) Picture of *N. benthamiana* spot infiltrated (dash circle) with empty vector on the left side and 144 candidate on the right side 7 days post inoculation (DPI) with *P. infestans* showing grey lesions in the spot inoculation site. (b) Means of the size of lesions induced by *P. infestans* on spot infiltration with pB7GWR2-EV and pB7GWR2-sp-144. (c) Lesion size mean induced by *P. infestans* on spot infiltration with pMdc43-spmRFP-EV and pMdc43-spmRFP-sp-144.

B. cinerea boost assay

B. cinerea has a necrotrophic lifestyle and was chosen to test the pathogenic effect of candidate 144. The infection was successful and very fast (Figure IV-12a): from 3 DPI, lesions started to overlap making the size measurement unreliable. Measurement at 2 DPI showed no difference in lesion size from the expression of the candidate RFP144 in the cytoplasm (Figure IV-12b) and the secreted version of RFP144 (Figure IV-12c) compared to empty vector control.

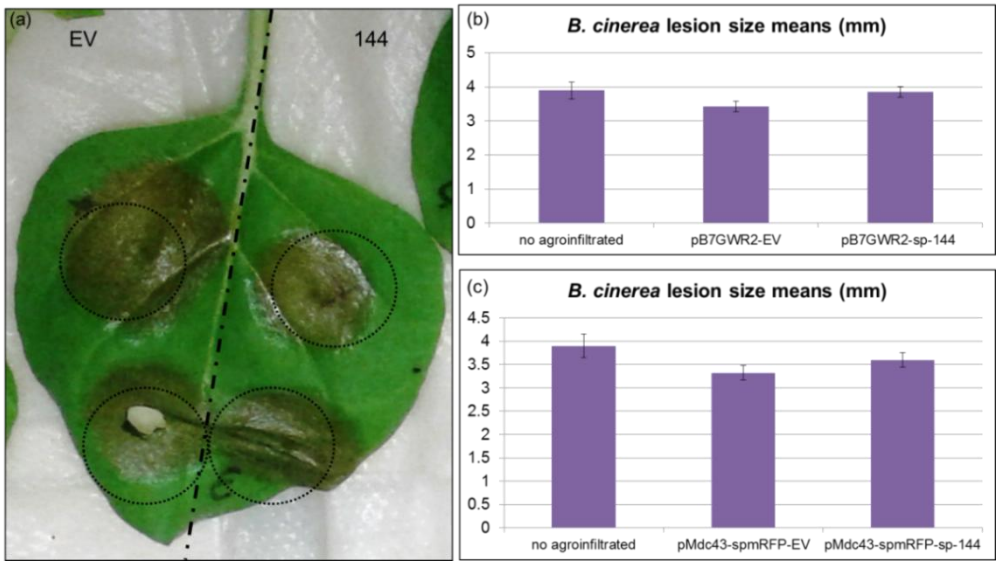

Figure IV-12: *B. cinerea* boost assay. (a) Picture of *N. benthamiana* spot infiltrated (dash circle) with empty vector on the left side and 144 candidate on the right side 4 days post inoculation (DPI) with *B. cinerea* showing brown and shiny lesions in the spot inoculation site. (b) Means of the size of the lesions induced by *B. cinerea* on spot infiltration with pB7GWR2-EV and pB7GWR2-sp-144 2 DPI. (c) Means of the size of the lesions induced by *B. cinerea* spot infiltration with pMdc43-spmRFP-EV and pMdc43-spmRFP-sp-144 2 DPI. Error bars represent standard deviation between biological reps.

IV.3.8. Does *R. commune* 144 candidate trigger accumulation of ROS in *N. benthamiana*

R. commune 144 candidate produced by *P. pastoris*

Infiltration of the putative protease inhibitor produced by *P. pastoris* and concentrated using a Vivaspin column into *N. benthamiana* leaves has previously been shown to trigger cell death. To determine if the cell death observed is due to recognition and hypersensitive response (HR) or due to toxic function, *N. benthamiana* leaves were infiltrated with fresh and inactivated by boiling protein followed by the study of reactive oxygen species (ROS), a strong marker of HR. Proteins were inactivated by heating at 95^{o}C for 1h. Each leaf was infiltrated with protein as shown in the leaf map (Figure IV-13A). DAB

straining was carried out 3 and 24h post infiltration. H_2O_2 was infiltrated at the sampling time to use as a visual control. ROS is characterised by small brown dots outside of the dark brown lesion spot caused by the mechanical infiltration (Figure IV-13B). No clear difference could be observed at 3h post infiltration between fresh and inactivated sample and between types of samples (Figure IV-13C-D). However, the 2 dilutions of protease inhibitor activated ROS 24h post infiltration when infiltrated fresh, but not when the protein was inactivated (Figure IV-13E-F).

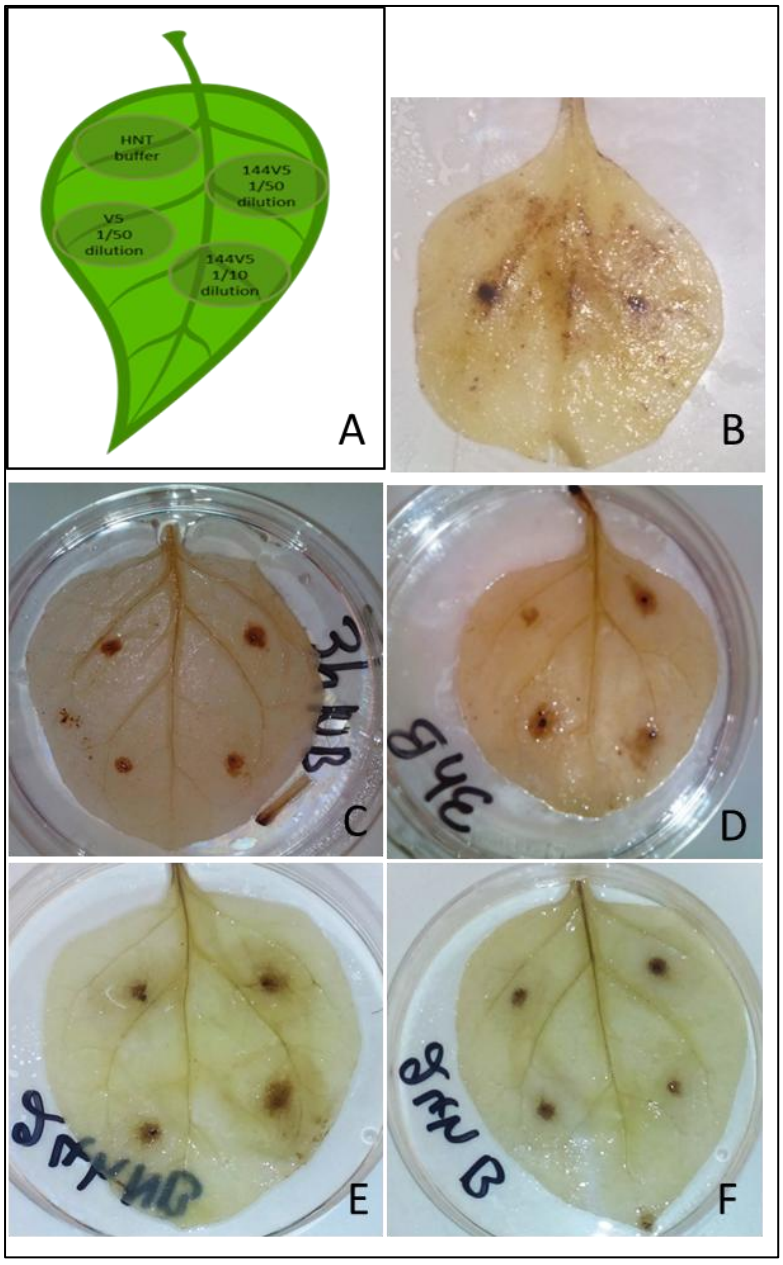

Figure IV-13: Map and picture of DAB staining experiment for ROS observation. A: map of sample infiltrated, B: DAB staining H_2O_2 control, C: DAB staining 3h post infiltration of fresh samples, D: DAB staining 3h post infiltration of inactivated samples, E: DAB staining 24h post infiltration of fresh samples, F: DAB staining 24h post infiltration of inactivated samples

Agrobacterium-mediated expression of *R. commune* 144 candidate.

DAB experiment was carried out following agroexpression of 4 different constructs: pEAQ-HT-EV (empty vector), pEAQ-HT-144 (previously showed to induce cell death), pEAQ-HT-GFP and pGrab-INF1 (as cell death positive control kindly provided by Fraser Murphy). These were infiltrated into the same *N. benthamiana* leaf following the map Figure IV-14a. DAB staining was carried out at 2 and 6 DPI. At 2 DPI, INF1 triggered ROS but no ROS could be detected on the protease inhibitor infiltration spot Figure IV-14c-d. At 6 DPI, leaves started to show cell death on the INF1 spot and a discoloration on the protease inhibitor spot Figure IV-14e. However, while DAB staining revealed ROS activation on the INF1 spot, no ROS activation was observed on the 144 spot Figure IV-14f.

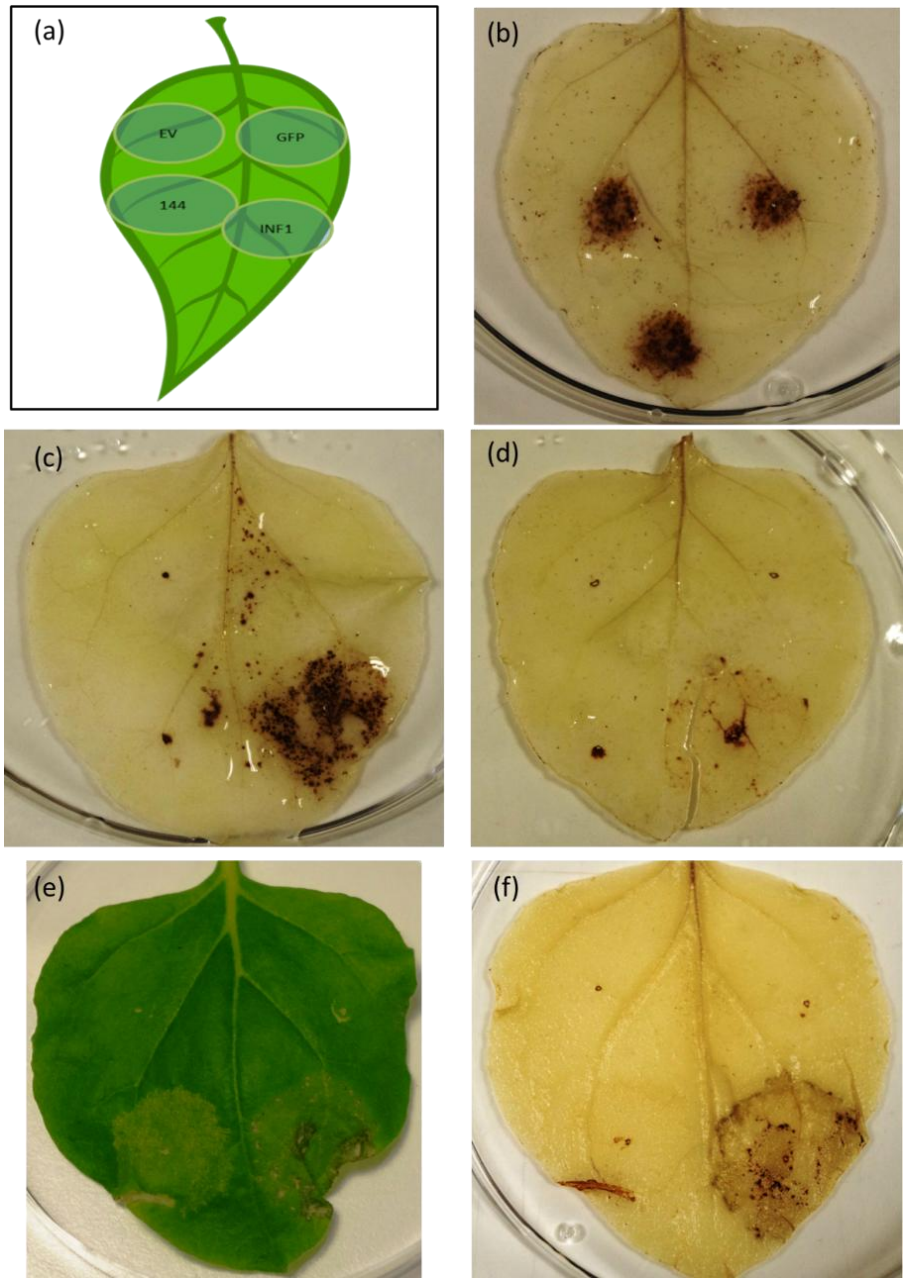

Figure IV-14: Map and picture of DAB staining experiment for ROS observation. A: map of samples infiltrated, B: DAB staining H_2O_2 control (not following the map), C, D: DAB staining 2 DPI, E: Picture of spot lesions induced 6 DPI, F: DAB staining 6 DPI.

IV.3.9. Study of the relative expression of HR marker genes during transient expression of the 144 candidate

Primer efficiency calculation

Primer efficiency was calculated for each primer pair used a slope of a standard curve generated using a 4-point serial dilution of cDNA mixed sample (E = 10^(-1/slope)-1) (Table IV-8).

Table IV-8: The efficiency of primers used for real time RT-PCR.

Primer pair	Slope	Amplification factor (E)	Efficiency (%)
EF	-3.2994	2.01	101.35%
L23	-2.9965	2.16	115.64%
PP2A	-3.4762	1.94	93.95%
MAPK	-3.2816	2.02	101.71%
nox	-3.31	2.01	100.50%
prx	-3.4111	1.96	96.41%
pr1	-3.3804	1.98	97.62%
hsp90	-3.3461	1.99	99.00%
sgt1	-3.3568	1.99	98.57%

Expression analysis

Another way of determining if the cell death observed is due to recognition and HR is to observe the expression of HR marker genes following the expression of the candidate The study of HR marker genes relative expression during transient expression of the candidate was carried including 3 biological reps and 6 HR markers: MAPK involved in signalling after PAMP recognition (Dodds and Rathjen 2010), NOX (NAPDH oxidase) and PRX (2-Cysteine peroxiredoxin) involved in ROS accumulation and detoxification respectively (Lara-Ortíz et al. 2003; Sevilla et al. 2015), pathogenesis-related 1 (PR1) involved in plant immunity (Zhang et al. 2012), molecular chaperone heat shock protein 90 (Hsp90) and SGT1, that plays a role in some early *R* gene-mediated plant defences (Austin et al. 2002). pEAQ-HT-144 is a construct used for transiently expressing the protease inhibitor which was previously identified to be triggering cell death. cDNA of non-infiltrated samples (NI), samples infiltrated with pEAQ-HT-empty vector (EV), samples infiltrated with pEAQ-HT-GFP (GFP), and samples infiltrated with pEAQ-HT-144 (candidate 144), produced to check the expression of candidate genes using the pEAQ-HT vector in *N. benthamiana* leaves were used for the relative expression analysis. In addition, a set of plants was infiltrated with pGrab-INF1 to overexpress INF1, a PAMP recognised by *N. benthamiana* as an HR control (Yaeno et al. 2011). The experiment was monitored by visual observation and DAB staining (previously described Figure IV-13) and ROS was observed in the part of the leaf expressing INF1 at 2 and 6 DPI. HR related genes (MAPK, NOX, PRX, PR1, HSP90, SGT1) relative expression was analysed on cDNA produced from *N. benthamiana* leaf discs collected 3 DPI from non-infiltrated samples (NI), pEAQ-HT-empty vector (EV)

sample, pEAQ-HT-GFP (GFP) sample, pEAQ-HT-144 sample (candidate 144) and pGrab-INF1. INF1 positive control did not work as expected as it did not trigger massive upregulation of any of the HR marker genes chosen maybe because 3 DPI was too late a time point. No significant difference (anova) in expression of any of the HR marker genes chosen was observed between the putative protease inhibitor and negative controls (Figure IV-15).

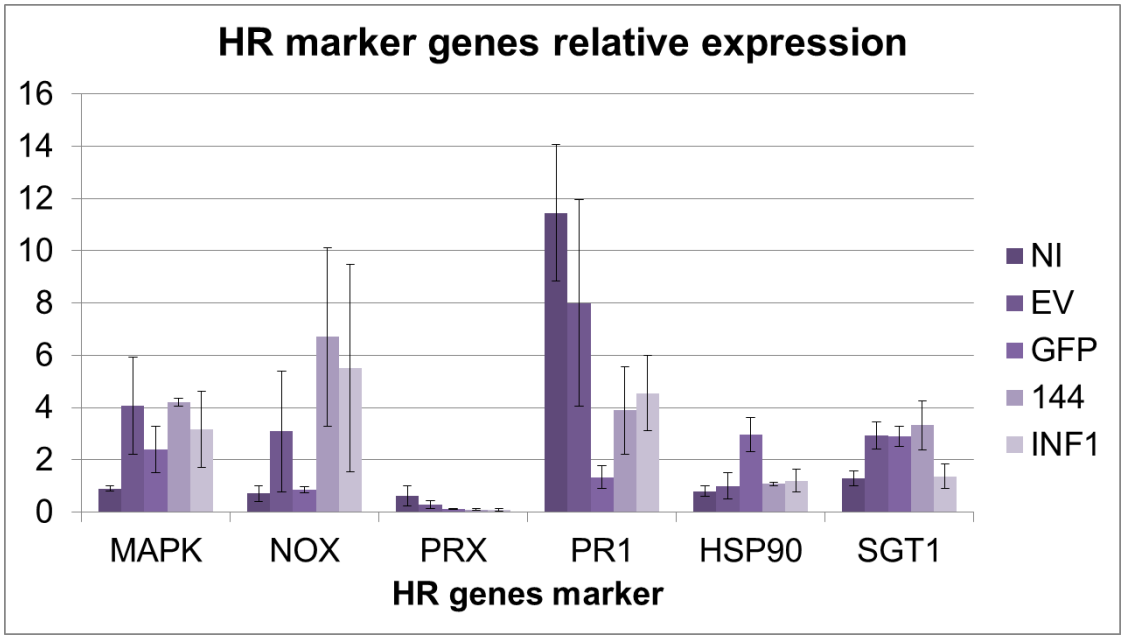

Figure IV-15: Relative expression of HR marker genes 5 days post infiltration (DPI). MAPK, NOX, PRX, PR1, HSP90 and SGT1 relative expression was studied on of empty vector pEAQ-ht (EV), pEAQ-ht-GFP (GFP), pEAQ-ht-144 (144) and pGrab-INF1 (INF1) infiltrated plants compared to non-infiltrated plants (NI). Error bars represent standard error between biological reps.

IV.4. Discussion

P. pastoris is broadly used to produce heterologous fungal effectors (Kombrink 2012) and appears to be a useful strategy and allowed the study of the effect of the protein in *N. benthamiana* and barley. In both plant species, 220 µg/ml and higher concentrations of candidate 144 protein triggered cell death and a positive correlation between the strength of the symptoms and the concentration of the protein was observed indicating that high concentration of candidate 144 was having a toxic effect in leaves and that the cell death was unlikely to be due to HR as HR usually happens with lower concentration of protein, for example, Flg22 is typically used as a control at 100 nM but it can cause HR at much lower concentration (Smith et al. 2014).

The fact that overexpression of protein mediated by *A. tumefaciens* in the apoplast triggered cell death or microscopically disrupted cells could be due to the accumulation of the protein in a small apoplast compartment where the quantity of the protein massively increases and raises the toxic level and leads to the phenotype. This cell disruption could also be due to secretion pathway issue due to the protein.

Production of reactive oxygen species (ROS) is a well-known plant process regulating several biological processes such as plant growth, development, senescence, stress adaptation and programmed cell death or HR (Pennell and Lamb 1997; Gechev et al. 2006) and as a consequence, looking for ROS activation is a good way to study HR. No evidence of ROS activation by our candidate 144 could be demonstrated even when lesion appeared at 6 DPI. This result suggests that the candidate 144 is not inducing HR or being recognised by the plant.

To confirm that the candidate 144 is not recognised and causing HR, expression of HR marker genes during the expression of candidate 144 was studied. MAPK was chosen because it is involved in signalling after PAMP recognition (Dodds and Rathjen 2010). NOX (NAPDH oxidase) and PRX (2-Cysteine peroxiredoxin) are involved in ROS production and detoxification respectively (Lara-Ortíz et al. 2003; Sevilla et al. 2015). Pathogenesis-related protein 1 (PR1) is induced by SA involved in plant immunity in particular against biotrophic fungi (Zhang et al. 2012), and molecular chaperone heat shock

protein 90 (Hsp90) and SGT1 play a role in early *R* gene-mediated plant defences (Austin et al. 2002). The study of HR marker genes did not show a clear difference in expression of any of them between the putative protease inhibitor and negative controls. The INF1 positive control did not work as expected and did not induce upregulation of any of the HR marker genes probably because 3 DPI was too late to observe the upregulation of these marker genes and maybe because it is cloned in a different expressing vector (pGrab) than the other constructs. From these result together with ROS assays, we can assume that the putative protease inhibitor is unlikely to induce HR. HR is usually a rapid response which usually becomes visible 24–48 h after the infiltration (Matsumura et al. 2003) and the fact that cell death induced by the candidate 144 was visible only from 6 DPI indicates that it is the accumulation of protein and the high concentration of protein which is probably toxic in the *N. benthamiana* and barley apoplast and induces cell death. It would have been good to repeat this experiment doing a time course trying to not miss the time when upregulation of HR genes should happen using INF1 positive control cloned into the pEAQ-HT plasmid. However, these experiments would have required a lot more time and effort to probably prove that the candidate 144 is not triggering HR as suggested by ROS experiment and it is not likely to act as a PAMP.

The fact that the candidate 144 does not trigger HR does not mean that the protein is not important for pathogenicity or does not play a role during the infection. The potential secretion of the protein suggests that it could still be involved in a yet unknown virulence process which should be investigated.

However, we were unable to confirm the protease inhibitor function of our 144 candidate by testing *in vitro* protease activity of apoplast in the presence of our candidate because the protease assay technique tried using TNBSA and adapted from (Tian et al. 2004) was unsuccessful maybe because the exact kit used by Tian et al. (2004) does not exist anymore and the adapted procedure was not high-standard enough or the apoplastic fluid extracted was not high-standard enough. In addition, it could have been a good idea to complement the assay by adding protease to the apoplast to supplement the natural protease content of the apoplast which could have been degraded during the procedure and or during the freeze drying.

The pull down assay and mass spectrometry to identify 144 candidate protein target allowed the identification of proteins which are unlikely to be 144 candidate protein targets as 144-V5 used for the pull down could not be detected in the sample meaning that the pull down assay did not pull down enough 144V5 protein to be detected and that identified proteins are probably unspecific. As an alternative, it would have been a good idea to use Anti-V5 Agarose Affinity Gel antibody from Sigma to pull down 144-V5 protein and its potential target(s).

Yeast-two-hybrid is a technique commonly used to identify effector targets but was not attempted because no library for apoplastic protein targets or membrane proteins was available in our lab. Moreover, there is a risk that this procedure would not work; the yeast two-hybrid procedure can be achieved with water soluble proteins but protein complexes occur in the nucleus, and if test proteins have other localization signals preventing them from localizing to the nucleus, two interacting proteins may be found to be non-interacting (Lu 2012).

The overexpression of candidate 144 in *N. benthamiana* plants did not boost the infection of *P. infestans* and *B. cinerea* but that result does not mean that candidate 144 does not play a role in the infection of barley by *R. commune.* So far, transient expression of the 144 protein heterologously in barley was attempted using the BSMV-VOX delivery system but the stability of the construct was not demonstrated and the fact that heterologous 144 protein was produced without any tag does not allow us to be sure that the protein was produced. In addition, barley plants putatively producing 144 through BSMV-VOX were not infected with *R. commune* to study the role of candidate 144 during *R. commune* colonisation of barley. Such an assay could have helped us to check whether the protein is being produced if it gave an advantage or disadvantage to *R. commune.* Biolistic particle bombardment techniques have been successfully used for transient gene expression in rice sheath cells indicating that this method is practical for host plant-microbe interaction studies and subcellular localisation (Wang et al. 2013), and could be adapted to study barley- *R. commune* interaction. As an alternative, the infection of *R. commune* mutants overexpressing candidate genes or KO mutants could be used to study the importance for pathogenicity of candidate effector.

IV.5. Conclusions

The function of candidate 144, a putative protease inhibitor, could not be confirmed and plant protein targets could not be identified. Pathogenicity tests on *N. benthamiana* using *P. infestans* and *B. cinerea* were not successful but this system is not optimal to study the pathogenicity effect of *R. commune* effectors and the lack of tools for functional studies in monocots did not allow further investigation. Disruption of *N. benthamiana* cells observed by confocal microscopy, cell death visually observed on *N. benthamiana*, necrosis visually observed on barley due to the presence of candidate 144 in the apoplast are likely to be due to a toxic effect as no proof of activation of the plant immune system was found by qPCR and DAB staining in *N. benthamiana*.

Despite the interesting putative function of candidate 144, it does not seem to play an important role in the *N. benthamiana* immune system, but further investigation would be needed to characterise its role in pathogenicity in barley.

V. Chapter 5: The role of salicylic acid in barley- *R. commune* interaction and the potential manipulation of its biosynthesis by *R. commune*

V.1. Introduction

Plant hormones are involved in many regulating processes and signalling, particularly in response to biotic stresses. Salicylic acid (SA) regulates plant defence responses against pathogens and pests, more specifically against biotrophic and hemibiotrophic pathogens in particular due to its ability to trigger plant cell death (Tanaka et al. 2015). Meanwhile, Jasmonic acid (JA) and ethylene (ET) regulate plant defences against necrotrophs (Bari and Jones 2009) such as *B. cinerea* (Ferrari et al. 2003) due to antagonistic effect on SA which inhibits the SA pathway and resistance to biotrophic pathogens. SA inhibition prevents plant cell death, a process that is advantageous to necrotrophic infection (Thaler et al, 2012). In addition, SA and other synthetic SA analogues have been shown to induce defence responses in rice and enhance resistance against the hemibiotrophic bacterial leaf blight pathogen *X oryzae* pv. *Oryzae* (Xu et al. 2013, De Vleesschauwer et al, 2014).

Biotic elicitors produced by plant pathogens or herbivore pests and priming agents rapidly activate the super induction of a range of plant defences leading to a faster and more robust pest and disease resistance and abiotic stress tolerance (Paré et al. 2005; Martinez-Medina et al. 2016). Priming is induced by chemical compound (volatile organic compounds, SA, JA, acibenzolar-S-methyl (BABA)), PAMPs and beneficial soil organisms (rhizobacteria) (Baccelli and Mauch-Mani 2016; Martinez-Medina et al. 2016). In the barley/*R. commune* pathosystem, the application of elicitors such as acibenzolar-S-methyl (ASM), BABA, and cis-jasmonate singly or in combination prior to infection led to an up-regulation of systemic acquired resistance (PR1), and increased activities of the defence-related enzymes (cinnamyl alcohol dehydrogenase (CAD), peroxidase (POX), and β-1,3-glucanase) (Walters et al. 2010; Walters et al. 2012). In

addition, priming-induced resistance of barley using saccharin provides systemic protection of barley against *R. commune* and powdery mildew in the field (Boyle and Walters 2006; Walters et al. 2008). So far, no study has been published describing SA priming of barley plants to protect them against *R. commune*.

SA is able to activate expression of plant pathogenesis-related (*PR*) genes, induces disease resistance and systemic acquired resistance (SAR) (Yalpani et al. 1991; Loake and Grant 2007). Studies suggest that SA is produced through two independent pathways in plant. SA is synthesised from phenylalanine, cinnamate and benzoate as the immediate precursor and regulated by phenylalanine ammonia lyase (PAL). However, 95% of SA is synthesised from isochorismate in the chloroplast but the enzyme converting isochorismate to SA remains unknown (Figure V-1) (Chen et al. 2009).

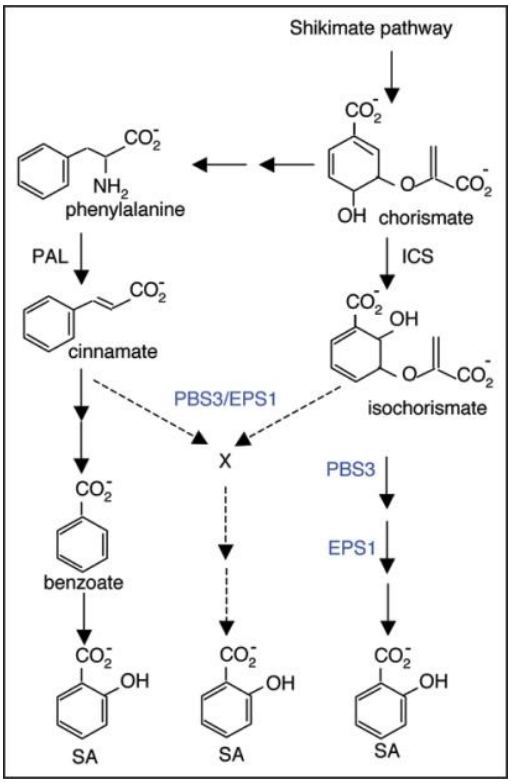

Figure V-1: SA production pathways discovered. (Chen et al. 2009)

With SA playing an important role in plant defences, pathogens developed strategies to disable the SA synthesis pathway. For example, chorismate mutase from the soybean cyst nematode *Heterodera glycines* have an important role in parasitism and is able to manipulate the SA pathway of the plants (Bekal et al. 2003). Moreover, during the infection of maize, *U. maydis*

uses a secreted chorismate mutase (Cmu1) to manipulate the SA biosynthesis pathway. Cmu1 was shown to be an important virulence factor, possibly dimerising with the maize homologue. It is thought to be diverting the chorismate substrate – a precursor for tyrosine and phenylalanine synthesis- from SA pathway to the prephenate pathway to disrupt the plant defence activation (Figure V-2). In addition, Cmu1 was able to move between plant cells (Djamei et al. 2011). Moreover, during the infection of *Arabidopsis* by the necrotrophic fungus *S. sclerotiorum* (Lib.) de Bary, SA-dependent defence induced a decrease of disease symptoms suggesting manipulation by the pathogen through a putative chorismate mutase SS1G_14320, which is highly expressed during infection, thereby questioning the current consensus regarding the necrotrophic lifestyle model of *S. sclerotiorum* (Nováková et al. 2014).

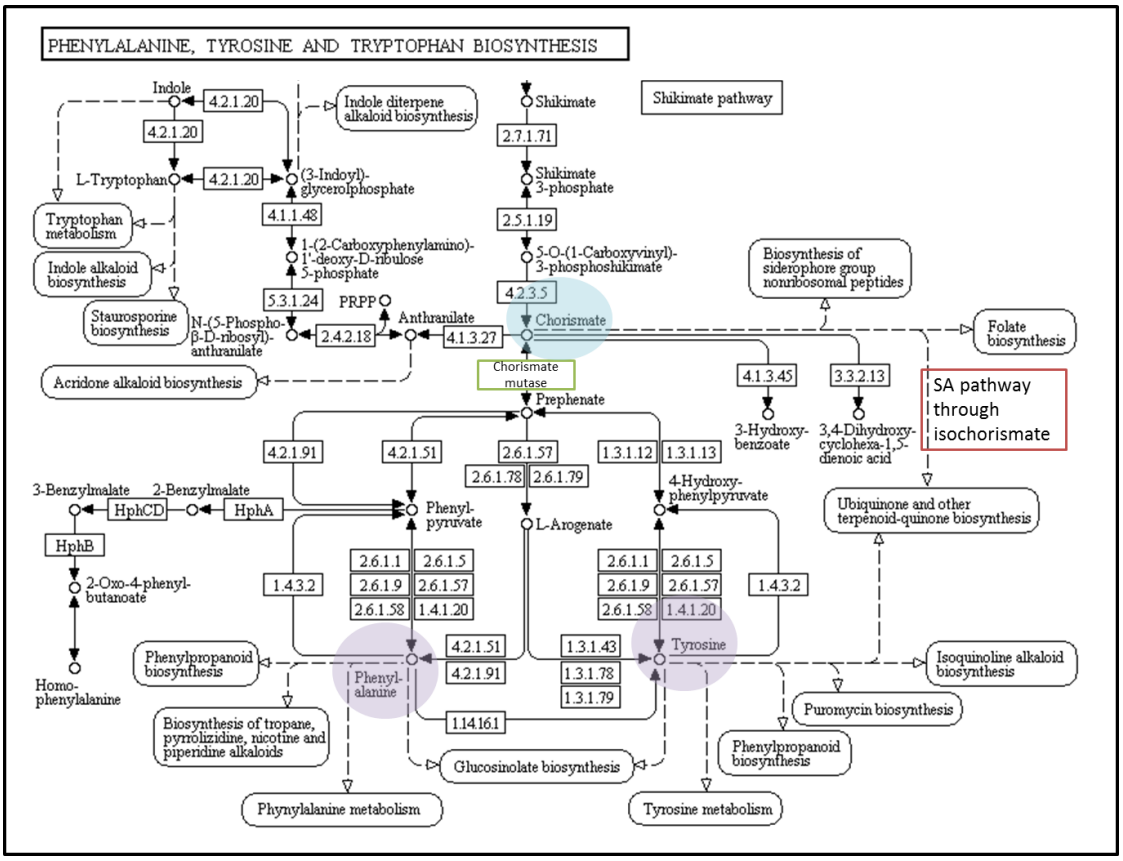

Figure V-2: Diagram illustrating metabolic processes involved in aromatic amino acid production from chorismate substrate adapted from KEGG website. Phenylalanine and tyrosine amino acids are shaded in purple, chorismate substrate is shaded in blue. The location of chorismate mutase is indicated in the green rectangle and the direction of the SA pathway through isochorismate is indicated in the red rectangle

In *P. sojae* and *V. dahlia*, isochorismate hydrolase (ISC) is required for full pathogenicity and suppresses salicylate-mediated innate immunity disease

resistance in soybean. The pathogens' ISC enzyme was shown to divert the isochorismate precursor away from SA production using Isochorismatase activity *in vitro*. Moreover, ICS does not have a conventional secretion signal and suggests the existence of a different and efficient delivery system of effectors (Liu et al. 2014). This shows that pathogens have developed at least two strategies to manipulate SA production (Figure V-3).

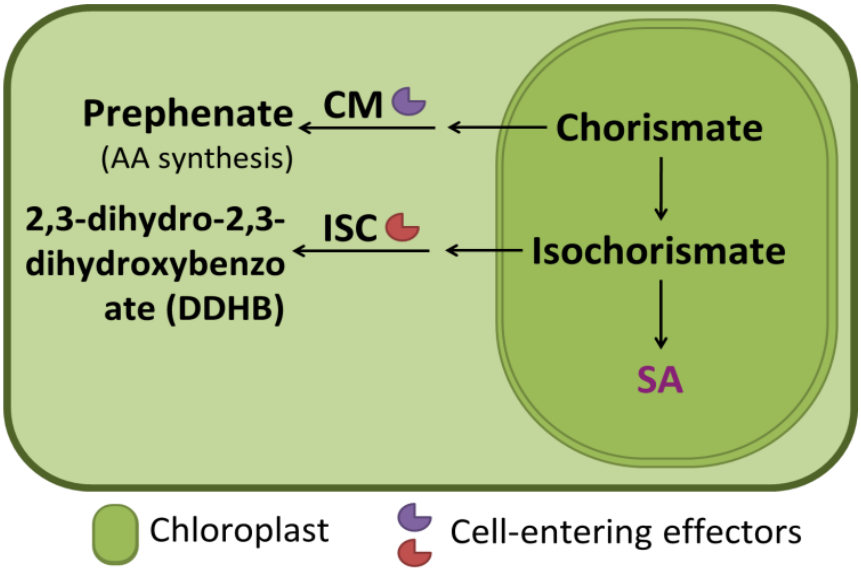

Figure V-3: Diagram illustrating the two layer pathogen strategy established to disrupt SA pathway production. Adapted from Liu et al. (2014).

Recent *R. commune* genome sequencing, assembly and annotation (Penselin et al. 2016) allowed the identification of a putative secreted chorismate mutase (RcCM) and an isochorismate hydrolase (RcISC) which appear to be interesting candidate effectors to study. *R. commune* may have developed a double layer of attack to manipulate SA production and regulate plant defence activation. Indeed, studying SA-related effectors would help us to better understand the ability of *R. commune* to infect barley. If we demonstrate that *R. commune* uses these effectors to manipulate the SA pathway of the plant, it would illustrate the biotrophic phase of the fungus, thereby confirming the hemibiotrophic lifestyle of *R. commune*. In addition, if we demonstrate that those SA-related effectors are important for pathogenicity, it would suggest that *R. commune* is able to translocate effectors from the apoplast to the plant cell to manipulate plant defence.

So far, in *R. commune, RcCM* and *RcISC* were shown to be upregulated during infection of barley and so potentially important for pathogenicity (Figure III-9).

The aim of this chapter is to study the role of SA during *R. commune* infection of barley by showing the implication of effectors on the manipulation of the SA plant defence pathway.

V.2. Materials and methods

V.2.1. Bioinformatics

Candidate effector sequences were compared to protein sequences in the NCBI database using https://blast.ncbi.nlm.nih.gov/Blast.cgi website. Protein conserved domains were identified using https://www.ncbi.nlm.nih.gov/Structure/cdd/wrpsb.cgi website. Multiple sequence alignments were generated using http://www.ebi.ac.uk/Tools/msa/ website.

V.2.2. Complementation of the *S. cerevisiae* mutant lacking chorismate mutase

Chorismate mutase complementation cassette generation

The *S. cerevisiae* ARO7 gene codes for the yeast homologue of the chorismate mutase. *S. cerevisiae* BY4741ΔYPR060C, Aro7 deletion strain, the corresponding parental strain (BY4741) and the plasmid pYES2 digested with *EcoR*1 and *Xba*1 were kindly provided by Dr Shin-Ichiro Hiraga (University of Aberdeen, UK). The *R. commune* chorismate mutase gene was amplified using primers designed to specifically amplify the gene and containing 5' extensions corresponding to the extremities of the digested plasmid region. Cloning and transformation was carried out in one step using previously described YRC. The presence of the RcCM insert in pYES2 vector was checked using primers used to generate PCR fragment. The BY4741ΔYPR060C strain was complemented by pYES2-RcCM and pYES2 as a control. The wild type strain BY4741 was complemented with pYES2 as a control.

S. cerevisiae chorismate mutase complementation growth assay

The complemented BY4741ΔYPR060C/pYES2-RcCM strain, knock out BY4741ΔYPR060C/pYES2 strain and wild type BY4741/pYES2 strain were grown overnight in 5 mL liquid SC-Ura medium. Each strain was serially diluted in sterile water to 1/5 starting from 10^5 cells/mL. 10 µL of 5 dilutions of each strain were spotted on plates of YPD control rich medium, -tyrosine (tyr) –tryptophane (try) –phenylalanine (phe) selective medium and -tyr –try –phe

selective medium supplemented with tyr, try and phe amino acids. Plates were left to dry before being sealed with parafilm and incubated at 30°C for 3 days.

V.2.3. SA *in vitro R. commune* growth assay

CZV8CM agar medium was supplemented with 10, 5, 1, 0.5, 0.1 mM of SA. *R. commune* conidia were scraped from a plate and re-suspended in sterile water. Conidia collected were diluted to 1/500, 1/200, 1/50 and 1/10 and 50 µL of each conidia dilution were spotted onto the CZV8CM agar medium supplemented with SA.

V.2.4. Gateway cloning

Gateway cloning for RcCM, RcISC and HVCM1 was processed as previously describes. Vectors used and generated are described in Table V-1.

Table V-1: List of vectors created and details of how they have been created, features and size of protein expressed.

Plasmid name	Antibiotic Resistance	function	Cloned from	Overexpressed protein size, kDa
pDONR207-sp-CM	gentamycin	Entry vector	CM candidate PCR without signal peptide and with stop codon	N/A
pDONR207-sp-CM-st	gentamycin	Entry vector	CM candidate PCR without signal peptide and without stop codon	N/A
pDONR207-ISC-st	gentamycin	Entry vector	ISC candidate PCR with stop codon	N/A
pDONR207-HVCM1-st	gentamycin	Entry vector	HVCM1 gene PCR without stop codon	N/A
pB7GWR2-sp-CM	spectinomycin	N-terminal RFP tagged	pDONR207-sp-CM	43.5
pMdc43-spmRFP-spCM-st	kanamycin	N-terminal RFP tagged secreted	pDONR207-sp-CM-st	43.5
pB7GWR2-sp-ISC	spectinomycin	N-terminal RFP tagged	pDONR207-ISC-st	48
pB7FGW2-HVCM1-st	spectinomycin	C-terminal GFP tagged	pDONR201-HVCM1-st	62
pB7GWF2-HVCM1-st	spectinomycin	N-terminal GFP tagged	pDONR207-HVCM1-st	62
pK7GW2-GFP	spectinomycin	GFP	N/A (empty vector)	27
pK7GW2-RFP	spectinomycin	RFP	N/A (empty vector)	28

V.2.5. *A. tumefaciens* transient expression of effector candidates in *N. benthamiana* to boost pathogen infection

A. tumefaciens transient expression of effector candidates in *N. benthamiana* to boost pathogen infection was processed as previously described using pB7GWR2-sp-CM and pMdc43-spmRFP-spCM.

V.2.6. Co-immunoprecipitation

Co-immunoprecipitation was carried out by collecting 36 leaf discs of 5 mm diameter from 4 dpi *N. benthamiana* plants transiently co-expressing RCCM and HV-CM1 proteins or transiently co-expressing RCCM with empty vector control. Frozen leaf material was grinded with a mortar and pestle in liquid nitrogen. 10 mL of GTEN extraction buffer was added (10 % glycerol, 25 mM Tris pH7.5, 1 mM EDTA, 150 mM NaCl, 2 % w/v PVPP, 10 mM DTT, 1X protease inhibitor cocktail (Sigma), 0.1% NP40 (Sigma)). Samples were centrifuged at 10000 x g to remove debris at 4°C and supernatant was transferred to a new tube. This step was repeated at least once more to remove as much debris as possible. 50 µL of extract were stored on ice to run as input on the SDS-PAGE. 20 µL of RFP-Trap® - ChromoTek beads were prepared per Co-IP by washing twice in washing buffet (10 mM Tris/Cl pH 7.5; 150 mM NaCl; 0.5 mM EDTA; 1x Plant Protease Inhibitor). RFP-Trap® was collected using magnetic stand in a 1.5 mL tube and washed 4 times with the washing buffer. Beads were resuspended in 75 µL of sample buffer (NuPAGE® LDS Sample Buffer (4X), 10 mM DTT) and boiled for 5 min at 95°C before separating protein sample from beads with the magnetic stand in a new tube ready for the SDS-PAGE.

V.2.7. Generation of mutants overexpressing tagged protein

Cassette construction

An overexpressing construct was generated using RcCM coding sequence tagged with HA epitope and the strategy of construction is described in Figure V-4.

Primers with specific extensions corresponding to recombination sites were used to amplify the Ptox promotor, candidate genes, Ptox terminator and

hygromycin resistance gene together with its promoter and terminator using Phusion taq PCR. The cassette with HA tag was generated by amplifying the candidate gene with specific extensions and HA sequence on the primer. Cassettes were assembled by YRC and screened as previously described for KO cassette generation.

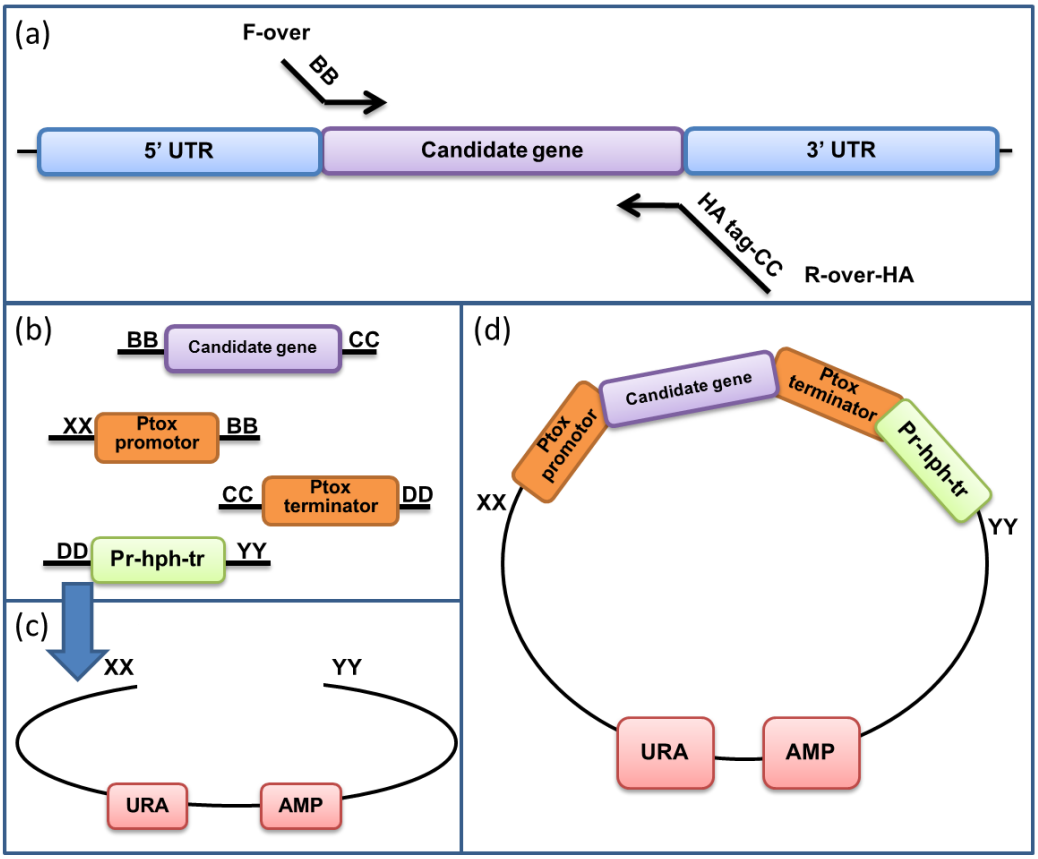

Figure V-4: Construct strategy for overexpressing HA epitope version of RcCM.

Precipitation of fungal secreted proteins

Transformed *R. commune* stains were grown for seven days in 10 mL YNB at 17°C shaking at 250 rpm. Fungal debris were removed by centrifugation. 85 µL of 2 % Na-deoxycholate (DOC) were added to the supernatant then vortexed for 1 min. Samples were incubated at room temperature for 15 min before adding 3330 µL 24 % trichloroacetic acid (TCA). Samples were vortexed for 1 min before centrifugation at 12000 x g for 30 min at 4°C. Pellets were washed once by centrifugation with acetone (-20°C) to remove excess of TCA and centrifuged at 12000 x g for 5 min at 4°C. Pellets were solubilised in sample loading buffer for SDS-PAGE before a dot blot.

Infection assay using transformants

Barley leaves were prepared for the inoculation by gently bending the second and/or third leaves of 2 week-old barley plants over a short tray placed upside down used as an inoculation platform standing on the tray parallel to the row of plants and described in more details in the next section. Barley leaves were drop inoculated with 2 10 µL drops of 214-GFP conidia suspension (10^7 spore/mL, 0.1% Tween 20) or transformant colonies conidia suspension (10^7 spore/mL, 0.1% Tween 20). 7 DPI, infected leaf sections were collected for protein extraction and solubilised in sample loading buffer for SDS-PAGE before a dot blot.

V.2.8. Effect of SA treatment of barley on *R. commune* infection

The effect of SA treatment of barley on *R. commune* infection was tested using detach leaf assay method and the alternative "attached" leaf assay. Four days prior treatments, plants were drench-treated with 400 mL of 1 mM SA (Sigma). A control plant tray was set up in the same conditions but drenched with water. Plants were infected with L73a or 214-GFP strain. Infection with 214-GFP strain allowed the monitoring of the growth of *R. commune* using confocal microscopy. Plants were grown in the lab at 18°C or in growth cabinet. (18°C, 16h light/8h dark). Disease was scored on SA treated plants and control plants following this key: 0: no lesion, 1: few necrotic spots in the drop inoculation region, 2: 50% of the drop inoculation region necrotic, 3: 100% of the drop inoculation region necrotic, 4: necrosis spreading out of the drop inoculation region. Samples were collected throughout the time course to study the expression of SA-related barley genes and SA-related *R. commune* putative effectors.

V.2.9. Real-time RT-PCR of SA related genes and barley reference genes

Elongation factor, tubulin A, ubiquitin and actin were chosen as endogenous controls during infection according to McGrann et al. (2015) and Ferdous et al. (2015). Real-time primers for SA-related genes and reference genes were found in the literature or designed manually (McGrann et al. 2015) (Table V-2).

Primer efficiency was calculated for each primer pair including *R. commune* primers previously described using a slope of a standard curve generated using a 4-point serial dilution of mixed cDNA sample ($E = 10^{(-1/slope)-1}$).

Table V-2: Primers used for transcriptional analysis.

Gene name	Primer name	Primer sequence 5'-3'
Actin	FHV-actin	agccacactgtgcccatttat
	RHV-actin	cagcgagatccaaacgaagaa
Elongation factor	HvEF1aF	atgattcccaccaagcccat
	HvEF1aR	acaccaacagccacagtttgc
Tubuline A	HvTUBAF	agtgtcctgtccacccactc
	HvTUBAR	agcatgaagtggatccttgg
Ubiquitine	HvUbiquitinF	gccgcaccctcgccgactac
	HvUbiquitinR	cggcgttggggcactccttc
PR1 (pathogenesis-related protein 1)	HvPR1F	agcacgaagctgcaggcgta
	HvPR1R	tctcgtccacccacagcttcac
PR3 (pathogenesis-related protein 3)	HvPR-3F	agttggccttgacaagaagcg
	HvPR-3R	cgcataacgtcaaggacgaag
PR5 (pathogenesis-related protein 5)	HvPR5F	ggagcttctccatcacgaac
	HvPR5R	gctgcaagctttggtcttg
PAL (phenylalanine ammonia lyase)	HVPalF	ttcgcatacgcagatgaccc
	HVPalR	tgacgtctctacgtcgtgct
ICS (isochorismatase)	HVICSF	aagaagcgcgccaattcatac
	HVICSR	ccccaccaaaccaaccaaca
PBS3: (4-substituted benzoates-glutamate ligase GH3.12)	HVPBS3F	gtacaggcagagcagggtg
	HVPBS3R	gcgccttgtactggttgatg
PBS3: (4-substituted benzoates-glutamate ligase GH3.12)	HVPBS3F2	gcactacgtggtgtactggg
	HVPBS3R2	cctcctccatctccaggcag
PBS3: (4-substituted benzoates-glutamate ligase GH3.12)	HVPBS3F3	acaagggcaccctggac
	HVPBS3R3	gatggagccgtccgcc

V.2.10 Infection of *Brachypodium distachyon* by *R. commune*.

B. distachyon BD21 lines were grown as described by Peraldi et al. (2014). Three weeks old plants were drop inoculated using 10 µL drops of conidia suspension (10^^{7} spore/mL, 0.1% Tween 20) and covered with an autoclave bag to maintain high humidity. Plants were kept at 18°C in the dark for the first 24 h after inoculation and at 18°C, 16h light and 8hdack for the rest of the infection.

V.2.11. PCR and agarose gels

Amplification of DNA fragments for yeast complementation

Amplification of DNA fragments to be used for cloning was carried out using Phusion high fidelity polymerase (NEB) following the manufacturer's recipe and

thermocycler condition using primers specifically designed to amplify selected fragments (Table V-3).

Table V-3: Primers used to generate PCR fragments for complementation. Green sequence is specific of the candidate gene. 5' black sequence is specific of the plasmid of integration

Gene	Primer name	Primer sequence (5'-3')
RcCM	F-rccm-com	CTAGTAACGGCCGCCAGTGTGCTGGAATTCATGCATTTCTCAACTCTCCTC
	R-rccm-com	CATAACTAATTACATGATGCGGCCCTCTAGATCATTCCTCACCACAGC

Amplification of DNA fragments for gateway cloning

Amplification of DNA fragments to be used for gateway cloning was carried out using *R. commune* or barley cDNA, Phusion high fidelity polymerase (NEB) following the manufacturer's recipe and thermocycler condition using primers specifically designed to amplify selected fragments (Table V-4).

Table V-4: Primers used to generate PCR fragments for gateway cloning. Green sequences are specific of the candidate gene. 5' black sequence is gateway extension.

Gene	Primer name	Primer sequence (5'-3')
RcCM	CM-spFattB1	GGGGACAAGTTTGTACAAAAAAGCAGGCTTCATGACAGAAACAAAGGATTGCAACGTATC
	CMRattB2	GGGGACCACTTTGTACAAGAAAGCTGGGTTTCATTCCTCACCACAGCC
	CM-stRattB2	GGGGACCACTTTGTACAAGAAAGCTGGGTTTTCCTCACCACAGCCCG
RcISC	ISC-FattB1	GGGGACAAGTTTGTACAAAAAAGCAGGCTTCATGGCGAAAACATTTAGAG
	ISC-RattB2	GGGGACCACTTTGTACAAGAAAGCTGGGTTCTAATTAATACTAGAGCTCTTAACCA
HVCM1	F-HVCM1topo	GGGGACAAGTTTGTACAAAAAAGCAGGCTTCATGGAGTTCAAGGTGGCATC
	R-HVCM1topo	GGGGACCACTTTGTACAAGAAAGCTGGGTTGTCCAGCCTCCTTAGCAAG

Amplification of DNA fragments for transformation cassette construction

Amplification of DNA fragments to be used for transformation cassette construction was carried out using Phusion high fidelity polymerase (NEB) following the manufacturer's recipe and thermocycler conditions using primers specifically designed to amplify selected fragments (Table V-5). Ptox fragments and Hygromycin fragment were amplified from pCAM-GFP. The Mcherry fragment was amplified from p74 vector. RcCM was amplified from *R. commune* cDNA.

Table V-5: Primers used to generate PCR fragments for transformation cassette construction. Green sequences are specific of the targeted sequence. 5' black sequences are YRC extensions. Red sequence is the HA epitope sequence.

Target sequence	Primer name	Primer sequence (5' 3')
Ptox promotor	F-Ptox-XX	GGAAGGGCGATCGGTGCGGGCCGTTTAAACgttaacgtcgacggtatcgattgg
	R-Ptox-BB	AGCTCCGGCACCAGCACCGGCACCAGCTCCCATggactatattcattcaatgtcagctatcgc
Ptox terminator	F-term-CC	GTATTCGTTAACTGTTAATTCATGACACAAGTAAAGCGGCCGCCCG
	R-term-DD	CGTAGAACTGGTTTGACTGTTTGACACTAActcatgtttgacagcttatcatc
Hygromycin +promotor and terminator	F-p-hph-t-DD	TTAGTGTCAAACAGTCAAACCAGTTCTACGACCGTCGACGTTAACTGATATTGAAG
	R-p-hph-t-YY	TGGAATTGTGAGCGGATAACAAGTTTAAACGATCACAGGCAGCAACGCTC
mCherry Tag	F-mch-AA	GTATCTCTCGAGAAAAGAGAGGCTGAAGCTatggtgagcaagggcgagg
	R-mch-CC	TTGTGTCATGAATTAACAGTTAACGAATACctacttgtacagctcgtccatgcc
RcCM	F-overCM-BB	GGAGCTGGTGCCGGTGCTGGTGCCGGAGCTATGCATTTCTCAACCCTCCTC
	R-overCM-AA	AGCTTCAGCCTCTCTTTTCTCGAGAGATACTTCCTCACCACAGCCCG
	R-over-CMHA-CC	TTGTGTCATGAATTAACAGTTAACGAATACAGCGTAATCTGGAACATCGTATGGGTATTCCTCACCACAGCCCG

Amplification of DNA fragments for mutant screening

Amplification of DNA fragments to be used for *R. commune* mutant genotyping was carried out using Phire polymerase (Fisher Scientific) following the manufacturer's recipe and thermocycler condition using two pairs of primers: one specific for the transformation cassette and one specific for actin for DNA quality control (Table V-6).

Table V-6: Table of primers used to screen for overexpressing mutant cassette integration.

Target sequence	Primer name	Primer sequence (5'-3')
Actin	Act fw 70	GGGACGACATGGAGAAGATCTGG
	Act rv 70	AGCTCGTATGACTTCTCCAAGCTGG
Cassette	BB fw	GGAGCTGGTGCCGGTGCTG
	DD rv	CGTAGAACTGGTTTGACTGTTTG

V.3. Results

V.3.1. Sequence similarity of RcCM and RcISC to proteins from other fungal species

RcCM

The RcCM protein sequence was analysed in order to identify conserved domains using NCBI Conserved Domain Search website and a chorismate mutase type II domain was detected (pfam01817, E-value=3.53e^{-17}) (Figure V-5). An 18 amino acid - long signal peptide was detected using SignalP 4.1 Server .

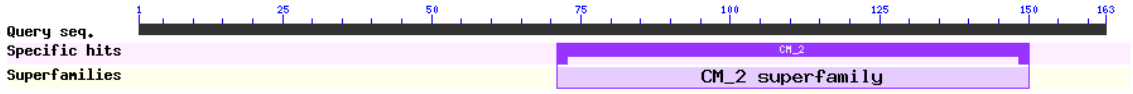

Figure V-5: Diagram illustrating the location of CM domain identified in the RcCM protein sequence.

The RcCM protein sequence was compared to secreted chorismate mutases of different pathogenic species using a BLASTp search. RcCM showed significant similarity to chorismate mutases from *S. sclerotiorum. Laccaria. bicolor, Puccinia graminis, Melamspora laricis* and *Melamspora larici-populina* (Table V-7 In addition, RcCM shares relatively high similarity with *S. sclerotiorum* and *L. bicolor* versions of chorismate mutase over most of the sequence, especially over the chorismate mutase type II domain (Figure V-6). RcCM was also compared to *S. cerevisiae* chorismate mutase version ARO7 but no significant sequence similarity was identified.

Table V-7: Results of comparison of RcCM against homologues from different fungal plant pathogens

Pathogen species	Query cover	E value	Identity
Sclerotinia sclerotiorum	93%	6.00E-64	63%
Laccaria bicolor	93%	9.00E-33	45%
Puccinia graminis	65%	8.00E-21	37%
Melamspora laricis	55%	3.00E-15	34%
Melamspora larici-populina	55%	3.00E-15	34%
Meloidogyne javanica	31%	0.1	25%
Heterodera glycines	35%	0.79	25%
Phytophtora ramorum	7%	6.3	38%

```
L.bicolor          MKLQ----YFLVGLAPFLHSS-LANSKPDFATACYGEVLPNLPAP--PENRTIPWGSPRI        53
S.sclerotiorum     MKFTTISQTLLLAFSPLAISATTPTQVSDPASVCYNSPVPTPSPI--NTNRTIPWGTPSY        58
R.commune          MHFSTLLLP----LMVLATVS-GTETKDCNVSSCYASPLPPLSPLSLTTSRPTPWGKPAF        55
                   *::          :  :   :         .: ** . :*         .*  ***.*

L.bicolor          V-NGSTTCCSSLDEVRTGIDVVDAQLLKLLLY--AKLREATRFKSTHDTVDVPSRDQQVI        110
S.sclerotiorum     TLPNGTTCCDSLDQVRAGINDINAQLVDLLAQRAAYVREATRFKATLGDVNVPSRNQEVI        118
R.commune          TLPNGTLCCDSLTQVRAGINAINAQLVELLAQRAAFVREATRFKRTIDSIDVPARDREVI        115
                   .  ..* **.** :**:**: ::***:.**    * :******* * . ::**:*:::**

L.bicolor          DNAMA--NATAFHLPQTIAKAVFTAIINTSVPFELCVFDSFHYDMEGGKCKRKIL     163
S.sclerotiorum     DGAVALANQTVPRLPEEIARGVFEAIINESVPFEECVWAISS-------------     160
R.commune          EGAVNASRKTEPRLPETIARAVFEAIINASVPFEECVFGESEAGC-----GEE--     163
                   :.*:   . *  :**: **:.** **** ***** **:
```

Figure V-6: Protein alignment of *R. commune* version of chorismate mutase with the most similar chorismate mutase versions from *S. sclerotiorum* and *L. bicolor.*

RcISC

The RcISC protein sequence was analysed looking for conserved domains using NCBI Conserved Domain Search website and a cysteine hydrolase domain containing isochorismatase was detected (cl00220, E-value=1.29e^{-42}) (Figure V-7). No secretion signal peptide was detected using the SignalP 4.1 Server website.

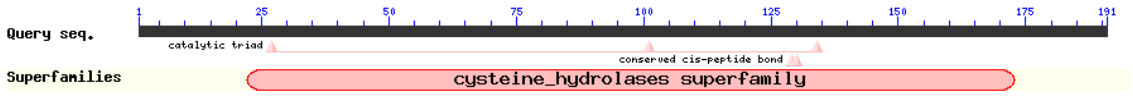

Figure V-7: Diagram illustrating the location of isochorismatase domain identified in the RcISC protein sequence

RcISC protein sequence was aligned against homologous proteins of different fungal plant pathogens (Table V-8). RcISC shares relatively high similarity with all the homologues tested (Figure V-8).

Table V-8: Comparison of RcISC with homologues from different phytopathogenic species.

Species	Query cover	E value	Identity
Marssonina brunnea	100%	4.00E-129	86%
Diaporthe helianthi	100%	4.00E-118	80%
Botrytis cinerea	99%	4.00E-113	77%
Sclerotinia sclerotiorum	99%	1.00E-109	74%
Fusarium oxysporum	97%	1.00E-104	70%
Fusarium graminearum	98%	4.00E-103	70%
Verticillium dahliae	98%	3.00E-97	66%

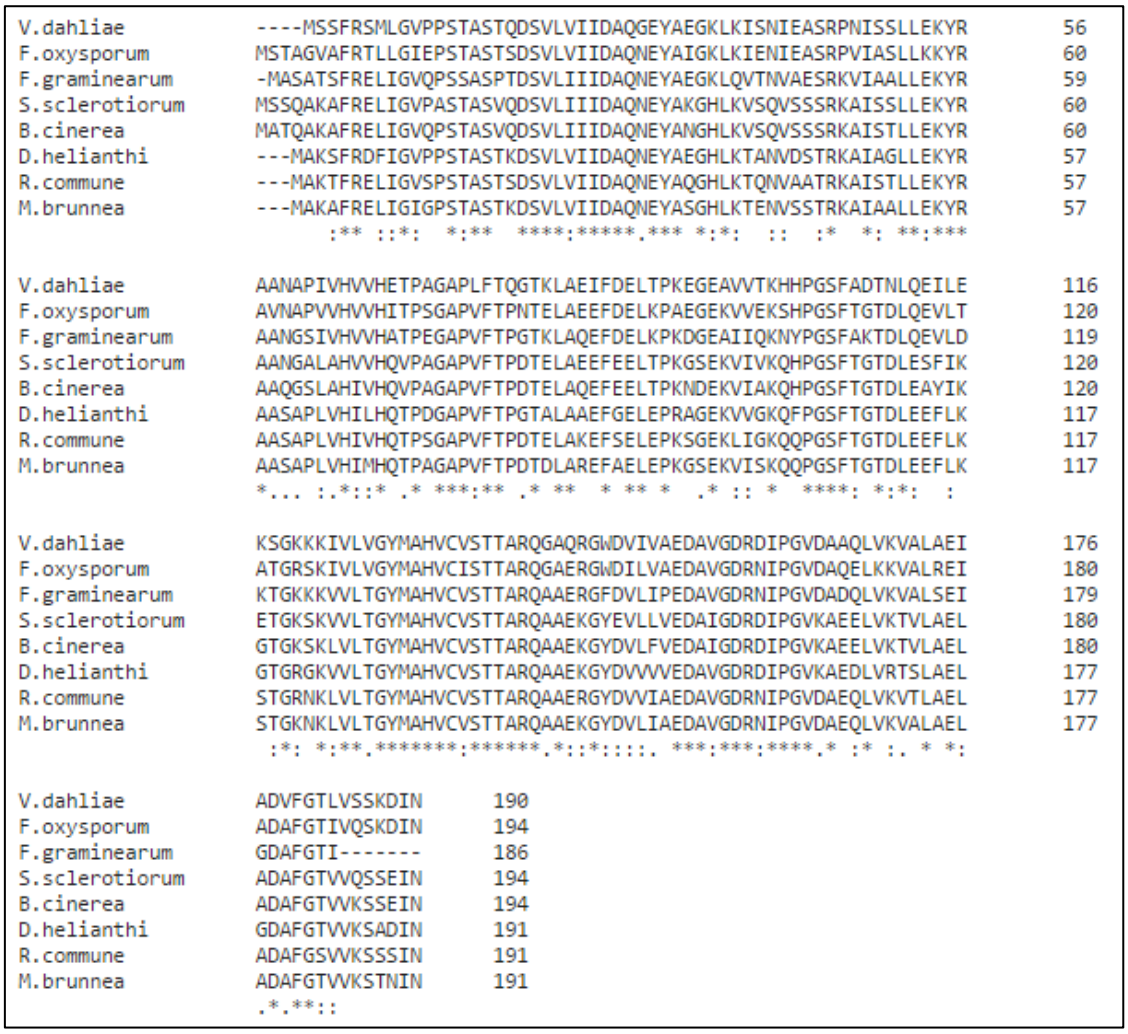

Figure V-8: Protein alignment of *R. commune* version of ISC with the homologues from other plant pathogenic species.

V.3.2. 2. RcCM can function as chorismate mutase in *S. cerevisiae*

Chorismate mutase enzymes are involved in the prephenate pathway necessary for the production of aromatic amino acids: phenylalanine and tyrosine (Figure V-2). Without the chorismate mutase enzyme, an organism cannot produce phenylalanine and tyrosine, so both amino acids must be obtained from the environment. The *S. cerevisiae* strain Δaro7 is knocked out for chorismate mutase and was used to confirm the function of RcCM by complementation. RcCM was cloned into pYES2 and pYES2-RcCM was transformed into Δaro7 to heterologously express RcCM when growing on galactose carbon source. pYES2-ev empty vector was transformed into the WT and Δaro7 as a control.

Five serial dilutions from 10^5 cells/mL of WT-pYES2-ev, Δaro7-pYES2-ev and Δaro7-pYES2-RcCM were grown on rich media (YPD) and appropriate selective media. WT-pYES2-ev successfully grew on all media. Δaro7-pYES2-ev only grew as expected on rich media YPD and selective media supplemented with the missing amino acids, but no growth was observed on media lacking aromatic amino acids. The complemented strain Δaro7-pYES2-RcCM grew on rich media YPD, selective media supplemented with the missing amino acids and selective media with galactose carbon source but not on selective media with glucose carbon source, showing that the induction of pYES2-RcCM by galactose in Δaro7 strain complemented the function of the yeast chorismate mutase aro7 (Figure V-9).

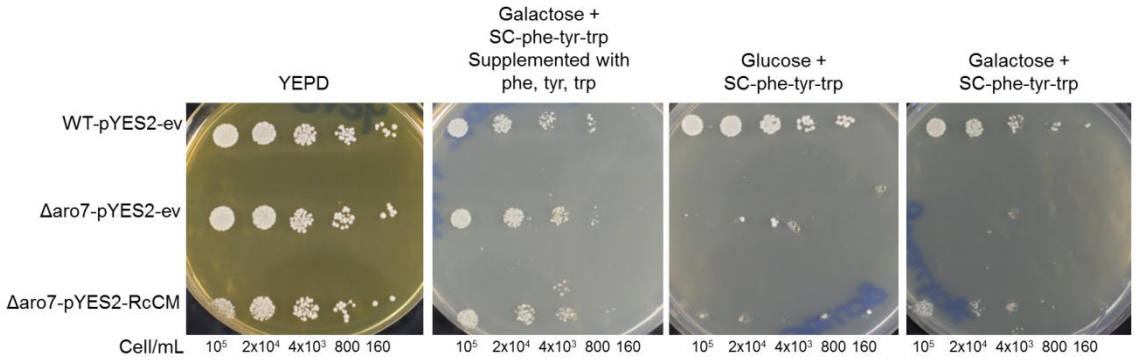

Figure V-9: Complementation of *S. cerevisiae* Δaro7 mutant with *R. commune* chorismate mutase. WT-pYES2-ev, Δaro7-pYES2-ev and Δaro7-pYES2-RcCM strains were grown for 3 days at 30°C on YPD rich media, galactose carbon source selective media lacking phenylalanine, tyrosine and tryptophan but supplemented with amino acid phenylalanine, tyrosine and tryptophan, selective media lacking phenylalanine, tyrosine and tryptophan with glucose carbon source and selective media lacking phenylalanine, tyrosine and tryptophan with galactose carbon source.

V.3.3. The effect of SA on *R. commune* growth *in vitro*

The growth of *R. commune* was observed on CZV8CM agar medium supplemented with 0.1, 0.5, 1, 5 and 10 mM of SA to see if SA has a direct effect on the growth of *R. commune*. The five dilutions of *R. commune* conidia suspension were spotted onto the medium following the map (Figure V-10a). Because SA was solubilised in ethanol prior to mixing with the growth media, the growth was observed on a plate supplemented with ethanol only. The concentration of SA in barley is usually quantified at around 1 nM (Ulferts et al. 2015), but higher concentrations of SA (from 0.1 to 1 mM) did not have any effect on the growth of *R. commune*. However, *R. commune* growth seems to be inhibited on plates containing high concentrations of SA, between 5 to 10

mM (Figure V-10b). SA does not seem to have a direct effect on *R. commune* growth except due to the natural antibiotic effect of the assay at high concentrations.

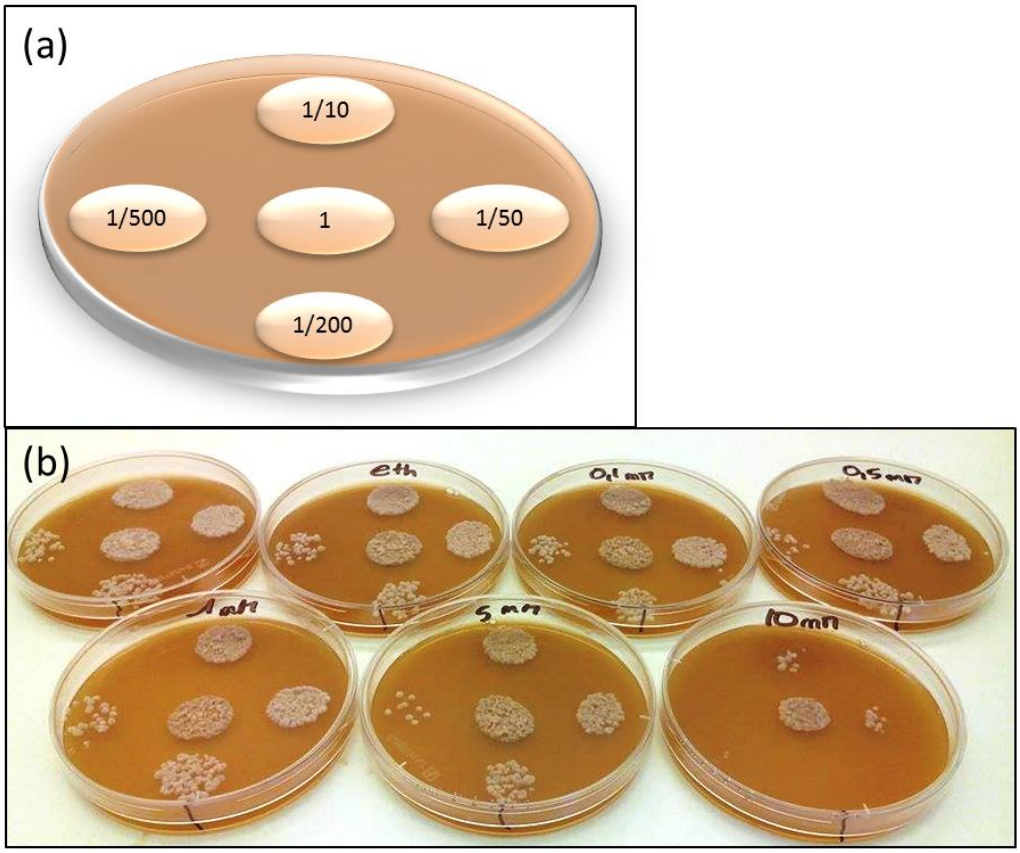

Figure V-10: *R. commune* growth on SA supplemented culture plates. (a) Map of the drop inoculation dilutions. (b) Picture illustrating the growth of *R. commune* on CZV8CM agar medium, CZV8CM agar medium supplemented with ethanol (eth) and CZV8CM agar medium supplemented with 0.1, 0.5, 1, 5 and 10 mM of SA.

V.3.4. Overexpression and subcellular localisation of RcCM and RcISC in *N. benthamiana*

RcCM and RcISC were cloned into different vectors to be overexpressed and tagged with mRFP in *N. benthamiana* using *A. tumefaciens* transient expression. Three expressing constructs were generated: pB7GWR2-sp-CM expressing an N-terminally mRFP-tagged version of *RcCM*, pMdc43-spmRFP-spCM-st expressing the N-terminally mRFP-tagged and secreted version of *RcCM*, and pB7GWR2-sp-ISC-st expressing the N-terminally mRFP-tagged version of *RcISC*.

The subcellular localisation was performed by confocal microscopy and showed that when RFP-CM was directed to the apoplast by secretion using pMdc43-

spmRFP-spCM-st, its subcellular location was comparable to pMdc43-spmRFP-EV vector expression (Figure V-11A,D). mRFP-CM and mRFP-ISC were soluble in the cytoplasm and passively diffused into the nucleus (Figure V-11B,C).

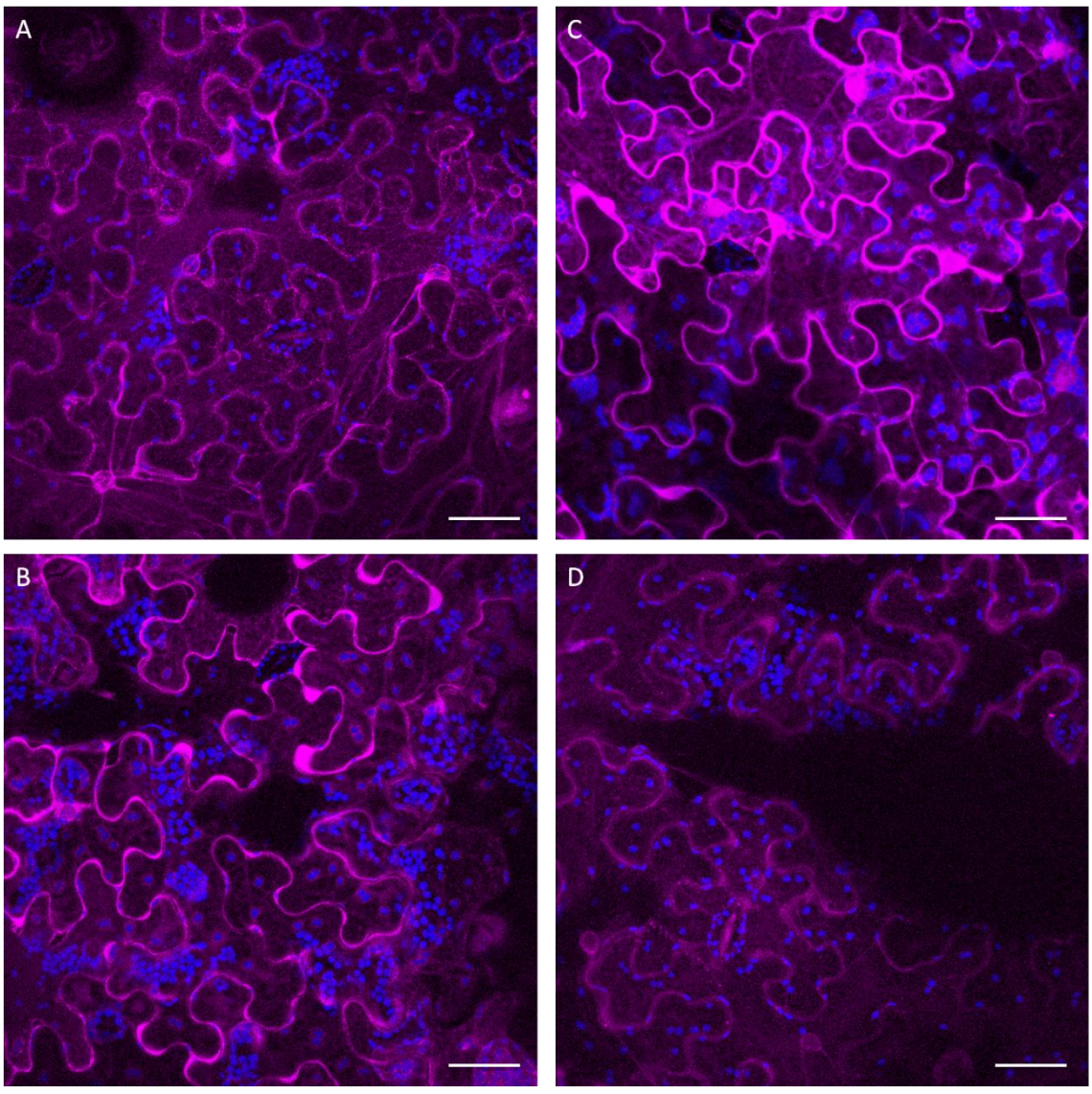

Figure V-11: Subcellular localisation of SA related *R. commune* effector 2 days post infiltration. A: pMdc43-spmRFP-spCM-st expression of RcCMRFP directed to the extracellular compartment (apoplast). B: pB7GWR2-sp-CM intracellular expression of RcCMRFP. C: pB7GWR2 –ISC-st intracellular expression of RcISCRFP, D: pMdc43-spmRFP-EV intracellular expression of mRFP. mRFP and chlorophyll autofluorescence channels are coloured in pink and in blue respectively. Scale bars represent 25 µm.

A Western blot with leaf disc samples collected 2 dpi was carried out to check for the presence of the mRFP tagged proteins. A faint mRFP band was detected in the pMdc43-spmRFP-EV sample but was not detected in the non-functional pB7GWR2-EV sample as expected. RFP-CM and ISC-mRFP were successfully detected as bands of the expected size expressed with pB7GWR2,

but mRFP-CM expressed with pMdc43-spmRFP-sp-CM-st looks slightly bigger than the one expressed with pB7GWR2-sp-CM. This bigger size is due to the linker between the signal peptide and mRFP sequence in pMdc43-spmRFP-sp-CM-st (Figure V-12).

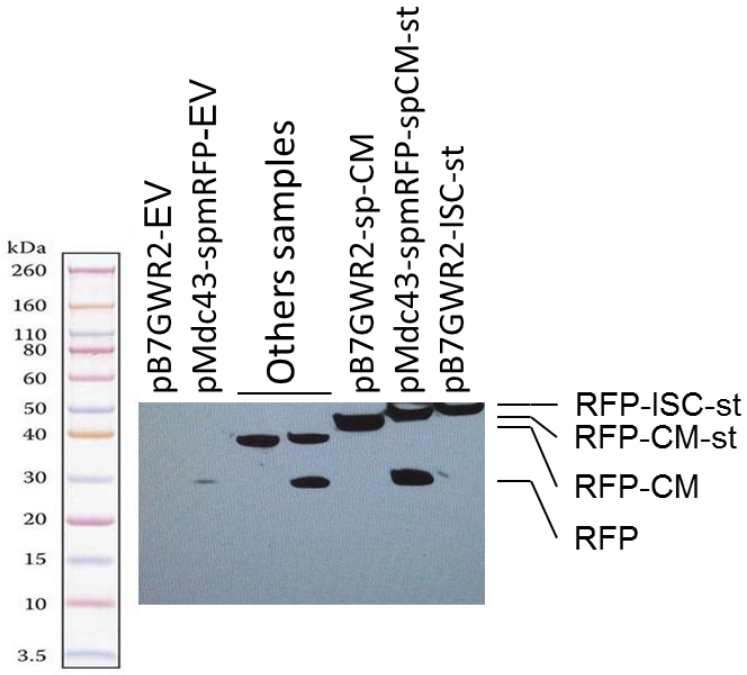

Figure V-12: Western blot using protein extract with RFP tagged proteins. Leaf disc samples were collected 2 days post infiltration with pB7GWR2-EV, pMdc43-spmRFP-EV, pB7GWR2-sp-CM, pMdc43-spmRFP-sp-CM-st and pB7GWR2ISC-st. Proteins were detected using the RFP antibody

V.3.5. The effect of overexpression of RcCM in *N. benthamiana* on infection with *P. infestans* and *B. cinerea*

In order to see whether the RcCM has an effect on pathogenicity, 3 weeks old plants of *N. benthamiana* were spot-infiltrated with an *A. tumefaciens* cell suspension carrying expression vectors. The infiltration was performed as 4 distinct 1.5 cm spots, where on one side the candidate effector was transiently expressed, and on the other side the empty vector was agroinfiltrated, followed by fungal inoculation 24 h after infiltration. If the effector tested has an effect on pathogenicity, the growth of the fungal pathogen may be boosted. With *R. commune* being unable to infect *N. benthamiana*, we tested *P. infestans* and *B. cinerea.* The secreted and the cytoplasmic versions of the chorismate mutase were tested separately with pMdc43-spmRFP-sp-CM and pB7GWR2-sp-CM respectively.

Does expression of RcCM in *N. benthamiana* have an effect on *P. infestans* infection?

Infection successfully took place (Figure V-13a) but no significant difference in lesion size could be observed between the expression of the candidate CM-RFP in the cytoplasm (Figure V-13b) and the secreted version of RFPCM (Figure V-13c) compared to the empty vector control at 7 dpi (t test, n=36).

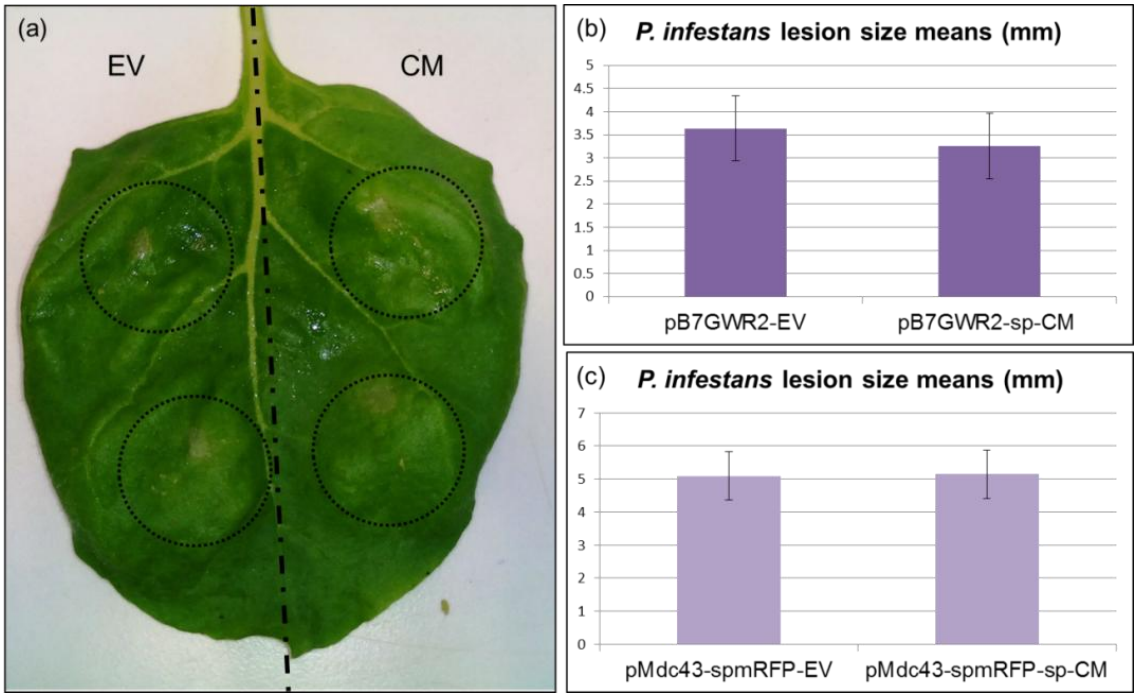

Figure V-13: *P. infestans* boost assay. (a) Picture of *N. benthamiana* spot infiltrated (dash circle) with empty vector on the left side and CM candidate on the right side 7 days post inoculation with *P. infestans* showing greys lesion in the spot inoculation site. (b) Lesion size mean (mm) induced by *P. infestans* on spot infiltration with pB7GWR2-EV and pB7GWR2-sp-CM. (c) Lesion size mean (mm) induced by *P. infestans* on spot infiltration with pMdc43-spmRFP-EV and pMdc43-spmRFP-sp-CM.

Does expression of RcCM in *N. benthamiana* have an effect on *B. cinerea* infection?

The infection of *N. benthamiana* with *B. cinerea* was successful and very fast (Figure V-14a): from 3 dpi, lesions started to overlap making the size measurement unreliable. Measurement at 2 dpi showed no significant difference in lesion size induced by the expression of the candidate RFP-CM in the cytoplasm (Figure V-14b) and the secreted version of RFP-CM (Figure V-14c) compared to empty vector control (t test, n=36).

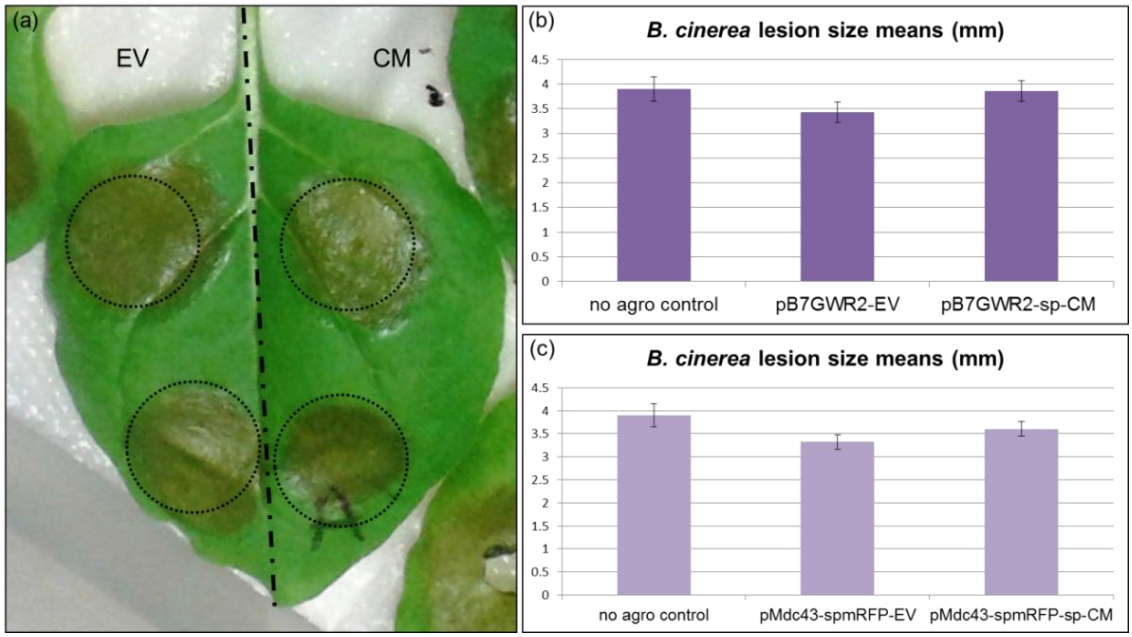

Figure V-14: *B. cinerea* boost assay. (a) *N. benthamiana* leaf spot infiltrated (dash circle) with empty vector on the left side and CM candidate on the right side 4 days post inoculation (DPI) with *B. cinerea* showing brown and shiny lesions in the spot inoculation site. (b) Lesion size mean (mm) induced by *B. cinerea* on spot infiltration with pB7GWR2-EV and pB7GWR2-sp-CM 2 dpi. (c) Lesion size mean (mm) induced by *B. cinerea* spot infiltration with pMdc43-spmRFP-EV and pMdc43-spmRFP-sp-CM 2 dpi.

V.3.6. Study of the dimerisation of RcCM with the barley homologue HVCM1

To be able to determine if RcCM is able to dimerise with the plant homologue as suggested in the study of Djamei et al. (2011) the barley plastid chorismate mutase 1 (HvCM1, accession: EU828765) was cloned into pB7FGW2 and pB7GWF2 vector to overexpress C-terminal GFP-tagged and N-terminal GFP-tagged version of the protein named pB7FGW2-HVCM1-st and pB7GWF2-HVCM1-st.

If dimerization happens, it should occur inside the plant cell so pB7GWR2-sp-CM with the RFP-CM version of *R. commune* was co-expressed with pB7FGW2-EV, pB7FGW2-HVCM1-st or pB7GWF2-HVCM1-st in *N. benthamiana* using *A. tumefaciens*. pB7GW2-RFP expressing free RFP kindly provided by Dr Sophie Mantelin was co-infiltrated with pB7FGW2-HVCM1-st or pB7GWF2-HVCM1-st as a control.

Four DPI after co-infiltration, the expression of proteins and subcellular localisation of expressed proteins was studied using confocal microscopy. All constructs were successfully expressed (Figure V-15). The free GFP was

localised in the cytoplasm and was passively diffusing into the nucleus (Figure V-15a). HVCM1 was localised in the cytoplasm no matter whether it was tagged N-terminally or C-terminally with GFP and was co-localising with RFP-RcCM (Figure V-15b,c).

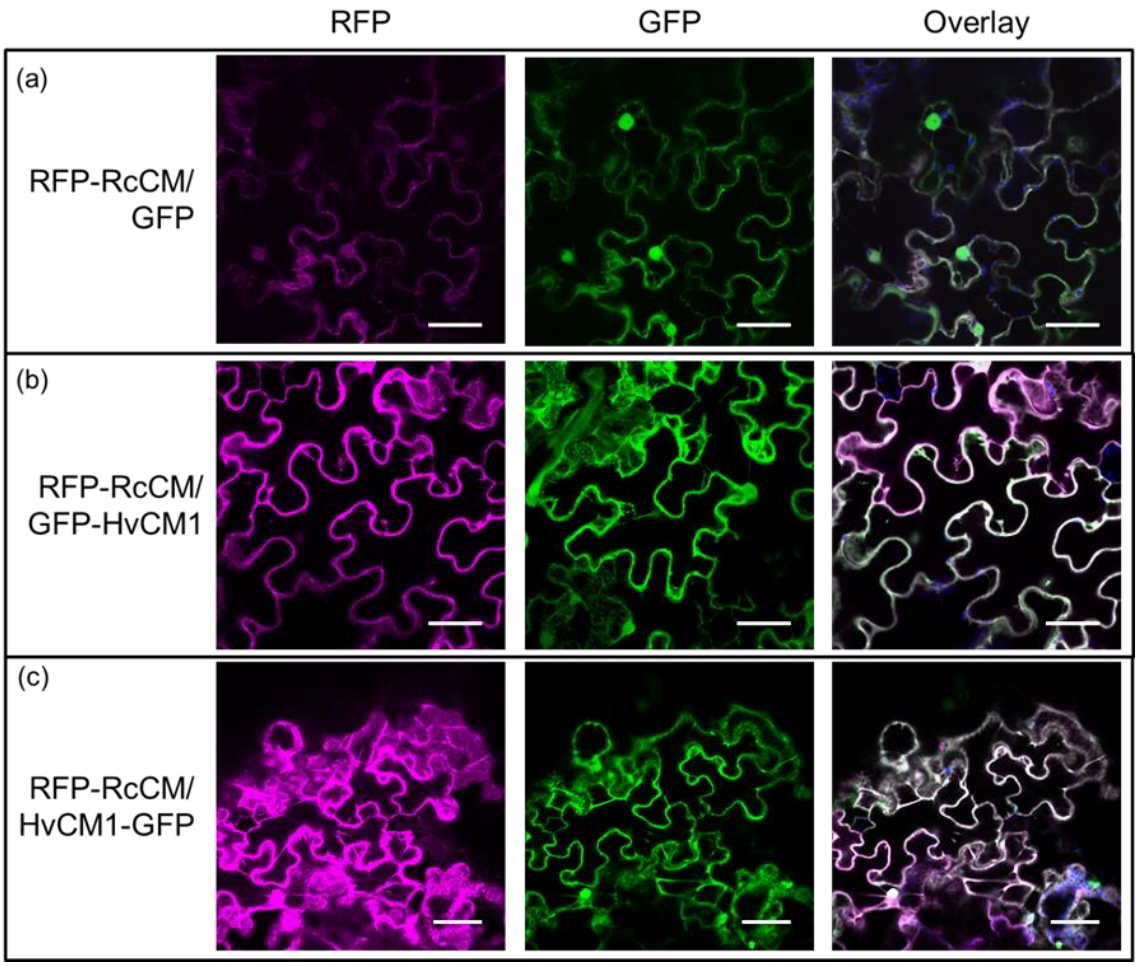

Figure V-15: Subcellular localisation of RcCM and HvCM1 4 DPI. (a) pB7GWR2-sp-CM and pB7FGW2-EV co-expression of RFP-RcCM and free GFP. (b): pB7GWR2-sp-CM and pB7FGW2-HVCM1-st co-expression of RFP-RcCM and GFP-HVCM1. (c) pB7GWR2-sp-CM and pB7GWF2-HVCM1-st co-expression of RFP-RcCM and HVCM1-GFP. RFP, GFP and chlorophyll autofluorescence channels are coloured in pink, green and blue respectively. Scale bars represent 25 µm.

Four DPI, RFP-CM was pulled down from protein extract of co-infiltrated leaves, with the aim of co-precipitating GFP-tagged HvCM. The presence of proteins was visualised by Western blot before immunoprecipitation in input samples and after immunoprecipitation in IP samples. The Ponceau staining of the membrane showed that Input samples had a comparable quantity of protein loaded but the RFP-RcCM/GFP sample was smeary and probably slightly degraded. IP samples showed very weak bands remaining due to pull-down washing which must have mostly retained RFP proteins (Figure V-16a). RFP

and RFP-CM could be perfectly detected in Input sample and in IP samples except for the RFP/GFP-HVCM1 IP sample which showed a very faint band. Adjusting the exposure time of the film to detect protein allows visualisation of different concentrations of proteins. To be able to visualise the presence of GFP on IP sample, the film had to be exposed for a long period involving overexposure for Input samples. In all IP samples, GFP and GFP-tagged versions of HVCM1 could be detected thanks to the long film exposure meaning that the IP did not specifically co-precipitate HVCM1 together with RcCM and that the GFP band was observed due to background. GFP-HVCM1 and HVCM1-GFP versions of GFP-tagged HVCM1 did not have the same size because GFP-HVCM1 does not have stop codon at the end of its coding sequence including an extra peptide on C terminal causing a size difference visible on the Western blot. Another consequence of the overexposure of the film is that GFP and GFP-tagged versions of HVCM1 could not be nicely visualised in Input samples and allowed visualisation of the degradation of the RFP-RcCM/GFP input samples (Figure V-16b).

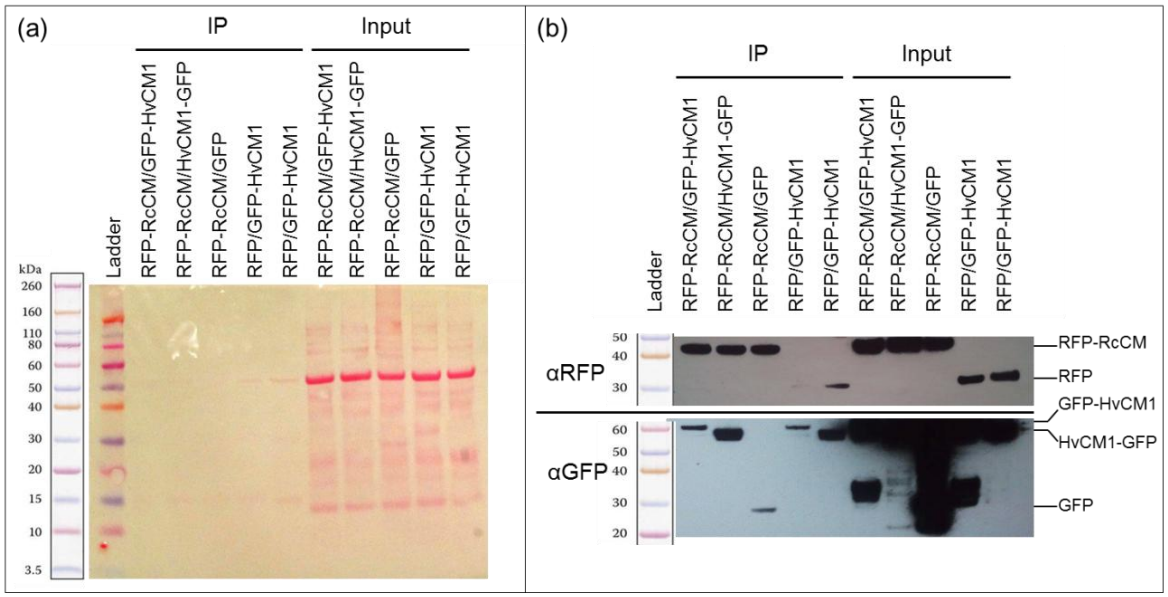

Figure V-16: Co-immunoprecipitation of HVCM1 with RcCM. (a) Ponceau staining of IP samples and Input samples (before IP). (b) Western blotting of IP sample and Input samples (before IP) with RFP antibody or GFP antibody.

V.3.7. Generation of an overexpressing HA-tagged RcCM *R. commune* mutant

YRC allowed the successful generation of a cassette to overexpress RcCM tagged with an HA epitope in *R. commune.* Expressing RcCM with an HA

epitope would help us to follow the localisation of RcCM during the infection and check if RcCM is able to be translocated into the plant cells. The cassette was transformed into *R. commune* and transformants were screened to detect the introduced cassette. The quality of transformant DNA extractions was poor but 4 colonies seem to have integrated the cassette (Figure V-17).

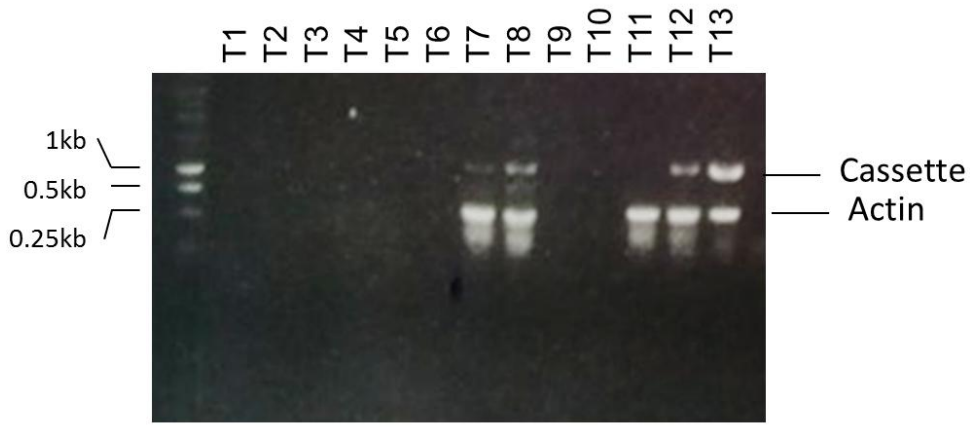

Figure V-17: Testing the *R. commune* transformants for HA-tagged RcCM integration. Actin band with expected size of about 250 bp is used as a control of DNA quality. The expected size of RcCM-HA band is about 800 bp.

The four positive colonies were grown in liquid media and secreted proteins were concentrated from the media to detect the secretion of the RcCM-HA under the control of the constitutive promoter and proteins were extracted from the tissue of *R. commune* positive colonies. In addition, the four positive colonies were used to infect barley plants and infected leaf tissue proteins were extracted to detect the presence of RcCM-HA in plant tissue. RcCM-HA was not detected in the liquid media from the fungal tissue, or from infected plant tissue from any of the positive colonies by dot blot using an HA antibody.

V.3.8. The Effect of SA treatment of barley on *R. commune* infection

Priming is a biochemical and molecular process which enhances plant defence through natural or synthetic chemicals (Conrath et al. 2015). Primed plants respond with faster and stronger activation of defence under stresses and priming provides benefits only under high disease pressure (Walters et al. 2008). Showing that priming barley plants with SA have an effect on the growth of *R. commune* could confirm the presence of a biotrophic phase in *R. commune* interaction with barley and its strategy of using CM and ISC during infection to prevent SA biosynthesis. Indeed, both enzymes could be produced

by the fungus to stop the plant producing SA. Plants were primed by drenching the soil with 1 mM of SA four days prior to inoculation.

A trial was carried out by inoculating detached leaves of plants previously primed or not with SA with *R. commune* 214-GFP strain. The growth of the fungus was monitored by confocal visualisation. No difference of growth could be observed at 5 and 13 DPI between the infection on primed plants and non-primed plants, and all samples appeared highly colonised. Detached leaf assays is a poorly adapted strategy to study the effect of SA priming of barley during infection with *R. commune.*

As an alternative, plants were infected using the attached leaf assay method. Unfortunately, plants grown in the lab were small and stressed due to the lack of light and the infection could not be carried out longer than 6 DPI and no lesions could be observed. However, confocal imaging allowed comparison of the growth of *R. commune* on primed and non-primed plants and a visual difference was observed. On non-primed plants, the fungus largely colonised outside of the dense inoculation spot with mycelial growth following the epidermal cell walls in a rectangular shape (Figure V-18a). On primed plant, the fungal growth was limited and random (Figure V-18b).

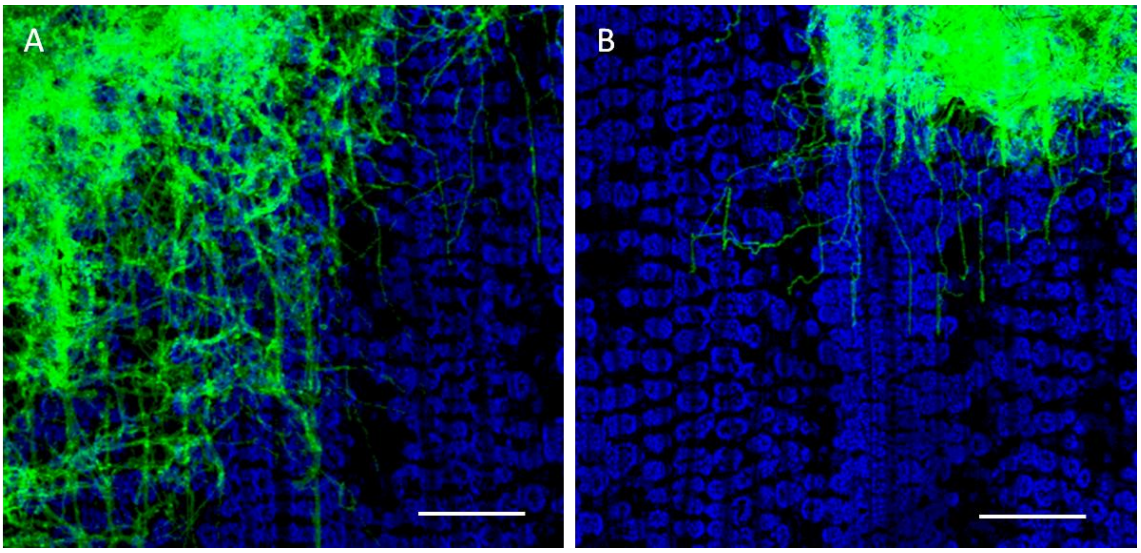

Figure V-18: Effect of SA treatment of barley on *R. commune* 214-GFP strain infection in the lab. Confocal imaging was carried out on infected leaves of barley cultivar Optic plants 6 DPI. A: barley not primed with SA, B: barley primed with SA. GFP and chlorophyll autofluorescence channels are coloured in green and in blue respectively. The scale bar represents 25 µm.

Infection by *R. commune* stain L73a successfully developed on plants grown in a growth cabinet prior to inoculation and lesions started to appear on non-

primed plants from 6 DPI. At 8 DPI, lesions started to appear on SA-treated plants as showed in Figure V-19a. Characteristic lesions started as yellow or light brown coloration at the inoculation point followed within the next day by a brown necrosis surrounded by the yellow/light brown coloration and finally expanding from the inoculation point. Water controls were included in the assay to show that lesions were due to the pathogen and not due to the solution containing detergent. Lesions were scored at 8 DPI and showed a significant difference between plants treated and not treated with SA (t-test, n>65, p=0.004) indicating that *R. commune* L73a development is slowed down in SA-primed plants (Figure V-19b).

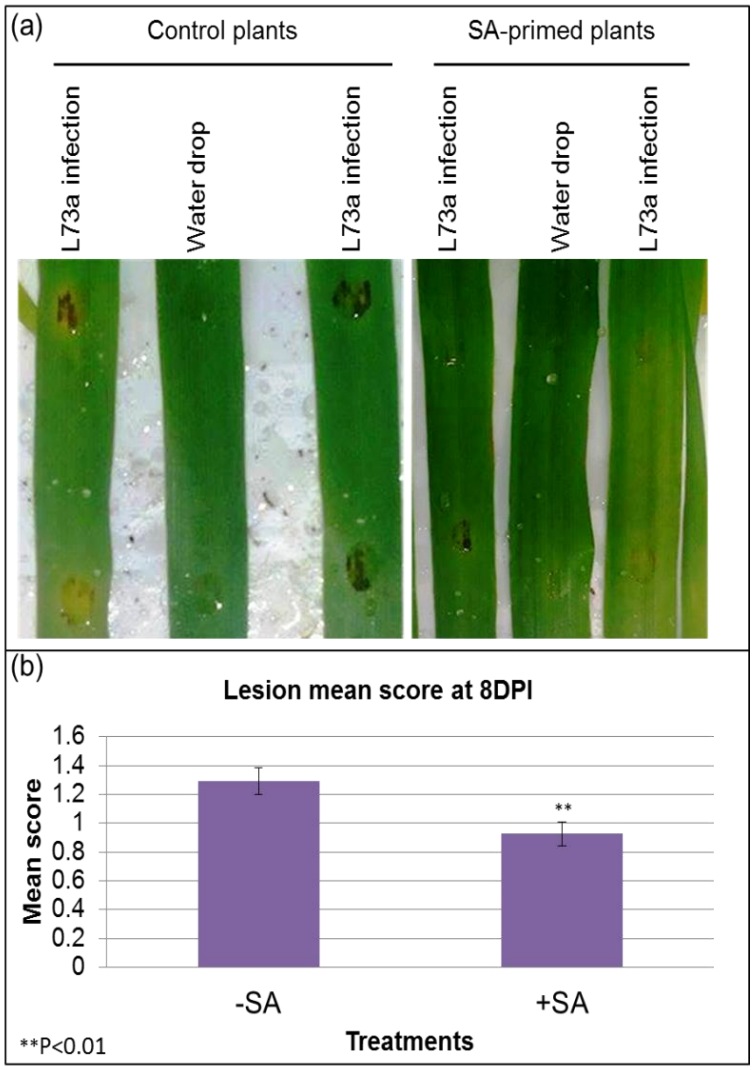

Figure V-19: Effect of SA treatment of barley on *R. commune* L73a strain infection in the lab. Optic plants were grown in a growth cabinet and infection was carried out in the lab. (a) Illustration of a subset of the representative lesions observed at 8 DPI on control plants (not treated with SA) and on plants treated with SA. (b) Plot illustrating the means of lesions observed at 8 DPI on control plants (-SA) and on plants treated with SA (+SA). Error bars represent the standard error.

Infection by *R. commune* strain L73a developed successfully and was very fast on plants grown and infected in growth cabinet compared to plants infected in the lab, as the characteristic lesions started to appear from 3 DPI (Figure V-20a). Lesions were scored throughout the time course and the trend showed that the number and size of lesions was higher on non-treated plants compared to SA-primed plants and showed a significant difference at 7 DPI (t-test: N=64, p= 0.010), indicating that even if the infection was very fast, *R. commune* strain L73a was slowed down on SA-primed plants (Figure V-20b).

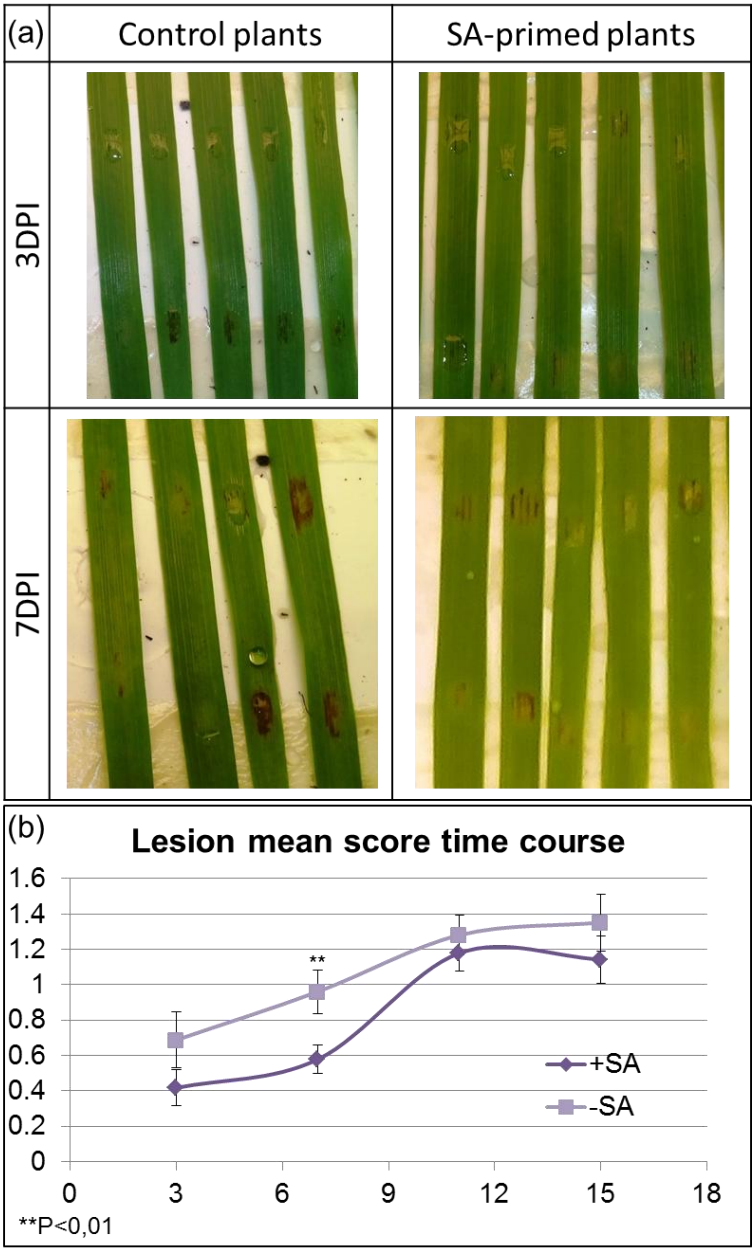

Figure V-20: Effect of SA treatment of barley on *R. commune* L73a strain infection in growth cabinet. Optic leaves were grown and infected in a growth cabinet (a) A subset of the representative lesions observed at 3 DPI and 7 DPI on control plants (Not treated with SA) and on plants treated with SA. (b) Plot illustrating the means of lesions score observed during the time course on control plants (-SA) and on plants treated with SA (+SA). Error bars represent the standard errors.

SA has been shown to have an indirect effect on *R. commune* through barley slowing down the colonisation by the fungus.

V.3.9. Transcriptional analysis of SA-related genes during *R. commune* infection

Primer efficiency was calculated for each primer pair using a slope of a standard curve generated using 4 serial dilutions of cDNA mixed sample ($E = 10^{(-1/slope)-1}$) (Table V-9).

Table V-9: The efficiency of primers used for real time RT-PCR.

	Primer pair	Slope	Amplification factor (E)	Efficiency (%)
Barley genes	**Elongation factor**	-3.31	2.01	100.50%
	Ubiquitine	-3.54	1.92	91.64%
	Tubuline A	-3.51	1.93	92.71%
	Actin	-3.32	2.00	100.00%
	PR1	-3.37	1.98	98.03%
	PR3	-3.79	1.84	83.59%
	PAL	-3.47	1.94	94.17%
	ICS	-3.47	1.94	94.17%
	PBS3	-4.73	1.63	62.71%
	PBS3 (pair 2)	-4.84	1.61	60.85%
	PBS3 (pair 3)	-6.36	1.44	43.66%
***R. commune* genes**	**Actin**	-2.93	2.19	119.48%
	RS5	-2.91	2.21	120.52%
	RS9	-3.10	2.1	110.17%
	RcCM	-2.95	2.18	118.33%
	RcISC	-3.04	2.13	113.08%

A preliminary qPCR time course using samples collected during the assay on plants grown in growth cabinet but infected in the lab allowed to study the expression of SA-related genes *PR1*. The priming effect of SA on *PR1* could be visualised by the significant difference of expression induced by the SA treatment (ANOVA: p= 0.009) from 0 DPI indicating a significant accumulation of transcript and suggested that *PR1* was primed by SA (Figure V-21). Two infected leaf sections were collected from primed and non-primed plants for a qPCR time course. Unfortunately, plants infected in the lab lacked light and the analysis could not be carried during the necrotrophic phase.

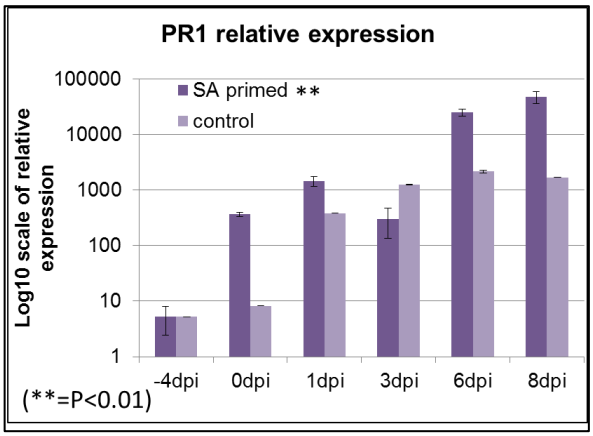

Figure V-21: Transcription profiling of SA-activated barley gene *PR1* during *R. commune* infection in the lab. SA primed indicates that plants were treated with SA by soil drenching 4 days before inoculation; control indicates that plants were not treated with SA. -4 dpi samples were collected on the drenching day before drenching, 0 dpi samples were collected the day of inoculation prior to inoculation, 1 dpi, 3 dpi, 6 dpi and 8 dpi samples were collected 1, 3, 6 and 8 dpi respectively. Error bars represent standard error of biological reps. LOG10 scale was chosen for Y axes to be able to visualise trending in both sets of samples and compare them with each other.

A qPCR time course using sample collected during the assay fully carried in the growth cabinet allowed to study the expression of genes during biotrophic phase and necrotrophic phase. Three leaf sections were collected from 4 different plant conditions: primed infected plants; non-primed infected plants; primed uninfected plants; and non-primed uninfected plants for a qPCR time course. Leaf sections were collected on the day of drenching and D0 as described previously corresponding to the infection day just before infection and 4 days after treatment for the SA effect, at D1, D2 and D3 corresponding to the penetration and asymptomatic phase, D7, D11 and D15 corresponding to the necrotic phase.

The transcription profiling of *PR1* revealed that it was upregulated during barley infection with *R. commune* and priming worked on barley plants, since plants treated with SA have accumulated 12 times more *PR1* than untreated plants prior to inoculation at 0 DPI but differences were not significant due to high biological variability (Two sample t test with treatment as group factor). At 2DPI, significant differences were observed between time course samples and between samples prior to treatment and infection (t test: N=6, p=0.022). At 1 DPI, the upregulation of *PR1* was stronger and faster in plants treated with SA thereby suggesting that priming worked by preparing the plant to protect itself against the pathogen (Figure V-22a). The trend of the graph showed a correlation between the days where the first lesions started to be visible and the peak of *PR1* upregulation, followed by a decrease in upregulation after 3 DPI.

No difference of timing could be observed due to the large variability between the biological repeats and the fact that infection happened very fast (Figure V-20). After the first lesion appeared, marking the end of the biotrophic phase and the start of the necrotrophic phase, *PR1* relative expression totally dropped compared to earlier time points, correlating with the switch of the plant from fighting against a biotrophic fungus to a necrotrophic one (Figure V-22a). In uninfected plants, *PR1* was not upregulated compared to SA-primed plants at 0 DPI confirming that upregulation observed during the infection is due to the fungal stimulus (Figure V-22b).

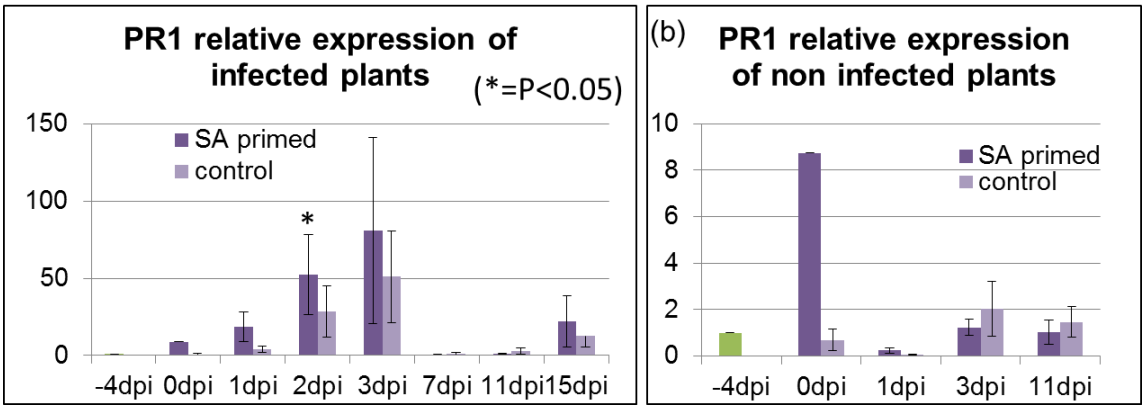

Figure V-22: Transcriptional profiling of SA-activated gene PR1 in infected and uninfected plants growth in a growth cabinet. SA primed indicates that plants were treated with SA by soil drenching 4 days before inoculation; control indicates that plants were not treated with SA. -4 days post inoculation (DPI) samples were collected on the drenching day before drench, 0 DPI samples were collected on the day of inoculation prior to inoculation. Samples were also collected at 1, 2, 3, 7, 11 and 15 DPI. Error bars represent standard errors of biological repeats.

Transcription profiling of *RcCM* showed a significant upregulation during infection compared to conidia and germinated conidia (t test: N=6); more specifically at the first two DPI corresponding to the biotrophic phase of the infection according to the lesion development. *RcCM* upregulation dropped from 3 DPI and slightly increased through the necrotrophic phase. Statistical difference in expression could be observed at 7 DPI between samples primed or not with SA (t test: N;3, p=0.023) and the pattern of the graph indicates that SA could have an effect on the expression of *RcCM* but no significant differences were observed (ANOVA; p=0.083) due to high biological variability (Figure V-23a).

Transcription profiling of *RcISC* showed a significant upregulation during infection compared to conidia and germinated conidia at 3, 7 and 11 DPI (t test: N=6). Statistical differences in expression could be observed at 1DPI (t test:

N;3, p=0.032) and 3 DPI (Two sample t test with treatment as group factor: N;3, p=0.017) between samples primed or not with SA, but high biological variability was observed at other DPI. From 3 DPI, the relative expression of *RcISC* was than in conidia and germinated conidia (Figure V-23b).

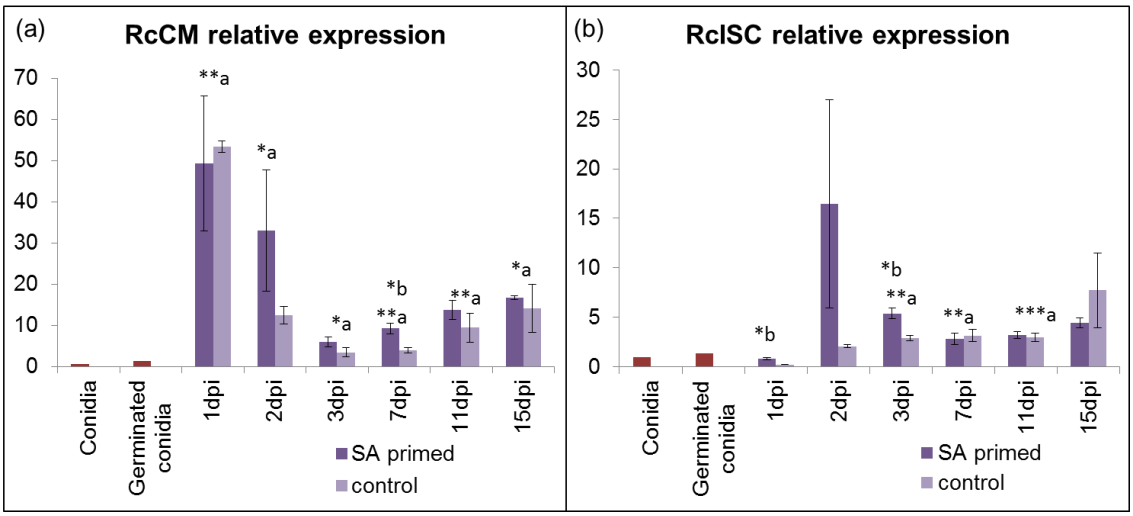

Figure V-23: Transcription profiling of SA-related *R. commune* effector genes during infection of SA-primed plants or control plants. SA primed indicates that plants were treated with SA by soil drenching 4 days before inoculation; control indicates that plants were not treated with SA. Conidia and germinated conidia samples (in red) were used as non-infection condition of expression, time course samples were collected 1, 2, 3, 7, 11 and 15 days post inoculation (DPI) respectively. Error bars represent standard errors of biological repeats. (*a) indicates significant differences between the corresponding time course sample and germinated conidia. (*b) indicates significant difference due to the SA treatment at the same time point. (a) Graph representing RcCM relative expression in SA-primed plants and control plants infected with *R. commune*. (b) Graph representing RcISC relative expression in SA primed plants and control plants uninfected with *R. commune.*

The expression of enzymes involved in the SA pathway (PAL, ICS and PBS3) was studied to see if infection of SA-primed plants was having any effect. PAL, ICS and PBS3 are involved in the 2 different production pathways of SA. PAL, ICS and possibly RcCM - if it manages to get into the plant cells - use chorismate as a substrate. ICS transforms chorismate into isochorimate which is possibly used as a substrate by RcISC - if it manages to get into the plant cells. The role of PBS3 is still unclear but its activity is dependent on isochorismate.

PBS3 transcription profiling could not be obtained as no satisfying primers could be designed.

PAL transcription profiling of infected plants showed a upregulation during the infection compared to prior treatment and infection samples but was only significant at 2DPI (t test; N=3, p=0.043). In addition, SA-primed plants

accumulated more PAL and *ICS* transcript than unprimed plants from 0 DPI in particular at 2DPI where significant difference were observed for PAL (t test: N=3, p=0.049) SA seems to self-prime and retro-control its production through the PAL and ICS SA pathway (Figure V-24a,c). *PAL* upregulation from 1DPI showed faster and stronger in SA-primed than non-primed plants until the time when the first lesions appeared (Figure V-20). During the biotrophic phase, (up to 3 DPI) *ICS* transcription profiling did not show upregulation in infected plants but a down regulation compared to the level of *ICS* before drenching. However, during the necrotrophic phase, the level of *ICS* increased up to the level of *ICS* before drenching and higher (Figure V-24c). No significant upregulation of *PAL* and *ICS* could be observed in uninfected plants (Figure V-24b, d).

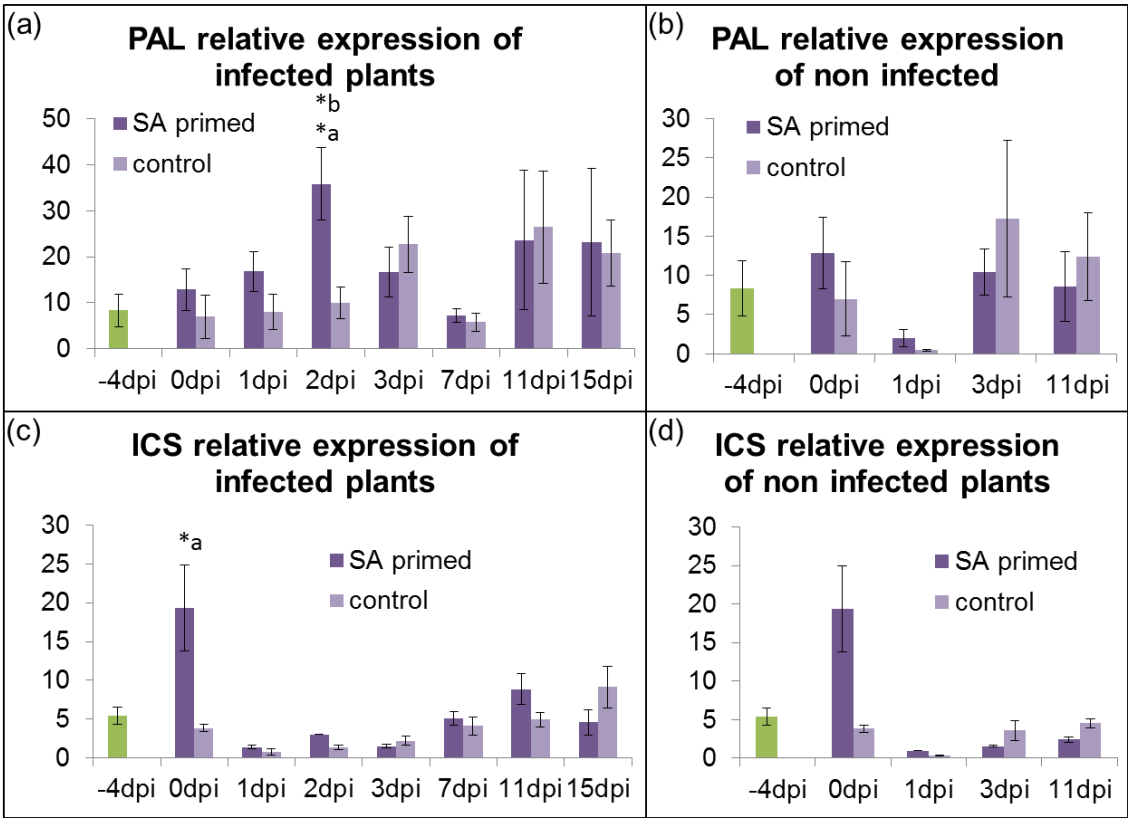

Figure V-24: Transcription profiling of SA pathway genes in *R. commune* infected and uninfected barley plants. SA primed indicates that plants were treated with SA by soil drenching 4 days before inoculation; control indicates that plants were not treated with SA. -4 DPI samples (in green) were collected on the drenching day before drenching, 0 DPI samples were collected on the day of inoculation prior to inoculation. Samples were also collected at 1, 2, 3, 7, 11 and 15 DPI. Error bars represent standard errors of biological repeats. (*a) indicates significant differences between the corresponding time course sample and sample prior treatment and infection. (*b) indicates significant difference due to the SA treatment at the same time point. (a) Graph representing *PAL* relative expression in SA-primed plants and control plants infected with *R. commune*. (b) Graph representing *PAL* relative expression in SA-primed plants and control plants non-infected with *R. commune.* (c) Graph representing *ICS* relative expression in SA-primed plants and control plants infected with *R. commune*. (d) Graph representing *ICS* relative expression in SA-primed plants and control plants uninfected with *R. commune*

The study of relative expression of SA pathway genes did not show a strong upregulation but biological variability was observed in biological replicates. The correlation between levels of expression of SA-related effectors and SA pathway genes was studied using Spearman's Rank Correlation (Table V-10). The higher correlation of 0.93 is observed during the biotrophic phase in SA-primed samples between RcISC and ICS.

Table V-10: Results of Spearman's Rank Correlation score between *R. commune* SA-related effector genes and barley SA-pathway genes

Time points	Samples	*R. commune* genes	Barleys genes	
			PAL	ICS
all time course	all samples	RcCM	-0.02	-0.19
		RcISC	-0.06	0.44
	SA primed	RcCM	0.12	-0.09
		RcISC	-0.05	0.26
	control	RcCM	-0.15	-0.32
		RcISC	0.01	0.53
Biotrophic phase (1-2dpi)	all samples	RcCM	0.06	-0.40
		RcISC	0.46	0.48
	SA primed	RcCM	-0.10	0.17
		RcISC	0.44	0.93
	control	RcCM	-0.38	-0.05
		RcISC	-0.29	-0.05
Necrotrophic phase (3-15dpi)	all samples	RcCM	-0.15	0.38
		RcISC	-0.19	0.05
	SA primed	RcCM	-0.35	0.21
		RcISC	-0.05	-0.35
	control	RcCM	0.12	0.33
		RcISC	-0.24	0.14

V.3.10. Use of *B. distachyon* as an infection model species.

To be able to prove that SA related genes have a role in host plants defences against *R. commune*. it would be interesting to infect barley mutant(s) disrupted for SA-related genes. However, generating barley mutants is an expensive and time consuming procedure. An alternative might be to use *B. distachyon,* a wild grass with a sequenced genome, which is already used as a model species of cereals, including as a pathosystem for infection with Fusarium head blight (FHB), *Oculimacula* spp. and *Ramularia collo-cygni* (Peraldi et al. 2011; Peraldi

et al. 2014).The other advantage of working *B. distachyon* is that it is fully sequenced, has a short stature and a rapid life-cycle (8 to 10 weeks) (Goddard et al. 2014) Moreover, there is a *B. distachyon* T-DNA collection available with annotated accessions which might have a mutant(s) with disruption or transcriptional enhancement in SA biosynthesis pathway genes (Thole et al. 2012). To be able to use *B. distachyon* mutant(s) first of all we need to show that *R. commune* is capable of infecting *B. distachyon*

The *B. distachyon* Bd21 line was infected by drop inoculation with two different strains of *R. commune* (L2A and 214-GFP) and the characteristic lesions of the infection were observed from 3 DPI and are illustrated at 6 DPI in Figure V-25.

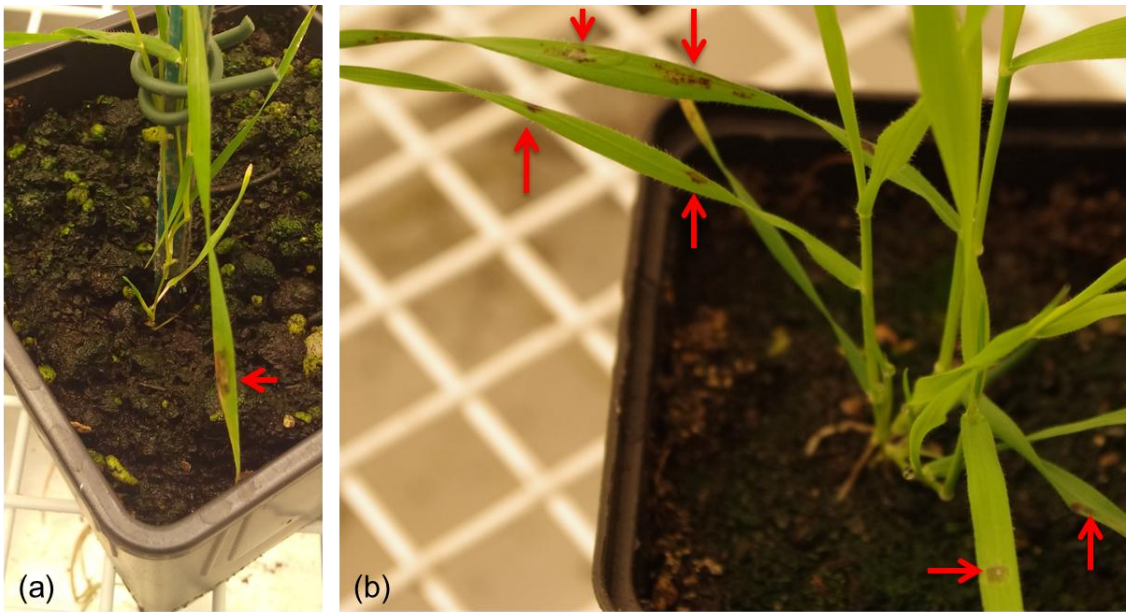

Figure V-25: Infection of *B. distachyon* Bd21 line with *R. commune* at 6DPI. *B. distachyon* leaves were drop inoculated with L2A strain (a) or 214-GFP strain(b). Red arrow indicates the location of the lesion.

The use of the 214-GFP fluorescent strain allowed the investigation to microscopically follow the growth of *R. commune* and infection of *B. distachyon* Bd21 line. At 2 DPI, superficial growth was observed within the inoculation spot (Figure V-26a). Confocal microscopy was coupled with transmitted light to be able to superimpose mycelial hyphae with shapes of barley cells allowing the visualisation of mycelial growth following the epidermal cell walls in a rectangular shape and proving the penetration of the fungus outside of the lesion and confirming the infection (Figure V-26b,c,d).

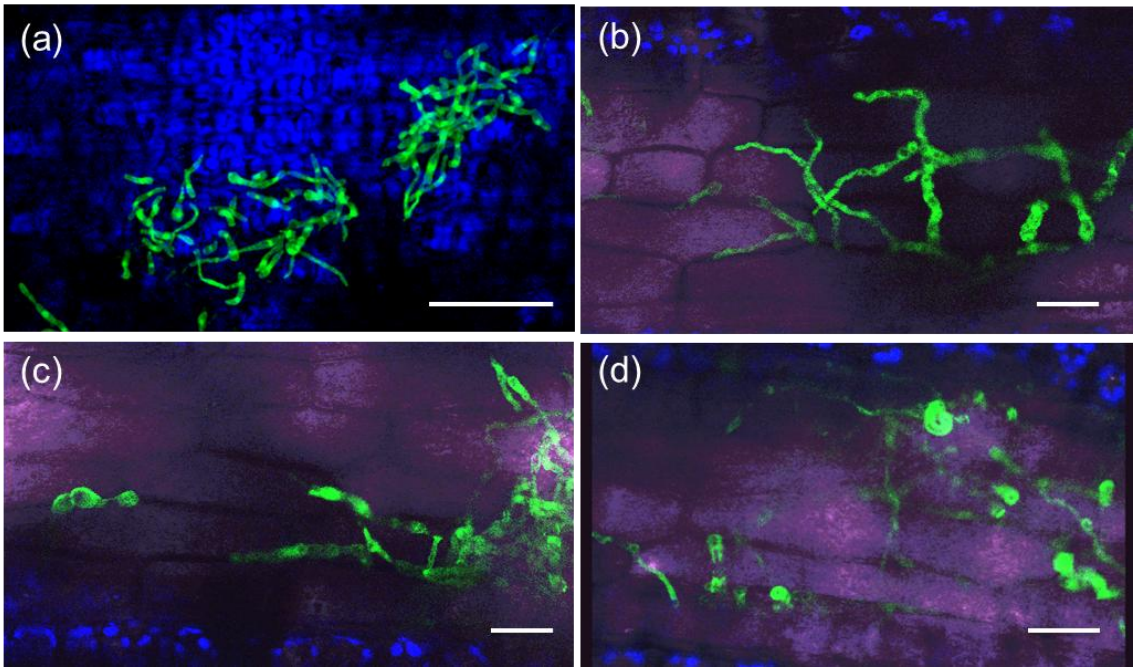

Figure V-26: Confocal microscopy pictures of the infection of *B. distachyon* Bd21 line by *R. commune*. (a) Leaf section infection spot is observed at 2DPI. Confocal microscopy was coupled with transmitted light and leaf sections were observed outside of the lesion at 7DPI (b-c) and 16 DPI (d). The scale bar represents 25 µm.

V.4. Discussion

RcCM

RcCM appeared to be an interesting candidate thanks to its conserved domain matching chorismate mutase, a function conserved among plants, plant microbes and pests (Jones et al. 2003; Djamei et al. 2011). Complementation of the yeast mutant confirmed the chorismate mutase activity of RcCM. However, it could have been a good idea to complement the assay by testing the yeast deleted CM strain complemented with the yeast gene to see the effect of the mutation and transformation on yeast fitness. *RcCM* was also shown to be upregulated during the infection and, in particular, prior to the first visible lesions, marking the end of the biotrophic phase and the start of the necrotic phase indicating that RcCM may be playing a role during the infection.

A. tumefaciens infiltration of *N. benthamiana* leaves leading to transient expression of RcCM in the plant cell or in the apoplast did not trigger visible symptoms microscopically or macroscopically, indicating that the protein is not being recognised by the plant. If *R. commune* manipulates the shikimate pathway through the translocation of the protein into the plant cell, the expected subcellular localisation of RcCM could be in the chloroplast (Maeda and Dudareva 2012). The subcellular localisation of RFP-RcCM in *N. benthamiana* indicated that the protein was in the cytoplasm and not in the chloroplasts. The RFP tag could be preventing the protein from localising into the chloroplast. However, plants also have cytosolic chorismate mutase (Maeda and Dudareva 2012) and Djamei et al. (2011) demonstrated that the *U. maydis* secreted chorismate mutase was localised in the cytosol of maize during the infection indicating that cytoplasmic localisation of RFP- RcCM could be real.

The importance for pathogenicity of RcCM could not be confirmed by using *P. infestans* or *B. cinerea* infection boost assays using *A. tumeaciens* transient expression in *N. benthamiana* plants as no change in infection speed was observed due to RcCM. However, the assay could have been complemented by studying the relative expression of SA-activated genes such as *PR1* and *PR3* and measuring the level of SA by HPLC during transient expression and infection to see if transient expression of RcCM was having an effect on SA-

pathway. Moreover, the tag may have caused RFP-RcCM to lose functionality, which would explain the lack of effect seen with RFP-RcCM on the *P. infestans* or *B. cinerea* infection. To check if the protein was functional, it would have been good to complement the yeast chorismate mutase knock-out mutant with the RFP-RcCM version. In the future, the importance for pathogenicity of RcCM could be tested by complementing CL13Δcmu1 *U. maydis* chorismate mutase knock out mutant (Djamei et al. 2011). An increase in pathogenicity would suggest that RcCM is able to be translocated and important for pathogenicity. Alternatively, no change of pathogenicity could indicate that RcCM could not be translocated into the host cell, but the importance for pathogenicity of RcCM could be tested with a synthetic gene containing the *U. maydis* translocation signal and *R. commune* CM domain.

Unfortunately, the lack of stable expression of RcCM using BSMV-VOX systemic expression did not allow the study of the role of RcCM during *R. commune* colonisation of barley. RcCM functional localisation being intracellular, microprojectile bombardments could be an adapted system to study barley *R. commune* interaction since it have been successfully used for transient gene expressions in single epidermal cells of cereal during cereal-mildew interaction (Panstruga 2004). As an alternative, *R. commune* mutants overexpressing RcCM-HA were generated to study the importance for pathogenicity of the candidate effector but no HA tagged proteins could be detected in the fungus, in the culture supernatant or in infected plant tissue. The fungus may not be producing enough protein, or the tagged CM may be too unstable to be detected, or RcCM-HA tertiary structure is preventing the detection though the HA epitope. It would have been good to check the expression by transcriptional analysis of *RcCM-HA* to be sure that the construct is functional; and to compare the expression of *RcCM* in WT and in *RcCM-HA* mutant to check if *RcCM* is not being silenced by the overexpression of *RcCM-HA*. RcCM-HA mutant strain would have been useful to study the subcellular localisation in the plant of RcCM during infection and to see whether or not *R. commune* is able to translocate effectors into the plant cell to manipulate the plant SA-pathway. It would have been a good idea to test the function and the detection of the HA tagged protein by complementing the yeast chorismate mutase knock-out mutant with RcCM-HA version.

The dimerization of RcCM with the barley chloroplastic homologue HvCM1 could not be proven even though both enzymes seem to localise in the cytoplasm. However, HvCM1 should have localised in the chloroplast, so it is possible that there were alterations of its function and conformation by the GFP tag preventing the translocation into the chloroplast. Moreover, according to the localisation of RFP-RcCM in *N. benthamiana*, it would have been more appropriated to study the dimerization with the cytosolic barley homologue HvCM2.

RcISC

RcISC appeared to be an interesting candidate thanks to its conserved domain matching isochorismatase hydrolase, a function conserved among plants, plant microbes and pest and newly identified as playing an important role during *P. sojae* and *V. dahlia* infection (Liu et al. 2014). *RcISC* was upregulated during the infection and in particular prior to the first visible lesions marking the end of the biotrophic phase and the start of the necrotrophic phase indicating that *RcISC* plays a role during the infection of barley by *R. commune*.

A. tumefaciens –mediated transient expression of RcISC in the cells of *N. benthamiana* did not trigger visible symptoms microscopically or macroscopically indicating that the protein was not recognised by the plant. The subcellular localisation of RFP-RcISC in *N. benthamiana* indicated that the protein was in the cytoplasm and not in the chloroplast. The RFP tag could be preventing the protein from localising in the chloroplast. However, PsIsc1 and VdIsc1, *P. sojae* and *V. dahlia* homologues of RcISC were localised in the cytosol of *N. benthamiana* during transient expression indicating that cytoplasmic localisation of RFP-RcISC could be real (Liu et al. 2014).

The importance for pathogenicity of RcISC was not studied and it remains unclear how RcISC could manage to be in the plant cell during the infection as it is lacking a conventional signal peptide and the protein is not predicted to be secreted by *R. commune* or translocated into the plant cell. However, PsIsc1 and VdIsc1 also lack conventional signal peptides but could be secreted by *P. sojae* and *V. dahlia* respectively through a new unconventional pathway (Liu et al. 2014). In the future, it would be good to check the importance for pathogenicity by generating knock-outs or overexpressing *R. commune* mutant

of RcISC. Alternatively, it would be interesting to complement PsIsc1 and VdIsc1 deletion mutants with RcISC to see if its function restores the pathogenicity of deletion strains (Liu et al. 2014).

In the future, the importance for pathogenicity of RcISC could also be tested by using *P. infestans* or *B. cinerea* infection boost assays using *A. tumefaciens* transient expression in *N. benthamiana* plants as done for RcCM complementation by studying the relative expression of SA- activated genes such as *PR1* and *PR3* and measuring levels of SA during transient expression and infection. In addition, the function of the protein could be tested by measuring the hydrolysis of isochorismate into DDHB as described by Liu et al. (2014).

The effect of SA signalling on *R. commune* interaction with barley

R. commune appeared not to be directly affected *in vitro* by SA at a concentration usually found in plants. However, SA seems to indirectly affect the growth and infection of *R. commune* via barley when SA is absorbed from the soil after drenching. This indirect effect of SA was already demonstrated in different plant/pathogen pathosystems such in *N. benthamiana/ A. tumefaciens* and in white clover/cyst nematodes where *N. benthamiana* plants treated with SA prior to infection showed decreased susceptibility due to a decrease of the growth and virulence of *A. tumefaciens* (Anand et al. 2008) and a decrease in the nematode multiplication was observed on white clover plants treated with SA prior to applying the cyst nematode (Kempster et al. 2001).

The fact that SA treatment has a negative effect on *R. commune* via barley indicates that SA-induced defence may play an important role during the infection with *R. commune.* In addition, the study of expression of SA-activated gene, *PR1,* during the infection with *R. commune* and SA treatment showed that *R. commune* itself could induce the activation of SA-activated genes. SA could efficiently prime barley plants, thus confirming the important role of SA during the infection of *R. commune* and as a consequence confirming the biotrophic phase of *R. commune*. Moreover, this hypothesis is supported by a previous study from Walters et al. (2014) who showed that the application of a combination of elicitors ASM, BABA, *cis*-jasmone (CJ)) could significantly control *R. commune* through the up-regulation of the expression of *PR1*. In

addition, the upregulation of SA-activated genes appeared to increase until the first symptoms induced by *R. commune* were visible, indicating a synchronisation between the expression of SA-activated gene, *PR1,* with the biotrophic phase of the infection, which ends with the switch to the necrotrophic phase marked by the first lesions. Indeed, proving the synchronisation between the first necrosis and the switching off of SA-related plant defence activation confirmed the existence of the biotrophic phase in barley interaction with *R. commune* during which barley uses SA to contain the spread of *R. commune* infection.

The study of genes involved in SA-pathways allowed us to visualise whether or not *R. commune* was manipulating SA pathways. *PAL* was slightly upregulated by the infection and seems to be accumulated in SA-primed plants which upregulated the expression of *PAL* faster and stronger than non-primed plants until the time when the first lesions appeared. SA seems to retro-control its own production through PAL SA pathway particularly in combination with infection to activate defence against the biotrophic phase of the fungus.

SA-primed plants seem to have accumulated more *ICS* transcript at 0 dpi than non-primed plants indicating that SA seems to retro-control its production though ICS SA pathway. The infection of *R. commune* does not seem to activate the expression of ICS. However, the necrotrophic phase of the infection shows an increasing upregulation of the level of ISC from the level of ISC before drenching. One hypothesis could be that *R. commune* is not triggering ICS during the infection. The other hypothesis is that *R. commune* could manipulate SA pathway through the down regulation of ICS observed during the biotrophic phase and through upregulation of ICS observed during the necrotrophic phase. Indeed, it is well known that SA provides systemic acquired resistance (SAR), protecting the plant from biotrophic pathogens, while JA protects the plant from necrotrophic pathogens, and synergistic and antagonistic interactions have been observed between SA and JA signalling defence processes (Beckers and Spoel 2006). *R. commune* could be down regulating SA pathways during the biotrophic phase to protect itself and stop its down-regulation of SA pathways during the necrotrophic phase to induce the now-ineffective SA pathway which at the same time represses the JA pathway effective during the necrotrophic stage of the infection. However, *R. commune*

does not need the necrotrophic phase to complete its life cycle and there is no evidence of *R. commune* benefiting from the necrotrophic phase, which indicates that it would be pointless for the fungus to fight against the JA pathway activation (Avrova and Knogge 2012). In addition, due to the antagonistic effect between SA and JA, JA pathway activation is an advantage for *R. commune* which suppresses SA pathway activation, which is demonstrated to be an efficient way to slow down the disease (Thaler et al. 2012).

Interestingly, the expression of the *Rc-ISC* fungal effector and the plant *ICS* are highly positively correlated during the biotrophic phase of infection in SA-primed plants. Theses enzymes could have an antagonistic effect due to the fact that the fungus subverts the plant defence mechanism by diverting chorismate and isochorismate using effector enzymes, thereby slowing down the plant defence pathway. The plant enzyme ICS accumulated due to SA-priming is overproducing isochorismate, thereby forcing the fungus to upregulate the *Rc-ISC* effector enzyme to use the overproduced isochorismate and to slow down the activation of SA pathway. The plant replies to this depletion by upregulation of *ICS* to overproduce isochorismate, again leading to an infinite upregulation fight between barley and *R. commune* for isochorismate level regulation until the start of the necrotrophic phase.

In addition, infection time courses showed that even if SA-priming is slowing down the disease - confirming the importance of SAR to control the disease - infection and symptoms still happen. This result indicated that SAR cannot totally stop the disease. However, the first lesions are associated with the end of the *PR1* and *PR3* SAR marker genes upregulation which is probably advantageous for the fungus, leaving the plants without SAR protection while the front of the infection moves away from the necrotic part of the leaf. This result suggests that *R. commune* benefits from the necrotrophic phase induced by the collapse of epidermal and mesophyll cells thanks to the switching off of biotrophic plant defence that it induces. As a consequence, to protect barley more efficiently against *R. commune*, it would be better to try treating plants regularly with SA, allowing the plants to re-activate SAR even after the first symptoms have appeared. However, Walters et al. (2011) showed that prior infection with *R. commune* compromises the plant’s ability to respond effectively

to elicitors, suggesting that supplementary treatments with SA would be inefficient and could explain why the efficiency of induced resistance in the field remains unproven (Herman et al. 2007).

Interestingly, *R. commune* infection appeared to be compatible with *B. distachyon* and it would have been a good idea to complement the study of SA-pathway interaction by using mutant of SA-related genes from the T-DNA *B. distachyon* library (Thole et al. 2012). However, seeds ordered took too long to arrive and could not be tested.

V.5. Conclusions

The study allowed identification of RcCM and RcISC, 2 effectors possibly involved in SA-pathway manipulation. The function of RcCM was confirmed and both genes were shown to be upregulated during infection indicating that they might have a role during infection. The importance for pathogenicity could not be proven yet but the assays attempted so far will be useful in choosing the most appropriate strategy.

The study of the indirect effect of SA on *R. commune* through barley was a success and showed that SA was an effective way of protecting the plant against *R. commune* by slowing down the disease, thereby suggesting the biotrophic phase of the fungus. In addition, the study showed that SAR marker genes *PR1* and *PR3* were upregulated during infection and until their switching off coinciding with the appearance of the first lesions, even if biotrophic interaction is still happening in the infection front moving away from the necrotic part of the leaf. This result could be evidence showing that *R. commune* manipulates the plant through the induction of symptoms and benefits from the switching off of biotrophic plant defence that induces symptoms. Moreover, a strong positive correlation during the biotrophic phase of infection in SA-primed plants was observed between the Rc-ISC fungal effector and the ICS, suggesting an endless upregulation fight between the plant and the pathogen aiming to regulate the level of isochorismatase, an important substrate of the SA pathway. This indicates that *R. commune* may be able to directly manipulate the SA pathway through RcISC, however it still unclear how RcISC manages to be translocated into the plant cells, and this hypothesis should be investigated..

VI. Chapter 6: Identification of resistance against *R. commune* in a spring barley collection

VI.1. Introduction

The main method of disease control of *R. commune* in the field is through fungicide application. However, *R. commune* is a highly genetically diverse pathogen and has developed insensitivity to previously effective fungicide classes (Avrova and Knogge 2012). Varietal resistance is an effective way of providing protection against initial infection and is another important method of disease control. Major resistance (*R*) genes trigger plant defence responses by directly or indirectly recognising the product of avirulence genes. However, due to the simple genetic architecture of this interaction, major gene-mediated resistance can be broken down after only a short period of commercial cultivation (Newton et al. 2001b; Abang et al. 2006), unless the avirulence gene product is essential to the pathogen. A number of studies have reported partial resistance genes that reduce rhynchosporium severity (Zhan et al. 2008). As these rely on less specific interactions with the pathogen, they are likely to be durable (Poland et al. 2009), but the limited magnitude of their effect means they are unlikely to offer a good level of varietal resistance if used in isolation. The use of resistant varieties carrying polygenic resistance (both major *R* genes and quantitative resistance) with complementary effects to control the disease in the field is the most sustainable and cost effective method of protecting the considerable breeding effort required to identify and incorporate resistance genes into elite varieties. However, the generation of polygenic resistance is not feasible for commercial breeders using only phenotypic selection and, as such, there is a requirement, not only for new sources of resistance, but also for the identification of closely linked markers for marker assisted breeding. Several major resistance genes and quantitative trait loci (QTL) against *R. commune* have already been mapped and were previously described. So far, none of these genes have been cloned.

In recent years, a number of genetic and genomic resources have been developed that make Genome Wide Association Scan (GWAS) methods feasible in barley. This approach allows significant genetic diversity to be sampled in a single experiment, as well as providing high resolution QTL mapping (Waugh et al. 2014a). For example, *Cellulose Synthase-like* genes; important for (1,3;1,4)-β-glucan synthesis significant in brewing and distilling and with positive impacts on human health; could be identified using a GWAS method for (1,3;1,4)-β-glucan content in the grain of contemporary two-row Spring and Winter barleys (Houston et al. 2014). GWAS methods were also used for disease resistance QTLs identification in, for example, Latin American barley germplasm, which allowed the identification of QTLs associated with Spot blotch (caused by *C. sativus*), stripe rust (caused by *P. striiformis* f. sp. *hordei*), and leaf rust (caused by *P. hordei*) (Gutiérrez et al. 2013). So far, no GWAS studies have been carried out for the identification of *R. commune* resistance.

This study describes the use of GWAS approaches to identify mapped and new resistance against *R. commune* in a collection of spring barley elite varieties.

VI.2. Materials and methods

VI.2.1. Germplasm and disease nursery trials

A collection consisting of 660 lines of spring barley (Table IX-1) was tested in field trials in a rhynchosporium disease nursery at the James Hutton Institute, Dundee, Scotland. This collection was collated as part of the IMPROMALT project (BBSRC: BB/K008188/1), and was chosen to represent diversity in current UK elite spring barley thus providing a resource of direct and immediate relevance to UK breeders. Disease assessments were conducted over the course of three growing seasons. For each of the trials, two replicates were sown using a randomized row-column design. Trials were sown as either 1.5 m^2, or 3 m^2 plots using a sowing rate of either 120 or 333 seeds/m^2 respectively (Table VI-1).

Table VI-1 Details of the field trials conducted for the GWAS analyses. Sowing date for each trial is shown along with the timing of sampling/ scoring by both date and growth stage.

Trial	Plot size, m2 sowing rate, (seed/m2)	Date sown	Disease assessment (Growth Stage)			Height assessment (Growth Stage)	Leaf sampling (Growth Stage)
H1413	1.5m^2	15/04/13	14/06/13 (29)	04/07/13 (62)	-	-	-
H1414	3m^2 (333)	11/04/14	05/06/14 (50)	10/07/14 (80)	-	18/07/15 (90)	-
H1415	3m^2	2/04/15	19/06/15	03/07/15	14/07/15	24/07/15	21/07/15

VI.2.2. Data collection and AUDPS calculation

Natural inoculum, present within the trial site (from crop debris built up over several years of field trials) was used for initial infection. To ensure disease establishment and development, overhead irrigation was applied to the trial on alternate days. Visible disease symptoms were assessed according to the method described by Looseley et al (2014). Briefly, plots were scored on a 1-9 scale, where 1 represented complete absence of disease symptoms, and 9 a complete coverage of all leaf surface by lesions. Disease symptoms were assessed 2-3 times per season by Dr Mark Looseley for the two first seasons and by myself during the last season. During the last trial season, leaf samples were collected for assessment of expression of candidate resistance genes. In the 2014 and 2015 trials, height was measured after plants had ripened. The barley growth stage (Zadoks et al. 1974) was recorded at each sampling point

for the first two years. A standardised area under the disease progress stairs (AUDPS) of each plot was calculated for all trials (Simko and Piepho 2012). Details of trials and timing of scores and sampling are provided in Table VI-1.

VI.2.3. Mean estimation using REML mixed models and standardisation

For each trial, individual line means were estimated using GenStat 18 software (VSN International 2011) by comparing different REML mixed models using a GenStat script kindly provided by Dr Mark Looseley. In each case, the fixed model comprised the barley line, and the random model included replicate. For more complex models, additional terms accounting for spatial effects were added to the random model. These included row and column effects as well as a residual term accounting for their interaction. The VSTRUCTURE procedure was used to specify a correlation model for the residual term using either a 1st order autocorrelation or identity structure. REML models were compared using a likelihood ratio test: the simplest model for which there were no significantly better models was used to estimate line means.

Estimated means from each year were standardised following the formula $z = \frac{x-\mu}{\sigma}$ where: x is the estimated mean of the line, μ is the mean of the population and σ is the standard deviation of the population.

Line means, across years, were estimated as combined estimated mean using GenStat 18 software (VSN International 2011) by comparing different REML mixed models as described previously, adding a year effect to the random model corresponding to different rep of each year.

VI.2.4. Statistical analysis of phenotypes

Shapiro–Wilk test for normality testing, correlation test and one way analysis of variance were run using GenStat 17 software (VSN International 2011).

VI.2.5. Genotypes and genetic map

510 of the 660 lines phenotyped in the field for resistance to Rhynchosporium had previously been genotyped using the 9K barley iSelect SNP genotyping platform described by Comadran et al. (2012). Lines are listed in supplementary

Table IX-1. This provided 6549 polymorphic markers amongst the phenotyped lines. SNPs with greater than 20% missing values or a minor allele frequency of less than 5% were excluded from further analysis in order to provide robust marker trait associations. The final marker set used for the GWAS comprised 5060 SNP markers. The map used was a consensus map kindly provided by Dr Bill Thomas made through the R package LPmerge to merge IBSC, PopSeq and BOPA maps into a consensus map (Muñoz-Amatriaín et al. 2011; Mayer et al. 2012; Ariyadasa et al. 2014).

VI.2.6. GWAS

Using GenStat and ISelect markers

Multiple environment association analyses (treating years as environments) were performed in GenStat using estimated line means of field disease and height scores along with the iSelect SNP genotypes of the 510 barley lines. Multiple environment association analyses for candidate QTLs as main effects or QTLxE interactions were performed using the QMASSOCIATION procedure of GenStat 17 using an Eigenanalysis mixed model to correct for population structure. Eigenanalysis uses principal component scores to examine the interrelations among a set of variables (markers) in order to identify the population structure of those variables. Multiple environment association analyses were also performed using the null mixed model for comparison. The VCMODEL option was used to select the best variance/covariance matrix model for environments (years) (this was the compound symmetry model indicating that all the variances and covariances are equal).

Using GenStat and exome capture SNPs

Multiple environment association analyses were performed using estimated line means of field disease scores and 148,770 exome capture derived SNPs from 130 barley genotypes provided by Dr Micha Bayer (unpublished data). Analyses were run individually for the 7 chromosomes as computer power was limiting the full data load on GenStat. Analyses were performed as described using the iSelect markers using Eigenanalysis mixed model.

Using GAPIT on R and ISelect SNPs

Association analyses were performed using the estimated combined (across year) line means of field disease scores and 5065 iSelect SNP data on 480 barley genotypes. Analyses were performed using the GAPIT package (Zhang et al. 2010) on R (Core 2013) both without correcting for population structure and by correcting population structure by specifying the number of principal components (PCs) using the PCA.total parameter. The best population structure correction was chosen based on the detection of significant principal components calculated using GenStat 17. The best population structure correction was also confirmed by observing QQ-plot of the negative logarithms of the p values from the GWAS using the number of PC compared to their expected p value under the null hypothesis of no association with the trait. In other words, QQ plots show the expected distribution of association test statistics across SNPs compared to the observed values. A clean QQ plot should show a solid line matching the null hypothesis until it sharply curves at the end representing the small number of true associations among the set of SNPs. QQ-plots showing low deviation from the null hypothesis indicate that the analysis adequately corrects for structure. QQ-plots sitting under the null hypothesis line indicate over correction.

Using GAPIT on R and exome capture SNPs

Association analyses were performed using the estimated combined line means of field resistance and 148,770 exome capture SNPs data of the 130 barley genotypes. Analyses were performed using the GAPIT package on R without correcting for population structure and by correcting population structure by specifying the number of principal components (PCs) using the PCA.total parameter. The best population structure correction in the 130 exome capture line was chosen based on the detection of significant principal components calculated using GenStat 17 and the iSelect genotyping data. The best population structure correction was also confirmed by observing QQ-plots.

Identification of significant QTL using ISelect data

The Bonferroni correction rejects null hypotheses when p-values are less than α/N (where α is the desired type 1 error rate) and N the number of independent

tests and indicate that the probability of false positives is no more than 0.05 (Glickman et al. 2014). The Bonferroni method with a genome wide significance threshold of 0.05 (and 5060 SNP markers) indicates that markers with a -log10p of greater than 5 are significant (-log10 (0.05/5060)=5.005). The false discovery rate (FDR) is the probability that a null hypothesis is true given that the null hypothesis has been rejected or, in other words, the proportion of false positives. Among tests, for any significance threshold chosen, the false discovery rate is the expected fraction of false positives (Glickman et al. 2014). The threshold was chosen to minimise the likelihood of discarding genuine associations and determining the rate of false positives expected.

The Bonferroni procedure with α=0.05 is considerably limiting the detection of significant associations by putting the threshold of -log10p at 5 for the AUDPS GWAS. This is due to dependent nature and linkage disequilibrium (LD) of SNP markers leading to over-correction when using Bonferroni adjustments which assume that all comparisons are independent. As a consequence, when marker density increases, the Bonferroni correction becomes more and more conservative despite the fact that linked SNPs on a chromosome tend to segregate together in blocks and are not independent (Johnson et al. 2010). Moreover, in the AUDPS GWAS, some associated markers with lower significance co-localised with already mapped resistance indicating that it would be appropriate to reduce the significance. Given that the aim of the analysis was to provide an initial survey of genetic variation in the association panel, a -log10p threshold of 2.9 (corresponding to a FDR lower than 15%) was chosen as compromise for the detection of AUDPS associated QTLs.

The Bonferroni procedure with α=0.05 is successfully allowing the detection of significant association by putting the threshold of -log10p at 5 for the Height GWAS. Markers with a -log10p of greater than 5 corresponding to a FDR lower than 0.1% were chosen as putative associated markers.

Significant marker sequences were used in a BLASTn search against the pseudomolecule sequence data from the Morex genome assembly (Mascher et al. 2016) to identify the physical location of each marker. Individual QTL were identified as multiple co-segregating markers. Associated markers were

considered as representing the same locus if up to 10 Mb or 10 cM apart from each other.

Identification of significant QTL using exome capture data

Due to the large number of SNPs present in the exome capture data and LD between SNP markers, the Bonferroni correction with α=0.05 is considerably limiting the detection of significant association by putting the threshold of -log10p at 6.5. If we use the same significance level as used for the iSelect data, markers with a -log10p of 2.9, the FDR is of 90% and appeared to be poorly adapted and overestimated due to LD. As a consequence, peak observed on the Manhattan plot where studied comparing them to the physical location of previously identified QTL and already mapped resistances.

VI.2.7. Location of previously reported resistance genes

The information for previously published major resistance genes, and other genes reported to affect *R. commune* resistance, along with their flanking markers were used to locate them on the iSelect map used in this study. The markers not represented on the iSelect map were mapped using a BLASTn search against the pseudomolecules from the Morex genome assembly (Mascher et al. unpublished). These positions were used to identify flanking iSelect markers (with known physical positions), allowing genetic intervals to be identified for the current map (Table VI-2).

Table VI-2: Locations of previously reported major resistance genes. Location are reported on the current ISelect map and their physical position. Marker with * are diagnostic markers followed by them physical location in parentheses

Gene	Chr	Reference	Flanking Marker	Flanking iSelect markers (position cM)	Genetic Interval size (cM)	Physical interval location (bp)
Rrs1	3H	(Hofmann et al. 2013)	11_0010-11_0823	BOPA1_11_10005-BOPA1_11_10728 **(57.89-58.84)**	0.95	489,991,522-491,895,585
Rrs2	7H	(Hanemann et al. 2009)	668A17_e11-2_SNP5 *	BOPA2_12_20201-BOPA2_12_31350 **(0.7-1.04)**	0.28	4,280,866-6,314,541
Rrs3	4H	(Grønnerød et al. 2002)	Hvm003-hvm068	BOPA2_12_11077-BOPA1_11_11513 **((50.82-63.69)**	12.87	166,878,536-574,975,817
Rrs4	3H	(Patil et al. 2003)	HVM060-WG940	BOPA1_11_20063-BOPA2_12_30090 **(83.77-94.63)**	10.86	576,629,513-598,143,391
Rrs12	7h	(Genger et al. 2003)	Bmag7-	BOPA1_11_10841- **(7.97-)**	-	13,838,040-
Rrs13	6H	(Abbott et al. 1995)	ABG378-MWG916	BOPA1_11_21032-BOPA1_11_20052 **(9.37-39.83)**	30.46	10,327,213-29,107,331
Rrs14	1H	(Yun et al. 2006)	CHRSTAR-Bmac0213	BOPA2_12_10420-BOPA1_11_20371 **(0-23.3)**	23.3	0-12,990,947
Rrs15 (2h)	2H	(Wagner et al. 2008)	GBM1281-GBM1121	BOPA1_11_21377-BOPA2_12_31284 (8.46-15.48)	7.02	12,212,577-21,581,768
Rrs15 (7h)	7h	(Genger et al. 2005)	-HVM49	-BOPA2_12_20079 **(-136.13)**	-	-647,664,938
Rrs16	4H	(Pickering et al. 2006)	MWG634-scsnp00600	BOPA2_12_31324-BOPA1_11_11136 **(0.7-19.57)**	18.87	639,959-11,733,569
sdw-1	3H	(Malosetti et al. 2011)	BOPA1_11_10867*	BOPA2_12_11338-BOPA2_12_30096 **(118.36-119.08)**	0.72	632,252,063-634,923,676
end 2h qtl	2h	(Looseley et al 2013, 2015)	11_10072-11_10085	BOPA1_11_10072-BOPA1_11_10085 **(149.91-153.82)**	3.91	751,886,745-758,851,137

VI.2.8. *Rrs1* phenotyping

Seedling resistance screens with *R. commune* isolates avirulent on barley lines containing *Rrs1* were performed using spray inoculation and visible disease scoring with strain LfL12F by our collaborators Dr Bianca Buettner and Dr Guenther Schweizer at the Bavarian State Research Center for Agriculture Institute for Crop Science and Plant Breeding. In addition, at the JHI, confocal microscopy with a GFP-expressing *R. commune* strain (214-GFP) was used to complement the spray inoculation phenotyping.

For the confocal assay, 2 seedlings of each selected line were grown at 17°C with 16h of light per day. The second and/or the third leaves of three weeks old seedlings were secured in a horizontal position to allow drop-inoculation. *R. commune* strain 214-GFP (Thirugnanasambandam et al. 2011) was grown on CZV8CM agar medium (Newton 1989) containing 100 µM hygromycin for 18 days at 18°C in the dark. Conidia were collected by scraping the mycelial mat with a spatula, re-suspending conidia in sterile distilled water (SDW), and filtering through a 60µm nylon filter (Millipore). The conidia suspension was centrifuged for 5 min at 1600 x g, the pellet was washed 3 times with 10 ml of SDW and the final inoculum adjusted to 10^6 spores/ml. Leaves of three weeks old seedlings were drop-inoculated at two locations with 10 µl of conidial suspension containing 0.1% Tween 20 (Sigma) and kept in the dark at 100% humidity for 2 days. Following this, plants were grown at 16h of light per day in plastic propagators to maintain high humidity.

Confocal imaging was performed at 11 days post inoculation (dpi) as described in Thirugnanasambandam et al. (2011) on a Leica SP2 confocal microscope using an excitation wavelength of 488nm. GFP fluorescence was imaged between 505 and 530nm and chlorophyll autofluorescence on a separate channel between 650 and 700nm. 17 UK spring barley lines predicted as *Rrs1* or non-*Rrs1* from the GWAS analysis were screened, supplemented by 2 spring barley lines carrying *Rrs1*: Atlas 46 ($Rrs1_{Turk}$, *Rrs2*) and SBCC145 ($Rrs1_{Rh4}$), and non-*Rrs1* cultivar Atlas (Rrs2). Lines were qualitatively differentiated by considering the lines with a mycelial growth following the epidermal cell walls in a rectangular shape to be susceptible and the line with a restricted randomised mycelial growth to be resistant (Looseley et al. 2015).

In addition, a seedling spray inoculation assay using *R. commune* isolate LfL12F (which is avirulent on *Rrs1, Rrs2* and *Rrs13*) was conducted as described in (Schweizer et al. 1995) to assess symptom development. Briefly, four seeds per test line were sown in 6x6 cm² pots. Pots were kept at 18°C for three days during germination and then at 16°C with 16 h light per day. 3 weeks after sowing, plants were spray inoculated with a suspension of 2.5 x 10^5 conidia and kept at 16°C in the dark at 100% humidity for 36 h. Subsequently, plants were kept at 16°C with 16 h light. Symptoms were assessed on a 1-4

scale with 0 representing no visible symptoms, 1 for very small lesions on edge and tip of leaf, 2 for small defined lesions on edge and basis of leaf, 3 for big, confluent lesions on the whole leaf and 4 for total collapse and drying-out of the leaf. 68 UK spring barley lines predicted as *Rrs1* or non-*Rrs1* from the GWAS analysis were screened supplemented by 3 spring barley cultivars carrying *Rrs1*: Atlas 46 ($Rrs1_{Turk}$, *Rrs2*), SBCC154 ($Rrs1_{Rh4}$) and SBCC145 ($Rrs1_{Rh4}$); Retriever winter barley line carrying *Rrs1*; Pelican 1745 winter barley line not carrying *Rrs1*; and Pewter spring barley line carrying *Rrs2*. Inoculated plants were scored at 15 dpi for resistance or susceptibility. Lines with a mean score higher than 1.5 were considered to be susceptible.

In order to improve the resolution of the mapping and identify the *Rrs1* allele detected by the analysis, resistance screens using spray inoculation of seedlings with the LfL12F *R. commune* isolate was performed on extra lines representing a more diverse collection of cultivated barley in order to maximise recombination. 56 Syrian/Jordanian barley landraces were chosen from the JHI barley collection. 9 elite winter barley cultivars were chosen including Retriever carrying *Rrs1* (Table VI-16). The line selection was complemented with lines carrying different allele of Rrs1 such as Atlas46 ($Rrs1_{TURK}$, *Rrs2*), Steudelli (*Rrs1, Rrs3*), Triton (*Rrs1, Rrs15*), Armelle ($Rrs1_{BRIER}$), Abyssinian-B19460 (*Rrs1, Rrs3*), CI11549 (*Rrs1, Rrs4*), SBCC145 ($Rrs1_{RH4}$), SBCC154 ($Rrs1_{RH4}$), CIHO-3515 ($Rrs1_{RH4}$, *Rrs13*).

VI.2.9. *Rrs1* interval and candidate gene identification

Physical locations of iSelect markers were obtained using a BLASTn search against the Morex genome assembly (Mascher et al. 2016). Additional SNPs from across the QTL4 (*Rrs1*) interval were obtained from a subset of 19 lines (which had been phenotyped for *Rrs1* resistance in the previous section) from exome capture and sequencing data (ref., unpublished). These SNPs were plotted in Flapjack (Milne et al. 2010) for haplotype visualisation around the physical location of the mapped marker associated with *Rrs1*. Gene content in the interval surrounding the haplotype was explored using the predicted high confidence gene models from the Morex genome assembly. These gene models were used to classify exome capture SNPs as synonymous or non-synonymous.

VI.2.10. SNP selection for the genotyping of *Rrs1* interval

The full set of exome capture SNPs in the 22 gene interval (from 489116071 to 491851065 bp) containing 19,551 polymorphic SNPs was studied selecting SNPs with polymorphic alleles genotypically differentiating 4 lines predicted to contain *Rrs1* (Beryllium, Brahms, SW_Macsena and Chieftain) from 5 lines predicted not to contain *Rrs1* (Drum, Jive, Aapo, Livet, Optic). Among markers within the interval, polymorphic SNPs between *Rrs1* and non-*Rrs1* lines were selected prioritising SNPs causing a non-synonymous change in annotated genes and SNPs surrounding these genes.

VI.2.11. Genotyping of *Rrs1* interval

156 lines were selected for genotyping of the *Rrs1* region using KASP assays. Among the 156 lines selected, lines carrying different alleles of *Rrs1* were used as controls. Syrian/Jordanian landraces and elite winter barley previously phenotyped for *Rrs1* resistance were chosen for the genotyping assay. In addition, lines were selected from the list of lines used in the GWAS including one that was phenotyped for *Rrs1* resistance supplemented with some extra lines used in the GWAS that were not phenotyped for *Rrs1* resistance but were predicted to carry *Rrs1* by the genotype at the best associated marker SCRI_RS_221644 (identified by the ISelect GWAS). List of lines and features are summarised in Table VI-16. 48 SNPs were selected from previously identified exome capture SNPs based on conserved polymorphism between predicted *Rrs1* and non-*Rrs1* lines, presence in a gene and being non-synonymous and distribution within genes from the interval. LGC Company designed primers for each SNP (Table VI-3).

Table VI-3: Table of primers used for the additional genotyping using exome capture selected SNPs

SNP name and position	F Primer Allele X	F Primer Allele Y	R Primer Common
chr3H_489987690	tctctaatccattttgattagtaccagt	ctctaatccattttgattagtaccagc	caactagtgaaacatttctccctgcttt
chr3H_489992342	gccatggcagggcgcgc	gccatggcagggcgcgg	cggtcgccgaccacctcca
chr3H_489994704	agccaatattttcatttttttatgaaggaaatt	agccaatattttcatttttttatgaaggaaatc	agaagtcataaaggcaggcaaaaccatat
chr3H_490138207	catggttccatgaattgtggtagg	gcatggttccatgaattgtggtagt	atatacttcgaggaggagtatttaaccaaa
chr3H_490140549	aactataccacgcaaagaaccacag	caactataccacgcaaagaaccacaa	caaaagttgtcgttgtgttatagggtgtt
chr3H_490185026	cttagccttatctaaattaactagacattttt	cttagccttatctaaattaactagacattttc	gatgatttttaacacaatatatctcatcat
chr3H_490222293	atcaattccatagttccacacagcc	gatcaattccatagttccacacagct	ggcaatcgagcgagggagtaataat
chr3H_490222504	cgagccagaacgggtaggc	gcgagccagaacgggtaggt	cctgcggcggccagagcat
chr3H_490224135	aatcctccaaaattcttatgaaattccttc	gaaatcctccaaaattcttatgaaattccttt	ggacataagttaggcggctctttgaa
chr3H_490225065	cacattgatacgccaaaccatgac	ccacattgatacgccaaaccatgat	gatggtctttggtctcttggcctat
chr3H_490225164	cccatgaaacaaacgatctcaatgc	ccccatgaaacaaacgatctcaatgt	gtagaggtatgatggtttgcggttgtt
chr3H_490225346	attgtaaaatcagtttcatgtgctcatttg	gtaaaatcagtttcatgtgctcatttt	cgttacagcctcttggctccatttt
chr3H_490226297	attgtagaattgtatttcttatagcccaac	aaattgtagaattgtatttcttatagcccaaa	tctgatatgcctactattctttgcatgttt
chr3H_490226443	gatggaggattaccacgagacga	atggaggattaccacgagacgg	caaaatgtcccctcggaggatcaa
chr3H_490226703	atttgtattagcttaaaatggcctttacg	catttgtattagcttaaaatggcctttaca	aggatttagcagatacgatttcttccgat
chr3H_490226807	acacgacttcgaagtacaatggg	agacacgacttcgaagtacaatgga	atcggaagaaatcgtatctgctaaa
chr3H_490226867	cctgaaaaagcctgctctgcag	atacctgaaaaagcctgctctgcaa	gttatcactctcccagtctcaacga
chr3H_490230968	gagaccgacgttccaaaagattctt	agaccgacgttccaaaagattctc	gcggatgctgaatgcatcaaacaaataat
chr3H_490231420	actaagcctacctagcctaagctt	ctaagcctacctagcctaagctc	catccgatttcaaccatcgttcgcaa
chr3H_490236800	ccacgtgttctataaatcccgcc	ccacgtgttctataaatcccgcg	acggttggcgagcgcccgt
chr3H_490237161	ggcttgcctcttccgccgt	gcttgcctcttccgccgg	gcacatggaatcgttgtaggtgcta
chr3H_490237629	gcaaggcgtggagatggcg	gcaaggcgtggagatggcc	cgctgcagtgctcaaccaatc
chr3H_490238268	gccaataattaacaactcatttgccag	gccaataattaacaactcatttgccac	aaaagaagtatcgatcgagagcaggat
chr3H_490238371	gttagttcaaatctagttttgtcatgctaaa	agttcaaatctagttttgtcatgctaag	aaaactatctattttggagttgccaaa
chr3H_490238420	ttggcaactccaaaatagatagtttta	tggcaactccaaaatagatagttttc	ccgacatctcctcccgtttccaa
chr3H_490238889	atagaacgggtagctgatctgcaa	agaacgggtagctgatctgcac	tctgatgacacctacgattcctcca
chr3H_490238963	cgccgactcgtactgcgga	gccgactcgtactgcggc	tcgcagaagatccccaggc
chr3H_490238966	cagaagatccccaggccagga	gaagatccccaggccaggg	tcagctacccgttctatctcgtc
chr3H_490238990	aggatgggcctcttgtcgtct	ggatgggcctcttgtcgtcc	ctggcctggggatcttctgc
chr3H_490239124	cccctgcccgagaccaaaaac	cccctgcccgagaccaaaaat	cgtgctgtcaggaaagtacagcag
chr3H_490239155	cgtgactttgcaacagggatcg	aacgtgactttgcaacagggatct	cgtgctgtcaggaaagtacagcag
chr3H_490239267	cccgatgagctgccaaacct	cccgatgagctgccaaaccc	gaggggcacttcatcatccgg
chr3H_490239383	gtgcacaaagacccgatcaac	ctgtgcacaaagacccgatcaag	cctggaattcctgacgaagaaggc
chr3H_490239682	tgtgcagccctgtacgtagg	gtgcagccctgtacgtagc	gatagagcatgccagacacacctg
chr3H_490239742	ctggcatgctctatcgggct	ctggcatgctctatcgggcc	cgaaccgtattaaccatatagacc
chr3H_490239753	aaccgtattaaccatatagaccgaact	ccgtattaaccatatagaccgaacg	tttttgccttccaaaacagccgtgc
chr3H_490243554	ctcttaggattttgcttggaaggg	ctctcttaggattttgcttggaagga	ctttgaaagcatacttttcaagtgaaccat
chr3H_490243586	aagggcactaatttatgactatatgcc	aaaagggcactaatttatgactatatgct	ccttcagagctatctttgaaagcatactt
chr3H_490244086	attaatggagagatcacggaggttg	aatggagagatcacggaggttt	accacagcccaaccactatcatctt
chr3H_490244130	gtggtgcattcagctgagt	gctgtggtgcattcagctgaga	actctagtcattgttggacgatctgta
chr3H_490244362	tcaccgtgagccaaaccgact	caccgtgagccaaaccgacc	cacccaaggaagattggtataaactgaat
chr3H_490245953	tgttgtttatactttatacagatacaatagt	gttgtttatactttatacagatacaatagc	tatttcttatggcagatgaaacaagtggt
chr3H_490246041	gggtggtcgatccctccact	ggtggtcgatccctccacc	cttaccacttgtttcatctgccataagaa
chr3H_490246263	gcccgcgacctctttcatgaat	cccgcgacctctttcatgaag	caagaactgcaaaggcggcgacaa
chr3H_490246360	gagccattgggcatgtactcgtt	agccattgggcatgtactcgtg	gcccctctgctagggttttgctt
chr3H_490246975	gggattcttctcggcaattccag	atgggattcttctcggcaattccat	gtcgtcgagatgctggagggta
chr3H_490258429	ggacatcaaagatttttgaaacgctca	gacatcaaagatttttgaaacgctcg	atgtatgtgttcgtagggatgagtgtttt
chr3H_493213107	gtccgccacgtaggaggag	cagtccgccacgtaggaggat	gagaaaagatggtccgggatggaaa

VI.2.12. Leaf sampling for transcriptional analysis

Three resistant (Casino, Chieftain and Westminster) and three susceptible (Aapo, Optic and Steffi) cultivars were selected for field sampling. Six leaves of approximatively 2 cm from six random plants from the same plot were pooled together. Green healthy tissue and infected tissue were collected in different tubes. Leaf tissue from 1 week-old uninfected seedlings of the same line were collected and used as an uninfected control for analysing barley transcript expression.

VI.2.13. RT-PCR assays

RT-PCR were run as previously described using specific primers (Table VI-4). For barley transcript quantification barley actin, tubulin, elongation factor and ubiquitin were used as constitutively expressed endogenous control genes (Table VI-4). For *R. commune* gene expression actin, c-4 methyl sterol oxidase and acyl-CoA desaturase were used as constitutively expressed endogenous control genes. Specific primers for each transcript, and of NIP1, are summarised in Table VI-4.

Table VI-4: List of primers for RT-PCR assays

Gene name	Primer name	Primer sequence 5'-3'
Actin	FHV-actin	AGCCACACTGTGCCCATTTAT
	RHV-actin	CAGCGAGATCCAAACGAAGAA
Elongation factor	HvEF1aF	ATGATTCCCACCAAGCCCAT
	HvEF1aR	ACACCAACAGCCACAGTTTGC
Tubuline A	HvTUBAF	AGTGTCCTGTCCACCCACTC
	HvTUBAR	AGCATGAAGTGGATCCTTGG
Ubiquitin	HvUbiquitinF	GCCGCACCCTCGCCGACTAC
	HvUbiquitinR	CGGCGTTGGGGCACTCCTTC
Transcript a	6tqpcrF	CAACCAGTGGAACGGAGGTG
	6tqpcrR	TGCTCAAGCTGCCTGCTATT
Transcript b	7qpcrF	TGGAATGGAAGCAGAGCACA
	7qpcrR	GCAACCGATGAATTGCCTGT
Transcript c	8qpcrF	GGTTTTCATCGGCTGCTTGT
	8qpcrR	ACCGGTGCTATCGCAGTAAA
NIP1	qpcr-NIP1F	TGCTTGGTTCCTGGGGATTG
	qpcr-NIP1R	TTGGAAGCCATTGCCACCTT

VI.2.14. Candidate transcript PCR and sequencing

Amplification of cDNA fragments was carried out using Phusion high fidelity polymerase (New England Biolabs) following the manufacturer protocol and thermocycler conditions using cDNA template and specific forward primer for each of 3 transcripts and a common reverse primer (Table VI-5). PCR fragment were sequenced using Rt-PCR primers.

Table VI-5: List of primers for transcript amplification

Primer name	Primer sequence 5'-3'	Amplicon size (bp)
Transcript a-F	ATGCCTCCCCTGCTCCTC	1827
Transcript b-F	ATGGCTCACCTACCACCACACTC	1977
Transcript c-F	ATGCCTCTCTTGCCCAGCC	1935
Transcript-R	TCAACTCAAGAGCACTTTTGGTGG	

VI.3. Results

VI.3.1. Statistical analysis of phenotypic data

The collection, collated as part of the IMPROMALT project, representing diversity in current UK elite spring barley was tested over 3 years for resistance to Rhynchosporium and for height in field trials at a Rhynchosporium disease nursery (Table 1).

Analysis of the 3 individual AUDPS estimated means

Rhynchosporium infection developed in each of the 3 years and standardised estimated means distribution was observed (Figure VI-1a). Shapiro-Wilk test for normality was used and AUDPS-2013 and AUDPS-2015 appeared to be normally distributed (p= 0.573 and p= 0.296 respectively) but AUDPS-2014 was not normally distributed (p= 0.042). Correlation between replicates for individual barley lines within each year trial was high (Figure VI-1b) and analysis of variance showed significant variation between barley genotypes ($p < 0.001$) (Table VI-6). A list of lines and standardised estimated means for each year are given in supplementary data Table IX-1.

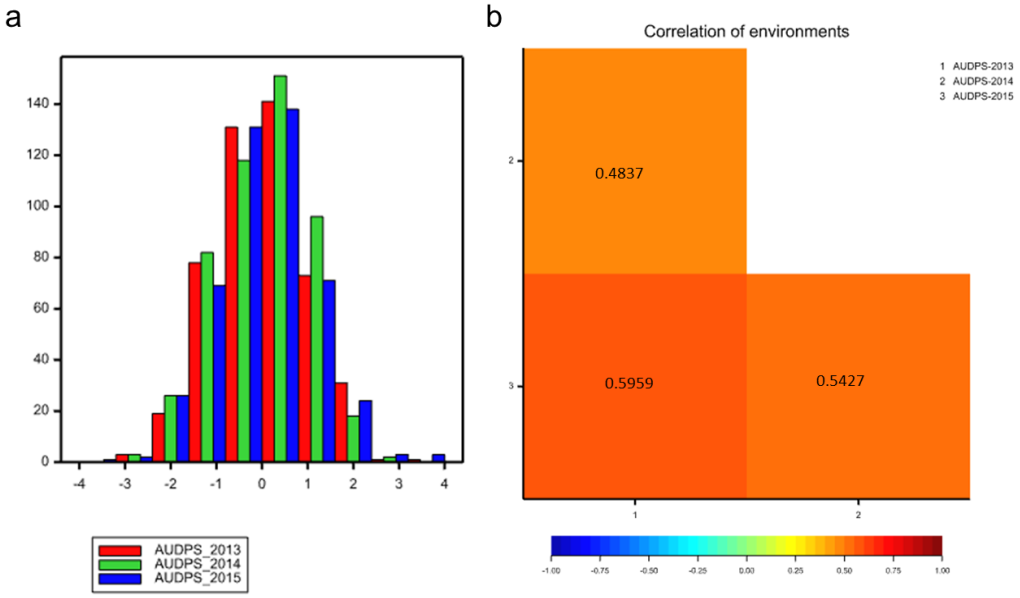

Figure VI-1: Statistical analysis of estimated AUDPS means. (a) Standardised estimated means distribution of the 3 years of data showing distribution of AUDPC-2013, AUDPC-2014, AUDPC-2015. (b) Correlation plot between AUDPC-2013, AUDPC-2014 and AUDPC-2015. The values indicate the correlation score between years tested. The x-axis shows the estimated standardized AUDPS mean and the y-axis shows the number of genotypes with that mean

Table VI-6: Analysis of variance table of the estimated AUDPS between the different genotypes tested. One way design ANOVA was run using the estimated AUDPS as variate and genotype as treatment. d.f.= degree of freedom, s.s.=sums of square, m.s.= means square, v.r.= Variance ratio, F test pvalue.

Source of variation	d.f.	s.s.	m.s.	v.r.	F pr.
Genotype	509	1043.829	2.0507	4.31	<.001
Residual	932	443.1195	0.4755		
Total	1441	1486.949			

Analysis of the combined AUDPS estimated mean

The 3 years combined estimated means showed a normal distribution (Shapiro-Wilk test for Normality p= 0.296) within the population (Figure VI-2). List of lines and their standardised estimated mean across years are listed in supplementary data Table IX-1.

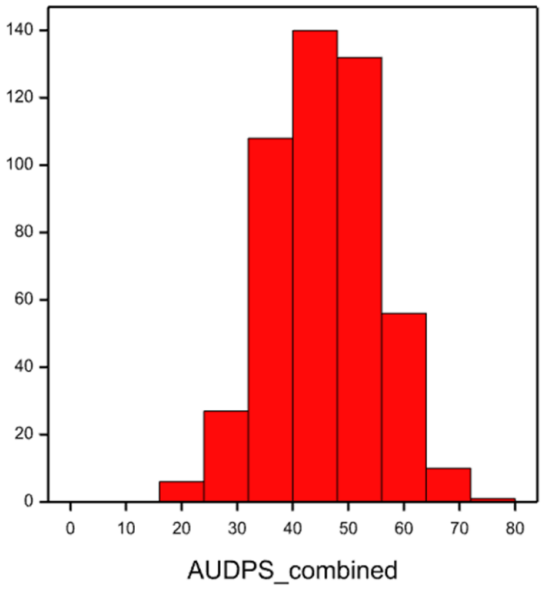

Figure VI-2: AUDPS standardised estimated means distribution showing normal distribution. The x-axis shows the estimated standardized mean combined AUDPS and the y-axis shows the number of genotypes with that mean.

Height phenotype

Height of plot in the field was measured in 2014 and 2015. The estimated standardized means of height showed a non-normal distribution both years (Shapiro-Wilk test for Normality Height-2014 p<0.001 and Height-2015 p <0.001) within the population (Figure VI-3).

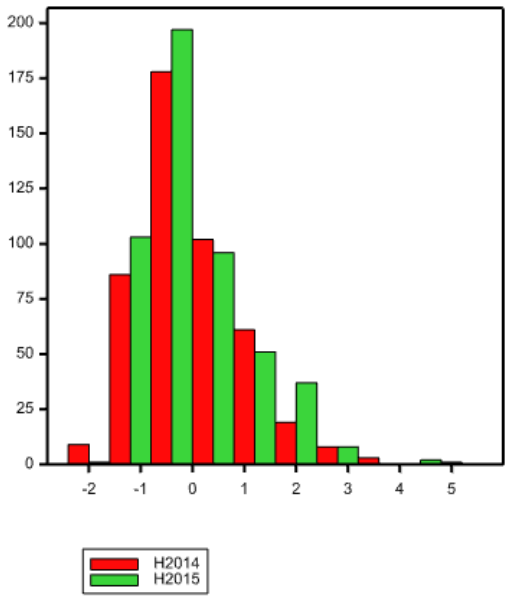

Figure VI-3: Statistical analysis of estimated height means. Height standardised estimated means distribution showing non-normal distribution of Height-2014 and height 2015. The x-axis shows the estimated standardized mean height and the y-axis shows the number of genotypes with that mean.

An attempt was made to improve the distribution of height phenotype by transforming the data and the best result was obtained by transforming at 1/X level with X being the estimated mean (Figure VI-4) and Height-2014 is normally distributed but Height-2015 is not normally distributed despite its improved normal pattern (Shapiro-Wilk test for Normality Height-2014 p=0.204 and Height-2015 p <0.001).

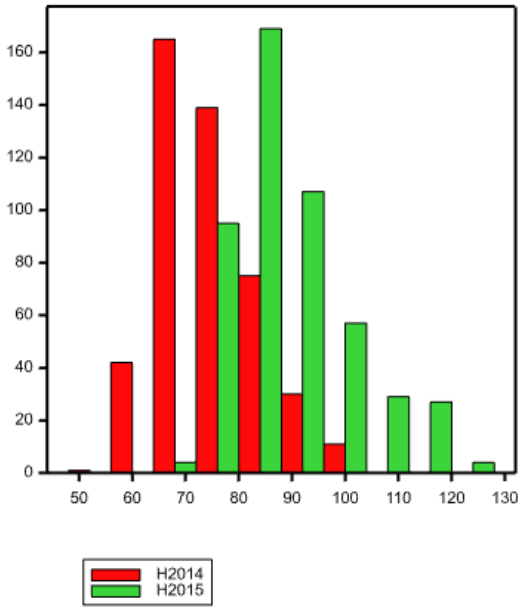

Figure VI-4: Statistical analysis of transformed estimated height means. Height transformed estimated means distribution showing an improved normal distribution of Height-2014 and height 2015. The x-axis shows the transformed standardized mean height and the y-axis shows the number of

A positive high correlation of 0.80 between estimated standardized means of 2014 and 2015 was observed. A list of lines and their standardised estimated mean for each year is listed in supplementary data Table IX-1.

Analysis of correlation between disease and height

Height is already known to be an important factor for disease resistance in previous studies thought to be due to the limited splash dispersion on tall cultivars (Looseley et al. 2015). Analysis of correlation between disease and height revealed a negative and high correlation of -0.3742 and -0.3063 ($p<0.01$ t test) in 2014 and 2015 respectively.

VI.3.2. GWAS using ISelect markers

Identification of the best method to use with the 510 barley genotypes

Multiple environment GWAS performed using the 3 years estimated line means of field resistance and the iSelect SNP data for the 510 barley genotypes was run without correcting for population structure using the null mixed relationship model. The QQ plot showed deviation from the null hypothesis indicating population structure (Figure VI-5) and the Manhattan plot showed high association across the genome (Figure VI-6).

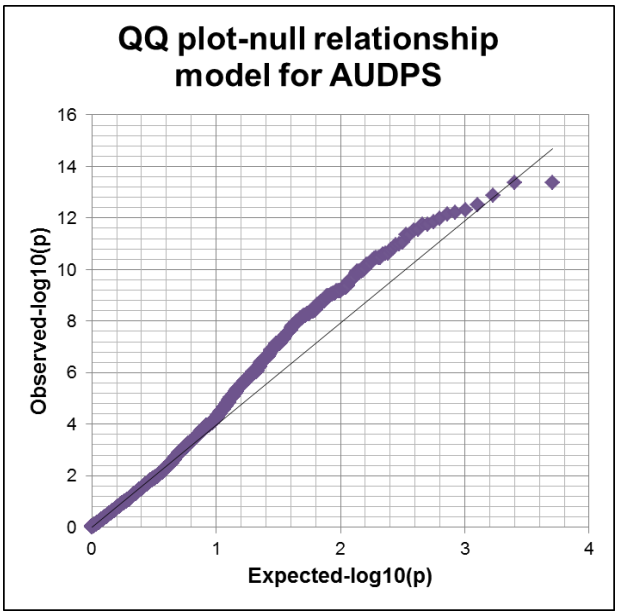

Figure VI-5: QQ-plot of the negative logarithms of the p values from the GWAS AUDPS null relationship. The negative logarithms of the p values (Purple Square) are showing deviation from the null hypothesis (dark line) indicating population structure.

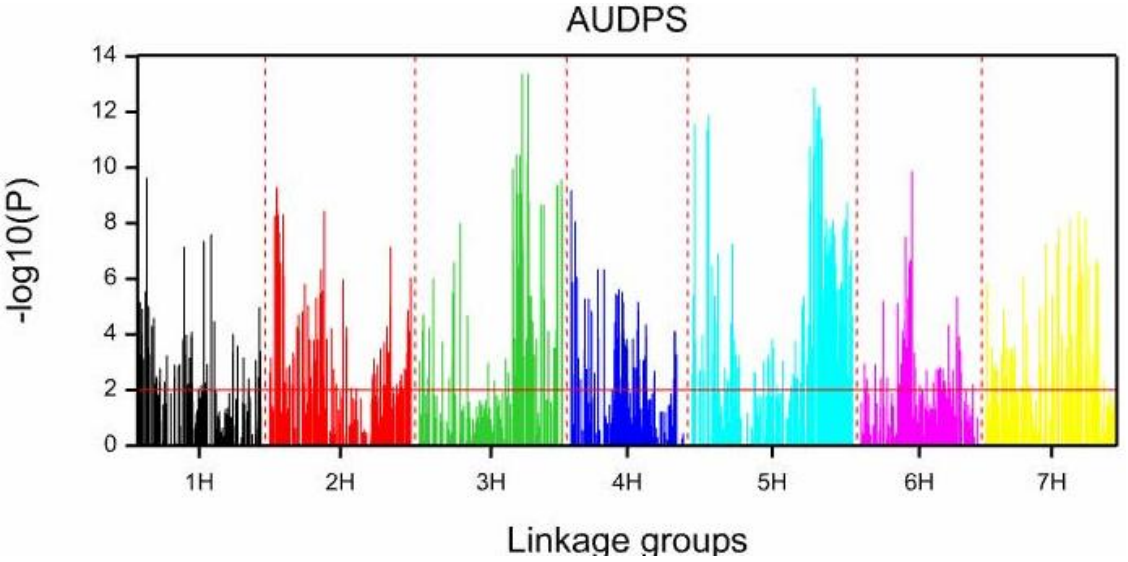

Figure VI-6: Manhattan plots of multi-environment GWAS analysis under null relationship model for AUDPS. The analysis included the 3-years of disease nursery trials. Peaks indicate marker association significance with AUDPS. Genetic positions of each of the markers tested is shown on the x axis, with the significance of the association (in –log10p units) shown on the y axis.

Multiple environment GWAS performed using estimated line means of height and the iSelect SNP data for the 510 barley genotypes was run without correcting for population structure using the null mixed relationship model. QQ plot showed high deviation from the null hypothesis line indicating population structure (Figure VI-7) and the Manhattan plot showed high levels of association across the genome (Figure VI-8).

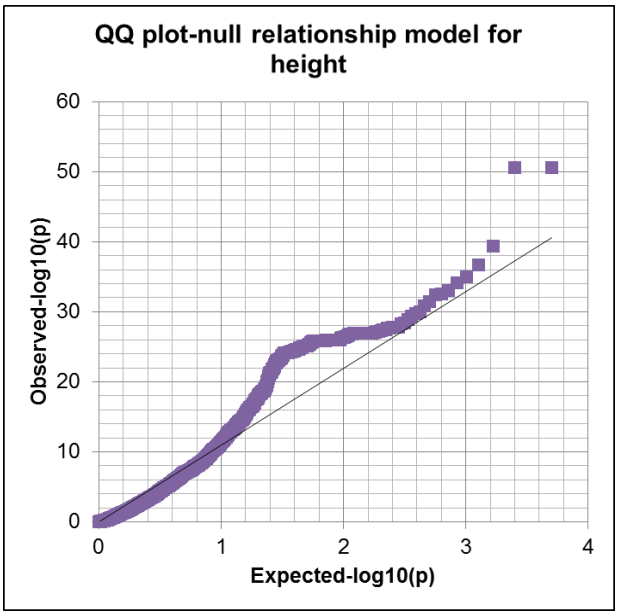

Figure VI-7: QQ-plot of the negative logarithms of the p values from the GWAS height null relationship model. The negative logarithms of the p values (purple squares) are showing strong deviation from the null hypothesis (dark line) indicating population structure.

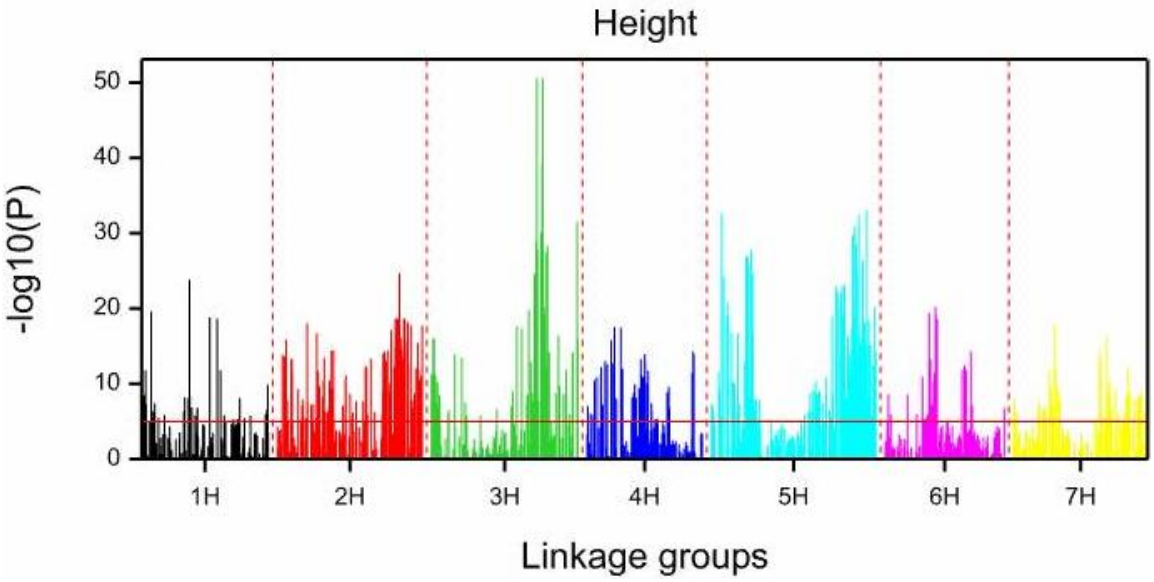

Figure VI-8: Manhattan plots of a multi-environment GWAS analysis under null relationship model for height. The analysis included 2 years data of disease nursery trials, and peaks indicate marker association significance with height. Genetic positions of each of the markers tested is shown on the x axis, with the significance of the association (in –log10p units) shown on the y axis

Multiple environment GWAS performed using estimated line means of field disease scores and the iSelect SNP data for the 510 barley genotypes was run, correcting for population structure using the Eigenanalysis mixed relationship model. The analysis detected six significant principal components indicating population structure among the spring barley collection (Table VI-7).

The QQ plot showed low deviation from the null hypothesis indicating that population structure was adequately controlled and that the GWAS result can be further analysed (Figure VI-9).

Table VI-7: Table of significant principal components detected by the Eigenanlysis multiple environment analysis

Axis	Tracy-Widom statistic	Eigenvalue	% Variance explained	Cumulative % Variance explained
axis 1	114.48	973830	9.47	9.47
axis 2	35.23	467014	4.54	14.01
axis 3	16.56	350883	3.41	17.42
axis 4	4.45	279151	2.71	20.13
axis 5	1.4	255947	2.49	22.62
axis 6	1.19	247134	2.4	25.03

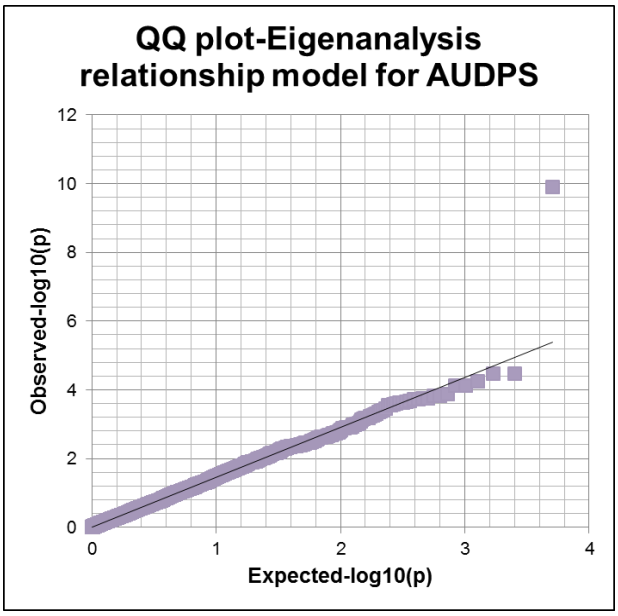

Figure VI-9: QQ-plot of the negative logarithms of the P values from the AUDPS GWAS Eigenanalysis relationship model. The negative logarithms of the p values (purple square) are showing poor deviation from the null hypothesis (dark line) indicating good correction for population structure.

The multiple environment GWAS identified a total of 20 significant QTL for AUDPS with a –log10p higher than 2.9. Five candidate QTLs showed consistent effects across years and fifteen showed evidence for QTLxE interactions. These are described in detail in Table VI-8 and Figure VI-11. Seven of these QTL locations coincided with known intervals of previously reported genes. QTL8 on 3H shares the marker 11_10005 synonym of marker 11_0010 which is associated with *Rrs1* in a study by Hofmann et al. (2013). QTL10 on 3H is co-localised with *Rrs4*, QTL1 on 1H is co-localised with *Rrs14*, QTL13 and QTL14 on 4H are both co-localised with *Rrs16*, QTL19 on 6H is co-localised with *Rrs13* and QTL12 on 3H is co-localised with *sdw1,* according to a map comparison of markers identified by Patil et al. (2003), Yun et al. (2006), Garvin et al. (2000), Pickering et al. (2006), Abbott et al. (1995), and (Pickering et al. (2006); Li et al. (2015)), respectively. In addition to these loci, 13 other QTL were detected on chromosomes 1H, 2H, 3H, 5H and 7H. Despite the location of QTL20 on chromosome 7H, it does not co-localise with *Rrs2* or *Rrs12* according to a map comparison of markers identifyed by (Hanemann et al. (2009); Marzin et al. (2016)) and Genger et al. (2003) respectively. In the same way, QTL3 on 2H did not co-localise with *Rrs15* according to a map comparison of markers identifyed by (Patil et al. (2003); Genger et al. (2005); Wagner et al. (2008);

Malosetti et al. (2011)). In addition QTL5, QTL6 and QTL7 on 2H did not co-localise with a QTL identified by Looseley et al. (2015).

Multiple environment GWAS performed using estimated line means of height and the iSelect SNP data for the 510 barley genotypes was run, correcting for population structure using the Eigenanalysis mixed relationship model. The QQ plot showed low deviation from the null hypothesis indicating that population structure had been adequately corrected for and that the GWAS result can be further analysed (Figure VI-10).

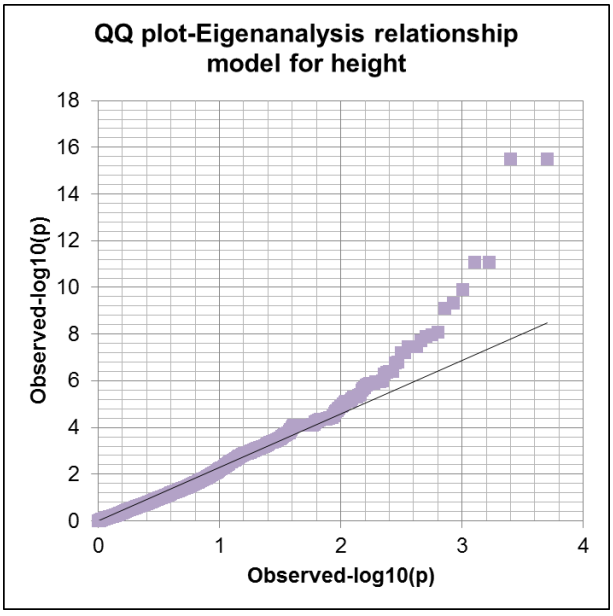

Figure VI-10: QQ-plot of the negative logarithms of the P values from the height GWAS Eigenanalysis relationship model. The negative logarithms of the p values (purple square) showing deviation from the null hypothesis (dark line) only for high –log10(p) indicating effective correction for population structure.

Eight significant associations for height (QTL1H, QTL2H, QTL3H, QTL4H QTL5H, QTL6H, QTL7H and QTL8H) were identified by the multi-environment association analysis. Four candidate QTLs with constant effects across yeas and four that showed evidence of QTLxE interactions were identified and are described in detail in Table VI-8 and Figure VI-11. QTL2H shares a marker location associated with *R. commune* resistance in the current study. This was QTL8, co-localising with the *R. commune* major resistance gene *Rrs1* located on 3H. QTL3H shares a marker location associated with the AUDPS QTL QTL11. QTL4H shares a marker location associated with the AUDPS QTL QTL12 and is co-localised with *sdw1,* according to a map comparison of markers identified by Patil et al. (2003).

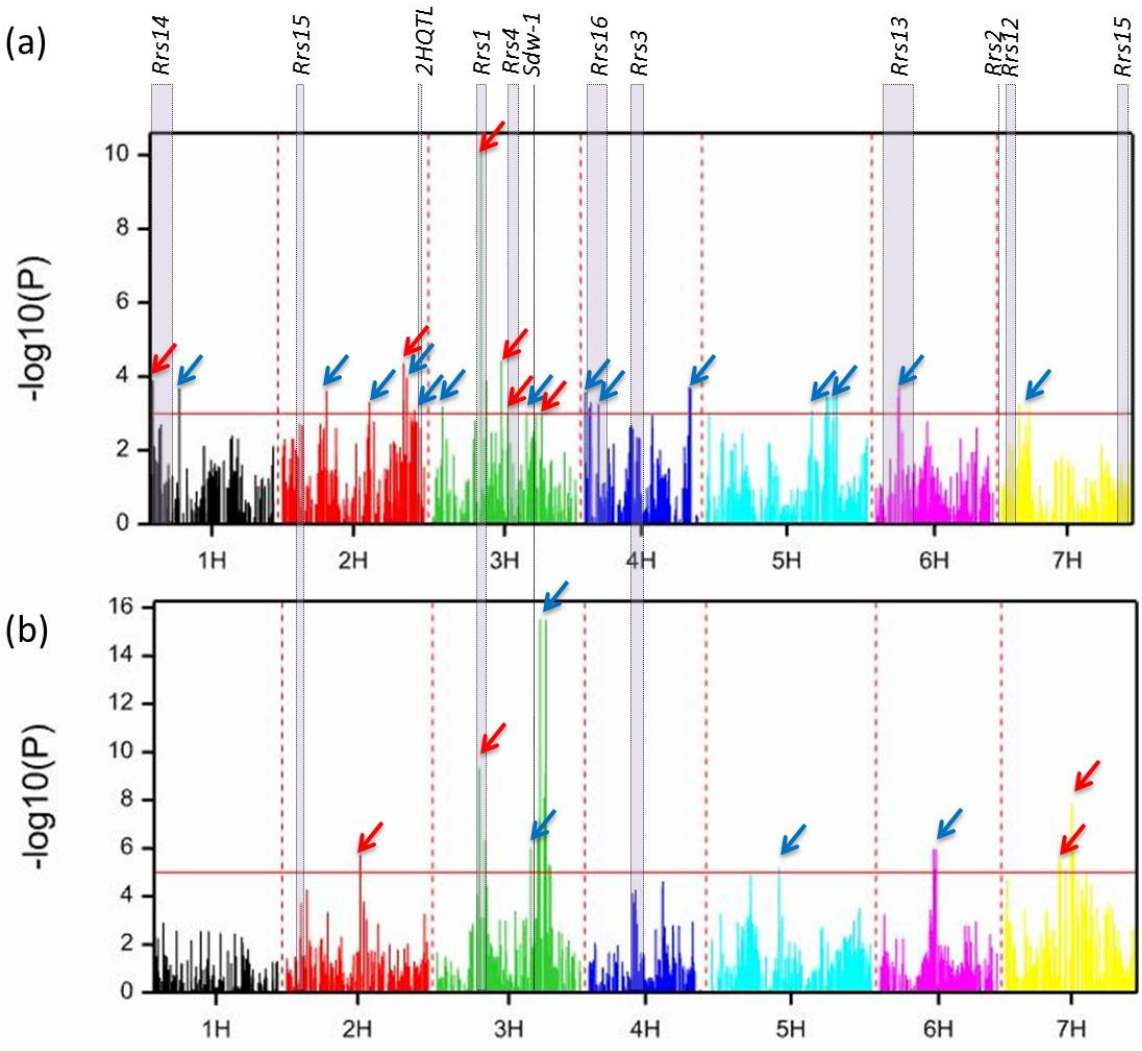

Figure VI-11: Manhattan plots comparing results from a multi-environment GWAS analysis on AUDPS and height. The analysis include was run using Eigenanalysis relationship model, peaks indicate marker associations significance with: (a). AUDPS; (b). Height. Genetic positons of each of the markers tested as shown on the x axis, with the significance of the association (in –log10p units) shown on the y axis. Map intervals for previously reported loci affecting *R. commune* resistance are indicated by lilac bars (or lines for diagnostic marker positions), with the locus name indicated between plots. The horizontal red lines represent the significance threshold of 2.9 for AUDPS and 5 for Height. Significant QTL are marked by arrows. Red arrows correspond to consistent QTL across years, Blue arrows correspond to inconsistent effects due to Gene-Environment interaction GxE. Genetic positions of each of the markers tested is shown on the x axis, with the significance of the association (in –log10p units) shown on the y axis.

Table VI-8: Summary of QTL identified in the GWAS for resistance against *R. commune* using GenStat and ISelect markers. SNP markers flanking the QTL are indicated, with marker positions shown in parentheses below. Best associated SNP markers are indicated, with marker positions shown below and its minor allele frequency (MAF). Fitted QTL effects are shown for each environment. Negative effects indicate that the resistant allele was contributed by the minor allele; positive effects indicate that the resistant allele was contributed by the major allele. Numbers in parentheses under QTL effects show the proportion of variance in estimated line means accounted for by best associated SNP parker of each QTL identified for each environment. Highlighted QTL correspond to QTL with GxE interaction

Traits	Name	Chr	Marker Interval (cM)	Peak marker (cM)	MAF (peak marker)	-log10p	Effect 2013	Effect 2014	Effect 2015
AUDPS	QTL1	1H	12_11311-12_30945	12_30945	0.078	3.88	0.2933	0.2933	0.2933
			(3.27-3.44)	3.44			(10***)	(4.6*)	(9***)
	QTL2	1H	11_10757-SCRI_RS_155382	11_10757	0.251	3.83	-0.1618	-0.0928	0.0557
			(32.08-32.08)	32.08			(7.4***)	(2.3)	0
	QTL3	2H	SCRI_RS_137093	SCRI_RS_137093	0.067	3.64	-0.1757	0.0513	0.2248
			47.78	47.78			(10.1**)	1.2	2.4
	QTL4	2H	11_20086	11_20086	0.339	3.29	-0.1825	-0.0747	0.0361
			94.48	94.48			(3.1)	1.5	2.2
	QTL5	2H	11_10376-SCRI_RS_202469	SCRI_RS_181112	0.41	4.47	-0.1848	-0.1848	-0.1848
			(131.38- 131.68)	131.38			(8.7***)	(3.1**)	(7.4***)
	QTL6	2H	SCRI_RS_138045-SCRI_RS_6458	SCRI_RS_138045	0.114	4.11	0.0809	0.171	0.3107
			(135.22-143.48)	135.22			1.4	1.9	4.2
	QTL7	3H	11_20595	11_20595	0.337	3.37	0.1018	0.0668	0.2025
			10.23	10.23			3.7	2.6*	6.4***
	QTL8	3H	SCRI_RS_221644-11_10005	SCRI_RS_221644	0.092	9.89	-0.5267	-0.5267	-0.5267
			(51.88-57.89)	51.88			(16.6***)	(6.1**)	(8.6*)
	QTL9	3H	SCRI_RS_227898	SCRI_RS_227898	0.187	4.24	-0.2673	-0.2673	-0.2673
			74.21	74.21			(5.6)	(0.7)	(1)
	QTL10	3H	SCRI_RS_208662	SCRI_RS_208662	0.175	2.92	0.2345	0.2345	0.2345
			81.38	81.38			(7.9***)	(3.6*)	2.7
	QTL11	3H	SCRI_RS_142438-	SCRI_RS_142438	0.253	2.98	0.1357	0.0184	0.1874
			101.58	101.58			(9.1***)	(3.6*)	(10.2***)
	QTL12	3H	SCRI_RS_138723-11_11172	11_11172	0.21	2.91	-0.1966	-0.1966	-0.1966
			111.82-118.36	118.36			(12.8***)	(7.9***)	(12.1***)
	QTL13	4H	12_30764-11_10319	12_30764	0.363	3.58	-0.0853	-0.0872	-0.2202
			(0-6.41)	0			(6.6***)	(4.7***)	(9.7***)
	QTL14	4H	SCRI_RS_197394-SCRI_RS_220110	SCRI_RS_197394	0.149	3.26	-0.018	0.0064	0.2103
			14.31-14.31	14.31			(2.5)	0.5	3.7
	QTL15	4H	SCRI_RS_9164-SCRI_RS_188829	SCRI_RS_9164	0.098	3.68	0.0273	-0.0024	0.282
			(113.4-114.9)	113.4			(0.3)	(0.4)	(7.3***)
	QTL16	5H	11_20259	11_20259	0.061	3.02	0.0693	0.2791	0.3617
			114.49	114.49			1.6	3.1	7
	QTL17	5H	SCRI_RS_175672-SCRI_RS_140356	SCRI_RS_175672	0.079	3.40	0.0908	0.2223	0.3659
			130.89-131.19	130.89			2.6	2.4	7.4**
	QTL18	5H	12_30400-SCRI_RS_9455	SCRI_RS_125263	0.391	3.76	-0.019	-0.1327	-0.2005
			(133.34-141.61)	141.47			(4.6*)	(4.6***)	(9.5***)
	QTL19	6H	11_20315-SCRI_RS_201251	SCRI_RS_201251	0.255	3.60	0.0595	0.105	0.2139
			(23.58-24.82)	24.82			0.5	1.7	3.8
	QTL20	7H	12_30530-SCRI_RS_138457	12_30530	0.163	3.18	0.1561	0.0749	0.2281
			(18.53-29.65)	18.53			(7.1**)	(2.9*)	(8.4***)
Height	QTL1H	2H	SCRI_RS_91810-SCRI_RS_137263	SCRI_RS_137263	0.187	5.71		-0.299	-0.299
			(79.99-80.09)	80.09					
	QTL2H	3H	11_10601 - SCRI_RS_173348	11_10601	0.263	9.32		0.3114	0.3114
			(45.43-52.02)	45.43					
	QTL3H	3H	SCRI_RS_142438	SCRI_RS_142438	0.253	6.02		-0.1667	-0.2424
			101.58	101.58					
	QTL4H	3H	SCRI_RS_150944 - 11_20612	11_11172	0.21	15.49		0.3593	0.4845
			(109.24-123.31)	118.36					
	QTL5H	5h	SCRI_RS_170151	SCRI_RS_170151	0.165	5.17		0.2762	0.166
			74.54	74.54					
	QTL6H	6H	11_102704- SCRI_RS_224297	SCRI_RS_237419	0.423	5.95		0.2248	0.0024
			(57.8-60.44)	57.98					
	QTL7H	7H	SCRI_RS_235584- SCRI_RS_175859	SCRI_RS_235584	0.4	5.59		0.2333	0.2333
			(57.97-59.26)	57.97					
	QTL8H	7H	11_10700 - SCRI_RS_231916	11_10209	0.433	7.90		0.2705	0.2705
			(70.96-73.9)	71.9					

QTL for resistance to Rhynchosporium identified 480 current UK elite spring barley using GAPIT analysis and ISelect genotype

The use of GenStat is limited by the amount of data. However the GAPIT (Zhang et al. 2010) package on R (Core 2013) can be used as an alternative to GenStat and is able to handle large numbers of markers as with exome capture data. the other advantage of GAPIT is that it uses Mixed Linear Model (MLM), one of the most effective methods for controlling false positives in GWAS studies (Zhang et al. 2010). However, the package does not implement multi-environment models, so a combined line means of field disease scores was calculated.

To see if GAPIT is a good alternative to GenStat, GWAS was performed using estimated combined line means of field disease scores and the iSelect SNP data for the 480 barley genotypes.

GWAS performed without correcting for population structure and (specifying 0 principal components (PCs) using the 'PCA.total' option) showed a light deviation from the null hypothesis (Figure VI-12a). The analysis was run correcting for population structure (specifying up to 6 principal components (PCs) using the 'PCA.total' option) according to the number of significant principal components detected in the 480 genotypes using GenStat. In this case, the QQ plot showed very similar profiles regardless of the population structure correction used (Figure VI-12b-g). The QQ plot specifying 3 PC seems to be the one showing the lowest deviation from the null hypothesis line, suggesting that this model is the best option to correct for population structure (Figure VI-12d). As a consequence, the GWAS was analysed correcting for population structure and by specifying 3 PC.

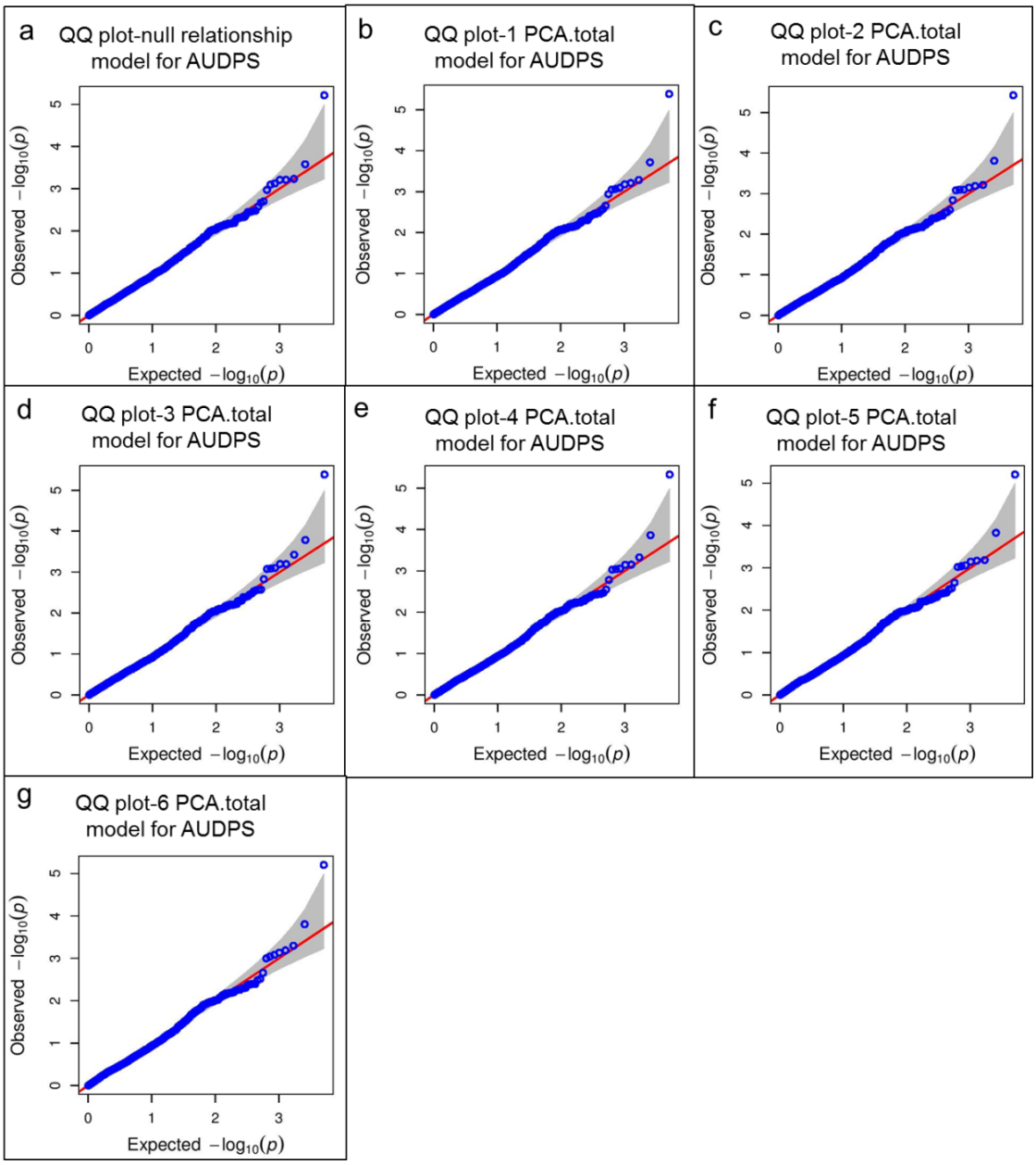

Figure VI-12: QQ-plot of the negative logarithms of the p values from the AUDPS GWAS using iSelect genotyping data. Null and up to 6 PC were specified to correct for population structure. (a) null relationship, (b) 1 PC, (c) 2 PC, (d) 3 PC, (e) 4 PC, (f) 5PC, (g) 6PC.

The GWAS identified 5 significant QTL (-log10 >2.9) for AUDPS using GAPIT package on R and are described in detail in Table VI-9 and Figure VI-13. Two of these QTL locations coincided with known intervals of previously reported genes (Table VI-2). QTL2C on 3H is flanked by the same markers as QTL8 identified during multi-environment association on GenStat co-localising with *Rrs1*; and QTL5C on 7H co-localises with *Rrs12* according to a map comparison of markers identified by Hofmann et al. (2013) and Genger et al. (2003) respectively. In addition, two of these QTL co-localise with QTL detected

during multi-environment association on GenStat. QTL1C on 1H co-localises with QTL2 and QTL3C on 3H co-localises with QTL9 (Figure VI-13).

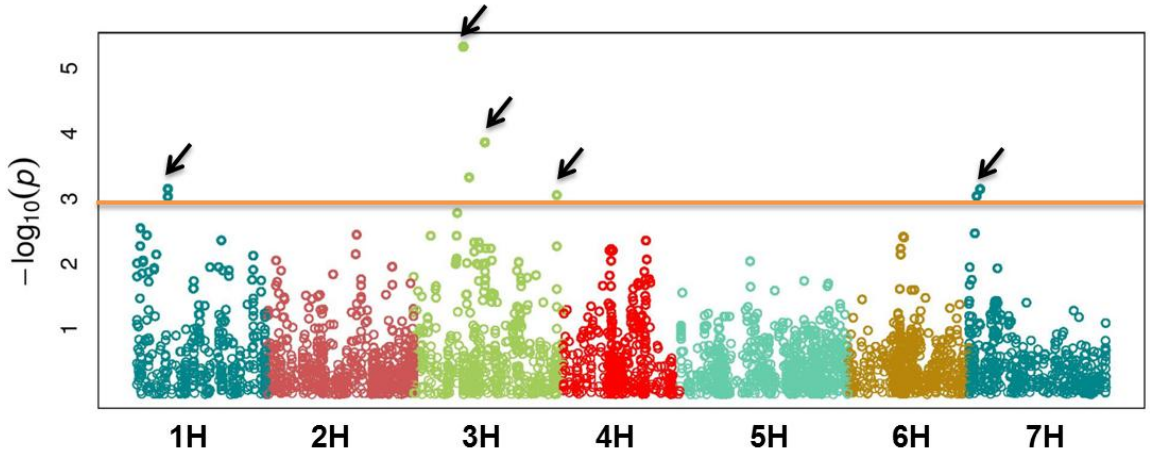

Figure VI-13: Manhattan plots of GWAS analysis using GAPIT and combined estimated AUDPS. 3 PCA were specified for population structure correction. ISelect genotype and combined estimated AUDPS means from 3-years of disease nursery trials was used. Rounds indicate marker association significance. Genetic positions of each of the markers tested is shown on the x axis, with the significance of the association (in –log10p units) shown on the y axis.

Table VI-9: Summary of QTL identified in the GWAS for resistance against *R. commune* using GAPIT and ISelect markers. SNP markers flanking the QTL are indicated, with marker positions below. Best associated SNP markers are indicated, with marker positions shown below and its minor allele frequency (MAF). Fitted QTL effects are shown for the combined estimated mean used as phenotype. Negative effects indicate that the resistant allele was contributed by the minor allele; positive effects indicate that the resistant allele was contributed by the major allele. Numbers in parentheses under QTL effects show the proportion of variance in estimated line means accounted for by best associated SNP parker of each QTL identified.

Name	Chr	Marker Interval (cM)	Peak marker (cM)	MAF peak marker	-log10p	Effect
QTL1C	1H	11_10757-SCRI_RS_155382	11_10757	0.243	3.15	-0.1454
		(32.08-32.08)	32.08			(7.3***)
QTL2C	3H	SCRI_RS_221644-11_10005	SCRI_RS_221644	0.069	5.33	-0.3483
		(51.88-57.89)	51.88			(16.5***)
QTL3C	3H	SCRI_RS_227898	SCRI_RS_227898	0.17	3.86	-0.1918
		(74.21)	74.21			(5.4)
QTL4C	3H	11_10694	11_10694	0.439	3.06	0.1407
		(149.25)	149.25			(6.2**)
QTL5C	7H	11_10841-SCRI_RS_155121	SCRI_RS_155121	0.316	3.15	-0.132
		(7.97-11.64)	11.64			(5.9**)

Genetic and physical location of each best iSelect marker associated in both GWAS

A table summarising all the QTL was generated indicating the name, along with the genetic and physical location of each peak marker (Table VI-10)

Table VI-10: Table summarising genetic and physical location of each best ISelect marker associated identified during GWAS of AUDPS

QTL	Chr	Best marker associated	Genetic position (cM)	Physical position (bp)
QTL1	**1H**	12_30945	3.44	1,913,903
QTL2/QTL1C	**1H**	11_10757	32.08	18,359,682
QTL3	**2H**	SCRI_RS_137093	47.78	51,223,264
QTL4	**2H**	11_20086	94.48	681,044,282
QTL5	**2H**	SCRI_RS_181112	131.38	726,082,735
QTL6	**2H**	SCRI_RS_138045	135.22	732,622,007
QTL7	**3H**	11_20595	10.23	11,725,047
QTL8/QTL2C	**3H**	SCRI_RS_221644	51.88	490,226,429
QTL9QTL3C	**3H**	SCRI_RS_227898	74.21	564,870,385
QTL10	**3H**	SCRI_RS_208662	81.38	574,659,697
QTL11	**3H**	SCRI_RS_142438	101.58	620,661,980
QTL12	**3H**	11_11172	118.36	632,247,047
QTL4C	**3H**	11_10694	149.25	684,467,546
QTL13	**4H**	12_30764	0	1,302,636
QTL14	**4H**	SCRI_RS_197394	14.31	8,808,903
QTL15	**4H**	SCRI_RS_9164	113.4	636,574,078
QTL16	**5H**	11_20259	114.49	594,978,246
QTL17	**5H**	SCRI_RS_175672	130.89	606,354,356
QTL18	**5H**	SCRI_RS_125263	141.47	620,106,313
QTL19	**6H**	SCRI_RS_201251	24.82	16,986,970
QTL5C	**7H**	SCRI_RS_155121	11.64	14,909,880
QTL20	**7H**	12_30530	18.53	23,576,066

VI.3.3. GWAS using exome capture SNPS data (a 130-lines subset from the GWAS lines have exome capture data)

QTL for resistance to Rhynchosporium identified in the 130 lines subset of the current UK elite spring barley using GAPIT analysis and exome capture SNPs data

A GWAS was performed using line means of each year and estimated combined line means (across years) of field disease scores and the exome capture SNP data for the 130 barley genotypes subset. This was run without correcting for population structure by specifying the 0 principal components (PCs) using the 'PCA.total' option. The QQ plot of this analysis showed a slight deviation from the null hypothesis indicating some population structure (Figure

VI-14a). The analysis was re-run correcting for population structure by specifying 4 principal components (PCs) using the 'PCA.total' option according to the number of significant principal components detected in the 130 subset genotypes using GenStat. The QQ plot sits under the null hypothesis line indicating overcorrection for population structure (Figure VI-14b). The analysis was also run correcting for population structure by specifying between 0 and 4 principal components (PCs) using the 'PCA.total' option but no better QQ plot was observed than that seen using 0 PC. As a consequence, the GWAS was analysed without correction for population structure.

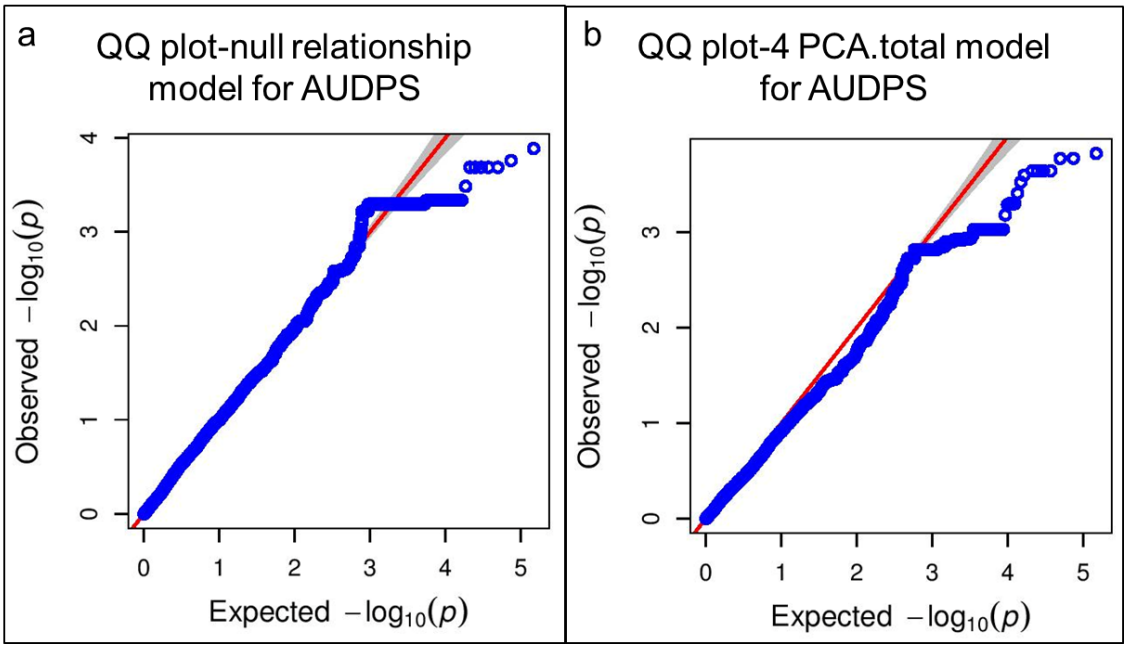

Figure VI-14: QQ-plot of the negative logarithms of the p values from the AUDPS GWAS using exome capture data. Two principal components (PCs) were tested: 0 (a) and 4 (b) to correct for population structure. The null relationship model shows a slight deviation from the null hypothesis (red line) only for high –log10(p) indicating population structure. The 4 principal components (PCs) relationship model sits under the null hypothesis line (red line)) indicating overcorrection for population structure.

The GWAS analysis was run for each years AUDPS estimated line means separately and using the combined estimate for the three years' field data. The Manhattan plot was produced using physical positions of SNPs (genetic position not being available for most markers) and provided an unusual graph pattern compared to genetic position based plots, preventing us from directly comparing GWAS results with each other (Figure VI-15). A general lower significance of marker test statistics and an increase in significance from the centromere to both directions of chromosome ends were observed, correlating with the density of SNPs markers. The analysis of 130 lines and 151k SNPs revealed no

significant associations for resistance, but clear peaks could be visualised on the Manhattan plot with some of them in the expected location of already mapped resistance loci; evidence of potential association. The best associated marker for each peak (using the cross-year AUDPS estimates means) with a significance higher than an arbitrary threshold of 2.3 (-log10p) were studied and compared to QTL identified using the ISelect genotypes known locations of published QTL summarised in Table VI-2 and Table VI-10. Results are summarised in Table VI-11.

QTL1EC is located on 1H co-localising with the *Rrs14* physical location (Yun et al. 2006). QTL2EC is located on 1H and co-localises with QTL2 and QTL1C. QTL3EC is located on 2H but 5Mb outside of *Rrs15* interval (Wagner et al. 2008). QTL4EC is located on 2H but 20 Mb from QTL3 and 10Mb outside of the *Rrs15* interval (Wagner et al. 2008). QTL5EC is located on 2H and could be co-localising with QTL4, QTL5, QTL6 or a QTL identified by Looseley et al. (2015) but is 12Mb far away from nearest QTL in the region of QTL4. QTL6EC is located on 3H and could be visually co-localised with QTL7 but is 12Mb physically distal. QTL7EC is located on 3H and co-localising with the *Rrs1* physical interval (Hofmann et al. 2013). QTL8EC on 3H is physically located in the *Rrs4* interval (Patil et al. 2003). QTL9EC on 4H is physically located in *Rrs3* interval (Grønnerød et al. 2002). QTL10EC on 5H is located 14 Mb away from QTL16. QTL11EC on 6H is overlapping with *Rrs13* and QTL12EC on 6H is just outside of the *Rrs13* interval (Abbott et al. 1995). QTL13EC located on chromosome 7H is 11Mb physically distal from *Rrs12*, but is overlapping with the physical interval of *Rrs2* (Hanemann et al. 2009). QTL14EC located on chromosome 7H is in the expected region of *Rrs12* but the lack of a right flanking marker in the published position of *Rrs12* does not allow confidence in concluding that they co-localise (Genger et al. 2003). QTL15EC and QTL16EC on 7H are in the expected region of *Rrs15* but the lack of a left flanking marker in the published position of *Rrs15* does not allow confidence in concluding that they co-localise, however, QTL16EC is only 8Mb far from the right flank of *Rrs15* (Genger et al. 2005).

In all QTL studied, the proportion of variance in estimated line means accounted for by the best associated SNP marker of each peak was high (in particular for peaks co-localising with *Rrs2* and *Rrs13* (Table VI-11)).

Among the years, peaks co-localising with *Rrs14*, *Rrs2* and *Rrs15* were observed while peaks co-localising with Rrs1, Rrs4, Rrs3 and Rrs13 were not detected in the AUDPS 2014 analysis.

Table VI-11: Summary of QTL identified in the GWAS for resistance against *R. commune* using GAPIT and exome capture SNPs data. SNP markers flanking the QTL are indicated, name correspond to the chromosome number followed by the base position. Best associated SNP markers are indicated and its minor allele frequency (MAF). Fitted QTL effects are shown for the combined estimated mean used as phenotype. Negative effects indicate that the resistant allele was contributed by the minor allele; positive effects indicate that the resistant allele was contributed by the major allele. Numbers in parentheses under QTL effects show the proportion of variance in estimated line means accounted for by best associated SNP marker of each peak identified.

Name	Chr	Marker Interval	Peak marker	MAF peak marker	-log10p	Effect
QTL1EC	1H	chr1H_4321467-chr1H_5278008	chr1H_5278008	0.473	2.374	0.169 (8.948*)
QTL2EC	1H	chr1H_17189650-chr1H_18780929	chr1H_17332256	0.419	2.327	-0.169 (9.801**)
QTL3EC	2H	chr2H_785623-chr2H_11396655	chr2H_7267388	0.450	2.701	0.190 (11.458**)
QTL4EC	2H	chr2H_30894120-chr2H_35067423	chr2H_32081728	0.403	2.857	0.198 (10.848**)
QTL5EC	2H	chr2H_688035797-chr2H_693200793	chr2H_693200269	0.093	2.378	0.289 (13.656*)
QTL6EC	3H	chr3H_23090327-chr3H_26653887	chr3H_23315087	0.372	3.484	0.223 (11.360***)
QTL7EC	3H	chr3H_491429053	chr3H_491429053	0.194	2.236	0.209 (10.287*)
QTL8EC	3H	chr3H_592449859-chr3H_593198968	chr3H_592563068	0.403	2.483	0.175 (9.896**)
QTL9EC	4H	chr4H_531536904-chr4H_534039771	chr4H_532859506	0.186	2.450	-0.240 (14.043**)
QTL10EC	5H	chr5H_636696667-chr5H_636944791	chr5H_636696667	0.202	2.395	-0.211 (12.913***)
QTL11EC	6H	chr6H_21437298-chr6H_21820887	chr6H_21437298	0.202	2.928	-0.242 (13.364***)
QTL12EC	6H	chr6H_30604705-chr6H_36199042	chr6H_30847918	0.109	3.336	0.334 (20.020***)
QTL13EC	7H	chr7H_625667-chr7H_8364406	chr7H_4097080	0.070	3.887	-0.442 (24.678***)
QTL14EC	7H	chr7H_27120203-chr7H_27160371	chr7H_27126150	0.364	2.626	-0.190 (10.443**)
QTL15EC	7H	chr7H_525988778-chr7H_537975086	chr7H_532055502	0.085	2.779	0.339 (17.17**)
QTL16EC	7H	chr7H_640702372-chr7H_641620715	chr7H_641092592	0.124	2.355	0.255 (13.72**)

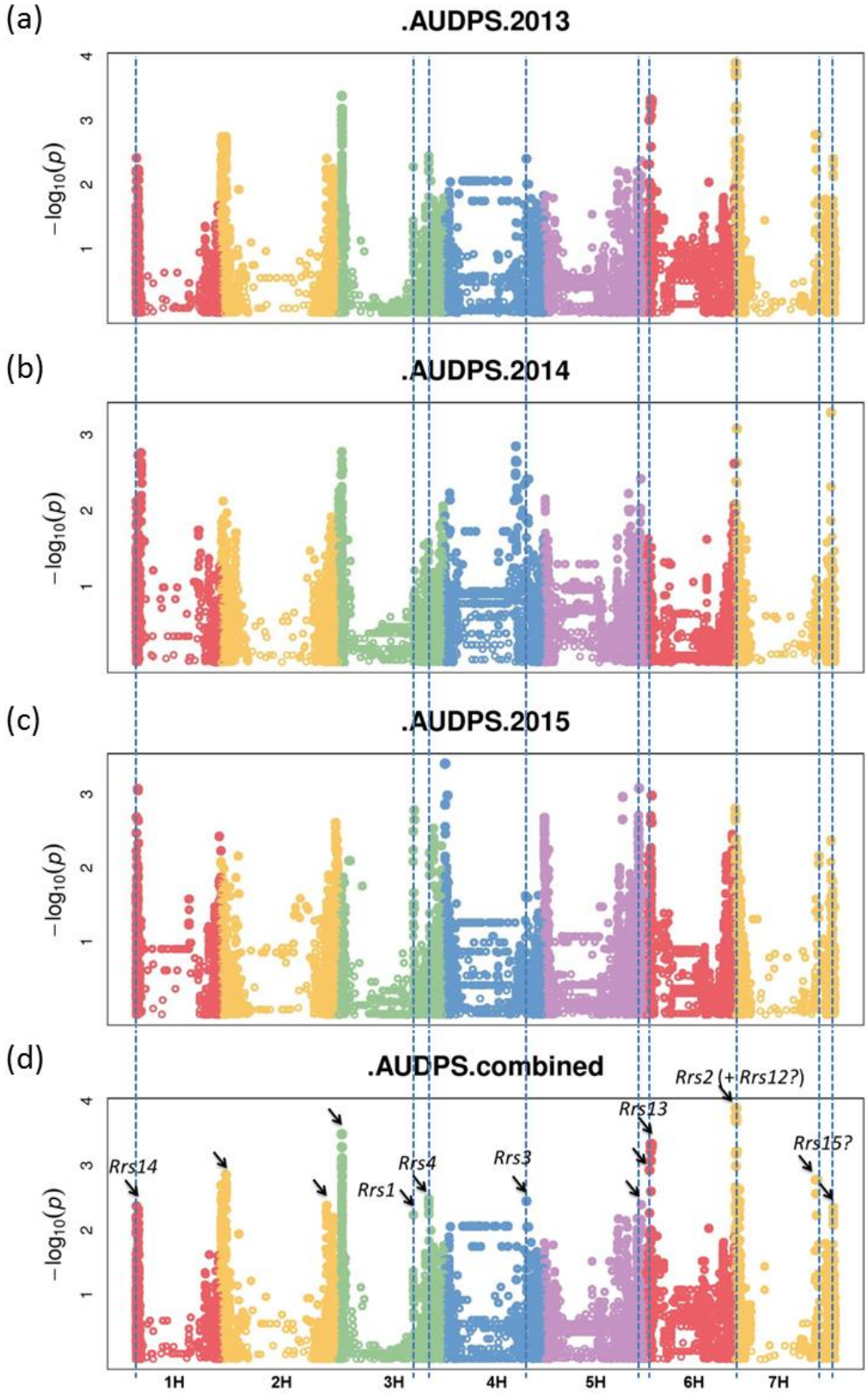

Figure VI-15: Manhattan plot of a GWAS for *R. commune* field disease scores with exome capture SNPs data. GAPIT was run using the 130 lines subset of the current UK elite spring barley and 2013 (a), 2014 (b), 2015 (c) and 3-years combined (d) estimated AUDPS means of disease nursery trials. Physical positons of each of the markers tested as shown on the x axis, with the significance of the association (in –log10p units) shown on the y axis. Peaks studied are marked by black arrows. Dashed blue lines represent the positions of already mapped resistances.

QTL for resistance to Rhynchosporium identified in the 130 lines subset of the current UK elite spring barley using GenStat multiple environment analysis and exome capture SNPs data

Multiple environment GWAS, performed on individual chromosomes using estimated combined line means of field disease scores across years and the exome capture SNP data for the 130 barley genotypes, was run, correcting for population structure using the Eigenanalysis mixed relationship. A Manhattan plot of each is shown in Figure VI-16.

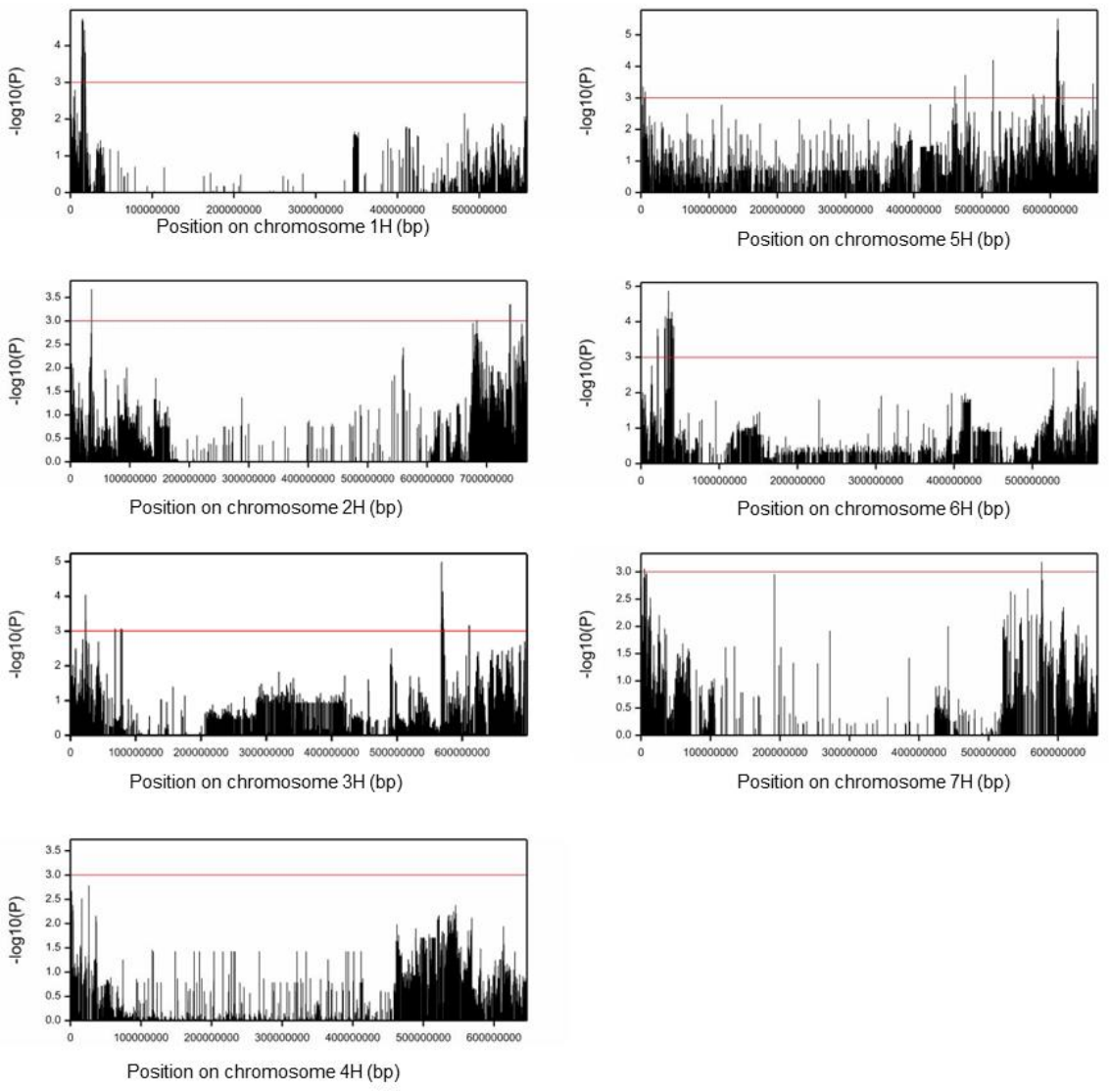

Figure VI-16: Manhattan plots of GWAS for *R. commune* field disease scores on the 130 lines subset of the current UK elite spring barley. Analyses were performed using multi environment methods, exome capture SNPs data, and 3-years combined estimates of AUDPS means. Physical positons of each of the markers tested is shown on the x axis, with the significance of the association (in –log10p units) shown on the y axis.

The analysis of 130 lines using individual chromosomes exome capture SNPs revealed 22 significant QTL (-log10>2.9). Associated intervals observed near already detected QTL positions were compared to the iSelect significant associated intervals and known location of published QTL (summarised in Table VI-2 and Table VI-10). Associations are summarised in Table VI-12. QTL1ECGS on 1H has an interval size of 4.6Mb and could be *Rrs14* as it is located 0.7Mb from it. QTL2ECGS on 2H has an interval size of 56Kb but is 30Mb away from *Rrs15*. QTL3ECGS on 2H has an interval size of 6.4Mb and is overlapping with QTL2. QTL4ECGS on 2H has an interval size of 0.8Mb and is 6.7Mb away from QTL6. QTL5ECGS on 3H has an interval size of 0.15Mb and is 11.4Mb away from QTL7. QTL7ECGS on 3H has an interval size of 3.6Mb and is located in the *Rrs4* interval. QTL8ECGS on 3H has an interval size of0.3Mb and is 9.8Mb away from QTL11. QTL9ECGS on 4H has an interval size of0.28Mb and could be *Rrs16* as it is localised 0.6Mb away from its published position. QTL15ECGS on 5H is located 3.1Mb away from QTL16. QTL16ECGS on 5H has an interval size is of4.8Mb and is located 2.9Mb away from QTL17. QTL17ECGS on 5H has an interval size is of2.6Mb and is overlapping with QTL18. QTL19ECGS on 6H has an interval size of 0.6Mb and is co-located with *Rrs13*. QTL20ECGS on 6H has an interval size of 11.7Mb and is 1.5Mb away from *Rrs13.* QTL21ECGS on 7H has an interval size of 71Kb and is located in *Rrs2* interval. QTL22ECGS on 7H could be co-localising with *Rrs15* but the lack of a left flanking marker for *Rrs15* does not allow confidence.

Table VI-12: Summary of QTL identified in the GWAS for resistance against *R. commune* using multi environment analysis on GenStat and exome capture SNPs data. SNP markers flanking the QTL are indicated, names correspond to the chromosome number followed by the base position. Best associated SNP markers are indicated and its minor allele frequency (MAF). Fitted QTL effects are shown for each year. Negative effects indicate that the resistant allele was contributed by the minor allele; positive effects indicate that the resistant allele was contributed by the major allele.

Name	Chr	Marker Interval	Peak marker	MAF peak marker	-log10p	Effect 2013	Effect 2014	Effect 2015
QTL1ECGS	1H	chr1H_13732370-chr1H_18413664	chr1H_14975300	0.104	4.73	6.208	-5.418	4.775
QTL2ECGS	2H	chr2H_35715134-chr2H_35771500	chr2H_35769278	0.164	3.67	-5.843	2.429	1.046
QTL3ECGS	2H	chr2H_677197341-chr2H_683621151	chr2H_683621151	0.317	3.02	-2.363	5.280	3.755
QTL4ECGS	2H	chr2H_739296286-chr2H_740074823	chr2H_739332154	0.431	3.35	3.775	-4.302	-3.017
QTL5ECGS	3H	chr3H_23160385-chr3H_23315087	chr3H_23160385	0.352	4.04	5.284	5.284	5.284
QTL6ECGS	3H	chr3H_68601737-chr3H_78996380	chr3H_77296980	0.054	3.06	-1.980	5.219	7.804
QTL7ECGS	3H	chr3H_567956233-chr3H_571631600	chr3H_568354860	0.086	4.98	4.284	-8.209	0.318
QTL8ECGS	3H	chr3H_610519454-chr3H_610813567	chr3H_610813567	0.365	3.17	-2.808	3.485	-2.033
QTL9ECGS	4H	chr4H_54593-chr4H_335856	chr4H_54593	0.417	3.55	3.485	-3.485	-3.485
QTL10ECGS	5H	chr5H_3439939-chr5H_6500441	chr5H_3439939	0.240	3.35	-2.087	-2.087	-2.087
QTL11ECGS	5H	chr5H_460609018	chr5H_460609018	0.291	3.37	-0.745	-2.455	-3.415
QTL12ECGS	5H	chr5H_475851495-chr5H_475851750	chr5H_475851750	0.190	3.72	-1.158	-1.850	-0.016
QTL13ECGS	5H	chr5H_516538937-chr5H_516539842	chr5H_516538937	0.392	4.20	-1.415	-2.429	-4.616
QTL14ECGS	5H	chr5H_575088852	chr5H_575088852	0.488	3.11	2.802	-3.932	-1.388
QTL15ECGS	5H	chr5H_590859825	chr5H_590859825	0.357	3.08	1.093	-2.633	-1.086
QTL16ECGS	5H	chr5H_609200353-chr5H_614070027	chr5H_611261749	0.109	5.51	3.984	-6.595	-4.051
QTL17ECGS	5H	chr5H_617558412-chr5H_620193673	chr5H_620193648	0.318	3.52	0.601	-0.537	-2.776
QTL18ECGS	5H	chr5H_662997463	chr5H_662997463	0.178	3.45	1.994	-2.641	-2.707
QTL19ECGS	6H	chr6H_21437298-chr6H_22047681	chr6H_21437298	0.208	3.80	-4.810	1.519	1.586
QTL20ECGS	6H	chr6H_30607489-chr6H_42369883	chr6H_35446631	0.093	4.86	5.960	-8.091	0.464
QTL21ECGS	7H	ch7H_5198704-ch7H_5269765	ch7H_5265173	0.054	3.06	-10.277	-10.277	-10.277
QTL22ECGS	7H	ch7H_576633390	ch7H_576633390	0.294	3.18	2.664	2.199	3.245

VI.3.4. *Rrs1* study

Resistance of barley lines predicted to contain *Rrs1* to *R. commune* strain recognised by *Rrs1*

Out of 510 barley lines used in the GWAS, 47 had the minor (resistant) allele of our best associated marker SCRI_RS_221644. In order to confirm the status of these putative *Rrs1*-carrying lines, a subset of barley lines predicted to contain *Rrs1* as well as lines predicted to lack *Rrs1* were tested alongside known *Rrs1*-containing (Atlas 46, SBCC145, SBCC154) or susceptible barley lines for

resistance to two *R. commune* strains (LfL12F and 214-GFP) which are avirulent on barley lines containing *Rrs1*. SBCC145 and SBCC154 were genotyped for the SCRI_RS_221644 SNP marker by sequencing, confirming the presence of minor allele of SCRI_RS_221644 in SBCC145 and SBCC154 lines, and indicating that these lines carry the *Rrs1* resistance.

The seedling spray inoculation assay with the *R. commune* isolate LfL12F confirmed that 21 out of 22 lines, predicted to contain *Rrs1,* were, indeed, resistant (Table VI-13). Details of lines, phenotypes and genotypes are summarised in supplementary data Table IX-2. Only cultivar Karry was susceptible despite the fact that it was carrying the SCRI_RS_221644 minor allele and Atlas 46 showed a heterogeneous phenotype despite the fact that it is reported to carry an *Rrs1* allele (Dyck and Schaller 1961) All lines predicted to lack *Rrs1* were susceptible except for four lines: SW 2808, Anaconda, Atlas (*Rrs2*) and Pewter (*Rrs2*). These lines, not carrying the SCRI_RS_221644 minor allele, appeared to be resistant, which was likely due to the presence of a separate gene conferring resistance to *R. commune* isolate LfL12F such as *Rrs2*, which is already known to confer resistance against LfL12F (Marzin et al. 2016).

Table VI-13: Summary of *Rrs1* predicted lines and phenotyping results. Lines carrying SCRI_RS_221644 minor allele were predicted as *Rrs1* lines; lines carrying SCRI_RS_221644 major allele were predicted as non-*Rrs1* lines.

	Strain, Phenotyping technique	
	LfL12F, spray inoculation	214-GFP, confocal microscopy
# resistant lines/ # *Rrs1* predicted lines tested	21/22	8/8
# susceptible lines/ # *Rrs1* predicted lines tested	1/22	0/8
# resistant lines/ # non-*Rrs1* predicted lines tested	4/51	2/10
# susceptible lines/ # non-*Rrs1* predicted lines tested	47/51	8/10

The confocal assay allowed the visualisation of barley leaf colonisation by *R. commune* strain 214-GFP outside of the dense inoculation spot in susceptible cultivars (Figure VI-17). However, due to graphic quality issues, we cannot perfectly observe and discriminate the phenotype on cultivars (Figure VI-17). Eight predicted *Rrs1* lines were resistant (Table VI-13, Figure VI-17). All lines predicted to lack *Rrs1* appeared to be susceptible except for two lines: Armelle and Acrobat, which were resistant to strain 214-GFP. These two lines were susceptible to *R. commune* isolate LfL12F suggesting that they have an

additional resistance gene (or a different allele of *Rrs1)* that recognises strain 214-GFP.

Phenotyping of *Rrs1* predicted lines (by the minor allele of SCRI_RS_221644 marker) indicated that SCRI_RS_221644 is able to discriminate *Rrs*1 lines but is not diagnostic. SCRI_RS_221644 must be tightly linked to *Rrs1*.

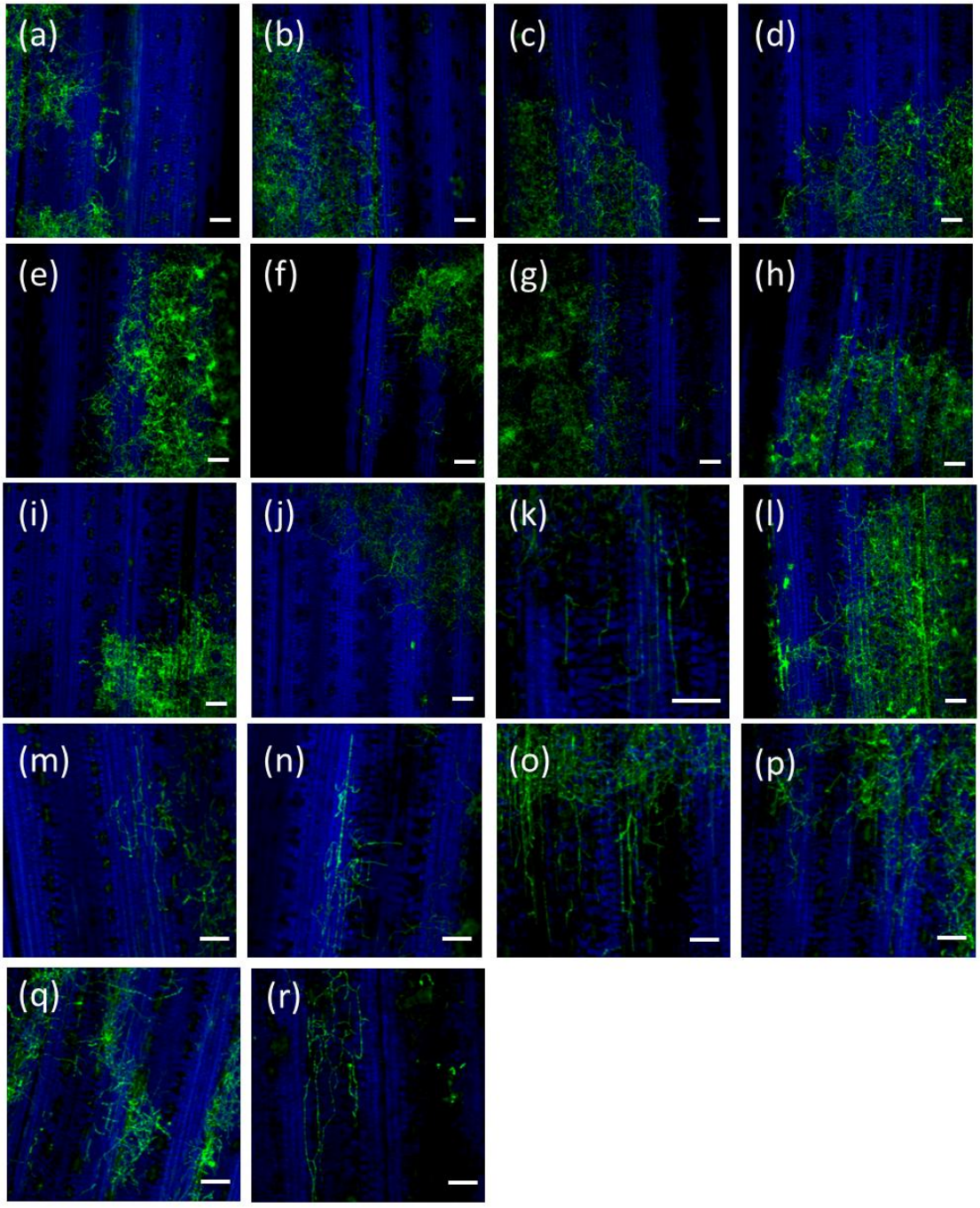

Figure VI-17: Confocal microscopy images showing GFP-214 *R commune* growth 11DPI on resistant and susceptible lines. Resistant lines: (a) Acrobat, (b) Armelle, (c) Atlas46, (d) Beryllium, (e) Cairn, (f) Casino, (g) Chieftain, (h) Corgi, (i) Acclaim and (j) SCBB145; Susceptible lines: (k) Akita, (l) Atlas, (m) Barabas, (n) Bulbul89, (o) Concerto, (p) Gizmo, (q) Imidis, (r) Nordal. GFP and chlorophyll autofluorescence channels are coloured in green and in blue respectively. The scale bar represents 25µm.

Rrs1 interval and candidate genes identification

The associated markers SCRI_RS_221644 and 11_10005 for the *Rrs1* interval could be mapped onto the Morex 3H pseudomolecule at 490,226,429bp and 489,991,523bp respectively. The subset of exome capture SNP data for the 19 lines screened for *Rrs1* resistance were plotted in Flapjack and used to visually identify a 0.8 Mb haplotype around the physical location of the markers associated with *Rrs1*, from 489,991,853bp to 490,817,329bp (Figure VI-18). Beryllium, Brahms, SW Macsena, Chieftain and Franklin are resistant lines and predicted to carry *Rrs1.* Drum, Jive, Aapo, Livet, Klaxon, Akita, Annabell, Ardilla, Baronesse, Ida and Optic are susceptible lines and predicted to not carry *Rrs1*. Pewter and Anaconda were resistant lines thanks to *Rrs2* resistance but are not predicted to carry *Rrs1*.

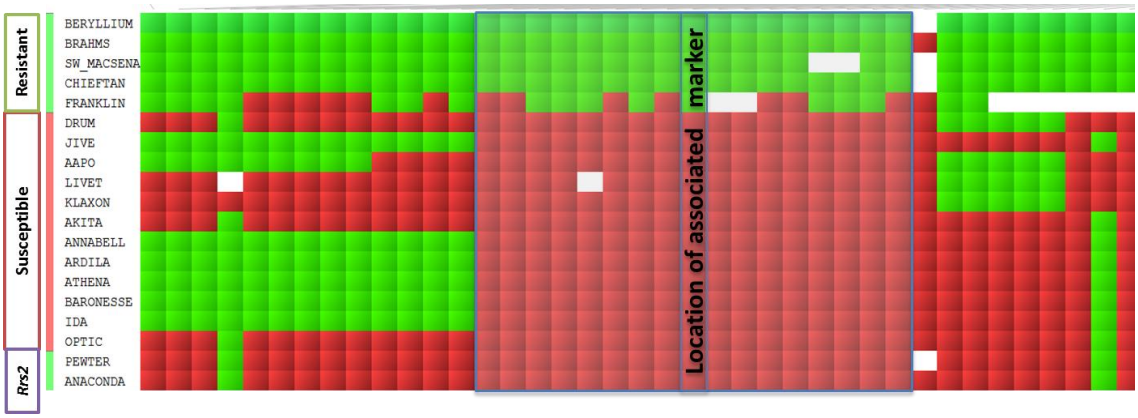

Figure VI-18: Diagram illustrating *Rrs1* haplotype identified using exome capture SNPs data and visualised using flapjack.

This interval was extended by 1 Mb on either side resulting in a 2.8 Mb interval which was explored in the new barley 3H pseudomolecule annotation revealing the presence of 22 genes summarised in Table VI-14.

Table VI-14: Gene content and annotation of the 2.8Mb interval corresponding to the physical interval containing *Rrs1*.

Gene	Location	# transcripts	Annotation	Pfam
HORVU3Hr1G063960	488714701-488716861	2	tRNA dimethylallyltransferase	PF01745
HORVU3Hr1G064040	489113573-489115813	4	Protein of unknown function (DUF1639)	PF07797
HORVU3Hr1G064070	489393734-489396105	6	Protein of unknown function (DUF1639)	PF07797
HORVU3Hr1G064080	489630358-489643914	7	zinc finger protein-related	PF01814, PF05495, PF14599
HORVU3Hr1G064100	489663696-489667102	4	unknown protein;	none
HORVU3Hr1G064110	489987777-490003929	19	Receptor-like protein kinase-like	PF13947, PF14380
HORVU3Hr1G064120	489987828-490006022	5	Alpha/beta hydrolase domain-containing protein 13	PF12695
HORVU3Hr1G064130	490134505-490244622	31	Protein kinase superfamily protein	PF13947, PF14380
HORVU3Hr1G064180	490222327-490226751	7	Protein kinase superfamily protein	PF13947, PF14380
HORVU3Hr1G064190	490224965-490228637	3	Zinc finger MYM-type protein	none
HORVU3Hr1G064200	490244656-490248080	3	receptor-like protein kinase 4	PF00704, PF07714
HORVU3Hr1G064230	490250334-490258624	17	Nucleotidylyl transferase superfamily protein	PF01467
HORVU3Hr1G064240	490251881-490254637	3	Reticulon family protein	PF02453
HORVU3Hr1G064290	490788416-490795983	4	serine/threonine protein phosphatase 2A	PF00149
HORVU3Hr1G064300	490796655-490805716	30	TFIIH basal transcription factor complex helicase XPB subunit	PF04851, PF13625, PF16203
HORVU3Hr1G064320	491037145-491038491	5	Glutathione S-transferase family protein	PF13410, PF13417
HORVU3Hr1G064340	491084331-491087583	5	Protein PLASTID MOVEMENT IMPAIRED 2	PF05701
HORVU3Hr1G064350	491353113-491353666	1	UDP-Glycosyltransferase superfamily protein	none
HORVU3Hr1G064370	491370347-491374436	8	RING/U-box superfamily protein	PF13639
HORVU3Hr1G064390	491376493-491383628	16	Alpha/beta fold hydrolase	PF12146
HORVU3Hr1G064410	491428834-491434720	52	Clathrin assembly protein	none
HORVU3Hr1G064420	491486104-491487212	1	hydroxyproline-rich glycoprotein family protein	none

The full set of exome capture SNPs in the 22 gene interval (from 489116071 to 491851065 bp) was kindly provided by Dr Micha Bayer. This interval contains a total of 19,551 polymorphic SNPs and was studied by selecting SNPs with polymorphic alleles that genotypically differentiated lines predicted to contain *Rrs1* (BERYLLIUM, BRAHMS, SW_MACSENA and CHIEFTAN) from lines

predicted to lack *Rrs1 (*DRUM, JIVE, AAPO, LIVET and OPTIC). Across the interval 1,126 SNPs were polymorphic between *Rrs1* and non-*Rrs1* lines. The study of the effect of selected SNPs identified non-synonymous SNPs at 5 different annotated genes within the interval: HORVU3Hr1G064110, HORVU3Hr1G064130, HORVU3Hr1G064180, HORVU3Hr1G064190 and HORVU3Hr1G064200. Two genes out of these five genes were unlikely to be *Rrs1*: a single non-synonymous SNP was found in the HORVU3Hr1G064110 gene, but the allele present in resistant lines was also the Morex reference allele: a fully susceptible line not carrying *Rrs1*; and HORVU3Hr1G064190, a gene that's function is annotated as transposon related. 16, 3 and 3 non-synonymous SNPs were found respectively in HORVU3Hr1G064130, HORVU3Hr1G064180 and HORVU3Hr1G064200 genes. 48 SNPs polymorphic between predicted *Rrs1* and non-*Rrs1* lines were selected for additional genotyping, prioritising SNPs causing amino acid changes in annotated genes and SNPs surrounding these genes. (Table VI-15).

Table VI-15: Table summarising markers chosen for genotyping. Names of SNPs correspond to the physical location of the SNPs on the genome. SNPs coloured in grey correspond to the SNPs outside of the interval, SNPs coloured in white correspond to SNPs located in intron or in-between coding sequences, SNPs coloured in blue correspond to SNPs located in the HORVU3Hr1G064110 gene, SNPs coloured in green correspond to SNPs located in the HORVU3Hr1G064180 gene, SNPs coloured in blue correspond to SNPs located in the HORVU3Hr1G064190 gene, SNPs coloured in red correspond to SNPs located in the HORVU3Hr1G064130 gene and SNPs coloured in orange correspond to SNPs located in the HORVU3Hr1G064200 gene.

		Susceptible					Resistant				
SNP name	Reference allele	DRUM	JIVE	AAPO	LIVET	OPTIC	BERYLLIUM	BRAHMS	SW_MACSENA	CHIEFTAN	SNP effect base on transcript
chr3H_489987690	T	T/T			C/C	C/C	T/T	T/T	T/T	T/T	NO SNP effect (border)
chr3H_489992342	C			G/G						C/C	AA change E-->D
chr3H_489994704	A	A/A		A/A		A/A				G/G	NO SNP effect (filling)
chr3H_490138207	C	C/C		C/C		C/C		A/A			AA change T-->N
chr3H_490140549	G	G/G						A/A			NO SNP effect (filling)
chr3H_490185026	A	A/A					G/G	G/G			NO SNP effect (filling)
chr3H_490222293	C	C/C		C/C	C/C	C/C	T/T				NO SNP effect (filling)
chr3H_490222504	G			G/G			A/A				AA change A-->T
chr3H_490224135	G	G/G					A/A			A/A	NO SNP effect (filling)
chr3H_490225065	G	G/G	G/G	G/G	G/G	G/G	A/A	A/A	A/A	A/A	AA change T-->M
chr3H_490225164	G	G/G	G/G	G/G	G/G	G/G	A/A	A/A	A/A	A/A	AA change A-->V
chr3H_490225346	C	C/C	C/C	C/C		C/C	A/A	A/A	A/A	A/A	NO SNP effect (filling)
chr3H_490226297	G	G/G	G/G	G/G	G/G	G/G	T/T	T/T	T/T	T/T	AA change L-->F

chr3H_490226443	A	A/A	A/A	A/A	A/A	A/A	G/G	G/G	G/G	G/G	AA change D-->G
chr3H_490226703	G	G/G	G/G	G/G	G/G	G/G	A/A	A/A	A/A	A/A	AA change R-->C
chr3H_490226807	C	C/C	C/C	C/C	C/C	C/C	C/C	C/C	C/C	C/C	AA change G-->E
chr3H_490226867	G	G/G	G/G	G/G	G/G	G/G		A/A	A/A	A/A	AA change T-->I
chr3H_490230968	T			T/T		T/T		C/C			NO SNP effect (filling)
chr3H_490231420	T			T/T						C/C	NO SNP effect (filling)
chr3H_490236800	G			G/G			C/C			C/C	NO SNP effect (filling)
chr3H_490237161	T	T/T		T/T	T/T		T/G	T/G	T/G	T/G	AA change S-->A
chr3H_490237629	G	G/G	G/G	G/G	G/G	G/G	G/C	G/C	G/C	G/C	AA change V-->L
chr3H_490238268	G		G/G	G/G			C/C		C/C	C/C	NO SNP effect (filling)
chr3H_490238371	A	A/A	A/A	A/A		A/A		G/G		G/G	NO SNP effect (filling)
chr3H_490238420	A	A/A	A/A	A/A		A/A		C/C	C/C	C/C	NO SNP effect (filling)
chr3H_490238889	T	T/T	T/T	T/T	T/T	T/T	G/G	G/G	G/G	G/G	AA change L-->V
chr3H_490238963	A	A/A	A/A	A/A	A/A	A/A	C/C	C/C	C/C	C/C	AA change I-->L
chr3H_490238966	T	T/T	T/T	T/T	T/T	T/T	C/C	C/C	C/C	C/C	AA change S-->P
chr3H_490238990	A	A/A	A/A	A/A	A/A	A/A	A/G	G/G	G/G	G/G	AA change R-->G
chr3H_490239124	C	C/C	C/C	C/C	C/C	C/C	C/T	C/T	C/T	C/T	AA change T-->I
chr3H_490239155	G	G/G	G/G	G/G	G/G	G/G	G/T	G/T	G/T	G/T	AA change A-->S
chr3H_490239267	T	T/T		T/T	T/T		C/C	C/C	C/C	C/C	AA change F-->L
chr3H_490239383	C	C/C		C/C	C/C		G/G	G/G	G/G	G/G	AA change N-->K
chr3H_490239682	G	G/G	G/G	G/G	G/G	G/G	C/C	C/C	C/C	C/C	AA change G-->A
chr3H_490239742	T	T/T		T/T	T/T		C/C	C/C	C/C	C/C	AA change L-->P
chr3H_490239753	A	A/A		A/A	A/A		C/C	C/C	C/C	C/C	AA change S-->R
chr3H_490243554	G	G/G	G/G	G/G	G/G	G/G	G/A	G/A	G/A	G/A	NO SNP effect (filling)
chr3H_490243586	C	C/C	C/C	C/C	C/C	C/C	C/T	C/T	C/T	C/T	AA change P-->L
chr3H_490244086	G	G/G	G/G	G/G	G/G	G/G	G/T	G/T	G/T	G/T	AA change V-->L
chr3H_490244130	T	T/T	T/T	T/T	T/T	T/T	T/A	T/A	T/A	T/A	AA change S-->R
chr3H_490244362	T	T/T	T/T	T/T	T/T	T/T	C/C	C/C	C/C	C/C	NO SNP effect (filling)
chr3H_490245953	T	T/T	T/T	T/T	T/T	T/T	C/C	C/C		C/C	AA change V-->A
chr3H_490246041	A	A/A	A/A	A/A	A/A	A/A	G/G	G/G		G/G	NO SNP effect (filling)
chr3H_490246263	A	A/A	A/A	A/A	A/A	A/A				C/C	AA change E-->D
chr3H_490246360	A		A/A			A/A	C/C				AA change N-->H
chr3H_490258429	A					A/A	G/G			G/G	AA change G-->E (border)
chr3H_493213107	G	G/G		G/G		G/G	T/T	T/T	T/T	T/T	NO SNP effect (border)

Additional genotyping of *Rrs1* interval

156 lines were genotyped using 48 SNPs which were polymorphic between predicted *Rrs1* and non-*Rrs1* lines. One of 48 SNPs did not produce data and no result was provided by LGC Genomics, chr3H_490226807 and chr3H_490244362 were monomorphic and chr3H_489992342 was monomorphic and showed high numbers of missing values (Table VI-16). Three

out of 156 lines, (used in duplicate) displayed a constant genotype indicating that the remaining assays were reliable.

Out of 156 lines genotyped, 138 lines were phenotyped with *R. commune* isolate LfL12F. However, this assay is not specific for *Rrs1* resistance and does not discriminate between *Rrs1*, *Rrs2, Rrs13* and potentially unknown resistances. To identify *Rrs1*-diagnostic SNPs, SNP marker candidates were eliminated if both alleles were found in susceptible lines. 9 lines showed high standard deviation of the score (Table VI-16). Lines were considered susceptible if the mean score of 4 plants was higher than 1.5, where 1 correspond to very small lesions on the edge and tip of the leaf and 2 to small defined lesions on the edge and base of the leaf. The full interval showed strong linkage disequilibrium but chr3H_490243586, chr3H_490244086 and chr3H_490244130 SNP markers showed the highest association with the trait thanks to the genotyping result of Syrian/ Jordanian landraces which provided a better resolution within the region (Figure VI-19, Table VI-16). Moreover, these 3 SNP markers specifically discriminated susceptible lines with the exception of 2 lines (with inconsistent phenotypes; showing high standard deviation which were thus removed from further analysis) (Table VI-16). These 3 markers were located in a 544bp interval, with identical genotypes in all the susceptible lines (Table VI-16). All three markers showed a heterozygote genotype in predicted *Rrs1* lines (Table VI-16). This result is likely to be due to the presence of homologous duplicated sequence in the barley genome. The 3 heterozygote calls were always associated together in resistant lines and were present in $Rrs1_{RH4}$ control lines SBCC145, SBCC154, CIHO-3515, and CI11549 (*Rrs1, Rrs4*) but all of the other *Rrs1* control line presented the susceptible allele. These 3 markers were all localised in a single gene: HORVU3Hr1G064130.

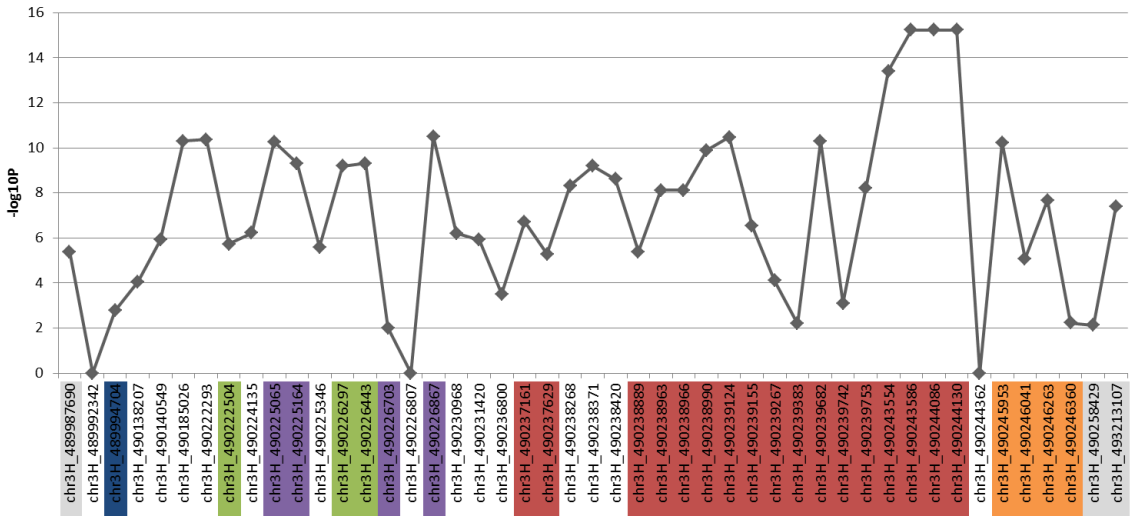

Figure VI-19: Plot of the –log10p (from a chi-squared test of association) of alleles of SNP markers in resistant lines compared to susceptible lines. Lines were considered as susceptible if the scores (means of 4 reps scored 15 days after infection) was higher than 1.5.. Names of SNPs correspond to the physical location of the SNPs on the genome. SNPs coloured in grey correspond to the SNPs outside of the interval, SNPs coloured in write correspond to SNPs located in introns or in-between coding sequences, SNPs coloured in blue correspond to SNPs located in HORVU3Hr1G064110 gene, SNPs coloured in green correspond to SNPs located in HORVU3Hr1G064180 gene, SNPs coloured in blue correspond to SNPs located in HORVU3Hr1G064190 gene, SNPs coloured in red correspond to SNPs located in HORVU3Hr1G064130 gene and SNPs coloured in orange correspond to SNPs located in HORVU3Hr1G064200 gene.

Table VI-16: Genotyping result of Rrs1 interval using lines selected. Scores are the means of 4 repeat scored 15 days after infection. Yellow mean score are inconsistent mean with high standard deviation. B allele= susceptible allele according to susceptible lines Beatrix and Concerto, A allele= opposite allele of Beatrix and Concerto, H= heterozygote call. Lines name with grey background are lines carrying SCRI_RS_221644 minor allele marker putatively predicting *Rrs1* line. Green line names are Syrian/ Jordanian landraces, red line names are winter barley cultivars. Names of SNPs correspond to the physical location of the SNPs on the genome. SNPs coloured in grey correspond to the SNPs outside of the interval, SNPs coloured in write correspond to SNPs located in intron or in-between coding sequences, SNPs coloured in blue correspond to SNPs located in HORVU3Hr1G064110 gene, SNPs coloured in green correspond to SNPs located in HORVU3Hr1G064180 gene, SNPs coloured in blue correspond to SNPs located in HORVU3Hr1G064190 gene, SNPs coloured in red correspond to SNPs located in HORVU3Hr1G064130 gene and SNPs coloured in orange correspond to SNPs located in HORVU3Hr1G064200 gene. SNPs genotype highlighted in pink shade are the only SNPs discriminating susceptible lines from resistant lines.

SNP physical location	chr3H_489987690	chr3H_489992342	chr3H_489994704	chr3H_490138207	chr3H_490140549	chr3H_490185026	chr3H_490222293	chr3H_490222504	chr3H_490224135	chr3H_490225065	chr3H_490225164	chr3H_490225346	chr3H_490226297	chr3H_490226443	chr3H_490226703	chr3H_490226807	chr3H_490226867	chr3H_490230968	chr3H_490231420	chr3H_490236800	chr3H_490237161	chr3H_490237629	chr3H_490238268	chr3H_490238371	chr3H_490238420	chr3H_490238889	chr3H_490238963	chr3H_490238966	chr3H_490238990	chr3H_490239124	chr3H_490239155	chr3H_490239267	chr3H_490239383	chr3H_490239682	chr3H_490239742	chr3H_490239753	chr3H_490243554	chr3H_490243586	chr3H_490244086	chr3H_490244130	chr3H_490244362	chr3H_490245953	chr3H_490246041	chr3H_490246263	chr3H_490246360	chr3H_490258429	chr3H_493213107	Phenotype	
Lines name (*known resistance*)																																															Mean	stdev
CONCERTO	B	B	B	B	B	B	B	B	B	B	B	B	B	B	B	B	B	B	B	B	B	B	B	B	B	B	B	B	B	B	B	B	B	B	B	B	B	B	B	B	B	B	B	B	B	B	B	3.33	0.77
BEATRIX	B	B	B	B	B	B	B	B	B	B	B	B	B	B	B	B	B	B	B	B	B	B	B	B	B	B	B	B	B	B	B	B	B	B	B	B	B	B	B	B	B	B	B	B	B	3.68	0.41
ATLAS46 (*Rrs1 TURK, Rrs2*)	A		A	B	B	B	B	B	B	B	B	B	B	B	B	B	B	B	B	B	B	B	B	B	B	B	B	B	B	B	B	B	B	B	B	B	B	B	B	B	B	B	B	B	B	1.56	1.45
STEUDELLI (*Rrs1, Rrs3*)	A		B	B	B	B	B	B	B	B	B	B	B	B	B	B	B	B	B	A	B	B	B	B	B			B	B	B		A	B	A		B	B	B	B	B	B	A	B	B		1.68	1.60
TRITON (*Rrs1, Rrs15*)	A		B	B	B	B	B	B	B	B	B	B	B	B	B	B	B	B	B	B	B	B	B	B	B	B	B	B	B	B	B	B	B	B	B	B	B	B	B	B	B	A	A	A	B	0.92	0.12
ARMELLE (*Rrs1 BRIER*)	A		B	B	B	B	B	B	B	B	B	B	B	B	B	B	B	B	B	B	B	B	B	B	B	B	B	B	B	B	B	B	B	B	B	B	B	B	B	B	B	A	B	A	B	4	0
ABYSSINIAN-B19460 (*Rrs, Rrs3*)	A		B	A	A	B		A	A	B	B	A	B	B		B	B	A	A	A	H	A		A					B	B	B	A	A			B	B	B	B	B	A	B	B	B	B	B	0	0
CI11549 (*Rrs1, Rrs4*)	B		B	A	A	B		A	A	B	B	A	B	B		B	B	A	A	A	H	H	B	B	B				B	B	H	A	A			B	B	B	B	A	A	B	B		B	B	0.38	0.38
SBCC145 (*Rrs1 RH4*)	B	B	B	B	A	B	B	A	A	B	B	A	B	B	B	B	B	B	B	B		B	B	B	B	A	B	B	B	A	B		B	B		H	H	H	H	B	B	B	B	B	B	B	0	0
SBCC154 (*Rrs1 RH4*)	A	B	B	B	B		B	B	A	B	A	A	A	A		B	A	A	A	B	B	B	B	B	B	B	B	B	B	B	B	B	B	B	B	B	H	H	H	H	B	B	B	B	B	B	B	0.09	0.29
CIHO-3515 (*Rrs1 RH4, Rrs13*)	A		B	A			B	B	A	B	A	A	A	A		B	A	A	A	B	B	B	B	B	B	B	B	B	B	B	B	B	B	B	B	B	H	H	H	H	B	B	B	B	B	B	B	0.25	0.25
BELGRAVIA	A		A	A	A	A	A	A	A	A	A	A	A	A	B	A	A	A	A	H	H	A	A	A	A	A	H	H	H	A	A	A	A	A	H	H	H	H	B	A	A	A	B	B	A	0	0
BERYLLIUM	A		A	A	A	A	A	A	A	A	A	A	A	A	B	A	A	A	A	H	H	A	A	A	A	A	H	H	H	A	A	A	A	A	H	H	H	H	B	A	A	A	B	B	A	0.44	0.32
BRAHMS	A		A	A	A	A	A	A	A	A	A	A	A	A	B	A	A	A	A	H	H	A	A	A	A	A	H	H	H	A	A	A	A	A	H	H	H	H	B	A	A	A	B	B	A	0	0
CAIRN	A		A	A	A	A	A	A	A	A	A	A	A		B	A	A	A	A	H	H	A	A	A	A	A	H	H	H	A	A	A	A	A	H	H	H	H	B	A	A	A	B	B	A	0	0
CASINO	A		A	A	A	A	A	A	A	A	A	A	A	A	B	A	A	A	A	H	H	A	A	A	A	A	H	H	H	A	A	A	A	A	H	H	H	H	B	A	A	A	B	B	A	0.31	0.54
CENTURY	A		A	A	A	A	A	A	A	A	A	A	A	A	B	A	A	A	A	H	H	A	A	A	A	A	H	H	H	A	A	A	A	A	H	H	H	H	B	A		A	B	B	A	0	0
CHIEFTAIN	A		A	A	A	A	A	A	A	A	A	A	A	A	B	A	A	A	A	H	H	A		A	A	A	H	H	H	A	A	A	A	A	H	H	H	H	B	A	A	A	B	B	A	0	0
CHRONICLE	A		A	A	A	A	A	A	A	A	A	A	A		B	A	A	A	A	H	H	A	A	A	A	A	H	H	H	A	A	A	A	A	H	H	H	H	B	A	A	A	B	B	A	0	0
FREJA	A		B	B	B	B	B	B	B	B	B	B	B	B	B	B	B	B	B	B	B	B	B	B		B		B	B	B		A	B	H		H	H	H	H	B	B	B	A	B	B		0	0
GARNER	A		A	A	A	A	A	A	A	A	A	A	A		B	A	A	A	A	H	H	A	A	A	A		H	H	H	A	A	A	A	A	H	H	H	H	B	A	A	A	B	B	A		
GRAPHIC	A		A	A	A	A	A	A	A	A	A	A	A	A	B	A	A	A	A	H	H	A	A	A	A	A	H	H	H	A	A	A	A	A	H	H	H	H	B	A	A	A	B	B	A	0	0
MAGELLAN	A		A	A	A	A	A	A	A	A	A	A	A		B	A	A	A	A	H	H	A	A	A	A	A	H	H	H	A	A	A	A	A	H	H	H	H	B	A	A	A	B	B	A	0	0
MINSTREL	A		A	A	A	A	A	A	A	A	A	A	A	A	B	A	A	A	A	H	H	A	A	A	A	A	H	H	H	A	A	A	A	A	H	H	H	H	B	A	A	A	B	B	A		
MONTOYA	A		A	A	A	A	A	A	A	A	A	A	A		B	A	A	A	A	H	H	A	A	A	A	A	H	H	H	A	A	A	A	A	H	H	H	H	B	A	A	A	B	B	A		
NSL_99-5363	A		A	A	A	A	A	A	A	A	A	A	A	A	B	A	A	A	A	H	H	A	A	A	A	A	H	H	H	A	A	A	A	A	H	H	H	H	B	A	B	A	B	B	A		
PROPINO	A		A	A	A	A	A	A	A	A	A	A	A		B	A	A	A	A	H	H	A	A	A	A	A	H	H	H	A	A	A	A	A	H	H	H	H	B	A	A	A	B	B	A		
PUBLICAN	A		A	A	A	A	A	A	A	A	A	A	A		B	A	A	A	A	H	H	A	A	A	A	A	H	H	H	A	A	A	A	A	H	H	H	H	B	A	A	A	B	B	A		
QUENCH	A		A	A	A	A	A	A	A	A	A	A	A		B	A	A	A	A	H	H	A	A	A	A	A	H	H	H	A	A	A	A	A	H	H	H	H	B	A	A	A	B	B	A		
REBECCA	A		A	A	A	A	A	A	A	A	A	A	A		B	A	A	A	A	H	H	A	A	A	A	A	H	H	H	A	A	A	A	A	H	H	H	H	B	A	A	A	B	B	A	0.31	0.54
SHUFFLE	A		A	A	A	A	A	A	A	A	A	A	A		B	A	A	A	A	H	H	A	A	A	A	A	H	H	H	A	A	A	A	A	H	H	H	H	B	A	A	A	B	B	A		
SUMMIT	A		A	A	A	A	A	A	A	A	A	A	A		B	A	A	A	A	H	H	A	A	A	A	A	H	H	H	A	A	A	A	A	H	H	H	H	B	A	A	A	B	B	A		
SW-2808	A		A	A	A	A	A	A	A	A	A	A	A		B	A	A	A	A	H	H	A	A	A	A	A	H	H	H	A	A	A	A	A	H	H	H	H	B	A	A	A	B	B	A	0	0
WESTMINSTER	A		A	A	A	A	A	A	A	A	A	A	A	A	B	A	A	A	A	H	H	A	A	A	A	A	H	H	H	A	A	A	A	A	H	H	H	H	B	A	A	A	B	B	A	0	0
22-004	A	B	B	A	A	B		A	A	B	B	A	B	B	A	B	B	A	A	A	H	A	A	A	A	A	A	H	H	H	A	A	A	A	A	H	H	H	H	B	A	A	A	B	B	B	1.13	0.38
22-013			B	H	A	H	A	A	A		H	A	H	H	A	B	A	A	A	H	H	A	A	A	A	A	H	H	H	A	A	A	A	A	A		H	H	H	H	B	A	A	A	B	H	B	1.19	0.32
30-010	B		B	B	A	A	A	A	A	A	A	A	A	A	B	A	A	A	A	H	B	A	A	A	A	A	H	H	H		A	A	A	A	H	H	H	H	B	A	A		B	B	B	0.25	0.43
34-030	A				A		A	A	A			A			B	A	A	A	A	H	H	A	A	A	A	H	H		H		A	A	A	A	H	H	H	H	B		A		B	B		0.19	0.21
34-076	A		B	A	A	A	A	A	A	A	A	A	A		B	A	A	A	A	H	H	A	A	A	A	A	H	H	H	A	A	A	A	A	H	H	H	H	B	A	A	A	B	B	A	0.56	0.57
58-019	A		A	B	A	A	A	A	A	A	A	A	A	A		A	A	A	A	H	B	A	A	A	A	A	A	A	B		A	A	A	A	H	H	H	H	B	A	A	A	B	B	A	0	0
66-016	A		B	A	A	A	A	A	A	A	A	A	A		B	A	A	A	A	H	H		A	A	A	A	H	H	H	A	A	A	A	A	H	H	H	H	B	A	A	A	B	B	B	0	0
66-023	A		B	A	A	A	A	A	A	A	A	A	A		B	A	A	A	A	H	H	A	A	A	A	A	H	H	H	A	A	A	A	A	H	H	H	H	B	A	A	A	B	B	B	0.81	0.48
66-024	A		B	A	A	A	A	A	A	A	A	A	A		B	A	A	A	A	H	H	A	A	A	A	A	H	H	H	A	A	A	A	A	H	H	H	H	B	A	A	A	B	B	B	0	0
67-007	A		B	A	A	A	A	A	A	A	A	A	A	A	B	A	A	A	A	H	H	A	A	A	A	A	H	H	H	A	A	A	A	A	H	H	H	H	B	A	A	A	B	B	A	0.38	0.38
67-017	A		B		A	A	A	A	A	A	A	A	A		B	A	A	A	A	H	H	A	A	A	A	A	H	H	H	A	A	A	A	A	H	H	H	H	B	A	A	A	B	B	B	0	0
JLB_08-005	B		B	B	A	A	A	A	A	A	A	A	A		B	A	A	A	A	H	B	A	A	A	A	A	H	H	H		A	A	A	A	H	H	H	H	B	A	A	A	B	B	B	0.50	0.31
RETRIEVER(*RRS1*)	A		A	A	A	A	A	A		A	A	A	A	A	B	A	A	A	A	H	H	A	A	A	A	A	H	H	H	A	A	A	A	A	H	H	H	H	B	A	A	A	B	B	A	0	0
SUZUKA	A		A	A	A	A	A	A	A	A	A	A	A	A	B	A	A	A	A	H	H	A	A	A	A	A	H	H	H	A	A	A	A	A	H	H	H	H	B	A	A	A	B	B	B		
WINSOME	A		A	A	A	A	A	A	A	A	A	A	A	A	B	A	A	A	A	H	H	A	A	A	A	A	H	H	H	A	A	A	A	A	H	H	H	H	B	A	A	A	B	B	A	0.13	0.22
30-031	B		B	B	A	A	A	A	A	A	A	A	A		B	A	A	A	A	H	B	A	A	A	A	A	H	H	H		A	A	A	A	B	B	B	B	B	A	A	A	B	A	B	3.88	0.22
09-049	B		B	B	A	A	A	A	A	A	A	A	A		B	A	A	A	A	H	B	A	A	A	A	A	H	H	H		A	A	A	A	B	B	B	B	B	A	A	A	B	A	B	4	0
12-002	B		B	B	A	A	A	A	A	A	A	A	A		B	A	A	A	A	H	B	A	A	A	A	A	H	H	H		A	A	A	A	B	B	B	B	B	A	A	A	B	A	B	2.44	0.57
19-011	A	B	B	A	A	B		A	A	B	B	A	B	B	A	B	B	A	A	A	H	H	A	A	A	A	B	B	B	B	H	A	A		A	B	B	B	B	B	A	B	B		B		2.5	0
19-034	A		B	A	A	B		A	A	B	B	A	B	B	A	B	B	A	A	A	H	H	A	A	A	A	B	B	B	B	B	A	A	B	A		A	B	B	B	B	B	A	B	A	B	3.81	0.21
66-058	B		B	A	A	B		A	A	B	B	A	B	B		B	B	A	A		H	H	A	A	A	A	B	B	B	B	H	A	A		A		A	B	B	B	B	A	B	B		B	4	0
49-048	A		B	A	A	B		A	A	B	B	A	B	B		B	B	A	A	A	H	H	A	A	A	A	B	B	B	B	H	A	A		A		A	B	B	B	B	A	B	B	B	B	4	0
49-025	A		B		B		B	A	A	B	B			B	A		B			A	B	B	A	A	A			A				A	B		B		B	B	B	B	B	B	A	A	B	4	0
SW-MACSENA	A		A	A	A	B		A	A	B	B	A	B	B		B	B	A	A		H	H	A	A	A	A	B	B	B	B	H	A	A		A		A	B	B	B	B	A	B	B		B	0	0
Steptoe	A		B			B	A	A	A	B	A	A	A			B	A	A	A		B	H	B	A	A	A	B	B	B	B	B	A	B	A	A	B	B	B	B	B	B	B	B	B	B		
FRANKLIN	A		B	A	A	B		A	A	B	B	A	B	B		B	B	A	A	A	H	A		A					B	B	H	A	A			B	B	B	B	B	A	B	B	B	B	B	0.75	0.204
GAIRDNER	A		B	A	A	B		A	A	B	B	A	B	B		B	B	A	A	A	H	H		A		B		B	B	H	A	A	B	H		B	B	B	B	B	A	B	B	B	B	B	0	0
42-008	B	B	B	A	A	B		A	A	B	B	A	B	B	A	B	B	A	A		B	H	B	B	B				B	B	A	A	A			B	B	B	B	B	A	A	B	B		B	4	0
SLB_03-026	B	B	B	A	A	B		A	A	B	B	A	B	B	A	B	B	A	A		B	H	B	B	B				B	B	A	A	A			B	B	B	B	B	A	A	B	B		B	4	0
05-053	B		B	A	A	B		A	A	B	B	A	B	B	A	B	B	A	A	A	H	H	B	B	B				B	B	H	A	A		A	B	B	B	B	B	A		B	B		B	4	0
22-065	B		B	A	A	B		A	A	B	B	A	B	B	A	B	B	A	A	A	H	H	B	B	B				B	B	H	A	A		A	B	B	B	B	B	A		B	B		B	2.75	0.47

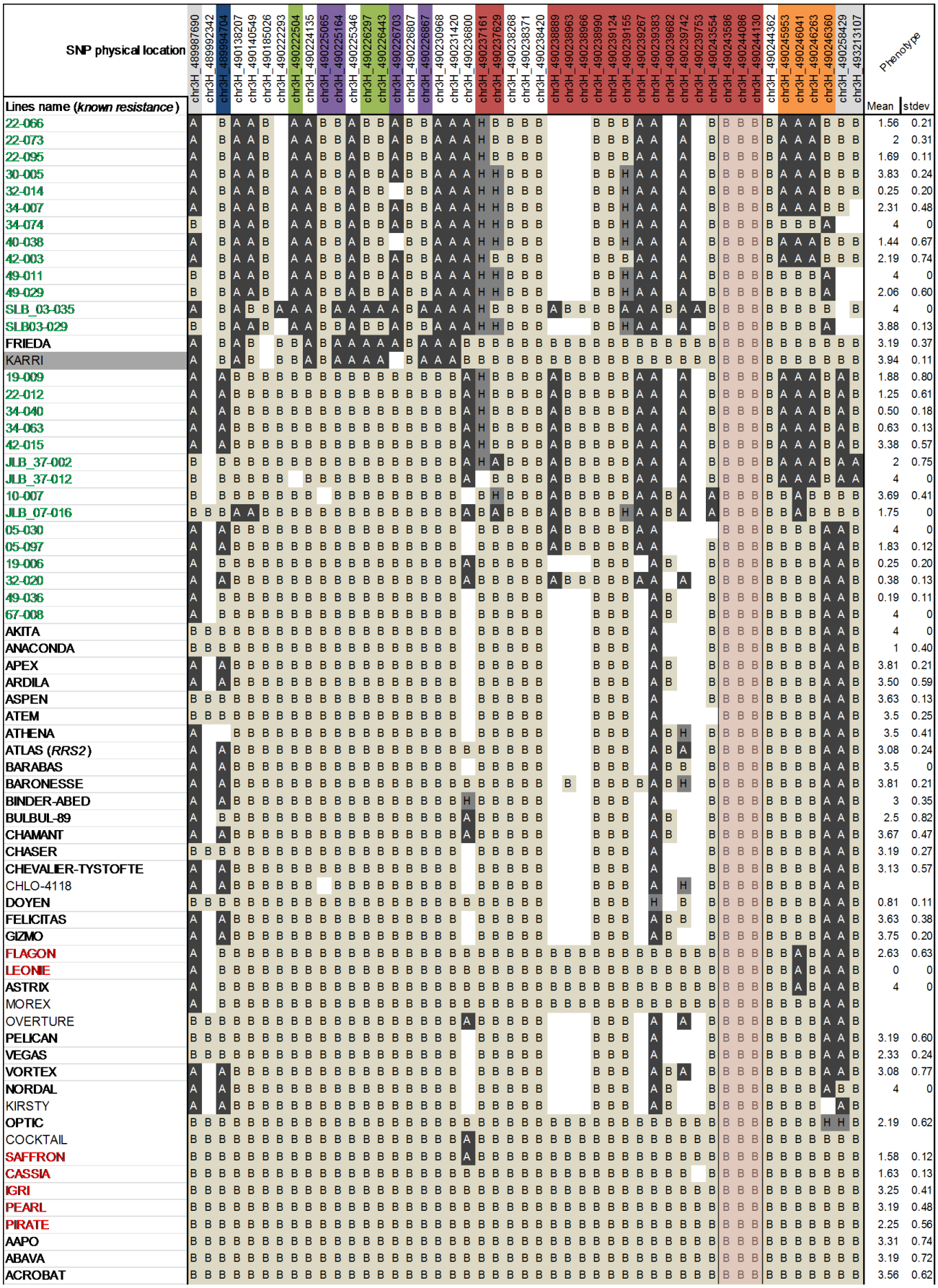
SNP physical location
chr3H_489987690
chr3H_489992342
chr3H_489994704
chr3H_490138207
chr3H_490140549
chr3H_490185026
chr3H_490222293
chr3H_490222504
chr3H_490224135
chr3H_490225065
chr3H_490225164
chr3H_490225346
chr3H_490226297
chr3H_490226443
chr3H_490226703
chr3H_490226807
chr3H_490226867
chr3H_490230968
chr3H_490231420
chr3H_490236800
chr3H_490237161
chr3H_490237629
chr3H_490238268
chr3H_490238371
chr3H_490238420
chr3H_490238889
chr3H_490238963
chr3H_490238966
chr3H_490238990
chr3H_490239124
chr3H_490239155
chr3H_490239267
chr3H_490239383
chr3H_490239682
chr3H_490239742
chr3H_490239753
chr3H_490243554
chr3H_490243586
chr3H_490244086
chr3H_490244130
chr3H_490244362
chr3H_490245953
chr3H_490246041
chr3H_490246263
chr3H_490246360
chr3H_490258429
chr3H_493213107
Phenotype
Lines name (known resistance)
Mean
stdev
22-066 1.56 0.21
22-073 2 0.31
22-095 1.69 0.11
30-005 3.83 0.24
32-014 0.25 0.20
34-007 2.31 0.48
34-074 4 0
40-038 1.44 0.67
42-003 2.19 0.74
49-011 4 0
49-029 2.06 0.60
SLB_03-035 4 0
SLB03-029 3.88 0.13
FRIEDA 3.19 0.37
KARRI 3.94 0.11
19-009 1.88 0.80
22-012 1.25 0.61
34-040 0.50 0.18
34-063 0.63 0.13
42-015 3.38 0.57
JLB_37-002 2 0.75
JLB_37-012 4 0
10-007 3.69 0.41
JLB_07-016 1.75 0
05-030 4 0
05-097 1.83 0.12
19-006 0.25 0.20
32-020 0.38 0.13
49-036 0.19 0.11
67-008 4 0
AKITA 4 0
ANACONDA 1 0.40
APEX 3.81 0.21
ARDILA 3.50 0.59
ASPEN 3.63 0.13
ATEM 3.5 0.25
ATHENA 3.5 0.41
ATLAS (RRS2) 3.08 0.24
BARABAS 3.5 0
BARONESSE 3.81 0.21
BINDER-ABED 3 0.35
BULBUL-89 2.5 0.82
CHAMANT 3.67 0.47
CHASER 3.19 0.27
CHEVALIER-TYSTOFTE 3.13 0.57
CHLO-4118
DOYEN 0.81 0.11
FELICITAS 3.63 0.38
GIZMO 3.75 0.20
FLAGON 2.63 0.63
LEONIE 0 0
ASTRIX 4 0
MOREX
OVERTURE
PELICAN 3.19 0.60
VEGAS 2.33 0.24
VORTEX 3.08 0.77
NORDAL 4 0
KIRSTY
OPTIC 2.19 0.62
COCKTAIL
SAFFRON 1.58 0.12
CASSIA 1.63 0.13
IGRI 3.25 0.41
PEARL 3.19 0.48
PIRATE 2.25 0.56
AAPO 3.31 0.74
ABAVA 3.19 0.72
ACROBAT 3.56 0.62

SNP physical location	chr3H_489987690	chr3H_489992342	chr3H_489994704	chr3H_490138207	chr3H_490140549	chr3H_490185026	chr3H_490222293	chr3H_490222504	chr3H_490224135	chr3H_490225065	chr3H_490225164	chr3H_490225346	chr3H_490226297	chr3H_490226443	chr3H_490226703	chr3H_490226807	chr3H_490226887	chr3H_490230968	chr3H_490231420	chr3H_490236800	chr3H_490237161	chr3H_490237629	chr3H_490238268	chr3H_490238371	chr3H_490238420	chr3H_490238889	chr3H_490238963	chr3H_490238966	chr3H_490238990	chr3H_490239124	chr3H_490239155	chr3H_490239267	chr3H_490239383	chr3H_490239682	chr3H_490239742	chr3H_490239753	chr3H_490243554	chr3H_490243586	chr3H_490244086	chr3H_490244130	chr3H_490244362	chr3H_490245953	chr3H_490246041	chr3H_490246263	chr3H_490246360	chr3H_490258429	chr3H_493213107	Phenotype	
Lines name (*known resistance*)																																															Mean	stdev
AZURE	B	B	B	B	B	B	B	B	B	B	B	B	B	B	B	B	B	B	B	B	B	B	B	B	B	B	B	B	B	B	B	B	B	B	B	B	B	B	B	B	B	B	B	B	B	B	3.31	0.27
BC-LINE-30 (*RRS13*)	B	B	B	B	B	B	B	B	B	B	B	B	B	B	B	B	B	B	B	B	B	B	B	B	B	B	B	B	B	B	B	B	B	B	B	B	B	B	B	B	B	B	B	B	B	B	2.19	0.37
CALGARY	B	B	B	B	B	B	B	B	B	B	B	B	B	B	B	B	B	B	B	B	B	B	B	B	B	B	B	B	B	B	B	B	B	B	B	B	B	B	B	B	B	B	B	B	B	B	2.63	0.38
CELEBRA	B	B	B	B	B	B	B	B	B	B	B	B	B	B	B	B	B	B	B	B	B	B	B	B	B	B	B	B	B	B	B	B	B	B	B	B	B	B	B	B	B	B	B	B	B	B	0	0
SCARLETT	B	B	B	B	B	B	B	B	B	B	B	B	B	B	B	B	B	B	B	B	B	B	B	B	B	B	B	B	B	B	B	B	B	B	B	B	B	B	B	B	B	B	B	B	B	B	2.5	0.53
TARM92	B	B	B	B	B	B	B	B	B	B	B	B	B	B	B	B	B	B	B	B	B	B	B	B	B	B	B	B	B	B	B	B	B	B	B	B	B	B	B	B	B	B	B	B	B	B	3.13	0.38
DIGGER (*RRS2*)	B	B	B	B	B	B	B	B	B	B	B	B	B	B	B	B	B	B	B	B	B	B	B	B	B	B	B	B	B	B	B	B	B	B	B	B	B	B	B	B	B	B	B	B	B	B	2.75	0.25
DRUM	B	B	B		B	B	B	B	B	B	B	B	B	B	B	B	B	B	B	B	B	B	B	B	B	B	B	B	B	B	B	B	B	B	B	B	B	B	B	B	B	B	B	B	B	B	3.58	0.31
HANNCHEN	B	B	B	B	B	B	B	B	B	B	B	B	B	B	B	B	B	B	B	B	B	B	B	B	B	B	B	B	B	B	B	B	B	B	B	B	B	B	B	B	B	B	B	B	B	B	3.13	0.94
KINNAN	B	B	B	B	B	B	B	B	B	B	B	B	B	B	B	B	B	B	B	B	B	B	B	B	B	B	B	B	B	B	B	B	B	B	B	B	B	B	B	B	B	B	B	B	B	B		
KLAXON	B	B	B	B		B	B	B	B	B	B	B	B	B	B	B	B	B	B	B	B	B	B	B	B	B	B	B	B	B	B	B	B	B	B	B	B	B	B	B	B	B	B	B	B	B	3.17	0.12
KYM	B	B	B	B		B	B	B	B	B	B	B	B	B	B	B	B	B	B	B	B	B	B	B	B	B	B	B	B	B	B	B	B	B	B	B	B	B	B	B	B	B	B	B	B	B	3.81	0.32
MARISOTTER	B	B	B	B	B	B	B	B	B	B	B	B	B	B	B	B	B	B	B	B	B	B	B	B	B	B	B	B	B	B	B	B	B	B	B	B	B	B	B	B	B	B	B	B	B	B		
NSL-98-5065	B	B	B	B	B	B	B	B	B	B	B	B	B	B	B	B	B	B	B	B	B	B	B	B	B	B	B	B	B	B	B	B	B	B	B	B	B	B	B	B	B	B	A	B	B	B	3.94	0.11
NSL-95-1257	B	B	B	B	B	B	B	B	B	B	B	B	B	B	B	B	B	B	B	B	B	B	B	B	B	B	B	B	B	B	B	B	B	B	B	B	B	B	B	B	B	B	B	B	B	B	2.75	1.27
CORGI	A		A	A	A	A	A	A	A	A	A	A	A		B	A	A	A	H	H	A	A	A	A	A	A	H	H	H	A	A	A	A	A	H	H	H	H	B	A	A	A	B	B	A	1	1.73
22-014	A	B	B	A	A	B		A	A	B	B	A	B	B	A	B	B	A	A	A	H	A	A	A	A	A	A	H	H	H	A	A	A	A	A	H	H	H	H	B	A	A	A	B	B	B	2.19	1.70
10-009	B		B	B	B	B	B	B	B	B	B	B	B	B	B	B	B	B	B	B	A	B	B	B	B	B	B	A	B	B	B	B	A	A			H	H	H	H	B	A	A	A	B	B	B	1.88	1.88
67-015	B		B	A		B	A	A	A	B	B	A	B	B	A	B	B	B	A	A	H	A	A	A	A	A	B	B	B	B	A	A		A		A	B	B	B	B	B	A	B	B	B	B	2.13	1.26
12-014	A	B	B	A	A	B		A	A	B	B	A	B	B	A	B	B	A	A		H	H	A	A	A	A	B	B	B	B	H	A	A		A		A	B	B	B	B	B	A	B	B		B	2.67	1.89
CROPTON	B	B	B	B	B	B	B	B	B	B	B	B	B	B	B	B	B	B	B	B	B	B	B	B	B	B	B	B	B	B	B	B	B	B	B	B	B	B	B	B	B	B	B	B		B	2	2
ATHENE	A		B	B	B	B	B	B	B	B	B	B	B	B	B	B	B	B	B	B	B	B	B	B	B	B	B	B	B	B	B	B	B	B	B	B	B	B	B	B	B	B	A	B	A	A	B	2.25	1.24

Characterisation of the candidate *Rrs1* gene HORVU3Hr1G064130 model

Transcripts that were generated as part of the genome annotation effort for the latest barley genome release were used to characterise the candidate *Rrs1* gene HORVU3Hr1G064130 (unpublished data). HORVU3Hr1G064130 transcripts were mapped against the barley cultivar Morex 3H pseudomolecule sequence and revealed that HORVU3Hr1G064130 has at least five exons (Figure VI-20a) putatively coding for different transcripts due to alternative splicing (Figure VI-20b). Three of the transcripts identified could be functional and code for proteins with different N-terminal regions, where the first three exons act as alternative starts for the 3 different transcripts, but the 2 last exons are shared and code for the C-terminal protein region containing the transmembrane domain and a protein kinase-like superfamily domain (PKc_like super family: cd14066) (Figure VI-20b). In this shared protein kinase-like domain are putatively located the 3 SNP markers that specifically discriminate susceptible lines leading to non-synonymous amino acid substitutions in the coding sequence (Figure VI-20b). The first exon represents the start of transcript HORVU3Hr1G064130.a, coding for a putative signal peptide, an extracellular cysteine-rich wall-associated receptor kinase galacturonan-binding domain (GUB_WAK_binding domain: pfam13947) followed by a cysteine-rich Wall-associated receptor kinase domain (WAK_assoc domain: pfam14380). The second exon represents the start of transcript HORVU3Hr1G064130.b,

coding for a putative signal peptide and a cysteine-rich wall-associated receptor kinase domain (WAK_assoc domain: pfam14380). The third exon represents the start of transcript HORVU3Hr1G064130.c, coding for a putative signal peptide and a cysteine-rich wall-associated receptor kinase domain (WAK_assoc domain: pfam14380). All HORVU3Hr1G064130 transcripts have a signal peptide and share the same protein kinase-like domain but have different WAK_assoc domains with poor amino acid identity (35% between the transcripts a and b, 28% between the transcripts a and c and 36% between the transcripts b and c) but only transcript a has a GUB_WAK_binding domain. Despite this variability, full HORVU3Hr1G064130 transcripts putatively code for a wall-associated receptor-like kinase and are around 55% identical over 96% of query covered to *Zea mays* homologues.

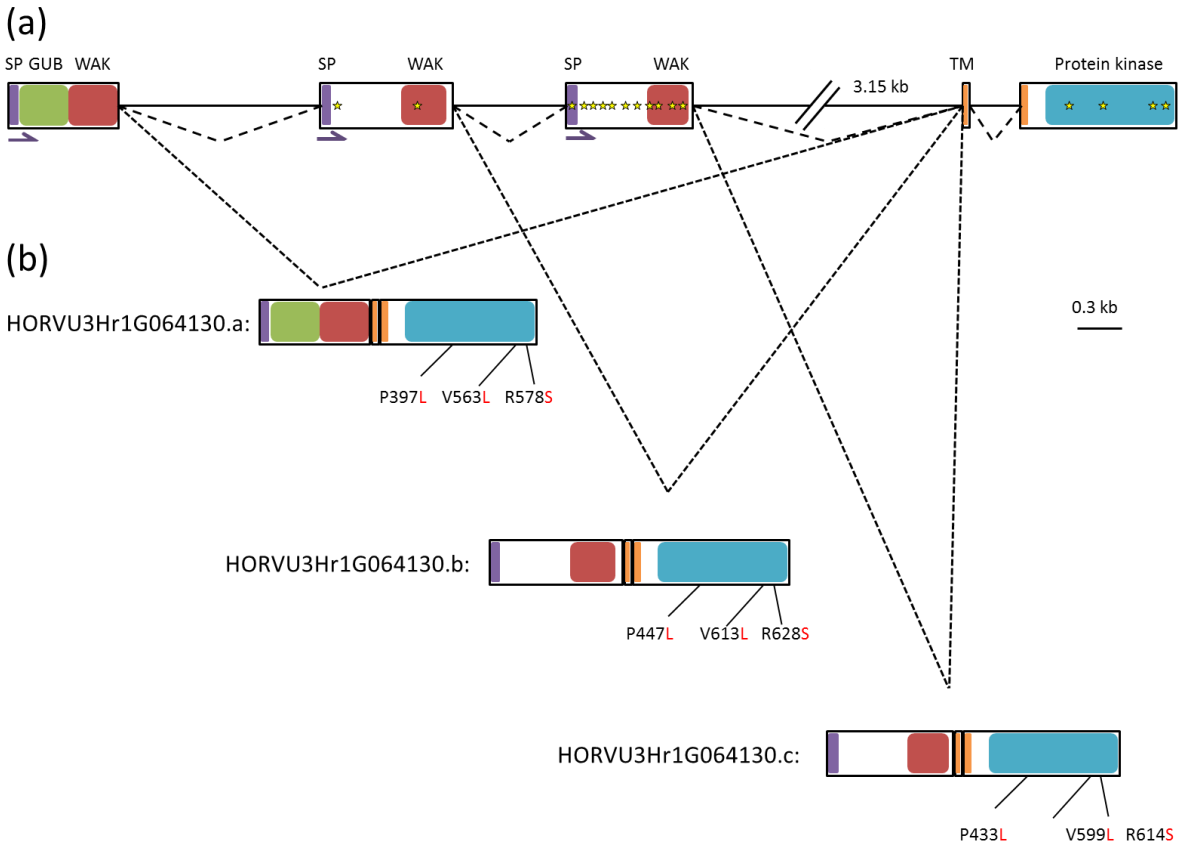

Figure VI-20: HORVU3Hr1G064130 gene model, transcript structure and non-synonymous amino acid SNP location in protein domain. (a) Gene structure of HORVU3Hr1G064130 gene and protein domain. Exons are represented as rectangular bars, and introns as black lines between the exons. Predicted domains are in colour: SP=start codon+signal peptide; GUB=wall-associated receptor kinase galacturonan-binding (GUB_WAK); WAK =wall-associated receptor kinase C-terminal (WAK_assoc); TM, transmembrane domain; protein kinase= protein kinase like superfamily domain. (b) Potentially functional transcript structure and location of non-synonymous amino acid SNP. Dashed line indicate splicing event necessary to generate each transcript. The number indicate the location of the amino acid in each transcript, the black letter indicate the reference amino acid allele (from Morex), the red letter indicate the alternative allele (from putative *Rrs1*)

PCR and RT-PCR of barley candidate gene transcripts and *R. commune* NIP1 effector

Primer efficiency was calculated for each primer pair using a slope of a standard curve generated using 4 serial dilutions of cDNA mixed sample ($E = 10^{(-1/slope)-1}$) (Table VI-17)

Table VI-17: The efficiency of primers used for qRT-PCR

	Primer pair	Slope	Amplification factor (E)	Efficiency (%)
Barley genes	Transcript a	-3.4851	1.94	93.61%
	Transcript b	-3.3559	1.99	98.60%
	Transcript c	-3.3834	1.97	97.50%
	C-term domain	-3.375	1.98	97.83%
***R. commune* genes**	NIP1	-3.7057	1.86	86.15%

Relative expression of *R. commune* NIP1 was measured from field samples (Figure VI-21). Due to the fact that not all strains carry NIP1 and that NIP1 relative expression analysis was normalised on reference genes expression present in all strains, the expression of NIP1 is underestimated in field samples compared to the germinated conidia sample. However the fact that we detected NIP1 in green leaf tissue shows that *R. commune* strains carrying NIP1 were present in the JHI nursery. No significant difference was observed between the expression of NIP1 regardless of the presence of *Rrs1* in the line studied (t test: n=3, p=0.17 for in green tissue, p=0.16 for necrotic tissue) and NIP1 was significantly upregulated in green tissue compared to necrotic tissue in *Rrs1* and non *Rrs1* lines (t test: N=3, p<0.01 for non *Rrs1* lines and p<0.05 for *Rrs1* lines (Figure VI-21).

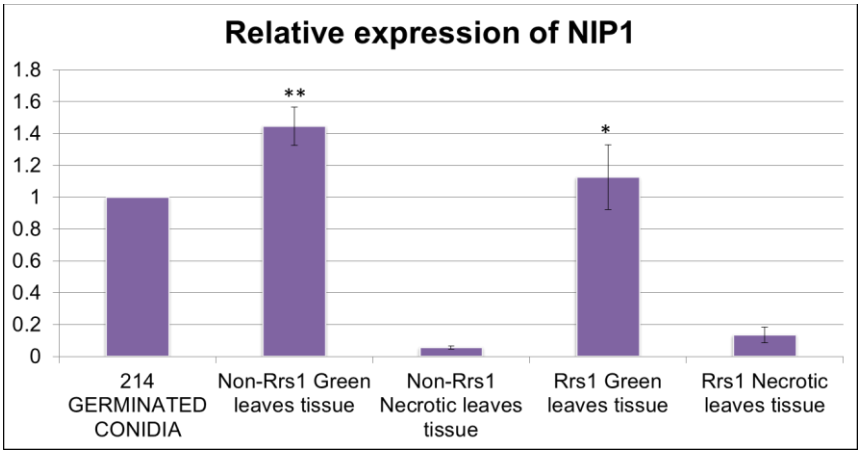

Figure VI-21: *R. commune* NIP1 effector relative expression. Mean of relative expression of NIP1 in non-*Rrs1* lines (Aapo, Optic and Steffi) and Rrs1 lines (Casino, Chieftain and Westminster) field samples (green leaves tissue and necrotic leaves tissue) compared to 214 germinated conidia. Error bars are standard deviation between lines. (* indicates significant differences of relative expression between green tissue and necrotic tissue of plants carrying *Rrs1* or not carrying *Rrs1*.

The relative expression of an *R. commune* endogenous gene was used to estimate the relative quantity of *R. commune* in the barley leaf section compared to the relative expression of barley endogenous genes estimating the relative quantity of barley cells per leaf section. This method assumes that the quantity of barley leaves collected for each sample was the same and allows differences in fungus quantity between susceptible and *Rrs1* predicted lines to be identified, indicating that lesions observed were caused by the fungus. The relative quantity of *R. commune* was highly variable between lines carrying or not carrying *Rrs1* (Figure VI-22). High quantity of fungus was estimated in necrotic leaves compared to green leaves and higher quantity of fungus was estimated in *Rrs1* green leaves compared to non-*Rrs1* green leaves but differences were not significant (t test: N=3, $p<0.05$) (Figure VI-22).

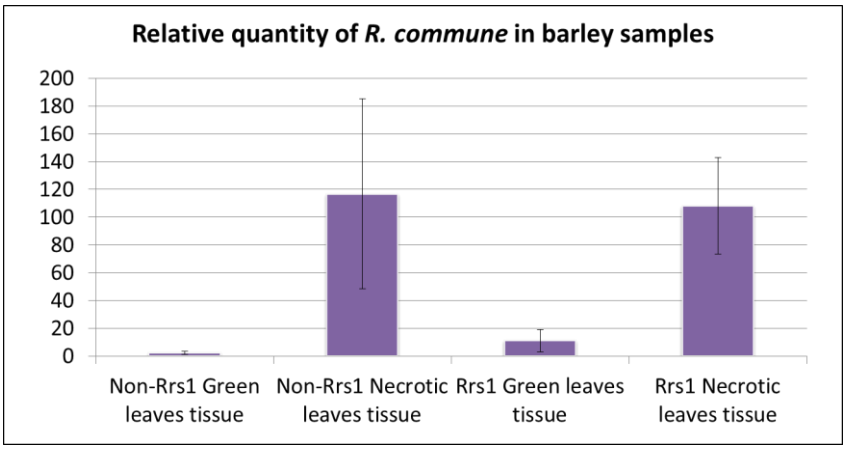

Figure VI-22: Mean of relative quantity of *R. commune* in non-*Rrs1* lines and *Rrs1* lines. Non *Rrs1* lines are: Aapo, Optic and Steffi. *Rrs1* line are: Casino, Chieftain and Westminster. Error bars are standard deviation between lines.

Transcripts were amplified from cDNA samples from Aapo, Steffi, Casino and Chieftain. PCR amplification of the 3 candidate transcripts showed that they were transcribed independently of the presence of *Rrs1* in all lines tested (Figure VI-23). The unique bright band of expected size for each sample indicates the splicing specificity on generating this transcript rather than non-functional mis-spliced product (Figure VI-23).

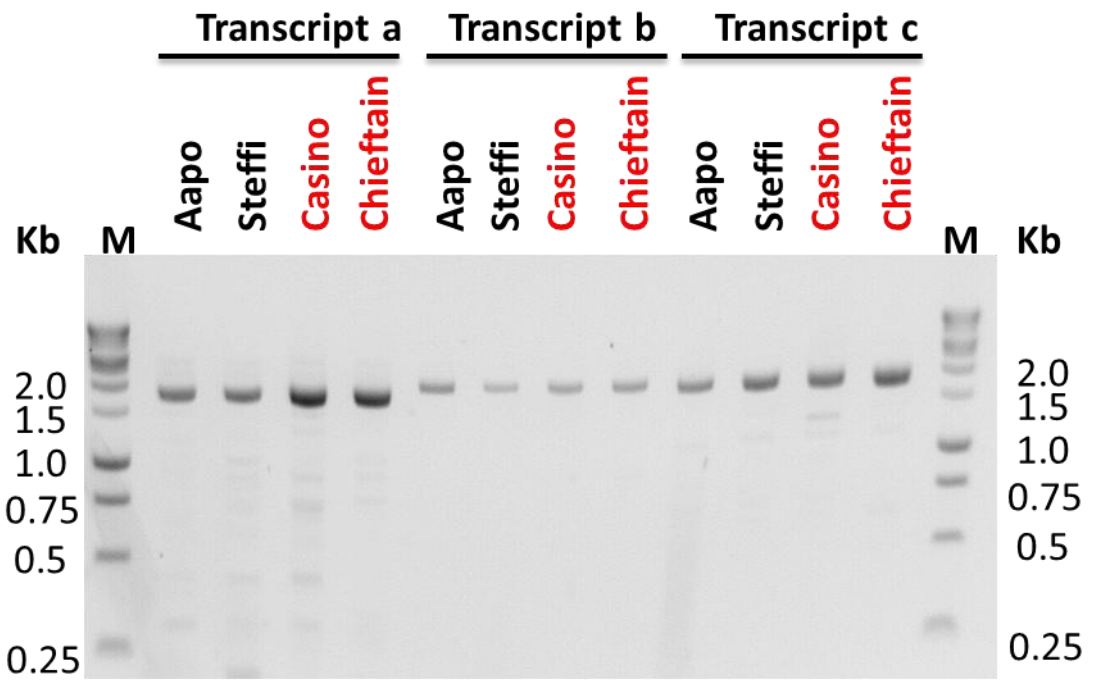

Figure VI-23: PCR amplification of the 3 transcripts in non-*Rrs1* lines and *Rrs1* lines. Non *Rrs1* lines: Aapo and Steffi. *Rrs1* lines in red: Casino and Chieftain. The expected size of PCR amplicon is 1827bp, 1977bp and 1935bp in transcript a, b and c respectively.

The 3 transcripts were partially sequenced from Aapo (non-*Rrs1*) and Casino (*Rrs1* predicted) and aligned against the Morex pseudomolecule (non-*Rrs1*) to check if the $Rrs1_{Rh4}$ discriminating SNP identified by the genotyping project were present in HORVU3Hr1G064130 transcripts studied. Many polymorphisms were visualised between Morex/Aapo and Casino corresponding to some of the SNPs selected in the genotyping project, causing the strong linkage disequilibrium observed in Figure VI-19. The C/T SNP located at the Chr3H_490243586 SNP location could be visualised at the expected location as Morex/Aapo and Casino were homozygous at this base location. This result suggests thatHORVU3Hr1G064130 is not *Rrs1* because putative *Rrs1* lines did not have the alternative allele discriminating the susceptible lines from the resistant lines (Figure VI-24).

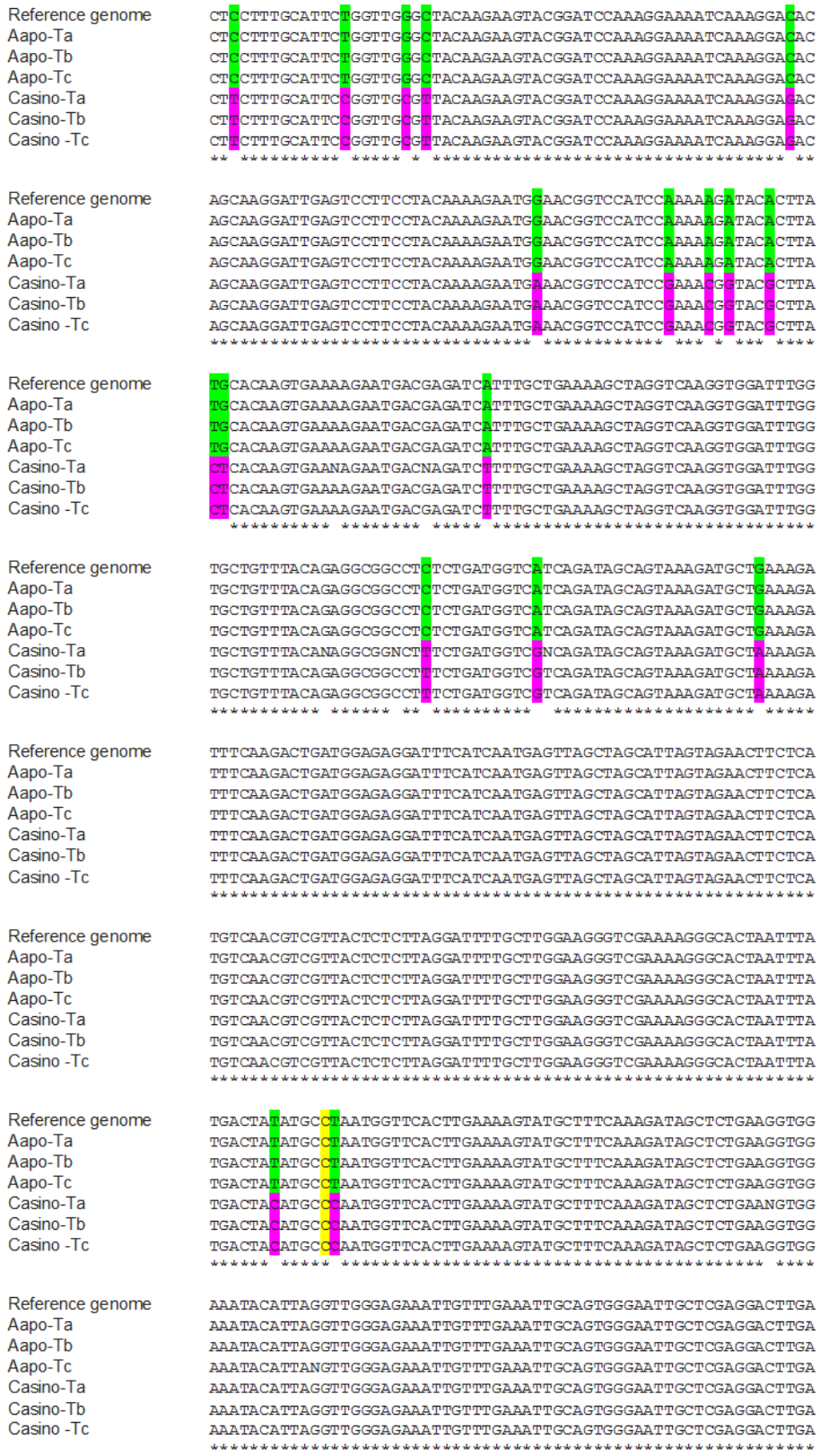

Figure VI-24: Partial sequencing alignment of the 3 HORVU3Hr1G064130 transcripts. Transcripts were sequenced from Aapo (non *Rrs1*) and Casino (*Rrs1*) barley lines and aligned against the reference genome Morex (non Rrs1) from chromosome 3 490,243,215 bp to 490,243,694 bp. Ta, Tb and Tc correspond to transcript a, b and c respectively. Bases highlighted in yellow, are bases located at chr3H_490243586 *Rrs1*$_{Rh4}$ discriminating SNP location with C on susceptible lines and C/T on *Rrs1Rh4* lines. Other SNPs discriminating Resistant and susceptible are highlighted in pink and green respectively.

Heterozygote calls in resistance lines must be due to a duplicated sequence identical to the fifth exon of HORVU3Hr1G064130 gene model. To find whether or not there is a duplicated sequence of the fifth exon of HORVU3Hr1G064130 gene model somewhere else in the genome, the 3' 800 bp of the last exon sequence containing the 3 *Rrs1*$_{Rh4}$ discriminating SNP was blasted against the pseudomolecule using the webblast.ipk website but no duplicated sequence could be found anywhere else in the genome except the location of HORVU3Hr1G064130 on 3H. Results of the blast are summarised in Table VI-18. Alignments of the 3' 800 bp of the last exon sequence containing the 3 *Rrs1*$_{Rh4}$ discriminating SNP with the 3 best blast match are in supplementary data.

Table VI-18: Table resuming result of blasting the C-terminal 800 bp of the last exon sequence containing the 3 *Rrs1Rh4* discriminating SNP was blasted against the pseudomolecule using the webblast.ipk website

Subject	Score	Identities (Query length)	Percentage	Expect
chr3H	1436	800/801 (800)	99	0
chrUn	185	342/498 (800)	68	6.00E-44
chr5H	176	352/514 (800)	68	3.00E-41
chr1H	109	345/526 (800)	65	4.00E-21
chr4H	50	97/137 (800)	70	0.003
chr2H	50	61/81 (800)	75	0.003
chr7H	44.6	33/39 (800)	84	0.14
chr6H	42.8	34/41 (800)	82	0.5

Thanks to the high polymorphism between susceptible and *Rrs1* predicted lines and the strong linkage disequilibrium in the HORVU3Hr1G064130 gene, the gene remains a good candidate and the relative expression of the 3 transcripts was studied together with the C-terminal domain potentially shared between family genes member containing *Rrs1*. The 3 candidate transcripts relative expression did not show any significant differential expression in seedling and field samples between *Rrs1* and non-*Rrs1* (t test: N=3, $p>0.05$) (Figure VI-25a). The transcript seems to be upregulated in field sample compared to uninfected seedling in *Rrs1* and non-*Rrs1* lines but differences were not significant. (t test: N=3). Transcript b is significantly upregulated in all field samples compared to uninfected seedling in *Rrs1* and non-*Rrs1* (t test: N=3, $p<0.05$) except for green leaf tissue of *Rrs1* lines samples. Transcript c is significantly upregulated in all

field samples compared to uninfected seedling in *Rrs1* and non-*Rrs1* (t test: N=3, $p<0.05$). The relative expression of the C-terminal domain of HORVU3Hr1G064130 gene was studied to see if an upregulation could be observed in *Rrs1* predicted lines compared to non-*Rrs1* lines which could be an evidence of the presence of an extra gene in *Rrs1* lines responsible for the resistance. The C-terminal domain is significantly upregulated in all field samples compared to uninfected seedling in *Rrs1* and non-*Rrs1* (t test: N=3, $p<0.05$) except for necrotic leaf tissue of non-*Rrs1* lines. (Figure VI-25a). However, relative expression of the C-terminal domain did not show any clear differential expression profile pattern between *Rrs1* and non-*Rrs1.*

The ratio of transcript relative expression differs between samples (Figure VI-25b). *Rrs1* seedling sample relative expression is similar to all non-Rrs1 samples with a majority of expression of transcript b while the transcript a ratio is almost double in *Rrs1* field samples reducing the proportion of transcript b (Figure VI-25b).

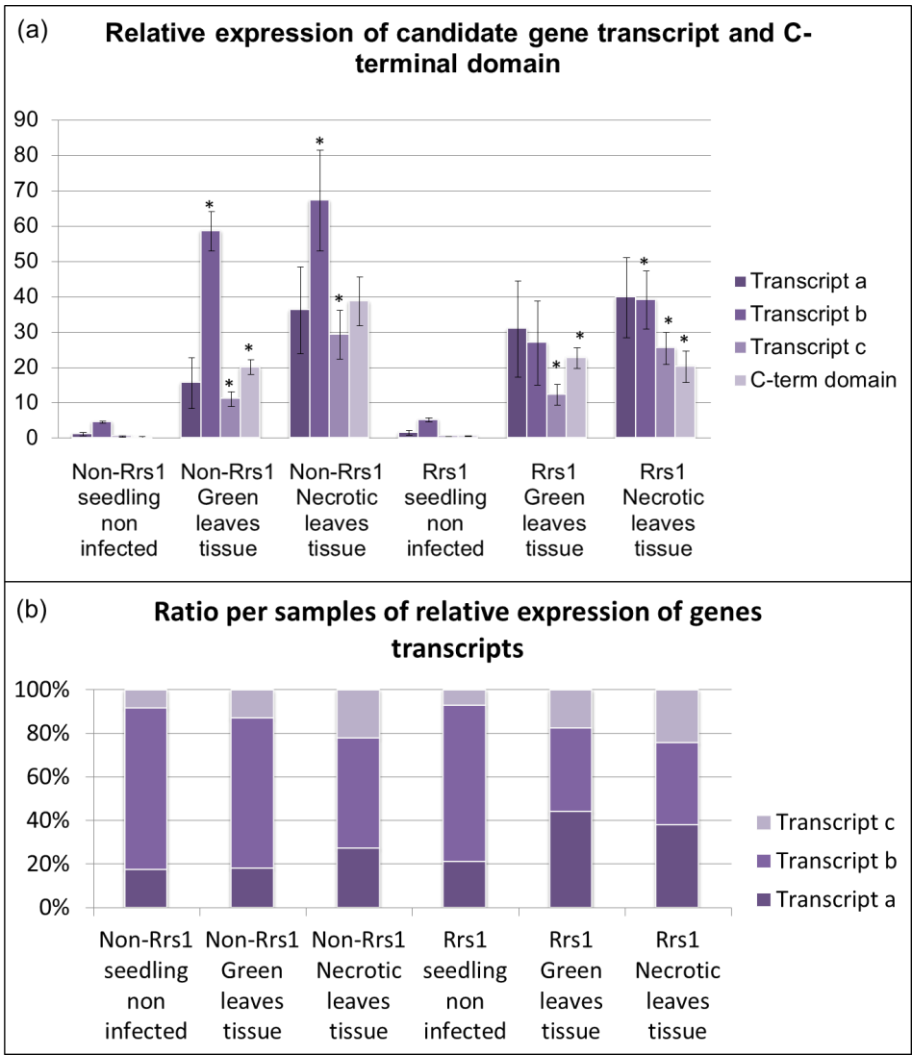

Figure VI-25: Transcriptional analysis of the transcripts. (a) Mean relative expression of candidate gene transcripts in non-*Rrs1* lines (Aapo, Optic and Steffi) and *Rrs1* lines (Casino, Chieftain and Westminster) field samples (green leaves tissue and necrotic leaves tissue) compared to uninfected seedlings. Error bars are standard deviations between lines. (b) Relative expression ratio of candidate gene transcripts per samples.

VI.3.5. *Rrs2* study

QTL13EC detected by the GWAS using exome capture data on GAPIT is located on chromosome 7H in the physical interval of *Rrs2.* Within the interval, the best associated SNP (chr7H_4097080) (with a –log10(p)=3.887) was located in HORVU7Hr1G002090, a gene with an unknown function but the minor allele significantly increases resistance in the field (Table VI-12). However, five SNPs: chr7H_5198704, chr7H_5199253, chr7H_5265173, chr7H_5269574 and chr7H_5269765 show an identical significance of –log10(p)= 3.687. Seven lines were carrying the minor allele of these five associated SNPs: Livet and Pewter, already known to carry *Rrs2* (Marzin et al. 2016); and Novello, Anaconda, Linden, Rasa and Kristaps which as

consequence could potentially carry *Rrs2* too. Interestingly, these 5 associated makers are localised 436 Kb far away from the *Rrs2* diagnostic marker described by Hanemann et al. (2009) in a 71Kb interval and which contain a single gene HORVU7Hr1G002820 described as an alpha dioxygenase from the heme-dependent peroxidase family (PF03098). Exome capture SNPs at chromosome 7H region from 3407000 to 8365000 were studied looking for SNPs discriminating predicted *Rrs2* lines: Livet (*Rrs2*), Pewter (*Rrs2*), Anaconda, Linden and Novello from susceptible lines: Colada, Cellar, Simba, Velvet and Taphouse. 177 SNPs perfectly discriminate *Rrs2* predicted lines from susceptible lines in the interval studied and 43 of them cause non-synonymous changes.

VI.3.6. Other mapped resistance

The lack of control lines carrying other resistances detected in the study prevented predictions being made regarding whether or not lines were carrying the detected resistance, but the location of best associated SNPs in the genome was studied.

Rrs3

QTL5ECP on 4H detected by the GWAS using exome capture data on GAPIT is physically located in *Rrs3* interval. The minor allele increased the resistance in the field. All the associated markers showed the same significance. The studied interval identified contains 14 annotated genes. Among the genes identified two Pathogenesis-related thaumatin superfamily protein (pfam: PF00314) and one UDP-Glycosyltransferase superfamily protein (pfam: PF00201) were found.

Rrs4

QTL8EC detected by the GWAS using exome capture data and QTL10 detected by the GWAS using iSelect data on 3H are physically located in *Rrs4* interval. The best associated SNP chr3H_592563068 major allele significantly increases the resistance in the field (Table VI-12). The studied interval identified contains three annotated genes, of which two are annotated as receptor kinases (PF07714). The best associated SNP is localised HORVU3Hr1G081050 gene annotated as receptor kinase (PF07714).

Rrs12

QTL14EC detected by the GWAS using exome capture data located on chromosome 7H is possibly in the expected region of *Rrs12* (Genger et al. 2003). The minor allele increased the resistance in the field. All the associated markers showed the same significance but the studied interval did not contain any annotated genes.

Rrs13

QTL11EC detected by the GWAS using exome capture data and QTL19 detected by the GWAS using ISelect data on 6H are both overlapping with *Rrs13.* The best associated marker chr6H_21437298 minor allele significantly increases the resistance in the field (Table VI-12) and is localised in HORVU6Hr1G011650, a gene coding for wall associated receptor kinase (PF07645, PF07714, PF13947).

Rrs14

QTL1 and QTL1EC on 1H identified by both GWAS methods are co-located with the *Rrs14* region (Garvin et al. 2000; Yun et al. 2006). In a population of the Australian cultivar Clipper with the wild barley *H. vulgare ssp. spontaneum* from Mehran, Iran (Garvin et al. 1997). QTL1 was shown to be an effective source of resistance in spring barley against naturally occurring *R. commune* populations thanks to the effect of the major allele. If this QTL is, indeed, *Rrs14*, then the interval was successfully reduced from 12.6 to 0.17 cM, corresponding to a physical interval of around 563 kb. The barley pseudomolecule gene annotation exploration of the 563 kb studied interval identified interesting potential candidate genes. Three out of the 14 genes annotated in the physical interval are disease resistance genes (pfam: PF00931) corresponding to NB-ARC domain protein. According to physical location of best associated markers, QTL1EC is distally located from QTL1 by about 2.5Mb but the best associated marker of QTL1EC is located in a gene annotated as disease resistance protein (pfam: PF00931)

Rrs15

QTL16EC on 7H detected by the GWAS using exome capture data (possibly localised in the expected region of *Rrs15)* is characterised by ten SNPs showing the same significance with the major allele increasing the resistance in the field (Table VI-12). The studied interval contains 26 genes but the ten best associated SNPs are located within an interval containing fifteen genes, including a cysteine-rich receptor-like protein kinase and a UDP-Glycosyltransferase superfamily protein Pfam: PF00201).

Rrs16

QTL13 on 4H detected by the iSelect GWAS was located in the *Rrs16* region. This interval is 3.5 cM or 3.8 Mb and contains a large number of genes (110 annotated genes) making it difficult to select potential candidate genes.

VI.4. Discussion

Statistical analysis of AUDPS phenotypic data showed a correlation between the different years and significant differences between the spring barley genotypes used, indicating that the phenotyping process was constant enough within the 3 different years of scoring and that there is variability between the different lines scored allowing us to proceed with the GWAS. Statistical analysis of height phenotypic data showed a strong correlation between 2014 and 2015 and significant differences between the genotypes of the spring barley collection used, indicating that the phenotyping process was constant enough within the 2 different years scored and that there is variability between the different lines scored allowing us to proceed with the GWAS.

Different GWAS strategies were attempted. Multiple environment association analyses were performed on GenStat allowing the identification of candidate QTLs as main effects or QTLxE interactions. This strategy was successfully used to identify QTL using iSelect genotyping data but appeared to be unadapted for large genotypic data files and did not allow the identification of QTL using full genome exome capture SNP data. As an alternative, multiple environment association analyses were performed on GenStat using individual chromosomes. The analysis was computationally intensive, requiring a long time to run but different (and less significant) QTL were detected due to the reduction of number of genotypes. For example: it considerably reduced the number of *Rrs1* lines (thus limiting its significance) but increased the proportion of *Rrs2* lines in the 130 genotypes subset, allowing its detection. The use of ISelect genotypic data and multiple environment association analyses performed on GenStat allowed the simultaneous analysis of 3 years-worth of phenotypic data and allowed the correction of population structure using an Eigenanalysis mixed model to fit the relationship. The analysis detected 6 principal components and improved the analysis compared with the null relationship model by reducing the level of spurious association. The second strategy attempted was using the GAPIT package on R. GAPIT allowed the detection of QTL using the 130 line exome capture subset using 151K SNPs markers. As QTLxE interactions are not incorporated into the GAPIT methods, the GWAS was run for individual years separately as well as a combined

estimate of the mean from the 3 years phenotypic data, allowing the detection of QTL having a consistent effect among the 3 years or at least strong enough in one year to be still detected using the combined estimated mean. This procedure allowed the identification of whether or not QTL were consistent. The GAPIT analysis uses MLM methods to control false positives in GWAS and incorporates population structure and cryptic relationships (Zhang et al. 2010). GAPIT was successfully run without correcting for population structure as the Manhattan plot did not show substantial difference, but the QQ plot showed evidence for overcorrection when trying to correct for population structure. GAPIT was also run using the ISelect genotypes and the combined phenotypic mean, which allowed the identification of QTL (although fewer than by using the GenStat multiple analysis). The reduction in the number of QTL identified may be due to the difference in the two methods (GAPIT uses a different method from GenStat to control false positives). Alternatively, the fact that the combined (across years) estimated mean was used could hide some of the association due to its inability to account for differential QTL expression across environments (years). In this respect, it would have been useful to run GAPIT on individual year's phenotypic data to see if any QTL were hidden by the use of combined estimated mean and thus reveal any potential QTLxE interactions in the analysis.

In order to interpret the results of the GWAS, a significance threshold needs to be set. For the GWAS using the ISelect set of genotype the Bonferroni method could have been used but the threshold would have been extremely conservative and set around 5, considerably limiting the detection of significant association due to LD between markers meaning that the true number of independent tests is far lower than the number of markers (Johnson et al. 2010). As an alternative, the false discovery rate method was used allowing the estimation of the false positive percentage for the threshold chosen. By choosing a significance threshold of 2.9, we assume that less than 15% were false positives but we allowed the identification of 20 different QTLs. Some of these may be false positive but the fact that QTL co-locate with known resistance genes is an additional line of evidence that increases the confidence in many of the QTLs detected. In addition, the ISelect genotypic data has already been successfully used by Houston et al. (2014) for a GWAS where the

significant threshold was set at 3 allowing the detection of QTLs in locations previously found to contain a QTL for the same trait. This indicates that adjusting the threshold to detect already mapped resistance should be appropriate. FDRs are usually set at 5% but are often found to be highly stringent, probably due to the the fact that all markers are considered as independent tests in the correction (Seren et al. 2012; Zegeye et al. 2014; Kumar et al. 2015). When 5% FDR was used by Houston et al. (2014), only 2 QTL were retained suggesting that this FDR is too stringent for the ISelect genotypic data. In addition, some published GWAS studies use a FDR of 10% and up to 30% to enrich for genes likely to affect the trait studied (De Rubeis et al. 2014; Horton et al. 2014). For the GWAS using the exome capture SNPs, the Bonferroni and FDR method appeared to be poorly suited. This issue is becoming more common due to high-throughput technologies such as whole genome single-nucleotide polymorphism (SNP) arrays which increase the number of SNPs in association studies (Lin and Lee 2012). As a consequence, clear peaks observed with an arbitrary significance of –log10p> 2.3 were studied comparing the physical location of the markers with previously identified QTL and already mapped resistances. Through this approach, the location of up to seven mapped resistances could be identified using the subset of 130 spring barley varieties used. In the future, this strategy can be used for the identification of already mapped resistance but it would be risky to try to identify new associations, where the comparison with better controlled analysis would be recommended. In addition, it would be good to reduce the number of SNPs by removing SNPs with complete LD which can increase the magnitude of the significance threshold without adding genotyping information (Johnson et al. 2010). Different mapped resistance could be detected using the different methods. The high marker density from the exome capture data provided a good coverage of the complete genome and allowed for increased resolution of interesting intervals and the exploration of the genome through the identification of SNPs haplotypes. Moreover, the fact that the analysis was processed on only 130 lines presented an unexpected advantage by reducing the number of lines carrying *Rrs1* and as a consequence reducing the significance of it but promoting the detection of several other mapped resistances.

The GWAS analysis detected twenty QTL that contributed to field resistance to Rhynchosporium in the spring barley association mapping panel using ISelect genotypes and allowed the precise narrowing down of the position of 7 previously-mapped resistances thanks to the high density of markers provided by exome capture data using the 130 subset of lines. The fact that seven of the ISelect detected QTL (QTL1, QTL8, QTL10, QTL12, QTL13, QTL14 and QTL19) and seven exome capture QTL (QTL1EC, QTL8EC, QTL9EC, QTL11EC, QTL13EC QTL14EC and QTL16EC) co-located with previously reported major resistance genes, coupled with the fact that these were generally consistent in their effects across years, and accounted for a high percentage of phenotypic variance, confirms the importance of major resistance genes to varietal resistance in UK spring barley, as well as demonstrating the effectiveness of combining GWAS with disease nursery data to identify meaningful resistance QTL. The associated markers identified in this study, reflect variation that currently exists within UK elite germplasm, and therefore represents a resource that can be used in routine marker screening in existing spring barley breeding programmes to increase levels of varietal resistance without the additional problems caused by introgressing resistance from exotic sources. Nevertheless, the ability to detect marker-trait associations using this technique depends on the allele frequency at QTL, and as such, it is likely that rare resistance genes were not detected by this analysis. As such, the resistance estimates for the varieties described in this study are likely to also represent a useful resource for further genetic investigations of resistance in spring barley.

QTL1 and QTL1EC on 1H appeared to be co-localising with *Rrs14* a resistance located near Bmac0213 marker identified in a population developed with the wild barley accession OUH602 as the donor parent (Yun et al. 2006). This resistance was also mapped 10.8cM away from HOR1 and 1.8 cM away from HOR2 by Garvin et al. (2000) in a population of the Australian cultivar Clipper with the wild barley *H. vulgare ssp. spontaneum* from Mehran, Iran (Garvin et al. 1997). The QTL1 major allele showed a consistent effect across the seasons and accounted for a high percentage of phenotypic variance (up to 10 %) a result in accordance with Garvin et al. (2000), who described a consistent protection for 2 consecutive years of up to 88 % less leaf damage observed on

the *Rrs14* line compared to Clipper. *Rrs14* is likely to be an effective source of resistance in spring barley against naturally occurring *R. commune* population and the QTL interval was successfully reduced from 12.6 to 0.17 cM, corresponding to a physical interval of around 563 kb. Due to the highly recombining location of the QTL on the end of the short arm of the chromosome and the impossibility to screen for *Rrs14* resistance only, no clear haplotype could be visualised using the exome capture SNP data. However, the barley pseudomolecule gene annotation exploration of the 563 kb interval identified interesting potential candidate genes. Three out of the 14 genes annotated in the physical interval are disease resistance genes (pfam: PF00931) corresponding to NB-ARC domain proteins: a plant resistance gene signalling motif (van der Biezen and Jones 1998) possibly used as a molecular switch that regulates the activity of the R protein (van Ooijen et al. 2008). The QTL1EC major allele accounted for a high percentage of phenotypic variance (up to 8.9 %). According to the physical location of the best associated markers, QTL1EC is distally located from QTL1 by about 2.5Mb, but the best associated marker of QTL1EC is located in a gene annotated as disease resistance protein (pfam: PF00931), like some of the genes present in the QTL1 interval.

Chromosome 3H, already described as a major source of resistance to Rhynchosporium (Zhan et al. 2008) contains 6 QTL in the current study (QTL7, QTL8, QTL9, QTL10, QTL11 and QTL12). QTL8 was the strongest QTL detected and co-localised with *Rrs1*, a major resistance gene which has previously been fine mapped in two large populations derived from Spanish barley landraces by Hofmann et al. (2013). In this study, the effect of QTL8 appeared to be consistent across years, and its contribution to phenotypic variance (between 6.1 to 16.6%) across the seasons studied was substantial enough to illustrate the effectiveness of *Rrs1* resistance. This decreasing of contribution for phenotypic variance is in accordance with the fact that *R. commune* already previously managed to avoid the effect of *Rrs1* resistance by losing the expression and/or the production of a recognised form of Nip1 in 45% of the isolates. The consistent effect confirms the efficiency of *Rrs1* in the field but suggests variation in the composition of pathogen populations across years. Indeed, previous studies have demonstrated that 45% of sampled isolates have lost the function of the corresponding avirulence product (NIP1) (Schurch et al.

2004). However, the fact that Nip1 could be quantified in field samples from 2015 (and the high QTL effect of QTL4) suggest that NIP1 strains are an important component of natural *R. commune* populations and that *Rrs1* remains an effective source of varietal resistance under realistic UK growing conditions. The GWAS approach used in this study allowed a significant reduction of the map interval to 0.24 Mb.

QTL10 and QTL8EC on 3H co-localised with *Rrs4*, resistance gene mapped by Patil et al. (2003) using a double haploid progeny from a cross between the susceptible cultivar Ingrid and the resistant accession CI 11549 (Nigrinudum). *Rrs4* is often confused with *Rrs1* due to their proximity, 22cM away from each other (Patil et al. 2003). In this study, QTL10 appears to be consistent across years and the percentage of phenotypic variance explained by variation at this locus within the 3 seasons (from 2.7% to 7.9%) was not negligible. However, the identified QTL only contains a single marker, preventing us from identifying an interval and candidate genes. The QTL8EC major allele accounted for a percentage of the phenotypic variance of 9.8% and the best associated SNP (chr3H_592563068) is located in the HORVU3Hr1G081050 gene, annotated as receptor kinase (PF07714), protein, well known for their role in plant defences activation (Goff and Ramonell 2007).

QTL12 on 3H co-localised with the semi-dwarfing gene *sdw1* mapped by Malosetti et al. (2011) around 11_10867 SNP marker. This QTL was also detected in our height GWAS as QTL4H and already identified as a resistance QTL in previous studies, thought to be due to the limited splash dispersion on tall cultivars (Looseley et al. 2012; Walters et al. 2012; Looseley et al. 2015). QTL12 shows a consistent effect through the season and seems to be an important source of resistance for spring barley due to the high percentage of phenotypic variance accounted for by this locus (up to 12.8%).

QTL13 and QTL14 on 4H are both co-localised with *Rrs16*, a resistance gene transferred from *Hordeum bulbosum* to barley and mapped by Pickering et al. (2006). According to physical location of flanking markers, QTL14 appeared to show better co-localisation with *Rrs16*. However, QTL14 shows an inconsistent QTL effect and QTL13 shows consistency and accounts for a high percentage of phenotypic variance (between 4.7 and 9.7%). The QTL13 interval is 3.5 cM

or 3.8 Mb and contains a large number of genes (110 annotated genes) preventing us from identifying candidate genes.

QTL5ECP on 4H co-localised with *Rrs3*, a resistance gene mapped by Bjørnstad et al. (2002) and Grønnerød et al. (2002) but not confirmed in a double haploid population from a cross between the susceptible Ingrid and the Ethiopian landrace Abyssinian due to heterogeneity in the Abyssinian accession (Grønnerød et al. 2002). The minor allele increased the resistance in the field. All of the associated markers showed the same significance. The interval identified contains 14 annotated genes. Among the genes, potentially interesting candidates were identified such as two Pathogenesis-related thaumatin superfamily proteins (pfam: PF00314) already known to provide resistance in wheat against stripe rust fungus (Wang et al. 2010) and one UDP-Glycosyltransferase superfamily protein (pfam: PF00201) already known to provide resistance in Arabidopsis against *P. syringae* (Langlois-Meurinne et al. 2005).

QTL19 and QTL11EC on 6H are overlapping with *Rrs13.* QTL19's best associated marker was inconsistent across the years and accounts for a small proportion of the phenotypic variance, but the best associated marker's (chr6H_21437298) minor allele of QTL11EC significantly increases the resistance in the field and is localised in HORVU6Hr1G011650, a gene annotated as a wall associated receptor kinase (Pfam: PF07645, PF07714, PF13947) with domains characteristic of Wall Associated Kinase receptors, known to be involved in plant pathogens response (Morris and Walker 2003).

QTL13EC on chromosome 7H is in the physical interval of *Rrs2.* Some of the best associated makers are in an interval which contains a single gene described as an alpha dioxygenase from the heme-dependent peroxidase family (PF03098) a potentially very interesting family known to have an important role in plant responses to pathogen attack, involved in ROS production and which were described as an effector target of *U. maydis* in maize (Hemetsberger et al. 2012). However, the study of exome capture SNPs in the QTL13EC region identified 177 SNPs which perfectly discriminate *Rrs2*-predicted lines from susceptible lines in the interval studied, 43 of them cause non synonymous changes. In the future, it would be interesting to set up a

genotyping project screening additional *Rrs2* lines and susceptible lines to reduce the number of discriminating SNPs in the interval and identify different candidate genes. However, previous study of *Rrs2* resistance suggests a local chromosomal rearrangement, alien introgression or inversion in *Rrs2* -carrying varieties (Hanemann et al. 2009) which indicates that using the pseudomolecule and exome capture data based on the Morex (not carrying *Rrs2*) assembly is not the appropriate technique to identify candidate genes, but such an approach could help to reduce the interval and locate the introgression.

QTL14EC located on chromosome 7H is possibly in the expected region of *Rrs12* (Genger et al. 2003) but the lack of a right flanking marker for the Rrs12 location does not allow confidence in concluding that they co-localise. The minor allele at this QTL increased the resistance in the field. All the associated markers showed the same significance but the interval did not contain any annotated genes.

QTL16EC on 7H possibly localised in the expected region of *Rrs15* but the lack of left flanking marker for the Rrs15 location does not allow confidence in concluding that they co-localise. Ten SNPs showing the same significance and with a major allele significantly increasing the resistance in the field were localised within the region of fifteen genes which contain a cysteine-rich receptor-like protein kinase and a UDP-Glycosyltransferase superfamily protein Pfam: PF00201); potentially interesting candidate genes (Park et al. 2001; Langlois-Meurinne et al. 2005).

In addition to these loci, 13 other QTL were detected on chromosomes 1H, 2H, 3H, 5H and 7H which did not co-localise with any known resitance. These QTLs could be potential new resistances but there is a possibility that they are false positive QTL. However, somes QTLs showed interesting characteristics such as QTL5 on 2H with a consistent effect through the years and accounting for a high percentage of phenotypic variance, possibly representing an undescribed major gene. It would be very interesting to study this region more deeply maybe using a recombinant population. So far, the QTL interval identified is less than 1cM (1.3Mb) which contains 25 genes. In addition, other QTLs identified with inconsistent effects across years could poteintialy be new

quantitative resitance loci which could be considered for pyramiding of resistance genes.

The study identified a number of overlaps between height and resistance to rhynchosporium. This may largely reflect the importance of height trait for controlling the disease in the field, however as height was measured in a trial with high levels of disease, this could also reflect the developmental effects of severe infection. QTL12 on 3H co-localised with the semi-dwarfing gene *sdw1,* mapped by Malosetti et al. (2011) around the 11_10867 SNP marker. This QTL was also detected in our height GWAS as QTL4H and already identified as a resistance QTL in previous studies, thought to be due to the limited splash dispersal on tall cultivars (Looseley et al. 2012; Walters et al. 2012; Looseley et al. 2015). QTL12 seems to be an effective source of resistance for spring barley due to its consistency and the high percentage of phenotypic variance accounted for by this QTL (up to 12.8%). However, tallness can be a detrimental agronomic trait and dwarfing gene are currently being used in breeding process for the development of modern cultivars with short and strong stalks providing resistance to lodging (responsible for yield and grain quality reduction) (Kuczyńska et al. 2013).

QTL8, is the most significant association detected by the GWAS analysis, and is co-located with *Rrs1*, a race specific resistance gene recognising NIP1, an effector secreted by some strains of *R. commune*. The peak marker for this QTL, allowed the prediction of spring barley lines carrying *Rrs1* resistance. The 214-GFP phenotyping using confocal microscopy confirmed the resistance on the 8 *Rrs1* predicted lines tested and identified resistance in 2 non *Rrs1* predicted lines but the figure of the picture of confocal are poor in quality and it would have been better to interpret the result in a quantitative way rather than qualitatively as illustrated in Looseley et al (2014). The phenotypic assay using LfL12F confirmed the resistance in 21 of 22 *Rrs1* predicted lines tested. Whilst some lines not carrying SCRI_RS_221644 minor allele showed resistance, this is consistent with the action of a second resistance gene in these lines. Indeed, the lines Atlas and Pewter are known to carry *Rrs2* resistance, which is known to be resistant to *Rrs2*. The high degree of association between genotype and phenotype showed that the best associated marker is tightly linked with *Rrs1* but not perfectly diagnostic. A 2.8 Mb interval surrounding the haplotype visually

identified using exome capture data was explored using the barley 3H pseudomolecule annotation, revealing the presence of 22 genes. A total of 19,551 polymorphic SNPs were identified in the 22 genes of the interval studied. 1,126 SNPs were polymorphic between predicted *Rrs1* resistant and susceptible lines. 48 SNPs were selected among the 1,126 polymorphic SNPs, prioritising SNPs causing amino acid change in genes, located in genes and distributed across these genes. Genotyping results allowed the identification of 3 markers perfectly discriminating the susceptible lines from *Rrs1* lines thanks to the use of Syrian and Jordanian landraces which improved the resolution within the *Rrs1* region and provided a good source of recombination which broke the UK cultivar haplotype thanks to their diversity and patterns of linkage disequilibrium.

The study of the effect of selected SNPs identified non-synonymous SNPs at 5 different genes within the interval but the 3 markers discriminating the susceptible lines were located in HORVU3Hr1G064130 gene. In resistant lines, genotype calls are all heterozygote, an unlikely result given the low rates of outcrossing in barley. The fact that all lines are heterozygous indicates that it is not an isolated problem with outcrossing in the seed stocks sampled. Instead, the heterozygote calls are likely to be due to duplicated sequence somewhere else in the genome. RNA-seq data allowed the identification of 3 potential functional transcripts generated by alternative splicing of HORVU3Hr1G064130 exons, potentially coding for proteins sharing the same C-terminal protein kinase domain. All 3 transcripts appeared to be expressed. The 3 transcripts were partially sequenced and many polymorphic SNPs were visualised between *Rrs1* predicted and susceptible lines corresponding to some of the SNPs selected for the genotyping project, accounting for the strong linkage disequilibrium. However, at the location of the discriminating Chr3H_490243586 SNP location the alternative allele present on resistant line was absent. Heterozygote calls in resistant lines must be due to a duplicated sequence with high homology to the fifth exon of the HORVU3Hr1G064130 gene model and tightly linked with the region identified according to the LD. However, no duplicated sequence could be found anywhere else in the genome. This result could be due to several reasons. Firstly, duplicated genes could be very frequent (in particular among the R genes families) contributing to a net gain of

R genes over of plant evolution (Panchy et al. 2016) but challenging their identification by causing numerous bioinformatics complications/artefacts, including mis-mapping and the associated false positive heterozygous SNPs. As a consequence, a number of very similar looking genes (containing *Rrs1)* may have been assembled into a single chimeric gene possibly annotated as the HORVU3Hr1G064130 gene. This would explain why no duplicated sequence can be identified on the pseudomolecule of the Morex assembly. The second hypothesis is that the heterozygote calls and the failure to find a duplicated sequence in the Morex pseudomolecule is because the true mapping target is not available, being absent from the genome of the Morex reference sequence. The fact that the 3 discriminating SNPs are heterozygotes in all the $Rrs1_{RH4}$ control lines SBCC145, SBCC154, CIHO-3515, and CI11549 (*Rrs1, Rrs4*) indicates that they may represent the $Rrs1_{RH4}$ allele of *Rrs1* and that the duplicated sequence is conserved among these lines. The fact that we cannot localise the duplicated sequence is because Morex does not carry *Rrs1*. The 3 discriminating markers may not inform precisely the location of *Rrs1* but they could potentially discriminate lines carrying $Rrs1_{Rh4.}$ All of the other *Rrs1* control lines presented the susceptible allele which is not surprising for Atlas46 ($Rrs1_{TURK}$*, Rrs2*) and Steudelli (*Rrs1, Rrs3*) which show an inconsistent phenotype (possibly due to an impure seed stock) which correlates with the susceptible genotype. Armelle ($Rrs1_{BRIER}$) presented the susceptible allele for the 3 markers identified and a susceptible phenotype indicating that the strain LfL12F used for the phenotyping is virulent on the $Rrs1_{BRIER}$ allele. 2 other *Rrs1* control lines Triton (*Rrs1, Rrs15*), and Abyssinian-B19460 (*Rrs1, Rrs3*) presented the susceptible allele for the 3 markers identified but were resistant to the strain LfL12F used for the phenotyping. Two possibilities could explain that result: the strain LfL12F is avirulent on these lines due to alternative resistant alleles of *Rrs1* or resistance to Lfl12 at a different locus such as *Rrs15* or *Rrs3* respectively carried by Triton and ABYSSINIAN-B19460.

So far, the relative expression of the C-terminal domain of the HORVU3Hr1G064130 gene did not show any clear differential expression profile between *Rrs1* and non-*Rrs1* lines. This result does not allow us to confirm whether or not there is a duplicated sequence of the C-terminal domain of the HORVU3Hr1G064130 gene. To test if there is a duplicated sequence in

Rrs1$_{Rh4}$ predicted lines, it would be useful to try to identify the number of copies of the C-terminal domain by qPCR using DNA or by southern blot. It would be also a good idea to fully sequence the three transcripts to see if the *Rrs1* predicted lines present the alternative resistant genotype of the two other *Rrs1*$_{Rh4}$ discriminating SNPs identified.

The triple transcript variant gene (having several discriminating SNPs) remains a potentially good candidate. Relative expression of the 3 transcripts and of the C-terminal only showed upregulation in field sample compared to non-infected seedlings independently of the presence of *Rrs1* in the lines tested. Differential expression between *Rrs1* and non-*Rrs1* lines is not absolutely required and receptors may not be upregulated by the disease as they are only required for the detection. Nevertheless, it would have been evidence of the importance of the gene if a significant difference was observed between the expression of our candidate genes in *Rrs1* and non-*Rrs1* lines. However, relative expression analysis reveals that transcript b ratio was doubled in *Rrs1* lines field samples compared to non-*Rrs1* lines field sample. This result could indicate that transcript b expression is prioritised in *Rrs1* lines.

The 3 markers discriminating the susceptible lines were located in the tyrosine kinase domain of HORVU3Hr1G064130 gene coding putatively for WAK family proteins. WAK are members of the receptor-like-kinase (RLK) family, a diverse family of transmembrane proteins with an intracellular kinase domain and various extracellular domains (Shiu and Bleecker 2001; Gish and Clark 2011). WAK are known to play an important role in cell expansion, pathogen resistance, heavy metal stress tolerance and wounding in *A. thaliana* (Zhang et al. 2005; Kohorn and Kohorn 2012). They serve as cell wall sensors and are known to be induced by pathogen attack and able to bind pectin fragments and oligogalacturonides (Sanabria et al. 2010; Kohorn and Kohorn 2012). Several studies describe WAK as resistance genes. *Htn1*=ZmWAK-RLK1, a member of the WAK-RLK family has been identified as a resistance gene candidate in maize against northern corn leaf blight, a disease caused by *E. turcicum*, a hemibiotrophic fungal pathogen (Hurni et al. 2015). The *Htn1* and *Rrs1* story present strong similarities; *Htn1* is described as a resistance conferring a quantitative partial resistance and a race-specificity against most strains. *Htn1*

has similar domain structure to our candidate gene in particular transcript a and has been identified using TILLING mutants in the serine tyrosine kinase domain. *RFO1*, a WAK was also identified to be providing a dominant resistance in *A. thaliana* against several races of Fusarium due to a single amino acid change in the kinase domain, but the fact that the WAK was providing resistance to different races dismissed the hypothesis of race specificity of the resistance (Diener and Ausubel 2005). These two examples show the importance of tyrosine kinase domain for resistance. Non-synonymous SNPs found in the kinase domain could be improving the transduction signal activating plant defence pathways more efficiently providing resistance. Moreover, OsWAK1 was shown to be induced by *M. oryzae* infection in rice and OsWAK1 constitutive expression provided resistance to the specific race (Li et al. 2009). In addition, Delteil et al. (2016) showed that OsWAK14, OsWAK91 and OsWAK92 were positively regulating quantitative resistance while OsWAK112d was a negative regulator of *M. oryzae* resistance. OsWAK91 was required for H_2O_2 production and able to activate defence gene expression during infection and OsWAKs were triggered by chitin and were partially controlled by the chitin receptor CEBiP (Delteil et al. 2016). WAK has also been described as being activated by PAMPs such as flagellin *in A. thaliana* and tomato (Rosli et al. 2013) and able to bind glycine rich proteins such as WAK1 in *A. thaliana* (Park et al. 2001). The WAK function is quite unexpected for the *Rrs1* resistance gene as it is expected to be able to recognise the NIP1 effect. However in the absence of cloned *R. commune* resistance genes, HORVU3Hr1G064130 remains a good candidate in particular due to the numerous polymorphic SNPs in the tyrosine kinase domain.

NIP1 is a secreted small protein in the apoplast, produced at early time points of the infection, able to pass through the cell wall and stimulate H+ ATPase pumps to disturb essential cellular process and force cell collapse (Wevelsiep et al. 1993; Rohe et al. 1995). Binding studies of NIP1 revealed a single class of binding sites with identical binding characteristics independent of the presence of the *Rrs1* resistance gene and independent of the avirulence activity of NIP1 suggesting that the *Rrs1* gene does not encode the NIP1 receptor and that an extra event is necessary for recognition and to trigger race-specific plant defence activation such as a hypothetical conformational change of the target

protein or an additional protein involved in the protein complex (van't Slot et al. 2007). As a consequence, Nip1 and candidate resistance WAK genes share the same subcellular localisation allowing a possible direct or indirect interaction. WAK are known cell wall sensors inducible by PAMPs (Sanabria et al. 2010; Rosli et al. 2013), the mechanism of inducing resistance signals could follow the conformational change hypothesis related to the cell wall which could release PAMPs such as pectin fragments to trigger plant defence. This could happen during NIP1 crossing through the cell wall on its way to weaken plant cells. Moreover, the fact that SNPs associated with the resistance are in the kinase domain of the identified WAK matches with the fact that binding of NIP1 seems to happen regardless of the presence of the *Rrs1* resistance gene. This result suggests that NIP1 may be activating the WAK independently of the presence the resistant allele, but that the resistance may come from amino acid changes in the kinase domain, allowing a more specific or more efficient activation of plant defence mechanisms compared to the same receptor which does not have these amino acid changes or which is a duplicated gene and as a consequence, conferring resistance to *NIP1* strains (Figure VI-26). Race specificity could be due to collateral effects of NIP1 crossing through the cell wall rather than protein recognition. Moreover, that theory would explain the partial resistance of *Rrs1* lines observed in the field despite the presence of non NIP1 producing strains. Cell wall modification must happen at later stages of infection through sensing this WAK activating *Rrs1* resistance signal, possibly too late to fully prevent the disease but enough to observe lines more resistant than average (Figure VI-26). To summarise, *Rrs1* could be a basal PTI type resistance advantaged by its ability to be triggered by NIP1 crossing early during infection and a good global resistance at later stage of infection. However, no proof of enzymatic activity of NIP1 was recorded. Nevertheless, it would be risky to neglect the theory of protein recognition of NIP1 by a WAK since the extracellular domain of the Arabidopsis wall-associated receptor kinase, WAK1 binds a glycine rich extracellular protein through its cysteine rich domain (Park et al. 2001); a shared feature with the cysteine rich protein NIP1 which contain 10 cysteine among its 82 amino acid (Rohe et al. 1995). Furthermore, the WAK family is expanded in monocots compared to *Arabidopsis* (Delteil et al. 2016) and WAK could have evolved to recognise

other types of elicitors such as effector proteins. It would be a good idea to find candidate resistance genes homologues in *B. distachyon*, check for the existence of mutated lines for that gene and compare the infection of *R. commune* on mutant line with WT.

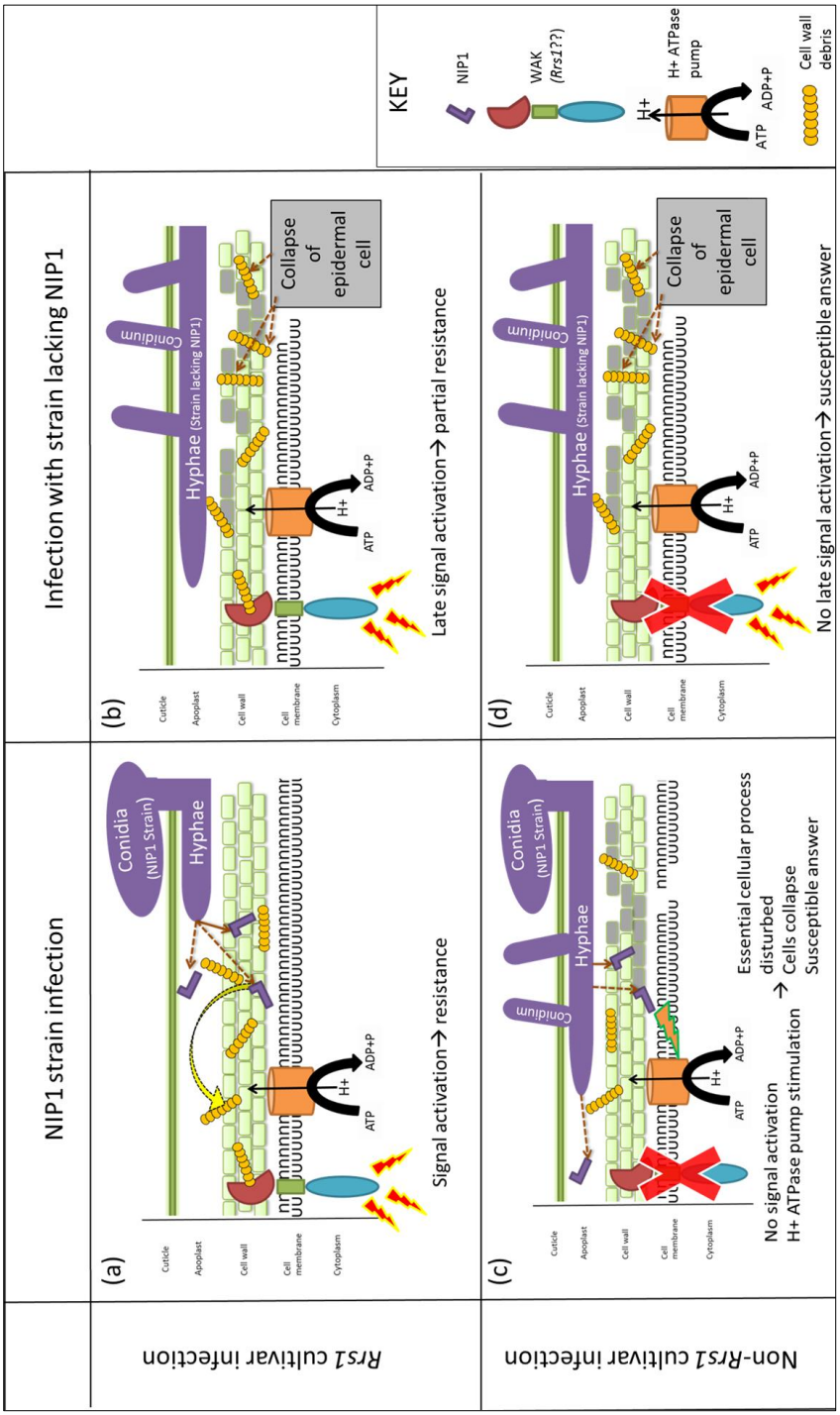

Figure VI-26: Diagrams illustrating resistance mechanisms if *Rrs1* is a WAK. (a) In the case of an infection of a *Rrs1* cultivar with *a R. commune* strain carrying NIP1, NIP1 is being secreted early during the infection and crossing the cell wall up to the cell membrane inducing cell wall modifications which release cell wall debris. WAK, acting as a cell wall sensor detects the cell wall modifications which activate plant defences and resistance. (b) In the case of an infection of a *Rrs1* cultivar with *a R. commune* strain not carrying NIP1, hyphae grow under the cuticle, inducing epidermal cell collapse. Cell collapse induces the release of cell wall debris being detected by WAK of neighbour cells inducing a late signal activation and partial resistance. (c) In the case of an infection of a non-*Rrs1* cultivar with *a R. commune* strain carrying NIP1, hyphae grow under the cuticle and secretes NIP1 crossing the cell wall up to the cell membrane. NIP1 stimulates H+ ATPase pump causing disturbance of essential cellular processes and cell collapse resulting in a susceptible response. (d)) In the case of an infection of a non-*Rrs1* cultivar with *a R. commune* strain not carrying NIP1, hyphae grow under the cuticle, induce epidermal cell collapse without activating late signals and resulting in a susceptible response.

VI.5. Conclusion

This study used the combination of 2 approaches to identify new and previously-mapped resistances against *R. commune* in a collection of elite spring barley. Most of the previously-mapped resistances were detected allowing us to reduce their map intervals, identifying new flanking markers and in some case, identifying strong candidate genes. However, the lack of control lines known to carry some of the resistances prevented the prediction of resistance in the lines.

The work has been mainly focussed on *Rrs1* resistance but has not yet allowed us to state whether the various described alleles of *Rrs1* are different alleles of the same gene or different, but tightly linked genes. All this work is based on the new Morex reference assembly that unfortunately is susceptible to *R. commune* and does not carry *Rrs1* resistance, meaning that *Rrs1* could be a gene that does not exist in Morex, which would agree with one of the hypotheses; suggesting that diagnostic markers identified for $Rrs1_{Rh4}$ allele are localised on a duplicated sequence absent from Morex but mis-mapped onto HORVU3Hr1G064130. Extra work will be needed to validate that candidate and understand whether or not *Rrs1* is a single gene or not.

VII. General discussion

This PhD project involved the use of two different approaches to identify genetic resistance against *R. commune* in barley: effectoromics and genomics.

The effectoromics methods based on recent sequencing data of *R. commune* (Penselin et al. 2016) allowed the bioinformatic identification of a list of fungal proteins presenting typical characteristics of effectors such as short cysteine-rich sequences with a secretion signal peptide (Saunders et al. 2012). My role was to select the most promising candidate effectors from a list of *R. commune* candidate effectors with homologues found in other fungal species. Looking for candidate effectors can be a disadvantage because a candidate shared between different species could be conserved due to its essential role for surviving and as a consequence, may not be involved in virulence or pathogenicity. However, the advantage of looking for candidate effectors that are shared between different species is that the protein homologues may have already been studied and contain conserved domains already known to play a pathogenicity-related role, particularly if the candidate is present in other plant pathogens. It was however important to not neglect candidate proteins with unknown function which could lead to the discovery of a potentially new kind of candidate effector.

The first approach used to reduce the number of candidates was to try to find genomic associations by studying DNA polymorphisms of candidate genes between different sequenced strains of *R. commune* and look for differential pathogenicity on different plant genotypes. This study was based on virulence testing of the different strains of *R. commune* on a selection of cultivars carrying known resistances. However, the variability of virulence testing results due to the loss of pathogenicity by strains over time and generated using the detached leaf assay method did not allow the identification of associations between the amino acid differences of the proteins and virulence/avirulence phenotypes on different barley cultivars. It would be a good idea to improve the virulence testing method, perhaps by using the “attached leaves assay” which involves working with plants that are less stressed than cut plants in the detached leaf

assay. Indeed, even if working with cut plants in small boxes takes up little space and seems to be a reliable way for virulence testing (Newton et al. 2001a), it is not a perfect method to test the virulence of *R. commune*. The whole plant assay is another successful methods used by Hofmann et al. (2013). In addition, it is essential to use refreshed *R. commune* cultures which often lose pathogenicity when repeatedly grown on media.

Moreover, effector candidates were chosen base on transcriptomics data indicating whether or not candidates were expressed at early stages of infection, the results of a relative expression analysis during infection, and their putative function. In addition, the difference in amino acid sequence between different strains was studied, as important candidate effectors must be present in all strains and be relatively conserved between *R. commune* stains. For this reason, putative candidate effector genes were selected based on their limited protein sequence variability within the 9 sequenced strains.

For the relative expression analysis, the infection time course was carried out in lab condition collecting pooled samples for each time point. Because the relative expression analysis is the leading step of the whole effector approach which allows us to select potentially interesting candidates, it would have been necessary to carry out the experiment with more rigour and I would not repeat that experiment in the same way in the future. Firstly, the use of pooled samples for each time points is introducing variability totally hidden within the sample which may have led to poor estimations of the relative expression of genes tested. Moreover, the lack of biological repeats does not allow statistical validation of any of these results and it would have been more appropriate to sample different biological replicates at each sampling than to pool samples even if the experiment would have require a lot more of time and consumables. To finish, I would run the experiment in a better controlled environment such as a climate cabinet, which seems more adapted to transcription analysis using plants (Erayman et al. 2015). Barley plants require more light than the light provided on the lab bench, which cause the development of weak and stressed plants which could be perfect victims for *R. commune* or contrariwise be activating resistance through the pathway shared between biotic and abiotic resistance (Fujita et al. 2006). For example, infection times courses related to SA assays were repeated under several plant growth conditions and a

difference of speed of the appearance of the first lesions was observed depending on the growth conditions of the plants. This result could be due to the fitness of the fungus which can often induce some variability of infection but the fact that better environmental growth condition increases the speed of infection could indicate that abiotically stressed plants were more resistant to the fungus a phenomenon previously described by Ben Rejeb et al. (2014) who describe that abiotic and biotic stresses can have a positive effect on plant by reducing the susceptibility to biotic stress. It would have been good to repeat that experiment in better conditions which would build confidence about the relative expression pattern of candidate effectors selected. However, the time course was used to study the relative expression of candidate effectors which may not be influenced by the environmental condition or the fitness of the plants and the relative expression of the *RcCDI1* effector control gene showed the expected pattern of upregulation previously obtained from experiments carried out with the same conditions with pooled samples and no biological reps, thereby confirming the repeatability of such infection time courses. In addition, relative expression analysis of most of the candidate effectors showed an upregulation during infection with different patterns of expression corresponding to different waves of effectors involved in different stages of the infection (Win et al. 2012). The majority of candidate genes showed an upregulation within the three first days of infection indicating that they must be important for the early stage of the infection which could be involved in suppressing immune responses or manipulating the host metabolism to increase nutrient availability (Koeck et al. 2011). However, since *R. commune* do not benefit from the necrotic phase of the infection (Avrova and Knogge 2012), it remains unclear what would be the function of late expressed effectors.

After relative expression analysis, candidate effectors were selected for functional characterisation using two main methods. The first method involves the generation of *R. commune* KO mutants through homologous recombination and gene replacement. The generation of KO mutants of an effector allows us to check whether or not a candidate effector is essential and as a consequence, a good candidate. Unfortunately, the efficiency of gene replacement by homologous recombination in *R. commune* is very low, with only 1-5 % of the transformants likely to be knock-outs depending on the gene and this strategy

never succeeded in our lab despite the efforts of several people. It would have been good to optimise this technique maybe collaborating with the group in Germany which is routinely generating *R. commune* KO mutant (Kirsten et al. 2012) before launching such a project. In addition to low efficiency of gene replacement knock-outs of essential genes are lethal, but we did not expect the effectors to be essential for *R. commune* survival in culture.

The second method involved the use of BSMV as a delivery system of our candidate effectors in barley plants. By screening a large number of barley lines, we were hoping to identify an *R* gene/ *Avr* gene interaction such as the well described Atlas46 Rrs1/ NIP1 interaction (Lee et al. 2012) which could have confirmed the effector function of the candidate gene and lead to the identification of a (potentially new) resistance gene by the observation of differential plant responses between the several barley lines used. However, it appears that BSMV constructs generated appeared to be highly unstable depending on the size of the effector and that BSMV itself induced necrosis. In addition, I discovered that no BSMV-WT control infection or test of stability were done together with the phenotyping, preventing any conclusions regarding whether the symptom observed were due to the insert or BSMV itself. In conclusion, the BSMV strategy is a very challenging technique which requires rigour which so far has not allowed reliable identification of an effector/ R gene interaction.

The pathology department of the JHI works on *P. infestans*, aphid and nematode pathogens; and makes routine use of *A. tumefaciens* - mediated transient expression in the *N. benthamiana* system (Goodin et al. 2008) to characterise candidate effectors. This procedure allowed identifying an interesting protein with a putative protease inhibitor function which potentially had a role related to pathogenicity. It induced cell death when produced in *N. benthamiana* which could be HR, a marker of recognition by the plant (Dangl and Jones 2001). The protein was also produced in a more adapted system; through *P.* pastoris (Damasceno et al. 2012). However, all the attempts to prove that the candidate effector was a good candidate which induces HR led to conclusion that it was simply toxic for the plant.

In theory, the effector strategy looks good, but the reality is that it is a challenging approach. The effectoromics approach to identify durable resistance against *R. commune* in barley is based on the fact that resistance genes recognising more essential *Avr* effector are likely to be more durable. That is why the work was focussed on the discovery of novel and essential *R. commune Avr* genes. However, the probability of finding a genuine effector among all the putative effectors which have a real effect is low mostly due to functional redundancy (Birch et al. 2008) and the fact that plants have a limited amount of *R* genes compared to the number of candidate effectors. Although creating durable resistance using gene for gene interaction with genes recognising more essential *Avr* effector may be a good idea but this strategy may be poorly adapted to *R. commune* because it puts a lot of pressure on a single resistance process which could rapidly lead to an adaptation of *R. commune*, which is well known for its genetic diversity and high rate of mutation within a few asexual cycles of fungal infection (Williams et al. 2003). More generaly, effectoromics is an interesting strategy for fundamental research which could lead to better understanding of the barley/ *R. commune* interaction and potentially find new ways to protect the plant.

In addition, *R. commune* does not infect *N. benthamiana,* which presents a need to develop new tools for transient expression of fungal proteins in barley to allow work in an adapted pathosystem to study *R. commune* candidate effectors. So far, most of works to transiently express proteins in monocots through viruses or co-bombardment have been focused on protoplasts (Matzeit et al. 1991; Ugaki et al. 1991; Panstruga 2004), a non-adapted method to the study of apoplastic effectors. However, more recently, a biolistic particle bombardment techniques has been successfully used for *in planta* transient gene expression in rice sheath cells (Wang et al. 2013), and could be adapted to study barley-*R. commune* interaction. Moreover, the compatibility of *R. commune* with the fully sequenced model cereal plant, *B. distachyon,* was tested. *B. distachyon* was shown to be compatible with major cereal pathogens showing various trophic lifestyles (Goddard et al. 2014) and preliminary results suggest that *B. distachyon* can be used as a host to study *R. commune* infection and could be used as an advantageous new tool for functional study

thanks for its a short stature, rapid life-cycle small genome and the availability of an annotated T-DNA mutant collection (Thole et al. 2012).

R. commune candidate effectors; RcCM and RcISC; were selected for functional characterisation because their putative function suggested involvement in the interference with the SA pathway. In *U. maydis*, a secreted CM was shown to be able to be translocated in the plant cell during infection and is thought to be manipulating the SA pathway from the cytoplasm by diverting the chorismate from the SA pathway (Djamei et al. 2011). RcCM chorismate mutase function was confirmed. In *P. sojae* and *V. dahlia,* unconventionally secreted ISC were identified and showed to be required for full pathogenesis, able to suppress salicylate-mediated innate immunity *in planta* and hydrolyse isochorismate *in vitro* (Liu et al. 2014). RcISC was shown to be localised in the same location as *P. sojae* and *V. dahlia* homologues when transiently expressed in *N. benthamiana.* However, it remains unclear how and whether RcCM and RcISC are translocated into the plant cell to manipulate the barley SA pathway and if they are important for pathogenicity. In addition, this study allowed a focus on a direct link between the SA pathway of barley and *R. commune* by studying the effect of SA priming of barley plants on *R. commune* infection. So far, only assays studying a combination of elicitors such as ASM (acibenzolar-S-methyl), BABA (acibenzolar-S-methyl) and CJ (cis-jasmonate) were attempted showing that *R. commune* could be controlled through barley priming which leads to the up-regulation of the *PR1*(Walters et al. 2014). SA is a compound triggering an immune response and effective defence against biotrophic pathogens (Glazebrook 2005) and the assay showed that SA-priming could slow down the disease. Transcriptional analysis showed that *R. commune* was activating *PR1* expression until the first lesion appearance indicating a synchronisation of the biotrophic plant defence activation with the fungal switch to the necrotrophic phase, suggesting the biotrophic phase of the fungus. In addition, the expression of the *RcISC* fungal effector and the plant *ICS* appeared to be highly positively correlated during the biotrophic phase of infection in SA-primed plants. This result suggest that proteins may have an antagonistic effect where the fungal enzyme RcISC subverts the plant defence mechanism by diverting chorismate and isochorismate thereby slowing down the SA plant defence pathway; and the plant compensates for the depletion by

upregulating the expression of the plant enzyme ICS to maintain the SA plant defence pathway. However work still needs to be done to be able to fully understand the mechanism.

Finally barley genomics were used to survey mapped and new resistance against *R. commune* in a collection of elite spring barley using GWAS. GWAS is broadly used in different domains such as human disease (Bush and Moore 2012) and plant breeding (Begum et al. 2015). In plant pathology, GWAS can be used for gene discovery using landraces for example (Gurung et al. 2014). but our GWAS aim to survey mapped and new resistance against *R. commune* in a collection of spring barley elite varieties This approach allowed identification of significant QTL for resistance to Rhynchosporium including seven of the known major resistance genes as well as new ones. The identification of QTL using GWAS is powerful but highly dependent on the decision of where to put the threshold which can be determined using different statistical methods and can be influenced by LD (Johnson et al. 2010). However, the fact that we successfully detected mapped resistances illustrated that the strategy was well adapted. However, the identification of QTL using GWAS requires a large sample size to obtain meaningful results and is limited when the QTL is poorly represented in the studied population (Korte and Farlow 2013). Markers closely linked with detected QTL were identified and the effect of each QTL was studied, producing valuable information which could help breeders to create new varieties with improved resistance to *R. commune* in the future. For example, this data could be used to do gene pyramiding, a strategy proved to enhances durable disease resistance (Fukuoka et al. 2015) by combining a selection of major genes and minor QTL. The best associated QTL detected in the GWAS was *Rrs1* proving that it remains an important source of resistance in the field. The access to the new barley genome assembly, transcriptional data and exome capture data (Mascher et al., unpublished) providing a high quantity of SNPs allowed narrowing down the location of the major resistance gene *Rrs1* and improving the knowledge about this complex resistance. At the beginning, genotyping data identified 3 SNP markers specifically discriminating one allele of *Rrs1*: $Rrs1_{Rh4}$. These SNPs appeared to be present in the tyrosine domain of a WAK but heterozygote in *Rrs1* lines, suggesting a duplicated gene. Resequencing of those gene transcripts in *Rrs1* and susceptible lines revealed

that both lines lacked the resistant allele at the diagnostic (heterozygote) SNPs, suggesting that the gene identified is not *Rrs1*. Gene duplications are common in particular among the *R* genes families (Panchy et al. 2016). Indeed, the results suggest that this resistance is due to the insertion (in *Rrs1* lines only) of a probably duplicated gene with a very similar tyrosine kinase domain, containing SNPs potentially improving the signal transduction activating plant defences. This new discovery is likely to lead to the identification of the first gene for resistance against *R. commune* and provide a useful breeding tool for improving the design of new varieties by allowing the incorporation of *Rrs1* resistance gene into new lines.

VIII. Bibliography

Abang MM, Baum M, Ceccarelli S, Grando S, Linde CC, Yahyaoui AH, Zhan J, McDonald BA (2006) Pathogen evolution in response to host resistance genes: Evidence from fields experiments with *Rhynchosporium secalis* on barley. Phytopathology 96:S2-S2

Abbott DC, Brown AHD, Burdon JJ (1991) Genes for scald resistance from wild barley (*Hordeum vulgare ssp spontaneum*) and their linkage to isozyme markers. Euphytica 61:225-231

Abbott DC, Lagudah ES, Brown AHD (1995) Identification of RFLPs Flanking a Scald Resistance Gene on Barley Chromosome 6. Journal of Heredity 86:152-154

Abe A, Kosugi S, Yoshida K, Natsume S, Takagi H, Kanzaki H, Matsumura H, Yoshida K, Mitsuoka C, Tamiru M, Innan H, Cano L, Kamoun S, Terauchi R (2012) Genome sequencing reveals agronomically important loci in rice using MutMap. Nat Biotech 30:174-178

Agarwal M, Shrivastava N, Padh H (2008) Advances in molecular marker techniques and their applications in plant sciences. Plant cell reports 27:617-631

AHDB (2016) Barley disease management guide

Ahuja I, Kissen R, Bones AM Phytoalexins in defense against pathogens. Trends in plant science 17:73-90

Akar T, Avci M, Dusunceli F (2004) Barley: Post-harvest Operations. Turkey, http://www.fao.org/

Alabi OJ, Kumar, P. L., and Naidu, R. A (2011) Cassava Mosaic Disease: A Curse to Food Security in Sub-Saharan Africa. APSnet Features

Alvarado MC, Zsigmond LM, Kovács I, Cséplö A, Koncz C, Szabados LM (2004) Gene trapping with firefly luciferase in Arabidopsis. Tagging of stress-responsive genes. Plant Physiology 134:18-27

Anand A, Uppalapati SR, Ryu C-M, Allen SN, Kang L, Tang Y, Mysore KS (2008) Salicylic Acid and Systemic Acquired Resistance play a role in attenuating cown gall disease caused by *Agrobacterium tumefaciens*. Plant Physiology 146:703-715

Ardvison J (1999) Effects of cultivation depth in reduced tillage on soil physical properties crop yield one pathogens. European Journal of Agronomy 9:2

Ariyadasa R, Mascher M, Nussbaumer T, Schulte D, Frenkel Z, Poursarebani N, Zhou R, Steuernagel B, Gundlach H, Taudien S (2014) A sequence-ready physical map of barley anchored genetically by two million single-nucleotide polymorphisms. Plant physiology 164:412-423

Armstrong MR, Whisson SC, Pritchard L, Bos JI, Venter E, Avrova AO, Rehmany AP, Bohme U, Brooks K, Cherevach I, Hamlin N, White B, Fraser A, Lord A, Quail MA, Churcher C, Hall N, Berriman M, Huang S, Kamoun S, Beynon JL, Birch PR (2005) An ancestral oomycete locus contains late blight avirulence gene *Avr3a*, encoding a protein that is recognized in the host cytoplasm. Proc Natl Acad Sci U S A 102:7766-7771

Austin MJ, Muskett P, Kahn K, Feys BJ, Jones JD, Parker JE (2002) Regulatory role of *SGT1* in early R gene-mediated plant defenses. Science 295:2077-2080

Avrova A, Knogge W (2012) Rhynchosporium commune: a persistent threat to barley cultivation. Molecular Plant Pathology 13:986-997

Avrova AO, Venter E, Birch PRJ, Whisson SC (2003) Profiling and quantifying differential gene transcription in Phytophthora infestans prior to and during the early stages of potato infection. Fungal Genetics and Biology 40:4-14

Ayesu-Offei E, Clare B (1970) Processes in the infection of barley leaves by *Rhynchosporium secalis*. Australian Journal of Biological Sciences 23:300-308

Baccelli I, Mauch-Mani B (2016) Beta-aminobutyric acid priming of plant defense: the role of ABA and other hormones. Plant Molecular Biology 91:703-711

Badr A, M K, Sch R, Rabey HE, Effgen S, Ibrahim HH, Pozzi C, Rohde W, Salamini F (2000) On the Origin and Domestication History of Barley (*Hordeum vulgare*). Molecular Biology and Evolution 17:499-510

Bari R, Jones JDG (2009) Role of plant hormones in plant defence responses. Plant Molecular Biology 69:473-488

Barrangou R, Fremaux C, Deveau H, Richards M, Boyaval P, Moineau S, Romero DA, Horvath P (2007) CRISPR provides acquired resistance against viruses in prokaryotes. Science 315:1709-1712

Baucher M, Halpin C, Petit-Conil M, Boerjan W (2003) Lignin: genetic engineering and impact on pulping. Critical Reviews in Biochemistry and Molecular Biology 38:305-350

Baulcombe D (2004) RNA silencing in plants. Nature 431:356-363

Beckers GJ, Spoel SH (2006) Fine-tuning plant defence signalling: salicylate versus jasmonate. Plant biology (Stuttgart, Germany) 8:1-10

Begum H, Spindel JE, Lalusin A, Borromeo T, Gregorio G, Hernandez J, Virk P, Collard B, McCouch SR (2015) Genome-Wide Association mapping for yield and other agronomic traits in an elite breeding population of tropical rice (*Oryza sativa*). PLoS ONE 10:e0119873

Bekal S, Niblack TL, Lambert KN (2003) A chorismate mutase from the soybean cyst nematode *Heterodera glycines* shows polymorphisms that correlate with virulence. Molecular plant-microbe interactions : MPMI 16:439-446

Ben Rejeb I, Pastor V, Mauch-Mani B (2014) Plant responses to simultaneous biotic and abiotic stress: molecular mechanisms. Plants 3:458-475

Bendahmane A, Querci M, Kanyuka K, Baulcombe DC (2000) Agrobacterium transient expression system as a tool for the isolation of disease resistance genes: application to the *Rx2* locus in potato. The Plant Journal 21:73-81

Birch PRJ, Boevink PC, Gilroy EM, Hein I, Pritchard L, Whisson SC (2008) Oomycete RXLR effectors: delivery, functional redundancy and durable disease resistance. Current Opinion in Plant Biology 11:373-379

Bjørnstad Å, Patil V, Tekauz A, Marøy AG, Skinnes H, Jensen A, Magnus H, MacKey J (2002) Resistance to scald (*Rhynchosporium secalis*) in Barley (*Hordeum vulgare*) studied by Near-Isogenic Lines: I. Markers and differential isolates. Phytopathology 92:710-720

Böhm H, Albert I, Fan L, Reinhard A, Nürnberger T (2014) Immune receptor complexes at the plant cell surface. Curr Opin Plant Biol 20

Boller T, Felix G (2009) A renaissance of elicitors: perception of microbe-associated molecular patterns and danger signals by pattern-recognition receptors. Annu Rev Plant Biol 60

Boller T, He SY (2009) Innate immunity in plants: an arms race between pattern recognition receptors in pants and effectors in microbial pathogens. Science 324:742-744

Boopathi NM. (2013) Genetic Mapping and Marker Assisted Selection. India: Springer.

Bos JI, Kanneganti TD, Young C, Cakir C, Huitema E, Win J, Armstrong MR, Birch PR, Kamoun S (2006) The C-terminal half of *Phytophthora infestans* RXLR effector *AVR3a* is sufficient to trigger R3a-mediated hypersensitivity and suppress INF1-induced cell death in Nicotiana benthamiana. Plant J 48:165-176

Bos JIB, Armstrong MR, Gilroy EM, Boevink PC, Hein I, Taylor RM, Zhendong T, Engelhardt S, Vetukuri RR, Harrower B, Dixelius C, Bryan G, Sadanandom A, Whisson SC, Kamoun S, Birch PRJ (2010) Phytophthora infestans effector *AVR3a* is essential for virulence and manipulates plant immunity by stabilizing host *E3 ligase CMPG1*. Proceedings of the National Academy of Sciences 107:9909-9914

Bouwmeester K, Han M, Blanco-Portales R, Song W, Weide R, Guo L-Y, van der Vossen EAG, Govers F (2014) The Arabidopsis lectin receptor kinase *LecRK-I.9* enhances resistance to *Phytophthora infestans* in Solanaceous plants. Plant Biotechnology Journal 12:10-16

Boyle C, Walters D (2006) Saccharin-induced protection against powdery mildew in barley: effects on growth and phenylpropanoid metabolism. Plant pathology 55:82-91

Bozkurt TO, Schornack S, Win J, Shindo T, Ilyas M, Oliva R, Cano LM, Jones AME, Huitema E, van der Hoorn RAL, Kamoun S (2011) *Phytophthora infestans* effector *AVRblb2* prevents secretion of a plant immune protease at the haustorial interface. Proceedings of the National Academy of Sciences 108:20832-20837

Brandizzi F, Hanton S, DaSilva LL, Boevink P, Evans D, Oparka K, Denecke J, Hawes C (2003) ER quality control can lead to retrograde transport from the ER lumen to the cytosol and the nucleoplasm in plants. Plant J 34:269-281

Brenchley R, Spannagl M, Pfeifer M, Barker GLA, D/'Amore R, Allen AM, McKenzie N, Kramer M, Kerhornou A, Bolser D, Kay S, Waite D, Trick M, Bancroft I, Gu Y, Huo N, Luo M-C, Sehgal S, Gill B, Kianian S, Anderson O, Kersey P, Dvorak J, McCombie WR, Hall A, Mayer KFX, Edwards KJ, Bevan MW, Hall N (2012) Analysis of the bread wheat genome using whole-genome shotgun sequencing. Nature 491:705-710

Brooks F (1928) Observations on *Rhynchosporium secalis* (Oud.) Davis, leaf blotch of barley and rye. New Phytologist 27:215-219

Brown A, Burdon J, Garvin D, Abbott D, Read B (1996) The effect of combining scald resistance genes on disease levels, yield and quality traits in barley. Theoretical and Applied Genetics 93:361-366

Brunner PC, SchÜRch S, McDonald BA (2007) The origin and colonization history of the barley scald pathogen *Rhynchosporium secalis*. Journal of Evolutionary Biology 20:1311-1321

Brutus A, Sicilia F, Macone A, Cervone F, De Lorenzo G (2010) A domain swap approach reveals a role of the plant wall-associated kinase 1 (*WAK1*) as a receptor of oligogalacturonides. Proc Natl Acad Sci USA 107

Bruun-Rasmussen M, Madsen CT, Jessing S, Albrechtsen M (2007) Stability of Barley stripe mosaic virus-induced gene silencing in barley. Molecular plant-microbe interactions : MPMI 20:1323-1331

Bush WS, Moore JH (2012) Chapter 11: Genome-Wide Association Studies. PLoS Computational Biology 8:e1002822

Cai H-w, Gao Z-s, Yuyama N, Ogawa N (2003) Identification of AFLP markers closely linked to the rhm gene for resistance to Southern Corn Leaf Blight in maize by using bulked segregant analysis. Molecular Genetics and Genomics 269:299-303

Cantu D, Segovia V, MacLean D, Bayles R, Chen X, Kamoun S, Dubcovsky J, Saunders DG, Uauy C (2013) Genome analyses of the wheat yellow (stripe) rust pathogen *Puccinia striiformis f. sp. tritici* reveal polymorphic and haustorial expressed secreted proteins as candidate effectors. BMC genomics 14:1

Cao H, Li X, Dong X (1998) Generation of broad-spectrum disease resistance by overexpression of an essential regulatory gene in systemic acquired resistance. Proceedings of the National Academy of Sciences 95:6531-6536

Carisse KX, Burnett PA, Tewari JP, Chen MH, Turkington TK, Helm JH (2000) Histopathological study of barley cultivars resistant and susceptible to *Rhynchosporium secalis*. Phytopathology 90:94-102

Carolan JC, Caragea D, Reardon KT, Mutti NS, Dittmer N, Pappan K, Cui F, Castaneto M, Poulain J, Dossat C, Tagu D, Reese JC, Reeck GR, Wilkinson TL, Edwards OR (2011) Predicted effector molecules in the salivary secretome of the pea aphid (*Acyrthosiphon pisum*): A dual transcriptomic/Pproteomic approach. Journal of Proteome Research 10:1505-1518

Carrington JC, Ambros V (2003) Role of microRNAs in plant and animal development. Science 301:336-338

Carris LM, Little CR, Stiles CM (2012) Introduction to fungi. The Plant Health Instructor

Cenis JL (1992) Rapid extraction of fungal DNA for PCR amplification. Nucleic Acids Research 20:2380

Ceoloni C (1980) Race differentiation and search for sources of resistance to *Rhynchosporium secalis* in barley in Italy. Euphytica 29:547-553

Chapman S, Kavanagh T, Baulcombe D (1992) Potato virus X as a vector for gene expression in plants. The Plant Journal 2:549-557

Chen S, Chronis D, Wang X (2013) The novel GrCEP12 peptide from the plant-parasitic nematode Globodera rostochiensis suppresses flg22-mediated PTI. Plant signaling & behavior 8

Chen W, Lee MK, Jefcoate C, Kim SC, Chen F, Yu JH (2014) Fungal cytochrome p450 monooxygenases: their distribution, structure, functions, family expansion, and evolutionary origin. Genome biology and evolution 6:1620-1634

Chen X (2009) Small RNAs and their roles in plant development. Annual Review of Cell and Developmental 25:21-44

Chen Z, Zheng Z, Huang J, Lai Z, Fan B (2009) Biosynthesis of salicylic acid in plants. Plant signaling & behavior 4:493-496

Chinchilla D, Bauer Z, Regenass M, Boller T, Felix G (2006) The Arabidopsis receptor kinase FLS2 binds flg22 and determines the specificity of flagellin perception. The Plant Cell 18:465-476

Chinchilla D, Zipfel C, Robatzek S, Kemmerling B, Nurnberger T, Jones JD, Felix G, Boller T (2007) A flagellin-induced complex of the receptor *FLS2* and *BAK1* initiates plant defence. Nature 448

Chisholm ST, Coaker G, Day B, Staskawicz BJ (2006) Host-microbe interactions: shaping the evolution of the plant immune response. Cell 124:803-814

Christou P (1992) Genetic transformation of crop plants using microprojectile bombardment. The Plant Journal 2:275-281

Comadran J, Kilian B, Russell J, Ramsay L, Stein N, Ganal M, Shaw P, Bayer M, Thomas W, Marshall D, Hedley P, Tondelli A, Pecchioni N, Francia E, Korzun V, Walther A, Waugh R (2012) Natural variation in a homolog of Antirrhinum CENTRORADIALIS contributed to spring growth habit and environmental adaptation in cultivated barley. Nature Genetics 44:1388-1392

Cong L, Ran FA, Cox D, Lin SL, Barretto R, Habib N (2013) Multiplex genome engineering using CRISPR/Cas systems. Science 339

Conrath U, Beckers GJ, Langenbach CJ, Jaskiewicz MR (2015) Priming for enhanced defense. Annual review of phytopathology 53:97-119

Consortium TG (2012) The tomato genome sequence provides insights into fleshy fruit evolution. Nature 485

Cooper JL, Till BJ, Laport RG, Darlow MC, Kleffner JM, Jamai A, El-Mellouki T, Liu S, Ritchie R, Nielsen N (2008) TILLING to detect induced mutations in soybean. BMC plant biology 8:9

Core R (2013) R: A language and environment for statistical computing

Damasceno LM, Huang C-J, Batt CA (2012) Protein secretion in *Pichia pastoris* and advances in protein production. Applied Microbiology and Biotechnology 93:31-39

Dangl JL, Jones JDG (2001) Plant pathogens and integrated defence responses to infection. Nature 411:826-833

Davis H, Fitt BDL (1990) Symptomless infection of *Rhynchosporium secalis* on leaves of winter barley. Mycological Research 94:557-560

Davis H, Fitt BDL (1992) Seasonal-changes in primary and secondary inoculum during epidemics of leaf blotch (*Rhynchosporium secalis*) on winter barley. Annals of Applied Biology 121:39-49

Davis H, Fitt BD, Evans R (1994) Atypical, green leaf blotch lesions on barley leaves infected by *Rhynchosporium secalis* (Oud.) Davis. New phytologist 127:139-145

Davis J (1922) Notes on parasitic fungi in Wisconsin–VII. Transactions of the Wisconsin Academy of Sciences, Arts, and Letters 20:399-411

Dawson IK, Russell J, Powell W, Steffenson B, Thomas WT, Waugh R (2015) Barley: a translational model for adaptation to climate change. New Phytologist 206:913-931

De Rubeis S, He X, Goldberg AP, Poultney CS, Samocha K, Ercument Cicek A, Kou Y, Liu L, Fromer M, Walker S, Singh T, Klei L, Kosmicki J, Fu S-C, Aleksic B, Biscaldi M, Bolton PF, Brownfeld JM, Cai J, Campbell NG, Carracedo A, Chahrour MH, Chiocchetti AG, Coon H, Crawford EL, Crooks L, Curran SR, Dawson G, Duketis E, Fernandez BA, Gallagher L, Geller E, Guter SJ, Sean Hill R, Ionita-Laza I, Jimenez Gonzalez P, Kilpinen H, Klauck SM, Kolevzon A, Lee I, Lei J, Lehtimaki T, Lin C-F, Ma/'ayan A, Marshall CR, McInnes AL, Neale B, Owen MJ, Ozaki N, Parellada M, Parr JR, Purcell S, Puura K, Rajagopalan D, Rehnstrom K, Reichenberg A, Sabo A, Sachse M, Sanders SJ, Schafer C, Schulte-Ruther M, Skuse D, Stevens C, Szatmari P, Tammimies K, Valladares O, Voran A, Wang L-S, Weiss LA, Jeremy Willsey A, Yu TW, Yuen RKC, The DDDS, Homozygosity Mapping Collaborative for A, Consortium UK, The Autism Sequencing C, Cook EH, Freitag CM, Gill M, Hultman CM, Lehner T, Palotie A, Schellenberg GD, Sklar P, State MW, Sutcliffe JS, Walsh CA, Scherer SW, Zwick ME, Barrett JC, Cutler DJ, Roeder K, Devlin B, Daly MJ, Buxbaum JD (2014) Synaptic, transcriptional and chromatin genes disrupted in autism. Nature 515:209-215

De Vleesschauwer D, Xu J, Höfte M, (2014) Making sense of hormone-mediated defense networking: From rice to Arabidopsis. Front. Plant Sci. 5, 1–15

Degrassi G, Devescovi G, Bigirimana J, Venturi V (2010) *Xanthomonas oryzae pv. oryzae* XKK.12 contains an AroQγ chorismate mutase that is involved in rice virulence. Phytopathology 100:262-270

Delteil A, Gobbato E, Cayrol B, Estevan J, Michel-Romiti C, Dievart A, Kroj T, Morel J-B (2016) Several wall-associated kinases participate positively and negatively in basal defense against rice blast fungus. BMC Plant Biology 16:1-10

Diener AC, Ausubel FM (2005) RESISTANCE TO *FUSARIUM OXYSPORUM* 1, a Dominant arabidopsis disease-resistance gene, iIs not race specific. Genetics 171:305-321

Dixon RA, Paiva NL (1995) Stress-induced phenylpropanoid metabolism. The Plant Cell 7:1085-1097

Djamei A, Schipper K, Rabe F, Ghosh A, Vincon V, Kahnt J, Osorio S, Tohge T, Fernie AR, Feussner I (2011) Metabolic priming by a secreted fungal effector. Nature 478:395-398

Dodds PN, Rathjen JP (2010) Plant immunity: towards an integrated view of plant-–pathogen interactions. Nat Rev Genet 11

Doehlemann G, Hemetsberger C (2013) Apoplastic immunity and its suppression by filamentous plant pathogens. New Phytol 198:1001-1016

Dong C-H, Rivarola M, Resnick JS, Maggin BD, Chang C (2008) Subcellular co-localization of Arabidopsis RTE1 and ETR1 supports a regulatory role for RTE1 in ETR1 ethylene signaling. The Plant Journal 53:275-286

Dong X (1998) SA, JA, ethylene, and disease resistance in plants. Curr Opin Plant Biol 1:316-323

Donnelly P (2008) Progress and challenges in genome-wide association studies in humans. Nature 456:728-731

Doudna JA, Charpentier E (2014) The new frontier of genome engineering with CRISPR-Cas9. Science 346:1258096

Duan X, Li X, Xue Q, Abo-El-Saad M, Xu D, Wu R (1996) Transgenic rice plants harboring an introduced potato proteinase inhibitor II gene are insect resistant. Nature biotechnology 14:494-498

Duggan DJ, Bittner M, Chen Y, Meltzer P, Trent JM Expression profiling using cDNA microarrays. Nat Genet

Dyck P, Schaller C (1961) Association of two genes for scald resistance with a specific barley chromosome. Canadian Journal of Genetics and Cytology 3:165-169

Edwards D, Batley J (2010) Plant genome sequencing: applications for crop improvement. Plant Biotechnology Journal 8:2-9

Elen O (2002) Plant protection in spring cereal production with reduced tillage. III. Cereal diseases. Crop Protection 21:195-201

Ellis JG, Lagudah ES, Spielmeyer W, Dodds PN (2014) The past, present and future of breeding rust resistant wheat. Frontiers in plant science 5:641

Endo M, Mikami M, Toki S (2014) Multi-gene knockout utilizing off-target mutations of the CRISPR/Cas9 system in rice. Plant and Cell Physiology

Erayman M, Turktas M, Akdogan G, Gurkok T, Inal B, Ishakoglu E, Ilhan E, Unver T (2015) Transcriptome analysis of wheat inoculated with Fusarium graminearum. Frontiers in Plant Science 6

Espinosa A, Guo M, Tam VC, Fu ZQ, Alfano JR (2003) The Pseudomonas syringae type III-secreted protein HopPtoD2 possesses protein tyrosine phosphatase activity and suppresses programmed cell death in plants. Molecular microbiology 49:377-387

Eulgem T (2005) Regulation of the Arabidopsis defense transcriptome. Trends in plant science 10:71-78

Eulgem T, Somssich IE (2007) Networks of WRKY transcription factors in defense signaling. Current Opinion in Plant Biology 10:366-371

Fekih R, Takagi H, Tamiru M, Abe A, Natsume S, Yaegashi H, Sharma S, Sharma S, Kanzaki H, Matsumura H, Saitoh H, Mitsuoka C, Utsushi H, Uemura A, Kanzaki E, Kosugi S, Yoshida K, Cano L, Kamoun S, Terauchi R (2013) MutMap+: genetic mapping and mutant identification without crossing in rice. PLoS ONE 8:e68529

Ferrari S, Plotnikova JM, de Lorenzo G, Ausubel FM (2003) Arabidopsis local resistance to Botrytis cinerea involves salicylic acid and camalexin and requires EDS4 and PAD2, but not SID2, EDS5 or PAD4. Plant J 35: 193–205

Ferdous J, Li Y, Reid N, Langridge P, Shi B-J, Tricker PJ (2015) Identification of reference genes for quantitative expression analysis of microRNAs and mRNAs in barley under various stress conditions. PLoS ONE 10:e0118503

Fitt BD, McCartney H, Walklate P (1989) The role of rain in dispersal of pathogen inoculum. Annual Review of Phytopathology 27:241-270

Fitt BD, Atkins SD, Fraaije BA, Lucas JA, Newton AC, Looseley ME, Werner P, Harrap D, Ashworth M, Southgate J, Phillips H, Gilchrist A (2010) Role of inoculum sources in Rhynchosporium population dynamics and epidemiology on barley. HGCA Final report. Project Number RD-2004-3099.

Flor H (1955) Host-parasite interaction in flax rust-its genetics and other implications. Phytopathology 45:680-685

Flor HH (1971) Current status of the gene-for-gene concept. Annual review of phytopathology 9:275-296

Fountaine JM, Shaw MW, Ward E, Fraaije BA (2010) The role of seeds and airborne inoculum in the initiation of leaf blotch (*Rhynchosporium secalis*) epidemics in winter barley. Plant Pathology 59:330-337

Frank B (1897) Über die Zerstörung der Gerste durch einen neuen Getreidepilz. Woch schrift Brauerei 14:518-520

Fry WE, Goodwin SB (1997) Resurgence of the Irish potato famine fungus. Bioscience 47:363-371

Fu J, Hettler E, Wickes B (2006) Split marker transformation increases homologous integration frequency in *Cryptococcus neoformans*. Fungal Genetics and Biology 43:200-212

Fujita M, Fujita Y, Noutoshi Y, Takahashi F, Narusaka Y, Yamaguchi-Shinozaki K, Shinozaki K (2006) Crosstalk between abiotic and biotic stress responses: a current view from the points of convergence in the stress signaling networks. Current opinion in plant biology 9:436-442

Fukuoka S, Saka N, Mizukami Y, Koga H, Yamanouchi U, Yoshioka Y, Hayashi N, Ebana K, Mizobuchi R, Yano M (2015) Gene pyramiding enhances durable blast disease resistance in rice. Scientific Reports 5:7773

Galletti R, Ferrari S, De Lorenzo G (2011) Arabidopsis MPK3 and MPK6 play different roles in basal and oligogalacturonide-or flagellin-induced resistance against *Botrytis cinerea*. Plant Physiology 157:804-814

Garvin DF, Brown AHD, Raman H, Read BJ (2000) Genetic mapping of the barley *Rrs14* scald resistance gene with RFLP, isozyme and seed storage protein markers. Plant Breeding 119:193-196

Garvin FD, Brown DAH, Burdon JJ (1997) Inheritance and chromosome locations of scald-resistance genes derived from Iranian and Turkish wild barleys. Theoretical and Applied Genetics 94:1086-1091

Gechev TS, Van Breusegem F, Stone JM, Denev I, Laloi C (2006) Reactive oxygen species as signals that modulate plant stress responses and programmed cell death. BioEssays 28:1091-1101

Genger RK, Williams KJ, Raman H, Read BJ, Wallwork H, Burdon JJ, Brown AHD (2003) Leaf scald resistance genes in *Hordeum vulgare* and *Hordeum vulgare spontaneum* parallels between cultivated and wild barley. Australian Journal of Agricultural Research 54:1335-1342

Genger RK, Nesbitt K, Brown AHD, Abbott DC, Burdon JJ (2005) A novel barley scald resistance gene: genetic mapping of the *Rrs15* scald resistance gene derived from wild barley, *Hordeum vulgare ssp spontaneum*. Plant Breeding 124:137-141

Gish LA, Clark SE (2011) The RLK/Pelle family of kinases. The Plant journal : for cell and molecular biology 66:117-127

Glazebrook J (2005) Contrasting mechanisms of defense against biotrophic and necrotrophic pathogens. Annu Rev Phytopathol 43:205-227

Glickman ME, Rao SR, Schultz MR (2014) False discovery rate control is a recommended alternative to Bonferroni-type adjustments in health studies. Journal of clinical epidemiology 67:850-857

Goddard R, Peraldi A, Ridout C, Nicholson P (2014) Enhanced disease resistance caused by *BRI1* mutation is conserved between *Brachypodium distachyon* and barley (*Hordeum vulgare*). Molecular Plant-Microbe Interactions 27:1095-1106

Goff KE, Ramonell KM (2007) The role and regulation of Receptor-Like Kinases in plant defense. gene regulation and systems biology 1:167-175

Goff SA, Ricke D, Lan T-H, Presting G, Wang R, Dunn M, Glazebrook J, Sessions A, Oeller P, Varma H (2002) A draft sequence of the rice genome (*Oryza sativa L. ssp. japonica*). Science 296:92-100

Gonsalves D, Ferriera S, Manshardt R, Fitch M, Slightom J (2000) Transgenic virus resistant papaya: New hope for controlling papaya ringspot virus in Hawaii. Plant Health Progress(plant Health Reviews) 21

Goodin MM, Zaitlin D, Naidu RA, Lommel SA (2008) *Nicotiana benthamiana*: its history and future as a model for plant-pathogen interactions. Molecular Plant-Microbe Interactions 21:1015-1026

Granett J, Omer A, Pessereau P, Walker M (1998) Fungal infections of grapevine roots in phylloxera-infested vineyards. VITIS-Journal of Grapevine Research 37:39

Greene EA, Codomo CA, Taylor NE, Henikoff JG, Till BJ, Reynolds SH, Enns LC, Burtner C, Johnson JE, Odden AR (2003) Spectrum of chemically induced mutations from a large-scale reverse-genetic screen in Arabidopsis. Genetics 164:731-740

Grønnerød S, Marøy AG, MacKey J, Tekauz A, Penner GA, Bjørnstad A (2002) Genetic analysis of resistance to barley scald (*Rhynchosporium secalis*) in the Ethiopian line `Abyssinian' (CI668). Euphytica 126:235-250

Gurung S, Mamidi S, Bonman JM, Xiong M, Brown-Guedira G, Adhikari TB (2014) Genome-wide association study reveals novel quantitative trait Loci associated with resistance to multiple leaf spot diseases of spring wheat. PLoS One 9:e108179

Gutiérrez L, Berberian N, Capettini F, Falcioni E, Fros D, Germán S, Hayes PM, Huerta-Espino J, Herrera S, Pereyra S, Pérez C, Sandoval-Islas S, Singh R, Castro A (2013) Genome-Wide

Association mapping identifies disease-resistance QTLs in barley germplasm from Latin America. In: Zhang G, Li C, Liu X (eds) Advance in barley sciences: Proceedings of 11th International Barley Genetics Symposium. Springer Netherlands, Dordrecht, pp 209-215

Guyon K, Balagué C, Roby D, Raffaele S. (2014) Secretome analysis reveals effector candidates associated with broad host range necrotrophy in the fungal plant pathogen Sclerotinia sclerotiorum. BMC Genomics. 15:336

Habgood R (1971) The transmission of *Rhynchosporium secalis* by infected barley seed. Plant Pathology 20:80-81

Habib H, Fazili KM (2007) Plant protease inhibitors: a defense strategy in plants. Biotechnology and Molecular Biology Reviews 2:68-85

Hahn M, Jungling S, Knogge W (1993) Cultivar-specific elicitation of barley defense reactions by the phytotoxic peptide NIP1 from *Rhynchosporium secalis*. Molecular plant-microbe interactions : MPMI 6:745-754

Hanemann A, Schweizer GF, Cossu R, Wicker T, Röder MS (2009) Fine mapping, physical mapping and development of diagnostic markers for the *Rrs2* scald resistance gene in barley. Theoretical and Applied Genetics 119:1507-1522

Hannon GJ, Rossi JJ (2004) Unlocking the potential of the human genome with RNA interference. Nature 431:371-378

Hansen L, Magnus H (1969) Leaf spot fungi on barley in Norway. Forskning og forsok i lanbruket 20:95-105

Harloff H-J, Emrani N, Jung C (2014) High throughput screening for detecting EMS mutations in oilseed rape (Brassica napus L.). Tagungsband der 64 Jahrestagung der Vereinigung der Pflanzenzüchter und Saatgutkaufleute Österreichs 25-26 November 2013, Raumberg-Gumpenstein:9

Heinsen E (1901) Beobachtungen uiber den neuen Getreidepilz Rhynchosporium graminicola. Jahrb d Hamburg wissenschaft Anstalten 3:43

Hemetsberger C, Herrberger C, Zechmann B, Hillmer M, Doehlemann G (2012) The *Ustilago maydis* effector Pep1 suppresses plant immunity by inhibition of host peroxidase activity. PLoS Pathog 8:e1002684

Heneen WK (2010) Cytogenetics and molecular cytogenetics of barley: a model cereal crop with a large genome. barley: Production, Improvement, and Uses 11:112

Herman M, Restrepo S, Smart C (2007) Defense gene expression patterns of three SAR-induced tomato cultivars in the field. Physiological and Molecular Plant Pathology 71:192-200

Hiremath PJ, Kumar A, Penmetsa RV, Farmer A, Schlueter JA, Chamarthi SK, Whaley AM, Carrasquilla-Garcia N, Gaur PM, Upadhyaya HD (2012) Large-scale development of cost-effective SNP marker assays for diversity assessment and genetic mapping in chickpea and comparative mapping in legumes. Plant biotechnology journal 10:716-732

Hittalmani S, Parco A, Mew TV, Zeigler RS, Huang N (2000) Fine mapping and DNA marker-assisted pyramiding of the three major genes for blast resistance in rice. Theoretical and Applied Genetics 100:1121-1128

Hofmann K, Silvar C, Casas AM, Herz M, Büttner B, Gracia MP, Contreras-Moreira B, Wallwork H, Igartua E, Schweizer G (2013) Fine mapping of the *Rrs1* resistance locus against scald in two large populations derived from Spanish barley landraces. Theoretical and Applied Genetics 126:3091-3102

Horbach R, Navarro-Quesada AR, Knogge W, Deising HB (2011) When and how to kill a plant cell: Infection strategies of plant pathogenic fungi. Journal of Plant Physiology 168:51-62

Horton MW, Bodenhausen N, Beilsmith K, Meng D, Muegge BD, Subramanian S, Vetter MM, Vilhjálmsson BJ, Nordborg M, Gordon JI, Bergelson J (2014) Genome-wide association study of *Arabidopsis thaliana* leaf microbial community. Nature Communications 5:5320

Houston K, Russell J, Schreiber M, Halpin C, Oakey H, Washington JM, Booth A, Shirley N, Burton RA, Fincher GB, Waugh R (2014) A genome wide association scan for (1,3;1,4)-β-

glucan content in the grain of contemporary 2-row Spring and Winter barleys. BMC Genomics 15:1-15

Houterman PM, Cornelissen BJC, Rep M (2008) Suppression of plant resistance gene-based immunity by a fungal effector. PLoS Pathog 4:e1000061

Hsu PD, Lander ES, Zhang F (2014) Development and applications of CRISPR-Cas9 for genome engineering. Cell 157:1262-1278

Hu T, Sun X, Zhang X, Nevo E, Fu J (2014) An RNA sequencing transcriptome analysis of the high-temperature stressed tall fescue reveals novel insights into plant thermotolerance. BMC Genomics 15:1147

Huang X-L, Ma J-B, Chen X, Wang X-J, Ding K, Han D-J, Qu Z-P, Huang L-L, Kang Z-S (2013) Genes involved in adult plant resistance to stripe rust in wheat cultivar Xingzi 9104. Physiological and Molecular Plant Pathology 81:26-32

Hubert DA, Tornero P, Belkhadir Y, Krishna P, Takahashi A, Shirasu K, Dangl JL (2003) Cytosolic HSP90 associates with and modulates the Arabidopsis RPM1 disease resistance protein. The EMBO Journal 22:5679-5689

Huffaker A, Ryan CA (2007) Endogenous peptide defense signals in Arabidopsis differentially amplify signaling for the innate immune response. Proceedings of the National Academy of Sciences of the United States of America 104:10732-10736

Hurni S, Scheuermann D, Krattinger SG, Kessel B, Wicker T, Herren G, Fitze MN, Breen J, Presterl T, Ouzunova M, Keller B (2015) The maize disease resistance gene Htn1 against northern corn leaf blight encodes a wall-associated receptor-like kinase. Proceedings of the National Academy of Sciences of the United States of America 112:8780-8785

Ichimura K, Shinzato T, Edaki M, Yoshioka H, Shirasu K (2016) SGT1 contributes to maintaining protein levels of MEK2DD to facilitate hypersensitive response-like cell death in *Nicotiana benthamiana*. Physiological and Molecular Plant Pathology 94:47-52

International V (2011) GenStat for Windows 14th Edition. VSN International, Hemel Hempstead, UK

Islam MT, Croll D, Gladieux P, Soanes DM, Persoons A, Bhattacharjee P, Hossain MS, Gupta DR, Rahman MM, Mahboob MG, Cook N, Salam MU, Surovy MZ, Sancho VB, Maciel JLN, NhaniJúnior A, Castroagudín VL, Reges JTdA, Ceresini PC, Ravel S, Kellner R, Fournier E, Tharreau D, Lebrun M-H, McDonald BA, Stitt T, Swan D, Talbot NJ, Saunders DGO, Win J, Kamoun S (2016) Emergence of wheat blast in Bangladesh was caused by a South American lineage of *Magnaporthe oryzae*. BMC Biology 14:84

Jacobs TB, LaFayette PR, Schmitz RJ, Parrott WA (2015) Targeted genome modifications in soybean with CRISPR/Cas9. BMC Biotechnology 15:16

Jeong JS, Kim YS, Redillas MCFR, Jang G, Jung H, Bang SW, Choi YD, Ha S-H, Reuzeau C, Kim J-K (2013) OsNAC5 overexpression enlarges root diameter in rice plants leading to enhanced drought tolerance and increased grain yield in the field. Plant Biotechnology Journal 11:101-114

Johansson EV, Nilsson AC, Östman EM, Björck IME (2013) Effects of indigestible carbohydrates in barley on glucose metabolism, appetite and voluntary food intake over 16 h in healthy adults. Nutrition Journal 12:1-12

Johnson RC, Nelson GW, Troyer JL, Lautenberger JA, Kessing BD, Winkler CA, O'Brien SJ (2010) Accounting for multiple comparisons in a genome-wide association study (GWAS). BMC Genomics 11:724-724

Jones JDG, Dangl JL (2006) The plant immune system. Nature 444:323-329

Jones JT, Furlanetto C, Bakker E, Banks B, Blok V, Chen Q, Phillips M, Prior A (2003) Characterization of a chorismate mutase from the potato cyst nematode *Globodera pallida*. Molecular Plant Pathology 4:43-50

Jones P, Ayres PG (1974) Rhynchosporium leaf blotch of barley studied during the subcuticular phase by electron microscopy. Physiological Plant Pathology 4:229-233

Jørgensen HL, De Neergaard E, Smedegaard-Petersen V (1993) Histological examination of the interaction between *Rhynchosporium secalis* and susceptible and resistant cultivars of barley. Physiological and Molecular Plant Pathology 42:345-358

Kadirvel P, Senthilvel S, Geethanjali S, Sujatha M, Varaprasad KS (2015) Genetic markers, trait mapping and marker-assisted selection in plant breeding. In: Bahadur B, Venkat Rajam M, Sahijram L, Krishnamurthy VK (eds) Plant biology and biotechnology, vol II., Plant genomics and biotechnologySpringer pp 65–88

Kamoun S, van West P, Vleeshouwers VG, de Groot KE, Govers F (1998) Resistance of *Nicotiana benthamiana* to *Phytophthora infestans* is mediated by the recognition of the elicitor protein INF1. The Plant Cell 10:1413-1426

Kamoun S (2006) A catalogue of the effector secretome of plant pathogenic oomycetes. Phytopathology 44:41

Kamthan A, Chaudhuri A, Kamthan M, Datta A (2016) Genetically modified (GM) crops: milestones and new advances in crop improvement. Theoretical and Applied Genetics 129:1639-1655

Kartha K, Chibbar RN, Georges F, Leung N, Caswell K, Kendall E, Qureshi J (1989) Transient expression of chloramphenicol acetyltransferase (CAT) gene in barley cell cultures and immature embryos through microprojectile bombardment. Plant cell reports 8:429-432

Katiyar-Agarwal S, Morgan R, Dahlbeck D, Borsani O, Villegas A, Zhu J-K, Staskawicz BJ, Jin H (2006) A pathogen-inducible endogenous siRNA in plant immunity. Proceedings of the National Academy of Sciences 103:18002-18007

Kay S, Hahn S, Marois E, Hause G, Bonas U (2007) A bacterial effector acts as a plant transcription factor and induces a cell size regulator. Science 318:648-651

Kempster V, Davies K, Scott E (2001) Chemical and biological induction of resistance to the clover cyst nematode *Heterodera trifolii*. in white clover *Trifolium repens*. Nematology 3:35-43

Kendall S, Hollomon DW, Ishii H, Heaney SP (1994) Characterisation of benzimidazole-resistant strains of *Rhynchosporium secalis*. Pesticide Science 40:175-181

Khan F (2015) Molecular markers: an excellent tool for genetic analysis. Journal of Molecular Biomarkers & Diagnosis 2015

Khoury CK, Achicanoy HA, Bjorkman AD, Navarro-Racines C, Guarino L, Flores-Palacios X, Engels JMM, Wiersema JH, Dempewolf H, Sotelo S, Ramírez-Villegas J, Castañeda-Álvarez NP, Fowler C, Jarvis A, Rieseberg LH, Struik PC (2016) Origins of food crops connect countries worldwide. Proceedings of the Royal Society B: Biological Sciences 283

Kim KH, Kang YJ, Kim DH, Yoon MY, Moon J-K, Kim MY, Van K, Lee S-H (2011) RNA-seq analysis of a soybean Near-Isogenic Line carrying bacterial leaf pustule-resistant and susceptible alleles. DNA Research 18:483-497

Kim MY, Lee S, Van K, Kim T-H, Jeong S-C, Choi I-Y, Kim D-S, Lee Y-S, Park D, Ma J, Kim W-Y, Kim B-C, Park S, Lee K-A, Kim DH, Kim KH, Shin JH, Jang YE, Kim KD, Liu WX, Chaisan T, Kang YJ, Lee Y-H, Kim K-H, Moon J-K, Schmutz J, Jackson SA, Bhak J, Lee S-H (2010) Whole-genome sequencing and intensive analysis of the undomesticated soybean (*Glycine soja* Sieb. and Zucc.) genome. Proceedings of the National Academy of Sciences 107:22032-22037

Kirsten S, Navarro-Quezada A, Penselin D, Wenzel C, Matern A, Leitner A, Baum T, Seiffert U, Knogge W (2012) Necrosis-inducing proteins of *Rhynchosporium commune*, effectors in quantitative disease resistance. Molecular Plant-Microbe Interactions 25:1314-1325

Kleemann J, Rincon-Rivera LJ, Takahara H, Neumann U, van Themaat EVL, van der Does HC, Hacquard S, Stüber K, Will I, Schmalenbach W, Schmelzer E, O'Connell RJ (2012) Sequential eelivery of host-induced virulence effectors by appressoria and intracellular hyphae of the phytopathogen *Colletotrichum higginsianum*. PLoS Pathog 8:e1002643

Knight J (2003) Crop improvement: A dying breed. Nature 421:568-570

Koch A, Kumar N, Weber L, Keller H, Imani J, Kogel KH (2013) Host-induced gene silencing of cytochrome P450 lanosterol C14alpha-demethylase-encoding genes confers strong resistance to Fusarium species. Proc Natl Acad Sci U S A 110:19324-19329

Koeck M, Hardham AR, Dodds PN (2011) The role of effectors of biotrophic and hemibiotrophic fungi in infection. Cellular microbiology 13:1849-1857

Kohorn BD, Kohorn SL (2012) The cell wall-associated kinases, WAKs, as pectin receptors. Frontiers in plant science 3:88

Kombrink A (2012) Heterologous production of fungal effectors in *Pichia pastoris*. Methods Mol Biol 835:209-217

Korte A, Farlow A (2013) The advantages and limitations of trait analysis with GWAS: a review. Plant Methods 9:29-29

Krattinger SG, Sucher J, Selter LL, Chauhan H, Zhou B, Tang M, Upadhyaya NM, Mieulet D, Guiderdoni E, Weidenbach D (2015) The wheat durable, multipathogen resistance gene *Lr34* confers partial blast resistance in rice. Plant biotechnology journal

Kuczyńska A, Surma M, Adamski T, Mikołajczak K, Krystkowiak K, Ogrodowicz P (2013) Effects of the semi-dwarfing *sdw1/denso* gene in barley. Journal of Applied Genetics 54:381-390

Kulkarni RD, Kelkar HS, Dean RA (2003) An eight-cysteine-containing CFEM domain unique to a group of fungal membrane proteins. Trends in biochemical sciences 28:118-121

Kumar V, Singh A, Mithra SVA, Krishnamurthy SL, Parida SK, Jain S, Tiwari KK, Kumar P, Rao AR, Sharma SK, Khurana JP, Singh NK, Mohapatra T (2015) Genome-wide association mapping of salinity tolerance in rice (*Oryza sativa*). DNA Research

Langlois-Meurinne M, Gachon CMM, Saindrenan P (2005) Pathogen-responsive expression of glycosyltransferase genes *UGT73B3* and *UGT73B5* is necessary for resistance to *Pseudomonas syringae pv tomato* in Arabidopsis. Plant Physiology 139:1890-1901

Lara-Ortíz T, Riveros-Rosas H, Aguirre J (2003) Reactive oxygen species generated by microbial NADPH oxidase NoxA regulate sexual development in *Aspergillus nidulans*. Molecular microbiology 50:1241-1255

Lee HK, Tewari JP, Turkington TK (2001) Symptomless infection of barley seed by *Rhynchosporium secalis*. Canadian Journal of Plant Pathology 23:315-317

Lee W-S, Hammond-Kosack KE, Kanyuka K (2012) Barley Stripe Mosaic Virus-mediated tools for investigating gene function in cereal plants and their pathogens: Virus-Induced Gene Silencing, Host-Mediated Gene Silencing, and Virus-Mediated Overexpression of heterologous protein. Plant Physiology 160:582-590

Lehnackers H, Knogge W (1990) Cytological studies on the infection of barley cultivars with known resistance genotypes by *Rhynchosporium secalis*. Canadian Journal of Botany 68:1953-1961

Li H, Zhou SY, Zhao WS, Su SC, Peng YL (2009) A novel wall-associated receptor-like protein kinase gene, *OsWAK1*, plays important roles in rice blast disease resistance. Plant Mol Biol 69

Li H, Chen G, Yan W (2015) Molecular characterization of barley 3H semi-dwarf genes. PLoS ONE 10:e0120558

Li L, Steffens JC (2002) Overexpression of polyphenol oxidase in transgenic tomato plants results in enhanced bacterial disease resistance. Planta 215:239-247

Ligterink W, Kroj T, zur Nieden U, Hirt H, Scheel D (1997) Receptor-mediated activation of a MAP kinase in pathogen defense of plants. Science 276:2054-2057

Lin W-Y, Lee W-C (2012) Improving power of Genome-Wide Association Studies with weighted false discovery rate control and prioritized subset analysis. PLOS ONE 7:e33716

Linsell KJ, Keiper FJ, Forgan A, Oldach KH (2011) New insights into the infection process of *Rhynchosporium secalis* in barley using GFP. Fungal Genetics and Biology 48:124-131

Liu D, Shi L, Han C, Yu J, Li D, Zhang Y (2012) Validation of reference genes for gene expression studies in virus-infected *Nicotiana benthamiana* using quantitative real-time PCR. PLoS One 7

Liu H-H, Tian X, Li Y-J, Wu C-A, Zheng C-C (2008) Microarray-based analysis of stress-regulated microRNAs in *Arabidopsis thaliana*. Rna 14:836-843

Liu T, Song T, Zhang X, Yuan H, Su L, Li W, Xu J, Liu S, Chen L, Chen T (2014) Unconventionally secreted effectors of two filamentous pathogens target plant salicylate biosynthesis. Nature communications 5

Liu Z, Ellwood SR, Oliver RP, Friesen TL (2011) *Pyrenophora teres*: profile of an increasingly damaging barley pathogen. Molecular Plant Pathology 12:1-19

Loake G, Grant M (2007) Salicylic acid in plant defence--the players and protagonists. Curr Opin Plant Biol 10:466-472

Looseley ME, Newton AC, Atkins SD, Fitt BDL, Fraaije BA, Thomas WTB, Keith R, Macaulay M, Lynott J, Harrap D (2012) Genetic basis of control of *Rhynchosporium secalis* infection and symptom expression in barley. Euphytica 184:47-56

Looseley ME, Keith R, Guy D, Barral-Baron G, Thirugnanasambandam A, Harrap D, Werner P, Newton AC (2015) Genetic mapping of resistance to *Rhynchosporium commune* and characterisation of early infection in a winter barley mapping population. Euphytica 203:337-347

Lu S (2012) Use of the yeast two-hybrid system to identify targets of fungal effectors. Methods Mol Biol 835:165-189

Lv D-K, Bai X, Li Y, Ding X-D, Ge Y, Cai H, Ji W, Wu N, Zhu Y-M (2010) Profiling of cold-stress-responsive miRNAs in rice by microarrays. Gene 459:39-47

Maeda H, Dudareva N (2012) The shikimate pathway and aromatic amino acid biosynthesis in plants. Annual review of plant biology 63:73-105

Malaker PK, Barma NCD, Tiwari TP, Collis WJ, Duveiller E, Singh PK, Joshi AK, Singh RP, Braun HJ, Peterson GL, Pedley KF, Farman ML, Valent B (2016) First report of wheat blast caused by *Magnaporthe oryzae* pathotype *triticum* in Bangladesh. Plant Disease 100:2330-2330

Malosetti M, van Eeuwijk FA, Boer MP, Casas AM, Elía M, Moralejo M, Bhat PR, Ramsay L, Molina-Cano J-L (2011) Gene and QTL detection in a three-way barley cross under selection by a mixed model with kinship information using SNPs. Theoretical and Applied Genetics 122:1605-1616

Manning VA, Chu AL, Scofield SR, Ciuffetti LM (2010) Intracellular expression of a host-selective toxin, *ToxA*, in diverse plants phenocopies silencing of a ToxA-interacting protein, ToxABP1. New Phytol 187:1034-1047

Marois E, Van den Ackerveken G, Bonas U (2002) The xanthomonas type III effector protein AvrBs3 modulates plant gene expression and induces cell hypertrophy in the susceptible host. Molecular plant-microbe interactions : MPMI 15:637-646

Martinez-Medina A, Flors V, Heil M, Mauch-Mani B, Pieterse CMJ, Pozo MJ, Ton J, van Dam NM, Conrath U (2016) Recognizing plant defense priming. Trends in plant science 21:818-822

Marzin S, Hanemann A, Sharma S, Hensel G, Kumlehn J, Schweizer G, Röder MS (2016) Are PECTIN ESTERASE INHIBITOR Genes Involved in Mediating Resistance to *Rhynchosporium commune* in Barley? PLoS ONE 11:e0150485

Massman J, Cooper B, Horsley R, Neate S, Dill-Macky R, Chao S, Dong Y, Schwarz P, Muehlbauer GJ, Smith KP (2011) Genome-wide association mapping of Fusarium head blight resistance in contemporary barley breeding germplasm. Molecular Breeding 27:439-454

Matsumura H, Reich S, Ito A, Saitoh H, Kamoun S, Winter P, Kahl G, Reuter M, Krüger DH, Terauchi R (2003) Gene expression analysis of plant host–pathogen interactions by SuperSAGE. Proceedings of the National Academy of Sciences 100:15718-15723

Matzeit V, Schaefer S, Kammann M, Schalk HJ, Schell J, Gronenborn B (1991) Wheat dwarf virus vectors replicate and express foreign genes in cells of monocotyledonous plants. The Plant Cell 3:247-258

Mayer K, Waugh R, Brown J, Schulman A, Langridge P, Platzer M, Fincher G, Muehlbauer G, Sato K, Close T, Wise R, Stein N (2012) A physical, genetic and functional sequence assembly of the barley genome. Nature 491:711-716

Mayer K, Rogers J, Dolezel J, Pozniak C, Eversole K, Feuillet C, Gill B, Friebe B, Lukaszewski A, Sourdille P, Endo T, Dolezel J, Kubalakova M, Cihalikova J, Dubska Z, Vrana J, Sperkova R,

Simkova H, Roger (2014) A chromosome-based draft sequence of the hexaploid bread wheat (*Triticum aestivum*) genome. Science 345

McCallum CM, Comai L, Greene EA, Henikoff S (2000) Targeting induced locallesions in genomes (TILLING) for plant functional genomics. Plant Physiology 123:439-442

McDonald B, Zhan J, Burdon J (1999) Genetic structure of *Rhynchosporium secalis* in Australia. Phytopathology 89:639-645

McDowell JM, Dangl JL (2000) Signal transduction in the plant immune response. Trends in biochemical sciences 25:79-82

McGrann GRD, Steed A, Burt C, Nicholson P, Brown JKM (2015) Differential effects of lesion mimic mutants in barley on disease development by facultative pathogens. Journal of Experimental Botany 66:3417-3428

Medzhitov R, Janeway CA (1997) Innate immunity: the virtues of a nonclonal system of recognition. Cell 91:295-298

Meindl T, Boller T, Felix G (2000) The bacterial elicitor flagellin activates its receptor in tomato cells according to the address–message concept. The Plant Cell 12:1783-1794

Melnyk CW, Meyerowitz EM (2015) Plant grafting. Current Biology 25:R183-R188

Memelink J, Verpoorte R, Kijne JW (2001) ORCAnization of jasmonate-responsive gene expression in alkaloid metabolism. Trends in plant science 6:212-219

Meng X, Zhang S (2013) MAPK cascades in plant disease resistance signaling. Annual Review of Phytopathology 51:245-266

Mengiste T (2012) Plant immunity to necrotrophs. Annual review of phytopathology 50:267-294

Merz PR, Moser T, Höll J, Kortekamp A, Buchholz G, Zyprian E, Bogs J (2015) The transcription factor *VvWRKY33* is involved in the regulation of grapevine (*Vitis vinifera*) defense against the oomycete pathogen *Plasmopara viticola*. Physiologia plantarum 153:365-380

Miah G, Rafii MY, Ismail MR, Puteh AB, Rahim HA, Islam KN, Latif MA (2013) A review of microsatellite markers and their applications in rice breeding programs to improve blast disease resistance. International Journal of Molecular Sciences 14:22499-22528

Milne I, Shaw P, Stephen G, Bayer M, Cardle L, Thomas WT, Flavell AJ, Marshall D (2010) Flapjack--graphical genotype visualization. Bioinformatics (Oxford, England) 26:3133-3134

Minoia S, Petrozza A, D'Onofrio O, Piron F, Mosca G, Sozio G, Cellini F, Bendahmane A, Carriero F (2010) A new mutant genetic resource for tomato crop improvement by TILLING technology. BMC research notes 3:1

Miya A, Albert P, Shinya T, Desaki Y, Ichimura K, Shirasu K (2007) CERK1, a LysM receptor kinase, is essential for chitin elicitor signaling in Arabidopsis. Proc Natl Acad Sci U S A 104

Morel JB, Dangl JL (1997) The hypersensitive response and the induction of cell death in plants. Cell death and differentiation 4:671-683

Morris ER, Walker JC (2003) Receptor-like protein kinases: the keys to response. Current opinion in plant biology 6:339-342

Morton RL, Schroeder HE, Bateman KS, Chrispeels MJ, Armstrong E, Higgins TJ (2000) Bean *α-amylase inhibitor 1* in transgenic peas (*Pisum sativum*) provides complete protection from pea weevil (*Bruchus pisorum*) under field conditions. Proceedings of the National Academy of Sciences 97:3820-3825

Mueller AN, Ziemann S, Treitschke S, Aßmann D, Doehlemann G (2013) Compatibility in the *Ustilago maydis*–maize interaction requires inhibition of host cysteine proteases by the fungal effector Pit2. PLoS Pathog 9:e1003177

Muñoz-Amatriaín M, Moscou MJ, Bhat PR, Svensson JT, Bartoš J, Suchánková P, Šimková H, Endo TR, Fenton RD, Lonardi S (2011) An improved consensus linkage map of barley based on flow-sorted chromosomes and single nucleotide polymorphism markers. The Plant Genome 4:238-249

Nakazawa M, Ichikawa T, Ishikawa A, Kobayashi H, Tsuhara Y, Kawashima M, Suzuki K, Muto S, Matsui M (2003) Activation tagging, a novel tool to dissect the functions of a gene family. The Plant Journal 34:741-750

Narusaka Y, Narusaka M, Seki M, Umezawa T, Ishida J, Nakajima M, Enju A, Shinozaki K (2004) Crosstalk in the responses to abiotic and biotic stresses in Arabidopsis: Analysis of gene expression in *cytochrome P450* gene superfamily by cDNA microarray. Plant Molecular Biology 55:327-342

Newton A (1989) Somatic recombination in *Rhynchosporium secalis*. Plant pathology 38:71-74

Newton A, Searle J, Guy D, Hackett C, Cooke D (2001a) Variability in pathotype, aggressiveness, RAPD profile, and rDNA ITS1 sequences of UK isolates of *Rhynchosporium secalis*. Zeitschrift fur Pflanzenkrankheiten und Pflanzenschutz 108:446-458

Newton AC, Searle J, Guy DC, Hackett CA, Cooke DEL (2001b) Variability in pathotype, aggressiveness, RAPD profile, and rDNA ITS1 sequences of UK isolates of *Rhynchosporium secalis*. Zeitschrift fur Pflanzenkrankheiten und Pflanzenschutz-Journal of Plant Diseases and Protection 108:446-458

Newton AC, Flavell AJ, George TS, Leat P, Mullholland B, Ramsay L, Revoredo-Giha C, Russell J, Steffenson BJ, Swanston JS, Thomas WTB, Waugh R, White PJ, Bingham IJ (2011) Crops that feed the world 4. Barley: a resilient crop? Strengths and weaknesses in the context of food security. Food Security 3:141-178

Nicaise V, Roux M, Zipfel C (2009) Recent Advances in PAMP-Triggered Immunity against Bacteria: Pattern Recognition Receptors Watch over and Raise the Alarm. Plant Physiology 150:1638-1647

NiÑO-Liu DO, Ronald PC, Bogdanove AJ (2006) *Xanthomonas oryzae* pathovars: model pathogens of a model crop. Molecular Plant Pathology 7:303-324

Ninomiya Y, Suzuki K, Ishii C, Inoue H (2004) Highly efficient gene replacements in Neurospora strains deficient for nonhomologous end-joining. Proceedings of the National Academy of Sciences of the United States of America 101:12248-12253

Nováková M, Šašek V, Dobrev PI, Valentová O, Burketová L (2014) Plant hormones in defense response of *Brassica napus* to *Sclerotinia sclerotiorum* – Reassessing the role of salicylic acid in the interaction with a necrotroph. Plant Physiology and Biochemistry 80:308-317

Nowara D, Gay A, Lacomme C, Shaw J, Ridout C, Douchkov D, Hensel G, Kumlehn J, Schweizer P (2010) HIGS: host-induced gene silencing in the obligate biotrophic fungal pathogen *Blumeria graminis*. The Plant Cell 22:3130-3141

Oerke E-C, Dehne H-W (2004) Safeguarding production—losses in major crops and the role of crop protection. Crop protection 23:275-285

Oldenburg KR, Vo KT, Michaelis S, Paddon C (1997) Recombination-mediated PCR-directed plasmid construction in vivo in yeast. Nucleic Acids Res 25:451-452

Oliver RP, Ipcho SV (2004) Arabidopsis pathology breathes new life into the necrotrophs-vs.-biotrophs classification of fungal pathogens. Mol Plant Pathol 5:347-352

Otim-Nape GW, Thresh JM (1998) The current pandemic of cassava mosaic virus disease in Uganda. In: Jones DG (ed) The Epidemiology of Plant Diseases. Springer Netherlands, Dordrecht, pp 423-443

Oudemans C (1897) Observations mycologiques. K Akad Wetensch Amsterdam

Verslag Wis en Natuurk Afd 6:86-92

Ow DW, Jacobs JD, Howell SH (1987) Functional regions of the cauliflower mosaic virus 35S RNA promoter determined by use of the firefly luciferase gene as a reporter of promoter activity. Proc Natl Acad Sci U S A 84:4870-4874

Ozoe S (1956) Studies on the Rhynchosporium scald of barley and its control. Bulletin of the Shimane Prefecture Agricultural Institute 1:1-122

Panchy N, Lehti-Shiu M, Shiu S-H (2016) Evolution of Gene Duplication in Plants. Plant Physiology 171:2294-2316

Panstruga R (2004) A golden shot: how ballistic single cell transformation boosts the molecular analysis of cereal–mildew interactions. Molecular Plant Pathology 5:141-148

Paré PW, Farag MA, Krishnamachari V, Zhang H, Ryu C-M, Kloepper JW (2005) Elicitors and priming agents initiate plant defense responses. Photosynthesis Research 85:149-159

Park AR, Cho SK, Yun UJ, Jin MY, Lee SH, Sachetto-Martins G, Park OK (2001) Interaction of the Arabidopsis receptor protein kinase *Wak1* with a glycine-rich protein, AtGRP-3. The Journal of biological chemistry 276:26688-26693

Park C-J, Caddell D, Ronald P (2012) Protein phosphorylation in plant immunity: insights into the regulation of pattern recognition receptor-mediated signaling. Frontiers in Plant Science 3

Patil V, Bjørnstad Å, Mackey J (2003) Molecular mapping of a new gene Rrs4CI 11549 for resistance to barley scald (*Rhynchosporium secalis*). Molecular Breeding 12:169-183

Pelgrom AJE, Van den Ackerveken G (2016) Microbial Pathogen Effectors in Plant Disease. eLS. John Wiley & Sons, Ltd

Pennell RI, Lamb C (1997) Programmed Cell Death in Plants. The Plant Cell 9:1157-1168

Penselin D, Munsterkotter M, Kirsten S, Felder M, Taudien S, Platzer M, Ashelford K, Paskiewicz KH, Harrison RJ, Hughes DJ, Wolf T, Shelest E, Graap J, Hoffmann J, Wenzel C, Woltje N, King KM, Fitt BD, Guldener U, Avrova A, Knogge W (2016) Comparative genomics to explore phylogenetic relationship, cryptic sexual potential and host specificity of Rhynchosporium species on grasses. BMC Genomics 17:953

Peraldi A, Beccari G, Steed A, Nicholson P (2011) *Brachypodium distachyon*: a new pathosystem to study Fusarium head blight and other Fusarium diseases of wheat. BMC Plant Biology 11:1

Peraldi A, Griffe L, Burt C, McGrann G, Nicholson P (2014) *Brachypodium distachyon* exhibits compatible interactions with *Oculimacula spp*. and *Ramularia collo-cygni*, providing the first pathosystem model to study eyespot and ramularia leaf spot diseases. Plant pathology 63:554-562

Perfect SE, Green JR (2001) Infection structures of biotrophic and hemibiotrophic fungal plant pathogens. Mol Plant Pathol 2:101-108

Perry JA, Wang TL, Welham TJ, Gardner S, Pike JM, Yoshida S, Parniske M (2003) A TILLING reverse genetics tool and a web-accessible collection of mutants of the legume *Lotus japonicus*. Plant Physiology 131:866-871

Pickering R, Johnston P (2005) Recent progress in barley improvement using wild species of Hordeum. Cytogenetic and genome research 109:344-349

Pickering R, Ruge-Wehling B, Johnston PA, Schweizer G, Ackermann P, Wehling P (2006) The transfer of a gene conferring resistance to scald (*Rhynchosporium secalis*) from *Hordeum bulbosum* into *H. vulgare* chromosome 4HS. Plant Breeding 125:576-579

Piron F, Nicolaï M, Minoïa S, Piednoir E, Moretti A, Salgues A, Zamir D, Caranta C, Bendahmane A (2010) An induced mutation in tomato eIF4E leads to immunity to two potyviruses. PLoS ONE 5:e11313

Pirona R, Eduardo I, Pacheco I, Da Silva Linge C, Miculan M, Verde I, Tartarini S, Dondini L, Pea G, Bassi D, Rossini L (2013) Fine mapping and identification of a candidate gene for a major locus controlling maturity date in peach. BMC Plant Biology 13:166

Poland JA, Balint-Kurti PJ, Wisser RJ, Pratt RC, Nelson RJ (2009) Shades of gray: the world of quantitative disease resistance. Trends in plant science 14:21-29

Polley R (1971) Barley leaf blotch epidemics in relation to weather conditions with observations on the overwintering of the disease on barley debris. Plant Pathology 20:184-190

Qi X, Niks RE, Stam P, Lindhout P (1998) Identification of QTLs for partial resistance to leaf rust (*Puccinia hordei*) in barley. Theoretical and Applied Genetics 96:1205-1215

Rafalski JA (2010) Association genetics in crop improvement. Current Opinion in Plant Biology 13:174-180

Rea PA (2007) Plant ATP-binding cassette transporters. Annu Rev Plant Biol 58:347-375

Rinaldo A, Gilbert B, Boni R, Krattinger SG, Singh D, Park RF, Lagudah E, Ayliffe M (2016) The *Lr34* adult plant rust resistance gene provides seedling resistance in durum wheat without senescence. Plant Biotechnology Journal

Ripke S, O'Dushlaine C, Chambert K, Moran JL, Kahler AK, Akterin S, Bergen SE, Collins AL, Crowley JJ, Fromer M, Kim Y, Lee SH, Magnusson PKE, Sanchez N, Stahl EA, Williams S, Wray NR, Xia K, Bettella F, Borglum AD, Bulik-Sullivan BK, Cormican P, Craddock N, de Leeuw C, Durmishi N, Gill M, Golimbet V, Hamshere ML, Holmans P, Hougaard DM, Kendler KS, Lin K, Morris DW, Mors O, Mortensen PB, Neale BM, O'Neill FA, Owen MJ, Milovancevic MP, Posthuma D, Powell J, Richards AL, Riley BP, Ruderfer D, Rujescu D, Sigurdsson E, Silagadze T, Smit AB, Stefansson H, Steinberg S, Suvisaari J, Tosato S, Verhage M, Walters JT, Multicenter Genetic Studies of Schizophrenia C, Psychosis Endophenotypes International C, Wellcome Trust Case Control C, Bramon E, Corvin AP, O'Donovan MC, Stefansson K, Scolnick E, Purcell S, McCarroll SA, Sklar P, Hultman CM, Sullivan PF (2013) Genome-wide association analysis identifies 13 new risk loci for schizophrenia. Nat Genet 45:1150-1159

Risk JM, Selter LL, Chauhan H, Krattinger SG, Kumlehn J, Hensel G, Viccars LA, Richardson TM, Buesing G, Troller A, Lagudah ES, Keller B (2013) The wheat *Lr34* gene provides resistance against multiple fungal pathogens in barley. Plant Biotechnology Journal 11:847-854

Robinson RA (1987) Host management in crop pathosystems. Macmillan Publishing Company

Rohe M, Gierlich A, Hermann H, Hahn M, Schmidt B, Rosahl S, Knogge W (1995) The race-specific elicitor, NIP1, from the barley pathogen, *Rhynchosporium secalis*, determines avirulence on host plants of the *Rrs1* resistance genotype. The EMBO Journal 14:4168-4177

Romer P, Hahn S, Jordan T, Strauss T, Bonas U, Lahaye T (2007) Plant pathogen recognition mediated by promoter activation of the pepper *Bs3* resistance gene. Science 318:645-648

Rosli HG, Zheng Y, Pombo MA, Zhong S, Bombarely A, Fei Z, Collmer A, Martin GB (2013) Transcriptomics-based screen for genes induced by flagellin and repressed by pathogen effectors identifies a cell wall-associated kinase involved in plant immunity. Genome Biology 14:1-15

Russell J, Mascher M, Dawson IK, Kyriakidis S, Calixto C, Freund F, Bayer M, Milne I, Marshall-Griffiths T, Heinen S, Hofstad A, Sharma R, Himmelbach A, Knauft M, van Zonneveld M, Brown JWS, Schmid K, Kilian B, Muehlbauer GJ, Stein N, Waugh R (2016) Exome sequencing of geographically diverse barley landraces and wild relatives gives insights into environmental adaptation. Nat Genet advance online publication

Sainsbury F, Thuenemann EC, Lomonossoff GP (2009) pEAQ: versatile expression vectors for easy and quick transient expression of heterologous proteins in plants. Plant Biotechnology Journal 7:682-693

Saitoh H, Fujisawa S, Mitsuoka C, Ito A, Hirabuchi A, Ikeda K, Irieda H, Yoshino K, Yoshida K, Matsumura H, Tosa Y, Win J, Kamoun S, Takano Y, Terauchi R (2012) Large-scale gene disruption in *Magnaporthe oryzae*identifies MC69, a secreted protein required for infection by monocot and dicot fungal pathogens. PLoS Pathog 8:e1002711

Sanabria NM, Huang JC, Dubery IA (2010) Self/nonself perception in plants in innate immunity and defense. Self/nonself 1:40-54

Sánchez-Vallet A, McDonald MC, Solomon PS, McDonald BA (2015) Is *Zymoseptoria tritici* a hemibiotroph? Fungal Genetics and Biology 79:29-32

Saunders DGO, Win J, Cano LM, Szabo LJ, Kamoun S, Raffaele S (2012) Using hierarchical clustering of secreted protein families to classify and rank candidate effectors of rust fungi. PLoS ONE 7:e29847

Savelkoul PHM, Aarts HJM, de Haas J, Dijkshoorn L, Duim B, Otsen M, Rademaker JLW, Schouls L, Lenstra JA (1999) Amplified-Fragment Length Polymorphism analysis: the state of an art. Journal of Clinical Microbiology 37:3083-3091

Scholthof HB, Scholthof KBG, Jackson AO (1996) Plant virus gene vectors for transient expression of foreign proteins in plants. Annual Review of Phytopathology 34:299-323

Schurch S, Linde CC, Knogge W, Jackson LF, McDonald BA (2004) Molecular population genetic analysis differentiates two virulence mechanisms of the fungal avirulence gene NIP1. Molecular plant-microbe interactions : MPMI 17:1114-1125

Schweizer G, Herz M, Mikolajewski S, Brenner M, Hartl L, Baumer M (2004) Genetic mapping of a novel scald resistance gene *Rrs15CI8288* in barley. Proceedings of the 9th international barley genetics symposium, Brno, Czech Republic, pp 258-265

Schweizer GF, Baumer M, Daniel G, Rugel H, Roder MS (1995) RFLP markers linked to scald (*Rhynchosporium secalis*) resistance gene *Rh2* in barley. Theor Appl Genet 90:920-924

Scofield SR, Huang L, Brandt AS, Gill BS (2005) Development of a virus-induced gene-silencing system for hexaploid wheat and its use in functional analysis of the *Lr21*-mediated leaf rust resistance pathway. Plant Physiology 138:2165-2173

Selin C, de Kievit TR, Belmonte MF, Fernando WGD (2016) Elucidating the role of effectors in plant-fungal interactions: progress and challenges. Frontiers in Microbiology 7:600

Seren Ü, Vilhjálmsson BJ, Horton MW, Meng D, Forai P, Huang YS, Long Q, Segura V, Nordborg M (2012) GWAPP: a web application for Genome-Wide Association mapping in Arabidopsis. The Plant Cell 24:4793-4805

Sevilla F, Camejo D, Ortiz-Espín A, Calderón A, Lázaro J, Jiménez A (2015) The thioredoxin/peroxiredoxin/sulfiredoxin system: current overview on its redox function in plants and regulation by reactive oxygen and nitrogen species. Journal of experimental botany:erv146

Shabab M, Shindo T, Gu C, Kaschani F, Pansuriya T, Chintha R, Harzen A, Colby T, Kamoun S, van der Hoorn RAL (2008) Fungal effector protein AVR2 targets diversifying defense-related cys proteases of tomato. The Plant Cell 20:1169-1183

Sheludko Y, Sindarovska Y, Gerasymenko I, Bannikova M, Kuchuk N (2007) Comparison of several Nicotiana species as hosts for high-scale Agrobacterium-mediated transient expression. Biotechnology and bioengineering 96:608-614

Shimizu T, Nakano T, Takamizawa D, Desaki Y, Ishii-Minami N, Nishizawa Y (2010) Two LysM receptor molecules, *CEBiP* and *OsCERK1*, cooperatively regulate chitin elicitor signaling in rice. Plant J 64

Shimono M, Sugano S, Nakayama A, Jiang C-J, Ono K, Toki S, Takatsuji H (2007) Rice *WRKY45* plays a crucial role in benzothiadiazole-inducible blast resistance. The Plant Cell 19:2064-2076

Shindo T, Kaschani F, Yang F, Kovács J, Tian F, Kourelis J, Hong TN, Colby T, Shabab M, Chawla R, Kumari S, Ilyas M, Hörger AC, Alfano JR, van der Hoorn RAL (2016) Screen of non-annotated small secreted proteins of *Pseudomonas syringae* reveals a virulence factor that inhibits tomato immune proteases. PLoS Pathog 12:e1005874

Shiu SH, Bleecker AB (2001) Plant receptor-like kinase gene family: diversity, function, and signaling. Science's STKE : signal transduction knowledge environment 2001:re22

Siewers V, Viaud M, Jimenez-Teja D, Collado IG, Gronover CS, Pradier JM, Tudzynski B, Tudzynski P (2005) Functional analysis of the cytochrome P450 monooxygenase gene *bcbot1* of *Botrytis cinerea* indicates that botrydial is a strain-specific virulence factor. Molecular plant-microbe interactions : MPMI 18:602-612

Simko I, Piepho HP (2012) The area under the disease progress stairs: calculation, advantage, and application. Phytopathology 102:381-389

Skoropad W (1959) Seed and seedling infection of Barley by *Rhynchosporium secalis*. Phytopathology 49:623-626.

Skoropad W (1966) Sporulating potential of *Rhynchosporium secalis* on naturally infected leaves of barley. Canadian Journal of Plant Science 46:243-247

Slade AJ, Fuerstenberg SI, Loeffler D, Steine MN, Facciotti D (2005) A reverse genetic, nontransgenic approach to wheat crop improvement by TILLING. Nature biotechnology 23:75-81

Smith JM, Salamango DJ, Leslie ME, Collins CA, Heese A (2014) Sensitivity to Flg22 is modulated by ligand-induced degradation and de *novo* synthesis of the endogenous flagellin-receptor FLAGELLIN-SENSING2. Plant Physiology 164:440-454

Solomon M, Belenghi B, Delledonne M, Menachem E, Levine A (1999) The involvement of cysteine proteases and protease inhibitor genes in the regulation of programmed cell death in plants. The Plant Cell 11:431-444

Sparkes IA, Runions J, Kearns A, Hawes C (2006) Rapid, transient expression of fluorescent fusion proteins in tobacco plants and generation of stably transformed plants. Nature protocols 1:2019-2025

Sperschneider J, Dodds PN, Gardiner DM, Manners JM, Singh KB, Taylor JM (2015) Advances and challenges in computational prediction of effectors from plant pathogenic fungi. PLoS Pathog 11:e1004806

Steiner-Lange S, Fischer A, Boettcher A, Rouhara I, Liedgens H, Schmelzer E, Knogge W (2003) Differential defense reactions in leaf tissues of barley in response to infection by *Rhynchosporium secalis* and to treatment with a fungal avirulence gene product. Molecular plant-microbe interactions : MPMI 16:893-902

Stergiopoulos I, de Wit PJ (2009) Fungal effector proteins. Annu Rev Phytopathol 47:233-263

Steuernagel B, Periyannan SK, Hernandez-Pinzon I, Witek K, Rouse MN, Yu G, Hatta A, Ayliffe M, Bariana H, Jones JDG, Lagudah ES, Wulff BBH (2016) Rapid cloning of disease-resistance genes in plants using mutagenesis and sequence capture. Nat Biotech 34:652-655

Stukkens Y, Bultreys A, Grec S, Trombik T, Vanham D, Boutry M (2005) NpPDR1, a pleiotropic drug resistance-type ATP-binding cassette transporter from *Nicotiana plumbaginifolia*, plays a major role in plant pathogen defense. Plant Physiology 139:341-352

Sucher J, Boni R, Yang P, Rogowsky P, Büchner H, Kastner C, Kumlehn J, Krattinger SG, Keller B (2016) The durable wheat disease resistance gene *Lr34* confers common rust and northern corn leaf blight resistance in maize. Plant Biotechnology Journal:n/a-n/a

Sukumaran S, Dreisigacker S, Lopes M, Chavez P, Reynolds MP (2015) Genome-wide association study for grain yield and related traits in an elite spring wheat population grown in temperate irrigated environments. Theoretical and Applied Genetics 128:353-363

Sullivan P, Arendt E, Gallagher E (2013) The increasing use of barley and barley by-products in the production of healthier baked goods. Trends in Food Science & Technology 29:124-134

Svitashev S, Young JK, Schwartz C, Gao H, Falco SC, Cigan AM (2015) Targeted mutagenesis, precise gene editing, and site-specific gene insertion in maize using *Cas9* and guide RNA. Plant physiology 169:931-945

Taggart PJ, Locke T, Phillips AN, Pask N, Hollomon DW, Kendall SJ, Cooke LR, Mercer PC (1999) Benzimidazole resistance in *Rhynchosporium secalis* and its effect on barley leaf blotch control in the UK. Crop Protection 18:239-243

Tai TH, Dahlbeck D, Clark ET, Gajiwala P, Pasion R, Whalen MC, Stall RE, Staskawicz BJ (1999) Expression of the *Bs2* pepper gene confers resistance to bacterial spot disease in tomato. Proceedings of the National Academy of Sciences 96:14153-14158

Takagi H, Tamiru M, Abe A, Yoshida K, Uemura A, Yaegashi H, Obara T, Oikawa K, Utsushi H, Kanzaki E, Mitsuoka C, Natsume S, Kosugi S, Kanzaki H, Matsumura H, Urasaki N, Kamoun S, Terauchi R (2015) MutMap accelerates breeding of a salt-tolerant rice cultivar. Nat Biotech 33:445-449

Takahashi T, Masuda T, Koyama Y (2006) Enhanced gene targeting frequency in *ku70* and *ku80* disruption mutants of *Aspergillus sojae* and *Aspergillus oryzae*. Molecular Genetics and Genomics 275:460-470

Tan KC, Phan HT, Rybak K, John E, Chooi YH, Solomon PS, Oliver RP (2015) Functional redundancy of necrotrophic effectors - consequences for exploitation for breeding. Front Plant Sci 6:501

Tanaka S, Han X, Kahmann R . 2015 . Microbial effectors target multiple steps in the salicylic acid production and signaling pathway . Frontiers in Plant Science 6 , 882

Tatum L (1971) The southern corn leaf blight epidemic. Science 171:1113-1116

Thackray D, Diggle A, Jones R (2009) BYDV PREDICTOR: a simulation model to predict aphid arrival, epidemics of Barley yellow dwarf virus and yield losses in wheat crops in a Mediterranean-type environment. Plant Pathology 58:186-202

Thaler JS, Humphrey PT, Whiteman NK (2012). Evolution of jasmonate and salicylate signal crosstalk. Trends Plant Sci. 17: 260–270

Thirugnanasambandam A, Wright KM, Atkins SD, Whisson SC, Newton AC (2011) Infection of *Rrs1* barley by an incompatible race of the fungus *Rhynchosporium secalis* expressing the green fluorescent protein. Plant Pathology 60:513-521

Thole V, Peraldi A, Worland B, Nicholson P, Doonan JH, Vain P (2012) T-DNA mutagenesis in *Brachypodium distachyon*. Journal of experimental botany 63:567-576

Thomas WTB, Powell W, Waugh R, Chalmers KJ, Barua UM, Jack P, Lea V, Forster BP, Swanston JS, Ellis RP, Hanson PR, Lance RCM (1995) Detection of quantitative trait loci for agronomic, yield, grain and disease characters in spring barley (*Hordeum vulgare L*.). Theoretical and Applied Genetics 91:1037-1047

Thompson SV, Swanson KS, Novotny JA, Baer DJ, Holscher HD (2016) Gastrointestinal Microbial Changes Following Whole Grain Barley and Oat Consumption in Healthy Men and Women. The FASEB Journal 30:406.401-406.401

Tian M, Huitema E, da Cunha L, Torto-Alalibo T, Kamoun S (2004) A Kazal-like extracellular serine protease inhibitor from *Phytophthora infestans* targets the tomato pathogenesis-related protease P69B. Journal of Biological Chemistry 279:26370-26377

Tian M, Benedetti B, Kamoun S (2005) A second kazal-like protease inhibitor from *Phytophthora infestans* inhibits and interacts with the apoplastic pathogenesis-related protease P69B of tomato. Plant Physiology 138:1785-1793

Till BJ, Reynolds SH, Weil C, Springer N, Burtner C, Young K, Bowers E, Codomo CA, Enns LC, Odden AR (2004) Discovery of induced point mutations in maize genes by TILLING. BMC plant biology 4:12

Till BJ, Cooper J, Tai TH, Colowit P, Greene EA, Henikoff S, Comai L (2007) Discovery of chemically induced mutations in rice by TILLING. BMC plant biology 7:1

Topping JF, Agyeman F, Henricot B, Lindsey K (1994) Identification of molecular markers of embryogenesis in *Arabidopsis thaliana* by promoter trapping. The Plant Journal 5:895-903

Tucker M, Moffat C, Ellwood S, Tan K-C, Jayasena K, Oliver R (2015) Development of genetic SSR markers in *Blumeria graminis f. sp. hordei* and application to isolates from Australia. Plant Pathology 64:337-343

Uauy C, Paraiso F, Colasuonno P, Tran RK, Tsai H, Berardi S, Comai L, Dubcovsky J (2009) A modified TILLING approach to detect induced mutations in tetraploid and hexaploid wheat. BMC plant Biology 9:1

Ugaki M, Ueda T, Timmermans MC, Vieira J, Elliston KO, Messing J (1991) Replication of a geminivirus derived shuttle vector in maize endosperm cells. Nucleic Acids Res 19:371-377

Ulferts S, Delventhal R, Splivallo R, Karlovsky P, Schaffrath U (2015) Abscisic acid negatively interferes with basal defence of barley against *Magnaporthe oryzae*. BMC Plant Biology 15:7

Ullstrup A (1972) The impacts of the southern corn leaf blight epidemics of 1970-1971. Annual review of phytopathology 10:37-50

van't Slot KA, Gierlich A, Knogge W (2007) A single binding site mediates resistance- and disease-associated activities of the effector protein NIP1 from the barley pathogen *Rhynchosporium secalis*. Plant Physiol 144:1654-1666

van der Biezen EA, Jones JDG (1998) The NB-ARC domain: a novel signalling motif shared by plant resistance gene products and regulators of cell death in animals. Current Biology 8:R226-R228

van Ooijen G, Mayr G, Kasiem MMA, Albrecht M, Cornelissen BJC, Takken FLW (2008) Structure–function analysis of the NB-ARC domain of plant disease resistance proteins. Journal of Experimental Botany 59:1383-1397

Varshney RK, Nayak SN, May GD, Jackson SA (2009) Next-generation sequencing technologies and their implications for crop genetics and breeding. Trends in Biotechnology 27:522-530

Verde I, Bassil N, Scalabrin S, Gilmore B, Lawley CT, Gasic K, Micheletti D, Rosyara UR, Cattonaro F, Vendramin E (2012) Development and evaluation of a 9K SNP array for peach by internationally coordinated SNP detection and validation in breeding germplasm. PLoS One 7

Vetukuri RR, Avrova AO, Grenville-briggs LJ, Van West P, Soderbon F, Savenkov EI, Whisson SC, Dixelius C (2011) Evidence for involvement of Dicer-like, Argonaute and histone deacetylase proteins in gene silencing in Phytophthora infestans. Molecular plant pathology 12:772-785

Voinnet O, Pinto YM, Baulcombe DC (1999) Suppression of gene silencing: A general strategy used by diverse DNA and RNA viruses of plants. Proceedings of the National Academy of Sciences 96:14147-14152

Wagner C, Schweizer G, Krämer M, Dehmer-Badani AG, Ordon F, Friedt W (2008) The complex quantitative barley–*Rhynchosporium secalis* interaction: newly identified QTL may represent already known resistance genes. Theoretical and Applied Genetics 118:113-122

Walters D, Paterson L, Havis N (2010) Control of foliar diseases of spring barley using resistance elicitors. The Dundee Conference Crop Protection in Northern Britain 2010, Dundee, UK, 23-24 February 2010. The Association for Crop Protection in Northern Britain, pp 91-96

Walters DR, Paterson L, Walsh DJ, Havis ND (2008) Priming for plant defense in barley provides benefits only under high disease pressure. Physiological and Molecular Plant Pathology 73:95-100

Walters DR, Paterson L, Sablou C, Walsh DJ (2011) Existing infection with *Rhynchosporium secalis* compromises the ability of barley to express induced resistance. European Journal of Plant Pathology 130:73-82

Walters DR, Avrova A, Bingham IJ, Burnett FJ, Fountaine J, Havis ND, Hoad SP, Hughes G, Looseley M, Oxley SJP, Renwick A, Topp CFE, Newton AC (2012) Control of foliar diseases in barley: towards an integrated approach. European Journal of Plant Pathology 133:33-73

Walters DR, Havis ND, Paterson L, Taylor J, Walsh DJ, Sablou C (2014) Control of foliar pathogens of spring barley using a combination of resistance elicitors. Frontiers in Plant Science 5:241

Wang R, Leng Y, Shrestha S, Zhong S (2016) Coordinated and independent functions of velvet-complex genes in fungal development and virulence of the fungal cereal pathogen *Cochliobolus sativus*. Fungal Biology 120:948-960

Wang S, Wong D, Forrest K, Allen A, Chao S, Huang BE, Maccaferri M, Salvi S, Milner SG, Cattivelli L, Mastrangelo AM, Whan A, Stephen S, Barker G, Wieseke R, Plieske J, Lillemo M, Mather D, Appels R, Dolferus R, Brown-Guedira G, Korol A, Akhunova AR, Feuillet C, Salse J, Morgante M, Pozniak C, Luo MC, Dvorak J, Morell M, Dubcovsky J, Ganal M, Tuberosa R, Lawley C, Mikoulitch I, Cavanagh C, Edwards KJ, Hayden M, Akhunov E (2014) Characterization of polyploid wheat genomic diversity using a high-density 90,000 single nucleotide polymorphism array. Plant Biotechnol J 12:787-796

Wang X, Tang C, Deng L, Cai G, Liu X, Liu B, Han Q, Buchenauer H, Wei G, Han D, Huang L, Kang Z (2010) Characterization of a pathogenesis-related thaumatin-like protein gene *TaPR5* from wheat induced by stripe rust fungus. Physiol Plant 139:27-38

Wang X, Wang H, Wang J, Sun R, Wu J, Liu S, Bai Y, Mun J-H, Bancroft I, Cheng F (2011) The genome of the mesopolyploid crop species *Brassica rapa*. Nature genetics 43:1035-1039

Wang Y-C, Klein TM, Fromm M, Cao J, Sanford JC, Wu R (1988) Transient expression of foreign genes in rice, wheat and soybean cells following particle bombardment. Plant Molecular Biology 11:433-439

Wang Y, Wu J, Kim SG, Kim ST, Kang KY (2013) A Transient Gene Expression Protocol for Subcellular Protein Localization and Protein Secretion Analyses in Rice

Waterhouse PM, Wang M-B, Lough T (2001) Gene silencing as an adaptive defence against viruses. Nature 411:834-842

Waugh R, Jannink JL, Muehlbauer GJ, Ramsay L (2009) The emergence of whole genome association scans in barley. Curr Opin Plant Biol 12

Waugh R, Flavell JA, Russell J, Thomas W, Ramsay L, Comadran J (2014a) Exploiting Barley Genetic Resources for Genome Wide Association Scans (GWAS). In: Tuberosa R, Graner A, Frison E (eds) Genomics of Plant Genetic Resources: Volume 1 Managing, sequencing and mining genetic resources. Springer Netherlands, Dordrecht, pp 237-254

Waugh R, Thomas B, Flavell A, Ramsay L, Comadran J, Russell J (2014b) Genome-Wide Association Scans (GWAS). Biotechnological Approaches to Barley Improvement. Springer, pp 345-365

Wevelsiep L, Kogel K-H, Knogge W (1991) Purification and characterization of peptides from *Rhynchosporium secalis* inducing necrosis in barley. Physiological and Molecular Plant Pathology 39:471-482

Wevelsiep L, Rupping E, Knogge W (1993) Stimulation of barley plasmalemma H+-ATPase by phytotoxic peptides from the fungal pathogen *Rhynchosporium secalis*. Plant Physiology 101:297-301

Williams K, Donnellan S, Smyl C, Scott L, Wallwork H (2003) Molecular variation in *Rhynchosporium secalis* isolates obtained from hotspots. Australasian Plant Pathology 32:257-262

Win J, Chaparro-Garcia A, Belhaj K, Saunders D, Yoshida K, Dong S, Schornack S, Zipfel C, Robatzek S, Hogenhout S (2012) Effector biology of plant-associated organisms: concepts and perspectives. Cold Spring Harbor symposia on quantitative biology. Cold Spring Harbor Laboratory Press, pp 235-247

Wroblewski T, Tomczak A, Michelmore R (2005) Optimization of Agrobacterium-mediated transient assays of gene expression in lettuce, tomato and Arabidopsis. Plant Biotechnology Journal 3:259-273

Wu G, Shortt BJ, Lawrence EB, Levine EB, Fitzsimmons KC, Shah DM (1995) Disease resistance conferred by expression of a gene encoding H2O2-generating glucose oxidase in transgenic potato plants. The Plant Cell 7:1357-1368

Wu L, Zhang Z, Zhang H, Wang XC, Huang R (2008) Transcriptional modulation of ethylene response factor protein JERF3 in the oxidative stress response enhances tolerance of tobacco seedlings to salt, drought, and freezing. Plant Physiol 148

Wu M, Chen A, Wang Z, Zhang J, Wang C, Li F, Wei P, Wang R, Luo Z, Wei C (2015) Plant microarray for gene expression profiling and their application. Journal of Agricultural Technology 11:93-105

Wulff B, Chakrabarti A, Jones D (2009) Recognitional specificity and evolution in the tomato-*Cladosporium fulvum* pathosystem. Molecular plant-microbe interactions 22:1191-1202

Xi K, Xue AG, Burnett PA, Helm JH, Turkington TK (2000) Quantitative resistance of barley cultivars to *Rhynchosporium secalis*. Canadian Journal of Plant Pathology-Revue Canadienne de Phytopathologie 22:217-223

Xie X, Song M-H, Jin F, Ahn S-N, Suh J-P, Hwang H-G, McCouch SR (2006) Fine mapping of a grain weight quantitative trait locus on rice chromosome 8 using near-isogenic lines derived from a cross between *Oryza sativa* and *Oryza rufipogon*. Theoretical and Applied Genetics 113:885-894

Xin Z, Wang ML, Barkley NA, Burow G, Franks C, Pederson G, Burke J (2008) Applying genotyping (TILLING) and phenotyping analyses to elucidate gene function in a chemically induced sorghum mutant population. BMC Plant Biology 8:1

Xu H-M, Kong X-D, Chen F, Huang J-X, Lou X-Y, Zhao J-Y (2015) Transcriptome analysis of *Brassica napus* pod using RNA-Seq and identification of lipid-related candidate genes. BMC Genomics 16:858

Xu J, Audenaert K, Höfte M, De Vleesschauwer D. (2013). Abscisic acid promotes susceptibility to the rice leaf blight pathogen *Xanthomonas oryzae pv. oryzae* by suppressing salicylic acid-mediated defenses. PLoS ONE 8:e67413 10.1371/journal.pone.0067413

Xu X, Pan S, Cheng S, Zhang B, Mu D, Ni P, Zhang G, Yang S, Li R, Wang J, Orjeda G, Guzman F, Torres M, Lozano R, Ponce O, Martinez D, de la Cruz G, Chakrabarti S, Patil V, Skryabin K, Kuznet (2011) Genome sequence and analysis of the tuber crop potato. Nature 475:189-195

Yaeno T, Li H, Chaparro-Garcia A, Schornack S, Koshiba S, Watanabe S, Kigawa T, Kamoun S, Shirasu K (2011) Phosphatidylinositol monophosphate-binding interface in the oomycete RXLR effector *AVR3a* is required for its stability in host cells to modulate plant immunity. Proceedings of the National Academy of Sciences 108:14682-14687

Yalpani N, Silverman P, Wilson TM, Kleier DA, Raskin I (1991) Salicylic acid is a systemic signal and an inducer of pathogenesis-related proteins in virus-infected tobacco. The Plant Cell 3:809-818

Yamaguchi Y, Pearce G, Ryan CA (2006) The cell surface leucine-rich repeat receptor for AtPep1, an endogenous peptide elicitor in Arabidopsis, is functional in transgenic tobacco cells. Proc Natl Acad Sci U S A 103:10104-10109

Yamanaka N, Morishita M, Mori T, Lemos NG, Hossain MM, Akamatsu H, et al. (2015). Multiple Rpp-gene pyramiding confers resistance to Asian soybean rust isolates that are virulent on each of the pyramided genes. Trop. Plant Pathol. 40, 283–290.

Yin C, Jurgenson JE, Hulbert SH (2011) Development of a host-induced RNAi system in the wheat stripe rust fungus Puccinia striiformis f. sp. tritici. Molecular plant-microbe interactions : MPMI 24:554-561

Yin X, Kropff MJ, Stam P (1999) The role of ecophysiological models in QTL analysis: the example of specific leaf area in barley. Heredity 82:415-421

Yoshida K, Saitoh H, Fujisawa S, Kanzaki H, Matsumura H, Yoshida K, Tosa Y, Chuma I, Takano Y, Win J (2009) Association genetics reveals three novel avirulence genes from the rice blast fungal pathogen *Magnaporthe oryzae*. The Plant Cell 21:1573-1591

Yu F, Huaxia Y, Lu W, Wu C, Cao X, Guo X (2012) GhWRKY15, a member of the WRKY transcription factor family identified from cotton (*Gossypium hirsutum L*.), is involved in disease resistance and plant development. BMC Plant Biology 12:1-18

Yun S, Gyenis L, Bossolini E, Hayes P, Matus I, Smith K, Steffenson B, Tuberosa R, Muehlbauer G (2006) Validation of quantitative trait loci for multiple disease resistance in barley using advanced backcross lines developed with a wild barley. Crop Science 46:1179-1186

Zadoks JC, Chang TT, Konzak CF (1974) A Decimal Code for the Growth Stages of Cereals. Weed Research 14:415-421

Zaffarano PL, McDonald BA, Linde CC (2011) Two new species of Rhynchosporium. Mycologia 103:195-202

Zegeye H, Rasheed A, Makdis F, Badebo A, Ogbonnaya FC (2014) Genome-Wide Association mapping for seedling and adultplant resistance to stripe Rust in synthetic hexaploid wheat. PLOS ONE 9:e105593

Zhan J, Fitt BDL, Pinnschmidt HO, Oxley SJP, Newton AC (2008) Resistance, epidemiology and sustainable management of *Rhynchosporium secalis* populations on barley. Plant Pathology 57:1-14

Zhang H-X, Blumwald E (2001) Transgenic salt-tolerant tomato plants accumulate salt in foliage but not in fruit. Nature biotechnology 19:765-768

Zhang H-X, Hodson JN, Williams JP, Blumwald E (2001) Engineering salt-tolerant Brassica plants: characterization of yield and seed oil quality in transgenic plants with increased vacuolar sodium accumulation. Proceedings of the National Academy of Sciences 98:12832-12836

Zhang S, Klessig DF (2001) MAPK cascades in plant defense signaling. Trends in plant science 6:520-527

Zhang S, Chen C, Li L, Meng L, Singh J, Jiang N, Deng X-W, He Z-H, Lemaux PG (2005) Evolutionary expansion, gene structure, and expression of the rice Wall-Associated Kinase gene family. Plant Physiology 139:1107-1124

Zhang Y, Dorey S, Swiderski M, Jones JDG (2004) Expression of *RPS4* in tobacco induces an AvrRps4-independent HR that requires EDS1, SGT1 and HSP90. The Plant Journal 40:213-224

Zhang Z, Ersoz E, Lai C-Q, Todhunter RJ, Tiwari HK, Gore MA, Bradbury PJ, Yu J, Arnett DK, Ordovas JM (2010) Mixed linear model approach adapted for genome-wide association studies. Nature genetics 42:355-360

Zhang Z, Wu Y, Gao M, Zhang J, Kong Q, Liu Y, Ba H, Zhou J, Zhang Y (2012) Disruption of PAMP-induced MAP kinase cascade by a *Pseudomonas syringae* effector activates plant immunity mediated by the NB-LRR protein SUMM2. Cell host & microbe 11:253-263

Zhu-Salzman K, Zeng R (2015) Insect response to plant defensive protease inhibitors. Annual review of entomology 60:233-252

Zipfel C, Felix G (2005) Plants and animals: a different taste for microbes? Curr Opin Plant Biol 8:353-360

Zipfel C (2014) Plant pattern-recognition receptors. Trends Immunol 35

IX. Supplementary DATA

Table IX-1: Table of the list of lines and them estimated means used for the GWAS. Lines in purple are lines with exome capture data.

Line name	AUDPS-2013	AUDPS-2014	AUDPS-2015	AUDPS-combined	Height-2014	Height-2015
995964	40.2		103.4	40.2		72.8
A 96-103		133.1			88.7	76.8
Aapo	52.2	137.2	101.1	52.2	78.4	68.8
Abacus	51.1	154.1	82.0	51.1	112.4	90.4
Abava	38.2	151.4	85.9	38.3	113.4	92.8
Acapella	46.0	166.5	87.8	46.1	79.2	66.9
Acclaim	36.0	162.1		36.0	95.0	
ACROBAT	44.1	174.5	103.5	44.1	78.9	71.4
Adonis	55.2	138.5	111.9	55.2	85.0	76.6
Agenda	44.1	168.0	134.6	43.9	81.2	72.6
Akcent	65.9	179.5	154.4	65.8	75.1	66.9
Akita	56.6	180.4	135.4	56.8	90.4	74.0
Akka	41.6	134.7	120.7	41.5	80.2	98.8
Alabama	45.1	174.7	107.5	45.0	81.6	59.3
Alexis	52.3	166.6	112.6	52.3	86.5	74.5
Alis	38.9	153.7	107.9	38.9	80.0	67.4
Alliot	53.3	162.0	106.0	53.3	90.5	73.9
Aluminium	51.2	154.5	95.8	51.2	89.1	70.5
ALVA	52.2	155.1	112.7	52.1	86.3	72.8
Ametyst	62.6	183.7	104.2	62.6	92.5	73.7
Amourette	52.3	130.6	110.8	52.2	78.9	61.0
ANACONDA	25.4	146.0	86.2	25.3	82.2	74.8
Anais	47.2	173.0	108.8	47.3	105.4	66.2
Anakin	51.4	119.6	100.4	51.3	86.8	65.4
Anla	38.6	160.4	87.1	38.6	98.1	86.1
Annabell	59.0	179.6	110.5	58.8	85.6	71.0
Anni	41.8	158.0	132.8	41.7	79.2	69.7
Ansis	44.2	152.4	95.1	44.3	79.4	71.0
Apex	47.3	124.4	102.1	47.3	83.1	77.9
Appaloosa	51.8	170.1	104.0	51.6	79.5	64.9
Aramir	41.9	139.1	94.9	41.8	101.9	85.2
Ardila	49.8	170.5	94.5	49.8	85.5	65.9
Armelle	29.2	100.7	45.3	29.3	111.5	95.8
Artisan		163.7			81.1	
ARVO	33.0	160.6	75.3	33.5	98.7	83.7
ASB 04-18	56.6	164.6				
Aspen	49.6	173.0	114.9	49.6	80.5	73.3
Astoria	61.1	144.0	101.7	61.0	80.0	69.7
Atem	35.6	129.8	73.3	35.7	108.8	91.7
Athena	56.1	164.9	116.2	56.2	93.2	78.5
Athos	32.7	159.5	88.3	32.8	98.9	88.9
Atlas	57.6	182.4	133.4	57.5	83.4	70.2
Atribut	51.9	165.1	132.7	51.9	89.4	71.7
Audio		174.5			79.0	67.3
Auriga	59.4	178.5	120.3	59.4	93.5	75.8
Avec	42.1	177.0	106.0	42.2	78.8	64.2
Azure	48.7	161.1	117.3	48.8	87.6	76.8
B83-12/21/5	60.7	190.0	105.6	60.7	82.1	60.2
Balalaika		132.7			81.1	62.5
Balder	33.9	113.7	81.9	33.9	108.8	83.4

Balder J	28.3	128.8	76.3	28.2	94.9	82.0
Balga	25.1	170.3	82.4	25.1	98.6	78.0
Barabas	35.4	160.5	103.0	35.3	79.6	67.2
Barke	43.1	121.8	93.1	43.2	88.4	71.0
Baronesse	40.0	135.8	97.0	39.9	107.2	82.0
Beatrix	58.3	176.7	117.5	58.3	80.6	69.0
Beka	17.0	144.9	72.3	17.0	115.2	88.2
Belgravia		131.0	88.4	36.8	92.4	77.5
Benchmark		165.7				90.0
Berac	43.6	164.0	83.8	43.6	103.5	85.0
Berenice	41.2	144.7	96.3	41.3	113.7	98.9
Berwick	47.0	162.3	95.6	46.8	107.7	74.9
Beryllium	52.6	153.7	93.6	53.1	82.4	63.7
Betzes	35.9	120.7	86.3	35.9	113.0	87.2
Binder	33.9	121.8	79.7	33.9	116.7	95.2
Binder Abed	38.5	129.3	84.3	38.5	120.5	96.9
Birgitta	33.8	135.9	88.1	33.6	105.0	95.4
BIRKA	38.0	136.0	72.0	38.0	101.5	84.4
Blenheim	59.9	159.8	121.9	60.0	92.1	80.1
Bogart	55.2	190.8	125.6	55.3	78.6	64.1
Bonus	38.4	144.9	55.4	38.3	99.8	84.8
Braemar	54.6	164.1	115.9	54.7	85.0	78.3
Brahms	48.7	165.9	108.5	48.6	89.7	72.6
Brazil	40.5	173.3	107.3	40.4	82.8	65.4
Brewster	48.8	127.3	103.6	48.8	101.1	82.2
Brise	60.7	167.7	126.4	60.7	78.6	71.5
Britta	42.3	131.4	87.1	42.3	112.0	93.2
Bulbul 89	52.3	142.4	104.8	52.3	98.2	84.1
Cabaret	44.2	132.5	56.4	44.1	81.4	59.4
Cairn	44.9	161.5		44.8	88.5	
Caja	31.2	137.0	93.5	31.2	100.5	74.2
Calgary	45.0	155.7	102.0	45.0	91.3	71.5
CALICO	42.6	171.8	105.4	42.6	83.7	64.6
Camargue	41.4	169.1	96.9	41.4	90.3	82.3
Cameo	44.0	170.9	96.9	43.9	92.8	74.4
Caminant	53.1	152.2	114.3	54.3	90.4	67.8
Camir	44.6	177.0	119.4	44.6	74.1	68.5
Campala	43.4	115.8	104.3	43.6	97.1	75.6
Canasta	63.2	174.3	107.8	63.1	76.8	68.1
Carafe	53.3		98.6	53.3	82.0	72.1
Carlsberg	31.8	113.3	69.4	31.7	95.9	89.0
Carvilla	62.9	154.1	125.7	62.9	75.1	65.5
Casino	23.9	126.8	83.9	23.9	91.7	75.3
Catalina	42.7	148.2	91.4	43.0	87.5	73.1
Cecilia	49.9	165.7	110.6	49.9	79.7	74.2
CELEBRA	40.1	177.2	96.1	40.0	98.8	72.1
Cellar	63.8	168.4	91.6	63.7	83.4	67.3
Centurion	60.7	178.0	130.5	60.8	76.6	61.9
Century	52.4	188.2	107.2	52.3	78.7	66.8
Ceylon	52.6	172.0	110.5	52.6	77.6	65.9
Chad	59.8		102.9	59.8	97.7	79.0
Chalice	51.3	174.2	119.0	51.4	79.6	68.0
Chamant	64.5	160.9	104.7	64.5	87.7	85.7
Chanell	29.9	134.3	97.6	29.9	90.0	72.8
Chariot	50.5	173.5	103.1	50.6	84.3	72.3
CHARM	53.2	150.3	89.6	53.1	88.3	69.5
Chaser	44.4	179.8	110.6	44.2	91.0	81.8
Checkmate		178.4			87.1	

Cheri	47.5	148.8	103.1	47.5	89.2	78.0
Chevalier Tystofte 1		125.3		25.7	164.0	128.6
Chieftain	42.2	201.7	84.5	42.2	82.6	70.2
Chime	49.4	159.7	98.6	49.5	79.0	74.9
Christina	58.3	175.2	112.5	58.2	81.6	64.5
Chronicle	37.7	137.0	84.3	37.7	90.6	75.3
Cicero	49.5	156.7	116.4	49.4	86.6	68.3
CILLA	41.0	182.7	103.7	41.1	110.5	85.8
Clansman	52.5	187.4	92.3	52.5	84.5	79.5
Claret	45.4	170.9	113.8	45.3	94.5	68.4
CLARITY	43.1	155.1	130.7	43.2	84.1	66.4
Class	46.0	158.3	98.5	46.1	79.8	71.1
Claude	46.2	150.9	119.0	46.3	84.8	72.4
Cocktail	37.1	166.9	96.2	37.1	80.9	66.4
Colada	76.2	169.5	127.5	76.1	77.1	64.1
Colston	34.4	110.1	91.9	34.5	87.4	80.2
CONCERTO	47.1	172.0	104.6	47.1	89.1	75.1
Conchita	39.8	165.4		39.8	84.2	
Cooper	51.1	146.3	105.8	51.2	74.7	64.0
Corgi	35.3	144.3	95.2	35.3	76.2	65.7
Cork	50.4	155.2	112.7	50.4	70.8	59.0
Corniche	51.7	160.8	98.1	51.7	93.5	76.1
Corsica	32.8	151.0	98.3	32.9	90.3	68.3
County	33.9	152.9	99.1	34.0	74.0	68.1
CPBT B67	47.1	172.3	109.6	47.0	77.5	63.2
CPBT B76	43.8	163.1	99.2	43.8	76.2	61.4
CPBT B80	48.7	179.6	105.1	48.7	72.5	56.5
Cribbage	40.5	164.0	100.2	40.3	91.2	71.0
Cristalia	41.9	183.2	101.9	42.0	80.4	73.4
Crooner		152.9	104.6	45.6	81.6	58.1
Cropton	49.9	144.7	112.6	50.2	83.9	67.6
Croydon	37.3	150.7	91.0	37.5	96.2	85.6
Crusader	41.3	142.1	120.5	41.4	101.0	66.6
Dallas	47.5	162.1	110.0	47.5	84.0	74.6
Dandy	35.4	139.0	87.3	35.4	100.3	86.7
Danuta	47.1	137.7	112.3	47.1	92.0	82.6
Deba Abed	58.8	162.9	101.8	58.8	82.9	72.6
Decanter	35.5	157.7	110.8	35.5	89.7	70.6
Delibes	43.2	162.6	110.9	43.3	88.0	64.7
DELTA	44.7	131.7	106.4	44.7	92.2	74.3
Derkado	54.9	169.0	142.7	55.2	82.3	65.6
Dew	42.9	162.3	95.5	42.9	79.2	69.8
Dialog	24.0	132.2	90.1	24.0	74.1	70.6
Diamant	57.1	179.2	115.4	57.2	81.1	76.9
Digersano	35.8	143.7	106.7	35.9	98.5	81.6
Digger	43.8	152.6	98.0	43.8	78.7	66.0
Dina	44.9	183.7	107.0	44.9	112.9	88.0
DOMEN	37.0	154.1	86.4	37.0	120.0	92.8
Doublet	60.1	168.8	128.0	60.1	75.5	74.1
Doyen	46.4	140.7	86.9	46.4	79.1	62.7
Drake	46.0	174.8	83.9	46.0	79.5	73.4
Draught	44.9	126.0	86.0	44.9	81.7	74.5
Dray	68.7	159.4	109.0	68.6	74.4	66.9
Drost	37.0	123.2	80.1	36.9	114.1	88.9
Drum	66.3	177.7	131.2	66.2	83.3	68.0
Egmont	35.3	141.2	93.1	35.3	102.6	90.6
Elantra	53.2	165.2	108.0	53.1	90.2	75.8

Elo	50.6	150.7	93.0	50.6	85.4	67.3
Emir	26.0	123.2	83.7	26.0	121.7	99.6
Esme	31.4	145.1	92.8	31.3	103.6	91.9
Eunova	47.6	137.3	103.6	47.7	98.5	81.9
Extract	48.2	157.8	97.8	48.1	90.6	74.4
Fairytale	42.7	158.1	101.5	43.5	92.4	77.2
Famin	60.5	187.0	154.9	60.6	79.3	68.1
Favorit	48.4	179.9	110.7	48.4	79.7	70.9
Felicie	42.6	157.8	98.6	42.8	89.9	78.6
Felicitas	40.0	162.6	128.9	40.0	89.3	68.6
Feltwell	62.0	154.6	108.8	62.2	75.1	62.9
Ferment	26.3	140.2	81.5	26.3	91.0	74.7
Fontana	65.2	177.5	128.5	65.1	75.3	67.9
Force	39.0	157.6	92.1	39.0		
Forensic	46.0	144.4		46.0	80.6	
FORMULA	47.8	159.3	114.8	47.7	85.3	61.4
Forum	58.6	159.6	124.1	58.6	73.8	63.5
Foxtrot	51.0	178.0	135.3	51.2	83.8	67.0
Fractal	46.9	152.3	102.8	46.8	87.7	69.8
Franklin	35.8	105.5	80.4	35.8	102.3	78.8
FREJA	37.6		94.4	37.7		85.2
Frieda	30.5	125.8	76.3	30.5	124.2	111.8
Gairdner	31.3	154.0	82.1	31.4	90.3	78.7
Galan	52.2	168.3	104.0	52.3	84.2	71.6
Gant	57.9	169.6	136.6	57.9	75.3	61.9
Garner	38.0	133.8		37.7	89.1	
Gate	57.6	135.7	109.6	57.6	91.6	77.7
Georgie	48.7	169.9	102.0	48.7	95.4	76.3
GERKRA	36.4	147.9	96.8	36.3	107.4	84.1
Gitane	41.9	150.3	76.7	42.0	100.7	78.1
Gizmo	50.1	167.8	125.1	50.0	89.5	75.7
Global	42.2	162.6	116.1	42.2	86.9	70.6
Gold	32.9	139.5	71.8	33.0	116.4	98.3
Golden Promise	44.2	166.8	92.3	44.2	82.6	69.1
Goldie	43.5	160.8	120.8	43.7	84.2	68.6
Golf	45.2	155.3	119.2	45.2	97.7	84.4
Gorm	34.3		78.2	34.3		81.9
GRANTA	49.8	176.8	119.6	49.8	75.4	60.6
Graphic	36.8	129.5	75.7	36.9	90.2	73.9
Gull	46.1	152.5	89.4	46.1	116.9	98.1
GUNDEL	41.8	179.2	126.4	41.9	90.2	74.5
GUSTAV	52.6	169.8	115.1	52.6	71.3	64.0
Hacker		142.9			88.0	
Hana	57.2	178.8	109.3	57.1	89.3	79.4
Hanka	57.4	174.7	122.9	57.4	78.9	76.3
Hanna	44.4	140.4	82.8	44.4		
Hannchen	63.0	182.9	112.9	63.1	90.3	72.6
Harriot	46.2	119.5	92.9	46.1	85.7	77.4
Harry	48.2	170.2	118.8	48.1	106.3	81.0
Hart	45.6	130.1	99.6	45.5	101.0	78.8
HASSAN	30.1	152.6	96.7	30.2	99.2	82.7
Heather	46.7		113.9	46.7		80.8
Helium	38.6	147.3	102.6	38.6	82.4	69.7
HELLAS	51.3	170.0	93.9	51.3	87.3	90.0
HELMI	40.8	130.5	102.9	40.8	112.4	90.1
HENLEY	48.2	146.2	94.6	48.2	96.0	76.0
Henni	61.5	187.5	128.2	61.4	82.2	69.0
Heris	45.5	158.7	81.0	45.5	79.5	82.5

Heron	37.6	149.7	105.0	37.6	76.8	74.1
Hopper	50.4	152.6	97.1	50.4	77.2	60.3
Horizon	64.2	172.5	108.0	64.2	80.9	69.6
HOST	53.8	142.6	91.4	53.7	87.2	60.3
Hydra	38.1	140.2	86.2	38.1	82.3	61.8
Hydrogen	39.8	126.8	88.3	39.8	86.0	68.9
Ida	42.4	191.6	90.5	42.3	97.7	75.4
Idumeja	45.9	152.9	111.3	46.0	89.0	85.1
Ilga	45.3	152.5	89.0	45.2	98.0	88.9
Imber	31.1	137.2	74.3	31.1	98.3	85.2
Imidis	55.7	160.9	113.0	55.3	74.9	67.6
Impala	39.5	153.0	79.4	39.4	111.8	87.0
Imula	32.1	160.2	126.1	31.8	102.6	87.3
INARI	50.2	180.5	109.0	50.0	85.6	73.6
Indola	51.1	160.0	104.6	51.1	81.4	74.9
Ingmar		157.1			82.6	71.3
Ingrid	39.8	127.3	76.6	39.8	103.0	76.4
Isabella	50.8	137.8	88.0	50.8	88.4	64.7
Isaria	29.2	142.5	80.2	29.2	136.7	110.0
Jacinta	54.1	162.2	114.2	54.1	79.5	60.3
Jarek	52.4	185.6	116.1	52.6	80.1	66.3
Jargon		169.3				
Jive	41.4	176.8	117.1	41.5	78.6	73.0
Jolika		157.4			92.2	70.7
Karat	56.3	180.3	116.7	56.5	86.6	68.4
KARRI	33.6	95.7	92.4	33.6	98.0	76.1
Kassima	57.7	163.9	139.3	57.8	86.4	66.4
Kenia	37.5	137.3	73.2	37.6	114.0	91.8
Keops	51.2	151.8	101.3	51.1	76.3	58.6
Kerstin		117.5			81.5	
Kinnan	27.3	157.4	113.1	27.4	84.8	80.0
Kirsty	39.0	178.6	107.0	39.0	83.7	66.4
Klaxon	38.3	166.8	90.4	38.4	99.3	83.4
Knightsbridge		148.6			83.5	69.8
Koral	48.6	172.0	135.2	48.7	90.6	74.5
Kristaps	42.2	157.4	99.6	42.3	99.0	82.2
Krona	64.9	196.7	113.2	64.8	86.0	77.1
Krystal	53.1	164.2	102.9	53.1	83.5	72.7
KWS Aurelia		182.6			72.7	
KWS Irina		164.3			76.8	
KWS Orphelia	39.8	153.3	104.1	39.7	75.0	62.7
Kym	41.6	125.2	98.5	41.6	89.5	75.3
Ladik	54.2	156.1	113.4	54.2	78.0	70.0
LAIRD	29.3	132.8	83.4	29.3	87.0	67.1
Landlord	34.0	163.5	95.1	34.0	79.5	71.8
Landora	42.4	151.4	92.2	42.5	93.3	82.9
Latvijas Vietejie	26.4	132.4	79.5	26.5	141.0	108.4
Leeni	55.5	194.7	157.6	55.6	83.7	77.8
Lenta	30.5	150.3	86.4	30.6	106.2	82.8
Lina	53.5	163.1	119.1	53.5		
Linden	43.6	151.1	74.2	43.6	118.3	72.9
Linga	33.3	151.8	94.0	33.3	87.2	78.9
Lithium	48.1	144.2	94.4	48.0	88.3	71.4
Livet	36.8	131.2	89.3	36.8	75.1	58.7
LOFA ABED	45.0	126.4	81.5	42.7	104.2	75.2
Lud	58.9	162.3	102.3	59.0	102.3	85.4
Lux	51.5	145.0	111.4	51.4	90.8	56.6
Lysiba	64.0	152.3	109.5	63.8	84.6	67.1

Lysimax	52.9	185.0	145.8	52.7	81.2	71.5
Macarena	53.2	161.0	102.6	53.2	77.2	67.5
Macaw	60.3	176.1	100.8	60.3	74.3	65.2
Madras	47.0	178.6	127.7	47.0	102.3	68.6
Magda	46.7	169.9	102.5	46.8		
Magdalena	35.0	145.1	96.0	35.1	84.7	66.7
Magellan	50.7	150.0	108.0	50.7	89.8	73.1
Magnif	34.0	148.0	80.1	34.0	108.7	83.0
Maja	42.6	132.2	86.1	42.6	103.2	85.1
Mala Abed		134.6				
Malt Jagger		131.2			76.1	
Maltby		153.3			83.0	61.6
Malva	36.0	155.4	71.6	35.9	95.3	85.6
Mandolin		173.1			73.8	57.5
Maraca		130.6			80.6	68.9
Maresi	51.5	180.2	124.6	51.6	85.1	68.7
Marionette	44.1	163.7	119.2	44.2	85.3	63.3
Maris Mink	51.3	175.5	101.1	51.3	82.5	68.8
Mars	60.4	166.5	100.3	60.4	82.4	74.5
MARTHE	52.4	188.1	108.1	52.2	81.5	64.6
Mary		193.6			83.1	
MAUD	62.6	177.3	123.4	62.5	81.7	73.4
Mauritia	43.7	166.9	85.8	43.7	79.3	67.1
Maypole	38.4	138.4	99.4	38.4	78.8	71.0
Melitta	65.1	173.4	120.6	65.2	82.1	70.6
Meltan	34.8	141.4	102.3	34.8	101.6	66.4
Mentor	47.5	161.9	145.3	47.4	81.9	70.9
Mercada	48.4	142.1	85.1	48.4	88.6	68.0
MIDAS	42.0	136.7	113.7	42.0	87.6	68.6
Mikado	54.0	175.1	114.5	54.1	77.2	68.7
Minstrel	48.2	161.5	94.3	48.3	82.7	70.1
Mirage	55.0	161.6		54.9	78.8	
Mona	46.6		97.0	46.7		74.2
Monika	43.3	151.0	88.7	43.3	86.3	65.9
Montoya	36.0	144.9	87.8	36.0	82.6	70.5
Moonshine 2RSB	49.6	126.8	125.8	49.6	83.6	61.1
Natasha	42.8	156.7	114.3	42.8	92.3	80.8
Natasia	35.1	151.9	89.1	35.1	80.4	69.5
NATHALIE	63.4	179.6	123.4	63.5	84.4	68.1
Nemex	48.5	185.2	113.0	48.4	106.7	78.0
Neruda	45.0	174.6	109.0	44.9	85.8	75.1
NFC Tipple	54.5	173.1	114.1	54.6	83.3	63.8
Nimbus	51.0	156.0	108.5	50.9	84.4	66.8
Nordal	39.9	155.7	85.2	39.9	106.5	84.9
Novello	30.1	134.0	108.9	30.1	89.9	68.6
Novum	46.3	156.2	104.4	46.3	72.3	56.8
NSL 95-1257	51.1	159.8	114.6	51.1	82.8	65.2
NSL 97-4552	52.5	173.8	130.8	52.5	91.0	71.2
NSL 97-4579	37.9	160.5	101.0	37.9	77.5	71.7
NSL 98-5065	57.5	154.2	103.9	57.5	113.9	75.5
NSL 99-5363	38.6	129.0	98.9	38.7	87.5	72.5
Nudinka	42.8	112.9	104.3	42.8	111.7	95.7
Odessa	23.1	141.4	81.4	23.3	79.4	78.1
Odin	33.9	134.1	102.4	33.8	95.6	85.3
Odyssey	39.0	135.3		38.8	86.5	
Okos	37.4	138.0	86.1	37.5	111.3	95.4
ONYX	38.8	171.9	88.3	38.9	112.4	95.7

Optic	52.7	164.1	127.7	52.6	86.5	68.6
Orbit	50.2	175.6	122.1	50.3	86.8	64.8
Orza	37.3	142.3	106.9	37.3	113.6	85.3
Otto	47.2	144.7	97.6	47.1	98.6	83.1
Overture	36.5	122.0	91.4	36.5	92.9	74.5
Oxbridge		136.0			79.3	65.3
Pallas	35.7	112.9	71.0	35.7	103.8	75.8
Paloma	48.4	165.5	108.9	48.4	90.4	73.2
Panther	49.8	148.8		49.9	80.5	
Paramount	45.4	159.6	117.2	45.6	82.3	76.1
Pasadena	56.7	149.5	114.9	56.8	82.4	71.6
PELICAN	41.0	#N/A	107.1	41.8		
Penthouse	40.8	#N/A	92.6	40.8		66.9
Perth		146.2			75.4	69.9
Perun	49.6	188.2	121.2	49.7	84.0	78.5
Pewter	34.8	141.5	72.8	34.8	89.4	65.9
Pitcher	51.6	183.4	94.3	51.6	77.9	77.5
Poet	48.7	158.7	95.2	48.6	78.8	76.2
Poker	49.8	165.0	93.8	49.7	84.7	73.4
Polygena	58.1	175.0	135.0	58.2	78.5	61.8
Pongo	42.3	154.2	106.2	42.2	78.5	72.9
Potter	32.9	157.2	90.0	33.0	81.2	67.3
Power	44.6	134.9	97.3	44.6	81.6	74.7
Prague	40.0	156.2	98.2	40.0	82.8	71.8
Prestige	35.6	140.1	114.9	35.6	86.6	72.1
Primera	51.0	161.0	116.3	51.1	94.9	77.0
Primus	48.6	167.3	110.1	48.7	88.9	69.5
Priora	38.3	138.4	97.3	38.3		
Prisma	55.6	176.9	105.0	55.6	87.6	75.8
Proctor	26.5	132.0	80.4	26.5	109.8	83.5
PROLOG	46.7	123.3	98.5	46.7	81.0	65.7
Propino	36.9	120.0	97.4	36.9	92.6	79.4
Prosa	38.6	158.7	85.7	38.7	91.1	80.4
Protege	40.0	157.2	106.8	40.0	79.2	73.6
Publican	21.0	156.8	93.1	20.8	87.7	65.9
Putney	49.9		108.8	50.0	78.9	58.7
Quartet	42.0	129.8	73.3	41.9	91.1	73.6
Quartz	52.9	160.1	111.1	52.8	101.5	85.4
Quench	38.7		97.4	38.7		68.1
Ragtime	47.4	186.6	124.6	47.5	74.0	74.6
Rainbow	60.3	167.0	119.8	60.3	86.2	73.1
Rakaia	51.4	146.3	96.7	51.3	75.0	66.6
Rangoon	21.9	117.0	84.9	21.8	92.0	75.1
Rapid	38.1	144.5	109.4	38.1	89.6	76.8
Rasa	34.6	157.4	90.8	34.7	105.9	78.3
Ratafia	49.0	165.5	100.4	49.0	92.5	69.3
Rebecca	39.1	149.2	110.9	39.1	84.8	75.4
Reggae	51.1	146.9	109.7	51.0	77.4	66.9
Renaissance		154.9			84.0	
Renata	39.0	119.4	86.3	38.9	115.8	96.1
Rhynchostar		136.1	100.9		88.1	68.3
Ria	41.9	133.6	100.9	41.9	90.7	75.6
Rika	50.8	152.4	106.2	50.8	114.1	87.3
RIVET	60.2		116.7	60.1		
Riviera	47.3	151.4	118.2	47.4	90.5	73.7
ROLAND	47.5	152.0	80.7	47.5	99.5	82.7
Romi	42.5	111.1	93.7	42.4	99.3	81.3
Roxana	40.4	177.0	113.0	40.3	85.3	77.0

Rubin	58.5	183.6	137.9	58.4	82.3	71.4
Ruja	43.7	126.7	96.2	43.7	108.8	92.1
Rummy	46.3	137.0	95.1	46.3	81.9	71.2
Rupal	42.7	164.2	85.9	42.6	89.5	73.9
SAANA	47.3	141.8	102.7	47.3	90.1	73.1
Sabel	54.1	157.2	120.9	54.2	71.6	75.8
Sacha	40.4	131.8	99.9	40.5	87.7	76.2
Safir	58.3	169.8	119.1	58.3	97.5	77.4
Salka	35.2	154.5	89.0	35.3	111.5	91.9
Saloon	47.6	172.1	111.1	47.7	85.7	70.7
Salve	42.9	134.2	90.2	43.0	107.8	87.1
SCANDIUM	38.2	176.4	121.3	38.1	84.7	62.2
Scarlett	50.6	153.7	113.0	50.7	87.3	77.6
Scout	43.5	180.2		43.4	86.7	
Sebastian	46.6	181.9	121.8	46.4	71.6	62.5
senat	38.6	143.6	75.9	38.4	106.2	82.3
Sencis	35.8	126.9	75.5	35.8	108.2	84.2
SHAKIRA	34.1	118.4	69.2	34.1	88.1	70.2
Shuffle		159.0			91.6	
Silicon	49.6	136.5	122.0	49.6	82.7	62.5
Simba	36.3	152.3	110.5	36.3	80.0	64.3
Simon	61.6	144.4	98.1	61.6	101.4	82.2
Sj 028117	52.5	176.2	98.9	52.3	81.5	66.7
Skagen	39.8	124.3	100.3	39.9	83.2	65.9
Skittle	37.2	150.7	86.5	37.3	89.5	71.4
Smilla	36.3	122.9	74.2	36.1	79.4	68.3
Snakebite	44.6	163.2		44.6	76.8	
Spartan	54.7	165.7	103.3	54.5	94.1	70.5
Spey	57.7	177.2	118.3	57.6	89.0	81.2
Spike	54.7	160.8	123.3	54.9	83.9	81.1
Spiral	29.5	125.6	92.5	29.5	92.7	77.8
Spire	63.4	171.8	112.3	63.4	84.5	65.6
Splash	56.0	176.4	122.6	56.0	76.1	74.3
Starlight	61.5	200.1	124.0	61.6	85.2	74.7
Static	55.1	156.5	103.9	55.0	81.9	68.4
Steffi	52.6	147.3	96.2	52.6	88.7	82.1
Steina	46.1	143.3	94.9	46.2	105.2	74.4
Stendes	34.1	114.2	79.4	33.9	112.4	90.3
Sultan	46.6	150.4	94.2	46.7	103.5	85.8
Summit	51.0	127.7	116.1	51.1	86.5	62.2
SW 2808	35.7	158.1	102.6	35.7	82.4	70.7
SW Catriona	58.0	176.1	111.0	58.1	82.6	71.8
SW MACSENA	30.0	131.7	97.4	30.1	89.2	70.7
SW Makof	51.5	172.9	121.8	51.5	86.9	67.3
SW Scania	53.4	167.6	116.1	53.3	76.9	73.8
SW Stella	43.5	167.2	109.7	43.5	84.0	66.5
Sweeney		160.3			81.7	63.5
SY Aboyne	40.3	158.2		40.3	90.1	
SY Barrell	48.7	142.6		48.7	79.4	
SY Taberna	43.1	179.9	102.6	43.1	88.6	69.6
SY Universal	30.9	129.1		31.0	93.1	
Tabora	38.3	177.6	103.9	38.4	87.1	75.0
Tamise		161.3			77.3	67.1
Tankard	53.2	198.1	132.1	53.2	80.7	77.8
Tapestry		163.3			85.9	69.6
Taphouse	57.5	164.9	101.4	57.5	84.5	69.1
Tardus	45.9	185.4	104.2	46.0	90.7	77.5
Tarm92	45.1	131.0	111.2	45.2	114.4	80.7

Tartan	47.6	157.2	116.4	47.5	80.7	74.6
Tavern	38.1	139.5	90.5	38.1	85.8	59.8
Tellus	43.2	157.3	85.8	43.2	93.9	77.2
Tennis	60.6	127.3	113.8	60.5	99.7	70.6
Terno	55.0	160.3	106.7	55.0	89.3	71.8
Thistle	38.1	133.1	97.9	37.9	79.8	63.5
Thrift	43.1	157.7	94.9	43.2	75.9	61.2
Thuringia	41.4	122.9	95.8	41.5	100.7	83.3
Timori	63.5	171.6	136.5	63.4	74.8	71.4
Toby	51.5	166.0	100.1	51.5	84.3	73.7
Tocada	50.6	190.7	120.0	50.5	87.4	74.5
Toddy	45.5	149.1	104.4	45.4	85.2	74.4
TOKEN	53.4	156.4	102.8	53.3	85.3	67.7
Torup	51.0	217.1	121.2	50.9	83.3	71.5
Toucan	47.7	150.4	108.5	47.9	90.1	71.2
Tremois	42.3	172.8	108.3	42.3	104.1	89.9
Trinidad	58.1	174.3	121.7	58.1	82.0	60.9
Trinity	48.9	155.5	114.3	48.9	78.4	67.7
Triumph	54.8	169.9	118.4	54.9	80.5	72.8
Troon	31.0	157.8	105.0	30.9	85.2	78.9
Trosa	48.6	159.6	112.9	48.7	80.5	67.7
Tucson	35.4	184.3	102.9	35.5	83.7	68.4
Turnberry	48.9	182.0	124.2	48.8	80.8	69.1
Tyne	56.7	167.7	85.6	56.6	82.8	66.8
TYRA	32.7	149.4	105.6	32.8	97.5	83.8
Union	52.3	151.0	93.7	52.4	110.9	98.7
Ursa	55.4	167.4	110.7	55.3	89.1	75.3
URSEL	38.0	139.4	84.4	37.9	92.8	87.5
Vada	42.2	160.5	95.0	42.3	115.0	88.8
Valticky	34.8	147.2	102.2	35.0	112.1	91.1
vankkuri	35.7	147.3	82.8	35.7	121.8	103.6
Varberg	33.9	154.4	74.6	34.0	94.1	65.9
VEGA	43.7	148.4	77.0	43.5	117.6	88.2
Vegas	52.2	169.7	120.5	52.2	90.0	81.3
Velvet	59.7	159.4	109.7	59.8	88.1	69.4
VIIVI	40.2	175.5	109.3	40.2	96.3	80.7
Villa	65.5		127.6	65.5		64.3
VIRGIL	37.6	213.2	96.0	37.6	84.5	70.8
VISKOSA	52.3	166.3	139.3	52.4	81.8	73.6
VIVENDI	53.7	172.0	116.7	53.7	84.4	64.8
Volla	40.1		77.2	40.2		100.6
Vortex	47.9	150.4	98.2	48.0	79.6	68.4
Waggon	64.6	159.2	135.3	64.7	80.1	71.8
Waldemar	36.8	185.3	122.1	36.7	74.5	52.1
Weitor	55.9	161.2	136.9	55.9	89.6	68.1
WELAM	52.5	158.8	90.2	52.4	115.4	85.7
Westminster	37.4	134.5	93.4	37.4	98.0	84.0
Wicket	57.3	110.6	105.7	57.3	83.8	60.8
Widre	55.1	188.9	118.5	55.1	74.4	61.8
Wing	45.2	144.8	94.4	45.2	115.6	82.6
Wisa	37.9	137.7	91.7	38.0	121.0	100.9
Wren	53.7	183.3	106.7	53.7	90.0	62.6
Yard		149.5			88.4	
Z91-103-21	48.7	184.5	116.0	48.7	78.8	66.0
Zenit	52.2	167.2	114.0	52.2	83.8	70.6
Zephyr	36.0	154.7	75.3	36.0	98.7	79.4

Table IX-2: *Rrs1* phenotyping on predicted *Rrs1* lines (using GWAS peak marker SCRI_RS_221644 genotype call). * lines where genotyped by sequencing

Barley lines	Disease reactions against *R. R. R.commune* isolates		Rrs1 allele prediction using SCRI_RS_221644 genotype call	Barley type
	LfL12F, spray inoculation	214-GFP, confocal microscopy		
Atlas 46 ($Rrs1_{Turk}$, Rrs2)	Susceptible	Resistant	Not genotyped	Spring
sbcc154 ($Rrs1_{Rh4}$)	Resistant	-	Rrs1*	Spring
sbcc145 ($Rrs1_{Rh4}$)	Resistant	Resistant	Rrs1*	Spring
Acclaim	Resistant	Resistant	Rrs1	Spring
Beriliyum	Resistant	Resistant	Rrs1	Spring
Cairn	Resistant	Resistant	Rrs1	Spring
Casino	Resistant	Resistant	Rrs1	Spring
Chieftain	Resistant	Resistant	Rrs1	Spring
Corgi	Resistant	Resistant	Rrs1	Spring
Gairdner	Resistant	Resistant	Rrs1	Spring
Brahms	Resistant	-	Rrs1	Spring
Celebra	Resistant	-	Rrs1	Spring
Century	Resistant	-	Rrs1	Spring
Chronicle	Resistant	-	Rrs1	Spring
Franklin	Resistant	-	Rrs1	Spring
Freja	Resistant	-	Rrs1	Spring
Graphic	Resistant	-	Rrs1	Spring
Magellan	Resistant	-	Rrs1	Spring
Rebecca	Resistant	-	Rrs1	Spring
Retriever	Resistant	-	Rrs1	Winter
SW Macsena	Resistant	-	Rrs1	Spring
Westminster	Resistant	-	Rrs1	Spring
Karri	Susceptible	-	Rrs1	Spring
Akita	Susceptible	Susceptible	non-Rrs1	Spring
Barabas	Susceptible	Susceptible	non-Rrs1	Spring
Bulbul 89	Susceptible	Susceptible	non-Rrs1	Spring
Concerto	Susceptible	Susceptible	non-Rrs1	Spring
Gizmo	Susceptible	Susceptible	non-Rrs1	Spring
Imidis	Susceptible	Susceptible	non-Rrs1	Spring
Nordal	Susceptible	Susceptible	non-Rrs1	Spring
Cropton	Susceptible	-	non-Rrs1	Spring
Aapo	Susceptible	-	non-Rrs1	Spring
Abava	Susceptible	-	non-Rrs1	Spring
Alexis	Susceptible	-	non-Rrs1	Spring
Annabell	Susceptible	-	non-Rrs1	Spring
Ardila	Susceptible	-	non-Rrs1	Spring
Aspen	Susceptible	-	non-Rrs1	Spring
Atem	Susceptible	-	non-Rrs1	Spring
Athena	Susceptible	-	non-Rrs1	Spring
Azure	Susceptible	-	non-Rrs1	Spring

Baronesse	Susceptible	-	non-Rrs1	Spring
Binder Abed	Susceptible	-	non-Rrs1	Spring
Calgary	Susceptible	-	non-Rrs1	Spring
Chamant	Susceptible	-	non-Rrs1	Spring
Chaser	Susceptible	-	non-Rrs1	Spring
Chevallier Tystofte	Susceptible	-	non-Rrs1	Spring
CPBT_C80	Susceptible	-	non-Rrs1	Spring
Drum	Susceptible	-	non-Rrs1	Spring
Felicitas	Susceptible	-	non-Rrs1	Spring
Frieda	Susceptible	-	non-Rrs1	Spring
Hannchen	Susceptible	-	non-Rrs1	Spring
Harriot	Susceptible	-	non-Rrs1	Spring
Ida	Susceptible	-	non-Rrs1	Spring
Jive	Susceptible	-	non-Rrs1	Spring
Klaxon	Susceptible	-	non-Rrs1	Spring
Kym	Susceptible	-	non-Rrs1	Spring
NSL 95-1257	Susceptible	-	non-Rrs1	Spring
NSL 98_5065	Susceptible	-	non-Rrs1	Spring
Pelican 1745	Susceptible	-	non-Rrs1	Winter
Rangoon	Susceptible	-	non-Rrs1	Spring
Scarlett	Susceptible	-	non-Rrs1	Spring
Vegas	Susceptible	-	non-Rrs1	Spring
Vortex	Susceptible	-	non-Rrs1	Spring
Apex	Susceptible	-	non-Rrs1	Spring
Beatrix	Susceptible	-	non-Rrs1	Spring
Optic	Susceptible	-	non-Rrs1	Spring
Steffi	Susceptible	-	non-Rrs1	Spring
Tarm 92	Susceptible	-	non-Rrs1	Spring
SW 2808	Resistant	-	non-Rrs1	Spring
Anaconda	Resistant	-	non-Rrs1	Spring
Atlas (Rrs2)	Resistant	Susceptible	non-Rrs1	Spring
Pewter (Rrs2)	Resistant	-	non-Rrs1	Spring
Acrobat	Susceptible	Resistant	non-Rrs1	Spring
Armelle	Susceptible	Resistant	non-Rrs1	Spring

Figure IX-1: Alignments of the 3' 800 bp of the last exon sequence containing the 3 *Rrs1*$_{Rh4}$ discriminating SNP with the 3 best blast match are in supplementary data.

```
> Query1 on chr3H
Length=699711114

 Score = 1443 bits (1600),  Expect = 0.0
 Identities = 800/800 (100%), Gaps = 0/800 (0%)
 Strand=Plus/Plus

Query  1          GTCATCAGATAGCAGTAAAGATGCTGAAAGATTTCAAGACTGATGGAGAGGATTTCATCA  60
                  ||||||||||||||||||||||||||||||||||||||||||||||||||||||||||||
Sbjct 490243424   GTCATCAGATAGCAGTAAAGATGCTGAAAGATTTCAAGACTGATGGAGAGGATTTCATCA  490243483

Query 61          ATGAGTTAGCTAGCATTAGTAGAACTTCTCATGTCAACGTCGTTACTCTCTTAGGATTTT  120
                  ||||||||||||||||||||||||||||||||||||||||||||||||||||||||||||
Sbjct 490243484   ATGAGTTAGCTAGCATTAGTAGAACTTCTCATGTCAACGTCGTTACTCTCTTAGGATTTT  490243543

Query 121         GCTTGGAAGGGTCGAAAAGGGCACTAATTTATGACTATATGCCTAATGGTTCACTTGAAA  180
                  ||||||||||||||||||||||||||||||||||||||||||||||||||||||||||||
Sbjct 490243544   GCTTGGAAGGGTCGAAAAGGGCACTAATTTATGACTATATGCCTAATGGTTCACTTGAAA  490243603

Query 181         AGTATGCTTTCAAAGATAGCTCTGAAGGTGGAAATACATTAGGTTGGGAGAAATTGTTTG  240
                  ||||||||||||||||||||||||||||||||||||||||||||||||||||||||||||
Sbjct 490243604   AGTATGCTTTCAAAGATAGCTCTGAAGGTGGAAATACATTAGGTTGGGAGAAATTGTTTG  490243663

Query 241         AAATTGCAGTGGGAATTGCTCGAGGACTTGAATATCTGCATAGAGGATGCAATACTCGCA  300
                  ||||||||||||||||||||||||||||||||||||||||||||||||||||||||||||
Sbjct 490243664   AAATTGCAGTGGGAATTGCTCGAGGACTTGAATATCTGCATAGAGGATGCAATACTCGCA  490243723

Query 301         TAGTGCATTTTGATATCAAGCCCCACAACATTCTATTGGATCAAAACTTCTGTCCAAAGA  360
                  ||||||||||||||||||||||||||||||||||||||||||||||||||||||||||||
Sbjct 490243724   TAGTGCATTTTGATATCAAGCCCCACAACATTCTATTGGATCAAAACTTCTGTCCAAAGA  490243783

Query 361         TCTCTGATTTCGGACTGGCCAAGCTGTGCCTGAACAAAGAAAGTATTATTTCCATTGGTG  420
                  ||||||||||||||||||||||||||||||||||||||||||||||||||||||||||||
Sbjct 490243784   TCTCTGATTTCGGACTGGCCAAGCTGTGCCTGAACAAAGAAAGTATTATTTCCATTGGTG  490243843

Query 421         GTGCAAGAGGAACAATAGGCTATATTGCTCCCGAGGTTTATTCGAAGCAATTCGGAGCAG  480
                  ||||||||||||||||||||||||||||||||||||||||||||||||||||||||||||
Sbjct 490243844   GTGCAAGAGGAACAATAGGCTATATTGCTCCCGAGGTTTATTCGAAGCAATTCGGAGCAG  490243903

Query 481         TGAGTAGCAAGTCCGATGTTTACAGCTATGGAATGATGGTTCTTGAGATGGTTGGGGCAA  540
                  ||||||||||||||||||||||||||||||||||||||||||||||||||||||||||||
Sbjct 490243904   TGAGTAGCAAGTCCGATGTTTACAGCTATGGAATGATGGTTCTTGAGATGGTTGGGGCAA  490243963

Query 541         GGGACAAGAACATCAGTCAAAATACTGAATCTAGCAGCCAGTATTTCCCACAGTGGATCT  600
                  ||||||||||||||||||||||||||||||||||||||||||||||||||||||||||||
Sbjct 490243964   GGGACAAGAACATCAGTCAAAATACTGAATCTAGCAGCCAGTATTTCCCACAGTGGATCT  490244023

Query 601         ATGAACATCTAGATGAATATTGTATTGGTGCTTCTGAGATTAATGGAGAGATCACGGAGG  660
                  ||||||||||||||||||||||||||||||||||||||||||||||||||||||||||||
Sbjct 490244024   ATGAACATCTAGATGAATATTGTATTGGTGCTTCTGAGATTAATGGAGAGATCACGGAGG  490244083

Query 661         TTGTGAGGAAGATGATAGTGGTTGGGCTGTGGTGCATTCAGCTGAGTTCTACAGATCGTC  720
                  ||||||||||||||||||||||||||||||||||||||||||||||||||||||||||||
Sbjct 490244084   TTGTGAGGAAGATGATAGTGGTTGGGCTGTGGTGCATTCAGCTGAGTTCTACAGATCGTC  490244143

Query 721         CAACAATGACTAGAGTCGTGGAGATGCTTGAAGGGAGCACAGCCGGCCTCGAATTGCCAC  780
                  ||||||||||||||||||||||||||||||||||||||||||||||||||||||||||||
Sbjct 490244144   CAACAATGACTAGAGTCGTGGAGATGCTTGAAGGGAGCACAGCCGGCCTCGAATTGCCAC  490244203

Query 781         CAAAAGTGCTCTTGAGTTGA  800
                  ||||||||||||||||||||
Sbjct 490244204   CAAAAGTGCTCTTGAGTTGA  490244223
```

```
> Query1 on chrUn
Length=249774706

 Score =  188 bits (208),  Expect = 5e-45
 Identities = 342/498 (68%), Gaps = 7/498 (1%)
 Strand=Plus/Plus

Query  43        ATGGAGAGGATTTCATCAATGAGTTAGCTAGCATTAGTAGAACTTCTCATGTCAACGTCG  102
                 |||| ||||| ||  | |||||| |    |||||| | || || |||||||| ||  | |
Sbjct  33143233  ATGGGGAGGAGTTTGTGAATGAGGTTATGAGCATTGGCAGGACCTCTCATGTGAATATTG  33143292

Query  103       TTACTCTCTTAGGATTTTGCTTGGAAGGGTCGAAAAGGGCACTAATTTATGACTATATGC  162
                 |||  || || |||||||| ||||| || || ||| | || || || ||||| || |||
Sbjct  33143293  TTAGCCTGTTTGGATTTTGTTTGGAGGGATCAAAACGAGCTCTTATATATGAGTACATGT  33143352

Query  163       CTAATGGTTCACTTGAAAAGTATGCTTTCAAAGATAGCTCTGAAGGTGGAAATACATTAG  222
                   |||||||| || || |  ||    | |  ||| | | |  |||    ||||   ||||
Sbjct  33143353  GCAATGGTTCCCTAGATAGATACATCTACTCAGAGAACCCAAAAG----AAATT--TTAG  33143406

Query  223       GTTGGGAGAAATTGTTTGAAATTGCAGTGGGAATTGCTCGAGGACTTGAATATCTGCATA  282
                 | |||||||   | | ||  || |   | ||||| ||||| ||||| |||||| ||||
Sbjct  33143407  GATGGGAGAGGCTCTATGCGATAGGGATTGGAATAGCTCGTGGACTGGAATATTTGCACC  33143466

Query  283       GAGGATGCAATACTCGCATAGTGCATTTTGATATCAAGCCCCACAACATTCTATTGGATC  342
                    | || || || || || || |||||||| || ||||| || || || ||  ||||
Sbjct  33143467  ATAGTTGTAACACACGGATCGTCCATTTTGACATTAAGCCTCAAAATATCCTTCTGGACA  33143526

Query  343       AAAACTTCTGTCCAAAGATCTCTGATTTCGGACTGGCCAAGCTGTGCCTGAACAAAGAAA  402
                 |  | || || ||||||||  | ||||| || || || || || ||||  | ||| || |
Sbjct  33143527  AGGATTTTTGCCCAAAGATTGCCGATTTTGGTCTAGCTAAACTATGCCATACCAAGGAGA  33143586

Query  403       GTATTATTTCCATTGGTGGTGCAAGAGGAACAATAGGCTATATTGCTCCCGAGGTTTATT  462
                 | |   |||| ||   |||||| |||||||||| || |  |||||||| || ||| | |
Sbjct  33143587  GCAAGCTTTCAATGATTGGTGCTAGAGGAACAATTGGATTCATTGCTCCAGAAGTTCACT  33143646

Query  463       CGAAGCAATTCGGAGCAGTGAGTAGCAAGTCCGATGTTTACAGCTATGGAATGATGGTTC  522
                 ||    | ||||||   ||    |  ||||| |||||||| || ||||||||||| | |
Sbjct  33143647  CGCGAAACTTCGGACTTGTTTCAACAAAGTCAGATGTTTATAGTTATGGAATGATGTTGC  33143706

Query  523       TTGAGATGGTTGG-GGCA  539
                 | |||||||||| ||||
Sbjct  33143707  TAGAGATGGTTGGAGGCA  33143724
```

```
> Query1 on chr5H
Length=670030160

 Score =  185 bits (204),  Expect = 6e-44
 Identities = 353/514 (68%), Gaps = 16/514 (3%)
 Strand=Plus/Minus

Query  43         ATGGAGAGGATTTCATCAATGAGTTAGCTAGCATTAGTAGAACTTCTCATGTCAACGTCG  102
                  ||||||| || ||  | |||||| | |  |||||||| || || || |||||||| || |
Sbjct  546110899  ATGGAGAAGAATTTGTAAATGAGGTCGTCAGCATTAGAAGGACATCCCATGTCAATGTTG
546110840

Query  103        TTACTCTCTTAGGATTTTGCTTGGAAGGGTCGAAAAGGGCACTAATTTATGACTATATGC  162
                  | || ||  | || || || ||||| || || || || || || || ||||| |||||||
Sbjct  546110839  TCACACTGCTTGGTTTCTGTTTGGAGGGTTCAAAGAGAGCCCTCATCTATGATTATATGC
546110780

Query  163        CTAATGGTTCACTTGAAAAGTATGCTTTCAAAGATAGCTCTGAAGGTGGAAATACATTAG  222
                  ||||||| ||||| || || |     | ||  || |  || |||     | | ||  | |
Sbjct  546110779  CTAATGGGTCACTGGACAAATTCATCTACACTGAGAATTC-GAA-----ACAAACTCTTG
546110726

Query  223        GTTGGGAGAAATTGTTTGAAATTGCAGTGGGAATTGCTCGAGGACTTGAATATCTGCATA  282
                  | |||||||||| | ||| || ||| |||| |||||  ||||| | || ||||| ||
Sbjct  546110725  GATGGGAGAAATTATATGAGATCGCAATGGGCATTGCCAGAGGATTGGAGTATCTTCACC
546110666

Query  283        GAGGATGCAATACTCGCATAGTGCATTTTGATATCAAGCCCCACAACATTCTATTGGATC  342
                  |||| || || || || ||  | || ||||| |||||||||| ||||| ||  | || |
Sbjct  546110665  GAGGGTGTAACACACGAATCATACACTTTGACATCAAGCCCCAGAACATCCTCCTAGACC
546110606

Query  343        AAAACTTCTGTCCAAAGATCTCTGATTTCGGACTGGCCAAGCTGTGCCTGAACAAAGAAA  402
                  |  |||||   ||||||||| | ||||| || ||||| ||| |||||     ||| || |
Sbjct  546110605  AGGACTTCGTCCCAAAGATCGCCGATTTTGGTCTGGCGAAGTTGTGCAACCCCAAGGAGA
546110546

Query  403        G-TA--TTATTTCCATTGGTGG--TGCAAGAGGAACAATAGGCTATATTGCTCCCGAGGT  457
                  | ||  | || || || | |||  |||  | || ||  | || |  || || || |||||
Sbjct  546110545  GCTACCTCATGTCGATGGATGGCATGC--GTGGTACGGTCGGGTTCATCGCGCCTGAGGT
546110488

Query  458        TTATTCGAAGCAATTCGGAGCAGTGAGTAGCAAGTCCGATGTTTACAGCTATGGAATGAT  517
                   |  |||| ||  ||||| |  |||   |  ||||| || || |||||||  || ||| |
Sbjct  546110487  CTTCTCGAGGCGGTTCGGGGTCGTGTCGACAAAGTCGGACGTGTACAGCTTCGGGATGGT
546110428

Query  518        GGTTCTTGAGATGGTTGGGGCAAGGGACAAGAAC  551
                  | |  | |||||||| || | ||||   ||||||
Sbjct  546110427  GCTCTTGGAGATGGTCGGAGGAAGG---AAGAAC  546110397
```